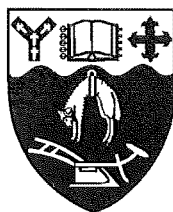


SPECIATION OF ALUMINIUM IN ENVIRONMENTAL SYSTEMS

A thesis submitted in partial fulfilment of the requirements for the degree of

Doctor of Philosophy in Chemistry

at the
University of Canterbury



by

Stuart L. Simpson

1996

ABSTRACT

This thesis is directed towards the development of a speciation protocol for Al in natural waters and soil solutions. Factors that might influence the accuracy of the speciation results are investigated.

The equilibrium reactions between aluminium(III) and (i) pyrocatechol violet (PCV) and (ii) 4-nitrocatechol have been studied by potentiometric titration in aqueous solution, $I = 0.10 \text{ M K(Cl)}$, 25.0°C . The adsorption behaviour of pyrocatechol violet on the surface of the aluminium-oxide hydroxide boehmite [$\alpha\text{-AlO(OH)}$] has been investigated. In this work, the experimental data for surface complexation were evaluated on the basis of the electrostatic constant capacitance model. The acidity constants of the surface hydroxy groups at the boehmite-solution interface were evaluated as a prerequisite to studying the ligand adsorption behaviour. This work and the equilibrium reactions between aluminium(III) and pyrocatechol violet (PCV) were performed at Umeå University, Sweden.

A comparison of the chromophores chrome azurol S (CAS), eriochrome cyanine R (ECR) and pyrocatechol violet (PCV) for the determination of Al was made. These studies were performed using computer modelling calculations. The pH and mass action effects were calculated for the representative 'interferents' citrate, oxalate, salicylate and fluoride. The effects of complexation kinetics on the use of PCV for the determination of 'labile' Al in the competitive systems: 'PCV- Al^{3+} -citrate' and 'PCV- Al^{3+} -oxalate' was investigated. These studies also validated the ' H^+ - Al^{3+} -pyrocatechol violet' equilibrium data for typical analytical conditions.

A preliminary survey was made of the electrochemical properties of a series of Al^{3+} -ligand systems using cyclic voltammetry. This was to identify redox-active ligands which may be used as electrochemical probes for Al. Flow injection analysis (FIA) methods for the determination of Al which exploit the indirect electrochemical detection of Al using the ligands pyrocatechol violet and tetrahydroxy-1,4-quinone were investigated.

The development of an Al^{3+} speciation procedure is described. It is based on a 2-s reaction with oxine-derivatised Fractogel positioned in a $22 \mu\text{L}$ column reactor in an FIA manifold. Al^{3+} (pre)concentrated on the column from a $650 \mu\text{L}$ sample was selectively eluted (via the rapid quantitative conversion of resin-bound Al^{3+} to the Al(OH)_4^- ion) with $150\text{--}250 \mu\text{L}$ of $0.02 \text{ mol L}^{-1} \text{ NaOH}$ and detected spectrophotometrically as the Al-CAS (chrome azurol S) complex at pH 5.0.

The resultant FIA method was tested for (i) the selective separation of reactive Al from Fe, (ii) the sequestering of Al from its citrate, oxalate, malonate and fluoride complexes and (iii) retention of Al-hydroxy polymers [*e.g.* $\text{Al}_{13}(\text{OH})_{32}^{7+}$] by the adsorbent. The method was applied to humic waters and soil solutions and the results for 'free' Al^{3+} were compared with those obtained by the previously published 7-s CAS

method. The method's detection limit and linear working range were evaluated. The potential for further development of this AI speciation technique is discussed.

ACKNOWLEDGEMENTS

I sincerely thank my supervisors Dr. H. Kipton J. Powell and Prof. Staffan Sjöberg for their generous support and encouragement throughout this work. Their guidance, wisdom and patience contributed greatly to the outcome of this project. I greatly appreciate Kip's dedication to this project and am very grateful to Staffan for inviting me to join his excellent 'solution chemistry group', Umeå University (Sweden), for a one year period of study leave and for his wonderful hospitality.

I would like to thank Dr. Alison J. Downard and Dr. Lars-Olof Öhman for many helpful discussions in the fields of electrochemistry and solution equilibria respectively. I would like to thank Dr. David J. Hawke for good cooperation and help throughout this project. I would also like to express my gratitude to Prof. Paul W. Schindler, University of Bern, Switzerland for valuable suggestions and stimulating discussion in the field of aqueous surface chemistry and to Dr. Per Persson for cooperation and deciphering information from vibrational spectra.

I would like to thank my good friends and colleagues Janne Nordin, Erkki Laiti, Agneta Nordin and Ingegärd Andersson for much guidance, assistance and cooperation during my period of study leave at Umeå University, Sweden. Further, I would like to thank all those who participated in making me feel very welcome during my stay in Umeå. Thanks for the hospitality.

I would also like to thank all other friends and colleagues, past and present, at the Chemistry Department for their fellowship and willing assistance. Special thanks to Brendon Laughton, Hamish, Glenn, Stu(2), Mike, Gill, Alex, Siân, Paul and Jens (Sloth), Janne, Erkki, Nils, Magnus, Camilla and Christer for creating a pleasant social environment both inside and outside the university.

I thank the University Grants Committee for the award of a University of Canterbury Doctoral Scholarship and the Swedish National Science Research Council for financial support during my stay in Sweden.

Finally, I would like to thank my parents, Neill and Barbara Simpson and my brothers Mike and Ali for their tremendous support.

TABLE OF CONTENTS

CHAPTER 1

THE ENVIRONMENTAL CHEMISTRY OF ALUMINIUM

SECTION A: THE CHEMISTRY OF ALUMINIUM IN THE ENVIRONMENT

1.1 ALUMINIUM IN THE ENVIRONMENT	1
1.1.1 Aluminium Transport And Release	2
1.1.2 Effects Of Acid Deposition	6
1.1.3 Speciation Of Aluminium In Natural Waters	8
(A) Al Hydrolysis	8
(B) Inorganic Al Species	9
(C) Organic Al Species	10
(D) Particulate and Colloidal Al Species	12

SECTION B: THE TOXICOLOGICAL EFFECTS OF ALUMINIUM TO PLANTS, AQUATIC ORGANISMS AND HUMANS

1.2 TOXICOLOGICAL EFFECTS OF ALUMINIUM	13
1.2.1 Aluminium Toxicity To Plants	13
(A) Morphological Damage	13
(B) Physiological Effects	14
(C) Tolerance Mechanisms	15
(D) Toxic Species	16
(E) Estimating Soil Toxicity	17
1.2.2 Aluminium Toxicity To Aquatic Biota	18
(A) Aluminium Toxicity to Invertebrates	19
(B) Aluminium Toxicity to Fish	20
1.2.3 Aluminium Toxicity To Humans	24
(A) Dialysis Related Disorders	24
(B) Alzheimer's Dementia	25
(C) Amyotrophic Lateral Sclerosis and Parkinson's Dementia	26
(D) Al Consumption	26

(E) Al Speciation in Biological Fluids	26
(F) Toxicity Mechanisms	27

SECTION C: THE MEASUREMENT AND SPECIATION OF ALUMINIUM AT ENVIRONMENTALLY SIGNIFICANT CONCENTRATIONS

1.3 Al MEASUREMENT	28
1.3.1 Speciation And Fractionation	28
(A) Driscoll Fractionation Protocol	29
(B) Kinetic Methods	30
1.4 OBJECTIVES OF THIS WORK	35

CHAPTER 2

NUMERICAL ANALYSIS

SECTION A: MATHEMATICAL TREATMENT OF POTENTIOMETRIC TITRATION DATA FOR THE DETERMINATION OF FORMATION CONSTANTS

2.1 THERMODYNAMIC TREATMENT OF AQUEOUS EQUILIBRIA	39
2.1.1 Ligand Protonation Equilibria	41
2.1.2 Metal-Ligand Equilibria	43
2.1.3 Formation Curves	44
(A) $Z(-\log h)$ Curves	44
(B) $\bar{n}(-\log [L])$ Curves	44
2.1.4 Evaluation Of The Equilibrium Model	45
(A) Data Collection	45
(B) Equilibrium Analysis	46
2.2 THERMODYNAMIC TREATMENT OF SURFACE COMPLEXATION	
2.2.1 Chemical Reactions At Metal Oxide-Water Interfaces	48
2.2.2 Chemical Modelling Of Surface Complexation	49
(A) The Triple Layer Model	50

(B) The Constant Capacitance Model	50
(C) The Diffuse Layer Model	52
2.2.3 The Constant Capacitance Model	52

SECTION B: THE MEASUREMENT OF pH

2.3 pH	55
2.3.1 pH Measurement	55

CHAPTER 3

EXPERIMENTAL METHODS

SECTION A: EXPERIMENTAL PROCEDURES AND APPARATUS

3.1 VOLUMETRIC EQUIPMENT	58
3.2 REAGENTS AND SOLUTION PREPARATION	58
3.2.1 Standard Alkali Solutions	59
(A) Procedure 1	59
(B) Procedure 2	59
3.2.2 Standard Acid Solutions	59
3.2.3 Electrolyte Solutions	60
3.2.4 Buffers	60
(A) Electrode Calibration Buffers	60
(B) Electrochemical and Spectrophotometric Buffers	60
3.2.5 Metal Ion Solutions	60
(A) Aluminium(III) Solutions	60
(B) Copper(II) Solutions	61
(C) Iron(III) Solutions	61
3.2.6 Ligand Solutions	61
(A) Pyrocatechol Violet	61
(B) 4-Nitrocatechol	61
(C) Chrome Azurol S	61

(D) Rhodizonic Acid and Tetrahydroxy-1,4-quinone	62
(E) Citric, Malonic, Oxalic and Salicylic Acids	62
(F) Fluoride	62
(G) Other Ligands	62
3.2.7 Microanalysis	62
3.2.8 Oxine Resin	62
(A) Reagents	62
(B) Brief Method	62
3.2.9 Boehmite Suspensions	63
3.3 FILTRATION AND CENTRIFUGATION	63
3.3.1 Filtration	63
3.3.2 Centrifugation	63
(A) Boehmite Work	63
(B) Soil Solutions	64
3.4 SPECTROPHOTOMETRIC TITRATION SYSTEM	64
3.5 ELECTROCHEMICAL INSTRUMENTATION	65
3.5.1 Voltammetry	65
3.5.2 Electrodes And Cells	65
3.5.3 pH Measurements	65
3.6 SPECTROPHOTOMETRY	65
3.6.1 Visible Absorption Spectra	65
3.6.2 Electrothermal Atomic Absorption Spectrophotometry	66
3.6.3 DRIFT Spectroscopy	66
3.7 FLOW INJECTION ANALYSIS	66
3.8 SPECIATION CALCULATIONS	66
3.9 SOIL SOLUTIONS AND HUMIC WATERS	66

SECTION B: POTENTIOMETRIC TITRATION SYSTEMS

3.10 TITRATION SET-UP AND OPERATION	67
3.10.1 Cell Assembly	67
(A) Titration System 1	67
(B) Titration System 2	67
3.10.2 Atmospheric Oxygen And Carbon Dioxide Removal	68
3.11 ELECTRODE SYSTEMS	68
3.11.1 Glass Electrodes / Reference Electrodes	68
(A) Preparation of the Silver-Silver (Chloride) Reference Electrode	68
(B) Use of the Silver Chloride Electrode	69
3.11.2 Hydrogen Electrodes	69
(A) Preparation of the Hydrogen Electrode	69
(B) Use of the Hydrogen Electrode	70
3.11.3 Electrode Testing And Calibration Procedures	70
(A) Electrode Calibration Procedures	70
(B) Testing of Glass Electrodes Against the Hydrogen Electrode	71
3.11.4 Coulometry	72
3.12 TITRATION PROCEDURE	73

CHAPTER 4**POTENTIOMETRIC STUDIES OF ALUMINIUM(III) - PYROCATECHOL VIOLET AND ALUMINIUM(III) - 4-NITROCATTECHOL EQUILIBRIA**

4.1 INTRODUCTION	74
4.1.1 Scope Of This Work	75

**SECTION A: POTENTIOMETRIC STUDIES OF ALUMINIUM(III)-
PYROCATECHOL VIOLET EQUILIBRIA**

4.2 PYROCATECHOL VIOLET	76
4.2.1 Experimental	77
(A) Chemicals and Analysis	77
(B) Spectrophotometric Determination of $\log K_1$	77
(C) Spectrophotometric Titrations	78
(D) Potentiometric Titrations	78
4.2.2 Data Treatment	79
(A) Potentiometry	79
(B) Spectrophotometry	80
4.2.3 Data, Calculations, Results	81
4.2.4 Discussion	87

**SECTION B: POTENTIOMETRIC STUDIES OF ALUMINIUM(III)-
4-NITROCATTECHOL EQUILIBRIA**

4.3 4-NITROCATTECHOL	93
4.3.1 Experimental	94
(A) Chemicals and Analysis	94
(B) Potentiometric Titrations	94
4.3.2 Data Treatment	95
4.3.3 Data, Calculations, Results	95
4.3.4 Discussion	98

CHAPTER 5**PYROCATECHOL VIOLET COMPLEXATION AT
THE BOEHMITE-WATER INTERFACE**

5.1 ADSORPTION OF ORGANIC LIGANDS AND METALS AT HYDROUS OXIDE SURFACES.	102
5.1.1 Introduction	102
5.1.2 Adsorption Of Natural Organic Matter	102
5.1.3 Adsorption Of Metals In The Presence Of Organics	103
5.1.4 Mechanisms Of Adsorption Of Ligands On Hydrous Oxide Surfaces	104
5.1.5 Surface Complexation Models	107
5.2 THE ADSORPTION BEHAVIOUR OF PYROCATECHOL VIOLET ON THE SURFACE OF BOEHMITE [α-AlO(OH)].	108
5.2.1 Introduction	108
5.2.2 Experimental	110
(A) Chemicals and Analysis	110
(B) Potentiometric Titrations	111
(C) Batch 'Adsorption' Titrations	111
(D) Spectrophotometric Studies	112
(E) Aluminium Analysis	112
(F) DRIFT Spectroscopy	113
5.2.3 Data Treatment	113
5.2.4 Data, Calculations And Results	114
(A) The 2-Component System	114
(B) The 3-Component System	115
(C) Spectrophotometric Studies	123
5.2.5 Discussion	123
(A) DRIFT Spectra	126
(B) Mechanism of Complexation	126
(C) Spectrophotometric Studies	129

CHAPTER 6

COMPARISON OF CHROMOPHORES AND REACTION KINETICS IN COMPETITIVE ' REAGENT-AL-LIGAND ' SYSTEMS

SECTION A: COMPARISON OF CHROMOPHORES CAS / ECR / PCV

6.1	INTRODUCTION	131
6.1.1	Scope Of This Work	134
6.1.2	Experimental	136
6.1.3	Results	139
	(A) Speciation in the Systems: $H^+ - Al^{3+}$ -Reagent and $H^+ - Al^{3+}$ -Ligand	139
	(B) Speciation in the Competitive $H^+ - Al^{3+}$ -Ligand-Reagent Systems	139
6.1.4	Discussion	143

SECTION B: $H^+ - Al^{3+}$ - PCV - CITRATE (OXALATE) REACTION KINETICS

6.2	INTRODUCTION	145
6.2.1	Scope Of This Work	147
6.2.2	Experimental	148
	(A) Chemicals and Analysis	148
	(B) Spectrophotometric Titrations	148
	(C) Al-PCV Stoichiometry and Linearity of Titration Curves	149
	(D) Batch Experiments with Other Ligands	149
6.2.3	Data Treatment	149
	(A) Data Analysis	149
	(B) Sensitivity Analysis	150
6.2.4	Results	150
	(A) Al-PCV Stoichiometry and Linearity of Titration Curves	150
	(B) Competitive Equilibria	151
	(C) Batch Experiments: <i>Kinetics of Other $H^+ - Al^{3+}$-Ligand-PCV Systems</i>	152

6.2.5 Discussion	153
(A) Competitive Equilibria	153
(B) Sensitivity Analysis	156
(C) Kinetics of Ligand-Exchange: Enhancements of Rate ?	157

CHAPTER 7

A SURVEY OF ELECTROCHEMICAL SENSOR LIGANDS FOR Al^{3+} AND THE DEVELOPMENT OF AN ELECTROCHEMICAL DETECTION SYSTEM FOR Al^{3+}

SECTION A: A SURVEY OF ELECTROCHEMICAL SENSOR LIGANDS FOR Al^{3+}

7.1 INTRODUCTION	159
7.1.1 Scope Of This Work	162
7.1.2 Experimental	163
(A) Chemicals and Analysis	163
(B) Voltammetric Equipment	166
(C) Cyclic Voltammogram Recording Procedures	166
7.1.3 Results	166
(A) Pyrocatechol Violet	168
(B) Rhodizonic Acid	172
(C) Tetrahydroxy-1,4-quinone	174
(D) Purpurin	175
(E) Pyridinones: Hmpp and Hdpp	178
(F) Other Ligands	179
7.1.4 Discussion	179
(A) Pyrocatechol Violet	179
(B) Rhodizonic Acid and Tetrahydroxy-1,4-quinone	181
(C) Other Ligands	182

SECTION B: DEVELOPMENT OF AN ELECTROCHEMICAL FLOW INJECTION ANALYSIS METHOD FOR THE DETERMINATION OF Al^{3+}

7.2 INTRODUCTION	183
7.2.1 Scope Of This Work	185
(A) Pyrocatechol Violet	185
(B) Tetrahydroxy-1,4-quinone	187
7.2.2 Experimental	189
(A) Chemicals and Analysis	189
(B) FIA Apparatus	189
7.2.3 Results	193
(A) Pyrocatechol Violet	193
(B) Tetrahydroxy-1,4-quinone	195
7.2.4 Discussion	196

CHAPTER 8

AN FIA METHOD FOR THE MEASUREMENT OF 'REACTIVE' ALUMINIUM (Al^{3+}) BY 2-s REACTION WITH OXINE-DERIVATISED FRACTOGEL

SECTION A: CHELATING RESINS FOR MATRIX SEPARATION AND PRECONCENTRATION OF METALS

8.1 INTRODUCTION	197
8.1.1 Matrix Separation And Preconcentration Procedures	198
8.1.2 Chelating Resins	200
(A) Al Targeting Chelating Resins	201
(B) Dithiocarbamate Resins	205
(C) 8-hydroxyquinoline Chelating Resins	207
(D) Other Chelators and Chelating Resins	208
(E) Solid Supports	210

**SECTION B: AN FIA METHOD FOR THE MEASUREMENT OF
'REACTIVE' ALUMINIUM (Al³⁺) BY 2-s REACTION WITH
OXINE-DERIVATISED FRACTOGEL**

8.2 INTRODUCTION	212
8.2.1 Scope Of This Work	216
8.2.2 Experimental	217
(A) Chemicals and Analysis	217
(B) FIA System and Protocol	218
(C) Model Ligand Solutions	220
(D) Al-Hydrolysis Solutions	221
(E) Natural Water and Soil Solutions	222
8.2.3 Results	223
(A) FIA Manifold Optimisation	223
(B) Model Ligand Systems	226
(C) Fe(III) Interferences	229
(D) Polymeric Hydroxy-Aluminium Species	230
(E) Column Fouling \ Stop-Flow Cleaning	232
(F) Application to Humic Waters and Soil Solutions	234
8.2.4 Conclusions	235

**CHAPTER 9
CONCLUSIONS**

9.1 INTERACTIONS OF PCV WITH Al³⁺ AND THE AL-OXIDE HYDROXIDE BOEHMITE	237
9.2 EVALUATION OF INTERFERENCES BY COMPUTER MODELLING AND EFFECTS OF COMPLEXATION KINETICS ON THE DETERMINATION OF 'LABILE' Al	238
9.3 DEVELOPMENT OF CHEMICAL AND/OR ELECTROCHEMICAL PROBES FOR THE AQUEOUS Al³⁺ ION (Al³⁺)	240

REFERENCES	243
-------------------	------------

CHAPTER 1

THE ENVIRONMENTAL CHEMISTRY OF ALUMINIUM

This chapter is divided into 3 parts.

SECTION A: This discusses the occurrence of Al, its speciation and transport in the environment.

SECTION B: The toxicological effects of aluminium to plants, aquatic organisms and humans is discussed.

SECTION C: Methods for the measurement of Al at environmentally significant concentrations is discussed, in particular, methods that measure the 'free' or 'rapidly labile' fractions of Al.

SECTION A: THE CHEMISTRY OF ALUMINIUM IN THE ENVIRONMENT

1.1 ALUMINIUM IN THE ENVIRONMENT

Aluminium is the most abundant metallic element in the earth's crust (comprising 8.3 % by weight); it is exceeded in abundance only by O (45.5 %) and Si (25.7 %), and is approached only by Fe (6.2 %) and Ca (4.6 %) [Greenwood and Earnshaw, 1984]. In nature aluminium occurs most widely in the form of igneous silicates (micas and feldspars), hydroxo oxide (*bauxite*) and as *cryolite* (Na_3AlF_6); it is therefore mostly insoluble and innocuous. On weathering, in temperate climates, the aluminium-silicates form clay minerals such as *kaolinite* [$\text{Al}_2(\text{OH})_4\text{Si}_2\text{O}_5$], *montmorillonite*, and *vermiculite* [Sposito, 1989].

The mechanisms controlling the concentration of Al^{*1} in soil and in aqueous systems in the environment are complex and poorly understood [Ritchie, 1994 and 1995]. Soil minerals are believed to be the primary source of Al in the environment. Through soil development, these large mineral pools of Al are gradually decomposed and Al^{3+} is made available to participate in biogeochemical processes. These reactions, which occur primarily as a result of weathering, proceed slowly due to the low solubility and slow dissolution kinetics of the soil minerals [Bloom, 1983]. The reactions are very pH dependent and are influenced by the Al-silicate source minerals, ligands present and cation exchange processes [Bache, 1986; Conyers, 1990; Ritchie, 1995]. Chemical weathering is

^{*1} In this document 'Al' is used to indicate all solution phase aluminium species. Al^{3+} is used to denote 'free' aluminium, i.e. $\text{Al}(\text{H}_2\text{O})_6^{3+}$.

primarily a result of H_2CO_3 or organic acid dissolution [Reuss and Johnson, 1985] or mineral hydrolysis, followed by the reprecipitation of Al as amorphous Al (hydr)oxides [Johnson *et al.*, 1981] or aluminosilicates [Lindsay, 1979]. Once available to the environment Al quickly becomes complexed by soil organic matter or adsorbed onto charged mineral surfaces as the free metal ion or organically complexed Al.

Due to the relatively low solubility of natural Al minerals, the concentrations of aluminium are usually low in most circumneutral waters. Reported values for Al in surface waters are $0.4 \mu\text{mol L}^{-1}$ [Stumm and Morgan, 1981] while for fresh water streams concentrations are typically near $9 \mu\text{mol L}^{-1}$ [Bowen, 1966]. Aluminium present as Al^{3+} , *i.e.* $\text{Al}(\text{H}_2\text{O})_6^{3+}$, represents only a very small fraction of the total aqueous Al in the environment. At near neutral pH's (6.0-8.0), Al is strongly hydrolysed and forms several insoluble complexes [Stumm and Morgan, 1981]. At both acidic and alkaline pH's the solubility of Al is enhanced [May *et al.*, 1979], increasing its availability for both biological and geochemical reactions. The presence of organic matter capable of complexing Al also increases Al solubility [Bloom *et al.*, 1979]. The availability of Al to the biota depends on solution pH, concentrations of complexing ligands (both inorganic, *e.g.* OH^- , F^- , SO_4^{2-} , and organic, *e.g.* humic matter), ionic strength and temperature. To a small extent living biomasses may also participate in the cycling of Al, however this will be almost insignificant since Al is neither a plant nor animal nutrient [Ehrlich, 1990].

There is particular interest in the effects of elevated concentrations of Al in soils and acidic freshwaters because of: (i) the role of Al as a pH buffer (dilute acidic waters); (ii) the influence Al may have on the natural cycling of trace metals, organic carbon and phosphate; and (iii) the potential toxicity of Al to many plants and aquatic organisms.

Some of the processes believed to contribute to aqueous Al in the environment are illustrated in Figure 1.1.

1.1.1 ALUMINIUM TRANSPORT AND RELEASE.— A variety of processes may contribute to the input of Al to aqueous environments [Driscoll and Schecher, 1990]. The composition of waters entering a surface drainage system of streams, rivers and lakes depends crucially upon (i) the hydrological pathway taken by the waters and (ii) the chemical, mineralogical and biological nature of the materials through which the waters percolate. The 'master variable' governing Al mobilisation is pH. The effects of pH are, however, modified by the mineral phase which is dissolving, by cation exchange and by the formation of soluble complexes with ligands [Bache, 1986]. Once present in the aqueous environment both particulate and dissolved transport of Al can occur; however, only the aqueous forms are immediately available for further chemical or biological transformations.

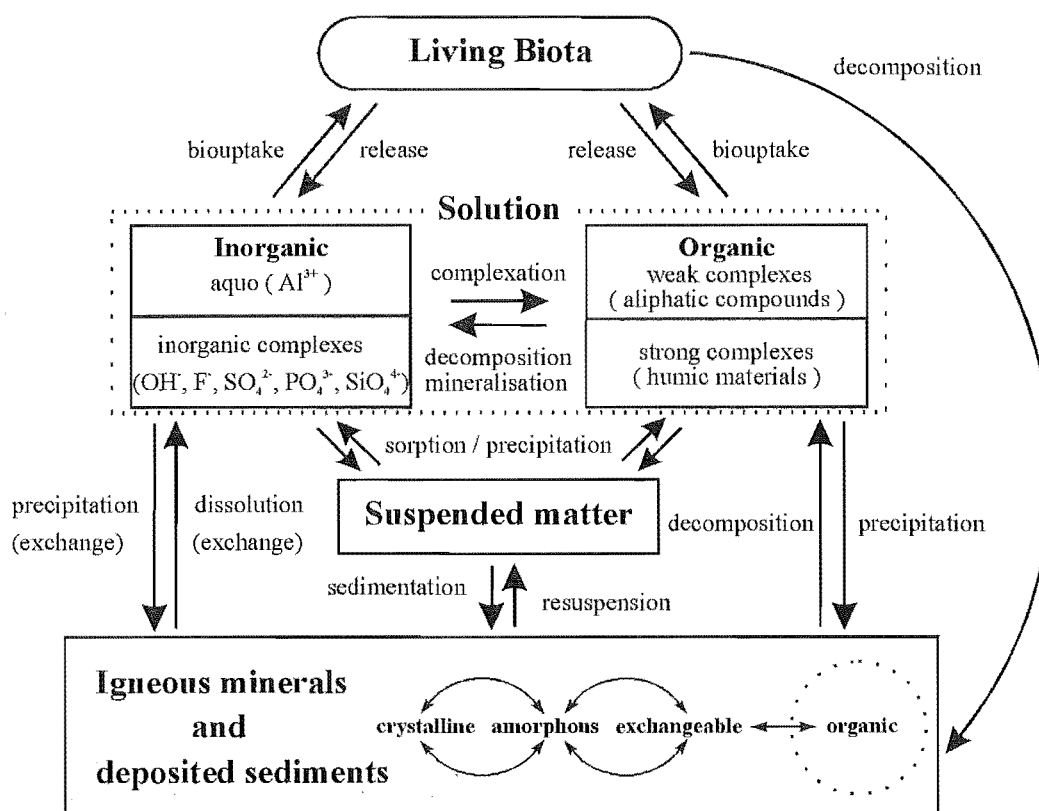


Figure 1.1 illustrates some of the processes believed to contribute to aqueous Al in the environment.

The primary input of Al to aqueous environments is through weathering of minerals in soils, whereas organically bound, exchangeable, interlayer and soluble complexed Al are sinks for Al released during mineral dissolution. The sinks provide the immediate sources of Al to the soil solution and hence, separately or collectively, may be seen as controlling the amount of Al in solution [Dahlgren and Walker, 1993; Hughes, 1994; Takahashi *et al.*, 1995]. The factors that contribute to the control of soil development will also affect the rate of mobilisation and transport of Al. Fundamental to understanding these processes is a knowledge of which solid phases are present, and the ability to model the phases that are regulating the Al concentrations in the complex soil and natural water environments [Gherini, 1985; Taugbøl *et al.*, 1994; Alveteg *et al.*, 1995; Grzyb, 1995; Tipping *et al.*, 1995].

Research [Johnson *et al.*, 1981; Bache, 1986] has indicated a number of solid phases that may control soil Al concentrations; these include amorphous or crystalline *gibbsite* [Al(OH)₃] [Cronan *et al.*, 1986], *kaolinite* [Al₂Si₂O₅(OH)₄], hydroxy sulfate minerals {e.g. *basalunite*, Al₄(OH)₁₀SO₄; *alunite*, KAl₃OH(SO₄)₂; or *jurbanite*, Al(OH)SO₄•5H₂O [Eriksson, 1981; Nordstrom, 1982; Nilsson and Bergkvist, 1983]}.

The dissociation of Al from soil organic matter has also been invoked to describe Al release [Bloom *et al.*, 1979; Cronan *et al.*, 1986; Dahlgren and Walker, 1993; Hughes, 1994; Takahashi *et al.*, 1995].

For different soil types, deviations from models based on these solid phases are apparent and simple solubility models are now often regarded as inadequate to explain the relationship between Al and pH in soil solutions [Bloom *et al.*, 1979; Neal *et al.*, 1989; Reuss *et al.*, 1990]. It is likely that several of these phases together control aqueous Al concentrations [Cronan *et al.*, 1986; Hughes, 1994]. In the long term, although Al is derived from mineral sources, the quantity released cannot necessarily be predicted from thermodynamics because morphological characteristics may result in kinetic considerations becoming as important as thermodynamic ones [Ritchie, 1994 and 1995]. Dahlgren and Walker (1993) measured Al release rates from soils dominated by hydroxy-Al interlayered silicates and Al-humic complexes. The results indicated that Al-humic complexes were strongly involved in regulating Al release rates. Recently, Alveteg *et al.* (1995) investigated the development of a kinetic alternative to modelling soil Al.

Secondary Inputs of Al into Aqueous Environments.— Colloidal matter present in soils as clay minerals and humus^{*2} is a source of negatively charged surfaces that can electrostatically adsorb cations. These particles diffuse through waters and are involved in relatively rapid cation exchange reactions and in the transport of salts percolating through soils. The most dominant exchangeable cation (after hydrogen ions) in acidic humic layers is calcium while that in the mineral subsoil layers is Al. The exchangeable Al fraction in acid soils thus provides a large reserve of adsorbed ionic Al that can be rapidly mobilised into soil solution and natural waters. The soil minerals that dominate the adsorption and exchange reactions are generally the secondary products of mineral dissolution, *i.e.* fine-grained, highly reactive minerals [Wilson, 1986]. However, much of the surface-adsorbed Al is bound very strongly by insoluble humic macromolecules or at (hydr)oxide or clay mineral surfaces and exchange processes occur slowly. The upper limit for solution Al concentrations in equilibrium with exchange systems is set by the solubility of the mineral phase.

Podzols typically form under coniferous forests and vegetation in cool humid climates (*viz.* West Coast, N.Z.). The process of soil podzolization strongly influences the mobilisation and transport of Al. This process involves the mobilisation of Al (along with Fe) by complexation with organic acids, leached from foliage as well as from decomposing forest litter, and the subsequent transport from upper to lower soil horizons [Lundstrom, 1993]. This Al is largely precipitated within the lower horizons and attributes little to the

^{*2} Humus: The insoluble (humins and humic acid) and soluble (fulvic acid) fractions of soil organic matter composed primarily of colloidal sized, weak polymeric acids of considerable aromatic character [Bloom (1981)].

Al transported from terrestrial to aquatic environments [David and Driscoll, 1984]. Recently, these traditional concepts of the translocation of Al and Fe in podzols have been challenged [Farmer, 1982; Farmer *et al.*, 1983; Childs *et al.*, 1983]. Farmer and co-workers suggest that aluminium is solubilised from the E(eluvial)-horizon as a silicate complex, followed by transport to the B-horizon where it is subsequently deposited as an aluminium silicate mineral (*viz.* *imogolite* or *proto-imogolite allophane*). During a second transport stage, soluble organic matter within this horizon re-mobilises the previously precipitated iron or aluminium silicates as alumino-organic complexes [Anderson *et al.*, 1982]. Wilson (1986) suggested that the weathering products involved in the mobilisation of Al from podzols are likely to be *proto-imogolite allophane* and hydroxy Al-interlayered *vermiculite* or *smectite*.

Bloom *et al.* (1979) concluded that hydrolysis of organically bound Al is a major source of buffering for acidic soil solutions and that exchange of Al^{3+} ions from organic matter controls the relationship between pH and Al^{3+} activity in acid soils of high variable charge cation exchange capacity. Their studies showed that the solubility of crystalline minerals or amorphous alumino-silicates has little direct influence on solution Al. Conyers (1990), upon studying several acidic Australian soils, suggested that leaching of silicic acid influences the extent of clay decomposition and hence Al solubility and that the relative sizes of the organic sink and mineral Al sources determine the influence of organic matter on Al solubility. Driscoll *et al.* (1985) observed that Al leached from organic horizons (undersaturated with respect to $\text{Al}(\text{OH})_3$ solubility) appeared to be largely organically complexed. In the lower soil horizons, inorganic Al concentrations were elevated and approached the solubility of $\text{Al}(\text{OH})_3$ (natural gibbsite).

Several authors have shown correlations between elevated dissolved organic carbon (DOC) and increased solution Al [Driscoll *et al.*, 1985; Driscoll, 1989]. The organic and inorganic Al fractions measured in natural waters are thus likely to originate from different soil sources (organic and mineral horizons, respectively) and different mechanisms of mobilisation (organic decomposition followed by Al complexation and dissolution of mineral sources by acid dissolution). In organic soil horizons, thermodynamic equilibrium between soil Al and solid phases is, quite probably, not often attainable in soils undergoing continuous inputs of exchangeable cations and anions and soil organic matter; here complexation kinetics (of Al with organic matter) are likely to most strongly influence the free Al concentrations [Walker *et al.*, 1990].

Reuss and Johnson (1985) highlighted the important role of CO_2 in the solubilisation and transport of Al. Calculations showed that for soils with low to moderately low exchangeable bases, the alkalinity^{*3} of the soil solution increases rapidly

^{*3} The *alkalinity* (Alk) of a water is its acid-neutralising capacity and can be defined as the concentration of all H^+ -ion acceptors minus the free H^+ -ion concentration [Stumm and Morgan, 1981], *i.e.* for the system : $\text{H}^+ - \text{Al}^{3+} - \text{CO}_2$, $\text{Alk} = [\text{HCO}_3^-] + 2[\text{CO}_3^{2-}] + [\text{OH}^-] - [\text{H}^+] - [\text{Al}^{3+}] - [\text{Al}(\text{OH})^{2+}] - [\text{Al}(\text{OH})_2^+]$.

with increases in CO_2 partial pressures while pH is only slightly affected. For soil solutions with positive alkalinities, their release from the soil environment results in rapid increases in pH due to degassing. Alternatively, waters with negative alkalinities (typical of acidic soils) remain acidic when released and subsequently degassed. The mechanism of Reuss and Johnson could account for the large changes in surface water pH observed (*cf.* 6.3 to 5.0 or less) associated with small changes in soil solution pH (*cf.* < 0.3). In soil environments, elevated partial pressures of CO_2 result in the formation of H_2CO_3 and its dissociation to H^+ and HCO_3^- . The resulting acidification increases Al dissolution and HCO_3^- acts as a counterion for Al transport. When the solution emerges from the soil to enter surface water, it equilibrates with atmospheric conditions (CO_2 degassing) resulting in the removal of HCO_3^- and the hydrolysis and precipitation of Al [as $\text{Al}(\text{OH})_3(\text{s})$].

1.1.2 EFFECTS OF ACID DEPOSITION.— Possibly the most important ecological consequence of acid deposition is the increased mobilisation and transport of soil Al [Johnson, 1979; Nilsson and Bergkvist, 1983; Johnson *et al.*, 1984; Mason and Seip, 1985]. Mineral acids from atmospheric deposition result in the remobilisation of Al either previously precipitated within soils during podzolisation or from soil exchange sites [Cronan and Schofield, 1979]. This Al may then be transported to adjacent surface waters. Acid deposition often results in considerable changes to the chemistry of surface waters without drastic changes occurring to the local soil systems [Seip, 1980; Reuss and Johnson, 1985].

Lakes and rivers become acidic when the input of acids exceeds the amount of bases produced in the catchment by weathering of rocks, and/or by reduction of strong acid anions within lake/watershed systems [Driscoll, 1989; Bailey *et al.*, 1995]. Catchments with largely siliceous bedrock geology are the most sensitive to acidification; in such areas, the alkalinity balance may become zero or even positive and proton concentrations equal to or greater than bicarbonate ion concentrations. At this end of the bicarbonate buffering system the pH is near 5.5 and represents a crucial point for the release of Al ions.

Soils that are low in exchangeable basic cations: Ca^{2+} , Mg^{2+} , Na^+ , K^+ , NH_4^+ , *e.g.* soils underlain by granitic (silicate) bedrock, are generally sensitive to the deposition of mineral acids (*e.g.* HNO_3 , H_2SO_4). In such soils the natural cycling of anions (*e.g.* SO_4^{2-} , NO_3^- , Cl^- , F^-) results in an increased mobility of acidic cations (H^+ , Al^{3+}) and the transport of these ions from the soil to surface waters [Gherini *et al.*, 1985]. In less acid-sensitive soils, the processes of dissolution or exchange of basic cations and/or retention of strongly acidic anions act to neutralise strong acids. The effects of Ca, present in acid

Alternatively alkalinity may be defined by the solution electroneutrality condition (the excess of positive charges over the anions of strong acids) generalised by : $\text{Alk} = [\text{Na}^+] + [\text{K}^+] + 2[\text{Ca}^{2+}] + 2[\text{Mg}^{2+}] + \dots - [\text{Cl}^-] - 2[\text{SO}_4^{2-}] - [\text{NO}_3^-] - \dots$.

rain-affected soils through leaching of CaSO_4 , on the mobilisation of Al was investigated by Berry *et al.* (1990). Ca, at concentrations typical of precipitation-induced CaSO_4 leachates, displaced significant quantities of protons in O_a (upper soil) horizons and subsequently increased Al solubility in the underlying soil horizons.

Johnson (1979) concluded that the neutralisation of strong acids is largely accomplished in the upper soil zone by rapid reaction with basic Al salts and by the leaching of bases from organic matter. Thus, by the time acid rain reaches the first small streams, its acidity has been greatly reduced. A 2-step process for the neutralisation of acid rain in the Hubbard Brook experimental forest (New Hampshire, U.S.A.) was proposed by Johnson *et al.* (1981). Initially, rapid neutralisation occurred by dissolution reactions of reactive Al within the soil zone. The second step involved neutralisation of both the hydrogen ion and Al acidity by chemical weathering of primary silicate minerals; this process involves the slow introduction of alkali and alkaline earth cations into the system (primarily Ca and Na). The soil zone was highlighted as the main site for Al acquisition by acid waters and the rate at which total neutralisation occurs closely follows the rate at which silicate minerals are weathered.

The long term capacity of a soil to neutralise acidity depends mainly on the dominant and weatherable mineral phases and the access of percolating solutions to the surfaces of these minerals. Prosser *et al.* (1993) compared soil acidification and Al concentrations under *Eucalyptus* forest and pasture. Differences in Al concentrations could be accounted for by the lag in Al response to acidification and greater complexation of Al with forest soil organic matter. The acidification of the forest floor, and resulting Al release, is broadly consistent with a net accumulation of organic anions. Bailey *et al.* (1995) monitored the acid-base chemistry and Al transport of an acidic, clear-water pond in the White mountains of New Hampshire. Al concentrations and speciation in the drainage waters changed with concentrations of natural organic matter.

The acidic decomposition of minerals is dependent on the type of acid involved; mineral acids (*e.g.* HNO_3 , H_2SO_4) or organic acids (*e.g.* oxalic, citric). Complexing acids extract more Al than do mineral acids at the same pH. Complexing acids bring about complete breakdown of mineral structures whereas mineral acids induce the formation of secondary minerals. Mineral acids are capable of depleting the exchangeable cations (such as Ca and Mg) from clay minerals much more rapidly than complexing ligands [Wilson, 1986].

The mobilisation of Al in laboratory-based soil columns exposed to acids [HNO_3 and H_2SO_4] and salt solutions [NH_4NO_3 and $(\text{NH}_4)_2\text{SO}_4$ fertilisers] was studied by Kotowski *et al.*, (1994). The greatest amounts of Al were mobilised from the illuvial (B_{hs}) and spodic (B_s) soil horizons. HNO_3 mobilised more Al than H_2SO_4 ; the degree of Al mobilisation by the salt solutions was between that observed for the two acids studied.

Lydersen *et al.* (1993) investigated the effect of addition of sulfuric acid to humic lake water (acidification from pH 5.6 to 4.1). Significant changes in the molecular weight distribution of organic complexes was observed for Fe and Al. It was suggested that increases in inorganic Al were primarily due to solubility and cation exchange reactions associated with high molecular weight Al-fractions.

1.1.3 SPECIATION OF ALUMINIUM IN NATURAL WATERS.— The chemistry of Al in natural waters and soil solution is very complex. Al is bound strongly by numerous inorganic ligands (*e.g.* OH^- , F^- , SO_4^{2-} , PO_4^{3-}) and a vast array of naturally occurring organic ligands including soil humics and smaller plant degradation or micro-organism secretion products (*e.g.* oxalic, citric and salicylic acids). As a result of extensive research, accurate thermodynamic data are available for Al complexes with inorganic species [Sposito, 1989; Pettit and Powell, 1995]. These data allow precise estimates of equilibrium concentrations for the complexes following input of total concentrations for the constituents and pH. Unfortunately there is a lack of reliable thermodynamic data for many of the organic constituents of these solutions. Also, considerable difficulty exists in estimating concentrations for organic constituents.

Dissolved Al exists as aquo Al, $[\text{Al}(\text{H}_2\text{O})_6]^{3+}$, as well as OH^- , F^- , SO_4^{2-} , PO_4^{3-} and organic complexes. In acidic surface waters of low ionic strength, the predominant forms of Al are the organic and F^- complexes. With further decreases in solution pH the concentration of inorganic forms of Al increases exponentially. The concentration of organic Al species is more strongly correlated with variations in total organic carbon (TOC) concentrations than by changes in surface water pH [Driscoll, 1989]. Temperature has been shown to influence the solubility of Al-minerals and the hydrolysis and molecular weight distribution of aqueous Al species [Lydersen *et al.*, 1990].

(A) Al Hydrolysis.— The speciation of Al is pH dependent. In acidic solutions ($\text{pH} < 4$) and in the absence of complexing ligands (other than hydroxide), Al is largely present as the aquo Al^{3+} ion, *i.e.* $[\text{Al}(\text{H}_2\text{O})_6]^{3+}$. As pH increases Al^{3+} quickly undergoes hydrolysis to form the species AlOH^{2+} and $\text{Al}(\text{OH})_2^+$ and small amounts of polynuclear species (*e.g.* $[\text{Al}_2(\text{OH})_2]^{4+}$; $[\text{Al}_3(\text{OH})_4]^{5+}$). At near neutral pH's (*ca.* 5.0-6.5) Al forms several highly polymerised and insoluble complexes (*e.g.* $[\text{Al}_6(\text{OH})_{12}(\text{H}_2\text{O})_{12}]^{6+}$; $[\text{AlO}_4\text{Al}_{12}(\text{OH})_{24+n} - (\text{H}_2\text{O})_{12-n}]^{(7-n)+}$ (Al_{13})).

The study of soluble hydroxy ions formed from Al^{3+} in aqueous solution is extremely complicated and the interpretation of experimental results is also difficult [Baes and Mesmer, 1976; Bertsch, 1990; Martin, 1991]. The Al dimer $\text{Al}_2(\text{OH})_2^{4+}$, which has been perceived as a significant Al-hydrolysis species [Baes and Mesmer, 1976], is currently believed to form to a much less significant extent [Öhman and Forsling, 1981; Brown *et al.*, 1985]. It is generally agreed, however, that (i) the species Al^{3+} , AlOH^{2+}

and $\text{Al}(\text{OH})_2^+$ dominate effects at $\text{pH} < 5$; (ii) the solubility of Al^{3+} decreases to a minimum near $\text{pH} 6.5$, with $\text{Al}(\text{OH})_3^0_{(s)}$ formation; and (iii) at higher pH values solubility increases again, with $\text{Al}(\text{OH})_4^-$ as the dominant solution species at $\text{pH} > 7$.

In the pH range 5-7 the wide range of high molecular weight polynuclear species proposed makes accurate calculations difficult. Variations in the model used has little effect at $\text{pH} < 5$ where Al^{3+} dominates, and at $\text{pH} > 7$ where $\text{Al}(\text{OH})_4^-$ dominates, but causes considerable differences in the distribution of AlOH^{2+} , $\text{Al}(\text{OH})_2^+$ and $\text{Al}(\text{OH})_3$ between $\text{pH} 5$ and 7 . Much controversy underlies the chemistry of Al hydrolysis and a number of excellent reviews are available on this subject [Baes and Mesmer, 1976; Bertsch, 1989; Nordstrom and May, 1989].

(B) Inorganic Al Species

Fluoride: Fluoride is present in significant concentrations in most surface waters and forms complexes which, except for some organic Al species, are claimed to be the most stable soluble species of this metal encountered in acidic waters [Driscoll and Schneider, 1989]. The stoichiometry of Al-F complexes varies with total F^- concentration; at lower F^- concentrations the species AlF^{2+} and AlF_2^+ dominate. As F^- concentrations increase, H_2O or OH^- ligands are successively displaced and the dominant species becomes AlF_3 . At higher pH values competition results in the displacement of F^- by OH^- ions and under alkaline conditions OH^- complexes dominate ($\text{pH} > 6$) [Martin 1988].

In natural waters concentrations of F^- are typically low ($5 \mu\text{mol L}^{-1}$, [Stumm and Morgan, 1981]) and the Al-F species AlF^{2+} and AlF_2^+ commonly form. Competition with organic ligands does not significantly modify the extent to which Al-F complexes form [Ares, 1990]. In acidic soils Al-F concentrations often appear negligible; this has been interpreted as indicating that Al-F complexes are easily transported because of their high solubility [Ares, 1990].

Sulfate: Sulfate, SO_4^{2-} , forms considerably weaker complexes with Al than F^- . At concentrations common in natural waters ($120 \mu\text{mol L}^{-1}$, [Stumm and Morgan, 1981]) Al-SO_4 complexes form only as minor species and these complexes form only at acidic pH 's. At lower SO_4^{2-} concentrations the species AlSO_4^+ dominates while at higher concentrations $\text{Al}(\text{SO}_4)_2^-$ forms. In environments subject to acid rain (H_2SO_4 , HNO_3), bioaccumulation of N results in SO_4^{2-} becoming the dominant anion in soil solution. The anion plays a very important role in the leaching and transport of base cations as well as Al^{3+} and H^+ in acidic soils.

Phosphate: Although soluble Al-phosphate complexes form and are more stable than sulfate complexes, phosphate, PO_4^{3-} , concentrations in natural waters are very low ($0.05 \mu\text{mol L}^{-1}$ [Gunneriusson, 1993]). Phosphate forms a number of highly insoluble species.

The inorganic anions HCO_3^- , Cl^- and NO_3^- (also found in natural waters) do not form important complexes with Al.

Silicon: The importance of aqueous Al-Si species is often alluded to in soil science. Such species are, however, likely to account for a major proportion of total inorganic monomeric Al in natural waters [Browne and Driscoll, 1992]. Silicic acid, $\text{Si}(\text{OH})_4$, is the principal dissolved form of Si in solutions at $\text{pH} < 8$ ($\text{pK}_a = 9.8$) and forms highly insoluble aluminosilicate species at near neutral pH's. Under dilute conditions, kinetics of precipitation are slow and it is reasonable to hypothesise that soluble Al-Si species would exist as intermediates in the weathering reactions of Al-Si minerals. Despite qualitative evidence that now exists for the formation of soluble Al-Si species [Chappell and Birchall, 1988; Exley and Birchall, 1992] reliable thermodynamic data for reactions are not available [Browne and Driscoll, 1992]. It is now accepted that silicic acid plays a significant role in the transport, bioavailability and toxicity of Al in the environment [Birchall, 1990]. Stumm and Morgan (1981) report median values for Si concentrations in freshwaters of $300 \mu\text{mol L}^{-1}$.

(C) Organic Al Species.— The diverse nature of dissolved organic matter present in natural water and the difficulties in quantifying total concentration of individual molecules makes a discussion of specific Al-organic interactions difficult [Ares, 1986; Schnitzer *et al.*, 1988; Grzyb, 1995; Schulten, 1995]. However, naturally occurring organic solutes play an important role in the solubility and speciation of Al [Lundstrom, 1993].

In organic soils the cation exchange capacity (CEC) is largely due to organic matter; much of the soluble Al in soils is associated with organic matter [Prosser *et al.*, 1993] and much of the Al in soil solutions and seeps appears complexed by organic ligands. Alumino-organic complexes are observed to predominate in highly organic soils [Driscoll *et al.*, 1985]. It is likely that biocycling of forest floor vegetation is of importance in Al transport in forest ecosystems [David and Driscoll, 1984]. Gamble *et al.* (1983) claimed that Al is bound more strongly to humic acids than any other metal ion except Cu, however it is most easily leached by acid. More recent studies have indicated, however, that soil-derived humic and fulvic acids bind Al in preference to Cu in the pH range 3.5 - 5.5 [Town and Powell, 1993]. Recently, Grzyb (1995) reported the development of a data analysis algorithm that may be used for estimating functional properties of dissolved organic matter (DOM) in aqueous environments. NOAEM (natural organic anion equilibrium model) includes metal-hydroxide complexes and is capable of predicting organically-bound Al.

The brown-coloured soluble humic substances that are common in waters leaching from organic horizons are possibly the most important organic ligands in soils. Soil humic substances (*viz.* humic and fulvic acids) are high molecular weight organic acids that display polyelectrolyte behaviour and thus exhibit a high potential for cation-

exchange [Schulten, 1995]. Humic substances contain substantial numbers of -COOH and phenolic -OH groups; metal binding by functional groups other than these contributes very little to the CEC of soil organic matter [Bloom, 1981]. The binding of Al and Fe by humic substances is important in podzol formation and in the stabilisation of soil aggregates. The ability of organic soil horizons to buffer acidic precipitation and affect Al release is potentially great due to the presence of humus-associated dissociable acidic functional groups. The interaction of humic and fulvic acids with clay minerals has been recognised for many years [Greenland, 1971].

For a natural water the modelling of interactions between Al and organic matter is a difficult task. Thermodynamic descriptions of Al-organic interactions in such media are confounded by the inherent complexity of the mixed ligand system which exhibits a large distribution of binding sites with varying affinity for Al [Gamble *et al.*, 1983; Evans, 1989; Schulten, 1995]. Furthermore, for the larger organics, such models must also contend with electrostatic interactions between ligand sites on the same molecules, configurational changes and aggregation [Stevenson and Vance, 1989]. Models have generally been formulated in terms of (i) a series of discrete binding sites with unique protonation constants, K_i , or (ii) a continuum of acidic functional groups ($\log K_a$ values). Titration data have been successfully modelled using two or four discrete protonation sites [Lövlgren *et al.*, 1987; Gregor and Powell, 1988].

For the reasons above, researchers often seek analytical descriptions of the organic characteristics of natural waters and soil solutions. Techniques have been developed which provide *operationally defined* yet useful quantification of aqueous organic Al. These *so-called* fractionation procedures are directed towards distinguishing between not only inorganic and organic Al but also at partitioning the organic Al into various groups (*e.g.* total Al, total monomeric Al, labile and nonlabile monomeric Al and acid soluble Al) [Stevenson and Vance, 1989]. These procedures will be discussed in more detail in SECTION C. The use of such techniques to study Al speciation, in particular Al-inorganic interactions, has in recent years resulted in a flurry of publications describing trends and water characteristics [Driscoll, 1989].

The ratio of organic carbon to Al-Org complexes generally decreases with soil depth [Driscoll *et al.*, 1985]. The solubility of alumino-organic substances decreases as the ratio of organic C to Al (and Fe) decreases. Concentrations of organic Al species are also observed to increase with decreasing solution pH, suggesting that (i) acidic soils have a higher concentration of NOM (natural organic matter) and Al complexed to NOM, or (ii) acidic conditions increase the mobility of these species (*i.e.* enhanced leaching of Al-organic solutes). The most commonly observed broad-based trends observed for natural waters are that (i) concentrations of inorganic Al increase exponentially with decreasing solution pH, and (ii) increasing organic monomeric Al correlates with increased dissolved organic carbon (DOC) levels [Johnson *et al.*, 1981; Driscoll, 1984].

The speciation characteristics of natural waters and soil solutions are complex and vary tremendously with small environmental changes. Spatial and temporal changes in speciation are common [Driscoll, 1985; Jeffries and Hendershot, 1989; Hughes *et al.*, 1994]. A vast amount of literature is now available regarding speciation of Al in watersheds around the world [Campbell *et al.*, 1983; LaZerte, 1984; Miller and Andelman, 1987; Jeffries and Hendershot, 1989]. However, problems associated with Al speciation and the environmental impact of processes such as acid precipitation are still not fully understood.

(D) Particulate and Colloidal Al Species.— During conditions of oversaturation, Al will hydrolyse, leading to formation of particulate Al oxyhydroxides. These materials are often colloidal in nature and remain suspended in solution. Colloidal Al oxides and hydroxides are plentiful in nature and provide a large array of sites which may adsorb metal ions and natural organic molecules [Davis, 1982 and 1984; Schautman and Morgan, 1994]. The cycling of phosphate, trace metals and dissolved organic carbon (DOC) is affected by adsorption processes occurring at these oxyhydroxide surfaces [Schautman and Morgan, 1994]. Tipping *et al.* (1989) studied the adsorption of Al by suspended stream particles. An empirical equation was developed based on Al^{3+} activity, pH and particle concentrations which could account for Al^{3+} adsorption. Calculations (taking dissolved humic substances into account) indicated that adsorbed Al may account for a significant proportion ($\geq 10\%$) of total monomeric Al. The complexation of Al^{3+} at the surface of *goethite* ($\alpha\text{-FeOOH}$) was investigated by Lövgren *et al.* (1990). A thermodynamic equilibrium model was developed involving two monodentate species; Al desorption was found to be extremely slow and showed poor reversibility.

SECTION B: THE TOXICOLOGICAL EFFECTS OF ALUMINIUM TO PLANTS, AQUATIC ORGANISMS AND HUMANS

1.2 TOXICOLOGICAL EFFECTS OF ALUMINIUM

1.2.1 ALUMINIUM TOXICITY TO PLANTS.— Elevated levels of soil Al have been shown to be toxic to several plant species including a number of commercially harvested food crops [Rosseland *et al.*, 1990; Blamey and Asher, 1993; Delhaize and Ryan, 1995]. The availability and phytotoxicity of Al depends on a number of abiotic and biotic factors including many of the factors controlling Al transport and release (discussed in SECTION A). Soil pH, Al concentrations and a number of other factors, including organic matter and clay contents of soils, are hypothesised as affecting Al toxicity to plants. Al has repeatedly been either hypothesised or demonstrated as a major contributing factor in forest decline [Cronan *et al.*, 1989; Arp and Strucel, 1989]. The extent of Al toxicity for any given soil is particularly dependent on the plant species [Parker *et al.*, 1989; Kinraide and Parker, 1990; Simon *et al.*, 1994a] along with factors such as plant age and growth stage [Wheeler, 1994].

Soil acidification is a problem that affects as much as 40 % of the world's arable lands [Haug, 1984]. Besides natural soil acidity, the use of fertilisers has contributed to the acidification of agricultural areas previously not suffering from Al toxicity. Acid rain in highly industrialised regions of the world has also been associated with accelerated rates of soil acidification. In highly acidic soils Al toxicity is probably the most important growth limiting factor [Blamey and Asher, 1993]. The costs of chemical amendments to problematic soils often outweigh the gains in production; the development of acid soil (Al and Mn) -tolerant plants may help reduce costs of crop production in such areas [Baligar *et al.*, 1993a,b].

(A) Morphological Damage.— The damage caused by Al to plants is most noticeable as deformations and reduced growth (decreased biomass yield) of both mature plants and seedlings. The most prominent feature of morphological damage is reduced root elongation [Pavan *et al.*, 1982; Hue *et al.*, 1986; Alva *et al.*, 1986b,c; Berggren and Fiskesjö, 1987; Ritchey *et al.*, 1988; Mookherji and Floyd, 1991]. However, toxicity also results in roots appearing stubby, swollen, brown and sometimes becoming brittle [Lee and Pritchard, 1984; Andersson, 1988; MacLean *et al.*, 1992].

Wagatsuma *et al.* (1987) indicated that morphological changes induced on roots by Al include: decrease in the turgescence of epidermal cells of the tip (barley); occurrence of small depressions (oats, rice); destruction of epidermal and outer cortex cells (maize) and cross-sectional deep cracks in the inner cortex cells (pea). From observations with the scanning electron microscope Wagatsuma *et al.* concluded that (i) root cell destruction

occurs most in the proximal cells and (ii) this destruction is not restricted to the meristematic region of the root. Results from studies by Gahoonia (1993) showed that the concentration of Al in the vicinity of roots (2 mm) may be considerably different from that in the bulk of the soil. In modeling studies of the interaction of Al^{3+} with plant membranes (Gouy-Chapman-Stern model), Kinraide *et al.* (1992) were able to more closely correlate root growth with the predicted activity of Al^{3+} at the surface of the plasma membrane than with the activity of Al^{3+} in the bulk solution.

Visible symptoms to plant tops are generally observed as secondary effects to those at the roots. Several investigations have indicated effects of Al on plant shoots, stems and leaves [Baligar *et al.*, 1987; Ritchey *et al.*, 1988; Rengel and Robinson, 1989; Baligar *et al.*, 1993a,b; Simon *et al.*, 1994a]. In studies of Al toxicity in tomato, Simon *et al.* (1994a) recorded (for 25 and 50 μM Al) reduction of leaf area, dry weight and stem length for growth experiments in dilute nutrient solutions (pH 4.0). Al affects nitrogen fixation [Hartel *et al.*, 1983; Mookherji and Floyd, 1991], photosynthesis by lowering chlorophyll content and reducing electron flow, reduces respiration activity and decreases protein synthesis [Roy *et al.*, 1988; Simon *et al.*, 1994b]. Aluminium is known to bind to DNA. The adverse effects of Al to plants are numerous; several good reviews have been published on this subject [Roy *et al.*, 1988; Andersson, 1988; Rengel, 1992; Delhaize and Ryan, 1995].

(B) Physiological Effects.— Al toxicity, although poorly understood, has been attributed to several physiological and biochemical processes. The levels of soil Al required to produce toxic symptoms are dependent on soil conditions (*i.e.* pH and composition) and on the species of plant. Symptoms of Al toxicity are usually first observed as structural and functional damage to roots: adverse effects occurring to plant mycorrhiza and inefficient uptake of water and absorption of nutrients.

The chemistry of these processes is believed to be very complex and considerable variation in Al tolerance is observed between different plant species, genotypes, strains or clones [Hartel *et al.*, 1983; Baligar *et al.*, 1987; Ritchey *et al.*, 1988; Mookherji and Floyd, 1991; Crush and Caradus, 1992; Baligar *et al.*, 1993a,b; Shann and Bertsch, 1993; Cline and Senwo, 1994]. Delhaize *et al.* (1993a) showed that Al-sensitive genotypes of wheat (*Triticum aestivum* L.) accumulate 5- to 10-fold more Al in their root apices than tolerant genotypes. In general, high Al concentrations reduce the mitotic activity of plant root systems resulting in stunted root growth (both depth and branching). This results in susceptibility to dehydration and poor nutrient adsorption.

In most plants, Al has been located in the nucleus and cell walls of meristematic cells. It also accumulates at high levels in epidermis, hypodermis, cortex, endodermis and to a small amount in immature xylem [Wagatsuma *et al.*, 1987]. The uptake of Al is believed to occur at the root cap and the mucilaginous secretion covering the epidermal

cells of the roots. In turn, specific binding of Al occurs at the mucilage by exchange adsorption on polyuronic acid, complexation with pectic substances and by formation of Al-polyhydroxy species [Roy *et al.*, 1988]. Al also interferes with the uptake, transport and use of several essential elements, including Cu, Zn, Ca, Mg, Mn, K, P and Fe [Lee and Pritchard, 1984; Baligar *et al.*, 1987; Rengel and Robinson, 1989; Baligar *et al.*, 1993a,b; Simon *et al.*, 1994a].

Ca in particular plays a very important role in the control of Al toxicity [Huang *et al.*, 1992; Rengel, 1992; Kinraide *et al.*, 1994; Ryan *et al.*, 1994; Delhaize and Ryan, 1995]. Interactions of Al with calcium pectate, a component of plant cell walls, has been the target of several recent investigations [Blamey *et al.*, 1993a,b]. Al reacts almost immediately with this material and has been hypothesised as the basis of aluminium-induced water stress and nutrient disorders. The effects of Al on plant physiology has been the subject of several good reviews [Haug, 1984; Roy *et al.*, 1988; Andersson, 1988; Rengel, 1992; Delhaize and Ryan, 1995].

(C) Tolerance Mechanisms.— The mechanisms of Al tolerance have been the subject of much recent research. Two general mechanisms of tolerance are apparent: reduced absorption of Al by the root or detoxification of Al after absorption (both mechanisms can operate in the same plant). It is also apparent that plants can be grouped according to where Al accumulates; accumulation in tops or in the roots. The tolerance of oats, buckwheat, hydrangea and blueberry to Al may be due to exclusion of Al ions by the plasmalemma in root cells [Wagatsuma *et al.*, 1987].

Levels of tolerance vary from species to species and appear to be controlled by one or more genes [Foy, 1983; Delhaize *et al.*, 1993a]. In the review by Andersson (1988) four general tolerance mechanisms were described; (i) active exclusion by the roots or exudation of chelating agents which will bind Al, (ii) immobilisation of excess Al in the roots, (iii) accumulation of Al in the tops coupled with a high internal tolerance and (iv) uptake of mineral nutrients independent of Al concentrations (possibly low nutrient requirements). In addition to these mechanisms, some crops appear to increase their Al tolerance by increasing the pH of their rhizosphere, thereby lowering the solubility and availability of Al.

Supply of various plant nutrients, *e.g.* N, Ca and P may also aid in tolerance to Al [Alva *et al.*, 1986b; Kinraide and Parker, 1987; Tanaka *et al.*, 1987]. Kinraide *et al.* (1992) found that the rhizotoxicities of Al^{3+} and La^{3+} were ameliorated by cations (C) in the order: $\text{H}^+ \approx \text{C}^{3+} > \text{C}^{2+} > \text{C}^+$. The ameliorative effects of Ca^{2+} were slightly greater than for other divalent cations; H^+ was much more effective than other monovalent cations.

Organic acids which form soluble complexes with Al will reduce toxicity [Tan and Binger, 1986]. It has been postulated that Al-tolerant plants may use secretion of organic acids to detoxify Al, either internally or in the rhizosphere [Miyasaka *et al.*, 1991; Delhaize *et al.*, 1993b]. Delhaize *et al.* (1993b) found that malic acid excretion was specifically stimulated by Al while neither La^{3+} nor Fe^{3+} were able to elicit this response. Much literature has been published on the subject of plant tolerance to Al toxicity [Roy *et al.*, 1988; Andersson, 1988; Delhaize and Ryan, 1995].

(D) Toxic Species.— In soil solutions Al^{3+} is in equilibrium with mononuclear hydroxy-Al species [*viz.* AlOH^{2+} , $\text{Al}(\text{OH})_2^+$]; at higher pH polynuclear Al may also coexist with Al^{3+} . Of these species current research supports the opinion that Al^{3+} is toxic [Pavan *et al.*, 1982; Hue *et al.*, 1986; Alva *et al.*, 1986a,c; Wright, 1987; Kinraide, 1991]. Increases in solution pH are generally found to relieve Al toxicity, which may indicate a differential toxicity of the monomeric hydrolysis products. However, some studies have indicated that one or more of the mononuclear hydroxy-Al ions is the principal toxic species [Helliwell *et al.*, 1983; Alva *et al.*, 1986c].

The difficulties in separating pH effects from Al speciation with respect to the toxicities of Al^{3+} and the mononuclear hydroxy-Al species has been discussed [Kinraide, 1991]. Kinraide *et al.* (1992) provided new evidence supporting the view that Al^{3+} is the primary toxic mononuclear Al species [rather than AlOH^{2+} and $\text{Al}(\text{OH})_2^+$]. These studies presented a number of arguments in favour of Al^{3+} toxicity ameliorated by H^+ *versus* amelioration because of reduced levels of the monomeric Al-hydrolysis species.

Recent studies have highlighted the high toxicity of polynuclear hydroxy-Al species [Parker *et al.*, 1988; Wagatsuma and Kaneko, 1987; Parker *et al.*, 1988 and 1989; Kinraide, 1991; Shann and Bertsch, 1993]. The species identified is the Al_{13} polymer, $\text{AlO}_4\text{Al}_{12}(\text{OH})_{24}(\text{H}_2\text{O})_{12}^{7+}$, exhibiting a toxicity at least 10 times that of Al^{3+} [Parker *et al.*, 1989]. Several studies support the notion that the physiological mechanisms of toxicity are different for mononuclear and polynuclear Al [Parker *et al.*, 1989; Shann and Bertsch, 1993].

The presence of polynuclear Al in soil solutions is controversial [Bache and Sharp, 1976; Bertsch, 1987; Furrer *et al.*, 1992]; if present, concentrations would be likely to be low and difficult to detect even at toxic levels [Parker *et al.*, 1989]. Polynuclear Al is likely to be strongly adsorbed by clay minerals or organic matter and exhibit slow exchangeability [Zelazny and Jardine, 1989]. However, Bertsch (1987) suggested that liming highly acidic soils may provide conditions conducive for the formation of the Al_{13} polynuclear species. A recent paper by Hunter and Ross (1991) provides evidence for the existence of the Al_{13} polynuclear species in the O_a horizon of an acidic forest soil. Several studies have indicated that the Al_{13} polynuclear species may form in the free space of plant roots [Kinraide, 1991].

Despite these studies it is still not clear which of these species is the primary cause of Al toxicity [Kinraide, 1991]. These problems have been related to difficulties in experimental design [Kinraide and Parker, 1989; Wheeler, 1994], problems which were re-addressed immediately but without resolve [Kinraide and Parker, 1989]. Kinraide (1991) concluded that polycationic Al, with charge > 2 is rhizotoxic (as are other polyvalent cations, *e.g.* Ga^{3+} , In^{3+} , La^{3+} [Kinraide and Parker, 1987; Kinraide *et al.*, 1992]). Furthermore, Kinraide also hypothesised that organic or inorganic ligands may reduce rhizotoxicity by reducing the charge on Al. Studies of polynuclear Al species are in particular very difficult; Bertsch (1987) identified OH/Al ratio, total Al, base injection rate, stirring rate and even choice of reaction vessel as factors influencing results. In growth studies dilute nutrient solutions more closely represent soil solution conditions than full-strength nutrient solutions.

Al toxicity is alleviated through the addition of salts such as CaCl_2 and NaCl *via* both a reduction in the activity of Al and as a direct physiological effect of the cation [Alva *et al.*, 1986a; Kinraide and Parker, 1987; Kinraide *et al.*, 1992]. Al complexed with F^- [Cameron *et al.*, 1986; MacLean *et al.*, 1992], with SO_4^{2-} [Tanaka *et al.*, 1987] or by soil organic matter and organic acids is less phytotoxic than Al^{3+} . In solution experiments with cotton (*Gossypium hirsutum*) Hue *et al.* (1986) grouped organic acids into three categories based upon their ability to detoxify Al: [i] strong (citric, oxalic, tartaric), [ii] moderate (malic, malonic, salicylic) and [iii] weak (succinic, lactic, formic, acetic, phthalic).

The effects of soluble Si on mobility of Al in soils has only recently begun to receive much attention. Silicon, although the second most abundant element in the lithosphere (27 wt. %), represents less than 0.05 % (by weight) in the biosphere [Deevey, 1970]. Si was found to alleviate the symptoms of Al toxicity to soybean and maize [Barcelo *et al.*, 1993; Baylis *et al.*, 1994]. These effects are most probably due to the formation of colloidal hydroxyaluminosilicate species [Birchall and Chappell, 1989].

(E) Estimating Soil Toxicity.— The concentration of Al in soil solution has been shown to be a better measure of Al toxicity than exchangeable Al. Soil solution Al concentrations better reflect the conditions in the vicinity of the soil-root interface. Many studies have indicated that Al toxicity symptoms are closely related to Al^{3+} activity and that monomeric Al is most toxic to root growth [Pavan *et al.*, 1982; Blamey *et al.*, 1983; Cameron *et al.*, 1986; Hue *et al.*, 1986]. Studies by Alva *et al.* (1986c) indicated that the sum of activities of monomeric Al species was the best index of Al toxicity (as measured by root length reduction) in soybean, subterranean clover, alfalfa and sunflower. Such correlations have been previously reported [Blamey *et al.*, 1983]. Parker *et al.* (1988), however, disagree that this sum is such a reliable toxicity index.

Results of Al toxicity studies in solution cultures often show poor agreement with soil solution studies [Hartel *et al.*, 1983]. The importance to agriculture in identifying the problems Al causes in soils with low pH buffering capacities is closely balanced with the high cost of applying lime relative to returns over the short term. Decreasing soil solution pH increases the monomeric fraction of soil Al, whereas, increased amounts of soil organic matter and organic acids reduce the availability of Al by complexation reactions. Soil Al concentrations are also dependent on the dominating clay minerals and the clay content of the soil. Soil tests for Al toxicity are hence plagued by complications in the speciation of Al in the complex soil environments.

The most commonly used measure of Al toxicity has been the activity of monomeric Al species. Wright *et al.* (1987) compared three methods for estimating phytotoxic aluminium in soil solution: 15 s 8-hydroxyquinoline, 30 s ferron and 30 min aluminon. Of these methods the 15 s 8-hydroxyquinoline method provided the best predictors of toxic Al. The soils studied were, however, low in organic matter and the suggestion was made for a further investigation of these techniques for measurements of Al in organic soils. A large number of methods have been developed for estimating total, labile (free) and non-labile Al, both prior to and since the study by Wright *et al.* These methods are discussed in SECTION C.

In developing soil tests for Al toxicity it has been common to use the Al concentration $[Al^{3+}]$ or activity $\{Al^{3+}\}$ together with another soil nutrient (*e.g.* Na, Ca, P) to obtain a more accurate correlation [Alva *et al.*, 1986b; Kinraide and Parker, 1987; Carr *et al.*, 1991]. In some soil types, *e.g.* many yellow earths of Western Australia, methods that estimate total Al may offer satisfactory correlations with Al toxicity [Carr and Ritchie, 1993]. It is clear from these findings that simple methods developed for the speciation of both monomeric and polymeric Al in soil solutions would be very beneficial to those studying soil science. Without methods for the separation of plant response to individual forms of Al, the screening of Al toxicity is likely to give erroneous results that can not be readily translated into effects expected in the field. Continued research shows that the currently 'best methods' still require much development [Whitten *et al.*, 1991a,b].

1.2.2 ALUMINIUM TOXICITY TO AQUATIC BIOTA.— High concentrations of Al in acidic river and lake waters are toxic to fish and freshwater invertebrates [Burrows 1977; Rosseland *et al.*, 1990]. Toxic effects are not only dependent on the species but also on the growth stage of the organism. In lakes and rivers the toxicity to, and possible bioaccumulation of Al in, aquatic organisms also depends on the Al species present [McCahon and Pascoe, 1989]. Al speciation is modified by pH, temperature, ionic strength (*viz.* Ca^{2+} concentrations) and concentrations of competing ligands, *e.g.* dissolved organic matter [see SECTION A (1.1.3)]. In acid waters containing significant concentrations of Al ($5\text{--}10\ \mu\text{mol L}^{-1}$) fish show fatal damage to gill structures and lose the

ability to maintain osmotic balance [Wood *et al.*, 1988; Rosseland *et al.*, 1992; Waring and Brown, 1995]. The most significant signs of Al toxicity to both planktonic and benthic invertebrates in acid waters are reductions in species populations [Rosemond *et al.*, 1992].

(A) Aluminium Toxicity to Invertebrates.— Invertebrates form a vital link in the food chain of freshwater and terrestrial ecosystems. The most sensitive invertebrates to Al were reported as being cladocerans while the most tolerant appear to be the molluscs. Al does not appear to biomagnify along food chains [Herrmann *et al.*, 1993]. In general, aquatic invertebrates are less sensitive to Al than fish [McCahon and Pascoe, 1989; McCahon *et al.*, 1989; Wren and Stephenson, 1991].

Al is often regarded as the most toxic metal to invertebrates in acidic waters. Havas and Likens (1985) reported that H^+ ions, at ecologically significant levels, exhibit a greater toxicity than Al to four species of invertebrates (*Daphnia*, *Holopedium*, *Chaoborus* and *Chironomus*). Al concentrations of 0.02-1.02 mg L⁻¹ were not found to cause significant damage to these species. Makie (1989) determined 96-h LC₅₀ values that are lethal to four groups of benthic macroinvertebrates (filter feeders, scrapers, shredders, predators). For all the invertebrates studied, LC₅₀ values reported were > 400 µg Al L⁻¹; higher than the highest levels of inorganic monomeric aluminium (325 µg L⁻¹) reported in central Ontario lakes. In studies concerning seven mollusc species, Mackie (1989) found that aluminium concentrations as high as 0.1 mg L⁻¹ at low pH did not cause harmful effects. Hall *et al.* (1985 & 1987) found that freshwater crustaceans were sensitive to both decreases in pH and elevated concentrations of Al.

Nyholm (1981) reported that pied flycatchers feeding in acidified catchments exhibited reduced reproductive function; elevated concentrations of Al in the diet of these birds was invoked to account for these findings. In studies of Al bioaccumulation and toxicity to the water flea (*Daphnia magna*), Havas (1985) found that adsorption and accumulation of aluminium occurs primarily in the respiratory structures of aquatic insects. Maximum Al toxicity and maximum bioaccumulation were observed at pH 6.5 (at 0.32 mg L⁻¹ Al). At pH 4.5, H^+ is the primary cause of toxicity; high concentrations of Al (> 1.02 mg L⁻¹) temporarily ameliorated this toxicity. Whole-body concentrations of Al in many invertebrates are observed to decrease with decreasing pH [Hall *et al.*, 1988]. Frick and Herrmann (1990) studied the accumulation of Al in mayfly nymphs. Significant accumulation was found to occur in the exuviae of the nymphs and consequently nymphs showed a decrease (70 %) in Al content upon moulting. Emerging adults contained lower amounts of accumulated Al resulting in no biomagnification unless terrestrial predators feed on mayfly or other insects before they make their final moult. However, small but significant amounts of Al were found to accumulate internally in the nymphs, thus providing a greater source of Al for bioaccumulation.

(B) Aluminium Toxicity to Fish.— Declines in fish populations in many soft-water streams has been attributed to acidification and release of toxic metal ions (*e.g.* Cd, Mn, Al). The most toxic species to fish in freshwater rivers and lakes appears to be the hydrogen ion, H^+ [Herrmann *et al.*, 1993]. Recently, however, numerous studies have highlighted the importance of Al in relation to fish survival rates [Schofield and Trojnar, 1980; Sadler and Turnpenny, 1986; Kramer *et al.*, 1986; McCahon *et al.*, 1989; Rosseland *et al.*, 1992].

Al has been demonstrated to affect egg hatching [Cleveland *et al.*, 1986] through reduction of ion uptake and the activity of the Na-K-ATPase in the embryo [Rosseland *et al.*, 1990; Rosseland *et al.*, 1992]. After hatching, Al affects gill ion and gas exchange processes [Wood *et al.*, 1988; McCahon *et al.*, 1989; Rosseland *et al.*, 1992; Waring and Brown, 1995] and loss of plasma ions (Na^+ , Cl^-) [Witters, 1986; Dalziel *et al.*, 1986; Rosseland *et al.*, 1992; Waring and Brown, 1995], in turn resulting in osmoregulatory failure [Witters, 1986; Booth *et al.*, 1988; Rosseland *et al.*, 1992]. Smaller changes in fish behaviour, *e.g.* feeding, is modified by Al exposure [Kramer *et al.*, 1986]. Recently, Brown and Whitehead (1995) reported increased release of catecholamines (adrenaline and noradrenaline) as a stress response in fish exposed to aluminium in acidic water.

Water Chemistry and Fish Mortality: The toxicity of Al depends of pH, calcium concentration and the presence of complexing ligands such as fluoride and dissolved organic matter, *e.g.* humic acid. Dissolved organic carbon concentrations and water hardness are the most important factors in ameliorating Al toxicity [Wood *et al.*, 1988; Gundersen *et al.*, 1994]. The chemistry exhibited by Al in natural waters is very complex and several authors have indicated that problems exist in accurately quantifying toxic responses in lakes and streams [Driscoll *et al.*, 1980; Sadler and Turnpenny, 1986; Kramer *et al.*, 1986; Weatherley *et al.*, 1990]. These difficulties are in-part related to rapid fluctuations in many of the chemical variables due to naturally occurring processes, *e.g.* chemical inputs due to snow melt.

Gundersen *et al.* (1994) studied Rainbow trout (*Oncorhynchus mykiss*) survival in alkaline waters (pH 7.14-8.58) with varying amounts of Al and hardness concentrations or Al and humic acid concentrations. Increased fish mortality was observed for waters with pH = 7.95-8.58 and was attributed to 10-fold higher filterable Al concentrations (*i.e.* $[Al(OH)_4]^-$). Hardness and humic acid protected against subacute Al toxicity; however, hardness was not observed to protect against Al-induced growth inhibition.

The loss of fish populations in acidic freshwaters has been frequently attributed to Al toxicity. Schofield and Trojnar (1980) reported that lakes (in the Adirondack mountain region of New York) diminished of brook trout (*Salvelinus fontinalis*) had mean Al concentrations of 0.29 mg L^{-1} whereas stocked lakes where the fish survived had Al concentrations of 0.11 mg L^{-1} . The concentrations of Al responsible for such effects are,

however, significantly higher than that required to affect fish behaviour, physiology and growth [Dalziel *et al.*, 1986; Buckler *et al.*, 1995; Laitinen and Valtonen, 1995; Waring and Brown, 1995]. Sadler and Turnpenny (1986) demonstrated that suppression of growth in brown trout occurred at concentrations above $20 \mu\text{g Al L}^{-1}$ at pH 4.4 to 5.2. Dalziel *et al.* (1986) found that a nominal addition of $8 \mu\text{g Al L}^{-1}$ to an artificial lake water at pH 4.5 and 4.0 reduced Na influx in brown trout significantly. In contrast, Waring and Brown (1995) found that labile monomeric Al concentrations of $12.5 \mu\text{g L}^{-1}$ in low organic content, soft water appear to be environmentally safe to brown trout.

During studies of Atlantic salmon (*Salmo salar*) exposed to Al concentrations ranging from 33 to $264 \mu\text{g L}^{-1}$ (pH 5.5), Buckler *et al.* (1995) monitored hatching success, mortality, growth, behaviour and tissue residues of Al. At this pH no effects on hatching were observed; however, larvae exposed to $124 \mu\text{g Al L}^{-1}$ at this pH incurred significant increases in mortality. Reduced growth was exhibited for larvae exposed to $71 \mu\text{g Al L}^{-1}$ and higher. The feeding behaviour of fish was inhibited among fish exposed to all Al concentrations; effects intensified as Al concentrations increased. Concentrations of whole-body tissue-Al were observed to increase with increasing Al concentrations; however, as the fish aged tissue-Al concentrations decreased again (*i.e.* not bioaccumulating).

Studies relating to the effects of Al on the hatching of eggs have consistently given differing results. Weatherley *et al.* (1990) and Buckler *et al.* (1995) both observed that hatching was independent of concentrations of monomeric aluminium. In contrast to these studies, Baker and Schofield (1982) demonstrated Al toxicity to eggs, with maximum toxicity at pH 5.2-5.5.

Toxicity Mechanisms: Considerable research has now been undertaken regarding the physiological effects of Al and the major toxicity mechanisms have become more apparent [Playle *et al.*, 1989; Dietrich and Schlatter, 1989; Exley *et al.*, 1991]. The most important effects are those of (i) ionoregulatory stress and (ii) respiratory system failure. Decreases in plasma Na^+ and Cl^- , red cell swelling and hemoconcentration are features of ionoregulatory toxicity. Respiratory toxicity involves reduction of blood oxygen and corresponding elevated blood carbon dioxide levels. The initial effects of respiratory stress (occurring at lower Al concentrations) are due to the impairment of gas exchange as a result of enhanced cell necrosis, proliferations, and fusions of the secondary lamellae in the gills which result in obstruction of the interlamellar space [Wood *et al.*, 1988; Dietrich and Schlatter, 1989; Rosseland *et al.*, 1992]. At higher Al concentrations, clogging of the gills (excessive mucus excretion) is observed [Kramer *et al.*, 1986; Rosseland *et al.*, 1992]; the ultimate cause of fish death. Exley *et al.* (1991) reviewed symptomatic evidence of toxicity and proposed that epithelial cell death is the general mechanism of Al-induced accelerated cell destruction and death to fish.

McCahon *et al.* (1989) studied the effects of acid, aluminium and lime additions on four fish species (salmon, trout, bullhead and charr) in an acidic Welsh stream. Al dosing was found to greatly increase fish mortalities with 100 % of salmon dead within 24 h in the stream zones dosed with solely Al or acid plus Al. Addition of lime decreased the rate of fish mortalities, however, even in this zone (Al at low pH with added limestone) all salmon were dead after 48 h. The ranking of species according to sensitivity to Al was salmon < trout < charr (no conclusion regarding bullhead). Previous studies [McCahon and Pascoe, 1989] in a soft-water stream (Wales) investigating the effects of sulfuric acid, aluminium sulphate and citric acid to salmon and trout gave similar results. Large mortalities were recorded in the acid/Al zone (in comparison to control and acid zones); mortalities were reduced in the citrate zone due to complexation of Al with citrate. Mortalities were hypothesised as being due to asphyxiation and hyperventilation; a result of clogging of gills by an excess of mucus produced in response to Al coating the gill surfaces. The speciation of Al in the toxic zones was dominated by labile inorganic Al, thus confirming previous studies hypothesising labile inorganic Al as the principal toxic species [Driscoll *et al.*, 1980]. The higher resistance of brown trout to acid Al-rich water than that of Atlantic salmon is now well established [Rosseland *et al.*, 1992].

Laitinen and Valtonen (1995) studied the cardiovascular, ventilatory and haematological responses of brown trout (*Salmo trutta* L.) to 0, 0.28 and 0.45 mg L⁻¹ Al added to a humic river water (pH 4.7, < 30 % labile Al). No mortalities were recorded during any exposure periods and acid stress alone was more important than effects from added Al. However, the acute responses in the heart and to fish ventilation rates (dose dependent) were greater in the presence of Al. Al did not appear to promote additional ionoregulatory stress. The responses in the humic water were significantly smaller than responses obtained in artificially prepared waters, indicating amelioration of effects of acid and Al stress by humic compounds.

The re-establishment of fisheries in lakes and rivers destroyed by acid deposition and Al release is frequently attempted by additions of mineral lime (*e.g.* CaCO₃) [Gee and Stoner, 1989]. However, Rosseland *et al.* (1992) reported that such additions can result in extremely toxic Al chemistry in the mixing zones between limed and acidic river waters. They found that in an acid stream (pH = 4.8, [Ca] = 1.3 mg L⁻¹, Al_i = 236 µg L⁻¹), LT₅₀ was 22 and 40 h for Atlantic salmon and brown trout, respectively. In the mixing zone between this river and a limed stream (pH = 4.8-6.5, [Ca] = 1.2-3.2 mg L⁻¹, Al_i = 50-240 µg L⁻¹), LT₅₀ was 7 h for both species.

Al Accumulation at Fish Gills: Possibly the most significant feature of Al toxicity to fish is the accumulation of Al on fish gills [Kramer *et al.*, 1986; Playle and Wood, 1990; Rosseland *et al.*, 1992]. The binding and accumulation of Al to fish gills has been proposed as the cause of respiratory and/or ionoregulatory disturbances [Booth *et al.*,

1988; Playle and Wood, 1989; Waring and Brown, 1995]. Booth *et al.* (1988) suggested two possible modes for Al toxicity (assuming toxicity was due to Al binding at gill surfaces), one based on solubility and the other based on speciation. Fish gills act as nucleating surfaces upon which Al can precipitate [Playle and Wood, 1990]. This precipitation and accumulation is likely to be due to the negative charge of the mucus layer (anionic sites: sulfate, carboxylate *etc.*) [Exley *et al.*, 1991; Wilkinson *et al.*, 1993; Poléo, 1995]. Fish respond to Al binding by increased discharge of mucus. This discharge distorts the bronchial epithelium resulting in increased diffusion distances for oxygen which leads to decreased arterial oxygen, the ultimate cause of respiratory stress [Wood *et al.*, 1988].

In studies of Al toxicity to common shiners (*Notropis cornutus*), Kramer *et al.* (1986) removed, killed and dissected fish that went into respiratory arrest. A build up of mucus at the gills was evident in all Al-doped fish; severely affected fish showed a complete loss of their epithelial layer. In static tests, loss of Al from solution was found to be proportional to the fish biomass. Tests using dead fish gave the same results as live fish, indicating that the organism itself provides an important Al sorption surface. In studies of rainbow trout Playle and Wood (1989) suggested that the pH in the gill bronchial micro-environment is raised above that of the inspired acidic soft water. These studies also indicated that much of the accumulated Al at fish gills is removed by extensive sloughing of Al bound by mucus.

Recently, Al polymerisation and, in particular, the role of 'Al₁₃' in Al-induced fish toxicity has received much attention [Flatten and Garruto, 1992; Exley *et al.*, 1994; Poléo, 1995]. Al is more toxic to fish in waters of pH around 5.0-5.5 than at lower pH; polynuclear species form readily in this pH range. Flatten and Garruto (1992) invoked polynuclear Al as playing an important role in Al toxicity, however, they did not present experiments to support this hypothesis. Recently, Exley *et al.* (1994) performed experiments aimed at elucidating the importance of Al polymerisation, exemplified by the polymer Al₁₃, as a mechanism of Al-induced toxicity. These studies showed clearly that Al₁₃ was not significantly more toxic to fish than the mononuclear Al³⁺ species. Poléo (1995) proposed that the growth of Al polymers on fish gill surfaces is more likely to be the cause of acute toxicity than precipitation of Al(OH)₃ or cellular internalisation of Al³⁺.

Tolerance Mechanisms: Tolerance mechanisms for fish species may include superior physiology (*e.g.* greater buffering capacity in the perivitelline fluid of the egg, osmotic stress tolerance) and behavioural adaptations (*e.g.* choice of spawning environment). Dissolved organic materials that complex Al reduce Al toxicity by competing for Al binding with gill epithelial binding sites.

Recent research has highlighted the role of silicon (present as silicic acid, Si(OH)₄, in natural waters) in mechanisms by which biological organisms reject Al and/or

reduce Al toxicity by the formation of hydroxyaluminosilicates [Birchall *et al.*, 1989; Birchall, 1990]. Birchall *et al.* (1989) studied Al toxicity to Atlantic salmon fry (*Salmo salar*) in acidic water (pH 5) at Al and Si [as $\text{Si}(\text{OH})_4$] concentrations of $7 \mu\text{mol L}^{-1}$ and $0.6 \mu\text{mol L}^{-1}$ respectively. 50 % of the salmon died within 24 h and all salmon were dead after 48 h. Severe damage to fish gills was observed. A second experiment was performed with a higher Si concentration ($93 \mu\text{mol L}^{-1}$); no fish deaths were observed and gill structures were largely unaffected. The formation of hydroxy-aluminosilicate species, presumably incapable of binding to gill epithelia, was hypothesised.

1.2.3 ALUMINIUM TOXICITY TO HUMANS.— Al intoxication as a consequence of long term haemodialysis, the treatment undertaken for renal failure patients, is the most well known form of Al toxicity in humans [Wills and Savory, 1983; Chazan *et al.*, 1991]. Many studies have, controversially, linked Al to the cause of the well known dementia Alzheimer's disease [Krishnan *et al.*, 1988; Doll, 1993]. The role of Al in several bone and other neurological disorders has also been suggested [McLaughlin, 1962; Gitelman, 1989; Garruto, 1991]. Geographic associations between concentrations of Al in drinking water and dementia have been hypothesised [Martyn *et al.*, 1989; Flaten, 1990; Forbes *et al.*, 1991].

The direction of this thesis is towards the environmental chemistry of Al. However, several interesting and important findings relating to Al toxicity have been advanced by studies of Al toxicity in humans. Therefore, a brief discussion is given to Al related disorders in humans and the speciation of Al in body fluids. A number of good reviews have been published on these subjects [Gitelman, 1989; Epstein, 1990; Doll, 1993; Winship, 1993; Martin, 1994]. The complexity of biological environments makes analytical protocols challenging [Tapparo *et al.*, 1995] and the interpretation of results difficult.

(A) Dialysis Related Disorders.— Neurological disorders in patients undergoing long term haemodialysis has been associated with or attributed to Al since 1972 [Alfrey *et al.*, 1972]. In a survey of the 18 dialysis centres in the U.K. [Parkinson *et al.*, 1979], a higher incidence of dementia was observed at centres with the highest Al concentrations in the water. Numerous studies have since confirmed the relationship between Al concentrations in dialysate fluids and the incidence of similar dementia [Chazan *et al.*, 1991].

When patients are treated with Al-containing dialysate, three disorders are commonly observed as a result of increased plasma Al (from *ca.* 0.2 to $10 \mu\text{mol L}^{-1}$): (i) microcytic anaemia (not responsive to iron therapy), (ii) vitamin D-resistant osteodystrophy (calcification and subsequent weakening of bones) and (iii) dialysis encephalopathy syndrome (DES) (a fatal neurological condition affecting speech and resulting in memory impairment and eventual dementia) [Wills and Savory, 1983; Winship,

1993; Martin, 1994]. The most common of these disorders is DES. Clinically, the disorder is described by progressive dementia and a speech disorder that progresses from stuttering to marked dysphasia. Motor abnormalities develop and personality changes occur resulting in patients no longer recognising friends [Winship, 1993].

Children or patients exhibiting minor renal disorders are often prescribed courses of $\text{Al}(\text{OH})_3$ (in the form of antacids) as a phosphate binding agent; encephalopathy has also been observed in these patients. In particular, ingestion of antacids in combination with citrate results in substantial increases in plasma Al concentrations [Slanina *et al.*, 1986].

(B) Alzheimer's Disease.— Alzheimer's disease (AD) is a progressive neurodegenerative disorder which results in permanent dementia. It is clinically characterised by a progressive deterioration of learning and memory which leads to severe impairment of judgement, language and motor function (usually occurring within 8 years) [Winship, 1993]. Elevated levels of Al have been found in the brains of AD victims [Krishnan *et al.*, 1988; Doll, 1993]. The role of Al in the progress of this neurological disorder is, however, still highly controversial [Krishnan *et al.*, 1988; Landsberg *et al.*, 1992; Doll, 1993].

Autopsies of AD victims [Candy *et al.*, 1986; Krishnan *et al.*, 1988; Good *et al.*, 1992] have revealed accumulation of Al in neurofibrillary tangle-bearing neurons of the brain. Also, Al-containing fibrillar amyloid proteins and senile plaques containing aluminosilicates are deposited in the brains. Comparisons of neurofibrillary tangles and amyloid cores of senile plaques with adjacent brain tissue have revealed that these sites contain the highest concentrations of Al. The senile plaques and neurofibrillary tangles have been found to contain Al, Fe and Si while plaque cores are particularly high in aluminosilicates [Gitelman, 1989; Martin, 1990; Doll, 1993; Winship, 1993]; however, Al and Fe are the only metals consistently present in these formations [Good *et al.*, 1992]. Uncertainty remains as to whether Al is directly involved in the deposition of amyloid proteins in brains and the consequent formation of the neurofibrillary tangles, or whether it accumulates as a secondary affect [Klatzo *et al.*, 1965; Krishnan *et al.*, 1988].

Several studies have highlighted possible demographic relationships between AD and Al in drinking water. However, these relationships are far less clear than similar relationships between Al concentrations in dialysate and incidence of dialysis disorders [Martyn *et al.*, 1989; Doll, 1993]. Treatment of AD patients with desferrioxamine [Wills and Savory, 1983; Winship, 1993] has been observed to result in less rapid deterioration in cognitive skills and in activities of daily living. Such evidence is also indicative of Al having an important role in AD.

(C) Amyotrophic Lateral Sclerosis and Parkinson's Dementia.— As a result of large case studies [Perl *et al.*, 1982; Garruto, 1991] Al has been hypothesised as having a role in amyotrophic lateral sclerosis (ALS) and Parkinsonism dementia (PD) in the native populations of western New Guinea, southern Guam and the Kii peninsula of Japan. In younger victims the disorder ALS prevails while older people suffer severe dementia associated with PD.

In both of these diseases, brain neurons are observed to undergo neurofibrillary degeneration into tangles. Unlike AD, plaque formation is not observed. A common feature of each of the districts where these disorders prevail has been the relatively high levels of exchangeable Al in soils and low concentrations of Mg^{2+} and Ca^{2+} .

(D) Al Consumption.— The sources of Al consumed by humans have been recently reviewed by several authors [Epstein, 1990; Winship, 1993; Martin, 1994; Reiber *et al.*, 1995]. Natural sources of daily consumable Al are typically low. Drinking waters average $0.02 \text{ mg Al L}^{-1}$ (possibly increased due to the use of alum, $Al_2(SO_4)_3$, as coagulation aid). The highest quantities of Al present in foods are tea (0.1-1 %, but poorly transferred to solution), herbs and spinach. The greatest sources of Al arise in food additives (alum baking powders, emulsifiers, anticaking agents) and pharmaceuticals (antacids, buffer aspirins, antiperspirants -*via* inhalation, vaccines).

(E) Al Speciation in Biological Fluids.— Biological systems are plentiful in 'hard' ligands, *e.g.* phosphate in membranes and ATP. The indiscriminative preference of Al for such ligands is likely to be the major reason for its toxicity to many organisms. Once present in the human body Al is quickly complexed by a number of common ligands (phosphate, citrate) and proteins (transferrin, catecholamines) [MacDonald and Martin, 1988; Martin, 1986 and 1994]. Ligands containing few carboxylate or phosphate groups are not likely to form important complexes with Al.

Blood plasma has pH *ca.* 7.4 and hence most uncomplexed Al is present as $Al(OH)_3$. Inorganic phosphate present in blood further decreases free Al^{3+} concentrations by the formation of insoluble Al-phosphates.

Citrate is probably the most important small ligand solubilising Al in body fluids [MacDonald and Martin, 1988; Martin, 1990]. Model calculations indicate that an appreciable fraction of the Al-citrate complexes is present in plasma as a neutral species ($AlCit^0$) which is of sufficient stability to preclude the formation of insoluble Al-hydroxide or Al-phosphates [Öhman, 1988; Slanina *et al.*, 1986]. This species may pass through cell membranes and thereby provide an important pathway for Al absorption into the body [Slanina *et al.*, 1986; Molitoris *et al.*, 1989; Domingo *et al.*, 1991]. Fromont *et al.* (1989) suggested that upon administration of Al in combination with citrate, enhanced adsorption

of Al occurs in the proximal bowel (*via* the paracellular pathway) due to the opening of cellular tight junctions.

The Fe-transport protein transferrin, whose sites are only 30 % occupied by Fe, is likely to account for the majority of Al in plasma and possibly provides the most important means for its transport in this fluid [MacDonald and Martin, 1988; Adreo and Glass, 1993]. Al^{3+} may be capable of displacing Mg^{2+} from phosphate binding sites on proteins (*e.g.* ATP) and consequently result in their disfunction [Martin, 1986; MacDonald and Martin, 1988; Adreo and Glass, 1993]. Ligand exchange rates of metal complexes found in biological fluids are also important in governing speciation [Martin, 1994]; Al^{3+} exchanges 10^4 times slower than Mg^{2+} and 10^7 times slower than Ca^{2+} [Birchall, 1990].

Recently, the presence of aluminosilicates in biological fluids has been highlighted as contributing significantly to the control of Al bioavailability [Birchall and Chappell, 1989; Birchall, 1990]. Martin (1990) indicated that up to 6 aluminosilicate species could be expected to exist in blood plasma in competitive equilibrium with citrate and transferrin. These findings draw new light to the presence of aluminosilicates found in the brains of AD victims [Candy *et al.*, 1986]. Netter *et al.* (1991) hypothesised that aluminosilicates may initiate or accelerate the formation of senile plaques and other cellular lesions in Alzheimer's disease victims. Several articles have directly or implicitly asked the question: "does silicon protect against aluminium toxicity ?" [Birchall, 1990; Fahal *et al.*, 1994].

(F) Toxicity Mechanisms.— The mechanisms relating to the neurotoxic effects of Al have been discussed in several of the reviews [MacDonald and Martin, 1988; Exley and Birchall, 1992; Adreo and Glass, 1993]. However, clear pathways by which Al acts are still far from clear. The reported effects on proteins and enzymes are many; possibly one of the most important is the disrupting effects Al has on the adenylate cyclase cascade [Adreo and Glass, 1993]. Al is also known to interfere with GTPase cycles and recently this was suggested as a cause of cell toxicity [Exley and Birchall, 1992].

Al affects brain tissue, including protein synthesis, axonal transport and neurotransmitter function. In AD, substantial evidence is now indicating that Al accumulation occurs in the grey matter. Sites include DNA-containing structures of the nucleus, the protein fractions of neurofibrillary tangles, the amyloid cores of senile plaques and cerebral ferritin [Winship, 1993]. Adsorbed Al has been reported to deposit in bone tissue [Eastwood, 1990].

SECTION C: THE MEASUREMENT AND SPECIATION OF ALUMINIUM AT ENVIRONMENTALLY SIGNIFICANT CONCENTRATIONS

1.3 AL MEASUREMENT

The toxicity of Al is dependent on its chemical form (*i.e.* its speciation) and is most commonly correlated with the sum of the free and labile forms. Thus the measurement of this fraction, rather than total Al, is of primary importance in soils and natural waters. Direct methods of analysis with sufficient sensitivity for environmental analysis (*e.g.* ion selective electrodes, atomic absorption spectrophotometry) are either not applicable to Al or do not achieve discrimination amongst different species. The lack of a direct method for the analysis of Al^{3+} has resulted in the development of a large number of indirect fractionation procedures. These techniques utilise operationally defined methodologies for the discrimination between the various aqueous forms of Al.

In recent years, a large variety of fractionation procedures have been developed in an attempt to distinguish between aqueous forms of Al. These techniques include dialysis, ultrafiltration or size exclusion chromatography [LaZerte *et al.*, 1988.; Lydersen *et al.*, 1992; Zernichow and Lund, 1995], ion chromatography [Jones *et al.*, 1988; Garcia Alonso *et al.*, 1989; Jones, 1991], ion exchange [Campbell *et al.*, 1983; Driscoll, 1984; Quintela *et al.*, 1993; Fairman *et al.*, 1994], chelating resins [Fernandez *et al.*, 1991; Ljunggren *et al.*, 1992; Quintela *et al.*, 1993; Hirayama *et al.*, 1994; Martín-Esteban *et al.*, 1995], F^- ion-selective electrode [Munns *et al.*, 1992; Ngila *et al.*, 1994], fluorimetry [Browne *et al.*, 1990a,b; Fairman and Sanz-Medel, 1993; Canizares and Luque de Castro, 1993; Baksi and Pal, 1994; Sutheimer and Cabaniss, 1995a,b], colorimetry [Hodges, 1987; Kerven, 1989; Fairman and Sanz-Medel, 1993] and kinetic methods [Lu *et al.*, 1994]. All of these procedures are operationally defined and undoubtedly detect somewhat different forms of Al. The direction of this thesis is not towards a comparison of these various fractionation procedures. The interested reader is directed towards a detailed discussion of these methods for further reference [Clarke, 1994; Sparén, 1994; Clarke *et al.*, unpub.]. Recent improvements in Al NMR techniques have advanced its use as a direct method for speciating Al in environmental samples, however, detection limits are still too high and species identification is difficult [Faust *et al.*, 1995; MacFall *et al.*, 1995].

1.3.1 SPECIATION AND FRACTIONATION.— In natural waters or soil extracts, the largest uncertainty in the evaluation of Al toxicity is caused by *operationally defined* results. This problem arises because of the inability of any fractionation procedure to accurately differentiate between aqueous and particulate Al, or between inorganic and organic forms of aqueous Al. Al determinations are usually made indirectly and often *via* the use of a complexing agent; for such a technique it is difficult to evaluate the extent to

which the complexing agent will desorb Al^{3+} from particulate matter or sequester Al^{3+} from naturally occurring ligands. Any method that disturbs the primary equilibria of a natural system, *e.g.* addition of a colorimetric reagent, will inevitably over-estimate toxic Al. This feature of all indirect techniques is the most important to consider when developing new speciation methodologies.

(A) Driscoll Fractionation Protocol.— Possibly the most commonly utilised procedure for fractionation of Al in waters is the technique described by Driscoll (1984). The fundamental steps of this method involve (i) the separation of organically complexed Al from inorganic Al through the uptake of the latter on a strong cationic exchange resin, and (ii) a separate rapid extraction or reaction of both inorganic and organic monomeric Al. Total Al is measured following acid digestion.

This procedure is now commonly referred to as 'Driscoll's method'; a schematic diagram of this procedure is given in Figure 1.3A.

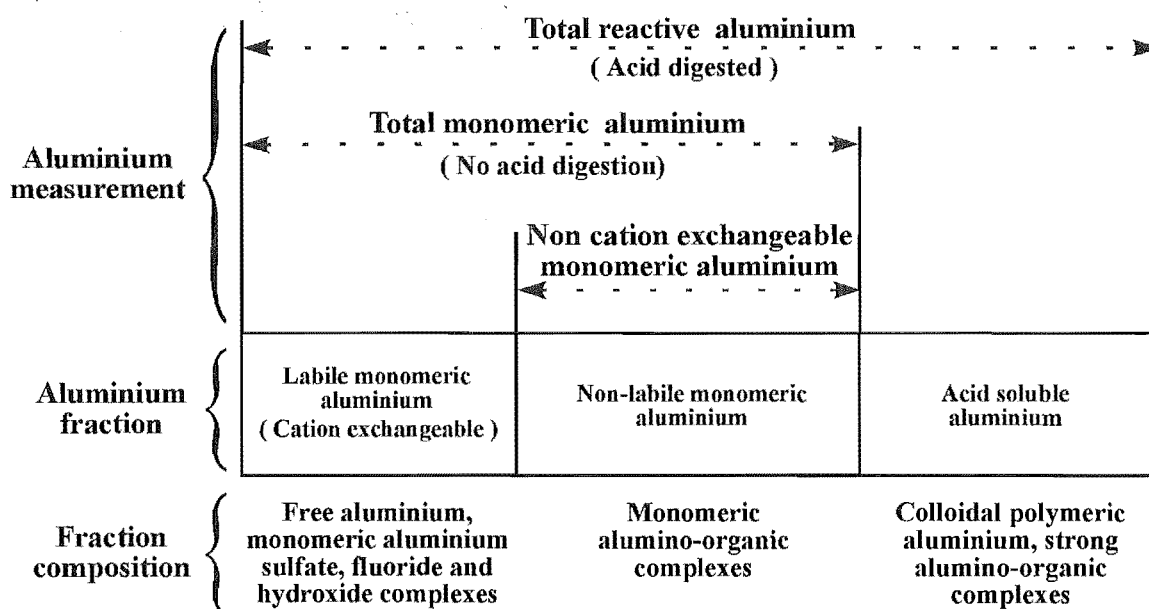


Figure 1.3A A sketch of Driscoll's scheme for aluminium fractionation (modified from Driscoll, 1984).

In this procedure three Al measurements are made, *total* Al (acid digested), *total monomeric* Al [rapid measurement using a suitable complexing agent, *e.g.* 15 s 8-hydroxy-quinoline (oxine) extraction at pH 8.3 into solvent or 10 min PCV reaction at pH 6.1], and *nonlabile monomeric* Al [separated from labile monomeric *via* a strong cation exchange column (Amberlite IR-120) followed by analysis of the eluent as monomeric Al]. This

procedure also results in the determination of two additional Al fractions; *acid soluble* Al is measured as the total Al less total monomeric Al and *labile monomeric* Al is determined as the difference between total monomeric and nonlabile monomeric Al. In Driscoll's original method the total monomeric Al in each fraction was measured by rapid extraction with 8-hydroxyquinoline in methyl isobutyl ketone [Barnes (1975)]. Many other researches have since attempted to further improve this methodology, either by change of reagent [Seip *et al.*, 1984; Sullivan *et al.*, 1986] or by increasing the precision and sample throughput by use of FIA [LaZerte *et al.*, 1988; McAvoy *et al.*, 1992; Fairman and Sanz-Medel, 1993]. In an inter-laboratory comparison [Fairman *et al.*, 1994] the Driscoll-pyrocatechol violet fractionation method was found to achieve relative standard deviations of 15 % for labile monomeric Al.

The inorganic Al species present in most waters are cationic and are assumed to be adsorbed by the cation exchange column. Conversely, organic species present in natural waters are predominantly anionic and are assumed not to be adsorbed. This concept is fundamental to Driscoll's speciation methodology. Unfortunately, however, if re-equilibration of the sample occurs during its passage through the exchange column (residence times range from 10 to 50 s), organic complexes will release Al, resulting in an overestimation of inorganic monomeric Al. Observations by a number of analysts indicate that dissociation of organic Al complexes does occur, is often variable, and depends on sample characteristics such as Al/C ratio [Backes and Tipping, 1987; Berggren, 1989; Dahlgren and Ugolini, 1989; Kerven, 1989]. Backes and Tipping's comparison of monomeric organic Al fractions (Al_{org}) of humic substances estimated by Driscoll's cation-exchange procedure (CE), and those obtained by equilibrium dialysis, indicated that the CE underestimates Al_{org} by up to 25 %. Berggren modified the cation exchange procedure to minimise dissociation of Al-complexes; however, sequestering of Al from Al-humic complexes was not completely overcome (mean = 7 %). The disturbance to the natural equilibrium position of a sample dominated by stable complexes (*e.g.* Al-humic materials) limits this method to one which provides good approximations (at best) of monomeric inorganic Al. Furthermore, the lack of testing of this methodology on model ligand or Al-hydrolysis systems leaves the operator guessing as to which species are measured in each fraction, *i.e.* is the cationic species, $[AlO_4Al_{12}(OH)_{24+n}(H_2O)_{12-n}]^{(7-n)+}$, commonly known as ' Al_{13} ' retained by cation exchangers?

(B) Kinetic Methods.— Kinetic methods for estimating toxic Al are currently the most preferred [Clarke *et al.*, 1992; Hawke and Powell, 1994; Clarke and Danielsson, 1995; Danielsson and Sparén, 1995; Fairman and Sanz-Medel, 1995]. These methods exploit the comparatively slow dissociation kinetics for Al complexes and employ short reaction

times with an Al selective reagent to discriminate between 'free' and complexed Al^{3+} . The reagent should react rapidly with the free Al so as to minimise the stripping of Al from comparatively stable, non-toxic complexes. The 'fast reactive' Al measured is representative of free and kinetically labile Al in the sample and is likely to contain monomeric inorganic Al as well as some labile organic species. The fast reactive fraction is measured directly, thus providing advantages over the Driscoll procedure where labile monomeric Al is taken as the difference between total monomeric Al and the non-labile Al fractions. As in Driscoll fractionation protocols, the fraction of Al measured by kinetic methods remains operationally defined, *i.e.* the measured fraction is dependent on the reagent used and on the contact time between sample and reagent.

Control of the reaction time in these methods is frequently achieved by use of a flow injection protocol. A typical manifold is shown in Figure 1.3B.

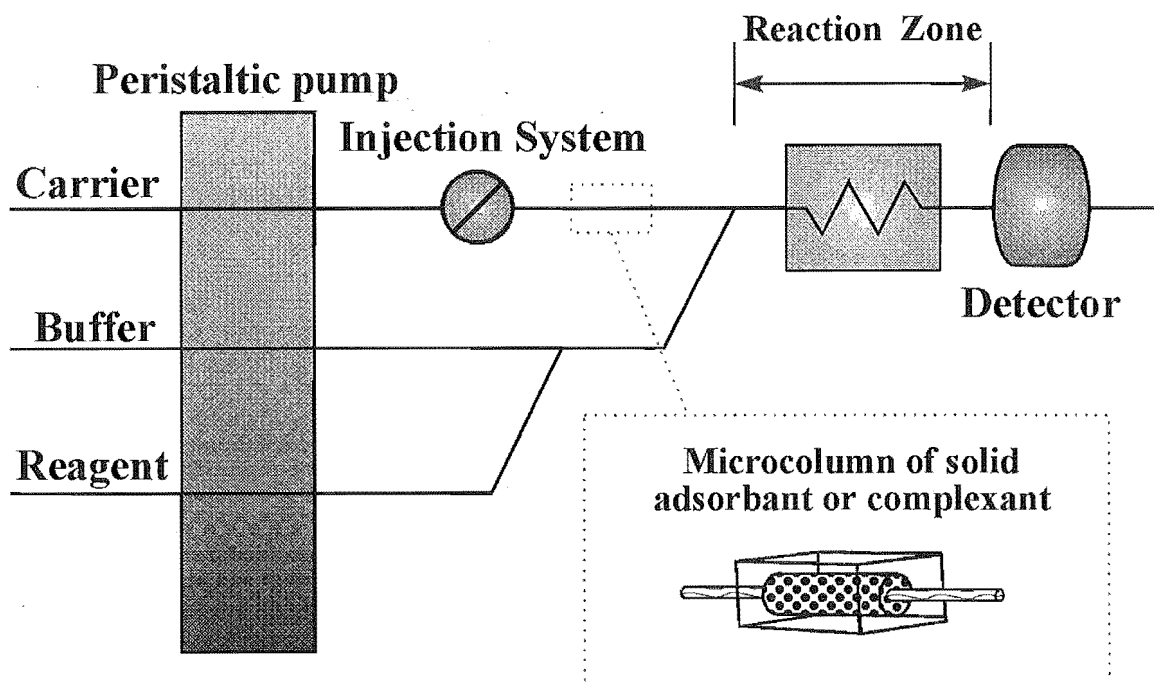


Figure 1.3B A typical flow injection manifold for the determination of rapidly reacting Al.

Kinetic methods (all FIA based) can be categorised into two groups; (i) *direct* and rapid reaction of Al with a suitable reagent with immediate detection and (ii) selective *capture* of reactive Al on a suitable adsorbent or chelating resin in a microcolumn with detection following elution. The direct approach has been the more utilised.

Direct Methods.— Clarke *et al.* (1992) developed a direct FIA oxine-solvent extraction method with a total reaction time of 7.4 s (2.3 s premix plus 5.1 s for solvent extraction). The technique requires on-line sample buffering (0.1 mol L⁻¹ acetate, pH 5.0) because reaction kinetics are pH dependent. This necessity may result in small changes in sample speciation occurring before reagent contact. Furthermore, the buffer contains 0.5 mol L⁻¹ hydroxylamine and 10 mmol L⁻¹ 1,10-*o*-phenanthroline to prevent interference from Fe³⁺. The reduction of Fe³⁺ (free and complexed) to Fe²⁺ by hydroxylamine and subsequent complexation with 1,10-*o*-phenanthroline results in ligands that were initially complexing Fe³⁺ becoming free. These ligands may immediately capture free Al and result in further disturbances to the samples' natural equilibria. The method also uses a comparatively high reagent concentration (4 mmol L⁻¹ oxine; 1.4 mmol L⁻¹ during premix and concentrated further during solvent extraction), which will tend to promote both a more rapid reaction with free Al and also greater sequestering of Al from organic complexes. Despite these potential problems, testing of the method against model ligand solutions (speciation computed by equilibrium modelling) provided good results for measured vs predicted free Al [Clarke *et al.*, 1992].

Hawke and Powell (1994) developed a somewhat less aggressive FIA method based on a 7 s reaction with CAS and spectrophotometric monitoring at the isosbestic point for a rapidly formed intermediate. This method uses a lower reagent concentration (35 µmol L⁻¹ at the detector) and has a lower detection limit than that of Clarke *et al.* (60 nmol L⁻¹ vs 200 nmol L⁻¹). In subsequent work Powell and Hawke (1995) have applied the method to determination of reactive Al in soil solutions and thus established pAl-pH correlations. They have also used it to determine Al-complexation capacities for NOM in waters and in soil solutions [Powell and Hawke, 1995; Hawke *et al.*, 1996].

Boudot *et al.* (1994) modified the widely used (Barnes/Driscoll) 15 s oxine extraction method for the speciation of Al in soil solutions and surface waters. Basically, (i) samples were forcefully injected (high turbulence) into buffered oxine to achieve thorough mixing, (ii) immediately methyl isobutyl ketone (MIBK) was injected (forcefully; terminated 5 s after sample injection) for extraction of the Al as the Al-hydroxyquinolate complex. Step '(ii)' was presumed to stop the reaction, however, a third step was used which may allow further reaction of Al that has not been extracted. In step (iii) the tubes were capped and shaken for a further 5-10 s to complete the extraction process. Analysis was performed spectrophotometrically; batch techniques gave greater precision than FIA. The method was tested on a large number of model ligand systems and gave satisfactory results. However, sequestering of Al from Al-fulvate complexes was significant at *ca.* 8 % (20 % in original 15 s extraction procedure).

Recently, Danielsson and Sparén (1995) modified and improved the method by Clarke *et al.* for the mechanised determination of low levels of quickly reactive Al in natural waters. The manifold system was simplified by combining the reductant, buffer

and reagent lines of the original FIA system. A graphite furnace atomic absorption spectrophotometric (GFAAS) detection system was used, giving a detection limit of 20 nmol L^{-1} and increased precision. Large sample volumes were required (pumped on-line) and sample throughput was *ca.* 10 sample h^{-1} . The largest drawback of this technique is the requirement for complicated and expensive apparatus.

Microcolumn Capture.— An alternative approach to speciation of metals is based on the selective capture of a metal ion (or its rapidly formed complex) on a suitable adsorbent or chelating resin in a microcolumn. Such methods can be selective (by choice of reagent or adsorbent) and involve preconcentration. This approach has only recently begun to be exploited and many existing adsorbents or chelating resins have not yet been tested for their suitability for the capture and subsequent measurement of free or reactive Al.

Fernández *et al.* (1991) utilised Chromotrope-2B immobilised on an anionic AG1-X8 exchanger to matrix separate and preconcentrate Al in a chelating microcolumn followed by spectrofluorimetric determination of the complex Al-5,7-dibromo-8-quinolate (extracted into ether). Optimum pH was 5.5 and the elements Cu^{2+} and Fe^{3+} were also partially retained by the resin. An FIA method was developed for Al in foods and dialysis concentrates but the possibility for analysis of natural waters was not examined.

The chelating properties of salicylideneamino-2-thiophenol derivatised glass beads towards Al^{3+} was investigated by Kobayashi and Miyazaki (1993). A method for FIA column preconcentration of Al at pH 5.5 was developed and interfering ions investigated. Of the ions tested for interference, Fe^{3+} was the most significant. This problem was overcome by use of the reducing agent hydroxylamine. Vilchez *et al.* (1993) examined the fluorescent complex of the Al-salicylidene-*o*-aminophenol for solid-phase spectrofluorimetric determination of Al^{3+} in natural waters. The complex was adsorbed on a dextran-type cation-exchange gel (Sephadex CM C-25) and determinations were made by batch procedure (optimum pH was 5.5-6.0). No interference was observed from Fe^{3+} at a 10,000-fold excess.

Desferrioxamine was used by Ljunggren *et al.* (1992) for preconcentration of aluminium ions *via* immobilisation on a modified porous glass, followed by GFAAS detection. Quantitative uptake of Al^{3+} (samples acidified with $1 \text{ mmol L}^{-1} \text{ HNO}_3$) was restricted to the pH range 5.5-6.0 (sample elution with $0.5 \text{ mol L}^{-1} \text{ HNO}_3$). Hirayama *et al.* (1994) immobilised CAS on a propylisothiuronium functionalised silica gel for the separation and preconcentration of Al in natural waters. Al was retained quantitatively above pH 5 and was eluted with $0.1 \text{ mol L}^{-1} \text{ HCl}$. The method was not developed, however, for the selective capture of free or reactive Al.

In an FIA procedure for speciation of Al in river and tap waters, Quintela (1993) reported the use of pyrocatechol violet (PCV) immobilised on Amberlite IR-120. Iron-

masking solutions containing 0.06 % 1,10-phenanthroline plus 3 % hydroxyl-ammonium chloride suppressed interference of Fe^{3+} up to $5.5 \mu\text{g mL}^{-1}$. A Driscoll type fractionation procedure was performed. Sarzanini *et al.* (1987) investigated two procedures for uptake of anionic Al(III)-PCV complexes on an anionic exchanger (Bio-Rad AG MP-1 macroporous anion-exchange resin). The first procedure involved pre-formation of Al(III)-PCV complexes followed by pumping through a column containing the exchanger. The second involved loading the resin with PCV and subsequent injection of the sample. The first procedure was deemed to be superior; this may be a result of the slow equilibration between PCV and Al(III).

Landing *et al.* (1986) synthesised an oxine-based chelating ion-exchange resin by immobilisation of oxine onto Fractogel TSK. The resin was found to be capable of chelating and thus concentrating Al, Mn, Fe, Co, Cu, Zn, and Cd from organic-rich freshwater samples. Subsequent research resulted in the development of FIA preconcentration procedures for Mn [Resing and Mottl, 1992], Al [Resing and Measures, 1994] and Fe [Measures *et al.*, 1995] in seawater. The method for Al utilised 2.5 mL sample volumes (pre-buffered; 0.02 mol L^{-1} acetate, pH 5.5) with maximum Al uptake occurring between pH 5.5 and 5.7. Captured Al was eluted by back-washing with 0.05 mol L^{-1} HCl and detected fluorimetrically with lumogallion. The detection limit was $\sim 0.15 \text{ nmol L}^{-1}$. Five interferents, previously reported for lumogallion-Al chemistry, including Cu^{2+} and Fe^{3+} were tested. No interferences were observed.

Fairman *et al.* (1995) used the hydrophobic XAD-2 resin in 'mini' columns ($88 \mu\text{L}$) to adsorb the Al(oxinate)_3 complex formed in an initial 2-3 s reaction of the sample with 2 mmol L^{-1} oxine in a FIA manifold. The method was also adapted to manual field processing of samples, with subsequent elution of the adsorbed complex (with 1.0 mol L^{-1} HCl) in the laboratory. The detection limit was 67 nmol L^{-1} (ICP-MS) and a RSD of 8 % was obtained at the $3.7 \mu\text{mol L}^{-1}$ level.

1.4 OBJECTIVES OF THIS WORK

The toxicity of Al is dependent on its chemical form (*i.e.* its speciation) and is most commonly correlated with the sum of the free and labile forms of Al. Thus the measurement of this fraction, rather than total Al, is of primary importance in soils and natural waters. No direct methods are available for the measurement of the free Al ion, Al^{3+} . Hence methods applicable to the speciation of Al require indirect approaches. Any method that disturbs the primary equilibria of a natural system will inevitably over-estimate free and labile forms of Al (toxic Al). Therefore, these procedures must accurately differentiate between aqueous and particulate Al, or between free, inorganic and organic forms of aqueous Al without altering the original sample composition.

Kinetic methods for estimating toxic Al are currently the most preferred. These methods exploit the comparatively slow dissociation kinetics for Al complexes and employ short reaction times with an Al selective reagent to discriminate between 'free' and complexed Al^{3+} . The reagent should react rapidly with the free Al so as to minimise the stripping of Al from comparatively stable, non-toxic complexes. The 'fast reactive' Al measured is representative of free and kinetically labile Al in the sample and is likely to contain monomeric inorganic Al as well as some labile organic species.

In this work, the development of a speciation protocol for Al in natural waters and soil solution was addressed. Fundamental to the development of a speciation technique is a knowledge (either chemical or theoretical) of the manner in which the reagent reacts with the target analyte. Furthermore, a knowledge of how the reagent interacts with other 'non-targeted' components of the analyte's natural matrix is also important. The ligand pyrocatechol violet (PCV) has been the most used reagent for the determination of Al. In the current work the interaction of this ligand with Al was investigated in detail.

The equilibrium reactions between Al and PCV were studied by potentiometry (and spectrophotometry) to develop a thermodynamic model describing these equilibria. Further to these studies, the potential complexation of PCV by naturally occurring (hydr)oxides was investigated through a thermodynamic study of the adsorption behaviour of PCV on the surface of the Al-oxide hydroxide boehmite. The latter of these studies was to provide information on the importance of colloids in natural waters and the potential for their interaction with 'Al-targeting' reagents.

The optimum conditions for the measurement of any metal ion by a reagent will depend strongly on the manner in which a reagent interacts with the metal. Most commonly, analysis conditions are optimised *via* a trial-and-error approach whereby the parameters such as pH and reagent concentration are manipulated to obtain the greatest detection signal. In speciation analyses, this optimisation procedure is further complicated

by the need to optimise the targeting of a single analyte species. An alternative to the trial-and-error approach is to carry out computer modelling using equilibrium constants. This approach is not often feasible due to the lack of appropriate data for either the interferent or the colorimetric reagent. Recently, however, equilibrium data have become available for the interaction of Al with the reagents chrome azurol S (CAS), eriochrome cyanine R (ECR) and, through the current studies, PCV. Modelling calculations were undertaken to compare the abilities of the reagents CAS, ECR and PCV to determine total Al in natural systems. The comparison is based on the competitive equilibria between the reagent and a ligand (potential interferent) with Al-complexing properties 'typical' of soils and natural waters. From these calculations, the applicability of each reagent to the determination of total Al, and implications to the assay of toxic Al are discussed.

The thermodynamic approach to assessing interferents and optimising analysis conditions is of limited use in the fine tuning of speciation protocol conditions. In natural water and soil environments, Al exists in competitive equilibria with a large number of naturally occurring ligands. Natural systems are quite 'dynamic' and the kinetics of chemical processes may be particularly important in controlling speciation. For speciation measurements it is desirable that the reagent should only interact with free Al, *i.e.* Al^{3+} , $\text{Al}(\text{OH})^{2+}$, $\text{Al}(\text{OH})_2^+$. Most reagents used for the determination of Al react rapidly and form strong complexes with Al. Unfortunately, these reagents are likely to sequester significant amounts of Al from both weak and moderate strength Al complexes.

The kinetics of complexation and dissociation processes affect the results obtained during the analysis of 'labile Al' and these effects may be different for different sample compositions. For this reason, an investigation was made of the time scales for the establishment of equilibrium in competitive Al-ligand-reagent systems (reagent = PCV). These studies also acted to validate the Al-PCV thermodynamic model under spectrophotometric conditions. Furthermore, the effect of the mixing-order in which the sample, reagent and buffer are combined, on speciation results was investigated. The implications for kinetic-based analysis of Al in samples differing in composition (*i.e.* presence or absence of a 'second' ligand) is discussed.

The measurement of Al is most easily performed using an indirect method whereby the response (spectrophotometric, fluorimetric, electrochemical) of a 'probe ligand' which complexes Al, can be monitored as a function of Al concentration. For this reason, the choice of ligand is of utmost importance to development of methods with both sufficient sensitivity and specificity for Al. Furthermore, methods which offer adequate sensitivity at a modest cost (of apparatus and reagents) are likely to find more widespread application than methods that require expensive apparatus and maintenance (*viz* ET-AAS, ICP-MS). Flow injection techniques utilising electrochemical detection may offer several advantages over other detection procedures (*e.g.* spectrophotometric or fluorimetric detection) in that analyses may be performed rapidly using relatively cheap apparatus.

The Al-binding and electrochemical properties of a series of ligands were evaluated with the intention that suitable ligands could be utilised in the development of an electrochemical method for the determination of Al. As an alternative to investigating ligands whose electrochemical response was expected to be perturbed by Al, a second indirect method for the electrochemical determination of Al was also considered. This novel procedure involved probing the electrochemistry of a secondary metal ion bound by a suitable ligand. The ligand's ability to complex Al should be such that, in its presence, the secondary metal ion is displaced quantitatively by Al, thus allowing this metal's electrochemistry to be exploited.

An unfortunate feature of indirect methods of analysis (whereby the response of a 'probe ligand' which complexes Al can be monitored as a function of Al concentration) is that these methods are prone to interference from other metal ions that interact with the 'probe' ligand. Fe^{3+} binds with the same types of ligands that complex Al^{3+} . In spectrophotometric and fluorimetric procedures interference from Fe^{3+} can often be masked using suitable 'masking agents', *e.g.* bipyridine/ or 1,10-phenanthroline/ascorbic acid. However, in electrochemical analyses of Al such masking agents are not appropriate because of the electroactivity of the reducing agent. Furthermore, Fe masking agents are less appropriate to speciation analyses because perturbation of Fe-NOM equilibria will also affect Al-NOM equilibria (NOM = natural organic matter).

FIA systems which incorporate a micro-column of suitable chelating resin (on-line) for the selective capture (matrix separation) and preconcentration of a test analyte may offer advantages over conventional speciation methods. In FIA on-line column procedures where an analyte is introduced to the flow system the operator is generally interested in (i) the complete (or reproducible) and selective 'capture' of the analyte species with the rejection of the interfering matrix to waste, followed by, the complete release of the analyte species to the detector, or alternatively (ii) the free passage of analyte to the detector and retention of interfering species. However, since both Al and Fe complex the same types of ligands then it is likely that Fe will be at least partially retained by chelating resins which complex Al. Hence scenarios, (i) and (ii) are not greatly applicable to the determination of Al in the presence of Fe (the interferent). This problem may be overcome by use of a method by which both Al and Fe are selectively retained by a chelating resin, followed by selective elution of one or both metals.

The final section of work in this thesis addresses the subject of on-line matrix separation and/or preconcentration for the flow-through speciation of Al in natural waters and soil solutions. The work is directed towards the development of an Al speciation technique which may be used without the use of additional masking agents for Fe. This technique will involve the direct measurement of 'reactive' Al through the selective capture of Al on a suitable chelating resin in a microcolumn (incorporated in an FIA system). The

factors which affect 'speciation' procedures (discussed throughout the earlier sections of work) are considered during the development of this new technique.

The resultant FIA method is tested for (i) the extent of separation between reactive Al and Fe, (ii) the sequestering of Al from its citrate, oxalate, malonate and fluoride complexes and (iii) retention of Al-hydroxy polymers [*e.g.* $\text{Al}_{13}(\text{OH})_{32}^{7+}$]. The method is applied to humic waters and soil solutions and the results for 'free' Al^{3+} are compared with those obtained from an alternative speciation method. The method's detection limit and linear working range are evaluated.

CHAPTER 2

NUMERICAL ANALYSIS

This chapter describes the mathematical treatment of potentiometric data for the evaluation of ligand protonation constants, formation constants for metal-ligand complexes and complexes at the surface of hydrous oxide particles. The chapter is divided into two parts.

SECTION A: A brief description of the non-linear least squares procedure used to calculate formation constants from titration data is given. The analysis of solution equilibria data for aqueous metal-ligand and surface-ligand(metal) complexation is addressed. The methodology behind the evaluation of a complete equilibrium model is discussed.

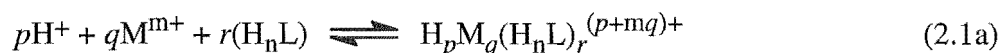
SECTION B: The conditions for accurate pH measurement are discussed.

SECTION A: MATHEMATICAL TREATMENT OF POTENTIOMETRIC TITRATION DATA FOR THE DETERMINATION OF FORMATION CONSTANTS

2.1 THERMODYNAMIC TREATMENT OF AQUEOUS EQUILIBRIA

The complete characterisation of an equilibrium system comprises (i) the determination of the stoichiometries of any species forming in significant quantities and (ii) the determination of each species' stability, as described by a thermodynamic equilibrium constant (commonly referred to as a formation constant). Thermodynamic equilibrium constants are a function of (a) temperature and (b) pressure. Methods frequently used for the study of solution equilibria include potentiometry, spectrophotometry, conductivity and calorimetry. The information provided by these methods on the equilibrium speciation is in the form of macroscopic measurements of individual species, *i.e.* a single measurement contains the sum of effects of all species present. Therefore, the characterisation of individual species (the equilibrium analysis) from this data must always be performed simultaneously with the quantification of the amount of each species (determination of formation constants).

For a three component system, the equilibrium condition may be described by the equation:



and

$$\begin{aligned}
 \beta_{p,q,r}^{th} &= \frac{\{H_p M_q (H_n L)_r\}^{(p+mq)+}}{\{H^+\}^p \{M^{m+}\}^q \{H_n L\}^r} \quad (2.1b) \\
 &= \frac{(\gamma_{H_p M_q (H_n L)_r})^{(p+mq)+}}{(\gamma_{H^+})^p (\gamma_{M^{m+}})^q (\gamma_{H_n L})^r} \cdot \frac{[H_p M_q (H_n L)_r]^{(p+mq)+}}{[H^+]^p [M^{m+}]^q [H_n L]^r} \\
 &= \frac{(\gamma_{H_p M_q (H_n L)_r})^{(p+mq)+}}{(\gamma_{H^+})^p (\gamma_{M^{m+}})^q (\gamma_{H_n L})^r} \cdot \beta_{p,q,r}
 \end{aligned}$$

where $\beta_{p,q,r}^{th}$ is the thermodynamic equilibrium constant of the species with stoichiometry p (proton), q (metal), r (ligand). $\{X\}$ is the activity, γ_X is the activity coefficient and $[X]$ is the concentration of component 'X'. The term, $\beta_{p,q,r}$, is a concentration dependent equilibrium constant.

The activity coefficient relates the activity of each species to its concentration. The activity of a species will be equal to its concentration only in infinitely dilute solutions. As ionic strength increases, ions of opposite charge interact leading to a decrease in their effective activity [Fischer & Peters, 1970]. Thus, the ionic strength of the medium will affect the measured value of the concentration quotient, $\beta_{p,q,r}$. Under experimental conditions of low ionic strength, changes in equilibrium speciation will affect the γ -values of all surrounding species. The equilibrium analysis [determination of (p,q,r) -stoichiometry and the corresponding β -values] of data determined under such conditions will be practically impossible.

This problem can be circumvented by using the constant ionic medium approach. This method utilises the principle that for a constant (and high) ionic strength medium, the activities of each of the participating ions and molecules remain practically constant as the ratio of reactant and product species is changed. In this situation, a concentration dependent equilibrium constant, $\beta_{p,q,r}$, can be defined which will be constant when the term describing an ion or molecule activity is constant under given experimental conditions.

$$\beta_{p,q,r} = \beta_{p,q,r}^{th} \cdot \frac{(\gamma_{H^+})^p (\gamma_{M^{m+}})^q (\gamma_{H_n L})^r}{(\gamma_{H_p M_q (H_n L)_r})^{(p+mq)+}} \quad (2.1c)$$

This condition has been shown to hold as long as the equivalent concentrations of the investigated species do not exceed about 10 % of the ionic strength of the medium [Biedermann, 1975]. Depending on whether predominantly anionic or cationic complexes form in the system, the total cation or anion concentration of the medium can be chosen to be held constant, *viz* $X \text{ mol L}^{-1} \text{ Na(Cl)}$ or $Y \text{ mol L}^{-1} \text{ (K)NO}_3$. In the present work, a constant ionic strength of $0.10 \text{ mol L}^{-1} \text{ K(Cl)}$ was used.

An obvious drawback of this approach is that the resulting (concentration) equilibrium constants are only valid in the ionic medium for which they were determined. For the application of such equilibrium data to other media, electrolyte theory must be applied to obtain the required data (*e.g.* standard-state data).

The speciation of metal ions in aqueous environments is often very complex. This makes complete characterisation of all species and the determination of their formation constants difficult. In the search for a thermodynamic model it is recommended that, whenever possible, the data be divided into sub-sets for the separate analysis of (i) ligand acid/base properties, (ii) metal ion hydrolysis, (iii) binary metal-ligand complexes and (iv) ternary complexes. All of these analyses are most easily performed using a non-linear least squares computer program. These programs enable the analyst to obtain immediate information regarding essential parameters such as 'goodness of fit'. They also provide outputs of residuals (*e.g.* $H_{\text{calc}} - H_{\text{exp}}$, where H is the total titratable acidity) which, like goodness of fit, reflect discrepancies between the experimental data and the model (essential for finding and eliminating systematic errors). In the present work the non-linear least squares computer program LAKE [Ingri *et al.*, 1996] was used for equilibrium analysis.

2.1.1 LIGAND PROTONATION EQUILIBRIA.— Most organic ligands can be treated as weak acids (H_nL). The titration of a weak acid with a strong base generates a series of species described by the two component equilibria (H^+ -Ligand):



where p can be a positive or negative integer (*i.e.* protonation or deprotonation respectively) and H_nL is the defined zero proton level for the ligand ($n = 0, 1, 2, \dots$).

A formation constant, $\beta_{p,q,r}$, is used to describe the equilibria in terms of the stoichiometry of each component p , q and r respectively. In the example described here, the formation constant may also be referred to as a protonation constant:

$$\beta_{p,0,I} = \frac{[H_{n+p}L^{p+}]}{[H_nL][H^+]^p} \quad (2.1.1b)$$

The law of mass action and the conditions for the concentrations applied to this reaction give equations (2.1.1c) and (2.1.1d), where h and c are the equilibrium concentrations of H^+ and H_nL respectively.

$$H = h + \sum p\beta_{p,0,I}h^p c - k_W h^{-1} \quad (2.1.1c)$$

$$C = c + \sum \beta_{p,0,I}h^p c \quad (2.1.1d)$$

In the potentiometric titration, the total concentration of protons (H) and ligand (C) are known from the initial concentration of titratable protons and the initial concentration of ligand, while h is measured potentiometrically as described in Chapter 3 (3.10-3.12). The experimentally determined quantities H and C are corrected for dilution.

The information from these equations is used to evaluate a function, Z_C , which will form a basis for the calculation of ligand protonation constants from the potentiometric titration data. Z_C is a function of $-\log h$ and describes the degree of protonation of a ligand:

$$Z_C[\text{exp}] = \frac{(H - h + k_W \cdot h^{-1})}{C} \quad (2.1.1e)$$

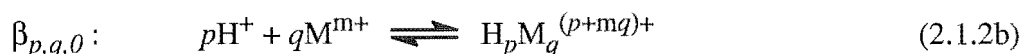
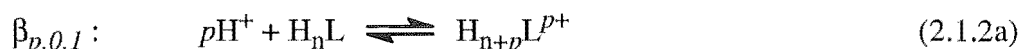
The function Z_C can be calculated from the experimentally determined values of H , C and h at each datum point in the titration. This value of Z_C is referred to as $Z_C[\text{exp}]$. The term k_W is the ionic product of water; $k_W = [H^+][OH^-]$.

Z_C can also be expressed as a function of the evaluated protonation constants of the ligand and of the equilibrium hydrogen ion concentration, h . This value is referred to as $Z_C[\text{calc}]$.

$$Z_C[\text{calc}] = \frac{\sum p\beta_{p,0,I}h^p}{1 + \sum \beta_{p,0,I}h^p} \quad (2.1.1f)$$

Hence, by assuming values for the $\beta_{p,0,1}$ of the ligand (defined by equation 2.1.1b), $Z_C[\text{calc}]$ can be determined at each datum point. By treating the β 's as variable parameters, the function $\Sigma(Z_C[\text{exp}]-Z_C[\text{calc}])^2$ may be minimised over all datum points by means of non-linear least squares analysis. In this way the formation constants may be determined (this procedure is discussed in more detail in Section 2.1.4).

2.1.2 METAL-LIGAND EQUILIBRIA.— The treatment of equilibrium data for a three-component system is approached in the same manner as the two component system. The system, $H^+-M^{m+}-H_nL$, can be described by equations of the general form:



where $\beta_{p,q,r}$, $\beta_{p,0,1}$ and $\beta_{p,q,0}$ are the formation constants for each reaction respectively, p can be a positive or negative integer (*i.e.* protonation or deprotonation respectively) and H_nL and M^{m+} define the zero proton level of these components (q , r and n are positive integers: 0,1,2, ...). Equation (2.1.2a) denotes ligand protonation, (2.1.2b) denotes hydrolysis of the metal ion and (2.1.2c) denotes the formation of three component complexes.

The law of mass action and the conditions for the total concentrations then give equations (2.1.2d-f), where $h = [H^+]$, $b = [M^{m+}]$ and $c = [H_nL]$ (free concentrations) and B is the total concentration of 'M'.

$$H = h + \sum p\beta_{p,0,1}h^p c + \sum p\beta_{p,q,0}h^p b^q + \sum p\beta_{p,q,r}h^p b^q c^r - k_W h^{-1} \quad (2.1.2d)$$

$$B = b + \sum q\beta_{p,q,0}h^p b^q + \sum q\beta_{p,q,r}h^p b^q c^r \quad (2.1.2e)$$

$$C = c + \sum \beta_{p,0,1}h^p c + \sum r\beta_{p,q,r}h^p b^q c^r \quad (2.1.2f)$$

The summations are taken over all species formed.

Correspondingly, the experimental data can be treated using these equations and an equilibrium model evaluated. However, the equilibria involved in metal-ligand complexation are often very complex and it may take many attempts to reach a final model. *i.e.* a large number of possible (p,q,r) -triplets exist (which define the stoichiometry

of the individual species) and many combinations of these may need to be tested before the best model is found. To aid in this process, several graphical procedures may be used. These are discussed in the next Section (2.1.3).

2.1.3 FORMATION CURVES.— The use of graphical methods to aid the analysis of experimental data is an important process in the evaluation of an equilibrium model. These methods allow the analyst to obtain general information on the behaviour of the system. The shape of different 'formation curves' may reveal information on a series of mononuclear complexes forming or the presence of polynuclear or ternary complexes. Alternatively, formation curves are useful for the identification of errors, *e.g.* random 'bad' points and systematic errors that need to be eliminated. Approximate values for relevant formation constants may be estimated which often aid in the computer refinement of larger models.

(A) **Z(-log *h*) Curves.**— Experimental data are possibly best visualised by the use of Z-curves. These curves are easily calculated and often form an integral part of model refinement. Z is defined as the average number of H⁺ (or OH⁻) bound per metal (B), Z_B, or ligand (C), Z_C, where Z_C is defined as:

$$Z_C[\text{exp}] = \frac{(H - h + k_w \cdot h^{-1})}{C} \quad (2.1.3a)$$

As discussed in Section 2.1.1, Z-curves can be calculated from the experimental data or, alternatively, evaluated from expressions involving the trial formation constants for the species forming over the relevant -log *h* range. A comparison between Z_C[exp]-curves in the absence and presence of the metal ion will reveal the -log *h* range for and the extent of complexation. Furthermore, significant contribution of mixed hydroxy metal-ligand species becomes evident if the value of Z_C exceeds *n* in H_{*n*}L.

(B) **\bar{n} (-log [L]) Curves.**— Often referred to as Bjerrum plots [Bjerrum, 1915], \bar{n} represents the average number of ligand molecules coordinated per metal ion. These curves reveal information on the extent to which a series of binary complexes, ML_{*n*}, may form. \bar{n} (-log [L^{*n*-}]) can be calculated from experimentally determined *H*, *B*, *C* and *h* data:

$$\bar{n}[\text{exp}] = \frac{\{C - (H - h + k_w \cdot h^{-1}) / Z_C[\text{calc}]\}}{B} \quad (2.1.3b)$$

where H is calculated from the zero proton level (H_2O , $\text{M}^{\text{m}+}$, $\text{L}^{\text{n}-}$) and $Z_{\text{C}}[\text{calc}]$ is defined as in Section 2.1.1.

Alternatively, \bar{n} may be expressed as a function of the trial formation constants for the metal and ligand species and of the equilibrium ligand concentration, $[\text{L}^{\text{n}-}]$:

$$\bar{n}[\text{calc}] = \frac{\beta_{0,1,1}[\text{L}^{\text{n}-}] + 2\beta_{0,1,2}[\text{L}^{\text{n}-}]^2 + 3\beta_{0,1,3}[\text{L}^{\text{n}-}]^3 + \dots}{1 + \beta_{0,1,1}[\text{L}^{\text{n}-}] + \beta_{0,1,2}[\text{L}^{\text{n}-}]^2 + \beta_{0,1,3}[\text{L}^{\text{n}-}]^3 + \dots} \quad (2.1.3\text{c})$$

Consequently, $\bar{n}[\text{exp}]$ can be determined for each datum point and a theoretical curve described by $\bar{n}[\text{calc}]$ can be calculated (much like comparing $Z_{\text{C}}[\text{exp}]$ and $Z_{\text{C}}[\text{calc}]$).

The formation of a series of mononuclear complexes, $\text{ML}_r^{(\text{m}-\text{n})+}$, is indicated over the $-\log h$ range for which the $\bar{n}[\text{exp}]$ data coincide with the $\bar{n}[\text{calc}]$ curve. This condition is independent of B/C ratios and concentrations. If the ligand forms only weak complexes with the metal, then hydrolysis of the metal may occur. The formation of hydroxy and/or polymeric species is indicated by deviations from the family of coincident plots. Therefore, such a series of mononuclear complexes is only commonly observed when the ligand forms quite stable complexes with the metal or large excesses of ligand have been used, or for metals less affected by hydrolysis.

2.1.4 EVALUATION OF THE EQUILIBRIUM MODEL.— The successful and scientifically convincing characterisation of an equilibrium system is determined by a number of prerequisites. The first of these is related to the collection of experimental data, both quality and information content; secondly we must consider the process of data evaluation.

(A) Data Collection.— (i) The experimental data upon which the analysis is based must be *true equilibrium data*. This necessitates that the reversibility of the system has been tested by performing both forward (increasing $-\log h$) and reverse (decreasing $-\log h$) titrations. (ii) For the analysis of a three component system, the underlying sub-systems, *e.g.* ligand protonation or metal ion hydrolysis, must be either well characterised or negligible. In some cases the careful selection of experimental conditions can aid in studies where, for example metal hydrolysis is not well understood. (iii) Equilibrium analysis is generally based on techniques that provide macroscopic measurements (sum of effects from all species present) to generate information on the equilibrium speciation. For this reason, data should be collected over as broad a range as possible with regard to total metal ion and ligand concentration, metal to ligand ratio and $-\log h$.

(B) Equilibrium Analysis.— Possibly the most important feature of any equilibrium analysis is that the presented model must give a good description of the experimental data. No systematic deviations should remain in the final model and the fit between experimental data and model curves should be within that expected for the technique used in the analysis.

Because of the complexity of many equilibrium systems often the best approach to equilibrium analysis is to evaluate the data in an unbiased manner, *i.e.* assume no knowledge of what species are likely to exist. In such a procedure, the analyst should investigate all possible combinations of (p,q,r) stoichiometries to establish the model which gives the best fit to the experimental data. In practise, this approach is often overlooked as the analyst is often familiar with a similar system which has been previously characterised. If this latter approach is used, the analyst must be careful to recognise any systematic deviations (whether small or large) and if present should return to the unbiased approach of data analysis.

Equilibrium models are usually developed for a specific purpose, *e.g.* modelling biofluids or natural waters. It is, therefore, of primary importance that the model should be valid for these conditions (*e.g.* pH range, ionic strength, temperature).

An Unbiased Search: The information obtained from the different types of formation curves can be used to outline a strategy for the processing of the available data. The purity of the ligand is often indicated by the shape of the Z_C curve (in the absence of metal). Estimates of acidic (or alkaline) impurities, often referred to as 'dirt', can be made and corrections for these introduced along with any adjustments to total ligand concentrations. Assuming an accurate knowledge of the ligand's acid/base properties, the analysis of three component data may be undertaken.

As mentioned in Section 2.1.3(B), coincident $\bar{n}(\log[L^n])$ curves indicates the presence of a series of $ML_r^{(m-n)+}$ complexes. The $-\log h$ range over which these complexes are observed to form may be used to evaluate approximate formation constants for this series of complexes. The next step (or steps) in the equilibrium analysis is the interpretation of the deviations from this 'mononuclear curve'. From this point forward, the \bar{n} -curve will not aid our search.

The search for a model explaining the data at $-\log h$ values beyond this series can be best performed by means of a procedure called a (p,q,r) -analysis. In this procedure it is assumed that within a certain data space region, only one new complex, $H_pM_qL_r$, is formed. Different p,q,r combinations are systematically tested (involving the refinement of the corresponding formation constant, $\beta_{p,q,r}$). The data region chosen should, at least partially, overlie the data space for which the model is already observed to 'fit', and all previously determined formation constants used to explain the data both within this range

and outside this range should be included but not altered. The 'best' species is the p,q,r combination that gives the lowest error squares sum $U = \Sigma(H_{\text{calc}} - H_{\text{exp}})^2$ or $U = \Sigma(Z_{\text{calc}} - Z_{\text{exp}})^2$. This p,q,r combination may represent a true stoichiometry of a species or it may also represent an average composition of two or more coexisting complexes. The species is, however, accepted into the model and the procedure is continued until the entire data range has been covered and adequately explained.

An important part of this unbiased approach is the careful examination of residuals ($\Delta H = H_{\text{calc}} - H_{\text{exp}}$) and Z-curves throughout the analysis and, in particular, when the final model has been reached. Any systematic deviations (as a function of $-\log h$, B , C or B/C) that are not within experimental uncertainties must be re-addressed. It is this process that is often the most time consuming and much time is often devoted to this repetitive but extremely necessary process.

The discussion of the above unbiased approach for the determination of a 'correct' equilibrium model is incomplete. Many variations to the methodology for reaching a final model are available to the analyst, *e.g.* division of data into smaller subsets defined by C/B ratios (and/or in combination with specified $-\log h$ intervals) followed by new (p,q,r) -analysis. The discussion does, however, provide the reader with some idea of the methodology behind this procedure. Sometimes the analyst can be 'lucky' and one species, past the initial ML_r series, is all that is required to explain the remaining data [Hedlund and Öhman, 1988; Marklund *et al.*, 1986]. In other cases, several p,q,r combinations may appear to give an equally good fit to the data; in such a situation it is not until the model is nearly complete before one of these combinations can be discarded. It is possible that initial attempts to model the data will reveal that further experiments are required to discriminate between two equally good models.

2.2 THERMODYNAMIC TREATMENT OF SURFACE COMPLEXATION

The use of potentiometric techniques to characterise the acid/base and complexing properties of hydrous oxide particle surfaces has become an active area of research during the last 20-25 years [Huang and Stumm, 1973; Hohl and Stumm, 1976; Davis, 1982; Sjöberg and Lövgren, 1993; Laiti *et al.*, 1995]. The thermodynamic equilibrium concepts that apply to solution coordination chemistry have been successfully applied to interactions at the particle/solution interface. A review of the literature, however, indicates the development of thermodynamic models that explain the physical and chemical nature of the mineral-water interface and the interaction of these interfaces with common ligands and metal ions is still quite limited.

2.2.1 CHEMICAL REACTIONS AT METAL OXIDE-WATER INTERFACES.—

The hydration of a metal oxide surface is depicted in Figure 2.2.1.

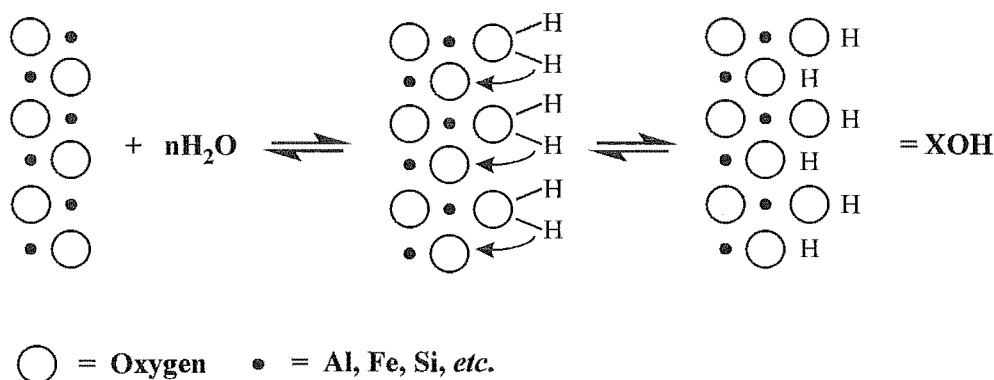


Figure 2.2.1 Hydration of a metal oxide surface [redrawn from Westall, 1986].

In this process, water groups adsorb to the oxide surface, hydrolysis occurs and surface hydroxyl groups are formed. This model assumes the formation of two distinct hydroxyl groups at the surface; differing in the plane of metal ions to which they are coordinated. In practise, however, edges of oxide surfaces and imperfections in faces (kinks or steps) will mean that many other coordination positions for hydroxyl groups will exist. For modelling purposes only the dominant surface hydroxyl groups depicted in Figure 2.2.1 will be considered.

The oxide surface hydration process can be interpreted in terms of a diprotic weak acid model [Davis *et al.*, 1978]. The model assumes an amphoteric character of the surface groups, $\equiv\text{XOH}$, and the formation of $\equiv\text{XOH}_2^+$ and $\equiv\text{XO}^-$ groups:



The law of mass action equations corresponding to these reactions are:

$$K_{a1}^s = \frac{[\equiv\text{XOH}][\text{H}^+]}{[\equiv\text{XOH}_2^+]} \cdot e^{+F\psi/RT} \quad (2.2.1c)$$

$$K_{a2}^s = \frac{[\equiv \text{XO}^-][\text{H}^+]}{[\equiv \text{XOH}]} \cdot e^{+F\psi/RT} \quad (2.2.1d)$$

where ψ (V) is the electrostatic potential, with respect to the bulk solution, at the mean plane of adsorption (used to correct for the coulombic energy changes of the surface). F is the Faraday constant (C mol^{-1}) and R is the gas constant ($\text{J K}^{-1} \text{mol}^{-1}$). The exponential term represents the electrostatic energy required to bring a charged species from the bulk solution to the plane of adsorption which has potential ψ . Material and charge balances can be derived for these expressions and the constants K_{a1}^s and K_{a2}^s evaluated. The evaluation procedure is, however, dependent on the assumptions regarding the complexation model used. The most common surface complexation models are discussed in Section 2.2.2.

The hydrous oxide surface (Figure 2.2.1) represents an array of complex forming donor groups which may coordinate metal ions, organic ligands or metal complexes from the bulk solution [Davis and Leckie, 1978; Kummert and Stumm, 1980; Davis and Leckie, 1980; McBride, 1982; Davis, 1984]. The metal ion at the oxide surface may be treated as a Lewis acid and the OH group may be replaced by coordinating ligands. The treatment of these surface complexes is addressed in Section 2.2.3 (constant capacitance model).

2.2.2 CHEMICAL MODELLING OF SURFACE COMPLEXATION.— Several surface complexation models have been developed for the description of adsorption/desorption reactions at the mineral-water interface. These models are based on several fundamental concepts and differ primarily in the description of the electric double layer. In the current models, this description is based on the work of Stern (1924), who used a series of layered planes, onto which species could be adsorbed by chemical or electrostatic interactions, to describe the interface.

Fundamental concepts:

- (a) The formation of surface complexes at the mineral-water interface occurs in a manner analogous to simple metal-ligand complexation reactions in solution.
- (b) Surface complexation equilibria can be quantitatively described by law of mass action equations.
- (c) A surface charge is created from the surface complexation reactions.
- (d) Charge dependent formation constants are required to account for the effect of surface charge on surface complexation.

(A) The Triple Layer Model.— The triple layer model, as depicted in Figure 2.2.2A, represents an extended version of the Stern model [Yates *et al.*, 1974]. The ions most strongly associated with the surface (*e.g.* H^+ and OH^- , inner sphere complexes of strongly bound metals and ligands) are assigned to the innermost plane where they contribute to a charge σ_0 and experience a potential ψ_0 . Less strongly bound ions (*e.g.* electrolyte ions K^+ , Na^+ , Cl^- , NO_3^- , SO_4^{2-} and organic anions), attracted to the surface by specific chemical and/or electrostatic interactions, are adsorbed at the inner Helmholtz plane (IHP) as outer sphere complexes. The charge in this plane is σ_1 and the ions experience a potential ψ_1 . Beyond the IHP is a layer of charge bound at the surface by electrostatic forces only. This layer is known as the diffuse layer, or the Gouy-Chapman layer. The innermost part of the diffuse layer is termed the outer Helmholtz plane (OHP). The charge-potential (σ_2 , ψ_2) relationships in the diffuse layer can be found by solving the Poisson-Boltzmann equation:

$$\sigma_2 = -(8\epsilon\epsilon_0RTc_b)^{1/2} \sinh \frac{F\psi_2}{2RT} \quad (2.2.2a)$$

where ϵ is the dielectric constant of water, ϵ_0 the permittivity of vacuum, R the molar gas constant, T the absolute temperature and c_b the electrolyte concentration in the bulk solution. The triple layer model can be regarded as composed of two constant capacitance layers (known as the compact layer with capacitances C_1 and C_2) and one diffuse layer. The total capacitance of the interface is given by the equation for three capacitances in series:

$$\frac{1}{C_{\text{total}}} = \frac{1}{C_{\text{compact}}} + \frac{1}{C_{\text{diffuse}}}$$

(B) The Constant Capacitance Model.— At high ionic strengths and high potentials, the diffuse layer capacitance (of the triple layer model) is much larger than the compact layer capacitance ($C_1 + C_2$). In such a case the total capacitance becomes approximately equal to the compact layer capacitance. The electrostatic model for this limiting case is known as the constant capacitance model (Figure 2.2.2B).

In the constant capacitance model all specifically adsorbed solutes are adsorbed in the same plane at the surface. Outer sphere complexation of weakly adsorbed electrolyte ions is not explicitly considered. The effects from these ions is included in the evaluated constants (which are regarded as conditional constants). The surface charge (σ_0) is neutralised by a plane of electrostatically attracted counter ions and a constant capacitance (c) is used to relate σ_0 to the surface potential (ψ_0):

$$\sigma_0 = c \cdot \Psi_0 \quad (2.2.2b)$$

No ionic strength dependence is included in the model, thus the capacitance and equilibrium constants determined are valid only for solutions of the same ionic composition.

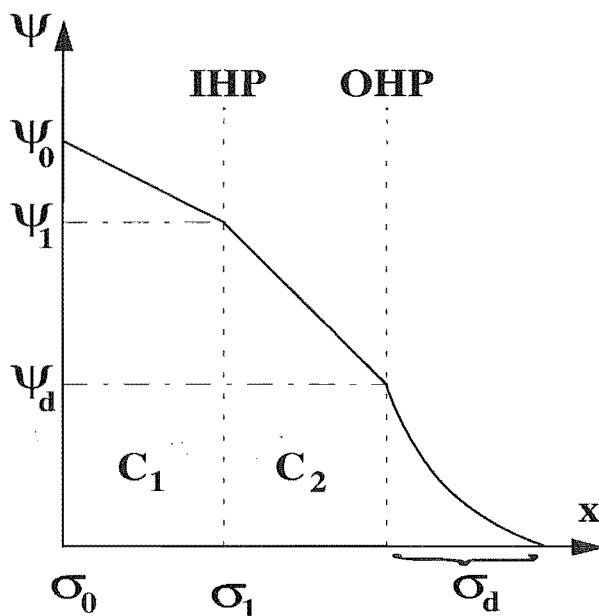


Figure 2.2.2A The Triple Layer Model

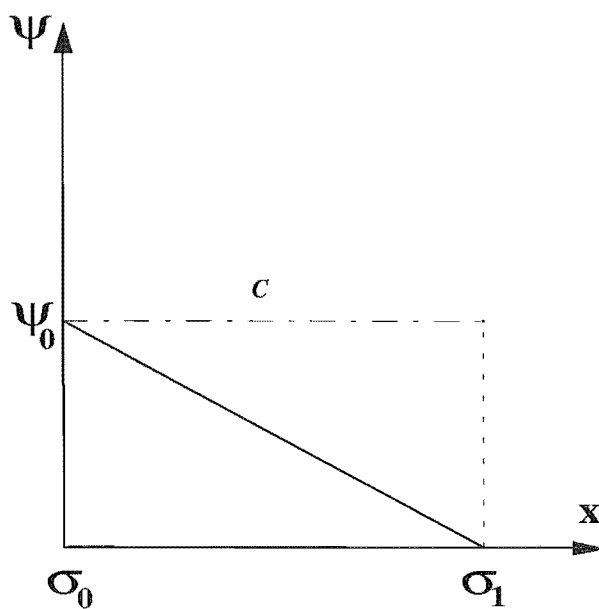


Figure 2.2.2B The Constant Capacitance Model

(C) **The Diffuse Layer Model.**— The second limiting case for the triple layer model is for solutions of low ionic strength and relatively low potentials. In this situation the diffuse layer capacitance (of the triple layer model) is much less than the compact layer capacitance and the total capacitance becomes approximately equal to the diffuse layer capacitance. This electrostatic model is known as the diffuse layer model (Figure 2.2.2C).

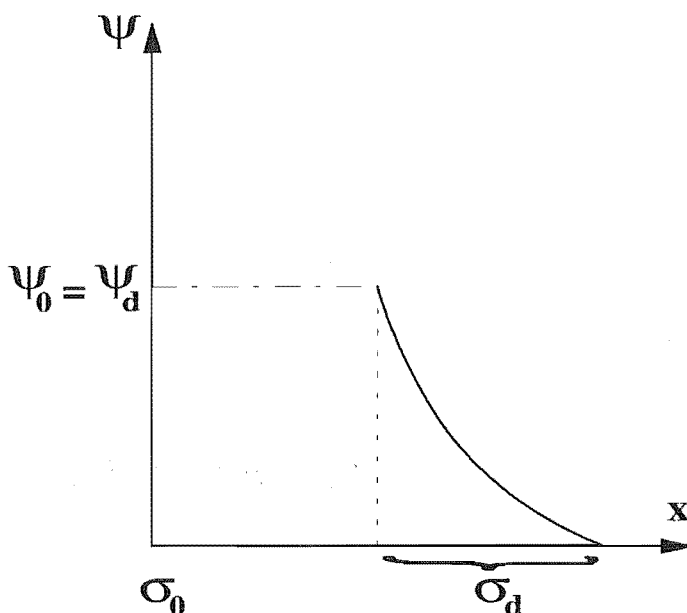


Figure 2.2.2C The Diffuse Layer Model

Like the constant capacitance model, only one plane of specifically adsorbed solutes is considered and outer sphere complexation of weakly adsorbed electrolyte ions is not explicitly considered. The electrostatically attracted counter ions are distributed throughout the diffuse layer and the surface charge-potential relationship is given by equation 2.2.2a (see triple layer model). Replacing c_b (bulk electrolyte concentration) with I (ionic strength) in this equation implies that this model is applicable for variable ionic strengths [Stone *et al.*, 1993].

Detailed discussions of the models described above have been the subject of several good reviews [Westall and Hohl, 1980; Westall, 1986; Davis and Kent, 1990; Schindler, 1990].

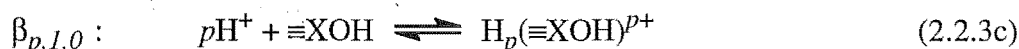
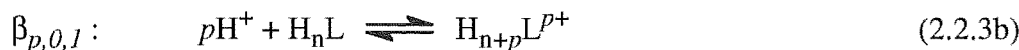
2.2.3 THE CONSTANT CAPACITANCE MODEL.— In the present studies the constant capacitance model was used for the evaluation of surface complexation equilibria. This model has been found to be quite adequate for describing ligand adsorption processes at the oxide mineral-water interface [Lövgren, 1991; Nilsson *et al.*, 1992; Laiti *et al.*, 1995] and the need for more complex models (*e.g.* triple layer model) has not been

required. The data treatment procedure for this model is discussed below. A ligand, H_nL , is used to illustrate the numeric analysis, however, the procedure is also applicable to adsorption of metal ions [Lövgren *et al.*, 1990].

Data Treatment.— The equilibria involving H^+ , $\equiv XOH$ and H_nL , can be expressed by the general equation:



The equilibria in the two 2-component systems, $H^+-(\equiv AlOH)$ and H^+-H_nL , can be expressed using the simplified equations (2.2.3b) and (2.2.3c) respectively:



It should be noted that $\beta_{p,q,r}$ and $\beta_{p,1,0}$ are conditional constants and thus must be corrected for the coulombic energy of the charged surface to obtain the corresponding intrinsic constants:

$$\beta_{p,q,r(int)} = \beta_{p,q,r} \cdot e^{zF\psi/RT} \quad (2.2.3d)$$

where z is the species charge and ψ is the potential at the oxide surface.

The law of mass action and the conditions for the total concentrations of H^+ (H), $\equiv XOH$ (B) and H_nL (C) give equations (2.2.3e-f), where h , b and c represent the free concentrations (mol dm^{-3}) of each component respectively.

$$H = h - K_W h^{-1} + \sum p \beta_{p,q,0(int)} \cdot e^{-(pF\psi/RT)} h^p b^q + \sum p \beta_{p,0,r} h^p c^r + \sum p \beta_{p,q,r(int)} \cdot e^{-(pF\psi/RT)} h^p b^q c^r \quad (2.2.3e)$$

$$B = b + \sum q \beta_{p,q,0(int)} \cdot e^{-(pF\psi/RT)} h^p b^q + \sum q \beta_{p,q,r(int)} \cdot e^{-(pF\psi/RT)} h^p b^q c^r \quad (2.2.3f)$$

$$C = c + \sum r \beta_{p,0,r} h^p c^r + \sum r \beta_{p,q,r(int)} \cdot e^{-(pF\psi/RT)} h^p b^q c^r \quad (2.2.3g)$$

The surface charge (in mol dm⁻³) is obtained from:

$$T_{\sigma} = \sum p\beta_{p,q,0(int)} e^{-(pF\psi/RT)} h^p b^q + \sum p\beta_{p,q,r(int)} e^{-(pF\psi/RT)} h^p b^q c^r \quad (2.2.3h)$$

or, in electrostatic units (C m⁻²):

$$\sigma = \frac{T_{\sigma} \cdot F}{s \cdot a} \quad (2.2.3i)$$

where F is the Faraday constant, s is the specific surface area (m⁻² g⁻¹) and a is the concentration of solid in g dm⁻³. Within the scope of the constant capacitance model, the surface potential, ψ , is related to the surface charge, σ , by the expression:

$$\sigma = c \cdot \Psi \quad (2.2.3j)$$

where c is the specific capacitance (C V⁻¹ m⁻²). Combining the last two equations gives:

$$\Psi = \frac{T_{\sigma} \cdot F}{s \cdot a \cdot c} \quad (2.2.3k)$$

In the calculations the least-squares computer program LAKE [Ingri *et al.*, 1996] was used in combination with the modelling program SOLGASWATER [Eriksson, 1979] modified to treat surface complexation according to the constant capacitance model. These calculations involved evaluating the mass balance equations (2.2.3e-f); the procedure or methodology employed was discussed in Section 2.1.3-2.1.4.

SECTION B: THE MEASUREMENT OF pH

2.3 pH

The concept of pH is unique amongst physicochemical quantities, in that $(-\log a_{\text{H}})$ involves a single ion activity coefficient which is immeasurable (Covington *et al.*, 1983). It is therefore defined operationally in terms of the method used to measure it.

The accurate measurement of pH is essential for the determination of thermodynamic equilibrium data *via* potentiometry. To this extent, very rigorous conditions are required defining 'pH' and attainment of thermodynamic equilibrium. The temperature dependence for the glass electrode is usually of the order of 1 mV deg^{-1} [Covington, 1969]. Therefore, it is essential that experiments are thermostated within $\pm 0.05 \text{ }^{\circ}\text{C}$ of the desired temperature.

In the present work, pH-drift conditions were managed by the computer which also controlled the autoburette. A 'delay time' was set for (i) the time period between acid/alkali addition and the first pH measurement and (ii) the period between successive pH measurements. The equilibrium condition was satisfied when a series of consecutive pH measurements agreed within a specified 'drift condition'. If the electrode drift condition was not satisfied (*i.e.* the drift limit exceeded) the data point was flagged and another delay period-(ii) initiated. After each pH measurement the drift condition was checked and the next burette addition was not made until the condition was obeyed. The adopted delay periods '(i)' and '(ii)' and the 'drift condition' are dependent on the system being studied and are given in the relevant Chapters (4 & 5).

2.3.1 pH MEASUREMENT.— The arrangement of the measuring cell can be divided into three parts: (i) the measuring electrode, (ii) the reference electrode and (iii) the liquid junction between the measuring compartment and the reference compartment. The hydrogen electrode is probably the best primary standard for measurement of pH, however, the development of reliable, easy to handle and fast responding glass electrodes has drastically reduced their use [Covington and Prue, 1955; Henry *et al.*, 1971].

The potential of single electrodes cannot be measured directly; it is therefore the potential difference (or electromotive force, e.m.f) between the glass electrode and the reference electrode that is determined. The quality of the reference electrode is therefore also of utmost importance. In potentiometry, two reference electrodes have been commonly employed for pH measurements: (i) the calomel (mercury-mercurous chloride) reference electrode or (ii) the silver-silver chloride (Ag/AgCl) reference electrode. The liquid junction of the calomel electrode consists of a semi-permeable diaphragm and the electrode compartment contains a concentrated salt solution (usually saturated KCl). The internal salt solution slowly permeates across the junction and means that liquid junction

potentials can be ignored. The most common approach for interconnecting the Ag/AgCl electrode with the glass electrode is *via* the use of a salt bridge. The alternative approach, in which both electrodes are immersed in the same solution, results in unstable potentials at the Ag/AgCl electrode. For the salt bridge arrangement, a liquid junction potential is created where the two solutions of different composition meet.

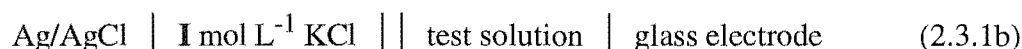
Despite the presence of the liquid junction potential, the Ag/AgCl electrode is probably the best reference electrode for pH measurements in solution equilibria studies. The calomel electrode releases small quantities of concentrated KCl into the test electrolyte solution and often results in significant changes in ionic strength over the duration of long titrations (>20 h). Furthermore, it is slow to reach temperature equilibrium and electrode potentials may vary with time (rarely reproducible to better than 3-4 mV) [Covington *et al.*, 1967].

At the liquid junction of the Ag/AgCl electrode, diffusion of ions will occur and create a liquid junction potential (E_j). The e.m.f of this cell can be written as:

$$E = E_+ - E_- + E_j \quad (2.3.1a)$$

where E_j is the potential caused by diffusion of ions across the liquid junction (E_+ and E_- are the potentials for the respective half-cells). In this cell, the construction of the liquid junction is very important and the design must be such that predictable and reproducible potentials are obtained. The half-cell design commonly called the 'Wilhelm' type [Forsling *et al.*, 1952] has been found to be ideal for these purposes. The liquid junction potentials of this half-cell have been found to be in fair agreement with the values predicted by the simple Henderson equation [Hefter, 1982]. Accurate expressions for the ionic medium dependence of this cell arrangement have been experimentally determined [Biedermann and Sillén, 1952; Sjöberg *et al.*, 1983].

The expression for the complete cell arrangement is:



where I denotes the concentration of the background electrolyte.

Assuming the activity coefficients to be constant, at 25 °C, the e.m.f of this cell (in mV) is given by:

$$E = E^\circ + 59.157 \cdot \log h + E_j \quad (2.3.1c)$$

where E° is the apparatus constant determined prior to each titration (see Chapter 3, 3.11.3) and the liquid junction potential, E_j , is calculated from:

$$E_j \text{ (mV)} = -49.7I^{-1} \cdot h + 21.4I^{-1} \cdot k_W \cdot h^{-1} \quad (2.3.1d)$$

where k_W is the ionic product of water and,

$$\log k_W = -14.013 + 1.022I^{1/2}/(1+I^{1/2}) - 0.22I \quad (2.3.1e)$$

In the present work a 0.10 M K(Cl) medium was used: $\log k_W = -13.775$ is the ionic product of water and $j_{ac} = -511.5 \text{ mV L mol}^{-1}$ and $j_{alk} = 238.7 \text{ mV L mol}^{-1}$ are assumed liquid junction parameters [Sjöberg *et al.*, 1983]. Refer to Chapter 3 [3.11.3(B), p71] for definitions of j_{ac} and j_{alk} respectively.

CHAPTER 3

EXPERIMENTAL METHODS

This chapter describes the experimental procedures and apparatus used throughout this thesis. It is divided into 2 parts.

SECTION A: A description of the analytical procedures for reagent and solution preparation and non-potentiometric apparatus is given.

SECTION B: The apparatus used for the potentiometric studies and the calibration procedures for the glass electrode are described .

SECTION A: EXPERIMENTAL PROCEDURES AND APPARATUS

3.1 VOLUMETRIC EQUIPMENT

All glassware was 'B' grade. Pipettes were calibrated by dispensing and weighing volumes of distilled water at constant temperature. Water density data (CRC Handbook of Chemistry and Physics) were used to convert the weight of water dispensed to volume at 25 °C. Titration burettes (ABU80 autoburette and 645, 655 Multi-Dosimats, Metrohm) were calibrated as above.

Volumetric glass and plasticware (for preparation and storage of solutions) was cleaned by soaking in *ca.* 10 % HNO₃ (BDH, AnalaR) for at least 24 h or in a solution *ca.* 90 % H₂SO₄, *ca.* 0.05 mol L⁻¹ Cr₂O₇²⁻ followed by 12 h soaking and repeat rinsing with triply distilled water (TDW). Other glassware and clean volumetric glassware was washed with detergents [Decon 90; Johnson Professional, Handdisk (pH = 6.5) and Merck, Extran (pH = 2.5 and 11.5)], rinsed thoroughly with TDW and stored after drying procedures (vacuum drying).

3.2 REAGENTS AND SOLUTION PREPARATION

Solutions were prepared in Milli-Q deionised water (resistance 18 MΩ) or freshly boiled distilled water (carbonate free). Unless otherwise specified, all working solutions (prepared from the respective standards) contained the appropriate amount of KCl to give a total ionic strength of 0.100 mol L⁻¹ K(Cl). Glass or teflon spatulas were used to dispense all solid samples. All solids were dried prior to use and stored in glass desiccators over CaCl₂ or silica gel. Light and temperature sensitive materials were stored under refrigeration (6 °C). Solutions sensitive to light were stored in clear glassware wrapped with aluminium foil. All titration solutions were stored at 25 °C.

3.2.1 STANDARD ALKALI SOLUTIONS (KOH).— Standard KOH solutions were prepared in the concentration ranges $0.1\text{--}0.3\text{ mol L}^{-1}$ and $0.01\text{--}0.04\text{ mol L}^{-1}$ respectively. Separate procedures, differing in strategy for the exclusion of carbonate contamination, were used in the preparation of these solutions. These procedures are outlined below and both appeared effective.

(A) **Procedure 1.**— Carbon dioxide-free water was prepared by boiling Milli-Q water for *ca.* 30 min and cooling in an ice bath under a stream of oxygen-free nitrogen. Using this water, KOH pellets (BDH, AnalaR) were rinsed rapidly to remove possible carbonate coatings (washings discarded), dissolved and made up to the appropriate volume. This solution was protected from intrusion of atmospheric CO_2 using a rubber stopper. The solution was then standardised by titration against weighed amounts of Tris HCl (Koch-light, puriss). KOH solutions were restandardised after 4 weeks and were used for a maximum of six weeks (no change in concentration was ever observed).

(B) **Procedure 2.**— Carbon dioxide-free water was prepared by boiling distilled water for *ca.* 30 min and cooling under a stream of oxygen-free argon. A saturated solution of KOH *ca.* $16\text{--}17\text{ mol L}^{-1}$ (Eka Nobel, Purissimum Pro Analyti) was prepared from CO_2 -free water following washing procedures described above. A quantity of this solution, *ca.* 30 mL, was passed through a porosity 4 sintered glass filter rapidly to remove $\text{K}_2\text{CO}_{3(s)}$ (which precipitates under saturated conditions) and *ca.* 10 mL of the filtrate was injected *via* a strong glass syringe into *ca.* 500 mL of freshly prepared carbon dioxide-free water under a flow of $\text{Ar}_{(g)}$ and sealed immediately. This solution was standardised the following day by titration against standard HCl solution [Bromocresol Green/Methyl Orange (3:1) indicator, BGMO]. From this standard alkali stock solution working alkali solutions were prepared accordingly with $I = 0.10\text{ mol L}^{-1}$ K(Cl) and sealed in Multi-Dosimat burettes (with a soda lime $\text{CO}_{2(g)}$ -trap inserted). These solutions were again standardised against standard HCl of an appropriate concentration *via* potentiometric titration.

3.2.2 STANDARD ACID SOLUTIONS (HCl).— Standard HCl solutions were prepared by dilution of concentrated HCl (BDH, AnalaR or Merck, Pro Analyti) with freshly boiled Milli-Q water. HCl standards with concentrations greater than 0.1 mol L^{-1} were standardised by titration (BGMO indicator) against weighed amounts of Tris [Fluka, Puriss Pro Analyti or Sigma (Trizma Base), reagent grade]. HCl standards with concentrations less than 0.1 mol L^{-1} were standardised by potentiometric titration (Gran potentiometry [Gran, 1952]) against standard alkali or coulometrically generated hydroxide.

3.2.3 ELECTROLYTE SOLUTIONS (KCl).— KCl (BDH, AnalaR or Merck, Pro Analysi) was dried at 120 °C for 12 h then stored in a desiccator over anhydrous CaCl_2 or silica gel. All electrolyte solutions were prepared by dissolving the appropriate weight of dry KCl. NaCl (BDH, AnalaR) electrolyte solutions were prepared similarly.

3.2.4 BUFFERS

(A) Electrode Calibration Buffers.— Three primary reference NBS standard buffers [Durst *et al.*, 1987] were used to calibrate the pH meter before electrochemical and spectrophotometric studies. All solids were BDH (AnalaR).

Phthalate Buffer: (pH = 4.006): 10.12 g of potassium hydrogen phthalate ($\text{KOOC.C}_6\text{H}_4\text{.COOH}$), dried at 110 °C, was dissolved in 1 L of triply distilled water.

Phosphate Buffer: (pH = 6.863): 3.388 g of potassium di-hydrogen phosphate (KH_2PO_4) and 3.533 g of di-sodium hydrogen orthophosphate (Na_2HPO_4), both dried at 40 °C, were dissolved in 1 L of triply distilled water.

Borax Buffer: (pH = 9.183): 3.80 g of di-sodium tetraborate decahydrate ($\text{Na}_2\text{B}_4\text{O}_7 \cdot 10\text{H}_2\text{O}$), not dried, was dissolved in 1 L of triply distilled water.

(B) Electrochemical and Spectrophotometric Buffers.— MES [2-(N-morpholino)ethanesulfonic acid] (Calbiochem), acetate (BDH, AnalaR) and ammonium acetate [ammonia/acetic acid] (BDH, AnalaR) were used as buffers for both preliminary electrochemical investigations and in electrochemical or spectrophotometric FIA studies. These materials were used as supplied without further drying or purification.

3.2.5 METAL ION SOLUTIONS

(A) Aluminium(III) Solutions.— Al(III) solutions were prepared by dissolving $\text{AlCl}_3 \cdot 6\text{H}_2\text{O}$ [ALFA (99.9995 %), or Baker Analysed, Reagent] in *ca.* 0.1 mol L⁻¹ HCl. The Al content of the 'ALFA' solution was determined by gravimetric analysis (in triplicate) of Al as the 8-hydroxyquinolate complex [Bassett *et al.*, 1978]. In the 'Baker' solution [0.10 mol L⁻¹ Al, 0.10 mol L⁻¹ HCl], the Al content was determined by back titration of excess EDTA with $\text{Pb}(\text{NO}_3)_2$ using xylenol orange indicator/hexamine [Bassett *et al.*, 1978]. $\text{Pb}(\text{NO}_3)_2$ was dried at 120 °C prior to the preparation of a 0.05 mol L⁻¹ primary standard solution. EDTA was dried at 80 °C prior to use. A 0.1 mol L⁻¹ EDTA solution was prepared from this material and standardised by titration against $\text{Pb}(\text{NO}_3)_2$, xylenol orange indicator/ HNO_3 /hexamine. Working solutions were prepared by dilution of Al stock solutions.

(B) Copper(II) Solutions.— A previously prepared Cu(II) stock solution [Town, 1991] *ca.* 0.1 mol L^{-1} was used to prepare all working stock solutions (*ca.* 2 mmol L^{-1}). This stock was prepared by dissolving $\text{Cu}(\text{NO}_3)_2 \cdot 3\text{H}_2\text{O}$ (BDH, AnalaR) in 1 mmol L^{-1} HCl and its concentration standardised gravimetrically as the benzoïn- α -oxinate and electrolytically by deposition on a platinum cathode [Bassett *et al.*, 1978].

(C) Iron(III) Solutions.— An Iron(III) stock solution was prepared by dissolving $\text{NH}_4\text{Fe}(\text{SO}_4)_2 \cdot 12\text{H}_2\text{O}$ (BDH, AnalaR) in 0.1 mol L^{-1} HCl (BDH, AnalaR) and Milli-Q water. This solution was not standardised.

3.2.6 LIGAND SOLUTIONS.— Ligand solutions were prepared in Milli-Q or triply distilled water containing the appropriate amount of KCl to give a total ionic strength of 0.10 mol L^{-1} KCl. Standard solutions were wrapped with aluminium foil and stored at 25°C . Ligand solutions for potentiometric work were standardised by potentiometric titration with standard KOH (Gran potentiometry, [Gran, 1952]) and were only used if the difference between the weighed and determined concentration was less than 2 %. Ligand solutions for electrochemical work were used without further purification (unless otherwise stated) and stored in the dark at 6°C .

(A) Pyrocatechol Violet (PCV).— Reagent grade PCV {pyrocatechol sulfonphthalein, 2-[(3,4-dihydroxyphenyl)(3-hydroxy-4-oxo-cyclohexa-2,5-dien-1-ylidene)methyl]benzenesulfonic acid, 3,3',4'-trihydroxy-fuchsone-2''-sulfonic acid} materials were obtained from the chemical companies: Koch-Light (now NBS Biologicals), Merck, Sigma and Aldrich. Following drying (under vacuum) at 105°C Koch-Light and Merck PCV were found to be the highest purity by visible absorption spectrophotometry (700-300 nm, $\lambda_{\text{max}} = 442 \text{ nm}$). Koch-Light, Merck and Sigma materials were used in experiments (see Chapters 4-8). PCV materials were dried to constant weight at 105°C under vacuum for 48 h to remove occluded acidic impurities (volatile) prior to solution preparation. Attempts at recrystallisation were unsuccessful. PCV solutions were membrane filtered ($-0.025 \mu\text{m}$). However, small residues of foreign acidic substances remained.

(B) 4-Nitrocatechol.— 4-nitrocatechol (Sigma) was used without further purification. Stock 4-nitrocatechol solutions were prepared in 0.02 mol L^{-1} HCl to prevent ligand oxidation and minimise biological activity.

(C) Chrome Azurol S (CAS).— Reagent grade CAS (3''-sulfo-2'',6''-dichloro-3,3'-dimethyl-4-hydroxyfuchson-5,5'-dicarboxylic acid) was obtained from Aldrich and used as supplied. The dye content of this sample was 61.5 %, as estimated by comparison with a recrystallised sample [Hawke *et al.*, 1995].

(D) **Rhodizonic Acid and Tetrahydroxy-1,4-quinone.**— Rhodizonic acid (1,2-dihydroxytetraquinone) was obtained from Sigma and used without further purification. Solutions were prepared daily under a nitrogen atmosphere to minimise possible oxidation and stored at 4 °C after use. The solid material was stored below 0 °C.

Tetrahydroxy-1,4-quinone (tetrahydroxy-1,4-benzoquinone) from Sigma was prepared in 0.01 mol L⁻¹ HCl.

(E) **Citric, Malonic, Oxalic and Salicylic Acids.**— Citric acid (BDH, AnalaR); malonic acid (Riedel-de Haën, AG); oxalic acid (Fisons, AR); salicylic acid (BDH, AnalaR). Solutions (5.0 mmol L⁻¹) were prepared by dissolving required weights of each ligand (after drying but without further purification) in Milli-Q water (0.001 mol L⁻¹ HCl).

(F) **Fluoride.**— NaF (BDH, AnalaR) was used without further purification. A 5.0 mmol L⁻¹ stock solution was prepared and stored in a plastic bottle.

(G) **Other Ligands.**— A variety of ligands were investigated for electrochemical response in the absence and presence of Al(III) or Cu(II). These ligands were used as supplied: Purpurin [1,2,4-trihydroxyanthraquinone] (Sigma), purpurogallin [2,3,4,6-tetrahydroxy-5H-benzo-cyclohepten-5-one] (Sigma), PAR [4-(2-pyridylazo)resorcinol] (Sigma), TAN [1,2-(thiazolyazo)-2-naphthol] (Sigma) and Tartrazine [3-carboxy-5-hydroxy-1-*p*-sulfophenyl-4-[(*p*-sulfophenyl)azo]pyrazole trisodium salt] (BDH). Samples of the pyridinones; Hmpp [3-hydroxy-2-methyl-4(1H)-pyridinone] and Hdpp [3-hydroxy-1,2-dimethyl-4-pyridinone] were obtained from Prof. C. Orvig (UBC, Canada) *via* Prof. S. Sjöberg (Umeå, Sweden).

3.2.7 MICROANALYSIS.— Elemental analysis of samples (C, H and N) was performed at the University of Otago (New Zealand).

3.2.8 OXINE RESIN.— 8-hydroxyquinoline (oxine) derivatised Fractogel resin was prepared using the method described by Landing *et al.* (1986). Two preparations were made using Fractogel TSK Toyopearl HW-65F (30-60 µm) and HW-40C (50-100 µm).

(A) **Reagents.**— Oxine (BDH, reagent grade), *p*-nitrobenzoyl chloride (Merck, CP), Et₃N (BDH, GPR), Na₂S₂O₄ (BDH, GPR), NaNO₂ (H&W, AnalaR), CH₂Cl₂ (Merck, spectroscopic). Ethanol, acetone, acetic acid, NaOH and HCl were all BDH, AnalaR. H₂O was triply distilled water.

(B) Brief Method

(i) **Resin Preparation:** 6 g of Fractogel resin slurry was rinsed 3 times with 100 mL of water to rinse away the NaN₃ preservative present. The resin was filtered through glass

filters [Whatman GF/D (4.25 cm)] and rinsed with (i) 2 times 50 mL 1.0 mol L⁻¹ NaOH, (ii) 3 times 50 mL H₂O, (iii) 2 times 50 mL 1.0 mol L⁻¹ HCl, (iv) 3 times 50 mL H₂O, (v) 2 times 50 mL ethanol, (vi) 2 times 50 mL acetone, (vii) 2 times 50 mL CH₂Cl₂ and allowed to air dry (1.0 g).

(ii) Immobilisation Procedure: The rinsed and dried resin was placed in 20 mL CH₂Cl₂, 1.05 mL Et₃N and 0.425 g *p*-nitrobenzoyl chloride and stirred for 12 h at 40 °C. The product was filtered, rinsed with 2 times 100 mL CH₂Cl₂ and allowed to air dry. Reduction of the nitro group was accomplished in 3 h at room temperature (16-20 °C) in a solution containing 1 g Na₂S₂O₄ / 21 mL H₂O. The product was filtered and rinsed with H₂O. Diazotisation of this material was achieved in 45 min at 0 °C in a 20 mL solution of 1 g NaNO₂ in 0.2 mol L⁻¹ acetic acid. The yellow product was filtered and rinsed with ice-cold H₂O. This product was added to 0.2 g oxine in 10 mL of 95 % ethanol for 45 min (0 °C) resulting in the formation of the red/orange oxine-derivatised gel.

(iii) Cleaning and Storage: The final product was filtered and rinsed with (i) 3 times 50 mL H₂O, (ii) 2 times 50 mL 0.5 mol L⁻¹ NaOH, (iii) 3 times 50 mL H₂O, (iv) 2 times 50 mL 1.0 mol L⁻¹ HCl, (v) 3 times 50 mL H₂O. The derivatised gel was stored in H₂O.

3.2.9 BOEHMITE SUSPENSIONS.— The boehmite used in the present study was finely powdered high purity, α-Al₂O₃ monohydrate, DISPERAL[®] product manufactured by Condea Chemie. The surface area was 180 m² g⁻¹ according to the BET method. Alumina stock suspensions, 20.00 g of boehmite L⁻¹ [0.10 mol L⁻¹ K(Cl)], were prepared at least two weeks prior to use. The total surface hydroxyl group concentration for such a suspension had been determined previously as 10.2 mmol L⁻¹ [Laiti *et al.*, unpub.].

3.3 FILTRATION AND CENTRIFUGATION

3.3.1 FILTRATION.— Coloured ligands (PCV, CAS), humic waters and soil solutions required filtration before use or storage. These solutions were filtered consecutively through 0.45 μm and 0.025 μm membrane filters (Schleicher & Schuell). A Sartorius SM 16510 filtration unit (capacity, 250 mL) was used for larger volumes (47 mm diameter filter); suction was applied *via* a water pump to effect filtration. For smaller sample volumes, a disposable syringe was used in conjunction with a hand held unit (Millipore, Swinex-2) to effect filtration through 25 mm filters. All filtration apparatus was free of metallic parts and was cleaned thoroughly (acid washed) before use.

3.3.2 CENTRIFUGATION

(A) Boehmite Work.— Beckman polypropylene (AY, 2.3x10 cm) centrifuge tubes (*ca.* 40 mL) were used for the containment of samples. Oxygen exclusion was achieved using argon gas. A Beckman J2-21 centrifuge using a JA-20 rotor and running at a speed of

16500 rpm (32900 g) for 30 min was used for centrifuging. The centrifuge was thermostated at 25 °C.

(B) Soil Solutions.— Becton Dickinson Labware polypropylene (FALCON[®] 2070, 2.5x10 cm) centrifuge tubes (50 mL) were used to accommodate the Teflon soil solution extraction tube (2x9 cm, with a 1 mm hole at bottom). A BTL bench centrifuge running at a speed of *ca.* 3500 rpm for 20 min at room temperature was used.

Extraction Protocol

(i) A circle of filter paper (Whatman 540, *ca.* 1.8 cm diameter) was cut and placed in the bottom of the soil solution extraction tube.

(ii) The soil solution extraction tube was firmly packed with soil (discarding roots, other pieces of vegetation and stones).

(iii) The filled soil solution extraction tube was placed in a centrifuge tube and capped.

(iv) Three tubes of equal weight (± 0.5 g) were centrifuged at *ca.* 3000 rpm for 20 min (room temperature).

(v) The soil solution extracted from each tube (*ca.* 3 mL) was immediately transferred to a syringe and filtered through a 0.025 μm membrane filter (Schleicher & Schuell) using a Swinex-25 (Millipore) into a new centrifuge tube (FALCON[®] 2096, 15 mL). The filter was changed if required.

(vi) Solutions that were not analysed within 4 h were stored refrigerated until 2 h before analysis. All analyses were performed within 36 h of extraction.

3.4 SPECTROPHOTOMETRIC TITRATION SYSTEM

CELL DESIGN.— A constant temperature titration cell was used to meet the demands of a system requiring rigorous exclusion of oxygen. The cell (total volume *ca.* 120 mL) was fitted with a lid and sealed by means of ground-glass flanges. Ground-glass ports were located in the lid. A larger port accommodated a Gilmont micrometer syringe passing through a bored rubber stopper; a second port contained a ground glass stopper with attached plastic strings suspending a small glass boat containing KOH pellets (BDH, AnalaR). Two small central ports accommodated a nitrogen gas line and microline tubing which connected the titration cell to a 70 μL spectrophotometric flow-cell *via* an Alitea C-4V peristaltic pump. A magnetic stirrer was used. Nitrogen gas was scrubbed *via* gas wash bottles with acidic vanadium(II) solution over a zinc (mercury) amalgam followed by pyrogallate in 1 mol L⁻¹ KOH solution. Both during the spectrophotometric measurements and for 2 h before, oxygen-free nitrogen was passed over the test solution.

A glass electrode/calomel electrode pair was used for pH measurements (see Section 3.11). Visible absorption spectra were recorded on a Perkin Elmer Lambda 2 UV-VIS spectrophotometer for a series of wavelengths as a function of pH.

3.5 ELECTROCHEMICAL INSTRUMENTATION

3.5.1 VOLTAMMETRY.— EG & G Princeton Applied Research equipment was used. Cyclic voltammograms (CVs) were obtained using either: (i) a PAR 173 potentiostat coupled to a PAR 175 universal programmer and a Graphtec WX 1200 recorder or (ii) a model 273 A potentiostat with computer recording.

3.5.2 ELECTRODES AND CELLS.— A three electrode 10 mL pyrex glass cell was used for all voltammetric studies. This consisted of a glassy carbon working electrode, a platinum wire counter electrode and a saturated calomel reference electrode (SCE). The design of these electrodes has been described previously [Xu, 1992].

Preparation and Treatment of the Glassy Carbon Electrodes: Glassy carbon electrodes were prepared from a 0.5 cm length of glassy carbon rod (0.3 cm diameter; Atomergic Chemetals, VC-10) sealed in a Teflon rod (0.7 cm diameter). Electrode contact with the glassy carbon was effected with a central copper rod.

Graphite electrodes were prepared from high-density graphite rod (0.6 cm diameter; PAR G0091) sealed in a Teflon rod (1.2 cm diameter). Electrode contact with the electrode was effected by a few drops of mercury and a copper wire.

Newly fabricated carbon electrodes were polished metallographically to a mirror-like finish using polishing papers followed by 9, 6, 3 and 1 μm diamond paste. The electrodes were washed with acetone (BDH, AnalaR) followed by washing with triply distilled water and dried with filter paper. Between experiments the electrode was briefly polished (*ca.* 2 min) with 1 μm diamond paste, rinsed with acetone and triply distilled water and dried with filter paper.

3.5.3 pH MEASUREMENTS.— A laboratory pH meter was used for solution pH measurements and prior to use the electrode was calibrated using standard buffer solutions (Section 3.2.4).

3.6 SPECTROPHOTOMETRY

3.6.1 VISIBLE ABSORPTION SPECTRA.— Visible absorption spectra were recorded on a Perkin Elmer Lambda 2 UV-VIS spectrophotometer, Hewlett Packard 8452A diode array spectrophotometer, Shimadzu UV-2100 UV-Visible recording

spectrophotometer or a GBC model 918 UV-Visible spectrophotometer. Quartz spectrophotometric cells (1 cm) were used for batch analysis, while a 70 μL flow-cell [Starna, 3 mm (i.d.) x 10 mm] was used for FIA spectrophotometric studies.

3.6.2 ELECTROTHERMAL ATOMIC ABSORPTION SPECTROPHOTOMETRY (ETAAS).— A Perkin-Elmer Zeeman/3030 Atomic Absorption Spectrometer (ETAAS) was used. HNO_3 was used as a modifier to minimise interference from the chloride medium.

3.6.3 DRIFT SPECTROSCOPY.— The diffuse reflectance spectra were obtained using a Bruker 113 IFS FTIR spectrometer equipped with a diffuse reflectance unit (Harrick Scientific Corp.) and a DTGS detector. The compartment was purged with nitrogen for 30 min prior to collection of spectra. KBr was used as the non-absorbing matrix and background. The DRIFT spectra were obtained from a mixture of 10 mg of the sample and 0.5 g KBr. All spectra were recorded by averaging 2048 scans at a resolution of 4 cm^{-1} .

3.7 FLOW INJECTION ANALYSIS (FIA)

An Alitea XV peristaltic pump was used to circulate solutions for all FIA studies. Microline (Cole Palmer) tubing of 0.51 mm i.d. was used to connect Ismatec tygon pump tubing, for manifold components and for reaction coils. Two injection systems were used: (i) a Rheodyne (5020) injection system (6-port) with 0.8 mm i.d. injection loops and (ii) a VICI actuator (CHEMINERT, C12-3110EH) injection system (10-port) with 0.76 mm i.d. injection loops. The injection loops used for both systems were Teflon and connected using Activon (Omnifit, OM2301) two-way Teflon-tube couplers. Threaded Teflon-tube end fittings and grippers (OM2110, OM2310) were used to connect microline to the injection system and to inserted columns (see Chapter 10). Other connections were effected using silicon tube (Pharmacia) of 1.1 mm i.d.

3.8 SPECIATION CALCULATIONS

Speciation calculations were performed using the computer program SOLGASWATER [Eriksson, 1979]. The version of this program available for this work was capable of including surface complexes described by the constant capacitance model [as formulated in Chapter 2 (2.2.3)].

3.9 SOIL SOLUTIONS AND HUMIC WATERS

All soils and waters were stored refrigerated prior to use.

SECTION B: POTENTIOMETRIC TITRATION SYSTEMS

3.10 TITRATION SET-UP AND OPERATION

The calibration procedures for the different electrode pairs are described in Section 3.11.3. The conditions which defined the 'establishment of equilibrium' were similar for both systems and met the requirements described in Chapter 2 (2.3). Further details regarding drift conditions, titrant addition rates and volumes, and numbers of datum points *etc.* are given in the relevant Chapters (4 & 5).

3.10.1 CELL ASSEMBLY.— Two potentiometric titration apparatus assemblies were used during the course of this thesis. These are described below.

(A) Titration System 1.— A constant-temperature titration cell (capacity *ca.* 50-100 mL) was used. The cell, constructed of pyrex glass, was fitted with an airtight lid and sealed by means of ground-glass flanges. Ground-glass ports were located in the lid to accommodate the electrode system, a nitrogen gas line and a burette tip. The circulation of thermostated water, 25 ± 0.05 °C, around the double walled titration cell was sufficient to maintain a constant temperature. The titration cell was mounted on a 1 cm polystyrene plate directly above of magnetic stirrer. A Teflon-coated magnetic stirrer bar was used. A Radiometer ABU80 autoburette was used to dispense standard KOH into the titration vessel. Nitrogen gas was used to prevent intrusion of atmospheric contaminants (see Section 3.10.2). A glass electrode was used in conjunction with a calomel reference electrode for $p[H^+]$ measurements. The automation of this equipment has been described in detail previously [Town, 1991].

(B) Titration System 2.— A constant-temperature titration cell (capacity *ca.* 25-90 mL) was used. The pyrex glass cell was clamped and sealed (*via* rubber O-ring) beneath a specially designed plastic lid which incorporated a series of snugly fitting entry ports for the insertion of electrodes, argon gas line and a burette tip or Pt-net (coulometry). Temperature was maintained constant by immersion of the cell in an oil-bath (HAAKE 21 PR, D8 thermostat, paraffin oil) thermostated at 25 ± 0.05 °C. A magnetic stirrer (HAAKE MRZ3, MRS control box) was positioned below the oil-bath; stirring was effected *via* a Teflon-coated magnetic stirrer bar. Both volumetric (KOH or HCl) and coulometric titrations were performed. Metrohm 645 or 655 Multi-Dosimats were used to dispense alkali (or acid) into the titration vessel. A glass electrode was used in conjunction with a Ag/AgCl reference electrode for $-\log h$ measurements. The coulometry system is described in detail in Section 3.11.4. Argon gas was used to prevent intrusion of atmospheric contaminants and is discussed in Section 3.10.2.

Mineral (Hydr)oxide Suspension Titrations

The titration systems described above were developed for the titration of liquid phases. Chapter 5 of this thesis deals with the adsorption of PCV onto a mineral oxide-hydroxide surface in aqueous media. A significant part of this investigation required the potentiometric titration of suspensions of this solid phase.

Titration of suspensions were made using titration system-2. The small changes in apparatus required for these titrations are now described. The homogeneity of the test suspensions was maintained by use of a mechanically driven teflon rotor situated approximately 5 mm above the bottom of the titration vessel (replacing magnetic stirrer). The Wilhelm bridge (Section 3.11.1B) for the Ag/AgCl electrode was modified in the design of the 'J-tip'; this was removed and replaced with a straight tip design to minimise blocking of this junction by the small suspended particles.

3.10.2 ATMOSPHERIC OXYGEN AND CARBON DIOXIDE REMOVAL.—

Atmospheric oxygen and carbon dioxide was removed from the titration cell (and test solutions) by purging with an oxygen-free inert gas; nitrogen or argon. Prior to reaching the titration cell the 'oxygen-free' gas was subjected to a series of oxygen traps; 0.1 mol L⁻¹ KCl (ionic medium), 10 % H₂SO₄, pyrogallol acid in 10 % NaOH and finally 0.1 mol L⁻¹ KCl again. The titration cell was purged with the oxygen-free gas for greater than 30 min prior to any measurements and throughout all titrations a continuous flow of gas was maintained over the solution.

3.11 ELECTRODE SYSTEMS

3.11.1 GLASS ELECTRODES / REFERENCE ELECTRODES.— Several glass electrodes were used in combination with different reference electrodes. A Russell SWR757 electrode was used in combination with a Russell CR5 calomel reference electrode using saturated KCl (BDH, AnalaR) as the electrolyte solution. Ingold type 201-NS electrodes were used in combination with a silver-silver chloride (Ag/AgCl) reference electrode.

(A) Preparation of the Silver-Silver (Chloride) Reference Electrode.— The electrode was prepared according to Brown (1934).

Construction: A Pt wire of length 1-2 cm (*ca.* 1 mm diameter) was welded to a Cu wire and sealed through a glass tube. The copper wire (for external connection purposes) was spring-like so as to prevent breakage of the Pt-Cu weld. The glass tube was well sealed around the Pt wire so as to prevent solution entry. A quick-fit joint was positioned near the top of the tube for fitting to the titration cell. The copper wire was sealed at the top to stop entry of moisture which may corrode the Pt-Cu weld.

Silver Surface Preparation: The Pt tip of the electrode was washed in warm conc. HNO_3 , rinsed thoroughly with Milli-Q H_2O and secondly ethanol and then heated in an ethanol flame until the tip was 'red hot'. Silver plating was effected by application of a 0.1 mA current for 24 h while positioned in 1 % $\text{KAg}(\text{CN})_2$ solution. During this time the wire formed a thin white Ag coating (plate). Immediately following this Ag plating the system was placed in a 100 mmol L^{-1} NaCl solution and anodised for *ca.* 2 h to form a chloride crust at the surface. The final surface appeared slightly pink.

(B) Use of the Silver Chloride Electrode.— The new electrode was placed in a Wilhelm bridge and a few drops of 0.5 mol L^{-1} AgNO_3 added to prevent the Ag plating from being decomposed during electrolysis. The 'complete' Wilhelm bridge (0.10 mol L^{-1} KCl) was allowed to stabilise for one week before use (sealed from air during this period).

Wilhelm Bridge: [Forsling *et al.*, 1952; Rossotti and Rossotti, 1961] Care should be taken to keep the bridge clear of any bubbles and the taps clear of grease build-up which may block solution flow. Between all titrations the Wilhelm bridge was flushed thoroughly with fresh electrolyte solution to prevent the build-up of impurities (which affect the liquid junction potentials). Silver chloride is both light and temperature sensitive, so these conditions must be kept constant throughout the titration.

3.11.2 HYDROGEN ELECTRODES.— The hydrogen electrode may be used directly to measure pH in solutions containing only water as the reducible species ($\text{H}_2\text{O} + \text{e}^- \rightleftharpoons \frac{1}{2}\text{H}_{2(\text{g})} + \text{OH}^-$). However, the hydrogen electrode takes considerably longer to reach equilibrium than a correctly functioning glass electrode. For this reason the hydrogen electrode is generally used only to calibrate the glass electrode which, in turn, is used to measure pH.

The Hydrogen electrode employed was of a modified Hildebrand design. The working of such electrodes has been described in detail [Rossotti and Rossotti, 1961; Bates, 1973].

(A) Preparation of the Hydrogen Electrode

Construction: A rectangular Pt foil, *ca.* (1.5x0.7) cm^2 , was welded to a Pt wire (H_2 torch). The Pt wire was sealed through a closed glass tube so that the Pt foil was positioned 2-3 mm from the base of the tube. The Pt wire was connected internally by a spring-like copper wire. The Pt foil (and external wire) was cleaned in warm conc. HNO_3/HCl (1:3), rinsed thoroughly with Milli-Q H_2O and secondly ethanol and then heated in an ethanol flame until it was 'red hot'.

Platinum Black Preparation: The clean Pt electrode was electrolysed for 3 min at 0.15 A in a $\text{PtCl}_4/\text{PbAc}_2$ solution to plate with 'black' (hence Platinum Black). [1g PtCl_4 dissolved in 30 mL H_2O ; add 0.1 mL 0.1 mol L^{-1} HCl and 20 mg PbAc_2 ; re-use (very expensive!)]. A small Pt electrode was used as the anode. If insufficient 'black' was obtained more PbAc_2 was added. Finally the foil was electrolysed (as cathode) in 0.1 mol L^{-1} H_2SO_4 (10 %) for 15 min at 0.15 A.

(B) Use of the Hydrogen Electrode.— The hydrogen electrode was housed in a glass (open bottom) tube (*ca.* 10 mm diameter). Near the bottom (*ca.* 8 mm) and on opposite sides of the tube, two small holes (*ca.* 5 mm dia.) were cut for the hydrogen gas to gently bubble out. The clean Pt-black electrode was carefully slid into this glass shield so that its end protruded (*ca.* 1 mm) from the bottom. The small holes at the base allowed the Pt-black surface to remain wet at the bottom (where the hydrogen gas never reached), to alternate wet/dry close to the gas exit holes and to remain dry above the holes. These conditions gave the desired properties to the catalytic Pt-black surface. Care was taken not to damage the Pt-black coating. The surface was washed with Milli-Q H_2O ; excess water was removed with a tissue by dabbing the end of the foil tip (without touching the main faces).

In the titration vessel, the solution volume was sufficient to prevent significant splashing of the test solution by the continuous bubbling of hydrogen. The glass electrodes requiring calibration, the Wilhelm bridges (J-tips) for the Ag/AgCl reference electrode and the coulometry electrodes (Pt-basket and Ag counter electrode, see Section 3.11.4) were all placed in this vessel. Finally the hydrogen electrode was inserted with a connection to the hydrogen gas tube. The hydrogen gas was subjected to the same O_2/CO_2 procedures as Argon gas. The gas outlet tube dipped slightly into the external oil-thermostat (for pressure maintenance). The titration vessel (extremely airtight) was allowed to equilibrate with respect to the hydrogen gas atmosphere (to constant pressure) for at least 1 h before initialisation of the coulometric titration procedure.

3.11.3 ELECTRODE TESTING AND CALIBRATION PROCEDURES.— Good e.m.f. data are dependent upon good electrode calibration procedures. In the present work, the electrode couples (glass electrode/reference electrodes) were calibrated as (i) $\text{p}[\text{H}^+]$ or as (ii) $-\log h$ probes respectively. Glass electrodes (and reference electrodes) are not immortal and will eventually malfunction. It is therefore desirable that response of the glass electrode is tested regularly. In the latter calibration procedure '(ii)' the response of the glass electrode was tested against the hydrogen electrode.

(A) Electrode Calibration Procedures.— Two methods were employed for the calibration of the electrode couples. Procedure '(i)' was used for the calibration of the glass electrode/calomel electrode pair and procedure '(ii)' was used for the calibration of

the glass electrode/silver-silver chloride electrode pair. In practise either method could be used for calibration purposes for each electrode couple.

(i) **$p[H^+]$ Calibrations:** $p[H^+]$ probe calibration was carried out by alkali titration of HCl (of known concentration) to pH *ca.* 11 in 0.10 mol L⁻¹ KCl electrolyte. Plotting pH (observed) against $p[H^+]$ (calc.) gave linear relationships ($r^2 \geq 0.99$) over the pH ranges 2.5-3.5 and 9.5-11.0. Electrodes were not used unless this condition was fulfilled.

(ii) **$-\log h$ Calibrations:** The Nernstian response of the glass electrodes was tested against the hydrogen electrode [described in Section 3.11.3(B)]. Correctly functioning electrodes were chosen from these results. The electrode was calibrated by means of an E° titration (to near pH 4.0) in a solution of known H^+ -concentration. This titration was performed coulometrically (as described in Section 3.11.4). Consequently, a series of calibration points was generated for which the hydrogen ion concentration, h , can be stoichiometrically calculated and $-\log h$ is known. If the ligand exhibits negligible acid/base properties for $-\log h \leq 3.5$, then the ligand may be present during this calibration procedure. Likewise, hydrolysis of Al is negligible below this point and the calibration is best performed in the presence of the metal ion.

(B) Testing of Glass Electrodes Against the Hydrogen Electrode.— An important part of the second electrode calibration procedure (discussed above) is the testing of the glass electrode before use. Glass electrodes were tested by comparing their response (one or several simultaneously) with the response of the hydrogen electrode.

The hydrogen electrode defines the pH scale, according to the equation:

$$E = E^\circ + \frac{g \cdot \log[H^+]}{p_{H_2}} + E_{j_{ac}}[H^+] + E_{j_{alk}}[OH^-] \quad (3.11.3)$$

where,

E = the measured potential, e.m.f, in mV.

E° = the E-zero of the electrode.

g = the Nernstian constant, 59.157 mV.

$E_{j_{ac}}$ = the liquid junction potential due to H^+ , -511.5 mV L mol⁻¹, @ 0.1 mol L⁻¹.

$E_{j_{alk}}$ = the liquid junction potential due to OH^- , 238.7 mV L mol⁻¹, @ 0.1 mol L⁻¹.

p_{H_2} = the partial pressure (of the hydrogen atmosphere).

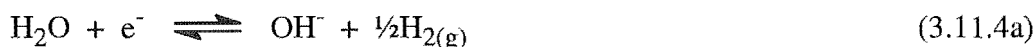
By titration of a solution containing equimolar concentrations of suitable buffers in the presence of both glass and hydrogen electrodes, data were collected which described the response of each electrode. For simplicity, pH measurements from the hydrogen electrode are now denoted pH_h (or E_h) while those of the glass electrode are

denoted pH_g (or E_g). [A suitable buffer system could contain, say, 6 mmol L^{-1} $\text{H}^+(\text{Cl}^-)$, 3 mmol L^{-1} each of NaOAc , $\text{NaH}_2\text{PO}_4 \cdot \text{H}_2\text{O}$ and $\text{B}(\text{OH})_3$ and 94 mmol L^{-1} NaCl ; giving $I = 0.10 \text{ mol L}^{-1}$ and initial $\text{pH} = 2.8$].

From this titration a plot of $E_h - E_g$ vs pH_h was constructed [pH_h is calculated using E_h in expression (3.11.3) above] and this plot indicates the pH range for which $\text{pH}_g = \text{pH}_h$ and hence the range over which the glass electrode will function accurately. The glass electrode is considered accurate if E_h and E_g differed by less than 0.3 mV over the pH_h range. It is common at higher pH s ($\text{pH} > 9.5$ -10) that the glass electrode begins to lose its accuracy and curvature will be observed in the plot. The glass electrode cannot be used accurately past such pH values. In the present studies the glass electrodes were only used if potentials were constant and reproducible within $\pm 0.3 \text{ mV}$ for $2 \leq -\log h \leq 9$.

3.11.4 COULOMETRY.— As an alternative to titrating with a strong base, coulometry offers a very precise method to gradually change the composition of the test solution. In such a titration, the pH is increased by coulometric addition of e^- which generate OH^- .

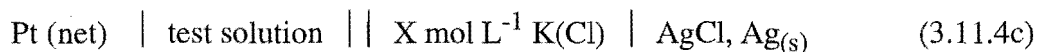
At the working electrode (Pt-net) the reaction is:



while at the counter electrode (silver rod) the reaction (3.11.4b) occurs:



A complete representation of the cell reaction is:



For this cell, the number of reduced protons is equal to the number of electrons passed through the cell. This quantity can be calculated from Faraday's law:

$$n_{e^-} = I \cdot t / 96485 \text{ A s mol}^{-1}$$

i.e. the addition of e^- (and hence OH^-) can be controlled through accurate control measures of electrical current and time.

Construction and Preparation.— A Pt-basket electrode was used in combination with a silver reference electrode for all experiments. The pre-made Pt-basket (20 mm x 5 mm) was positioned at the end of a Pt-wire (1 mm diameter) passing through a rubber stopper.

The basket was cleaned prior to use by washing in warm acid [conc. HNO_3/HCl (1:3)] and thoroughly rinsed in TDW followed by ethanol. The basket was then heated in an ethanol flame until 'red hot' and used immediately after cooling. The silver reference electrode was prepared from a flat sheet of silver (1 mm thickness). This was moulded into a cylindrical spiral and sealed into a plastic quick-fit lid with araldite glue. This electrode was connected to the titration system *via* a second Wilhelm bridge [0.10 mol L^{-1} $\text{K}(\text{Cl})$ electrolyte].

3.12 TITRATION PROCEDURE

The details regarding the titration procedures for the two titration set-ups differ primarily in the electrode systems and their calibration. The general procedure for potentiometric titrations of ligand or metal-ligand solutions and mineral (hydr)oxide or mineral (hydr)oxide-ligand suspensions is now described.

All solutions were equilibrated at 25°C before volumes were dispensed and the test solution was purged with inert gas for 30 min before commencing a titration. Before every titration the electrode pair [glass/calomel, glass/Ag-AgCl] was calibrated as described in Section 3.11.3. For titration system-1, the electrolyte used for the calibration was removed before addition of the investigated test solution. In the case of titration system-2 the test solution (ligand/metal-ligand *etc.*) was added to the calibration electrolyte so as to minimise disturbances to the electrode system. In the case of metal-ligand titrations, the investigated metal ion, Al, was present in this calibration solution. Following the final addition of ligand to the test solution, *ca.* 30 min was allowed for pH stabilisation before the titration was commenced. The titrant was then dispensed *via* an automated procedure similar to that described previously by Town (1991). (Note: titration systems-1 and -2 used different autoburettes). At the completion of every titration the electrodes were re-calibrated again to permit correction for any drift in the electrode response over time (assumed linear during the course of the titration).

CHAPTER 4

POTENTIOMETRIC STUDIES OF ALUMINIUM(III) - PYROCATECHOL VIOLET AND ALUMINIUM(III) - 4-NITROCATÉCHOL EQUILIBRIA

4.1 INTRODUCTION

Aluminium has long been recognised for its toxicity toward plants, aquatic organisms and humans [Chapter 1 (1.2)]. In natural systems Al exists in a competitive equilibrium with a large number of naturally occurring ligands. In waters and soil solutions Al is most frequently observed to be tightly bound by various forms of natural organic matter (NOM), *eg.* humic substances. Also present in such systems are various forms of inorganic Al and Al-hydrolysis species.

The toxicity of Al is dependent on its chemical form (*i.e.* its speciation) and is most commonly correlated with the sum of the free and labile forms. Thus the measurement of this fraction, rather than total Al, is of primary importance in soils and natural waters. As discussed in Chapter 1 (1.3), no direct methods exist that are either applicable (achieve discrimination amongst different species) or sensitive enough for the analysis of environmental concentrations of Al.

The speciation (characterisation and quantification) of Al in an aquatic system is generally approached using two methods (used separately or in combination with each other). The first approach involves the use of a fractionation procedure [see Chapter 1 (1.3)] to separate, and hence speciate, Al prior to its analysis. All fractionation procedures are operationally defined and undoubtedly detect somewhat different forms of Al. This means that there is no fundamental connection between the Al content of the fraction and the actual chemical species that are being assigned to the fraction. Reaction kinetics, which result in time dependent re-equilibration of samples during analysis, also severely affects the ease of use of these procedures. Small changes in operating conditions (which would, for example, be expected between different laboratories) may result in large differences in speciation results.

The second approach commonly used for chemical speciation in aquatic systems is the use of chemical modelling [Schecher and Driscoll, 1987 and 1988; Lewis *et al.*, 1988; Öhman and Sjöberg, 1988; Bi, 1995]. In this approach, thermodynamic data are used together with total and/or free concentrations of reacting components in order to calculate the equilibrium concentrations of individual species. This approach has advantages over the analytical fractionation approach, in that it provides the analyst with predictive capabilities. The analytical approach reveals information only on the 'current situation' and can give no information on the consequences of a change in chemical conditions. However, several drawbacks also exist in the use of this theoretical approach.

The validity of much thermodynamic data is questionable and, further, large amounts of 'required' data often does not exist in the database. In this procedure, the results obtained are directly related to the validity and completeness of the thermodynamic model. Another difficulty regarding the theoretical approach is that the reacting components must be well characterised; the organic components of natural systems are, in particular, very difficult to characterise.

As mentioned above, the toxicity of Al is most commonly correlated with the sum of the free and labile forms. Therefore, in toxicity studies, methods that can accurately discriminate between this fraction and all other Al fractions (*e.g.* strongly complexed or adsorbed Al) are the most useful. Of the large number of Al fractionation procedures that have been developed for this purpose, the most commonly employed are those using a suitable Al-complexing reagent (to achieve this discrimination) [Hodges, 1987; Royset, 1985; Kerven, 1989; Clarke *et al.*, 1992; Hawke and Powell, 1994].

4.1.1 SCOPE OF THIS WORK.— This thesis is directed towards the development of techniques for the speciation of Al in environmental samples. An integral part of this work involved the investigation of new and/or commonly used ligands for the analysis of Al. As discussed above, a knowledge the reaction(s) between the equilibrium components based on thermodynamic data is invaluable to understanding a system's speciation. If this data is available for the reaction between a chemical reagent and the target metal, it provides the analyst with the ability to investigate experimental conditions quickly and avoid performing unnecessary experiments, *i.e.* experiments that will not work in theory are unlikely to work in practise.

Pyrocatechol violet (PCV) and 4-nitrocatechol (4ncat) are ligands that are well known for their ability to complex Al. However, a lack of thermodynamic data exists for the reaction of these ligands with Al. In particular, no accurate data exists for the Al^{3+} -PCV equilibria and the data regarding the Al^{3+} -4ncat system has not been determined over either pH or ligand/metal ranges applicable for the use of 4ncat in the determination of Al. In the present work the equilibria between Al and (i) PCV and (ii) 4ncat have been studied.

The chapter is divided into 2 parts.

SECTION A: The equilibrium reactions between aluminium(III) and pyrocatechol violet (PCV) have been studied by potentiometric titration in aqueous solution, $I = 0.10 \text{ M K(Cl)}$, 25.0°C . This work was performed at Umeå University, Sweden.

SECTION B: The equilibrium reactions between aluminium(III) and 4-nitrocatechol were studied by potentiometric titration in aqueous solution, $I = 0.10 \text{ M K(Cl)}$, 25.0°C .

SECTION A: POTENTIOMETRIC STUDIES OF ALUMINIUM(III)-PYROCATECHOL VIOLET EQUILIBRIA

4.2 PYROCATECHOL VIOLET (PCV)

A range of metallochromic dyes have been used for spectrophotometric or FIA-spectrophotometric analysis of Al in environmental systems, *e.g.* pyrocatechol violet (PCV) [Røyset, 1985; Dougan and Wilson, 1974], chrome azurol S (CAS) [Hawke and Powell, 1994], eriochrome cyanine R (ECR) [Røyset, 1985], oxine [Hodges, 1987] and aluminon [Røyset, 1985]. Several comparisons have been made between selected ligands [Røyset, 1985; Hawke and Powell, 1994; Hodges, 1987]. Thermodynamic data for the reaction between Al and these reagents are scarce.

Several spectrophotometric studies of equilibria between Al and PCV (H_4L , Figure 1) have been reported [Tikhonov and Bakhtina, 1984; Chiacchierini *et al.*, 1974]. However, none of these has adequately analysed the equilibria. In a potentiometric study the formation of three complexes was proposed and equilibrium constants were given [Goïna *et al.*, 1970], however the values are anomalously high for 'catecholate' ligands. The lack of reliable data for H^+-Al^{3+} -PCV equilibria contributes to confusion over what Al species are being targeted during spectrophotometric analyses *e.g.*, in the 60 s measurements of reactive Al in soil solutions [Kerven *et al.*, 1989].

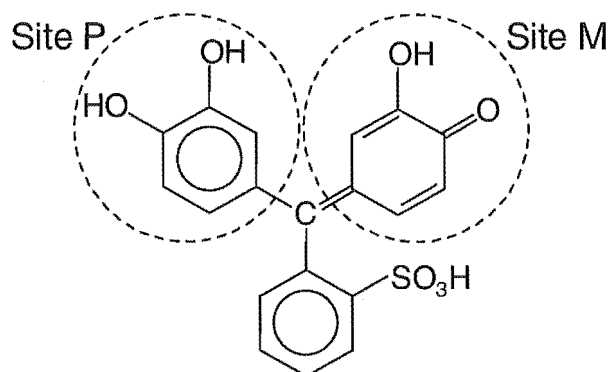


Figure 4.2 Pyrocatechol violet (PCV, H_4L). 'Site P' and 'Site M' designate the 'catechol' and 'maltol' functionalities respectively.

4.2.1 EXPERIMENTAL

(A) **Chemicals and Analysis.**— All solutions were prepared from CO₂-free, boiled Milli-Q water and all working solutions were prepared in 0.10 mol L⁻¹ K(Cl) (Merck, *p.a.*), dried at 120 °C.

(i) **Pyrocatechol Violet Solutions:** PCV: pyrocatechol sulfonphthalein, 2-[(3,4-dihydroxyphenyl)(3-hydroxy-4-oxo-cyclohexa-2,5-dien-1-ylidene)methyl]benzene sulfonic acid or 3,3',4'-trihydroxy-fuchsone-2''-sulfonic acid is depicted in Figure 4.2.

Reagent grade PCV materials were obtained from the chemical companies Aldrich, BDH, Koch-Light (now NBS Biologicals), Merck and Sigma. The dye content of each of these materials was examined by spectrophotometric analysis of the Al-PCV complex (pH 6.2). The results indicated a large range of dye contents (and metal impurities); Koch-Light and Merck had absorbances twice that of Aldrich. Aldrich, BDH and Sigma materials were excluded from the present studies.

PCV (Koch-Light or Merck) was dried to constant weight at 110 °C under vacuum to remove occluded acidic impurities [see 'Dirt acid'; Section 4.2.1(D)] prior to solution preparation. Attempts at recrystallisation were unsuccessful. PCV solutions were membrane filtered (<0.025 µm). However, small amounts of foreign acidic substances remained. The PCV and 'dirt acid' concentrations in ligand stock solutions were determined from potentiometric titration data using the computer program LAKE [Ingri *et al.*, 1996]. The PCV content was found to be within 1-2 % of the value expected from weighing; the remaining weight was assumed to be that of occluded water or 'dirt acid'.

(ii) **Aluminium Solutions:** A stock solution of Al³⁺ (*ca.* 0.1 mol L⁻¹) was prepared from Baker Analysed Reagent in *ca.* 0.1 mol L⁻¹ HCl and was standardised as described in Chapter 3 [3.2.5(A)]. The Al³⁺ content determined was within 0.1 % of the weighed amount.

(iii) **Standard Alkali (KOH) and Acid (HCl) Solutions:** Standard HCl (BDH, AnalaR) solutions were prepared and standardised as described in Chapter 3 [3.2.2]. Carbonate-free KOH (Eka Nobel, *p.a.*) solutions were prepared and standardised according to Chapter 3 [3.2.1(B)]. Dilute (*ca.* 0.01-0.04 mol L⁻¹) KOH solutions were standardised potentiometrically against standard HCl.

(B) **Spectrophotometric Determination of log K₁.**— This determination required rigorous exclusion of oxygen. The thermostatted cell and the spectrophotometric apparatus required for these measurements were described in Chapter 3 [3.4]. In these studies 5 titrations were performed with [PCV] = 30-80 µmol L⁻¹. This solution (*ca.* 50 mL) was deoxygenated at *ca.* pH 4.5 and titrated to *ca.* pH 11.5. At this pH ~ 99 % of

the ligand is present as HL^{3-} . The pH was measured using a glass electrode/calomel electrode pair {refer to Chapter 3 [3.11.3(A)] for calibration procedure, $p[H^+]$ }. The response of this electrode system was assumed to remain linear to $pH = 13$.

Ligand absorption spectra were determined for 6 wavelengths (in the range 460-550 nm) as a function of pH (11.5-12.8). The molar absorptivity for the fully deprotonated species, ϵ_{A^-} , was determined following addition of $KOH_{(s)}$ to the cell.

(C) Spectrophotometric Titrations.— Spectrophotometric titrations of Al-PCV solutions were undertaken using the spectrophotometric apparatus described in Chapter 3 [3.4] (without the 'KOH boat'). Two titrations were performed with (i) $[PCV] = 60 \mu\text{mol L}^{-1}$, $[Al^{3+}] = 15 \mu\text{mol L}^{-1}$ (ligand/metal = 4.0) and (ii) $[PCV] = 70 \mu\text{mol L}^{-1}$, $[Al^{3+}] = 40 \mu\text{mol L}^{-1}$ (ligand/metal = 1.75).

(D) Potentiometric Titrations.— The titration set-up and cell arrangement is described in Chapter 3 [3.10.1(B)]. The electrode pair was calibrated for the measurement of $-\log h$ as described in Chapter 3 [3.11.3A(ii)]. The free H^+ concentration, h , was determined by measuring the e.m.f. of the cell described by equation 2.3.1b (see Chapter 2). In the present investigation, the combined data from the E_0 calibration titrations (coulometric reductions of H^+ in a dilute HCl solution) were used to calculate a value of j_{ac} [the 'acid' liquid junction potential; see Chapter 2 (2.3.1) and Chapter 3 (3.11.3B)]. In this calculation, a plot of $(E - 59.157 \cdot \log h)$ vs. $-\log h$ will give a straight line of slope j_{ac} and intercept E_0 . The junction potential, j_{ac} , was determined as $-519.8 \text{ mV L mol}^{-1}$ ($3\sigma = 34.2 \text{ mV L mol}^{-1}$) which is in good agreement with the (literature) value used in the calculations [Chapter 2 (2.3.1)].

The conditions defining the establishment of pH equilibrium [see 'delay times', Chapter 2 (2.3)] were similar for all the titrations, however, longer equilibrium periods were used at $C/B < 2$ (where C and B denote the total concentrations of PCV and Al respectively). The delay time following the addition of each aliquot was the same as that between measurements. In titrations with $C/B > 2$ this delay time was 3 min, whereas for titrations with $C/B < 2$ a delay time of 6 min was employed. The equilibrium condition was satisfied when stable potentials within $\pm 0.1 \text{ mV}$ ($0.0017 -\log h$) were obtained. All titrations typically contained 15-40 data points. Titrations for determination of the dissociation constants $\log \beta_{-1,0,1}$ and $\log \beta_{-2,0,1}$ for PCV and $\log k_D$ for the 'dirt acid' were performed separately within the ranges $0.002 \text{ mol L}^{-1} \leq C \leq 0.01 \text{ mol L}^{-1}$ and $2.0 \leq -\log h \leq 9.5$.

In three-component titrations B and C were varied within the limits $0.0004 \text{ mol L}^{-1} \leq B \leq 0.006 \text{ mol L}^{-1}$ and $0.002 \text{ mol L}^{-1} \leq C \leq 0.010 \text{ mol L}^{-1}$, covering C/B ratios in the range 1-10. Dilution titrations were performed at $C/B = 1$ by addition of aliquots of Al-PCV solution (prepared *via* titration to $3.5 \leq -\log h \leq 4.0$) to pure ionic medium.

The reproducibility and reversibility of equilibria were tested by performing both forward (increasing $-\log h$) and backward (decreasing $-\log h$) titrations.

Coulometric titration of PCV: The ability to perform coulometric titrations throughout this work was an appealing concept due to the much higher precision of coulometric generation of OH^- over volumetric addition [described in Chapter 3 (3.11.4)]. However, the ability to use coulometry for the titration of any material is dictated by whether or not the material will interfere in the coulometric procedure (see equation 3.11.4a, Chapter 3), *i.e.* this may happen if the ligand can be easily oxidised or reduced.

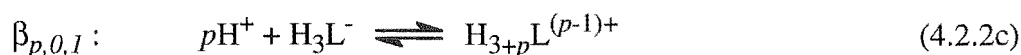
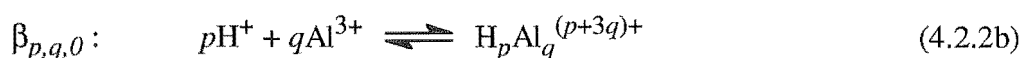
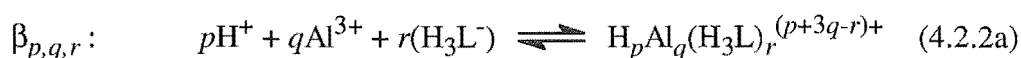
Preliminary investigations revealed that PCV affected (by an indeterminate side reaction) the coulometric generation of e^- (and hence OH^-) and coulometry could not be used for the study of the acid/base and complexing properties of this ligand. This phenomenon has been reported previously for catechol [Öhman and Sjöberg, 1983].

Dirt acid: Metallochromic reagents (*e.g.* PCV, CAS, ECR) available from any manufacturer are often found to contain large quantities of foreign substances. The initial titration of PCV revealed the presence of considerable amounts of a 'dirt acid' (an unknown impurity which exhibits acid/base properties). From a comparison of Z_C -curves, the dirt acid could be observed to account for almost 10 % of titratable protons at $-\log h \sim 4.5$ (but in total represented < 2 % of total titratable protons).

The PCV materials were purified as described above [4.2.1A(i)] and the dirt acid impurities [suspected to be acetic acid impurities] largely removed under vacuum. Any remaining acidic impurities were accounted for by inclusion of a fourth component in the calculations (*i.e.* $\text{H}^+ - \text{Al}^{3+} - \text{PCV} - \text{'Dirt'}$), which exhibited a single protonation constant, k_D , in the model.

4.2.2 DATA TREATMENT

(A) **Potentiometry.**— Data treatment assumed the presence of three-component equilibria of the general form (4.2.2a) and the two-component equilibria (4.2.2b) and (4.2.2c):



The law of mass action and the conditions for the total concentrations then give equations (4.2.2d-f), where equilibrium concentrations $b = [\text{Al}^{3+}]$ and $c = [\text{H}_3\text{L}^-]$. The summations are taken over all species formed: $\beta_{p,q,r}$, $\beta_{p,0,1}$ and $\beta_{p,q,0}$ are the equilibrium constants for the reactions (4.2.2a), (4.2.2b) and (4.2.2c), respectively.

$$H = h + \sum p\beta_{p,0,1}h^p c + \sum p\beta_{p,q,0}h^p b^q + \sum p\beta_{p,q,r}h^p b^q c^r - k_{\text{W}}h^{-1} \quad (4.2.2d)$$

$$B = b + \sum q\beta_{p,q,0}h^p b^q + \sum q\beta_{p,q,r}h^p b^q c^r \quad (4.2.2e)$$

$$C = c + \sum \beta_{p,0,1}h^p c + \sum r\beta_{p,q,r}h^p b^q c^r \quad (4.2.2f)$$

The aluminium hydrolysis species, defined according to equation (4.2.2b), used in the calculations were: AlOH^{2+} ($\log \beta_{-1,1,0} = -5.33$), $\text{Al}(\text{OH})_2^{2+}$ ($\log \beta_{-2,1,0} = -10.91$), $\text{Al}_3(\text{OH})_4^{5+}$ ($\log \beta_{-4,3,0} = -13.13$), $\text{Al}_{13}(\text{OH})_{32}^{7+}$ ($\log \beta_{-32,13,0} = -107.41$) and $\text{Al}(\text{OH})_4^-$ ($\log \beta_{-4,1,0} = -23.46$) [Öhman *et al.*, 1983; Brown *et al.*, 1985].

Because the dissociation of the sulfonate proton occurs at $-\log h < 1$ [Wakley and Varga, 1972], the zero proton level is defined as a triprotic species, H_3L^- . The least-squares computer program LAKE [Ingri *et al.*, 1996] was used to determine sets of p, q, r triplets and the corresponding equilibrium constants that 'best' fit the experimental data [see Chapter 2 (2.1.4)]. The best model was the one which gave the lowest error squares sum $U_{\text{ZC}} = [(H_{\text{calc}} - H_{\text{exp}})/C]^2$. Goodness of fit parameters are expressed as $U_{\text{ZC}}(pr)_q \times 10^{-3}$ and $\sigma(Z_C)$ where p, q, r designate the species present (*i.e.* $U_{\text{ZC}}(00)_0$ is U_{ZC} before new species were included) and $Z_C(-\log h) = (H - h + k_{\text{W}}h^{-1})/C$.

(B) Spectrophotometry.— The constant $\log K_1$ was calculated by Ågren's method [Ågren, 1955]. The determined value of $\log K_1$ was converted into the cumulative constant, $\log \beta_{-3,0,1}$, where $\log K_1 = \log K_{-3,0,1} - \log K_{-2,0,1}$.

Ågren's method: A modified version of Ågren's equation was used for the calculation of the first protonation constant, K_1 , for the reaction:



This reaction is related to the hydrolysis reaction:



for which

$$K_b = \frac{[\text{HA}][\text{OH}^-]}{[\text{A}^-]} = K_w \cdot K_1 \quad (4.2.2i)$$

Given that the extinction coefficient, ϵ , for the fully deprotonated ligand is known (*i.e.* ϵ_{A^-} is known), then the modified version of Ågren's equation can be used:

$$\frac{[\text{HA}]_{\text{tot}}}{\text{Abs}} = \frac{1}{\epsilon_{\text{HA}}} + \left\{ [\text{OH}^-] \frac{\text{Abs} - \epsilon_{\text{A}^-} - [\text{HA}]_{\text{tot}}}{\text{Abs}} \right\} \frac{1}{K_b \epsilon_{\text{HA}}} \quad (4.2.2j)$$

4.2.3 DATA, CALCULATIONS, RESULTS.— The experimental results showing the complexation behaviour of the system are illustrated by the function $Z_C(-\log h)$, *i.e.* the average number of OH^- reacted per ligand, plotted as a function of $-\log h$ (Figure 4.2.3A).

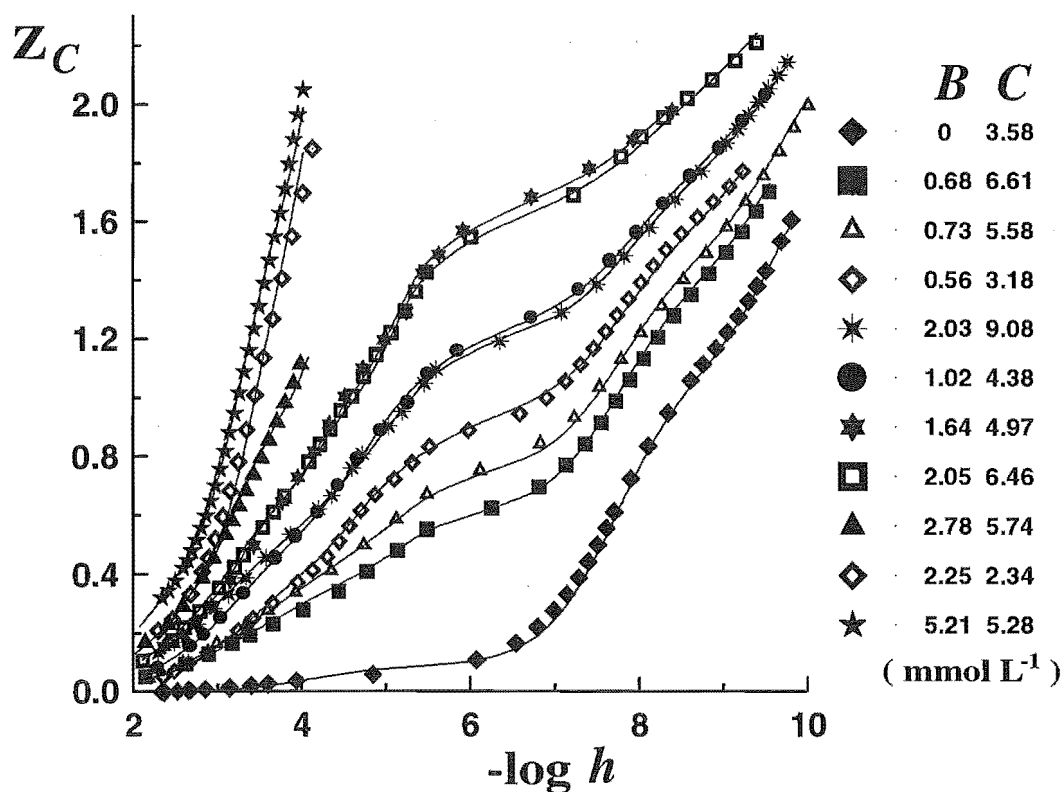


Figure 4.2.3A Part of the experimental data plotted as curves $Z_C(-\log h) = (h - H - k_w \cdot h^{-1})/C$ for C/B ratios 1, 2, 3, 4.5, 5.7, 7.5, 10 and ∞ . The Z_C function was calculated over the zero proton level H_2O , Al^{3+} , H_3L^- . All symbols represent total concentrations of Al and PCV. The curves were calculated using the constants in Table 4.2.3.

The data used to calculate $\log \beta_{-1,0,1}$ and $\log \beta_{-2,0,1}$ and $\log k_D$ for the 'dirt acid' comprised 15 titrations with *ca.* 600 data points ($\log h$ range 2.2-9.8). The calculations established $\log \beta_{-1,0,1} (\pm 3\sigma) = -7.71 \pm 0.01$, $\log \beta_{-2,0,1} = -17.49 \pm 0.02$ and $\log k_D = -4.1 \pm 0.3$. The first protonation constant was calculated spectrophotometrically as $\log K_1 = 12.72 \pm 0.03$, giving $\log \beta_{-3,0,1} = -30.21 \pm 0.05$. Concentrations of 'dirt acid' and values of $\log k_D$ differed slightly between PCV stock solutions. No PCV solution was used for studying the H^+ - Al^{3+} -PCV system if the difference between the weighed and determined concentration of PCV was greater than 2 %.

Prior to numerical analysis of the three-component system, a simulation of the expected complexation properties of pyrocatechol violet was made by using the substances catechol [Öhman and Sjöberg, 1983] and maltol [Hedlund and Öhman, 1988] in equal and representative concentrations. Here catechol is taken to approximate the 1,2-dihydroxyaryl binding site (site 'P') and maltol the 2-hydroxy-*p*-quinomethide site (site 'M') of pyrocatechol violet. From the calculations it was seen that the 'maltol' site would be expected to dominate Al binding at lower $-\log h$ values, whereas the 'catechol' site would not be expected to bind a significant fraction of Al until $-\log h > 7$.

The analysis of the three-component data, comprising 27 titrations with 780 data points was broken into two parts. The first comprised data with $C/B \geq 4$, selected to avoid any effects from possible polymeric-hydroxo species that might exist at lower ratios. Initial calculations indicated that the formation of polynuclear species would be negligible under these conditions. The model calculation for 'PCV' as described above had indicated that a series of mononuclear 'maltol' complexes, $Al(H_2L)^+$, $Al(H_2L)_2^-$ and $Al(H_2L)_3^{3-}$, could be expected to form at lower $-\log h$ values. The formation constants for these three species were evaluated from data for 10 titrations (182 datum points with $2.2 \leq -\log h \leq 4.0$) by use of the program LAKE. The equilibrium constants obtained were $\log \beta_{-1,1,1} = -0.19 \pm 0.05$; $\log \beta_{-2,1,2} = -1.05 \pm 0.05$ and $\log \beta_{-3,1,3} = -2.53 \pm 0.09$. NOTE: The use of a Bjerrum plot [see Chapter 2, 2.1.3(B)] was not applicable to this system because the proton displaced during complexation was that of the 'maltol' moiety ($\log \beta_{-2,0,1} - \log \beta_{-1,0,1} = -9.78$). At the $-\log h$ range over which this complexation occurs the proton of the 'catechol' moiety has not yet been displaced, *i.e.* it is usually displaced before the proton of the maltol moiety ($\log \beta_{-1,0,1} = -7.71$). This anomaly causes the Bjerrum expression to be either not applicable to this system or very complex and difficult to understand.

These three species were then considered as known and a complete *pqr*-analysis (the testing of single *p,q,r* triplets or combinations of *p,q,r* triplets) was performed on 10 titrations (175 datum points, $3.7 \leq -\log h \leq 7.0$) to find species which best explained the experimental data up to $-\log h = 7.0$. These calculations, for which U_{ZC} values are given in Figure 4.2.3B(i), indicated four compositions that could equally well explain most of the experimental data (circled values). However, a comparison of experimental Z_C curves

with theoretical ones revealed systematic residuals still remaining, thereby indicating a need for at least one further species to be included in the model. A second pqr -analysis was therefore undertaken which successively included one of the four 'best' species indicated in Figure 4.2.3B(i) in combination with a second species with another p, q, r composition. The results of these calculations indicated significant improvement in U_{ZC} for only two of the four 'best' species. These results are presented in Figures 4.2.3B(ii) and 4.2.3B(iii). For the other two 'best' species no improvement could be obtained by including a second species. Figure 4.2.3B shows that the combination of the species $(-4, 1, 2)$ ($\log \beta_{-4,1,2} = -10.26 \pm 0.10$) and $(-5, 1, 3)$ ($\log \beta_{-5,1,3} = -13.03 \pm 0.13$) gives the best fit to the experimental data, $U_{ZC}(pr)_q \times 10^{-3} = 0.72$ and $\sigma(Z_C) = 0.004$. These constants can be ascribed to the products $\text{Al}(\text{HL})_2^{3-}$ and $\text{Al}(\text{HL})_2(\text{H}_2\text{L})^{5-}$ respectively.

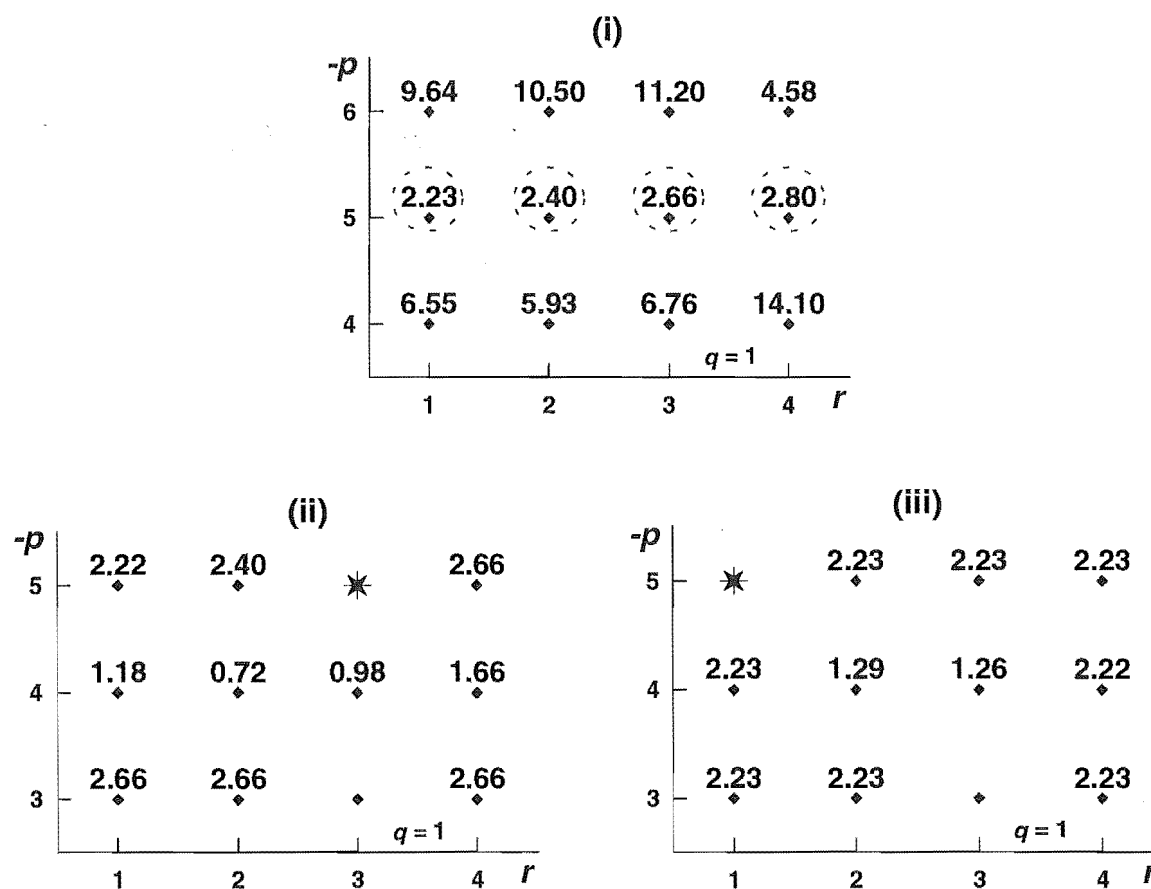


Figure 4.2.3B Results of the pqr -analysis concerning the range $3.7 \leq -\log h \leq 7.0$. The diagrams give the error squares sums $U_{ZC}(pr)_q \times 10^{-3}$, assuming one new complex in (i) and two new complexes in (ii) and (iii) respectively. The four 'best' species are circled in Figure (i). In (ii) and (iii) the complex assumed known, from (i), has been starred and the $U_{ZC}(pr)_q$ value given is the error squares sum for the combination of this species, also refined, with another p, q, r species, as shown. In the calculations, equilibrium constants

for Al hydrolysis and the species $\text{Al}(\text{H}_2\text{L})^+$, $\text{Al}(\text{H}_2\text{L})_2^-$ and $\text{Al}(\text{H}_2\text{L})_3^{3-}$ have been assumed to be known, *cf.* the absence of error squares sum at $(-3,1,3)$. The calculations were based on 175 datum points giving an initial sum of squares, $U_{ZC}(00)_0 \times 10^{-3} = 60.9$.

For the remaining data, to $-\log h = 9.6$, the logical species remaining that could be included in the model were $(-6,1,3)$ *i.e.* $[\text{Al}(\text{HL})_3^{6-}]$ followed by the stepwise deprotonated species $(-7,1,3)$ $[\text{Al}(\text{HL})_2\text{L}^{7-}]$, $(-8,1,3)$ $[\text{Al}(\text{HL})\text{L}_2^{8-}]$ and $(-9,1,3)$ $[\text{AlL}_3^{9-}]$. Statistical approximations [Perrin *et al.*, 1981] were used to provide initial estimates of the equilibrium constants for the latter two of these species. Calculations indicated that there would be no measurable concentration of AlL_3^{9-} below $-\log h = 9.6$ and this species was not included in further analysis. Use of this series of complexes adequately explained all remaining data. In a final calculation on this data set (10 titrations and 447 data points, $2.2 \leq -\log h \leq 9.6$) the equilibrium constants for all the above species except $(-9,1,3)$ were varied on the whole data set.

The second part of these calculations involved the analysis of data at $C/B < 3.5$. These calculations involved the use of 14 titrations, including 3 dilution titrations, and 280 datum points over the range $2.2 \leq -\log h \leq 4.2$. An initial comparison of experimental and theoretical curves indicated almost no remaining Z_C residuals for $3.0 < C/B < 3.5$, however very large deviations could be seen at $C/B < 2.1$. Once again, *pqr*-analyses were performed on the experimental data to obtain the sets of *p,q,r* triplets giving the lowest value of U_{ZC} and thus best explaining the data. Preliminary analyses indicated that simple mononuclear species had little effect on improving the fit. Results from *pqr*-analyses with $q = 1, 2, 3, 4$ or 5 showed that the species that could 'best' explain the data were those with $r/q = 1$ and $2 \leq q \leq 4$. However, no single species was adequate to explain all the data; therefore combinations of two species with $r/q = 1$ were considered. These calculations indicated that the combination of a species with $r = q = 3$ and another with $r/q = 1$ could adequately explain the data. The final result from these calculations was the inclusion of one species with $r = q = 3$ ($\log \beta_{-6,3,3} = -5.07 \pm 0.05$) and another species with $r = q = 6$, ($\log \beta_{-16,6,6} = -23.2 \pm 0.2$). This gave $U_{ZC}(pr)_q \times 10^{-3} = 6.6$ and $\sigma(Z_C) = 0.02$, where $U_{ZC}(00)_0 \times 10^{-3} = 415.4$. The effect of these two species on the equilibrium constants determined for data with $C/B > 4$ was checked *via* a calculation using both data sets over the range $2.2 \leq -\log h \leq 9.6$. The result of this calculation indicated that the polynuclear species described above had very little effect on the species forming at higher values of C/B . The final results for all species forming in the binary and ternary systems are given in Table 4.2.3 and the fit of experimental data to the resulting theoretical curves has been visualised in Figure 4.2.3A.

Table 4.2.3 Binary and ternary complexes in the H^+ - Al^{3+} -pyrocatechol violet system. The equilibrium constants ($\beta_{p,q,r}$) are given according to the reaction: $p\text{H}^+ + q\text{Al}^{3+} + r(\text{H}_3\text{L}^-) \rightleftharpoons \text{H}_p\text{Al}_q(\text{H}_3\text{L})_r^{(p+3q-r)+}$.

p, q, r	$\log (\beta_{p,q,r} \pm 3\sigma)$	Proposed product formula
$(-1, 0, 1)$	-7.71 ± 0.01^a	H_2L^{2-}
$(-2, 0, 1)$	-17.49 ± 0.02^a	HL^{3-}
$(-3, 0, 1)$	-30.21 ± 0.05^a	L^{4-}
$(-1, 1, 1)$	-0.23 ± 0.04	$\text{Al}(\text{H}_2\text{L})^+$
$(-2, 1, 2)$	-1.02 ± 0.03	$\text{Al}(\text{H}_2\text{L})_2^-$
$(-3, 1, 3)$	-2.57 ± 0.06	$\text{Al}(\text{H}_2\text{L})_3^{3-}$
$(-4, 1, 2)$	-10.21 ± 0.09	$\text{Al}(\text{HL})_2^{3-}$
$(-5, 1, 3)$	-13.03 ± 0.11	$\text{Al}(\text{H}_2\text{L})(\text{HL})_2^{5-}$
$(-6, 1, 3)$	-21.10 ± 0.14	$\text{Al}(\text{HL})_3^{6-}$
$(-7, 1, 3)$	-30.46 ± 0.25	$\text{Al}(\text{HL})_2\text{L}^{7-}$
$(-8, 1, 3)$	-40.75 ± 0.46	$\text{Al}(\text{HL})\text{L}_2^{8-}$
$(-9, 1, 3)$	-52.0 (estimate)	AlL_3^{9-}
$(-6, 3, 3)$	-5.07 ± 0.05	$\text{Al}_3(\text{H}_2\text{L})_3(\text{OH})_3^0$
$(-16, 6, 6)$	-23.2 ± 0.2	$\text{Al}_6(\text{H}_2\text{L})_6(\text{OH})_{10}^{4-}$

^aWhere for the protonation of L^{4-} , $\log K_n = 12.72, 9.78$ and 7.71 for $n = 1-3$ respectively.

With this final model, no systematic deviations remained. The computer program SOLGASWATER [Eriksson, 1979] was used to calculate distribution diagrams. These are presented in Figure 4.2.3C.

Spectrophotometric Titration Results.— The results from the spectrophotometric titrations were not used directly in the model development. They did, however, provide some information on the validity of the model at lower concentrations (*i.e.* potentiometric concentrations are millimolar whereas spectrophotometric concentrations are typically micromolar).

A series of isosbestic points were present in the titration spectra. Model calculations of solutions with identical composition to those used in the titrations were made using the computer program SOLGASWATER (using the equilibrium constants given in Table 4.2.3). These results are presented in Figure 4.2.3D, where the experimentally determined and theoretical isosbestic point ranges are represented by the solid and broken lines respectively.

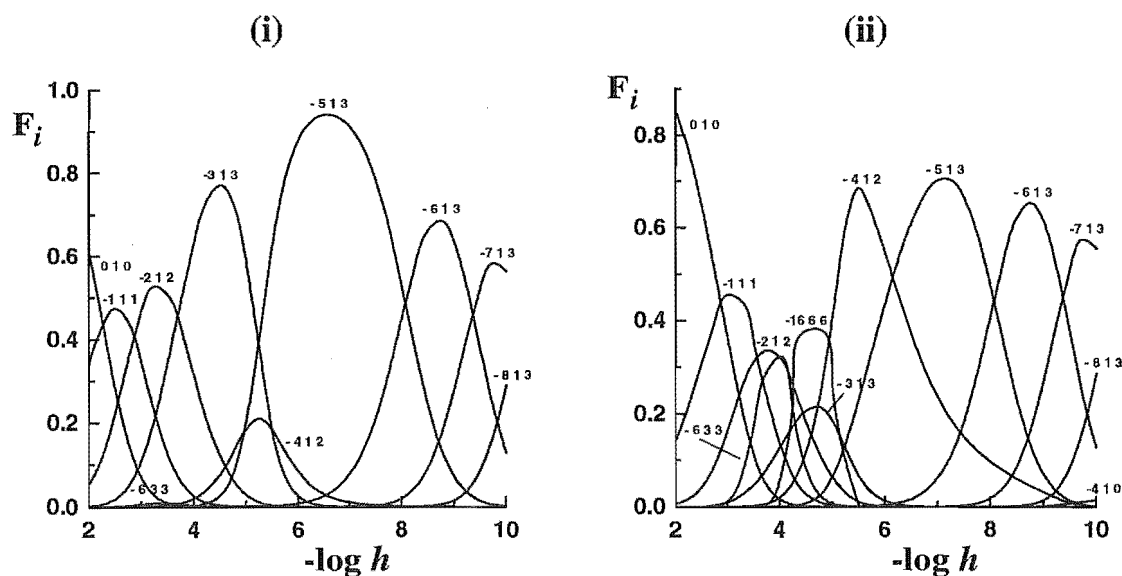


Figure 4.2.3C Distribution diagrams $F_i(-\log h)_{B,C}$ for millimolar concentrations of PCV and Al^{3+} : (i) $C = 10.0 \text{ mmol L}^{-1}$, $B = 1.0 \text{ mmol L}^{-1}$, (ii) $C = 3.0 \text{ mmol L}^{-1}$, $B = 1.0 \text{ mmol L}^{-1}$. F_i is defined as the ratio of the aluminium concentration in an equilibrium species to the total aluminium concentration.

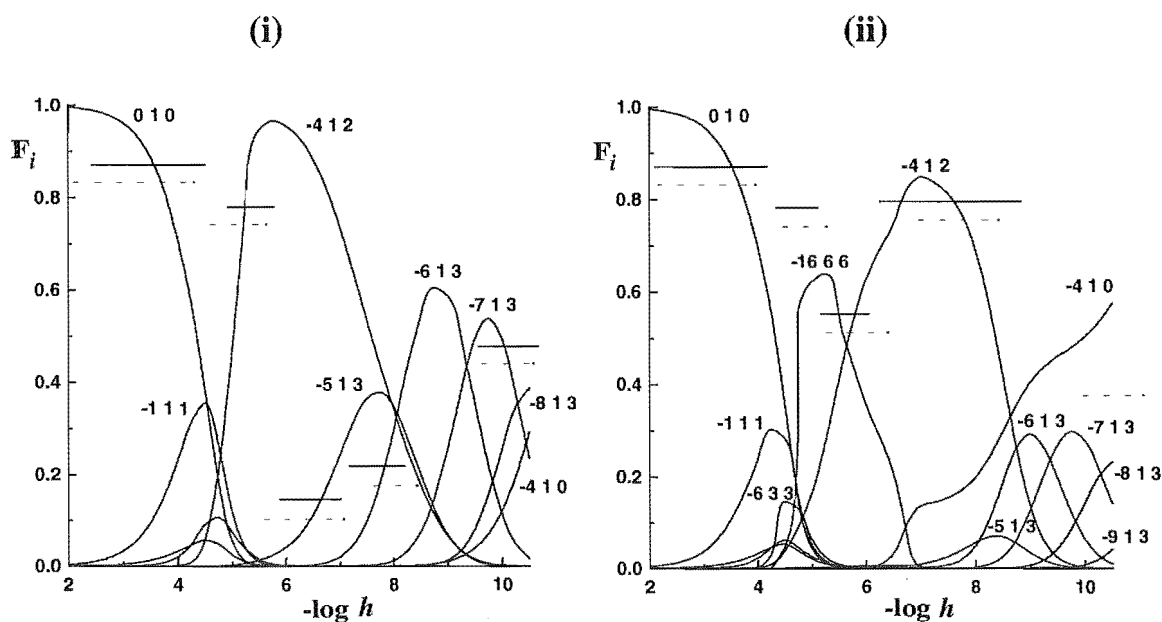


Figure 4.2.3D Distribution diagrams $F_i(-\log h)_{B,C}$ for solutions of identical composition to those of the spectrophotometric titrations. Definitions and conditions as for Fig 4.2.3C. (i) $[\text{PCV}] = 60 \text{ } \mu\text{mol L}^{-1}$, $[\text{Al}^{3+}] = 15 \text{ } \mu\text{mol L}^{-1}$ (ligand:metal = 4) and (ii) $[\text{PCV}] = 70 \text{ } \mu\text{mol L}^{-1}$, $[\text{Al}^{3+}] = 40 \text{ } \mu\text{mol L}^{-1}$ (ligand:metal = 1.75). Here the experimentally determined and theoretical isosbestic point ranges are represented by the solid (—) and broken lines (----) respectively.

The speciation of the Al-PCV system is very complex at lower C/B ratios. However, the $-\log h$ ranges for the isosbestic points found experimentally appear to match those expected for the calculated distribution of Al-PCV species.

4.2.4 DISCUSSION.— The ligand deprotonation constants $\log \beta_{n,0,1}$ reported in Table 4.2.3 are in reasonable agreement with those reported by other workers at the same ionic strength $\{(-7.77; -17.52)$ [Saraswat *et al.*, 1979] and $(-7.90; -17.84)$ [Biryuk and Ravitskaya, 1970]; $n=1,2\}$. However, the values determined previously for the third deprotonation constant $(-11.71$ and -11.82 , $n = 3$ respectively) are significantly lower than the value reported here [$\log (\beta_{-3,0,1} / \beta_{-2,0,1}) = -12.72$]. This difference may be related to the propensity of PCV to undergo oxidation at high $-\log h$ values and the resulting difficulty in accurately determining this dissociation constant. In our study $\log K_1$ was determined under strictly oxygen free conditions. This value can be compared with that for catechol $(-13.43$, Table 4.2.4).

Table 4.2.4 Deprotonation and stability constants for catechol^a and maltol^b

Compound	p,q,r	$\log (\beta_{p,q,r})$	formula
Catechol (H ₂ L)	$(-1,0,1)$	-9.26^c	HL ⁻
	$(-2,0,1)$	-22.69^c	L ²⁻
	$(-2,1,1)$	-5.80	AIL ⁺
	$(-4,1,2)$	-14.83	AIL ₂ ⁻
	$(-6,1,3)$	-28.54	AIL ₃ ³⁻
Maltol (HL)	$(-1,0,1)$	-8.38^c	L ⁻
	$(-1,1,1)$	-0.13	AIL ²⁺
	$(-2,1,2)$	-0.96	AIL ₂ ⁺
	$(-3,1,3)$	-2.67	AIL ₃ ⁰

^a0.1 M KCl [Kennedy and Powell, 1985], ^b0.6 M NaCl [Hedlund and Öhman, 1988].

^cWhere for the protonation of catechol, L²⁻, $\log K_1 = 13.43$ and $\log K_2 = 9.26$ and for maltol, L⁻, $\log K_1 = 8.38$.

The order in which the -OH groups deprotonate may be deduced from the spectral shifts occurring with changes in $-\log h$ and from the structure of the PCV molecule. The large colour change from orange/red ($\lambda_{\max} = 442$ nm) to blue/violet ($\lambda_{\max} = 585$ nm) that accompanies the first deprotonation indicates that proton loss is from the 1,2-dihydroxyaryl moiety; probably the *para*-OH. Deprotonation of the hydroxy

group on the *p*-quinomethide moiety would not be expected to develop enough electron delocalisation for such a colour change. This assignment of protonation constant indicates that in PCV the 1,2-dihydroxyaryl moiety has a significantly higher acidity than does catechol (-9.26, Table 2). This can be rationalised in terms of the electron withdrawing properties of the *p*-quinomethide moiety. A direct comparison of the acidity of the 2-hydroxy-*p*-quinomethide moiety with model compounds is not possible but it is noted that the -OH group is significantly less acidic than the -OH in maltol (Table 4.2.4).

Regarding the three-component system, the species in this series, $\text{Al}(\text{H}_2\text{L})_n$, $n = 1-3$, which form at $-\log h < 4.5$ are probably chelates between Al^{3+} and the 2-hydroxy-*p*-quinomethide (site M) moiety. At higher $-\log h$ values the species forming more likely involve the 1,2-dihydroxyaryl (site P) moiety of PCV, Figure 4.2. These deductions are based on the simulation of expected complexation properties of PCV. Catechol is an appropriate model for the 1,2-dihydroxyaryl moiety on PCV, and maltol should approximate to the binding properties of the 2-hydroxy-*p*-quinomethide moiety. The inductive effects for maltol will be significantly different due to the pyranone oxygen. At intermediate $-\log h$ values there is the possibility of mixed site binding. This is consistent with the species composition $(-5, 1, 3)$ *i.e.* $\text{Al}(\text{H}_2\text{L})(\text{HL})_2^{5-}$.

A comparison may be made between the present results (Table 4.2.3) and the Al equilibria for catechol and maltol (Table 2). Similarities are apparent between the constants obtained for the species $(-1, 1, 1)$, $(-2, 1, 2)$ and $(-3, 1, 3)$ of maltol $[\text{AlL}_n]$ and PCV $[\text{Al}(\text{H}_2\text{L})_n]$. However, significant differences are noted for the species $(-4, 1, 2)$ and $(-6, 1, 3)$ of catechol $[\text{AlL}_2, \text{AlL}_3]$ in comparison to PCV $[\text{Al}(\text{HL})_2, \text{Al}(\text{HL})_3]$. In the Al^{3+} -PCV system the equivalent species form at a lower $-\log h$ than in the Al^{3+} -catechol system. This can be explained by the much larger first (and larger second) deprotonation constant for the 1,2-dihydroxyaryl moiety in PCV compared to that of catechol. Modelling calculations indicated that the 'catechol' site would not bind a significant fraction of Al until $-\log h > 7$. Because of the stronger binding by the 1,2-dihydroxyaryl moiety in PCV, this site begins to dominate Al binding at *ca.* $-\log h = 5$, *i.e.* lower than predicted from the modelling and consistent with the higher acidity of the 1,2-dihydroxyaryl moiety of PCV. The only other stability constants for the H^+ - Al^{3+} -PCV system were determined by Goina *et al.* (1970). Their results ($\log K_n = 25.12, 22.27$ and 20.74 , $n = 1-3$ respectively) are anomalously high compared with other catecholate ligands.

The observation that a series of one proton reactions occurs at $-\log h > 8$ is consistent with (i) complexes having the 1,2-dihydroxyaryl moiety binding to Al (as in $\text{Al}(\text{HL})_3^{6-}$, $\text{Al}(\text{HL})_2\text{L}^{7-}$ *etc.*), and (ii) the assignment of the second protonation constant of the free ligand to the -OH group on the 2-hydroxy-*p*-quinomethide moiety. The $\text{p}K_a$ calculated for formation of $\text{Al}(\text{HL})\text{L}_2^{8-}$ from $\text{Al}(\text{HL})_2\text{L}^{7-}$ (10.29) is significantly higher than the $\text{p}K_a$ of the group presumed to be deprotonating (9.78 for the free ligand); it is

also higher than that estimated from statistical considerations ($9.36 + \log 3$) where $\log \beta_{-7,1,3} - \log \beta_{-6,1,3} = 9.36$. This observation may indicate that disturbance of the charge distribution by the Al centre significantly affects the dissociation of the conjugated pendant -OH group; an apparent shift of > 0.4 occurs in the pK_a of the uncoordinated 2-hydroxy-*p*-quinomethide proton. Further, conjugation within the ligands means that the pendant 2-hydroxy-*p*-quinomethide groups are not electronically independent. Dissociation of one such group (to form $\text{Al}(\text{HL})_2\text{L}^{8-}$) affects the net phenoxide electron density about the Al^{3+} centre and lowers the acidity of the remaining pendant groups. A similar phenomenon has been reported previously for Al-protocatechuic acid complexes [Kennedy and Powell, 1985] where the apparent pK_a of the carboxy group was shifted $\sim +0.4$. This contrasts with ligand systems where the coordinated and pendant groups are not conjugated; for example in the $\text{Al}(\text{dopamine})_3$ complexes dissociation constants for the non-coordinated $-\text{NH}_3^+$ groups are statistically related.

Deprotonated pyrocatechol violet (H_2L^{2-}) can be represented by resonance structures involving conjugation between the 2-hydroxy-*p*-quinomethide (M) site and the monoprotinated 1,2-dihydroxyaryl site (P) (as depicted in Figure 4.2.4A).

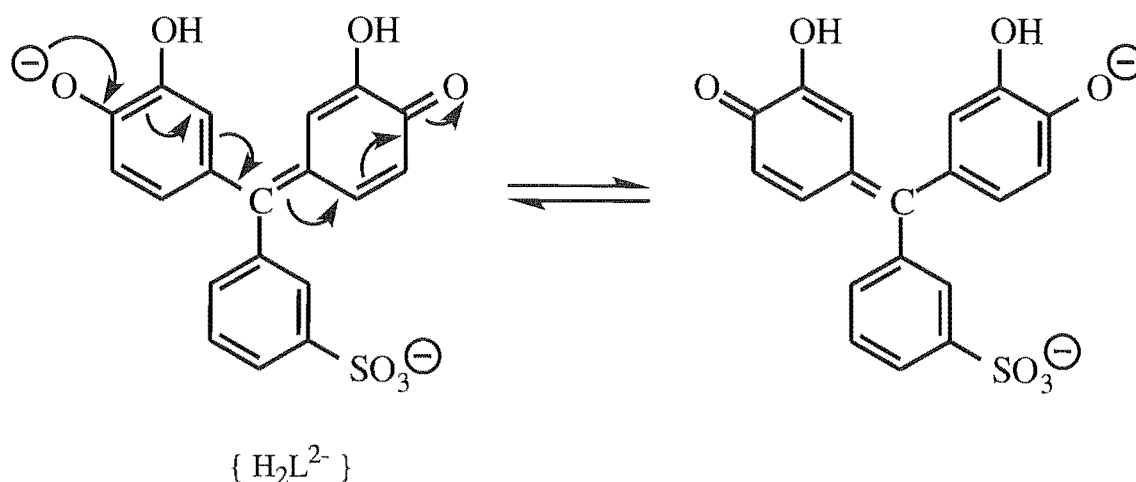


Figure 4.2.4A Possible resonance structures of the deprotonated pyrocatechol violet moiety, H_2L^{2-} .

The conjugation in the pyrocatechol violet moiety H_2L^{2-} provides a mechanism for Al^{3+} bound at site M to become bound by site P without altering its chelation position. The complex merely undergoes a deprotonation and an intramolecular electron shift. The formation of $\text{Al}(\text{HL})_2^{3-}$ from the tri-coordinated $\text{Al}(\text{H}_2\text{L})_3^{3-}$ species can be thought of as

arising from such a mechanism. The transition from a tris species $\text{Al}(\text{H}_2\text{L})_3^{3-}$ to a bis species $\text{Al}(\text{HL})_2^{3-}$ with increasing $-\log h$ may be rationalised in terms of the change in electron density surrounding the Al^{3+} centre. The charge stabilisation effected by two deprotonated 1,2-dihydroxyaryl moieties is, apparently, at least equivalent to three deprotonated 2-hydroxy-*p*-quinomethide moieties, resulting in a species of similar or greater stability.

Titration at lower *C/B* ratios indicated the species $(-6,3,3) [\text{Al}_3(\text{H}_2\text{L})_3(\text{OH})_3^0]$ and $(-16,6,6) [\text{Al}_6(\text{H}_2\text{L})_6(\text{OH})_{10}^{4-}]$ are formed at $-\log h < 4.2$ (Figure 4.2.3C). These titrations were terminated at $-\log h < 4.2$ due to precipitation (observed in solutions with *C/B* = 1); this may be due to formation of polymerised or uncharged species. Calculations using the final constants indicated that these species exist up to $-\log h \approx 6.5$. It is possible that they represent the summation of a larger series of polynuclear mixed hydroxo species.

The verification of $(-16,6,6)$ in the model required to fit the data at the higher $-\log h$ values was aided by dilution titrations. For these data polymers of low nuclearity were unable to explain the large systematic deviations recorded. The minimum in U_{ZC} was found at a nuclearity of six, whereby further increases in the nuclearity resulted in increased values of U_{ZC} . In studies of the related phthalein dye CAS (which has salicylate and *p*-quinomethide-2-carboxylic acid residues), linear Al-CAS polymers (*e.g.* $\text{Al}_x\text{H}_{-x}\text{L}_{1+x}$, $x = 4$ or 5) were reported forming at $2.5 < -\log h < 6$ [Hawke *et al.*, 1995]. The formation of such polymers is not possible for PCV because deprotonation and coordination of the 1,2-dihydroxyaryl moiety does not occur below $-\log h \approx 4$. Therefore these polymers must involve either hydroxy and/or *o*-quinonoid (O^-) bridges between adjacent Al^{3+} ions. Such polymeric units have been established for Al at low $-\log h$ in a great number of systems with organic ligands *e.g.* in the citrate, $[\text{Al}_3(\text{OH})(\text{alkoxide})_3]$ [Öhman, 1988], and lactate and propionate complexes, $[\text{Al}_2(\text{OH})_2\text{L}]$ [Marklund, 1990; Marklund and Öhman, 1990].

Spectrophotometric Analysis of Aluminium.— Determinations of Al in environmental samples are often carried out spectrophotometrically using the formation of an Al-PCV complex at $-\log h \approx 6$. From spectrophotometric molar ratio plots it has been found that the Al:PCV ratio is 1:2 near pH 6 under spectrophotometric conditions ($[\text{PCV}]$ *ca.* 20 μM , $[\text{Al(III)}]$ 0–10 μM). SOLGASWATER calculations were made using the constants from these studies (Table 4.2.3) to determine the species in solution at $-\log h = 6$ at spectrophotometric concentrations. The dominant species forming at $-\log h = 6$ was $\text{Al}(\text{HL})_2^{3-}$ (Figure 4.2.4B), consistent with spectrophotometric molar ratio plots. This species dominates in the $-\log h$ range *ca.* 4.9–8.0. However its formation is (near) quantitative (> 95 %) only in the range $-\log h = 5.6$ –6.5.

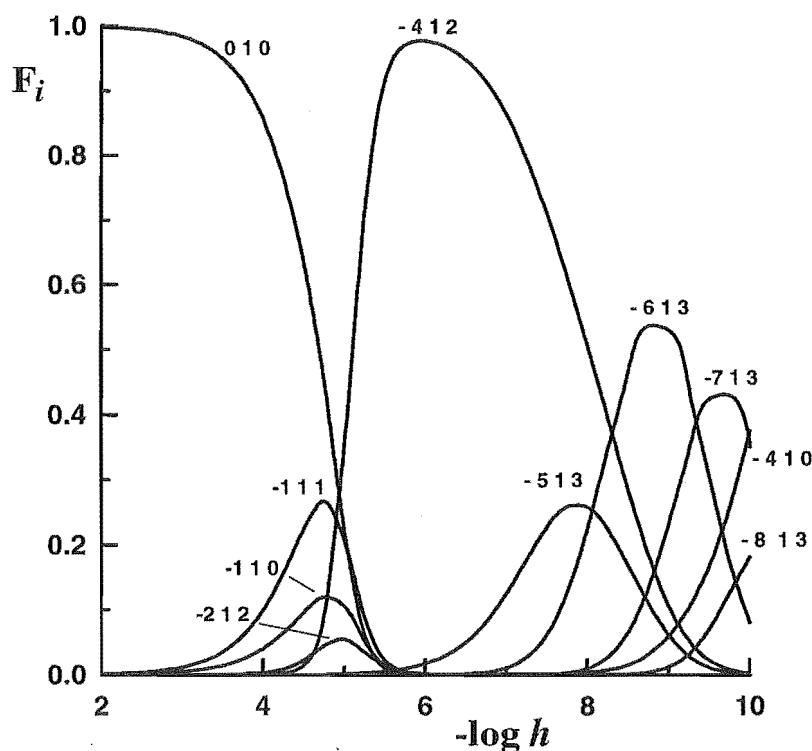


Figure 4.2.4B Distribution diagrams $F_i(-\log h)_{B,C}$ for micromolar concentrations, $C = 20 \mu\text{mol L}^{-1}$ and $B = 4 \mu\text{mol L}^{-1}$. Definition and method as for Figure 4.2.3C.

The suitability of a ligand for the analysis of Al will be impaired if the ligand interacts with untargeted materials. Mineral oxides and clay materials are abundant in many natural waters and soil solutions. Much is within the colloidal range and would not be removed by a $0.45 \mu\text{m}$ filter. Therefore the potential solubilising effects of PCV on natural mineral oxides was investigated by making a number of model calculations using the computer program SOLGASWATER. In these calculations a hypothetically one molar solution of gibbsite [$\log^* K_{s0} = 8.309$, Palmer and Wesolowski (1992)] was equilibrated with water and PCV. From Figure 4.2.4C it can be seen that even at very low concentrations PCV increases the solubility of gibbsite over a large $-\log h$ range (if equilibrium is attained). At a typical analytical $-\log h$ (6.0) and PCV concentration ($30 \mu\text{mol L}^{-1}$) the effect of gibbsite (assuming equilibrium) would be to enhance the apparent concentration of Al in solution by *ca.* $5 \mu\text{mol L}^{-1}$. Attainment of equilibrium may require extremely long reaction times. It would, however, introduce a significant error in a typical working range of $0.5\text{--}10 \mu\text{mol L}^{-1}$ Al. These calculations indicate that the error arising from the gibbsite dissolution will be minimised if (i) PCV is not used in large excess for spectrophotometric measurements, (ii) the $-\log h$ is kept as low as possible within the allowable window (5.8–6.6) for quantitative formation of $\text{Al}(\text{HL})_2^{3-}$, and (iii) the reaction time is short to ensure minimal dissolution of gibbsite.

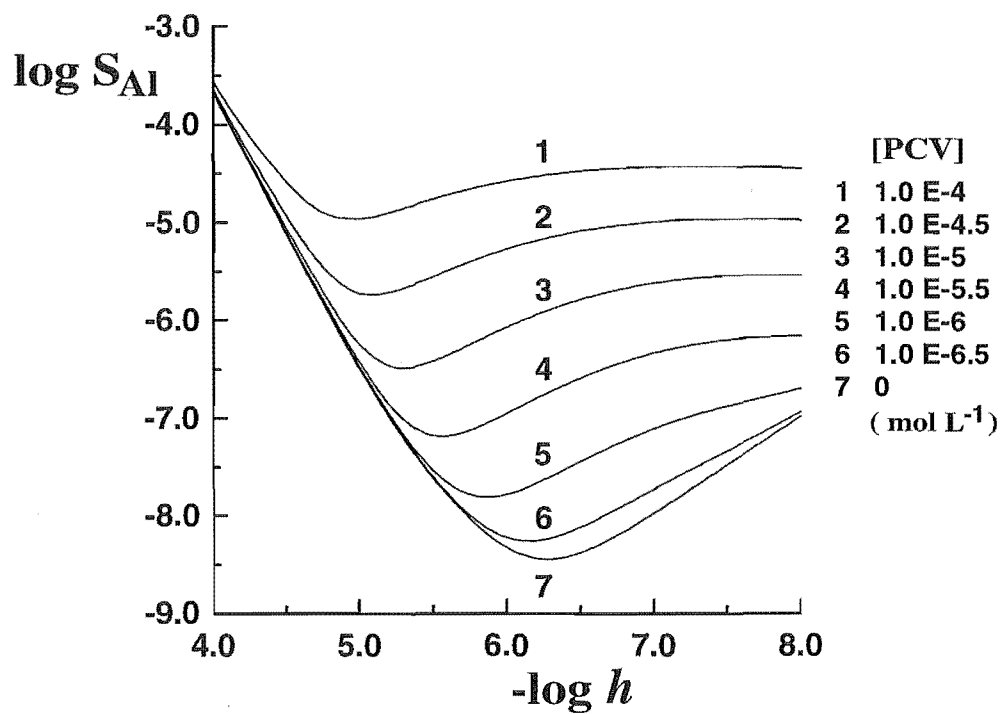


Figure 4.2.4C The effects of pyrocatechol violet on the calculated solubility of gibbsite { $\log^* K_{s0} = 8.309$; [Palmer and Wesolowski, 1992]}.

SECTION B: POTENTIOMETRIC STUDIES OF ALUMINIUM(III)- 4-NITROCATECHOL EQUILIBRIA

4.3 4-NITROCATECHOL (4NCAT)

A significant, and on-going, project of this research group involves the investigation of amperometric and voltammetric techniques for the electrochemical analysis of Al. This work involves the characterisation of the solution equilibria and the electrochemical behaviour of ligands that form stable complexes with Al and may produce a useful electrochemical response, which is suitably modified on binding to Al. The electrochemical analysis of Al is discussed in Chapter 7.

The ligand, 4-nitrocatechol (4ncat, Figure 4.3) has been investigated by this group [Lenihan, 1994] for the purpose of developing an FIA amperometric technique for Al analysis. 4ncat is known to form a very stable complex with Al, which will form quantitatively in the $1\text{--}10\text{ }\mu\text{mol L}^{-1}$ Al range ($10\text{--}50\text{ }\mu\text{mol L}^{-1}$ ligand). Stability constants have been reported for the complexes AlL^+ , AlL_2^- and AlL_3^{3-} (where $\text{H}_2\text{L} = 4\text{ncat}$) from measurements in solutions with ligand:metal (C/B) ratios 3:1 to 6:1 and millimolar concentrations [Häkkinen, 1984c]. The pH ranges used in the calculation of these constants was pH 3.0 - 6.25. Under these conditions there was no evidence for the formation of ternary, hydroxy-Al-ligand species, which, by analogy with other 1,2-dihydroxyaryl- systems, may be expected to form [Öhman and Sjöberg, 1983; Kennedy and Powell, 1985].

In the studies by Lenihan (1994) it was found that 4ncat will be most useful, for electroanalysis of Al, at pH 9.0. Unfortunately, data were not collected to this pH in the studies by Häkkinen, and hence the model may not be valid above pH 6. Furthermore, the model was developed using only data at higher C/B ratios. It would be desirable to know whether any other species are likely to exist at lower C/B ratios.

In the present work the deprotonation and Al^{3+} formation constants for 4ncat have been redetermined.

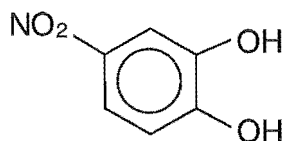


Figure 4.3 4-nitrocatechol (4ncat, H_2L).

4.3.1 EXPERIMENTAL

(A) **Chemicals and Analysis.**— All solutions were prepared from CO₂-free, boiled Milli-Q water and all working solutions were prepared in 0.10 M KCl (BDH, AnalaR), dried at 120 °C.

(i) **4-Nitrocatechol Solutions:** 4ncat, 1,2-Dihydroxy-4-nitrobenzene is depicted in Figure 4.3. Reagent grade 4ncat was obtained from Sigma and used without further purification. Microanalysis established the composition: C, 46.51 %; H, 3.18 %; N, 9.10 % (cf. calc. for C₆H₅O₄N: C, 46.46 %; H, 3.25 %; N, 9.03 %. Stock 4ncat solutions were prepared in excess 0.02 mol L⁻¹ HCl to prevent ligand oxidation and minimise biological activity.

(ii) **Aluminium Solutions:** A stock solution of Al³⁺ (ca. 0.08 mol L⁻¹) was prepared from AlCl₃·6H₂O [ALFA (99.9995 %)] in ca. 0.05 mol L⁻¹ HCl and was standardised as described in Chapter 3 [3.2.5(A)].

(iii) **Standard Alkali (KOH) and Acid (HCl) Solutions:** Standard HCl (BDH, AnalaR) solutions were prepared and standardised as described in Chapter 3 [3.2.2]. Carbonate free KOH (BDH, AnalaR) solutions (ca. 0.2-0.3 mol L⁻¹) were prepared and standardised according to Chapter 3 [3.2.1(A)].

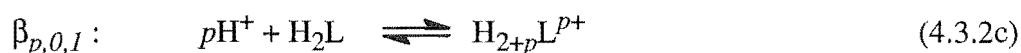
(B) **Potentiometric Titrations.**— The titration set-up and cell arrangement is described in Chapter 3 [3.10.1(A)]. The electrode pair was calibrated for the measurement of p[H⁺] as described in Chapter 3 [3.11.3A(i)]. Throughout titrations with $C/B < 2.0$, the minimum addition rate (125 μL min⁻¹) of alkali was used to minimise the localised formation of polymeric Al³⁺ hydrolysis products. The conditions defining the establishment of pH equilibrium [see 'delay times', Chapter 2 (2.3)] differed for each titration (longer equilibrium periods used at lower C/B ratios). Generally solution pH was monitored at 3-6 min intervals after the addition of each aliquot until the means of 3 successive replicates (30 measurements) gave stable readings within ± 0.002 p[H⁺].

Titrations for determination of the dissociation constants log β_{-1,0,1} and log β_{-2,0,1} for 4ncat were performed separately within the ranges 0.0015 mol L⁻¹ ≤ C ≤ 0.004 mol L⁻¹ (where C = total concentration of 4ncat). Each titration consisted of ca. 90 datum points in the range 3.0 ≤ p[H⁺] ≤ 11.0.

In three-component titrations B and C were varied within the limits 0.0004 mol L⁻¹ ≤ B ≤ 0.0012 mol L⁻¹ and 0.0007 mol L⁻¹ ≤ C ≤ 0.0025 mol L⁻¹, covering C/B ratios in the range 1-4 (B denotes the total Al concentration). Titrations typically had 100-140 data points for $C/B > 2.0$ and 15-25 data points for $C/B = 1.0$.

4.3.2 DATA TREATMENT

Potentiometry.— Data treatment assumed the presence of three-component equilibria of the general form (4.3.2a) and the two-component equilibria (4.3.2b) and (4.3.2c):



The law of mass action and the conditions for the total concentrations are applied to these equilibria to give the equations 4.2.2d-f (see Section 4.2). Where, $b = [\text{Al}^{3+}]$ and $c = [\text{H}_2\text{L}]$.

The Al^{3+} hydrolysis constants (defined according to equation 4.3.2b) were from Brown *et al.* (1985). The formation constants for $\text{Al}(\text{OH})_4^-$ ($\log \beta_{-4,1,0}$) and $\text{Al}(\text{OH})_3$ ($\log \beta_{-3,1,0}$) were calculated by the method of Millero and Schreiber (1982) from the thermodynamic constants of Palmer and Wesolowski (1992) and Nordstrom and May (1989) respectively [assuming $\gamma(\text{Al}(\text{OH})_4^-) = \gamma(\text{OH}^-)$]. These Al hydrolysis species were: AlOH^{2+} ($\log \beta_{-1,1,0} = -5.33$), $\text{Al}(\text{OH})_2^{2+}$ ($\log \beta_{-2,1,0} = -10.91$), $\text{Al}_3(\text{OH})_4^{5+}$ ($\log \beta_{-4,3,0} = -13.13$), $\text{Al}_{13}(\text{OH})_{32}^{7+}$ ($\log \beta_{-32,13,0} = -107.41$), $\text{Al}(\text{OH})_3$ ($\log \beta_{-3,1,0} = -17.32$) and $\text{Al}(\text{OH})_4^-$ ($\log \beta_{-4,1,0} = -23.3$).

The least-squares computer program SUPERQUAD [Gans *et al.*, 1985] was used to determine sets of p, q, r triplets and the corresponding equilibrium constants that 'best' fit the experimental data [see Chapter 2 (2.1.4)]. The best model was determined visually from SUPERQUAD outputs of residuals and from goodness of fit parameters, χ^2 and σ .

4.3.3 DATA, CALCULATIONS, RESULTS.— The data used to calculate $\log \beta_{-1,0,1}$ and $\log \beta_{-2,0,1}$ comprised 12 titrations with *ca.* 1000 datum points. The calculations established $\log \beta_{-1,0,1} (\pm 3\sigma) = -6.67 \pm 0.02$ and $\log \beta_{-2,0,1} = -17.55 \pm 0.08$.

Prior to numerical analysis of the three-component system, the data determined by Häkkinen (1984c) was used to calculate distribution diagrams. These calculations provided information on the pH range at which the species AlL^+ , AlL_2^- and AlL_3^{3-} could be expected to form under the conditions used in the present experiments. It also indicated the important pH ranges over which binary or polymeric $\text{Al}_q(\text{OH})_n^{(3q-n)+}$ species are likely to form.

The analysis of the three-component data comprised 12 titrations with *ca.* 1100 datum points. For titrations with $C/B \sim 1$, the titration curves showed a well defined inflection at $p[H^+]$ 4.6 (corresponding to titration of excess acid and formation of AIL , *i.e.* 2 moles of OH^- per mole of Al^{3+}) followed by a second buffer region (characterised by excessive drift above $p[H^+]$ 5.25) and an inflection at $p[H^+]$ 6.4 [consistent with the formation of equimolar AIL_2 and $Al(OH)_3$]. For $C/B \sim 2$, titration curves showed a minor inflection at $p[H^+]$ 4.0 (corresponding to formation of AIL) and a major inflexion at $p[H^+]$ 5.9 (corresponding to formation of AIL_2) followed by a third buffer region characterising the formation of $Al(OH)L_2^{2-}$. Calculations used data up to $p[H^+]$ 8.2. The titrations at $C/B > 3$ showed inflexions at $p[H^+]$ 4.0 and 5.25 and a major inflexion at $p[H^+]$ 8.0, corresponding to the stepwise formation of AIL^+ , AIL_2^- and AIL_3^{3-} respectively.

For titration with $2.0 < C/B < 3.0$, Z_C [the moles of protons titrated per mole of ligand, see Chapter 2 (2.1.3) for definition] exceeded 2.0 at $p[H^+] > ca. 6$ indicating a contribution of hydroxy species to the protonation equilibria. For titrations with $1.0 < C/B < 1.2$, Z_C exceeded 2.0 at $p[H^+] > 4.75$; this indicated the contribution of metal-hydroxy and (possibly) metal-hydroxy-ligand species to the equilibrium model.

The non-linear least squares analysis of the data was effected in terms of the equilibria: $pH^+ + qAl^{3+} + r(H_2L) \rightleftharpoons H_pAl_q(H_2L)_r^{(p+3q)+}$. The final results for all species forming in the binary and ternary systems are given in Table 4.3.3.

Table 4.3.3 Binary and ternary complexes in the H^+ - Al^{3+} -4-nitrocatechol system. The equilibrium constants ($\beta_{p,q,r}$) are given according to the reaction: $pH^+ + qAl^{3+} + r(H_2L) \rightleftharpoons H_pAl_q(H_2L)_r^{(p+3q)+}$.

p,q,r	$\log (\beta_{p,q,r} \pm 3\sigma)$	Proposed product formula
(-1,0,1)	-6.67±0.02	HL^-
(-2,0,1)	-17.55±0.08	L^{2-}
(-2,1,1)	-3.80±0.04	AIL^+
(-4,1,2)	-9.66±0.05	AIL_2^-
(-5,1,2)	-17.17±0.45	$AIL_2(OH)^{2-}$
(-6,1,3)	-18.27±0.07	AIL_3^{3-}

With this final model the computer program SOLGASWATER [Eriksson, 1979] was used to calculate distribution diagrams. These are presented in Figure 4.3.3.

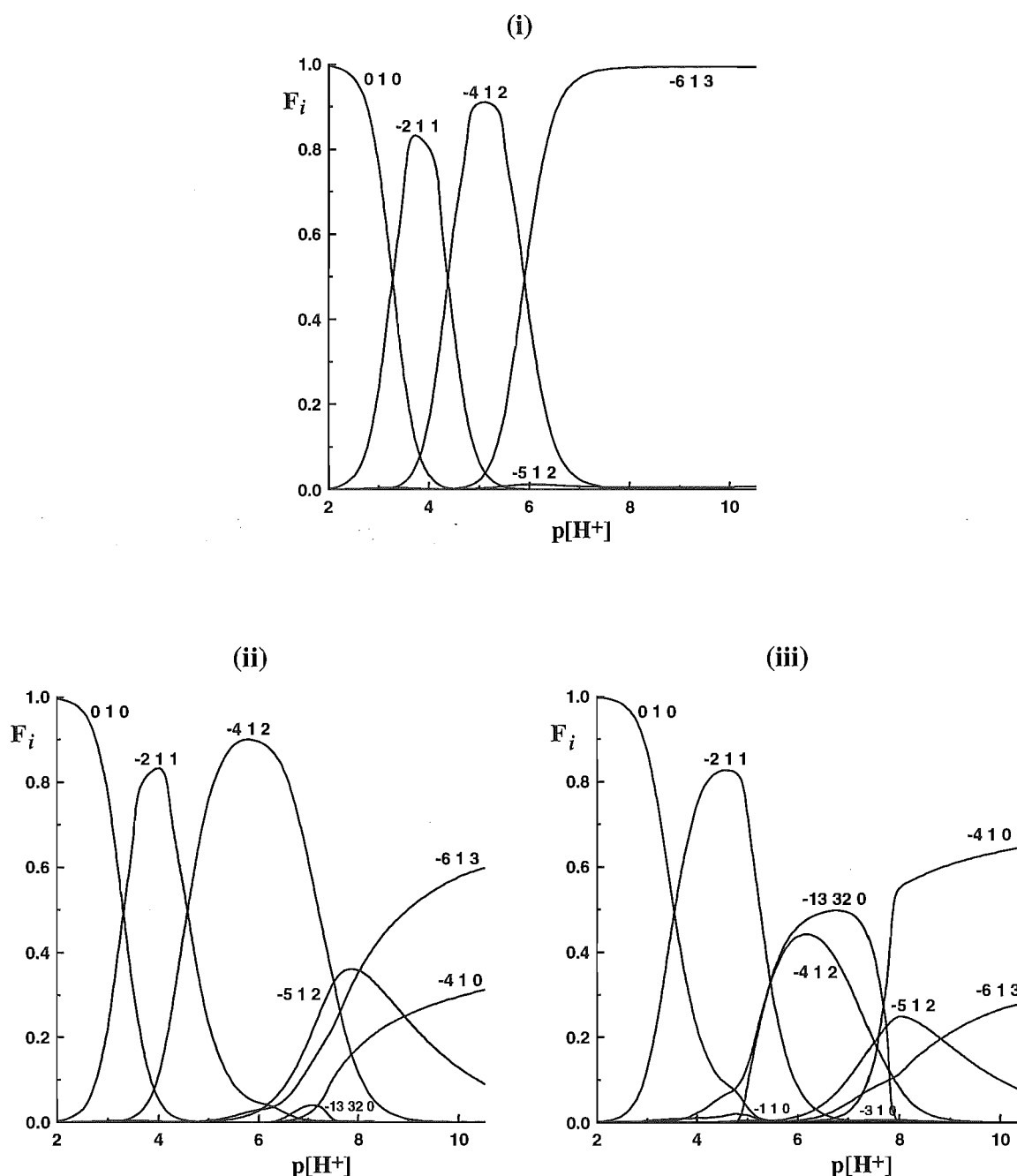


Figure 4.3.3 Distribution diagrams $F_i(p[H^+])_{B,C}$ for millimolar concentrations of 4ncat and Al^{3+} . F_i is defined as the ratio of the aluminium concentration in an equilibrium species to the total aluminium concentration. The calculations have been performed with the computer program SOLGASWATER with the equilibrium constants given in Table 4.3.3. (i) $[4ncat] = 2.0 \text{ mmol L}^{-1}$; $[Al^{3+}] = 0.5 \text{ mmol L}^{-1}$, (ii) $[4ncat] = 2.0 \text{ mmol L}^{-1}$; $[Al^{3+}] = 1.0 \text{ mmol L}^{-1}$ and (iii) $[4ncat] = 1.0 \text{ mmol L}^{-1}$; $[Al^{3+}] = 1.0 \text{ mmol L}^{-1}$.

4.3.4 DISCUSSION.— The protonation constants (25 °C, 0.1 mol L⁻¹ medium) for 4ncat have been determined by a number of researchers. The results from the present work are in good agreement with this previous work (Table 4.3.4).

Table 4.3.4A Protonation constants for 4-nitrocatechol (0.1 mol L⁻¹ medium, 25 °C)

Medium (0.1 mol L ⁻¹)	log $\beta_{1,0,0}$	log $\beta_{2,0,0}$	reference
KCl	10.88(10)	17.55(08)	This work
KCl	10.95	17.73	Pichet <i>et al.</i> , 1967
KCl	10.88	17.65	--- (spectrophotometrically)
KCl	10.71	17.57	Hakoila <i>et al.</i> , 1972
KCl	10.64	17.42	--- (spectrophotometrically)
KNO ₃	10.74	17.44	Jameson and Wilson, 1972
KCl	10.83	17.53	Häkkinen, 1984c
KNO ₃	11.00	17.55	Das, 1989

Häkkinen (1984) has determined the formation constants for the complexes with Al³⁺, Cd²⁺ and Be²⁺ [Häkkinen, 1984c], Mg²⁺, Ca²⁺, Sr²⁺ and Ba²⁺ [Häkkinen, 1985], Cu²⁺ and Zn²⁺, [Häkkinen, 1984a] and Mn²⁺, Co²⁺, Ni²⁺ and Fe³⁺ [Häkkinen, 1984b], all in 0.1 mol L⁻¹ KCl, 25 °C. Data for the Ca²⁺ and Ni²⁺ complexes are reported for 0.1 mol L⁻¹ KNO₃, 25 °C [Jameson and Wilson, 1972] and for Ga²⁺ in 0.1 mol L⁻¹ KCl at 25 °C [Pichet *et al.*, 1967].

In Häkkinen's studies of the Al-4ncat system, titrations were limited to high *C/B* ratios (3-6) and the pH range 3.0-6.25. It was necessary for the present work to establish the speciation at lower *C/B* ratios (as may arise in FIA or voltammetric analysis) and in the pH range used for electroanalytical determinations [*ca.* pH 9; Lenihan, 1994]. The high *C/B* ratios used by Häkkinen would conceal the existence of metal-hydroxy-ligand species. Such species have been characterised in many Al³⁺-1,2-dihydroxyaryl systems. Both AlL(OH) and AlL₂(OH)²⁻ have been reported for 1,2-dihydroxynaphthalene-4-sulfonic acid [Öhman *et al.*, 1983] and for catechol, protocatechuic acid and catechin [Öhman and Sjöberg, 1983; Kennedy and Powell, 1985]. The present work established the existence of the AlL₂(OH)²⁻, log $\beta_{-5,1,2} = -17.2 \pm 0.4(3\sigma)$. Evidence for the existence of AlL(OH) was equivocal. It is, if formed, a very minor species around pH 5 in titrations at low *C/B* ratios; for this pH and stoichiometry pH drift is problematic. The characterisation of AlL₂(OH)²⁻ highlights the importance of measuring formation constants over a wide range of solution stoichiometries and pH. It also emphasises that calculations using published

formation constants should not employ solution stoichiometries or pH ranges widely different from those used in the experimental determinations.

The constants $\log (\beta_{p,q,r} \pm 3\sigma)$ determined in this work are given in Table 4.3.4B and compared with Häkkinen's β_n values (after conversion to $\beta_{p,q,r}$ using his protonation constants). The results for complexes AlL_n are in excellent agreement. Data are also given for other substituted 1,2-dihydroxyaryl ligands.

Table 4.3.4B Comparison of ternary complexes in the H^+-Al^{3+} -4ncat system with Häkkinen's β_n values and other substituted 1,2-dihydroxyaryl ligands. All constants have been converted into the $\log \beta_{p,q,r}$ format using protonation constants from the relevant papers. Hence, the equilibrium constants ($\log \beta_{p,q,r}$) are given according to the reaction: $pH^+ + qAl^{3+} + r(H_2L) \rightleftharpoons H_pAl_q(H_2L)_r^{(p+3q)+}$.

Ligand	Species [†] :	AlL^+	AlL_2^-	$AlL_2(OH)^{2-}$	AlL_3^{3-}
	$\log \beta_{p,q,r}$ (p,q,r):	(-2,1,1)	(-4,1,2)	(-5,1,2)	(-6,1,3)
4ncat ^a		-3.80	-9.66	-17.17	-18.27
4ncat ^b		-3.79	-9.68	-	-18.28
Catechol ^c		-4.54	-13.20	-21.17	-23.40
Protocatechuic acid ^c		-4.26	-13.03	-20.64	-22.19
Catechin ^c		-3.33	-12.63	-20.95	-22.68
1,2-dihydroxynaphthalene- 4-sulfonic acid ^d		-5.34	-13.12	-21.15	-24.47

^a This work; ^b Häkkinen (1984c); ^c Kennedy and Powell (1985) and Kennedy *et al.* (1984); ^d Öhman and Sjöberg (1983).

[†] Here L represents the equivalent 1,2-dihydroxyaryl ligand (H_2L), *i.e.* the protons displaced during Al complexation are from the 'catechol' moiety.

From Table 4.3.4B, the greater stability of Al complexes with 4ncat compared with other 1,2-dihydroxyaryl ligands can be observed. Only the equivalent catechin species, AlL^+ , is observed to be of greater stability in comparison to the corresponding Al-4ncat species.

The high stability of the Al-4ncat complexes is of great importance to the use of 4ncat in the electroanalysis of Al in dilute solutions. In comparison to other 1,2-dihydroxyaryl ligands, 4ncat will quantitatively complex Al at (i) lower pH and (ii) lower concentrations of both metal and ligand. Both of these properties are very desirable and

will allow significantly lower detection limits to be obtained with this ligand. The Al-complexing properties of this ligand are presented as distribution diagrams (Figure 4.3.4) calculated for environmental concentrations of Al and micromolar concentrations of 4ncat (typical for FIA analysis).

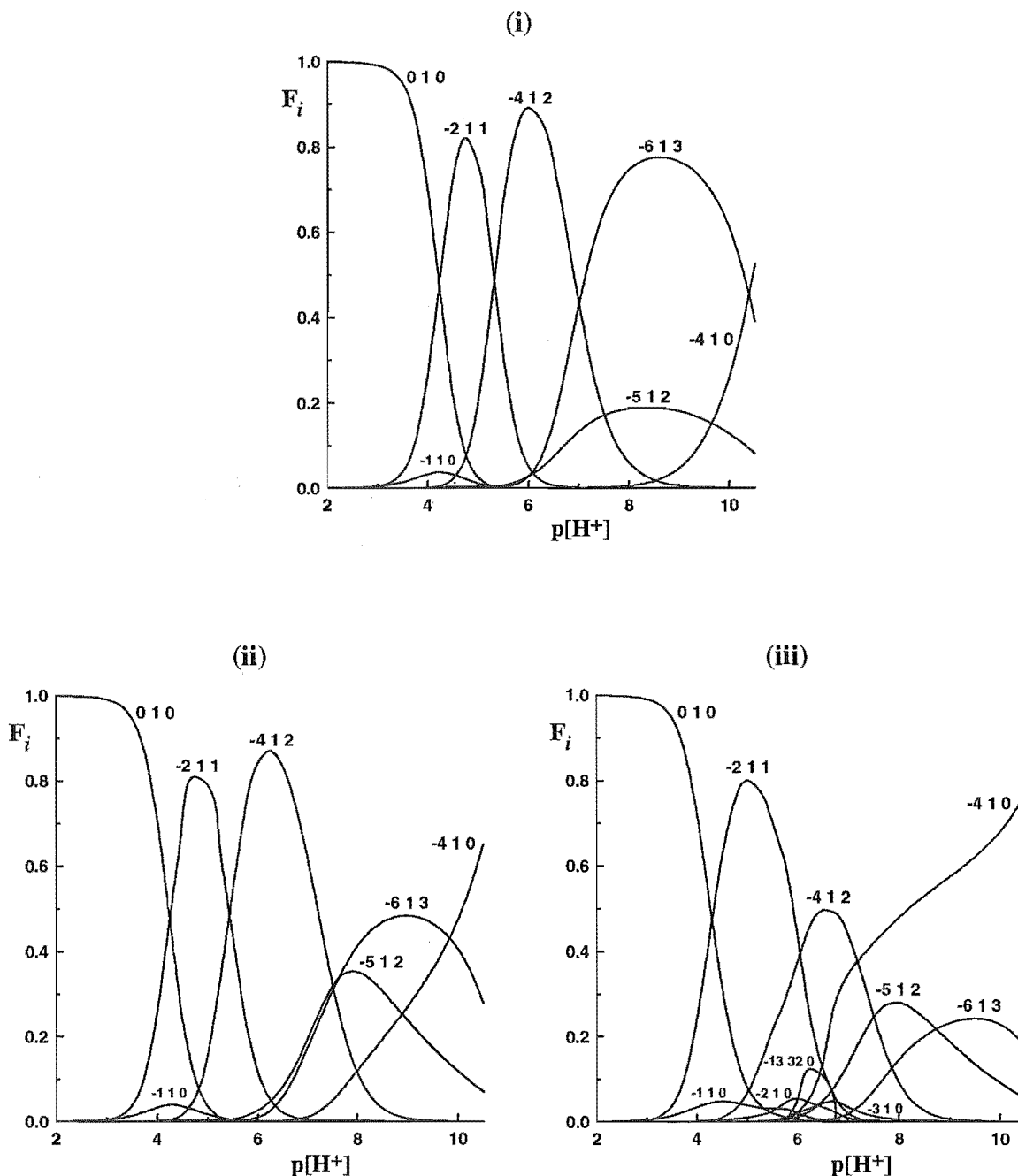


Figure 4.3.4 Distribution diagrams $F_i(-\log h)_{B,C}$ for micromolar concentrations of 4ncat and Al^{3+} (typical concentrations at the detector in FIA analysis). Definitions and conditions as for Figure 4.2.4. (i) $[4ncat] = 25 \mu\text{mol L}^{-1}$; $[Al^{3+}] = 5 \mu\text{mol L}^{-1}$, (ii) $[4ncat] = 25 \mu\text{mol L}^{-1}$; $[Al^{3+}] = 10 \mu\text{mol L}^{-1}$ and (iii) $[4ncat] = 25 \mu\text{mol L}^{-1}$; $[Al^{3+}] = 20 \mu\text{mol L}^{-1}$.

The distribution curves shown in Figure 4.3.4 indicate that the species $\text{AlL}_2(\text{OH})^{2-}$ will form in the pH range desired for FIA electroanalysis of Al. Furthermore, a significant excess of ligand is required (at *ca.* pH 9) to avoid the formation of the aluminate ion $[\text{Al}(\text{OH})_4^-]$ during analysis.

The results presented in Figure 4.3.4 are for thermodynamic equilibrium conditions. In FIA work (as in most analytical methods) equilibrium is never reached; therefore, the analyst cannot be sure whether the secondary species [*e.g.* AlL_2 , $\text{AlL}_2(\text{OH})$ or AlL_3] have sufficient time to form [Hawke *et al.*, 1994]. Hawke *et al.* investigated the metallochromic reagents CAS, ECR and PCV for the kinetic determination of reactive Al. These methods involved very short reaction times between the reagent and Al and it was observed that, under the time-scale of the studies, Al formed a 1:1 complex with PCV (*ca.* pH 6.2). Thermodynamic calculations indicate (see Figure 4.2.4A) that the dominant species forming should be that of $\text{Al}(\text{PCV})_2$ (*i.e.* a 1:2 complex).

The problems which chemical kinetics cause in the use of thermodynamic data for approximating experimental systems used for analysis is discussed in Chapter 6.

CHAPTER 5

PYROCATECHOL VIOLET COMPLEXATION AT THE BOEHMITE-WATER INTERFACE

5.1 ADSORPTION OF ORGANIC LIGANDS AND METALS AT HYDROUS OXIDE SURFACES

5.1.1 INTRODUCTION.— The potential of naturally occurring surfaces, *viz* iron (hydr)oxides (goethite), aluminium (hydr)oxides (alumina, boehmite, bayerite and gibbsite), clays (kaolinite and montmorillonite), in affecting the speciation of metals and adsorption of organic ligands has received a considerable amount of interest recently [Schindler, 1981; Sigg and Stumm, 1981; McBride, 1982; Davis, 1984; Tipping *et al.*, 1989; Nilsson *et al.*, 1992; Gutzman and Langford, 1993; Laiti *et al.*, 1995]. In natural waters, sediments and soil solution these minerals exist as colloids with large surface areas on which adsorption (of anions or cations) or complexation (of organic or inorganic anions) may occur. Fe and Al oxides are the predominant organic matter adsorbing surfaces present in soils and water systems. Si oxides with negatively charged surfaces in the pH range of natural waters are usually quite inert towards organics.

The importance of solid surfaces in the control of coagulation, sedimentation, adsorption and other processes has highlighted the need for their inclusion in chemical or geochemical models. The properties of mineral surfaces are believed to be controlled by the physical and chemical processes occurring at the solid/liquid interface and are critically dependent on the coordinative reactions taking place at this interface.

5.1.2 ADSORPTION OF NATURAL ORGANIC MATTER.— Davis (1981 and 1982) investigated the adsorption of dissolved natural organic matter (NOM) on several hydrous oxides, including γ -alumina. Results revealed that under conditions 'typical' for natural waters, hydrous oxide surfaces were almost completely covered with organic material. Maximum adsorption for alumina was at pH 5, with almost no adsorption at pH 10. It could be inferred from the results that the major adsorbing species were phenolic or other weakly acidic moieties. The importance of molecular weight on surface adsorption affinities was investigated by Davis and Gloor (1981). The alumina surface, exposed to lake water, exhibited a strong negative charge indicating a high degree of organic adsorption. It was found that organic compounds with molecular weight in excess of 1000 formed strong complexes at the surface of γ -alumina, whereas organics with weights less than 500 were only weakly adsorbed. The pH-dependent adsorption of humic and fulvic acids on Al and Si oxides was investigated by Schulthess and Huang (1991). The results indicated that the Al sites present on the Al oxide (δ - Al_2O_3) and kaolinite strongly

adsorbed organics. Al sites strongly adsorbed organic matter even at very high pH values, while Si sites adsorbed very little above pH 4.

5.1.3 ADSORPTION OF METALS IN THE PRESENCE OF ORGANICS.— A number of researchers have reported studies indicating that ligands bound at oxide surfaces can both enhance and inhibit metal adsorption [Davis and Leckie, 1978]. Greenland (1971) found that organic matter bound to clays facilitated irreversible adsorption for Fe^{3+} and Al^{3+} . Ca^{2+} exhibited reversible adsorption under such conditions, indicating that metals which can form strong complexes with organic matter are not readily desorbed from particle surfaces. The metal ion Cu^{2+} has been the most investigated in regard to adsorption behaviour at organically-coated oxides surfaces. This can, in part, be related to its ease of analysis and its affinity for a wide range of naturally occurring ligands (*i.e.* oxygen and nitrogen donors).

The effect of surface bound organics on the metal uptake at a hydrous oxide surface was investigated by Davis and Leckie (1978). An amorphous iron oxide surface was subjected to both Cu^{2+} and several organic ligands including salicylic, protocatechuic (PCCA), glutamic, picolinic (2-carboxypyridine) and 2,3-pyrazinedicarboxylic (PDCA) acids. Strong adsorption behaviour was exhibited by aromatic compounds with adjacent carboxylic or phenolic groups (*e.g.* PDCA and PCCA). The maximum adsorption of picolinic acid was observed to occur at a pH close to the pK_a of the carboxylic group, while PDCA has a steep desorption edge near pH 6 suggesting that surface complexation involves both carboxylic groups. The effects these ligands imparted on Cu adsorption differed considerably depending on the functionalities present on each ligand. Cu uptake was increased by glutamic acid and PDCA, *i.e.* these ligands contain sufficient complexing functionalities form mixed ligand-surface-metal complexes. Alternatively, picolinic acid effectively impaired adsorption by complexation in solution.

Elliot and Huang (1979) attempted to suggest a mechanism for the combined adsorption of Cu^{2+} and the organic ligands nitrilotriacetic acid (NTA), glycine (Gly) and aspartic acid (Asp) on γ -alumina. The observed adsorption sequence was $\text{CuAsp} > \text{CuNTA} > \text{CuGly}$. The adsorbing Cu-Asp species, the divalent CuAsp_2^{2-} entity, was perceived as experiencing a greater coulombic attraction for the positive alumina surface than the somewhat less adsorbed CuAsp^0 species or the CuNTA^- univalent anion. The lowest adsorption was exhibited by CuGly^+ which could be expected to be electrostatically repelled from the charged oxide surface. Thus electrostatic interactions appeared to be an important adsorption mechanism for the complexed Cu. Optimum adsorption conditions were when ligand/Cu was 1.0. Adsorption of Cu species decreased as this ratio was increased. This behaviour can be easily attributed to competitive adsorption by the ligand.

Davis (1984) extended his earlier studies to consider the adsorption of trace metals on organically coated oxide surfaces. The complexation of Cu^{2+} with the adsorbed

organic matter was found to be stronger than complexation by the clean oxide (alumina) surface while, in contrast, the adsorption of Cd^{2+} was affected very little by the presence of organic material at the surface. The distribution of Cd between the aqueous and surface phases appeared to be controlled by surface hydroxyl complexation whereas Cu adsorption (and solution speciation) was dominated by organic matter complexation. The complexation of Cu could be adequately modelled using apparent stability constants for the surface-bound Cu-ligand species of similar magnitude to values found for solution phase equilibria.

The interaction of humic substances with Cu^{2+} at an alumina surface was investigated by Oden *et al.* (1993). The presence of NOM was found to affect the uptake of Cu^{2+} for all organic matter sources studied at pH 6.2 and 7.2 (the two pHs studied). The facilitatory or inhibitory effects of the humic materials on Cu transport appeared mixed; many binding mechanisms could be implied from the results.

These results highlight the importance of considering colloidal particles as coated with natural organic compounds rather than clean oxide surfaces when considering the fate (distribution) of metals. Also from this research it appears that the presence of large quantities of organic adsorbents on hydrous oxide surfaces could considerably mask the properties of the underlying solid, thus raising the question of 'whether adsorption models based on clean oxide surfaces are useful for a description of natural systems'. An understanding of the surface complexation behaviour of these complex systems cannot, however, be developed without a sound knowledge of the behaviour of the underlying systems. Therefore, in order to understand the properties of naturally occurring oxide surfaces, *i.e.* those covered with NOM, it is beneficial that models are initially developed for these surfaces in the absence of NOM.

5.1.4 MECHANISMS OF ADSORPTION OF LIGANDS ON HYDROUS OXIDE SURFACES.— Robarge and Corey (1979) used an Al-saturated ion exchange resin to investigate the adsorption of phosphate by hydroxy-aluminium species. The Al-saturated resin was subjected to alkali to create a hydroxylated surface and the adsorption of phosphate was studied at low ionic strengths. Results indicated that the hydroxy-Al species were the primary phosphate adsorbing species. Maximum phosphate adsorption corresponded to the point where the amount of adsorbing surface was high and competition from hydroxyl ions for adsorption sites was minimal.

Of a large range of low molecular weight organic ligands, aromatic acids with functional groups in the ortho position (in particular carboxylic and hydroxy substituents) have been found to adsorb most strongly at oxide surfaces. Kummert and Stumm (1980) investigated the adsorption behaviour of the aromatic acids, benzoic, phthalic and salicylic acid, and catechol on the surface of $\gamma\text{-Al}_2\text{O}_3$ using both adsorption and potentiometric titration curves. Complex formation was interpreted in terms of the formation of 1:1

complexes between a surface hydroxy group ($\equiv\text{AlOH}$) and a single phenolic or carboxylic group (loss of H_2O). At higher pH values bidentate species were postulated to be formed with a single Al on the surface. Inner sphere complexes were indicated to form in each case. In studies of the adsorption of catechol on gibbsite, boehmite and noncrystalline alumina [McBride, 1988], adsorption was attributed to $\equiv\text{AlOH}$ groups situated on edge sites. Conflicting with the model proposed by Kummert and Stumm, a 1:1 binuclear complex was depicted as forming at these edge sites. Evidence of this behaviour was derived from both competitive studies with phosphate and acetate and from the nature of the infrared spectra of surface bound species at pH 7. Only phosphate was found to compete effectively with catechol for adsorption sites.

Much work has been undertaken towards identifying the parameters of greatest importance (for modelling purposes) in the adsorption mechanisms of oxide surfaces. Stone *et al.* (1993) investigated the effects of pH and ionic strength on the adsorption of a series of alcohols and substituted aminophenols on oxide surfaces, including Al_2O_3 . The most basic phenol groups ($\text{p}K_{\text{a}} > 9.9$) exhibited very low or no adsorption on these surfaces; each compound existing as protonated or neutral species at pH values below the pH_{zpc} (pH of the zero proton charge, *i.e.* net charge at the surface equals zero). Phenols with $\text{p}K_{\text{a}}$'s substantially less than the pH_{zpc} exhibited adsorption properties which were greatest for those surfaces with high surface charge densities (*e.g.* Al_2O_3 which acquires a higher positive surface charge than most oxides). They adsorbed strongly at more acidic pH values. Non-specific adsorption (arising from long-range electrostatic forces) could completely explain the data. Aminophenols and a pyridinemethanol species did not adsorb strongly on Al_2O_3 due to the lower affinity of Al toward nitrogen donor groups. The conclusion was drawn that adsorption of organic ligands on such surfaces arises from a combination of both long-range electrostatic type interactions and near-range physical and chemical interactions. The effects of pH and ionic strength on adsorption processes was described as a direct consequence of (i) stoichiometry of surface complex formation, (ii) mass balance equations for ligands, protons and surface sites, and (iii) Poisson-Boltzmann terms which relate ion concentrations at the oxide/water interface to concentrations in bulk solution.

The relationship between the amount of adsorption and the isoelectric pH (pH_{iep}) for the adsorption of phosphate and arsenate on a variety of hydrous oxide surfaces [$\gamma\text{-Al}_2\text{O}_3$, amorphous $\text{Al}(\text{OH})_3$, anatase and crystalline $\text{Fe}(\text{OH})_3$] was studied by Anderson and Malotky (1979). These protolyzable ions are found to adsorb specifically on oxide surfaces resulting in a lower pH_{iep} and raised pH_{zpc} . Adsorption is dependent on both chemical and electrostatic forces. Anderson and Malotky's studies involved the use of linearised isoelectric adsorption isotherms which allowed the calculation of surface dissociation constants and hence the ability to model the adsorption- pH_{iep} dependence of the systems. It was interpreted from the studies that a suitable model does not require the

use of multiple adsorption sites and adsorption potential does not vary with pH. The adsorption characteristics of a series of amino polycarboxylic acids on $\gamma\text{-Al}_2\text{O}_3$ were modelled employing hydrogen bond formation as the principle adsorption process (Bowers and Huang, 1985). Surface binding energies were in support of such a model, however, the correlations between observed and model data were not high.

Surface complexation of organic ligands is primarily thought to involve the formation of inner-sphere complexes between a metal ion at the surface and the adsorbing ligand. Studies of the fluorescent complexes formed between aluminium and 8-hydroxy-quinoline-5-sulfonate at the aluminium oxide-water interface (Hering and Stumm, 1991) provided strong evidence for such species. Ogawa (1991) used IR spectroscopy to investigate the orientation of benzoic acid and terephthalic acid adsorbed on an alumina surface. Both acids adsorbed through the carboxylate anion with a vertical conformation of the benzene ring relative to the surface plane. Terephthalic acid also adsorbed as a dicarboxylate anion in a close-to-horizontal orientation.

A number of studies have considered the competitive nature of adsorbates on aluminium oxide surfaces. The competitive adsorption of phosphate and oxalate anions as a function of pH and order of addition was studied by Violante *et al.* (1991). Both anions competed strongly for adsorption sites, decreasing the total adsorption of the other respectively. Oxalate dominated adsorption at acid pH values while the ability of phosphate to displace oxalate increased with increasing pH. Schulthess and McCarthy (1990) investigated the competitive effects of carbonate on the adsorption behaviour of acetic acid on $\gamma\text{-Al}_2\text{O}_3$ over a wide pH range. The observed affinity for adsorption of the aqueous ions on Al oxide was $\text{OH}^- > \text{CO}_3^{2-} > \text{acetate} (\text{AcO}^-) > \text{Cl}^-$. This indicated the importance of controlling the concentrations of such ions in adsorption studies.

Thomas *et al.* (1989a) investigated the importance of alumina porosity on the adsorption mechanisms of polar molecules. Two aluminas of similar surface area and electrical properties, but with differing textural properties (pore size/area) were studied in conjunction with two surfactants. The studies revealed, as expected, that the pore walls bear the most reactive sites and that the more porous of the two aluminas was the most reactive. The most reactive surface sites were interpreted to be the $\equiv\text{AlOH}_2^+$ sites which would be situated at surface edges and on pore walls; adsorption on the external surface would begin only once these sites had been filled (*i.e.* at high ligand concentrations). The possibility of surface complexation reactions, specific adsorption involving hydrogen bonding and ion exchange were each hypothesised as explanations for increased adsorption with increasing pH. All of these mechanisms were considered plausible for adsorption on external surface sites. The structure of the adsorbed layer was found to be independent of alumina porosity. These studies were followed by adsorption experiments involving salicylate and the above alumina materials [Thomas *et al.*, 1989b]. Adsorption

was greatest on the more porous alumina material and the same mechanisms for adsorption were considered most important.

The processes of dissolution and precipitation of mineral phases is also influenced by complexation reactions occurring at the surfaces of minerals. The influence of ligands on dissolution processes, *e.g.* ligand-promoted dissolution, has been investigated [Furrer and Stumm, 1983 and 1986].

The mechanisms involved in the adsorption of ligands and metals at the surface of mineral oxides are now becoming better understood. Much of the current research is now being directed towards the modelling of these processes. The topic of 'adsorption mechanisms in aquatic surface chemistry' has been the subject of a number of good reviews or book topics [Stumm, 1986; Westall, 1987; Schindler, 1990; Stone, 1991; Schindler and Sposito, 1991].

5.1.5 SURFACE COMPLEXATION MODELS.— A large number of surface complexation models have been developed in recent decades [Sposito, 1983; Schindler and Stumm, 1987; Davis and Kent, 1990]. The more common of these include the constant capacitance model [Schindler and Gamsjäger, 1972; Hohl and Stumm, 1976; Schindler, 1981], the diffuse layer model [Stumm *et al.*, 1970; Huang and Stumm, 1973], and the triple layer model [Stern, 1924; Davis *et al.*, 1978]. These models have been addressed in Chapter 2 (2.2). The fundamental concepts underlying each of these models are essentially the same, however differences exist in the manner by which the surface charge and potential of the interfacial region is described. In each model surface adsorption takes place at a finite number of specific coordination sites; mass balance equations are used to describe the surface adsorption reactions; and interactions at the surface result in a series of surface charges and potentials. Each of these models can adequately describe the surface reactions of aluminium oxides sufficiently well (Westall and Hohl, 1980).

The assumption is made in most surface models that a proton becomes progressively more difficult to remove with each incremental removal of protons. The idea is taken into account by the introduction of an exponential term into the model equations which assumes that the surface charge causes a change in reactivity between the ions at the surface and in the bulk solution, which is described by a Boltzmann distribution. The resulting constants determined for these models are conditional constants and must be corrected for the coulombic energy of the surface charge to obtain the corresponding 'intrinsic constants' [see Chapter 2 (2.2.3)]. Sposito (1983) observed that 'these surface complexation models are *too* successful'. From the large number of models it is 'very difficult to choose which model is more realistic, or establish why the Boltzmann distribution correction term is necessary'.

Schulthess and Sparks (1987) described a two site model for aluminium oxide which considered the effects of competitive pH- and salt-dependent reactions. The model successfully accounted for the proton isotherm behaviour of the aluminium oxide surface with mass balance equations, while the use of intrinsic equilibrium constants and exponential terms was avoided. Despite the success of the model derived by Schulthess and Sparks, the three 'commonly used models' mentioned above [discussed in Chapter 2 (2.2.2)] have been very successful in explaining the adsorption behaviour of many metals and ligands at a variety of naturally occurring surfaces.

The model used in the present study (the constant capacitance model) has been successfully used in treating the adsorption behaviour of metals and ligands at the surfaces of goethite [Lövgren, 1990; Nilsson, 1992; Nilsson, 1995]; γ -alumina [Laiti *et al.*, 1995]; boehmite [Laiti and Öhman, unpub.] and zinc- and lead-sulfides [Rönnngren *et al.*, 1991; Sun *et al.*, 1991; Rönnngren, 1992].

5.2 THE ADSORPTION BEHAVIOUR OF PYROCATECHOL VIOLET ON THE SURFACE OF BOEHMITE [α -AlO(OH)]

5.2.1 INTRODUCTION.— Colloids in natural waters, sediments and soil solution represent large surface areas on which adsorption (of anions or cations) or complexation (of organic or inorganic anions) may occur. These surfaces carry a significant proportion of the humic substances 'dissolved' in natural waters and thus could control the availability of ligands that mask Al toxicity.

This thesis is concerned with the determination of Al in natural waters and soil solutions. As discussed in Chapter 1 (1.3), the most common methods for performing these analyses involve the use of a reagent (*e.g.* metallochromic or redox-active ligands) that will complex Al. The surfaces present in natural waters have the potential to complex these reagents and interfere in Al determinations. In particular, any variety of aluminium oxide (or iron oxide) is likely to adsorb reagents suitable for Al complexation. Furthermore, possible ternary complexes (*e.g.* surface-ligand-metal) may form or the surfaces may undergo ligand-promoted dissolution (which in the case of aluminium oxides will result in an over-estimation of measured Al).

In terms of stoichiometry, there is only one form of aluminium oxide, namely, *alumina* (Al_2O_3). However, large varieties of polymorphs, hydrated species, *etc* exist depending on formation conditions [Cotton and Wilkinson, 1988; Fredrikson, 1993]. Two forms of anhydrous Al_2O_3 exist, α - Al_2O_3 and γ - Al_2O_3 , differing in the packing of the Al and oxide ions. α - Al_2O_3 occurs in nature as the mineral *corundum*; it is stable at high temperatures and is prepared by heating any hydrous oxide above 1000 °C. γ - Al_2O_3 is obtained by dehydration of hydrous oxides at low temperatures (~450 °C). In contrast to

$\gamma\text{-Al}_2\text{O}_3$ which readily takes up water and dissolves in acids, $\alpha\text{-Al}_2\text{O}_3$ is very hard and resistant to hydration and attack by acids. Alumina also exists in several important hydrated forms corresponding to the stoichiometries $\text{AlO}(\text{OH})$ (*boehmite* and *diaspore*) and $\text{Al}(\text{OH})_3$ (*gibbsite* and *bayerite*).

The phase chosen for the present studies, boehmite [$\alpha\text{-AlO}(\text{OH})$], has been found to be relatively stable under the conditions chosen for this work [Laiti and Öhman, unpub.]. Unlike other alumina materials, *e.g.* γ -alumina, boehmite does not undergo rearrangements on contact with water [Laiti and Öhman, unpub.]. The material also reaches equilibrium quickly in 0.10 mol L^{-1} medium, thus enabling immediate titration.

In the present study the adsorption behaviour of the metallochromic indicator pyrocatechol violet, H_4L (Figure 5.2.2), on the surface of the aluminium-oxide hydroxide boehmite [$\alpha\text{-AlO}(\text{OH})$] has been investigated. The interaction of boehmite with organic ligands has been reported from a limited number of studies [McBride and Wesselink, 1988; Madsen and Blokhuis, 1994; Laiti and Öhman, unpub.]. The interaction of PCV with aluminium minerals is of interest due to its common use in spectrophotometric analysis of Al in natural waters and soil extracts [Kerven *et al.*, 1989].

The concept of treating surface complexation as thermodynamic equilibria in the same manner as solution equilibria is new to the scientific arena. In this approach a hydrous oxide surface is regarded as a polyelectrolyte consisting of amphoteric functional groups which are capable of forming complexes. In this work, the experimental data for surface complexation were evaluated on the basis of the electrostatic constant capacitance model [Schindler and Gamsjäger, 1972]. The model is based on a linear relationship between the charge at the inner Helmholtz plane, representing the specifically adsorbed ions, and the surface potential. This model was chosen for these studies due to its simplicity. The assumptions and numeric analysis regarding this model are discussed in Chapter 2 (2.2.3). The acidity constants of the surface hydroxy groups at the boehmite-solution interface were evaluated as a prerequisite to studying the ligand adsorption behaviour. This work was performed at Umeå University, Sweden.

5.2.2 EXPERIMENTAL

(A) **Chemicals and Analysis.**— All suspensions and solutions were prepared, in a laboratory thermostatted at 25.0 ± 0.5 °C, from CO₂-free, boiled Milli-Q water and all working solutions were prepared in 0.10 mol L^{-1} KCl (Merck, *p.a.*; dried at 120 °C).

(i) **Boehmite Suspensions:** Finely powdered high purity boehmite, $\alpha\text{-Al}_2\text{O}_3$ monohydrate (DISPERAL, Condea Chemie), was used. The surface area was $180 \text{ m}^2 \text{ g}^{-1}$ according to the BET method. Boehmite suspensions were prepared at least two weeks prior to use (equilibration period) as $20.00 \text{ g (boehmite) L}^{-1}$ ionic medium. The total surface hydroxyl group, $\equiv\text{AlOH}$, concentration for such a suspension had been determined previously as 10.2 mmol L^{-1} [Laiti and Öhman, unpub.] using the procedure described by Hohl and Stumm (1976). The determination involves the measurement of the maximum exchange capacity of the $\equiv\text{AlOH}$ groups *{i.e.}* $[\equiv\text{AlOH}]_{\text{tot}} = [\equiv\text{AlOH}_2^{2+}] + [\equiv\text{AlOH}] + [\equiv\text{AlO}^-]$. This is achieved by addition of known amounts of strong acid or base to a suspension followed by back titration, analysis of unreacted protons (calculated from $-\log h$ measurements) and calculation of the surface site concentration. Corrections are made for surface dissolution (both in the acidic and alkaline directions) which affects both suspension pH and particle concentration.

(ii) **Pyrocatechol Violet Solutions:** PCV: 2-[(3,4-dihydroxy-phenyl)(3-hydroxy-4-oxocyclohexa-2,5-dien-1-ylidene)methyl]benzene sulfonic acid is depicted in Figure 5.2.2. PCV (Merck) solutions were prepared and standardised as described in Chapter 4 [4.2.1(A)].

(iii) **Standard Alkali (KOH) and Acid (HCl) Solutions:** Standard HCl (BDH, AnalaR) solutions were prepared and standardised as described in Chapter 3 [3.2.2]. Carbonate-free KOH (Eka Nobel, *p.a.*) solutions were prepared and standardised according to Chapter 3 [3.2.1B]. Dilute (*ca.* $0.01\text{--}0.04 \text{ mol L}^{-1}$) KOH solutions were standardised potentiometrically against standard HCl.

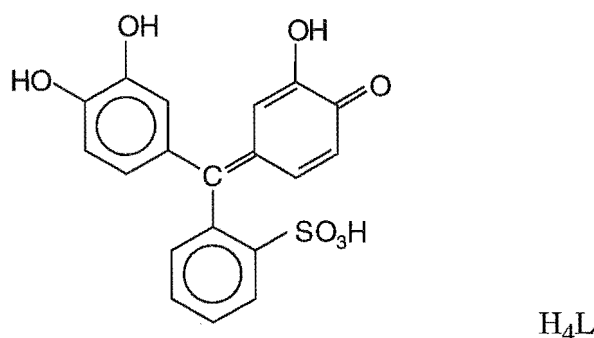


Figure 5.2.2 Pyrocatechol violet (PCV, H_4L).

(B) Potentiometric Titrations.— The titration set-up and cell arrangement is described in Chapter 3 [3.10.1(B)] - 'mineral (hydr)oxide suspension titrations'. The electrode pair was calibrated for the measurement of $-\log h$ as described in Chapter 3 [3.11.3A(ii)]. The free H^+ concentration, h , was determined by measuring the e.m.f. of the cell described by Equation 2.3.1b (see Chapter 2).

During titrations of boehmite in the absence of PCV ($5.0 \leq -\log h \leq 10.0$) the initial total concentration of boehmite ($\equiv AlOH$ sites), B , was varied between the limits $0.0015 \text{ mol L}^{-1} \leq B \leq 0.0102 \text{ mol L}^{-1}$. During the three-component titrations ($5.0 \leq -\log h \leq 9.0$), the ratio between B and the total concentration of PCV, C , was held constant. The initial concentrations of B and C were varied within the limits $0.0027 \text{ mol L}^{-1} \leq B \leq 0.0097 \text{ mol L}^{-1}$ and $0.0010 \text{ mol L}^{-1} \leq C \leq 0.0049 \text{ mol L}^{-1}$, covering C/B ratios in the range 0.10-1.78.

The conditions defining the establishment of pH equilibrium [see 'delay times', Chapter 2 (2.3)] were the same for all the titrations. The delay time (30 min) following the addition of each aliquot was the same as that between measurements. In both systems equilibrium times varied considerably with the value of $-\log h$ and were generally shorter at lower $-\log h$ values. The criterion accepted for stable readings was a drift in the measured potential of less than 0.3 mV h^{-1} ($0.005 -\log h \text{ h}^{-1}$). Typical equilibration times between each addition were 6 h. All titrations typically contained 8-20 datum points.

The reproducibility and reversibility of equilibria were tested by performing both forward (increasing $-\log h$) and backward (decreasing $-\log h$) titrations.

(C) Batch 'Adsorption' Titrations.— Spectrophotometric batch titrations (PCV adsorption) were undertaken to determine the amount of PCV, $H_3L^-_{(aq)}$, remaining in solution after a period of exposure to a boehmite suspension. Beckman polypropylene (AY, $2.5 \times 10 \text{ cm}$) centrifuge tubes (*ca.* 40 mL) were used for the containment of samples throughout the experiments. Oxygen exclusion was achieved using argon gas. A Beckman J2-21 centrifuge using a JA-20 rotor running at 16500 rpm (32900 g) for 30 min at 25°C was used for centrifugation. The spectrophotometer used for the analysis of PCV was a Shimadzu UV-2100 UV-Visible recording spectrophotometer.

The titrations were carried out by the addition of a desired aliquot of boehmite suspension to a centrifuge tube, followed by bubbling with argon gas for at least 20 min. Aliquots of ionic medium, PCV and acid or alkali were then added quickly, but with care not to create a local excess of acid or alkali which may promote dissolution. The vessel was closed (with further care taken to exclude air) and mixing effected immediately. The total amounts of these constituents added were such that $-\log h$ values of 4.5-9.5 would be obtained. Homogeneity of suspensions was maintained by means of an end-to-end rotating test tube holder running at approximately 30 rpm.

In these experiments B and C were varied within the limits $0.004 \text{ mol L}^{-1} \leq B \leq 0.010 \text{ mol L}^{-1}$ and $0.0017 \text{ mol L}^{-1} \leq C \leq 0.0043 \text{ mol L}^{-1}$, covering C/B ratios in the range 0.21-1.06. After a period of 72 h equilibration the test suspensions were centrifuged and an aliquot of the supernatant was removed and acidified to $-\log h = 3.5$. The concentration of PCV was then analysed *via* the spectrophotometric measurement of $\text{H}_3\text{L}^-_{(\text{aq})}$ at 442 nm ($\epsilon = 1.50 \times 10^4$).

(D) Spectrophotometric Studies.— The adsorption of PCV at micromolar concentrations on boehmite (at concentrations typical of a natural water) was investigated. These studies were performed in the same manner as the spectrophotometric 'batch adsorption titrations' described above [5.2.2(C)]; however the work was performed in a different laboratory and without the care of temperature control or an inert atmosphere.

Becton Dickinson Labware polypropylene (FALCON[®] 2070, $2.5 \times 10 \text{ cm}$) centrifuge tubes (50 mL) were used for the containment of samples throughout the experiments. A BTL bench centrifuge running at a speed of *ca.* 4000 rpm for 20 min at room temperature was used for centrifuging. The spectrophotometer used for the analysis of PCV was a Hewlett Packard 8452A diode array spectrophotometer.

The titrations were carried out by the addition of a desired aliquot of boehmite suspension to a centrifuge tube, followed by aliquots of buffered ionic medium and PCV. The ionic medium was 0.05 mol L^{-1} MES (Calbiochem) buffer/ 0.05 mol L^{-1} KCl (BDH, AnalaR) at pH = 6.1. The boehmite stock solution was prepared as described above [5.2.2(A)] as 5.0 g L^{-1} (2.56 mmol L^{-1} total surface hydroxyl group, $\equiv\text{AlOH}$, concentration) and allowed to equilibrate for two weeks. A 5 mmol L^{-1} PCV (Koch-Light) stock solution was used. Homogeneity of suspensions was maintained by means of an end-to-end rotating device running at approximately 20 rpm. NOTE: This rotation device was not as efficient as the end-to-end rotator used in the 'batch titrations' above [5.2.2(C)] and boehmite was observed to stick to the tube walls.

In these experiments the total concentration of PCV (C) was $20 \text{ } \mu\text{mol L}^{-1}$ and the total concentration of boehmite (B) was varied within the range $B = 0\text{--}100 \text{ mg L}^{-1}$ ($0\text{--}51 \text{ } \mu\text{mol L}^{-1}$ total surface hydroxyl group, $\equiv\text{AlOH}$, concentration). After a period of 72 h equilibration the test suspensions were centrifuged and an aliquot of the supernatant was removed and acidified to $-\log h = 3.5$. The concentration of PCV was then analysed *via* the spectrophotometric measurement of $\text{H}_3\text{L}^-_{(\text{aq})}$ at 442 nm ($\epsilon = 1.50 \times 10^4$).

(E) Aluminium Analysis.— The concentration of Al^{3+} at equilibrium in batch titrations was analysed to ascertain the extent of surface dissolution. A Perkin-Elmer Zeeman/3030 atomic absorption spectrometer (ETAAS) was used. HNO_3 was used to minimise interference from the chloride medium. From batch titrations a total of 23 samples in the

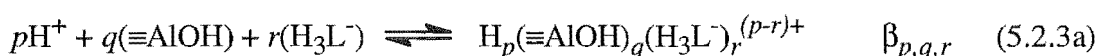
range $5.0 \leq -\log h \leq 9.5$ were analysed. Two potentiometric titrations, taken to $-\log h > 8.5$, were sampled (at completion) and analysed.

(F) DRIFT Spectroscopy.— Diffuse reflectance infrared spectra were collected to provide structural information relating to possible surface bound species. The spectra were obtained using a Bruker 113 IFS FTIR spectrometer equipped with a diffuse reflectance unit (Harrick Scientific Corp.) and a DTGS detector. The compartment was purged with nitrogen for 30 min before collecting spectra. KBr was used as the non-absorbing matrix and background. Spectra were obtained from a mixture of 10 mg of the sample and 0.5 g KBr and were recorded by averaging 2048 scans at a resolution of 4 cm^{-1} . Spectra were recorded for centrifuge residues from several batch titration samples covering the range $5.5 \leq -\log h \leq 8.0$. Prior to analysis residue samples were allowed to dry slowly under Ar. In order to subtract out the effects of the 'clean' boehmite surface and free PCV, the spectra of pure boehmite and PCV solids were also obtained.

5.2.3 DATA TREATMENT

Potentiometry.— The zero proton level defined in these studies treats the hydroxylated boehmite surface as $\equiv\text{AlOH}$; it considers the ligand, PCV, as a triprotic species, H_3L^- , because the protonation of the sulfonate group occurs at $-\log h < 1$ [Wakley and Varga, 1972]. The boehmite surface contains hydroxyl groups that can bind and/or release protons and can also take part in complexation reactions with metal ions and ligands.

The equilibria involving H^+ , $\equiv\text{AlOH}$ and PCV, can be expressed by the general equation:



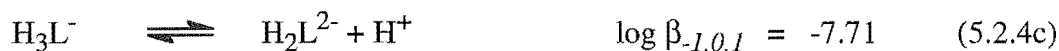
The equilibria in the two 2-component systems, $\text{H}^+-(\equiv\text{AlOH})$ and $\text{H}^+-\text{H}_3\text{L}^-$, can be expressed using the simplified equations (5.2.3b) and (5.2.3c) respectively:



It should be noted that $\beta_{p,q,r}$ and $\beta_{p,1,0}$ are conditional constants and thus must be corrected for the coulombic energy of the charged surface to obtain the corresponding intrinsic constants. This data treatment and the derivation of the corresponding mass balance expressions is discussed in Chapter 2 (2.2.3).

In the calculations the least-squares computer program LAKE (capable of treating multi-method data) [Ingri *et al.*, 1996] was used in combination with the modelling program SOLGASWATER [Eriksson, 1979] modified to treat surface complexation using the constant capacitance model. These calculations involved evaluating the mass balance equations [see Chapter 2 (2.2.3)] and were performed in an iterative procedure for the two data sets (potentiometric and batch data respectively). For LAKE calculations the best model was the one which gives the lowest error squares sum $U_{Z_B} = [(H_{\text{calc}} - H_{\text{exp}})/B]^2$. LAKE computations were performed using a Sun SPARC station.

5.2.4 DATA, CALCULATIONS AND RESULTS.— The present investigation was divided into two parts. The first involved the determination of the acid/base properties of the boehmite surface, as described by equations (5.2.4a) and (5.2.4b); in the second series of experiments the adsorption behaviour of PCV at the boehmite-medium interface was investigated. The initial investigation was performed as a series of potentiometric titrations, whereas in the 3-component system both potentiometric and spectrophotometric batch titrations were performed. The equilibrium constants describing the acid/base reactions of PCV, (5.2.4c) and (5.2.4d), were taken from Table 4.2.3 (Chapter 4).



(A) The 2-Component System.— H^+ -{Boehmite}

The acid/base hydrolysis reactions of the boehmite surface were studied in 5 potentiometric titrations (43 datum points) in the range $5.0 \leq -\log h \leq 10.0$. These data are shown in Figure 5.2.4A, where Z_B represents the average number of H^+ reacted per $\equiv\text{AlOH}$ group, $Z_B(-\log h) = (H - h + k_{\text{w}}h^{-1})/B$. The reversibility was tested in three of these titrations. The system was found to be completely reversible when titrations were reversed prior to reaching $-\log h$ values at which surface dissolution was likely to occur. Surface dissolution was negligible over this $-\log h$ range ($5.0 \leq -\log h \leq 9.0$) and during the time scale of these experiments. The constants evaluated, $\log \beta_{1,1,0(\text{int})}$ and $\log \beta_{-1,1,0(\text{int})}$, and the capacitance, c , are given in Table 5.2.4A. These values are in excellent agreement with those obtained by Laiti and Öhman (unpub.).

Table 5.2.4A

Species	p, q, r	$\log (\beta_{p, q, r(int)} \pm 3\sigma)$	Previous Studies ^a
$\equiv\text{AlOH}_2^+$	(1,1,0)	7.46 ± 0.04	7.47
$\equiv\text{AlO}^-$	(-1,1,0)	-9.87 ± 0.12	-9.81
specific capacitance		$1.002 \pm 0.028 \text{ F m}^{-2}$	0.92

^aLaiti and Öhman, (unpub.).

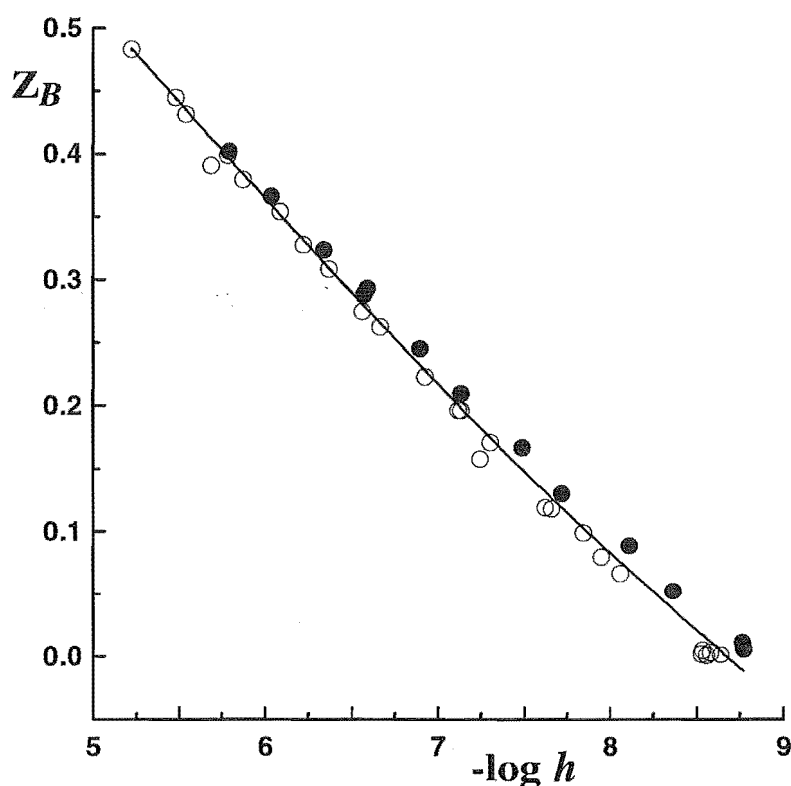


Figure 5.2.4A Experimental data from titrations of boehmite in $0.10 \text{ mol L}^{-1} \text{ K}(\text{Cl})$ plotted as Z_B versus $-\log h$ curves. Z_B is defined as the average number of protons reacted per $\equiv\text{AlOH}$. The symbols, filled and open, represent forward (increasing $-\log h$) and backward (decreasing $-\log h$) titrations respectively. The line was calculated using the proposed model.

(B) The 3-Component System.— H^+ -{Boehmite}-PCV

The results for the 3-component system are illustrated in Figures 5.2.4B and 5.2.4C. In Figure 5.2.4B, Z_B , the average number of H^+ reacted per surface site, $\left\{ \begin{smallmatrix} \equiv\text{AlOH} \\ \equiv\text{AlOH} \end{smallmatrix} \right\}$, has been plotted $[Z_B(-\log h) = (H-h+k_w h^{-1})/B]$. The fraction of PCV

adsorbed, α_i [$i = \Sigma(H_n L^{n-4})_{\text{ads}}$], versus $-\log h$ is plotted in Figure 5.2.4C. From these Figures it is clear that PCV is adsorbed to the boehmite surface. Preliminary calculations also showed that the proton effects caused by this adsorption are quite small. Regarding these observations, it is apparent that significant information on possible surface complexation reactions will be derived from the adsorption data.

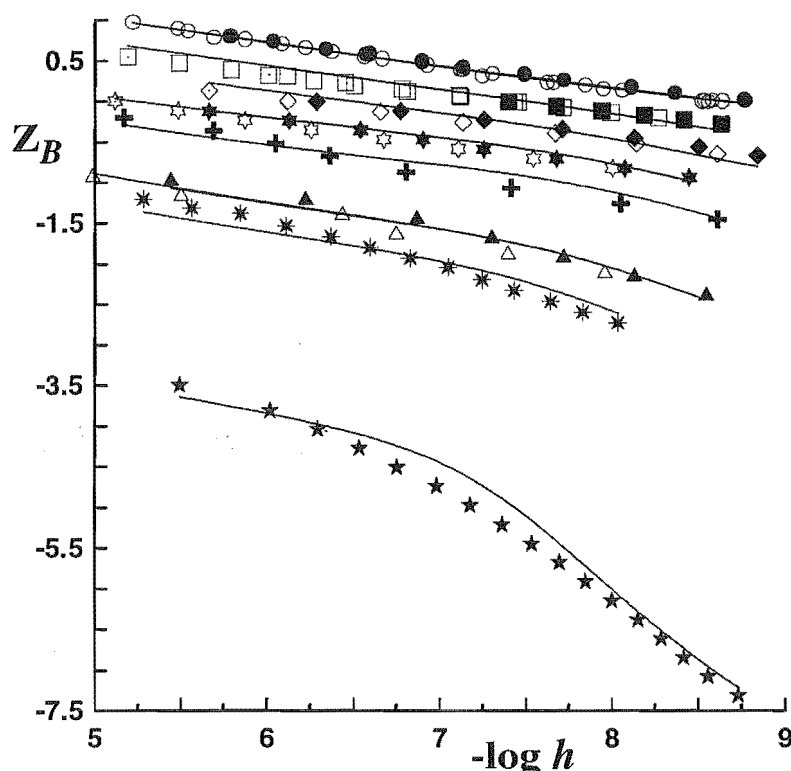


Figure 5.2.4B Part of the experimental data plotted as Z_B curves where Z_B is the average number of protons reacted per $\left\{ \begin{smallmatrix} \equiv \text{AlOH} \\ \equiv \text{AlOH} \end{smallmatrix} \right\}$. Both forward (increasing $-\log h$) and backward (decreasing $-\log h$) titrations are shown as described for Figure 5.2.4A. The lines were calculated using the proposed model. The quotient $[\text{PCV}]_{\text{tot}} / \left[\left\{ \begin{smallmatrix} \equiv \text{AlOH} \\ \equiv \text{AlOH} \end{smallmatrix} \right\} \right]_{\text{tot}} = 0$ (●), 0.20 (■), 0.44 (◆), 0.64 (★), 0.84 (+), 1.40 (▲), 1.68 (✱) and 3.56(★).

The evaluation of the model for the 3-component system involved testing of single complexes and combinations of complexes with different compositions. Monodentate, bidentate and bridging complexes were tested. Initial calculations indicated that mononuclear complexes could not provide an adequate fit to experimental data. Any combination of mononuclear species that provided even a crude fit to adsorption data resulted in very large proton effects.

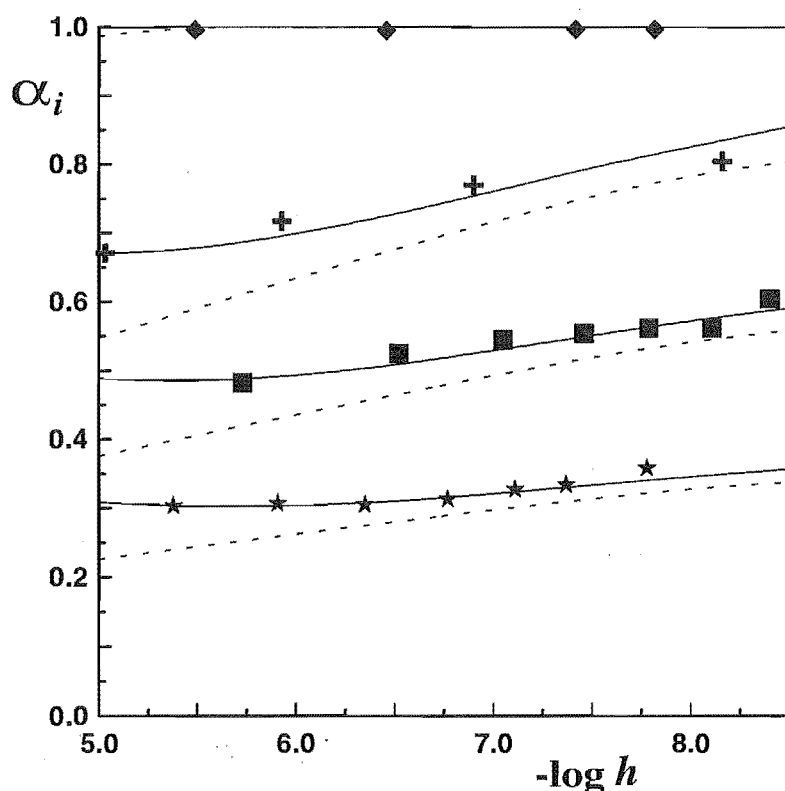


Figure 5.2.4C Adsorption curves, α_i vs $-\log h$, for PCV at the boehmite surface. α_i represents the ratio between surface bound PCV, $\left\{ \begin{smallmatrix} \equiv \text{AlOH} \\ \equiv \text{AlOH} \end{smallmatrix} \right\} \text{PCV}$, and aqueous PCV, $\sum H_n L^{n-4}$ ($n=1-4$). The solid lines were calculated using the proposed model (final model). The dashed lines were calculated using a 'single species' model (see 'Model evaluation' later in this Section). The quotient $[\text{PCV}]_{\text{tot}} / \left[\begin{smallmatrix} \equiv \text{AlOH} \\ \equiv \text{AlOH} \end{smallmatrix} \right]_{\text{tot}} = 0.42$ (\blacklozenge), 0.84 ($+$), 1.25 (\blacksquare) and 2.10 (\star).

For batch titrations carried out with an excess of PCV to surface hydroxyl groups {i.e. $[\text{PCV}]/[\equiv \text{AlOH}] > 1$ }, information can be derived relating to the stoichiometry of surface complexes forming. In Figure 5.2.4D, a plot of the fraction of PCV adsorbed multiplied by the ratio $[\text{PCV}]/[\equiv \text{AlOH}]$ versus $-\log h$ is shown. From this graph it is apparent that the surface complexes forming will have stoichiometries ($\text{PCV}/\equiv \text{AlOH}$) less than 1 (and most likely 0.5). Further calculations indicated that the dominating species would be binuclear, i.e. the PCV molecule bridging two metal centres.

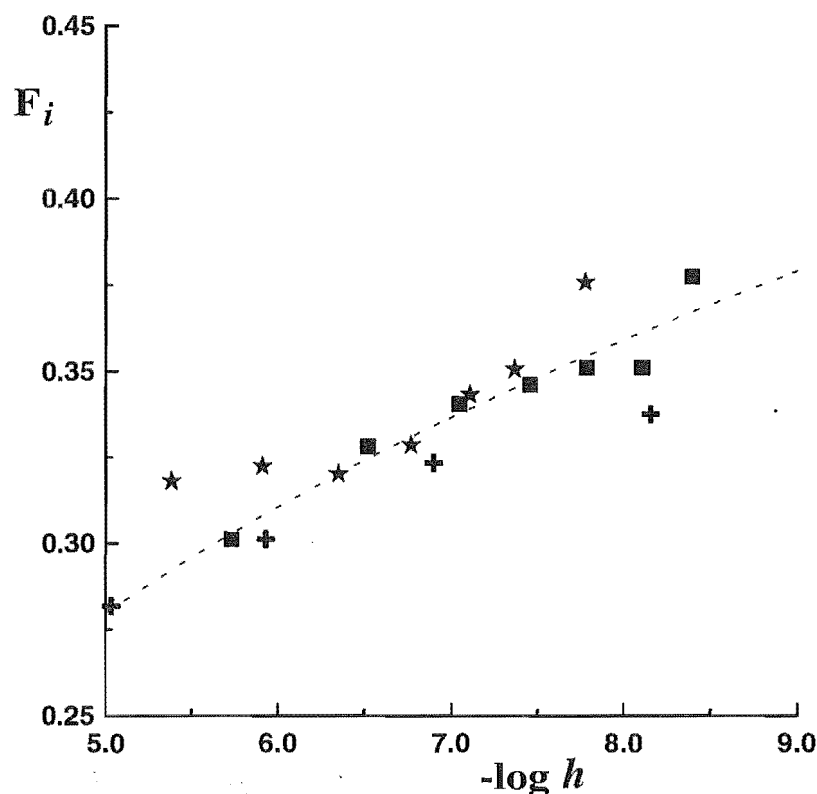
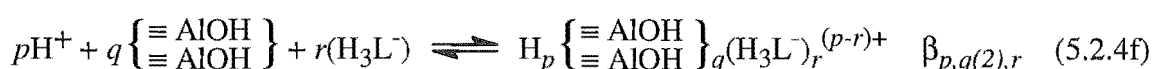
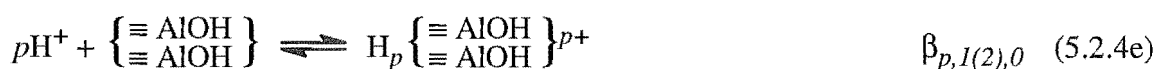


Figure 5.2.4D A plot of the fraction of PCV adsorbed multiplied by the ratio $[\text{PCV}]/[\equiv\text{AlOH}]$, F_i , versus $-\log h$. The symbols represent the corresponding data shown in Figure 5.2.4C. The dashed line represents the data trend.

As a result of these observations, the zero proton level was redefined to treat a surface site as $\left\{ \begin{smallmatrix} \equiv \text{AlOH} \\ \equiv \text{AlOH} \end{smallmatrix} \right\}$. Here $\left\{ \begin{smallmatrix} \equiv \text{AlOH} \\ \equiv \text{AlOH} \end{smallmatrix} \right\}$ designates a binuclear binding site where the adjacent hydroxy groups are identical and dependent. The total concentration of $\left\{ \begin{smallmatrix} \equiv \text{AlOH} \\ \equiv \text{AlOH} \end{smallmatrix} \right\}$ sites, B' , is half the total surface hydroxy concentration, *i.e.* 5.1 mmol L^{-1} in stock suspensions. New expressions for the general 2-component, $\text{H}^+ - \left\{ \begin{smallmatrix} \equiv \text{AlOH} \\ \equiv \text{AlOH} \end{smallmatrix} \right\}$, and 3-component, $\text{H}^+ - \left\{ \begin{smallmatrix} \equiv \text{AlOH} \\ \equiv \text{AlOH} \end{smallmatrix} \right\} - \text{PCV}$, equilibria are:



where $q(2)$ specifies bidentate $\left\{ \begin{smallmatrix} \equiv \text{AlOH} \\ \equiv \text{AlOH} \end{smallmatrix} \right\}$ sites. The basis for the revised treatment of the 2-component and 3-component systems and their corresponding equilibrium constants is explored in the Discussion.

Complexation in the $\text{H}^+ - \left\{ \begin{smallmatrix} \equiv \text{AlOH} \\ \equiv \text{AlOH} \end{smallmatrix} \right\}$ -PCV system was studied in 10 potentiometric titrations (143 data points) in the range $5.0 \leq -\log h \leq 9.0$ ($0.20 \leq C/B' \leq 3.56$) and 5 batch titrations (27 data points) in the range $5.0 \leq -\log h \leq 8.5$ ($0.42 \leq C/B' \leq 2.10$). An upper $-\log h$ value of 8.0 was used if the titration was to be reversed. The dissolution of the surface at $-\log h > 8.5$ was found to be greater in the presence of PCV than in its absence. In batch titrations the $-\log h$ range was restricted by oxidation of the ligand (oxygen could not be excluded as thoroughly as in the potentiometric titrations). The complexation reactions were found to be quite reversible at C/B' ratios less than 1.68 (as evident in Figure 5.2.4B); the reversibility was not tested at ratios greater than this. Only with an excess of surface sites ($B'/C \geq 2$) was all PCV adsorbed from solution. As a result of the weak adsorption behaviour it was not possible to perform experiments whereby complete surface saturation was reached. Such experiments are often important in determining the stoichiometry of adsorption processes.

Model Evaluation: The evaluation of the model was performed as a series of iterative calculations utilising both the least-squares program LAKE and the modelling program SOLGASWATER. Based on potentiometric data only, a series of single species models were evaluated. Each of these adequately explained the potentiometric data, however, for most of them very poor fits to adsorption data were obtained. Of these models the best description of both potentiometric and batch titration data involved the formation of the species with stoichiometry $[-1, 1(2), 1]$, $\log \beta_{-1, 1(2), 1(int)} = 1.52$. The fit of this species to the batch titration data is indicated in Figure 5.2.4C (dashed line). No other single-species model calculated, based on either data set, could provide a better fit to the batch titration data without resulting in a very unsatisfactory fit to potentiometric data.

Systematically testing of p, q, r -combinations for the equilibria described in Equation 5.2.4f was undertaken to investigate combinations of complexes that could better explain the data. These calculations revealed that the dominating species in the equilibria would have the stoichiometry $[-1, 1(2), 1]$ but a secondary species was needed to improve the fit to the batch titration data. The inclusion of the species $[0, 1(2), 1]$ into the model improved the fit to adsorption data {in combination with the species $[-1, 1(2), 1]$ }, however, a much greater improvement of fit was obtained by including the species $[1, 1(2), 1]$ into the model. The species $[+2, 1(2), 1]$ and $[-2, 1(2), 1]$ were also tested. The possibility of including all three species $\{[-1, 1(2), 1], [0, 1(2), 1]$ and $[1, 1(2), 1]\}$ was considered. However, there was insufficient data to fit these three species accurately and

the fit, in comparison to the model with just two species $\{[-I,I(2),I]$ and $[I,I(2),I]\}$, could not be improved.

The final model contained two species: $[I,I(2),I]$, $\log \beta_{I,I(2),I(int)} = 12.50 \pm 0.25$ and $[-I,I(2),I]$, $\log \beta_{-I,I(2),I(int)} = 2.75 \pm 0.20$. The errors given here are based upon a visual inspection (sensitivity analysis) of the fit to the experimental data. At no stage during the calculations was any attempt made to adjust the acid/base equilibrium constants or the specific capacitance for the boehmite surface. The final constants are given in Table 5.2.4B along with the revised ($\left\{ \begin{smallmatrix} \equiv \text{AlOH} \\ \equiv \text{AlOH} \end{smallmatrix} \right\}$ site) acid/base equilibrium constants. Distribution diagrams for the batch titrations are presented in Figure 5.2.4E.

Table 5.2.4B

p,q,r	$\log (\beta_{p,q(2),r(int)} \pm 3\sigma)$	Proposed formula
$[I,I(2),I]$	12.50 ± 0.25	$\left\{ \begin{smallmatrix} \equiv \text{AlOH}_2 \\ \equiv \text{AlOH} \end{smallmatrix} \right\}^+ \text{H}_3\text{L}^-$ or $\left\{ \begin{smallmatrix} \equiv \text{Al} \\ \equiv \text{Al} \end{smallmatrix} \right\} \text{H}_2\text{L}$
$[-I,I(2),I]$	2.75 ± 0.20	$\left\{ \begin{smallmatrix} \equiv \text{AlOH} \\ \equiv \text{AlOH} \end{smallmatrix} \right\} \text{H}_2\text{L}^{2-}$ or $\left\{ \begin{smallmatrix} \equiv \text{Al} \\ \equiv \text{Al} \end{smallmatrix} \right\} \text{L}^{2-}$
$[-2,I(2),0]$	-19.74	$\left\{ \begin{smallmatrix} \equiv \text{AlO} \\ \equiv \text{AlO} \end{smallmatrix} \right\}^{2-}$
$[-I,I(2),0]$	-9.57	$\left\{ \begin{smallmatrix} \equiv \text{AlOH} \\ \equiv \text{AlO} \end{smallmatrix} \right\}^-$ or $\left\{ \begin{smallmatrix} \equiv \text{AlO} \\ \equiv \text{AlOH} \end{smallmatrix} \right\}^-$
$[1,I(2),0]$	7.76	$\left\{ \begin{smallmatrix} \equiv \text{AlOH}_2 \\ \equiv \text{AlOH} \end{smallmatrix} \right\}^+$ or $\left\{ \begin{smallmatrix} \equiv \text{AlOH} \\ \equiv \text{AlOH}_2 \end{smallmatrix} \right\}^+$
$[2,I(2),0]$	14.92	$\left\{ \begin{smallmatrix} \equiv \text{AlOH}_2 \\ \equiv \text{AlOH}_2 \end{smallmatrix} \right\}^{2+}$
specific capacitance	$1.002 \pm 0.028 \text{ F m}^{-2}$	

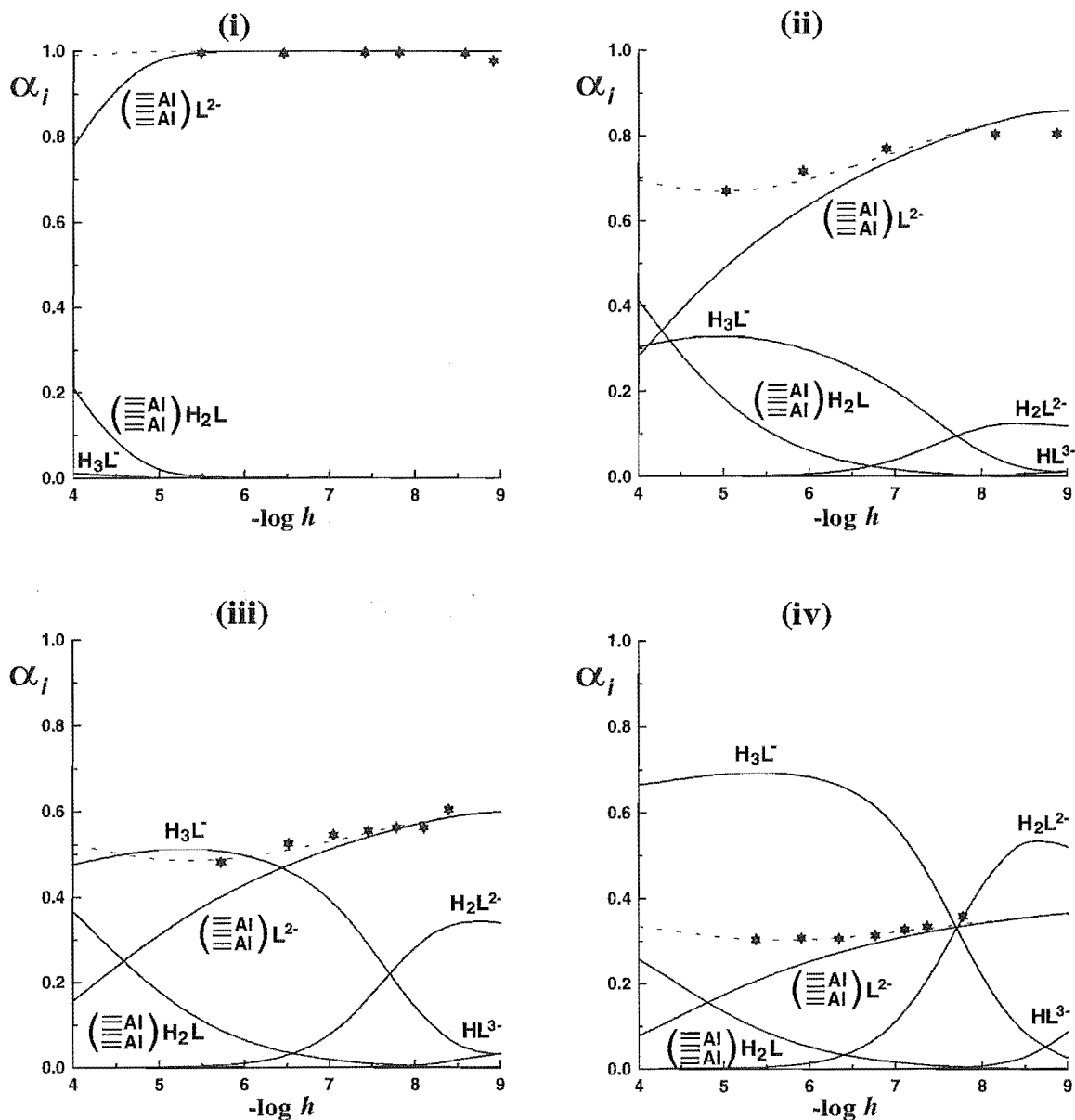


Figure 5.2.4E Distribution diagrams for the batch adsorption titrations with $[\text{PCV}]_{\text{tot}}/[\{\equiv\text{AlOH}\}]_{\text{tot}} =$ (i) 0.42, (ii) 0.84, (iii) 1.25, and (iv) 2.10. α_i defined in Figure 5.2.4C. The solid lines denote the species forming, the symbols represent experimental data and the dashed line was calculated using the proposed model.

The DRIFT spectra are shown in Figure 5.2.4F. Although precautions were taken to prevent degradation of the samples (*e.g.* oxidation of bound ligand) it was noted that for samples prepared at $-\log h \geq 7$ spectra were not reproducible after a period of exposure to air (≤ 30 min).

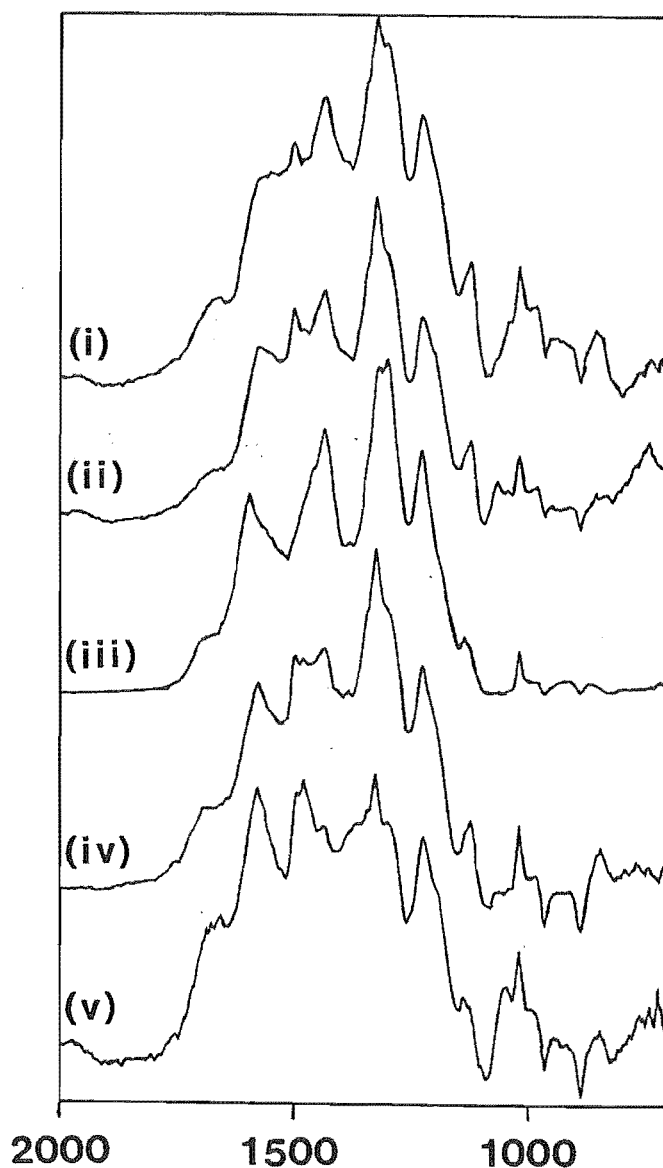


Figure 5.2.4F DRIFT spectra for several batch titration residues. The approximate $-\log h$ for the samples were (i) 5.0, (ii) 5.0, (iii) 6.0, (iv) 7.0 and (v) 8.0.

(C) Spectrophotometric Studies.— Typically natural waters contain Fe or Al oxide materials at concentrations *ca.* 10 mg L^{-1} [Cosby *et al.*, 1981; Laxen, 1985]. Such 'surfaces' may adsorb reagents during speciation analyses of these waters. Therefore the adsorption of PCV at micromolar concentrations on boehmite (at concentrations typical of a natural water) was investigated. Model calculations were made using the computer program SOLGASWATER and the experimental model described in Table 5.2.4B to predict 'expected' amounts of PCV adsorbed from solutions ($\text{pH} = 6.1$) containing varying amounts of boehmite. Batch experiments were performed with solutions (suspensions) containing $20 \text{ } \mu\text{mol L}^{-1}$ PCV and varying amounts of the Al-oxide hydroxide boehmite ($0\text{--}100 \text{ mg L}^{-1}$). The results from these studies are shown in Figure 5.2.4G.

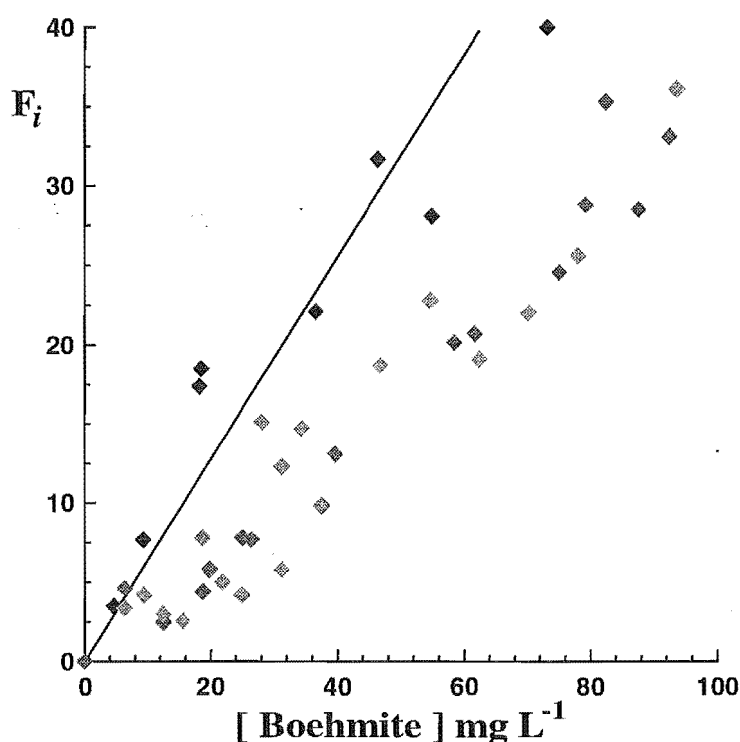


Figure 5.2.4G The adsorption of PCV ($20 \text{ } \mu\text{mol L}^{-1}$) onto boehmite [$0\text{--}100 \text{ mg L}^{-1}$ ($0\text{--}51 \text{ } \mu\text{mol L}^{-1}$ total surface hydroxyl group, $\equiv\text{AlOH}$, concentration)]. F_i represents the percent of PCV present as a surface bound species. The solid line denotes the fraction of adsorbed PCV, F_i , calculated from the equilibrium model. The differently shaded symbols represent different experiments respectively.

5.2.5 DISCUSSION.— The acid/base constants and specific capacitance reported for boehmite are in excellent agreement with those determined by Laiti and Öhman [Table 5.2.4A]. In Figure 5.2.5A(i) the distribution diagram is presented for the titration of a

10.2 mmol L⁻¹ boehmite [$\equiv\text{AlOH}$] solution. The constant capacitance model appeared quite suitable for providing a description of surface equilibria under these conditions.

During the analysis of the 3-component system initial calculations, performed using the equilibrium expressions (5.2.3a) and (5.2.3b), indicated that the dominating surface bound species would be binuclear. To avoid problems arising in the mass balance equations, the zero proton level was redefined to treat a surface site as $\left\{ \begin{smallmatrix} \equiv\text{AlOH} \\ \equiv\text{AlOH} \end{smallmatrix} \right\}$. In this treatment, the 2-component system is described by the formation of the 4 possible hydrolysis species: $[-2,1(2),0]$, $[-1,1(2),0]$, $[1,1(2),0]$ and $[2,1(2),0]$, i.e. $\left\{ \begin{smallmatrix} \equiv\text{AlO} \\ \equiv\text{AlO} \end{smallmatrix} \right\}^{2-}$, $\left\{ \begin{smallmatrix} \equiv\text{AlOH} \\ \equiv\text{AlO} \end{smallmatrix} \right\}^-$, $\left\{ \begin{smallmatrix} \equiv\text{AlOH}_2 \\ \equiv\text{AlOH} \end{smallmatrix} \right\}^+$ and $\left\{ \begin{smallmatrix} \equiv\text{AlOH}_2 \\ \equiv\text{AlOH}_2 \end{smallmatrix} \right\}^{2+}$. The determination of their corresponding equilibrium constants could not be made on such few data over the limited $-\log h$ range. This calculation was made statistically [King, 1965] from the values determined earlier (Table 1), giving $\log \beta_{-2,1(2),0(int)} = -19.74$, $\log \beta_{-1,1(2),0(int)} = -9.57$, $\log \beta_{1,1(2),0(int)} = 7.76$ and $\log \beta_{2,1(2),0(int)} = 14.92$, and stepwise protonation constants, $\log K_n$ ($n=1-4$), 10.17, 9.57, 7.76 and 7.17 respectively. The specific capacitance, c , was not changed. In this manner, the formation of binuclear species at the surface could be treated correctly. In Figure 5.2.5A(ii), the distribution of the acid-base species is presented in accord with this newly defined model. Because this is strictly a mathematical manipulation, the resulting fit between data and model curves (U_{Z_B}) is identical to the previous model involving just two species.

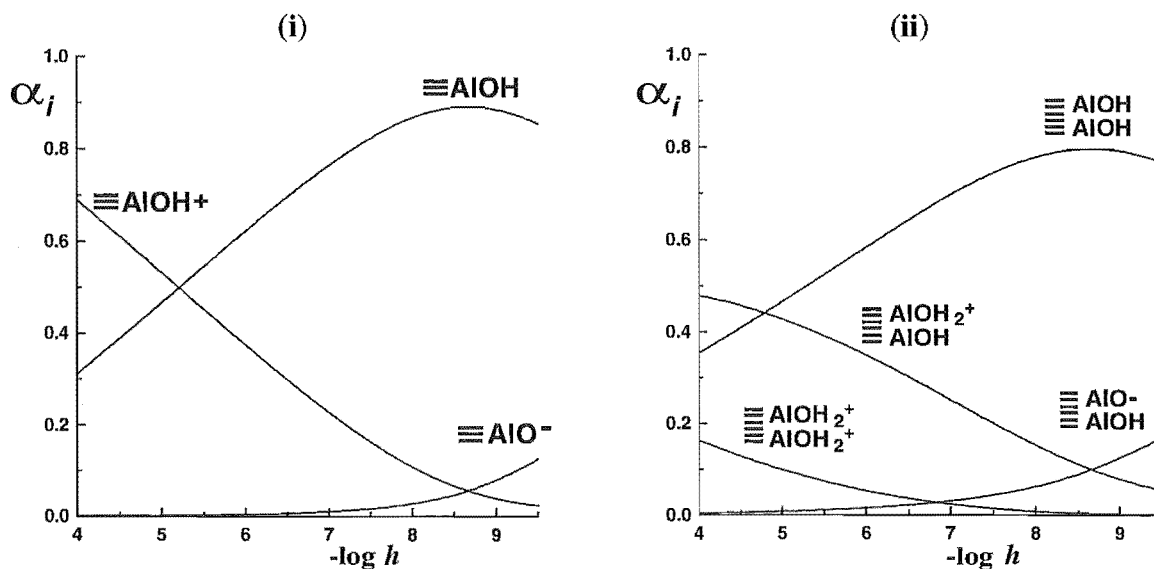


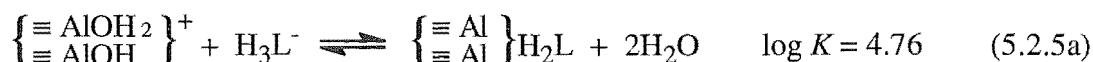
Figure 5.2.5A Distribution of species for boehmite suspension. (i) $[\equiv\text{AlOH}]_{\text{tot}} = 10.2 \text{ mmol L}^{-1}$ and (ii) $\left\{ \begin{smallmatrix} \equiv\text{AlOH} \\ \equiv\text{AlOH} \end{smallmatrix} \right\}_{\text{tot}} = 5.1 \text{ mmol L}^{-1}$. α_i represents the ratio between the concentrations of the individual surface species and the total surface concentration.

From spectrophotometric measurements of free ligand concentrations, no desorption edge was found within the $-\log h$ range studied (Figure 5.2.4C). The lack of either adsorption or desorption edges is consistent with the large $-\log h$ range over which PCV complexes Al^{3+} [Chapter 4 (4.2.3)]. The adsorption of PCV is slightly enhanced in more alkaline suspensions indicating that the main interaction is not just electrostatic but involves surface complexation.

Over the time scale of batch titrations, PCV considerably enhanced surface dissolution at $-\log h \geq 8.5$ whereas for $-\log h$ values 5.0-8.0 surface dissolution was negligible. No surface dissolution was observed during potentiometric titrations; this may be due to the shorter exposure to high $-\log h$. The dissolution studies of aluminium oxide-C in the presence of 8-hydroxyquinoline-5-sulfonate at $\text{pH} = 7.65$ [Hering and Stumm, 1991] indicated continuous ligand-promoted dissolution occurred over time periods > 1 h. In the present experiments dissolution did not occur as quickly, indicating that the Al-PCV surface complexation is weaker or that the interaction of PCV at two surface hydroxy sites may inhibit immediate dissolution of individual Al ions.

In Chapter 4 (Figure 4.2.4C) the expected dissolution effect of PCV on the naturally occurring aluminium oxide 'gibbsite' was predicted. From these calculations it was found that PCV could be expected to increase the dissolution of the oxide over a wide $-\log h$ range. These calculations did not take surface complexation into account. The present study indicated that PCV is adsorbed to the aluminium hydroxide colloids. The model developed to describe this adsorption behaviour involved two species $[I, I(2), I]$ and $[-I, I(2), I]$ with $\log \beta_{p,q(2),r(int)} = 12.50 \pm 0.25$ and 2.75 ± 0.20 respectively. A calculation, using this model, indicated that in the presence of excess PCV, 1 mg L^{-1} ($\mu\text{g L}^{-1}$) of boehmite will remove approximately 0.1 mmol (μmol) PCV from solution. Such adsorption could contribute significant errors in the measurement of Al (or other metal species) in natural waters or soil solution. It is likely that such problems arise for other metallochromic reagents also.

It is possible to calculate a constant for the first equilibrium occurring in the boehmite-PCV system:



The constant for the surface complexation (5.2.5a) may also be compared with values determined for the complexation of phthalate and phenylphosphonate at the boehmite-water interface. In the case of phthalate outer sphere complexation has been postulated *via* the reaction: $\equiv\text{AlOH}_2^+ + \text{L}^{2-} \rightleftharpoons \equiv\text{AlOH}_2^+\text{L}^{2-}$, with $\log K = 1.78$ [Nordin *et al.*, (unpub.)]. Outer sphere complexation is considerably weaker than inner

sphere complexation and this difference is, in part, reflected in the lower $\log K$ for this reaction. For phenylphosphonic acid, a binuclear binding model is proposed [Laiti and Öhman, (unpub.)]. This reaction has a formation constant, $\log K = 9.53$ for $\left\{ \begin{smallmatrix} \equiv \text{AlOH} \\ \equiv \text{AlOH} \end{smallmatrix} \right\} + \text{H}_2\text{L} \rightleftharpoons \left\{ \begin{smallmatrix} \equiv \text{Al} \\ \equiv \text{Al} \end{smallmatrix} \right\} \text{L}$. It is well known that phosphate adsorbs strongly to mineral surfaces [Violante *et al.*, (1991); Nilsson *et al.*, (1992)]. The greater strength of binding by phenylphosphonic acid to boehmite reflects both of these properties.

(A) DRIFT Spectra.— Solution complexation studies [Chapter 4 (4.2.3)] indicated that the 2-hydroxy-*p*-quinomethide moiety dominates Al^{3+} binding at $-\log h \leq 4.5$ and at higher $-\log h$ values there is a shift to phenoxide binding (at the 1,2-dihydroxyaryl moiety). The DRIFT studies (Figure 5.2.4F) did not aid the modelling process but provided valuable information relating to the structure of the species at the surface. The spectra are indicative of inner sphere complexes forming. In general the spectra appeared similar and mostly independent of $-\log h$. However, the intensity of the absorption band at 1685 cm^{-1} , characteristic of $\nu(\text{C}=\text{O})$, increased with increasing $-\log h$. This may indicate that the 2-hydroxy-*p*-quinomethide moiety, which contains such a functional group, is becoming less surface bound as $-\log h$ increases. Catechol, 1,2-dihydroxybenzene, has major absorption bands at 1495 and 1255 cm^{-1} [McBride and Wesselink, 1988]. The decrease in absorption near 1495 cm^{-1} with increasing $-\log h$ may indicate that the 1,2-dihydroxyaryl moiety of PCV is interacting with the surface and becoming progressively more bound. The DRIFT studies indicate that a shift in the binding mode of the surface bound species may occur with increasing $-\log h$.

In an infrared study of catechol adsorption on boehmite [McBride and Wesselink, 1988] binuclear complexation was invoked. Their studies were in contrast to an earlier study of catechol adsorption on γ -alumina [Kummert and Stumm, 1980] where the mode of binding was assumed to be *via* a mononuclear complex. In this work the formation of two binuclear complexes provides a good description of the surface adsorption processes for PCV at the boehmite-water interface.

(B) Mechanism of Complexation.— Several structural descriptions of the surface bound species are plausible. Although PCV is significantly larger than catechol, it contains two metal binding sites (*i.e.* 2-hydroxy-*p*-quinomethide and 1,2-dihydroxyaryl moieties). The PCV molecule is $\sim 1 \text{ nm}^2$ (based on the catechol structure) and the distance between donor atom pairs $\sim 0.25 \text{ nm}$. The surface area and total surface hydroxyl group concentration of boehmite imply $\sim 1 \left\{ \begin{smallmatrix} \equiv \text{AlOH} \\ \equiv \text{AlOH} \end{smallmatrix} \right\} \text{ site nm}^{-2}$. Based on this information and the model developed, three possible surface binding modes are apparent. PCV may bind *via* (a) one moiety involving two 'sufficiently close' surface hydroxyl groups $[\equiv \text{AlOH}]$, *i.e.* at a $\left\{ \begin{smallmatrix} \equiv \text{AlOH} \\ \equiv \text{AlOH} \end{smallmatrix} \right\}$ site, (b) both chelate moieties simultaneously to non-paired (*i.e.* more

widely spaced) surface hydroxy groups or alternatively, (c) one moiety to a mononuclear surface site while the dimensions of the molecule and/or weaker interactions from the other moiety prevent a second (neighbouring) $\equiv\text{AlOH}$ group from dissociating (in accord with the acid/base properties).

Studies by Laiti and Öhman (unpub.) indicated that phenylphosphonic acid (PPA) is coordinated to one proton active site and 'blocking' the other (possibly hydrogen bonding). The two binding moieties of PPA are closer than those in PCV implying that the surface hydroxyl groups involved must be closer than that indicated by the surface concentration (*i.e.* the surface hydroxyl groups are not evenly distributed and are more or less 'paired', thus forming a bidentate 'site'). Ogawa (1991) studied the adsorption of benzoic acid on an alumina surface and concluded that adsorption occurred predominantly in the vertical orientation. The structure of PCV would indicate that if it was bound vertically then both complexing moieties would not be in a favourable position for strong binding. Complexation *via* the 1,2-dihydroxyaryl moiety, with a second $\text{p}K_a > 12$, would be unlikely to occur at low $-\log h$ values unless orientations were favourable. Therefore, if both functionalities are simultaneously involved in surface binding, PCV must interact at a shallow angle to the surface so that both moieties are in favourable orientations. The DRIFT spectra indicated a shift in binding modes as a function of $-\log h$. If the 2-hydroxy-*p*-quinomethide moiety is to be considered as unbound at higher $-\log h$ values, as a result of increased phenoxide binding, then it is likely that only one binding site of PCV is required for complex formation.

These observations indicate that PCV attaches to the boehmite surface predominantly *via* complexation at one moiety and this complexation involves two $\equiv\text{AlOH}$ groups. If the surface hydroxyl groups are not close enough for this interaction then it must be invoked that the second $\equiv\text{AlOH}$ group is affected by a mechanism not involving direct complexation. A mechanism for the complexation is proposed (Figure 5.2.5B). Details regarding the intermediate steps [(b) and (c)] have been discussed previously [Chapter 4 (4.2.4)]. The PCV molecules bound at the surface are likely to affect the surface potential description provided by the constant capacitance model. Preliminary calculations in which the charge on PCV was varied indicated that the negatively charged sulfonate group does affect the behaviour of PCV at the surface. PCV (H_3L^-) was given a charge of -1 in the model and the two species, $[1,1(2),1]$ and $[-1,1(2),1]$, have net charges of 0 and -2 respectively.

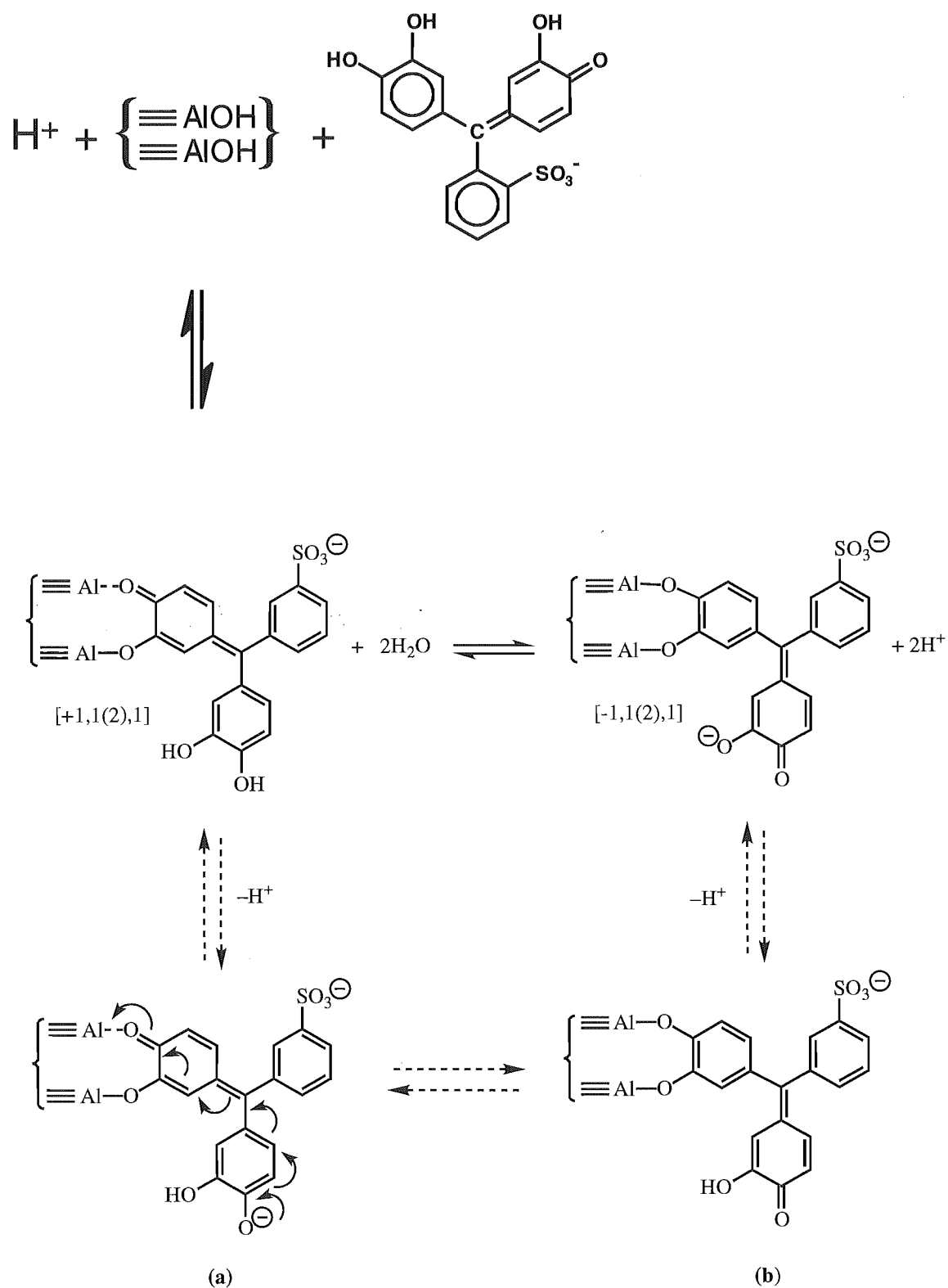


Figure 5.2.5B Proposed mechanism for PCV binding at the boehmite-water interface.

The study of this system involved the use of 3 techniques aimed at providing information on solution equilibria and the complexation reactions taking place. A series of potentiometric titrations at different ratios of ligand concentration to number of surface sites were performed to obtain accurate and detailed information relating to proton stoichiometry during possible complexation reactions. Batch titrations, involving the equilibration of a boehmite-PCV suspension and subsequent analysis of free PCV and Al^{3+} , were performed to provide information on total PCV adsorption and possible dissolution effects at the surface. Benefit was gained from combining potentiometric and ligand adsorption data into one calculation, with simultaneous minimisation of errors (between model and data). It was also important, however, to balance the weighting in such a calculation so that data of higher accuracy took preference in the final model calculation.

(C) Spectrophotometric Studies.— The adsorption of PCV at micromolar concentrations on boehmite (at concentrations typical of a natural water) was investigated. From Figure 5.2.4G it is apparent that a major discrepancy exists between the model used in the calculations and the experimental conditions. There are, however, several possible sources of error that may account for most of this discrepancy.

The conditions (temperature control, inert atmosphere, pH measurement and purity of the components) used in the development of this model were very well controlled. In the experiments discussed here the experimental conditions were 'far less controlled', *i.e.* the experimental conditions were designed to imitate the 'average experimental conditions' used by an analyst performing Al speciation experiments. Temperature control is often not employed by analysts and an inert atmosphere would never be considered in Al analysis; pH measurements are typically made using a laboratory pH meter (*i.e.* ± 0.1 units).

In these experiments it was observed that boehmite 'stuck' to the walls of the centrifuge tubes. If the boehmite became attached to the walls immediately during an experiment then this could result in a loss of PCV-adsorbing surface sites and, hence, an expected increase in free $\text{PCV}_{(\text{aq})}$ relative to model predictions. During the batch experiments (used for model development) centrifugation was performed in a temperature controlled centrifuge, *i.e.* the samples did not over-heat during centrifugation. Temperature control was not possible in the centrifuge used in the latter experiments (discussed here). Samples were noticeably 'warm' when removed from the centrifuge and this may have resulted in small sample re-equilibration during centrifugation (20 min). No temperature control (room temperature *ca.* 16–18 °C) was used throughout the adsorption period (72 h).

Possibly the most important source of error in the design of these experiments may have been the use of a buffer. Schulthess and McCarthy (1990) highlighted the

importance of controlling the concentrations of electrolyte ions in adsorption studies. These studies investigated the competitive nature of carbonate and acetic acid for adsorption sites on $\gamma\text{-Al}_2\text{O}_3$ over a wide pH range. In the present studies, the system used during model development contained only the components: ' H^+ -boehmite-PCV- K^+ - Cl^- '. However, during the experiments discussed here, a buffer was necessary for maintaining the pH of each batch at $\text{pH} = 6.1$. The buffer used was 0.05 mol L^{-1} MES [2-(N-morpholino)ethanesulfonic acid]; this 'ligand' has a pK_a of 6.1 (25°C). At pH 6.1 the boehmite surface can be expected to be predominantly positively charged; this may be sufficient to electrostatically attract the negatively charged buffer, $\{\text{C}_6\text{H}_{12}\text{NO}\}-\text{SO}_3^-$, ions (approximately 50 % of the MES) and result in some blocking of surface sites. Although electrostatic adsorption of sulfate complexes is likely to be very weak, the great excess of the buffer over PCV (0.05 mol L^{-1} MES vs $20 \text{ }\mu\text{mol L}^{-1}$ PCV) makes this the best explanation for the discrepancies observed in Figure 5.2.4G.

From Figure 5.2.4G it is clear that PCV will be adsorbed by oxide particles at concentrations typical of natural waters. For a $20 \text{ }\mu\text{mol L}^{-1}$ PCV solutions approximately 5 % could be expected to become adsorbed by oxide particles at 10 mg L^{-1} . The results also highlight the difficulties in quantitatively predicting surface adsorption from model systems developed using 'clean systems', *i.e.* only small differences between the system the model was developed for and the 'new' experimental conditions may result in predictions becoming quite 'unsatisfactory'.

CHAPTER 6

COMPARISON OF CHROMOPHORES AND REACTION KINETICS IN COMPETITIVE 'REAGENT-AL-LIGAND' SYSTEMS

This chapter describes the evaluation of interferences for three metallochromic reagents (using computer modelling) and the effects of complexation kinetics on the determination of 'labile' Al in the presence of two Al complexing ligands. It is divided into 2 parts.

SECTION A: A comparison of the chromophores chrome azurol S (CAS), eriochrome cyanine R (ECR) and pyrocatechol violet (PCV) for the determination of Al was made. These studies were performed using computer modelling calculations. The pH and mass action effects were calculated for the representative 'interferents' citrate, oxalate, salicylate and fluoride.

SECTION B: The effects of complexation kinetics on the use of PCV for the determination of 'labile' Al in the competitive systems: 'PCV-Al³⁺-citrate' and 'PCV-Al³⁺-oxalate' was investigated. These studies also validate the 'H⁺-Al³⁺-pyrocatechol violet' equilibrium data (presented in Chapter 4) for typical analytical conditions.

SECTION A: COMPARISON OF CHROMOPHORES CAS / ECR / PCV

6.1 INTRODUCTION

The interest in reagents with the ability to determine (i) 'total Al' and (ii) 'free or labile Al' has increased considerably in recent years. In the first of these determinations, 'total Al' should represent the total aqueous Al concentration of an analyte solution. In contrast, a determination of 'free or labile Al' should measure only the fraction of Al that is free or weakly bound (hence labile). This fraction typically comprises the hexaaquo Al ion $\text{Al}(\text{H}_2\text{O})_6^{3+}$, monomeric Al-hydroxy species, inorganic Al-ligand complexes (AlX , *e.g.* $\text{X} = \text{F}^-$, PO_4^{3-} , SO_4^{2-}), or labile Al-organic complexes (AlL , *e.g.* $\text{L} = \text{phthalate}$, salicylate).

Techniques for the determination of 'total Al' are often more accurate than those for the determination of 'free or labile Al' and do not involve the operational definitions fundamental to the latter. Techniques applicable to the determination of 'free or labile Al' (the Al of greatest environmental concern) have been discussed in Chapter 1 (1.3). Common to both of these methods is the use of a reagent (R) that will form a strong complex, Al-R , and exhibit desirable properties (*e.g.* spectrophotometric, electrochemical)

that allow its accurate measurement. Spectrophotometric analyses have been the most utilised [Røyset, 1985; Hawke and Powell, 1994; Hodges, 1987].

As discussed in Chapter 4 (4.2) numerous chromogenic reagents have been investigated for the spectrophotometric or FIA-spectrophotometric analysis of Al in environmental systems, *e.g.* pyrocatechol violet (PCV), chrome azurol S (CAS), eriochrome cyanine R (ECR), 8-hydroxyquinoline (oxine), ferron and aluminon. The characteristics of each of these reagents (*e.g.* optimum pH, λ_{\max} and molar extinction coefficient, ϵ , for the Al-reagent complex) differ significantly. Likewise, the functional groups involved in Al complexation, the thermodynamic stability and the stoichiometry of the resulting Al-reagent complex differ for each of these reagents. The particular characteristics of the reagent and the Al-reagent complex affect the method's sensitivity. Furthermore, these characteristics affect the degree to which other Al-complexing ligands may interfere in Al determinations.

A number of researchers have compared chromogenic reagents and discussed their applicability to the determination of Al in natural waters [Røyset, 1985; Røyset and Sullivan, 1986; Hodges, 1987; Lewis *et al.*, 1988; Hawke and Powell, 1994] or in the assay of phytotoxic aluminium [Wright *et al.*, 1987; Noble *et al.*, 1988; Parker *et al.*, 1988; Alva *et al.*, 1989].

Determining Aluminium in Natural Waters: Røyset (1985) compared the reagents PCV, aluminon, ECR and ECR/CTA (cetyltrimethylammonium bromide) for the FIA-spectrophotometric determination of Al in water. The most sensitive of these methods was the ECR/CTA technique [detection limit (D.L.) = $1 \mu\text{g Al L}^{-1}$], compared with a D.L. of $5 \mu\text{g Al L}^{-1}$ for the PCV and ECR techniques. The potential interferents fluoride, phosphate and iron were investigated and tolerance levels discussed. Fe interferences could be masked in all methods by using suitable reagents (*e.g.* hydroxylammonium chloride/1,10-phenanthroline or ascorbic acid). Phosphate interferences were negligible at PO_4^{3-} concentrations typical of natural waters. Fluoride, however, exhibited significant interference in all methods, particularly for the ECR/CTA and aluminon methods. The PCV and ECR methods were not significantly affected by fluoride at concentrations below 0.5 mg L^{-1} (typical of natural waters).

The potential interference from dissolved humic substances on PCV, ECR and oxine methods was investigated by Røyset and Sullivan (1986). These organic acids form stable complexes with Al and will potentially result in underestimations of both total monomeric and nonlabile monomeric Al [NOTE: for 'Driscoll fractionation protocols' labile monomeric Al (often correlated with toxicity) is calculated as the difference between these two fractions]. Interference was apparent in all three methods at dissolved organic carbon (DOC) concentrations above 10 mg L^{-1} and the interpretation of Al speciation for methods using Driscoll's fractionation protocol [as described in Chapter 1 (1.3)] becomes

increasingly difficult at higher DOC concentrations. Furthermore, interferences were observed to be pH dependent (as may be expected for substances exhibiting a variety of complexing moieties *e.g.* phenolic and carboxylic groups).

Hodges (1987) compared five procedures for the speciation of Al. The reactive Al values obtained by the oxine method (15 s) correlated well with those from the indirect fluoride electrode procedure in predicting Al^{3+} and 'toxic Al' [$\text{Al}^{3+} + \text{AlOH}^{2+} + \text{Al}(\text{OH})_2^+$] concentrations. However, the studies also indicated the difficulty in using chromogenic reagents (ferron and oxine) for estimating Al^{3+} and toxic Al concentrations in natural waters with high DOC concentrations.

The monomeric Al concentrations estimated using PCV, oxine and fluoride electrode methods in the presence of a variety of organic ligands (including humic and fulvic acids) were investigated by Lewis *et al.* (1988). Ligands with phenolic and/or carboxylic groups in ortho positions caused significant reduction in apparent monomeric Al concentrations. The greatest reductions were caused by citric acid and CDTA. The extent of these effects was dependent on ligand configuration and complexing moieties present, the stability of the measured Al-ligand complex, pH and reaction kinetics. Furthermore, the studies indicated that (if not controlled adequately) factors such as (i) measurement pH, (ii) reagent concentration and Al/reagent ratio, and (iii) dissociation kinetics of the Al-ligand complex relative to the kinetics of the measurement reaction, will significantly affect the value of monomeric Al estimated.

Recently Hawke and Powell (1994) compared the chromogenic reagents CAS, ECR and PCV for the kinetic determination of reactive Al in natural waters and soil solutions. The effects of pH, ionic strength, buffer composition and reagent concentration were investigated. PCV was found to be more aggressive towards 'complexed' Al than CAS and ECR. Furthermore, the absorbance for the Al-PCV complex ($\lambda_{\text{max}} = 580 \text{ nm}$) was observed to vary with time. Mass action effects observed using different reagent concentrations highlighted the potential for stripping of Al from labile Al-ligand complexes. These effects were dependent on the complexing characteristics of both the reagent and the ligand, *i.e.* the complexing moieties present and both the lability and stability of the Al-ligand(reagent) complexes. The lowest D.L. for the determination of 'kinetically-labile' (10 s reaction) and 'equilibrium reactive' (10 min reaction) was obtained for CAS (D.L. = 60 nmol L^{-1}).

Assaying Phytotoxic Aluminium: The use of chromogenic reagents for the assay of phytotoxic Al in soil and nutrient solutions has been subject to considerable research recently. Numerous studies have indicated that the presence of anions including SO_4^{2-} and F^- alleviate Al toxicity in culture solutions [Chapter 1 (1.2)]. Wright *et al.* (1987) showed that oxine (15 s reaction) and aluminon (30 min reaction) were better predictors

of phytotoxic Al in soil solutions than ferron (30 s reaction). However, the extent to which these reagents may strip Al from organically complexed forms was not investigated.

A comparison of aluminon and oxine methods for the assaying of phytotoxic Al in the presence of F^- was investigated by Noble *et al.* (1988). These studies were performed in nutrient solutions for which the concentrations of Al^{3+} and Al-F complexes were predicted using the computer program GEOCHEM. Significant correlations (non-linear, $r^2 > 0.97$) were found between (i) 'predicted' Al^{3+} and (ii) labile Al (oxine method) and soybean tap root length. The aluminon method measured a significant fraction of the Al complexed by F^- and tap root length was poorly correlated with this measurement.

Alva *et al.* (1989) evaluated the oxine, aluminon and ferron Al assay techniques. These studies were, in particular, directed towards the use of these reagents to measure Al^{3+} while excluding Al complexed by F^- and SO_4^{2-} from the measured fraction (the effect of reaction time was investigated). All three methods were observed to effectively exclude Al complexed by F^- , however the reagents failed to exclude Al complexed by SO_4^{2-} (regardless of reaction time). It is therefore likely that these reagents will overestimate phytotoxic Al in the presence of high concentrations of SO_4^{2-} (*i.e.* high $AlSO_4^+$ concentrations). For soil solutions with high $AlSO_4^+$ concentrations, the use of computer-based speciation modelling, following the complete characterisation of anion and cation concentrations, may be a better predictor of Al toxicity than currently available methods.

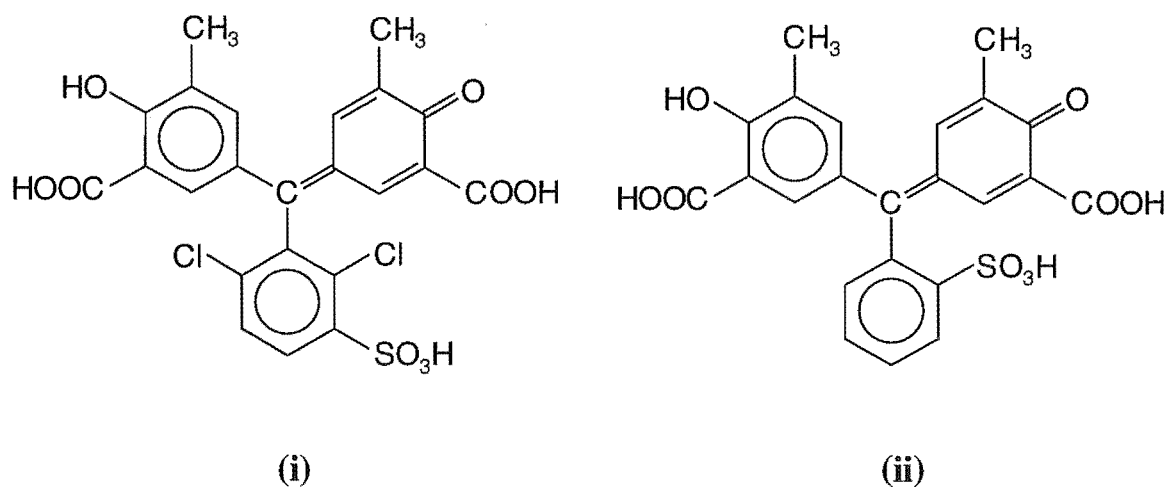
The ability of a method to differentiate between monomeric and polymeric hydroxy-Al species is also of relevance to assaying phytotoxic Al. Parker *et al.* (1988) investigated the reagents oxine, aluminon and ferron for this purpose. The three reagents were ranked in the order: oxine > ferron > aluminon, with respect to precision in estimating mononuclear Al in solutions with molar ratios of OH/Al up to 2.25. The studies demonstrated the use of ferron for the kinetic analysis of the mononuclear Al fraction.

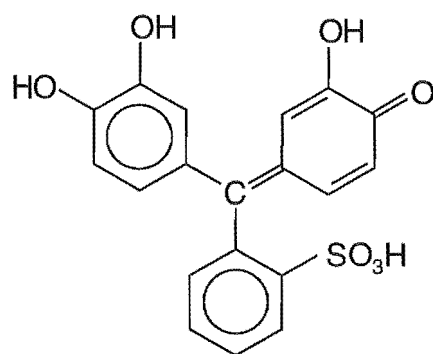
6.1.1 SCOPE OF THIS WORK.— Recently, thermodynamic speciation models (computer based) have been employed to predict solution 'Al-toxicity' by calculating theoretical distributions of the various Al species present in the solution. These calculations utilise solution pH and the total concentrations of Al and other cations and anions in solution. Unfortunately, when this approach is applied to natural systems (in contrast to synthetic solutions) the analysis of all cations and anions (including organic ligands) must be undertaken. This is a tedious procedure and often the organic components cannot be accurately characterised. Therefore, this approach has been utilised only when the analyte solution can be easily characterised, or for synthetic solutions (*e.g.* nutrient solutions).

As discussed above, a number of research groups have compared various reagents for their ability to measure Al in the presence of potentially interfering cations and anions common to natural waters and soil solutions (*e.g.* Fe^{3+} , F^- , PO_4^{3-} , SO_4^{2-} and organic acids *viz* citric, malonic, humic and fulvic acids *etc.*). These studies have been performed experimentally and, because of their time-consuming nature, the concentration ranges of reagent and 'interfering' ligands as well as pH are often limited (*i.e.* interferents are usually evaluated experimentally under narrowly defined analytical conditions).

A complementary approach to evaluating interferences is to carry out computer modelling studies using equilibrium constants. This approach is not often feasible due to a lack of appropriate equilibrium data for either the interferent or the colorimetric reagent. Recently, however, equilibrium constants have been published for two commonly used Al chromophores: chrome azurol S (CAS) [Hawke *et al.*, 1995], and eriochrome cyanine R (ECR) [Hawke *et al.*, 1996]. In Chapter 4 the equilibrium constants for pyrocatechol violet (PCV) were determined. In Figure 6.1.1 the structures of the three metallochromic reagents (i) CAS, (ii) ECR and (iii) PCV are given.

In the present work a comparison is made between the abilities of the reagents CAS, ECR and PCV to determine total Al in natural systems. This comparison is based on calculations for competitive equilibria between the reagent (R) and ligand (L) for Al. The ligands (potential interferents) used were citrate, oxalate, salicylate and fluoride (representing ligands with Al-complexing properties 'typical' of soils and natural waters) and the calculations were made over the pH range 4.5 - 6.5. The pH and mass action effects of the representative interferents on the 3 chromophores were calculated. The implications of the calculations for assays of total Al and toxic Al are discussed.





(iii)

Figure 6.1.1 Structures of the metallochromic reagents (i) CAS, (ii) ECR and (iii) PCV.

6.1.2 EXPERIMENTAL

Modelling calculations for the effect of interfering ligands on CAS, ECR and PCV assays for Al were performed using the computer program SOLGASWATER [Eriksson, 1979]. The chosen pH range (4.5 - 6.5) reflects the pH of natural systems (especially soil solutions), and encompasses the pH optima for chromophore complexation. The calculations used a pH scale based on concentration, $p[H^+]$, rather than activity, $pa(H^+)$, as used by most analysts. However, the 2 scales are sufficiently similar for the purposes of this study.

Choice of model ligands was constrained by availability of stability constants. The ligands chosen were the strong organic complexant citrate [Öhman, 1988], the weaker complexants oxalate [Sjöberg and Öhman, 1985] and salicylate [Öhman and Sjöberg, 1983] and the strong inorganic complexant fluoride [Nordstrom and May, 1989]. Stability constants for the chromophores were from: CAS [Hawke *et al.*, 1995], ECR [Hawke *et al.*, 1996] and PCV [Chapter 4, Table 4.2.3] and, as for the Al^{3+} hydrolysis constants, were determined for $I = 0.1 \text{ mol L}^{-1}$. The Al^{3+} hydrolysis constants were from Brown *et al.* (1985). The formation constant for $Al(OH)_4^-$ ($\log \beta_{-4,1,0}$) was calculated by the method of Millero and Schreiber (1982) from the thermodynamic constant of Palmer and Wesolowski (1992) [assuming $\gamma(Al(OH)_4^-) = \gamma(OH^-)$]. Constants were not available for all the ligands at $I = 0.1 \text{ mol L}^{-1}$, but were available at $I = 0.6 \text{ mol L}^{-1}$ (F^- : $I = 0.53 \text{ mol L}^{-1}$). While the difference in ionic strengths was not ideal, it was a consistent factor.

The constants for the reagents CAS and ECR are given in Table 6.1.2A (constants for PCV are given in Chapter 4, Table 4.2.3) along with the Al^{3+} hydrolysis constants. The thermodynamic data for the ligands (citrate, oxalate, salicylate and fluoride) were obtained from the references cited above and are given in Table 6.1.2B.

Table 6.1.2A Thermodynamic data for the systems: $H^+ - Al^{3+}$ -reagent (R) (where R = CAS or ECR) and $H^+ - Al^{3+}$ (aluminium hydrolysis). The equilibrium constants ($\beta_{p,q,r}$) are given according to the reaction: $pH^+ + qAl^{3+} + rR^{3-} \rightleftharpoons H_pAl_qR_r^{(p+3q-3r)+}$.

Species	(p,q,r)	log $\beta_{p,q,r}$
CAS (L^{3-})		
LH_1^{4-}	(-1,0,1)	-11.64
HL^{2-}	(1,0,1)	4.64
H_2L^-	(2,0,1)	6.93
AlH_1L^-	(-1,1,1)	2.01
$Al_2H_1L_2^-$	(-1,2,2)	12.92
$Al_3H_2L_2^+$	(-2,3,2)	12.29
$Al_4H_4L_5^{7-}$	(-4,4,5)	26.57
$Al_4H_3L_5^{6-}$	(-3,4,5)	31.35
ECR (L^{3-})		
HL^{2-}	(1,0,1)	4.42
H_2L^-	(2,0,1)	6.93
AlH_1L^-	(-1,1,1)	1.75
$Al_3H_2L_2^+$	(-2,3,2)	13.44
$Al_4H_3L_5^{6-}$	(-3,4,5)	29.07
$Al_4H_4L_5^{7-}$	(-4,4,5)	25.30
$Al_4H_5L_5^{8-}$	(-5,4,5)	20.67
Al-hydrolysis		
$AlOH^{2+}$	(-1,1,0)	-5.33
$Al(OH)_2^+$	(-2,1,0)	-10.91
$Al_3(OH)_4^{5+}$	(-4,3,0)	-13.13
$Al(OH)_4^-$	(-4,1,0)	-23.30
$Al_{13}(OH)_{32}^{7-}$	(-32,13,0)	-107.41
K_w	(-1,0,0)	-13.78

Table 6.1.2B Thermodynamic data and equilibrium constants ($\beta_{p,q,r}$) for the systems: H^+ - Al^{3+} -ligand (L), where L = citrate, oxalate, salicylate and fluoride respectively.

Species	(<i>p, q, r</i>)	$\log \beta_{p,q,r}$
Citric acid (H_3L)		
H_2L^-	(-1,0,1)	-2.77
HL^{2-}	(-2,0,1)	-6.85
L^{3-}	(-3,0,1)	-12.07
$AlHL^+$	(-2,1,1)	-2.68
AIL^0	(-3,1,1)	-4.92
AIL_2^{3-}	(-6,1,2)	-12.53
$Al_3(OH)(H_{-1}L)_3^{4-}$	(-13,3,3)	-21.77
$Al(H_{-1}L)^-$	(-4,1,1)	-8.48
$AlOH(H_{-1}L)^{2-}$	(-5,1,1)	-14.71
$Al_3(OH)_4(H_{-1}L)_3^{7-}$	(-16,3,3)	-47.11
Oxalic acid (H_2L)		
HL^-	(-1,0,1)	-0.97
L^{2-}	(-2,0,1)	-4.54
$AlHL^{2+}$	(-1,1,1)	1.40
AIL^+	(-2,1,1)	1.43
AIL_2^-	(-4,1,2)	1.85
AIL_3^{3-}	(-6,1,3)	1.26
$Al_3(OH)_3L_3^0$	(-9,3,3)	-4.28
$Al_2(OH)_2L_4^{4-}$	(-10,2,4)	-4.62
Salicylic acid (H_2L)		
HL^-	(-1,0,1)	-2.72
L^{2-}	(-2,0,1)	-15.82
AIL^+	(-2,1,1)	-3.05
AIL_2^-	(-4,1,1)	-8.39
$AlOHL_2^{2-}$	(-5,1,2)	-15.99
$Al(OH)_2L_2^{3-}$	(-6,1,2)	-23.31
Fluoride (F^-)		
HF	(1,0,1)	3.14
AlF^{2+}	(0,1,1)	6.13
AlF_2^+	(0,1,2)	11.15
AlF_3^0	(0,1,3)	15.00

Concentrations chosen for the modelling reflected analytical and regulatory requirements. The WHO guideline for total Al in drinking water ($7.4 \mu\text{mol L}^{-1} = 0.2 \text{ ppm}$) was used. Chromophore concentrations were $20 \mu\text{mol L}^{-1}$ (typical of kinetic FIA methods [Hawke and Powell, 1994]) and $100 \mu\text{mol L}^{-1}$ (typical of conventional colorimetry). This range also allowed exploration of mass action effects. Ligand concentrations were $20 \mu\text{mol L}^{-1}$ (citrate, fluoride, oxalate) or $500 \mu\text{mol L}^{-1}$ (salicylate).

6.1.3 RESULTS

(A) Speciation in the Systems: $H^+ \text{-} Al^{3+}$ -Reagent and $H^+ \text{-} Al^{3+}$ -Ligand.— The speciation of the $H^+ \text{-} Al^{3+}$ -reagent(R) and $H^+ \text{-} Al^{3+}$ -ligand(L) systems has been described fully in the relevant papers. In brief, the equilibria of CAS and ECR are very similar and dominated by the formation of a single monomeric species at the concentrations and pH range chosen for these studies (4.5 - 6.5). Small amounts of polymeric species form over this pH range. Unlike CAS and ECR, at spectrophotometric concentrations PCV does not complex Al strongly over this entire pH range [see Figure 4.2.4B (Chapter 4)]. At $\text{pH} < 5.5$ complexation is incomplete and a mixture of species is formed, including polymeric species at lower PCV/Al ratios. At $\text{pH} > 5.5$ complexation is strong and dominated by the formation of the species $Al(PCV)_2$.

Citrate binds Al strongly ($> 90 \%$) over the chosen pH range and at $\text{pH} > 5.7$ greater than 99 % of Al is complexed by citrate. Increased ligand and/or metal concentrations do not significantly affect the outcome of these results. Oxalate binds $> 90 \%$ of Al at $\text{pH} < 5.5$ whereas at higher pH values oxalate is displaced by OH^- . Salicylate binds $> 80 \%$ of Al over the chosen pH range with maximum binding at $\text{pH} = 5.5$. Fluoride, at $\text{pH} < 5.5$, complexes greater than 80 % of Al but as pH increases above this value OH^- quickly displaces fluoride and there is almost no complexation at $\text{pH} = 6.5$. For these ligands, lower ligand concentrations and lower ligand/Al ratios increase the rate at which OH^- displaces the ligand, especially over pH ranges where binding is not optimal.

(B) Speciation in the Competitive $H^+ \text{-} Al^{3+}$ -Ligand-Reagent Systems

(i) Citrate: Citrate binds Al very strongly (Figure 6.1.3A). Addition of the chromophores to the modelling calculation showed that neither CAS nor ECR are effective in sequestering Al from citrate. At $20 \mu\text{mol L}^{-1}$ chromophore concentration, CAS and ECR removed $< 10 \%$ of Al from citrate at pH 4.5, decreasing to $< 2 \%$ at pH 6.5. In contrast, PCV showed decreasing interference from citrate (increasing sequestration of Al) with increasing pH. Increasing each chromophore concentration fivefold, from $20 \mu\text{mol L}^{-1}$ to $100 \mu\text{mol L}^{-1}$, decreased citrate interference. At the optimum pH for each chromophore determined by the original investigators {CAS, pH 5.0 [Pakalns, 1965]; PCV, pH 6.2 [Dogan and Wilson, 1974]; ECR, pH 5.5 [Hill, 1966]}, the amount of sequestered Al

increased 3-fold (CAS, 7 \rightarrow 23 %; PCV, 30 \rightarrow 90 %), or 4-fold (ECR, 1.5 \rightarrow 6 %). For PCV at 100 $\mu\text{mol L}^{-1}$, increasing the pH from 6.2 to 6.5 led to negligible citrate interference. The above calculations clearly demonstrate the importance of both pH and mass action effects in controlling interference levels. However, equilibration in the H^+ - Al^{3+} -PCV (20 $\mu\text{mol L}^{-1}$) - citrate system requires in excess of 300 min at pH 6.2 (see SECTION B of this Chapter).

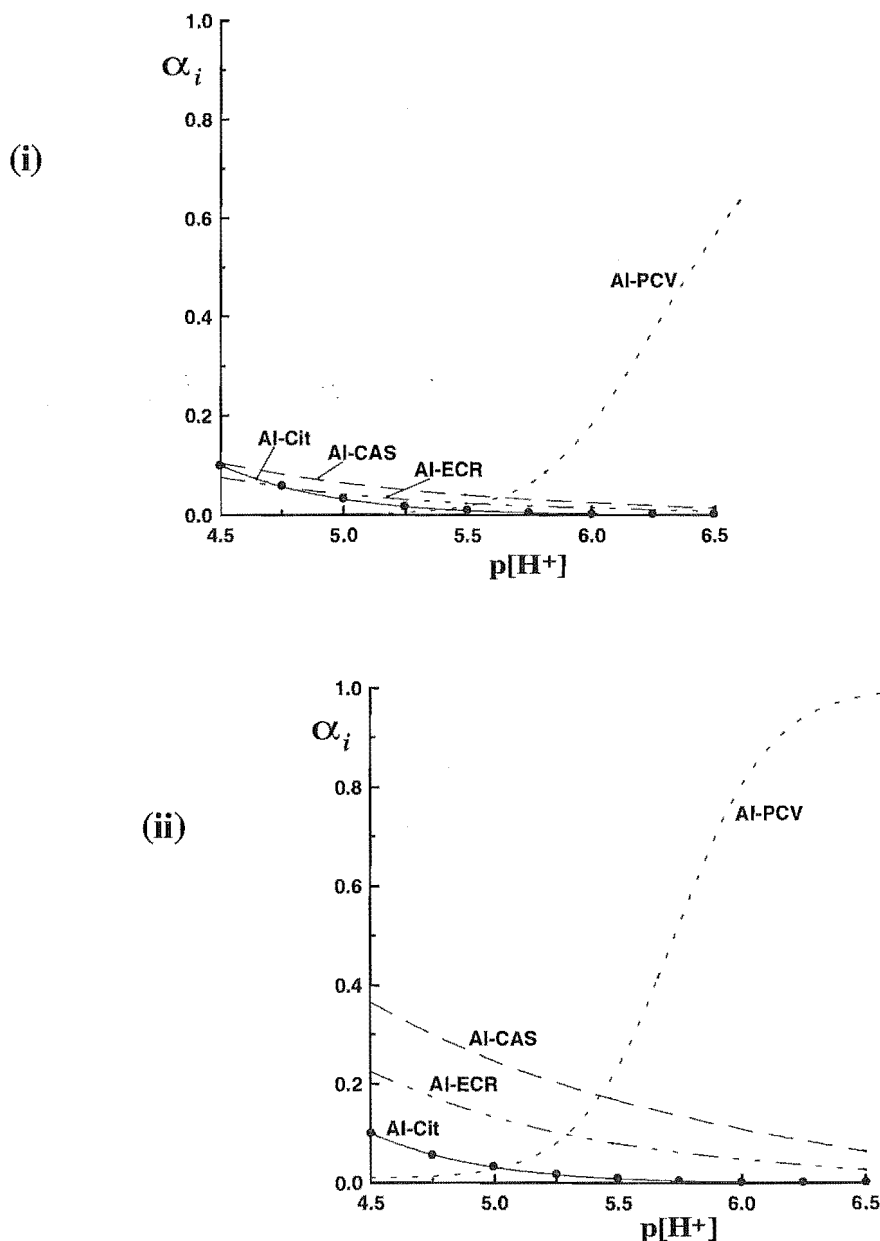


Figure 6.1.3A Calculated Al speciation in the presence of 20 $\mu\text{mol L}^{-1}$ citrate, and (i) 20 $\mu\text{mol L}^{-1}$ chromophore and (ii) 100 $\mu\text{mol L}^{-1}$ chromophore at 7.4 $\mu\text{mol L}^{-1}$ total Al. α_i represents the fraction of Al complexed by each chromophore. Also shown is the fraction of non-complexed Al in the absence of chromophore ($\text{---}\bullet\text{---}$).

(ii) **Oxalate:** Oxalate is a significantly weaker ligand than citrate. Thus, at $20 \mu\text{mol L}^{-1}$ oxalate and $20 \mu\text{mol L}^{-1}$ PCV [Figure 6.1.3B(i)], oxalate showed negligible interference at $\text{pH} \geq 6.0$. In contrast to citrate, oxalate interference with CAS and ECR determinations of Al decreased with increasing pH up to pH 6.2. This is a consequence of the different pH dependence of complexation, with Al complexation by oxalate being essentially complete at $\text{pH} < 4.5$. CAS and ECR showed least interference at pH 5.8 - 6.2.

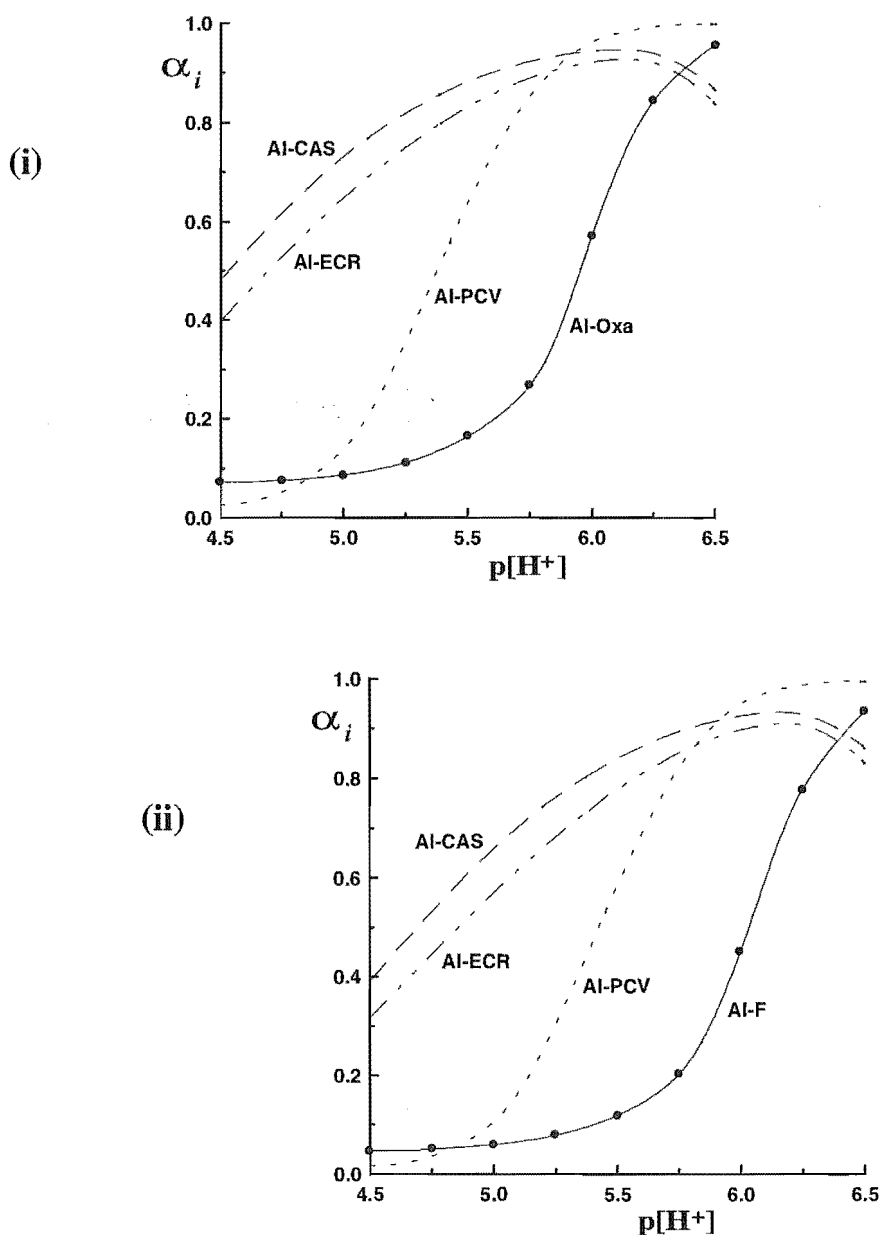


Figure 6.1.3B Calculated Al speciation in the presence of $20 \mu\text{mol L}^{-1}$ oxalate (i) or fluoride (ii), and $20 \mu\text{mol L}^{-1}$ chromophore at $7.4 \mu\text{mol L}^{-1}$ total Al. Refer to Figure 6.1.3A for definitions and description of curves.

(iii) **Fluoride:** Fluoride [Figure 6.1.3B(ii)] gave similar results to oxalate. Al complexation by both oxalate and fluoride decreased substantially at $\text{pH} > 5.5$, a consequence of the comparative strength of Al^{3+} hydrolysis.

(iv) **Salicylate:** Acid-base effects were clearly demonstrated by salicylate (Figure 6.1.3C). The fraction of Al bound by $20 \mu\text{mol L}^{-1}$ ligand in the absence of chromophore increased to a maximum around $\text{pH } 5.5$, then decreased through competition from hydrolysis. The relatively high pH for maximum binding, compared with oxalate and fluoride, is due to the weakly acidic phenolic proton ($\text{p}K_{\text{a}} \approx 12$) on salicylate. At $500 \mu\text{mol L}^{-1}$ salicylate and $20 \mu\text{mol L}^{-1}$ chromophore, PCV sequestered virtually all of the Al above $\text{pH } 6.3$. Increasing the CAS or ECR chromophore concentration to $100 \mu\text{mol L}^{-1}$ essentially removed the interference shown in Figure 6.1.3C.

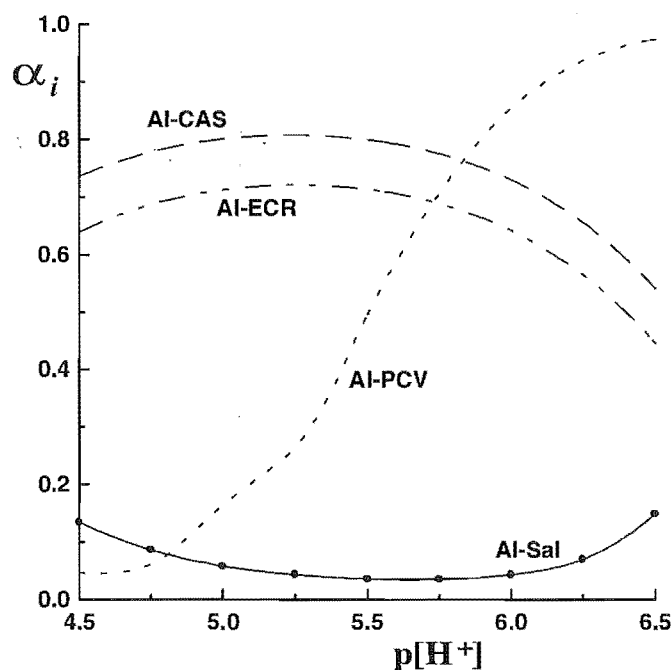


Figure 6.1.3C Calculated Al speciation in the presence of $500 \mu\text{mol L}^{-1}$ salicylate and $20 \mu\text{mol L}^{-1}$ chromophore at $7.4 \mu\text{mol L}^{-1}$ total Al. See Figure 6.1.3A for definitions and description of curves.

6.1.4 DISCUSSION

The equilibrium calculations showed that PCV is the chromophore least susceptible to interference from Al-binding ligands. Because of its low background absorbance at the wavelength and pH used for analysis, it is also the chromophore for which mass action effects can best be utilised. By using high PCV concentrations and a relatively high pH (≈ 6.5), interference from the ligands discussed in the present study should be minimal for common environmental samples (assuming equilibrium in the analyte-chromophore-interferent reaction).

The results of the equilibrium interference calculations showed that PCV's susceptibility to interference decreased with increasing pH, regardless of the competing ligand. In contrast, CAS and ECR reflected the pH dependence of Al complexing by the interferent ligand. With assays using CAS and ECR, the pH at which the competing ligands interfered least was in the order citrate ($\text{pH} < 4.5$) < salicylate ($\text{pH} 5.2$) < oxalate \approx fluoride ($\text{pH} 6.1$) (from Figures 6.1.3A-C). Organic matter from soils and natural waters contains both salicylate and carboxylate functional groups. Therefore, manipulating pH to minimise interference when using CAS or ECR is a futile exercise in soil and water analysis.

Using mass action effects to overcome interference is limited by the blank absorbance. At the respective λ_{max} and pH optima, the extinction coefficients for the pure chromophores are 5400 {CAS [Hawke *et al.*, 1995]}, 11100 {ECR [Hawke *et al.*, 1996]} and 1500 {PCV [these studies]}. If an upper limit on blank absorbance of 0.7 was imposed, then maximum chromophore concentrations would be $130 \mu\text{mol L}^{-1}$ (CAS), $63 \mu\text{mol L}^{-1}$ (ECR) and $470 \mu\text{mol L}^{-1}$ (PCV). Therefore, the greatest potential for use of mass action effects is with PCV.

The focus of regulatory requirements is on the determination of total Al. However, much current research is aimed at measuring the toxic fraction. In the sense that the chromophore should not sequester Al bound to naturally occurring ligands, this requires that interference be maximised rather than minimised. Figures 6.1.3A-C show that all chromophores (but particularly PCV) overestimate free Al^{3+} , irrespective of ligand. The results therefore support other work [Hawke and Powell, 1994] showing that PCV is unsuitable for determinations of free (toxic) Al because of its aggressiveness towards complexed Al. While PCV causes minimal disruption of the primary equilibria at low pH (4.8 - 5.0), low spectrophotometric sensitivity at this pH may cause such analyses to be of little practical value. The most promising use of Al chromophores is therefore in kinetic, rather than equilibrium assays [Hawke and Powell, 1994].

The significance of the slow equilibria in the H^+ - Al^{3+} -PCV system under spectrophotometric conditions has been previously demonstrated by Hawke and Powell (1994). In experiments carried out in a flow injection system they demonstrated that

several hours were required for complete colour development with Al^{3+} standards. For experimental studies, slow equilibria may result in interference assessments being operational in nature. For modelling studies, the result may be interference assessments which do not match the effects experienced in routine analysis.

SECTION B: H^+ - Al^{3+} - PCV - CITRATE (OXALATE) REACTION KINETICS

6.2 INTRODUCTION

In natural water and soil environments, Al exists in competitive equilibria with a large number of naturally occurring ligands. The relative rates at which Al species are formed in these complicated multiple ligand systems will be important in describing the distribution of Al species, *i.e.* natural systems are quite 'dynamic' and the kinetics of chemical processes may be particularly important in controlling speciation. If equilibrium is assumed (as it was in SECTION A of this Chapter) these factors will be overlooked. Pankow and Morgan (1981) indicated that often the condition of thermodynamic equilibrium may be rarely obtained in natural water environments.

The rate of Al complexation has only recently been addressed in the context of environmental systems [Lopez-Quintela *et al.*, 1984; Plankey *et al.*, 1986; Plankey and Patterson, 1987]. Plankey *et al.* investigated fluoride and fulvic acid complexation respectively, and complexation was found to be strongly pH and temperature dependent. Plankey *et al.* (1995) studied the kinetics of Al complex formation with three different soil fulvic acids (in the pH range 2.4-3.6). Two kinetically different Al binding sites were distinguished in all three fulvic acids and although quite different Al binding behaviour was observed for each acid the proton binding behaviour was quite similar. When the experiments were carried out in acetate buffered solutions the nature of Al complexation was significantly affected. In the presence of buffer Al bound first at the less acidic sites of the fulvic acid (apparently salicylic acid moieties), whereas in the absence of buffer the Al was bound at the stronger acid sites. Recently, a kinetic analysis was applied to the speciation of Al in river water and snow [Lu *et al.*, 1994]. The application of this iterative convolution method proved successful in kinetically distinguishing Al species according to their dissociation rate constants.

The dynamics of Al complexation in multiple ligand systems was studied by Anderson and Bertsch (1988). These studies were undertaken in the presence of fluoride (F^-), oxalate (Ox) and citrate (Cit) using an ion chromatographic speciation method to calculate rate constants (k_f) for the formation of each species. The results contrasted with the accepted concept that concurrent reactions are assumed to proceed *via* independent kinetic pathways. The rate constant for the formation of AlF^{2+} , for example, was observed to increase in the presence of Ox and Cit . In contrast, the rate constant for the formation of $AlOx^-$ was much more rapid than that of AlF^{2+} and was unaffected by the presence of F^- . The rate of complexation of Al by Cit was sufficiently fast that a rate constant could not be measured.

The rate enhancing effects of Ox and Cit on the formation of AlF^{2+} observed in the studies by Anderson and Bertsch may be attributed to one of two possible mechanisms: (i) a mixed complex transition state is formed where the rapidly complexing ligands Ox and Cit form a 'reduced charge Al-species' with greater rates of water exchange, which creates favourable conditions for the penetration of F^- and displacement of the inner sphere Ox or Cit, or (ii) F^- may exchange directly with the inner sphere Ox or Cit. Another unusual observation from these studies was that the formation of AlCit in the presence of F^- initially exceeded the thermodynamically predicted concentration, followed by a slower re-equilibration to a lower solution concentration (as the slower formation of Al-F species proceeded). This behaviour was not observed for the formation of AlOx^- in the presence of F^- . These studies highlight the importance of understanding multiple ligand systems and their importance in controlling dynamic concentrations of metal ions and metal ligand complexes in the environment.

Al speciation analyses: The application of any reagent to the determination of total Al or for performing speciation analyses (*e.g.* measurement of free or labile Al) is limited, to some extent, by the aggressiveness of the reagent towards Al complexed by other ligands, *e.g.* NOM. In measurements of total Al using chromogenic reagents, samples are usually acidified prior to analysis. This acidification is assumed to result in the complete release of complexed Al and thus enables its reaction and subsequent determination with a suitable reagent. The release of Al from stable or inert complexes is, however, controlled by chemical kinetics and therefore the complete release of Al from these complexes (upon acidification) may not occur unless reaction times are sufficiently long. In contrast to total Al determinations, for speciation measurements it is desirable that the reagent should only interact with free Al, *i.e.* Al^{3+} , $\text{Al}(\text{OH})^{2+}$, $\text{Al}(\text{OH})_2^+$.

Most reagents used for the determination of Al react rapidly and form strong complexes with Al. Unfortunately, these reagents sequester significant amounts of Al from both weak and moderate strength Al complexes. Many reagents (*e.g.* PCV), if given time, sequester Al from stable Al-organic complexes. This feature of all speciation techniques renders the results 'operationally defined' according to the thermodynamics and the reaction kinetics of the overall 'reagent-Al-ligand(s)' system(s). Many speciation techniques developed recently have based their 'speciation protocol' on the reaction kinetics of a suitable reagent with Al [Clarke *et al.*, 1992; Hawke and Powell, 1994].

Lewis *et al.* (1988) investigated the effects of humic and fulvic acids and various other ligands on the determination of monomeric Al. As discussed in SECTION A (6.1) the extent to which a competing ligand may affect results is dependent, to some degree, on the kinetics of both the measurement reaction and the dissociation of Al-ligand complexes. The strongly Al-complexing ligands citrate and CDTA caused the greatest reduction in determined monomeric Al. Tartrate caused a significantly larger reduction in monomeric

Al concentrations determined by PCV and oxine methods than did malate (despite their similar structures).

The comparison of the oxine, ferron and aluminon methods for differentiating between mono- and polynuclear hydroxy-aluminium complexes made by Parker *et al.* (1988) also addressed the 'unavoidable' question of chemical kinetics. Many of the polynuclear Al species that have been proposed as forming in water or soil environments are generally viewed as metastable products (by-products of oxide dissolution processes or precursors to oxide formation). The toxicity of these species may, however, vary greatly [Chapter 1 (1.2)]. The reaction of oxine with mononuclear Al was found to be essentially instantaneous whereas ferron and aluminon reacted more slowly and allowed the mixtures of mono- and polynuclear Al-hydroxide species to be kinetically modelled as two simultaneous reactions.

Bartlett *et al.* (1987) described a method utilising PCV for the kinetic fractionation of reactive Al in soil solutions. The method operationally identified three fractions of Al as rapidly reacting (RR), moderately rapidly reacting (MR) and totally reactive (TR). The RR fraction (from 20 soil extracts) was correlated with the oxine Al measured by the James *et al.* (1983) method. Other studies have also indicated that PCV and oxine react with similar labile forms of Al [Sullivan *et al.*, 1986].

6.2.1 SCOPE OF THIS WORK.— The model calculations in SECTION A of this Chapter were used to determine the degree of interference expected from several naturally occurring ligands (*viz* citrate, oxalate, salicylate and fluoride) on the measurement of total Al by the chromophores CAS, ECR and PCV. The direction of much current research is, however, now towards the speciation of Al in natural water and soil samples, *i.e.* the measurement of the 'free and labile' fraction of Al, rather than just the determination of total reactive Al.

The recent recognition that natural systems are quite dynamic has challenged the use of 'equilibrium approximations' as a tool for the analysis of metal ion speciation [Langford and Cook, 1995]. As highlighted above, the kinetics of complexation and dissociation processes will affect the results obtained during the analysis of 'labile Al' and these affects may be different for different sample compositions.

The aim of this SECTION was to (i) validate the H^+-Al^{3+} -PCV model (determined in Chapter 4) for spectrophotometric conditions and (ii) investigate the time scales for the establishment of equilibrium in the competitive systems: H^+-Al^{3+} -citrate-PCV and H^+-Al^{3+} -oxalate-PCV.

The model validation studies were performed using experimental conditions [*i.e.* concentrations of Al, PCV, ligand (citrate, oxalate) and pH] identical to those used in the model calculations (SECTION A of this Chapter). The two ligands chosen for this work,

citrate and oxalate, exhibit strong and moderate binding affinities for Al respectively and were expected to result in significant effects (as predicted from the calculations) that could be accurately measured. Preliminary studies investigated the stoichiometry (molar ratio) of the dominant Al-PCV species forming in the absence of competing ligand. The effect of equilibration time on these molar ratio curves was investigated.

6.2.2 EXPERIMENTAL

(A) **Chemicals and Analysis.**— All solutions were prepared from CO₂-free, boiled Milli-Q water and all working solutions were prepared in 0.10 mol L⁻¹ KCl (Merck, *p.a.*), dried at 120 °C.

(i) **Pyrocatechol Violet Solutions:** PCV is depicted in Figure 6.1.1(iii). A 5.0 mmol L⁻¹ PCV (vacuum dried Koch-Light) stock solution (prepared in 1 mmol L⁻¹ HCl) was used for all experiments. This solution was not standardised, however its purity was believed to be at least 97 % dye content.

(ii) **Ligand Solutions:** Citric acid (BDH, AnalaR) and oxalic acid (Fisons, AR) solids were used after drying (silica gel, 25 °C) but without further purification. 5.0 mmol L⁻¹ stock solutions were prepared.

(iii) **Aluminium Solutions:** A 2.0 mmol L⁻¹ Al stock solution was prepared in 0.02 mol L⁻¹ HCl by dilution of the 'ALFA' stock solution described in Chapter 3 [3.2.5(A)].

(iv) **Alkali (KOH) and Acid (HCl) Solutions:** HCl solutions were prepared by dilution of concentrated HCl (BDH, AnalaR). Carbonate-free KOH (BDH, AnalaR) solutions were prepared according to Chapter 3 [3.2.1(A)]. These solutions were not standardised.

(v) **Buffer Solution:** A MES (Sigma) buffer solution (pK_a = 6.1 at 25 °C) was prepared *ca.* 0.05 mol L⁻¹ (pH = 6.2).

(B) **Spectrophotometric Titrations.**— These measurements required rigorous exclusion of oxygen. The thermostatted cell and the spectrophotometric apparatus required for these measurements was described in Chapter 3 [3.4] (without the 'KOH boat'). Absorbance data were recorded using a Hewlett Packard 8452A diode array spectrophotometer.

A Radiometer PHM 64 research pH meter was used for pH measurements; this instrument was calibrated against standard buffers (phthalate, pH 4.01 and phosphate, pH 6.86) prepared according to the experimental section [3.2.4(A)]. An Alitea XV peristaltic pump was used to circulate the test liquid through microline tubing (Cole Palmer, 0.51 mm i.d.) to a 70 µL flow-cell [Starna, 3 mm (i.d.) x 10 mm] positioned in the spectrophotometer.

Titration procedure: Titrations of mixtures of Al^{3+} ($7.4 \mu\text{mol L}^{-1}$), citrate ($20 \mu\text{mol L}^{-1}$; or oxalate, $100 \mu\text{mol L}^{-1}$), plus PCV ($20 \mu\text{mol L}^{-1}$ or $100 \mu\text{mol L}^{-1}$) were carried out in 0.10 mol L^{-1} KCl at 25°C (after 150 min pre-equilibration) from pH 5.0 to pH 6.5. Equilibration times between KOH additions were varied in the range 45 - 400 min. Additions of all reagents were made *via* a calibrated micro-pipette or 25 mL glass pipette.

The test solution (*ca.* 50 mL), used for obtaining a blank signal, contained 0.02 mol L^{-1} MES buffer and the desired amounts of all equilibrium components except PCV. The 'spectrophotometer blank' was usually measured at pH 5.0 and was made directly before addition of PCV. Adjustment of pH was effected by small additions ($< 2.5 \text{ mL}$ total) of CO_2 -free KOH solution.

Equilibration: The metal-ligand system was initially allowed to equilibrate in the absence of PCV at pH *ca.* 5.0. This equilibration period was *ca.* 60 min for solutions containing oxalic acid (or in the absence of ligand) and *ca.* 120 min for solutions containing citric acid. Such long equilibration periods are both necessary and sufficient for equilibration in these systems [Öhman, 1988].

(C) Al-PCV Stoichiometry and Linearity of Titration Curves.— Two preliminary studies were undertaken before the competitive spectrophotometric titrations: (i) the stoichiometry of the dominant Al-PCV species forming (pH 6.2) in the absence of competing ligand was investigated and (ii) the linearity of Al-PCV spectrophotometric titration curves at pH 6.2 was checked and the effect of equilibration time (following each incremental addition of Al) on the slope of these curves investigated. These studies were performed with the same apparatus and experimental conditions as discussed above $\{[\text{PCV}] = 20 \mu\text{mol L}^{-1} \text{ or } 100 \mu\text{mol L}^{-1}\}$. The spectra were measured following a 10-20 min equilibrium period after each addition of Al.

(D) Batch Experiments With Other Ligands.— A series of experiments were performed comparing Al-PCV reaction rates for solutions initially containing PCV and a 'second' ligand. The ligands citrate, oxalate, malonate, salicylate and fluoride were investigated. In these 'batch' experiments aliquots of ligand and PCV were added to MES buffer solution (pH = 6.2) and allowed to equilibrate for 10 min. Al was then added and the formation of the Al-PCV complex observed visually.

6.2.3 DATA TREATMENT

(A) Data Analysis.— The calculation of the fraction of Al measured by PCV was performed as a ratio of the spectrophotometric signal [λ_{max} (Al-PCV) = 578 nm] for experiments performed in the presence and absence of competing ligand. The only corrections made to these measurements were from the 'background absorption' for the free ligand (PCV) at this wavelength [calculated using changes at λ_{max} (PCV) = 442 nm]

and small effects from dilution. Total errors for each datum point shown in the Figures (6.2.4A-C) are estimated as $< 2.5\%$.

The model curves were calculated using the computer program SOLGAS-WATER [Eriksson, 1979] and the thermodynamic equilibrium data described in SECTION A (6.1.2) of this Chapter.

(B) Sensitivity Analysis.— The sources of thermodynamic data used for the H^+ - Al^{3+} -PCV and H^+ - Al^{3+} -ligand systems were given in SECTION A (6.1.2). As discussed in that SECTION, no reliable constants were available for all the H^+ - Al^{3+} -ligand systems in 0.1 mol L^{-1} media. The constants used were for 0.6 mol L^{-1} media and were considered accurate and suitable for those studies. The differences in ionic strength ($I = 0.1$ vs. 0.6) may, however, impose small errors in this work.

In order to determine the size of any possible ionic strength effects, a sensitivity analysis was performed. In this calculation small variations were made to the constants of the dominating Al-ligand species (*viz* the major species appearing in Figures 6.2.5A & B). These effects were considered in relation to the data measured above. All calculations were performed using the computer program SOLGASWATER.

6.2.4 RESULTS

(A) Al-PCV Stoichiometry and Linearity of Titration Curves.— These results are presented in Figure 6.2.4A for $20 \mu\text{mol L}^{-1}$ and $100 \mu\text{mol L}^{-1}$ PCV solutions respectively.

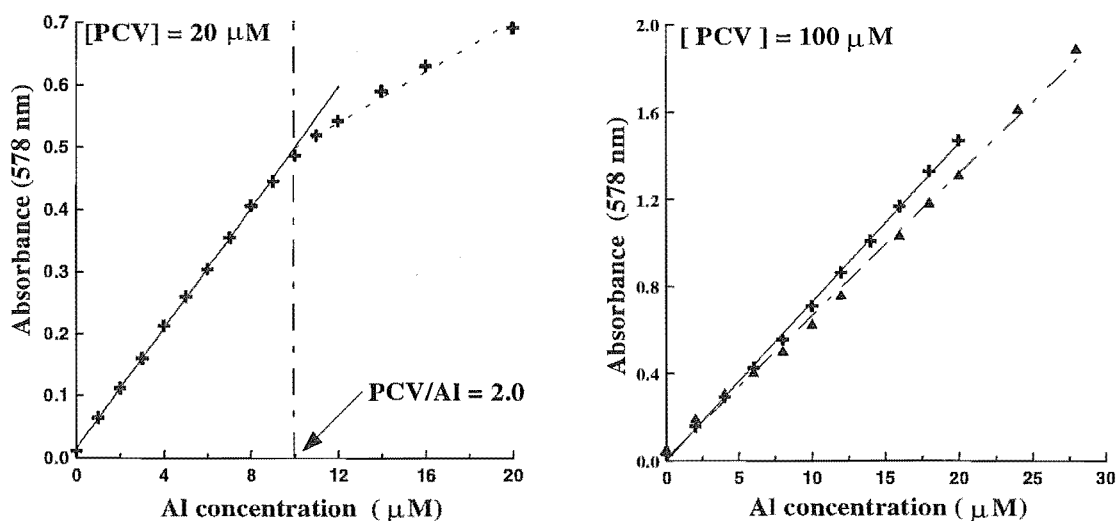


Figure 6.2.4A Titration curves for $20 \mu\text{mol L}^{-1}$ and $100 \mu\text{mol L}^{-1}$ PCV solutions (pH 6.2). Equilibration times between additions of Al (and measurement of spectra) were 15 min for the $20 \mu\text{mol L}^{-1}$ PCV titration and 10 min (dashed line) and 20 min (solid line) respectively for the $100 \mu\text{mol L}^{-1}$ PCV titrations.

From the $20 \mu\text{mol L}^{-1}$ PCV titration curve it is apparent that the dominant species forming at pH 6.2 has the stoichiometry $\text{Al}(\text{PCV})_2$ (*i.e.* $\text{PCV}/\text{Al} = 2.0$). This is in accord with the thermodynamic model (see Chapter 4, Figure 4.2.4B). At $100 \mu\text{mol L}^{-1}$ PCV, the curve remains linear ($r^2 > 0.99$) over the entire Al concentration range investigated, *i.e.* the 'limiting' stoichiometry for $\text{Al}(\text{PCV})_2$ is not reached. It is apparent from these curves (10 min and 20 min equilibration times respectively) that the Al-PCV reaction is quite time dependent. This feature was particularly important in the design of the subsequent competitive ligand titration experiments.

(B) Competitive Equilibria

(i) *The H^+ - Al^{3+} -citrate-PCV system:* The results for titrations in the presence of citrate are shown in Figure 6.2.4B, expressed as the fraction of Al measured by PCV (F_i).

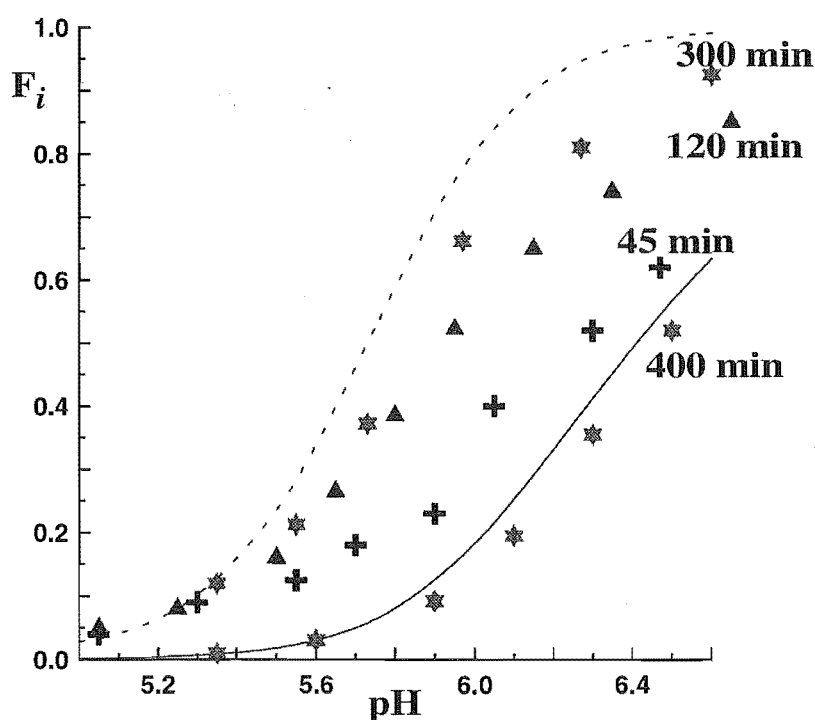


Figure 6.2.4B Spectrophotometric titration of the H^+ - Al^{3+} -citrate-PCV system. The titration mixtures comprised $7.4 \mu\text{mol L}^{-1}$ Al^{3+} , $20 \mu\text{mol L}^{-1}$ citrate and $20 \mu\text{mol L}^{-1}$ (solid line) or $100 \mu\text{mol L}^{-1}$ (dashed line) PCV respectively. Here F_i is the fraction of Al measured by PCV [calculated as described in the 'data treatment' (6.2.3)]. Three experiments are shown for the $100 \mu\text{mol L}^{-1}$ PCV titrations (with equilibration times of 45, 120 and 300 min respectively) whereas only one experiment (400 min equilibration time) is shown for the $20 \mu\text{mol L}^{-1}$ PCV titration.

In all the Al^{3+} -citrate-PCV titrations the measured Al (*i.e.* Al-PCV) depended strongly on the equilibration time following KOH additions. The experiments for $100 \mu\text{mol L}^{-1}$ PCV titrations (Figure 6.2.4B) clearly show the extent of these affects. Acceptable fits of measured Al to that predicted from the model calculations were obtained only for equilibration times ≥ 300 min.

(ii) **The H^+ - Al^{3+} -oxalate-PCV system:** The results for titrations in the presence of oxalate are shown in Figure 6.2.4C. In this system acceptable fits were also obtained, however, the equilibration times required for oxalate were much shorter (150-180 min) than those for citrate.

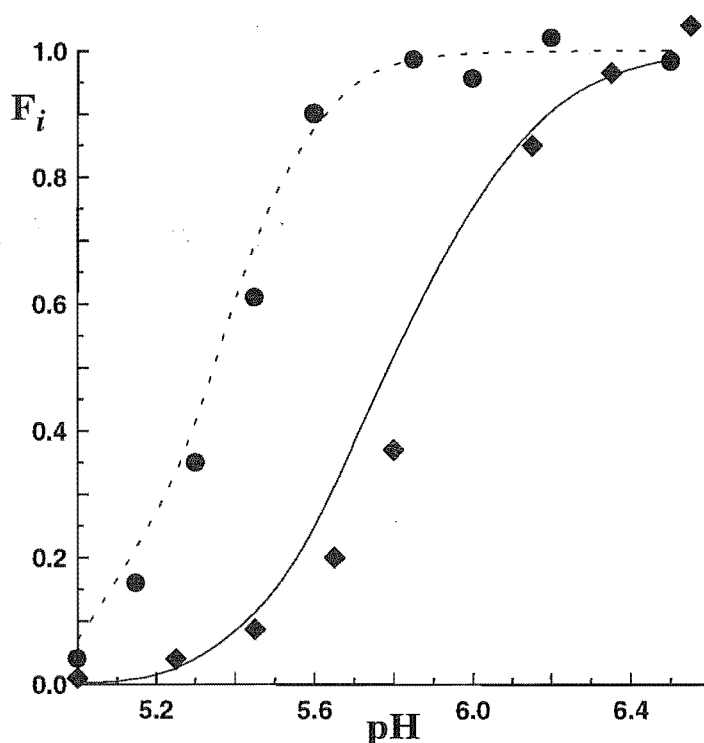


Figure 6.2.4C Spectrophotometric titration of the H^+ - Al^{3+} -oxalate-PCV system (equilibration time of 150 min). The titration mixtures comprised $7.4 \mu\text{mol L}^{-1}$ Al^{3+} , $20 \mu\text{mol L}^{-1}$ oxalate and $20 \mu\text{mol L}^{-1}$ (solid line) or $100 \mu\text{mol L}^{-1}$ (dashed line) PCV respectively. The definition of F_i is given in Figure 6.2.4B.

(C) **Batch Experiments: Kinetics of Other H^+ - Al^{3+} -Ligand-PCV Systems.**— A series of experiments were performed comparing Al-PCV reaction rates for solutions initially containing PCV and a 'second' ligand, *viz* citrate, oxalate, malonate, salicylate or fluoride (pH 6.2). When Al was added the initial rates of colour development (visually determined) were oxalate \approx F \approx malonate $>$ salicylate \gg no competing ligand $>$ citrate.

After leaving these solutions to equilibrate for 24 h all solutions appeared the same colour indicating that PCV eventually displaced Al quantitatively from all of these ligands.

6.2.5 DISCUSSION

(A) Competitive Equilibria.— The experimental results for the competitive equilibria with citrate and oxalate (Figures 6.2.4B and C) confirm the applicability of the determined PCV constants (which were obtained potentiometrically) to spectrophotometric conditions. Also apparent from these experiments is the large differences in the kinetics of the respective citrate and oxalate equilibria.

In the experiments with citric acid and $100 \mu\text{mol L}^{-1}$ PCV (Figure 6.2.4B) the time required to reach equilibrium was investigated in detail. The initial experiment used equilibration times of 45 min between pH adjustments. It quickly became apparent that either the model or experimental conditions were inappropriate. Increased delay periods between measurements resulted in significantly better results. Using equilibration periods of 300-400 min only very small changes in spectral absorbance occurred after this period (regarded as negligible).

For the oxalic acid system (Figure 6.2.4C) problems were also initially encountered as a result of inadequate equilibration time. The first experiments performed both in the presence and absence of oxalate used 30 min delays between measurements. Using these data to calculate the measured fraction of Al, results greater than 100 % were obtained at $\text{pH} \geq 5.8$. Later experiments revealed that this effect was due to kinetic enhancements of the reaction of PCV with Al in the presence of oxalate [see Section 6.2.5(C) for discussion] relative to standards. Specifically, Al-PCV standards did not achieve equilibrium within 30 min. In all final experiments, for oxalic acid and 'PCV only' studies, equilibration times were 150-180 min (after this delay period changes in spectral absorbance with time were negligible).

The differences in the kinetics of these two ligand systems may be best explained by considering the structure of the ligands and also by looking at the speciation present (thermodynamic equilibrium) during the titrations. Distribution diagrams are presented in Figures 6.2.5A & B for the speciation present in solutions 'identical' to those used in the current experiments.

For the H^+ - Al^{3+} -citrate-PCV system the speciation calculations indicate that Al-citrate species dominate the equilibria over the lower pH range ($\text{pH} < 6.0$) for both reagent concentrations and up to *ca.* $\text{pH} = 6.2$ for the $20 \mu\text{mol L}^{-1}$ PCV titrations. The polymeric species $(-13,3,3)$ $[\text{Al}_3(\text{OH})_4(\text{H}_{-1}\text{Cit})_3^{7-}]$ is predicted as forming to *ca.* 5-10 % in both titrations, whereas the dominating Al-Cit species has the stoichiometry $(-4,1,1)$ $[\text{Al}(\text{H}_{-1}\text{Cit})^-]$.

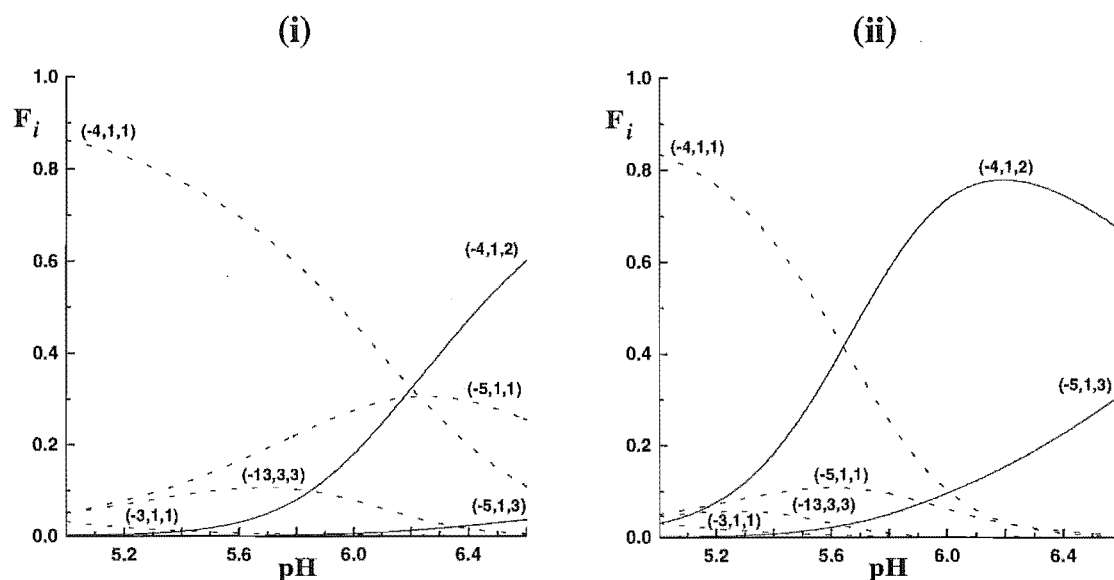


Figure 6.2.5A Distribution diagrams F_i for 7.4 $\mu\text{mol L}^{-1}$ Al, 20 $\mu\text{mol L}^{-1}$ citrate and (i) 20 $\mu\text{mol L}^{-1}$ or (ii) 100 $\mu\text{mol L}^{-1}$ PCV. F_i is defined as the ratio of the aluminium concentration in an equilibrium species to the total aluminium concentration. The dashed lines represent Al-ligand species whereas the solid lines represent Al-PCV species. The p, q, r stoichiometries are given (where r is the 'ligand' or PCV respectively).

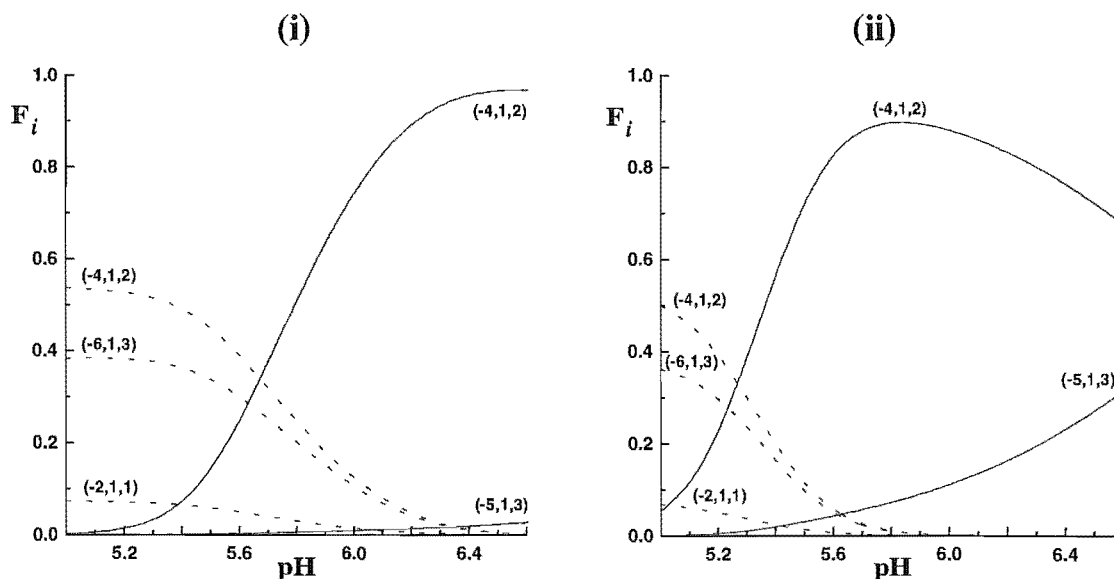


Figure 6.2.5B Distribution diagrams F_i for 7.4 $\mu\text{mol L}^{-1}$ Al, 20 $\mu\text{mol L}^{-1}$ oxalate and (i) 20 $\mu\text{mol L}^{-1}$ or (ii) 100 $\mu\text{mol L}^{-1}$ PCV. Refer to Figure 6.2.5A for definitions and description of curves.

Öhman (1988) found that Al-citrate equilibria proceed very slowly *via* complicated equilibrium reactions. In the present studies very slow equilibria were observed. These observations are consistent with the observations of Öhman and indicate that in kinetic analyses of 'monomeric Al', Al-citrate species are likely to be unmeasurable. Marjerrum *et al.* (1978) ascribed the low rate of dissociation of multidentate ligands (*viz* citrate) relative to unidentate ligands to the high thermodynamic stability of their complexes. The direct displacement of Al from these ligands by unidentate ligands could be expected to be very limited. PCV is a multidentate ligand and forms complexes of high stability with Al, however, the 'chelation' of Al by citrate inhibits the displacement of Al from citrate complexes.

Al complexation by oxalate is significantly weaker than that by citrate, the speciation in this system is less complicated and three 'stepwise' Al-oxalate species are observed to form (Figure 6.2.5B). The equilibration time required to reach a 'stable absorbance' for this system was considerably shorter than that required for the citrate system. Oxalate, although multidentate, is smaller than citrate and the approach to Al by PCV is likely to be less sterically hindered.

Two mechanisms can be considered for the formation of Al-PCV species from the Al bound by citrate and oxalate: (i) PCV reacts with and complexes 'free Al' (Al^{3+}) and law-of-mass-action results in continuous re-equilibration of the Al-ligand systems until both the PCV and the ligand equilibrium conditions are fulfilled (*i.e.* dissociation of Al^{3+} from the Al-citrate complex must occur before PCV reacts), alternatively (ii) PCV may form an initial 'encounter complex' (mixed ligand transition state) with the Al-ligand species which subsequently undergo ligand displacement and formation of the Al-PCV species. Such mechanisms for ligand-exchange reactions have been previously proposed [Hering and Morel, 1990]. Both of these mechanisms could be expected to occur slowly as a result of slow ligand- and/or PCV-Al equilibria. In studies of the kinetics of Al-citrate complexation, Mak and Langford (1983) assumed a dissociative mechanism [*i.e.* mechanism '(i)' above] for the ligand exchange between Al-citrate and the metal-fluorochromic reagent Calcein Blue. Their results suggested that the dissociation of Al from the Al-citrate complex is the rate determining step in ligand exchange.

The considerable time dependence of the Al measured in the presence of citrate is consistent with the very slow attainment of equilibrium in the Al^{3+} -citrate system observed in potentiometric studies [Öhman, 1988]. Although the kinetics of Al^{3+} -citrate equilibria is perhaps an extreme example, these results clearly highlight the importance of allowing sufficient equilibration time. This applies to both experimental assessments of interference, and to routine analysis.

The significance of slow equilibration in the Al^{3+} -PCV system under spectrophotometric conditions has been previously demonstrated [Hawke and Powell,

1994]. In these experiments, carried out in a flow injection system, it was shown that several hours were required for complete colour development with Al^{3+} standards. For experimental studies, slow equilibration may result in interference assessments being operational in nature. For modelling studies, the result may be interference assessments which do not match the effects experienced in routine analysis.

(B) Sensitivity Analysis.— The stability constants used for the ligands were determined in 0.6 mol L^{-1} media. Although they were very suitable for the intended comparisons made in SECTION A of this Chapter the small effects of ionic strength differences may result in small errors in this work, *i.e.* in these studies the ionic strength was 0.1 mol L^{-1} for all species.

To determine the size of any possible ionic strength effects, a 'sensitivity analysis' was performed. In these calculations small variations were made to the constants of the dominating Al-ligand species (*i.e.* those in Figures 6.2.5A & B). The effect of these variations is presented in Figure 6.2.5C.

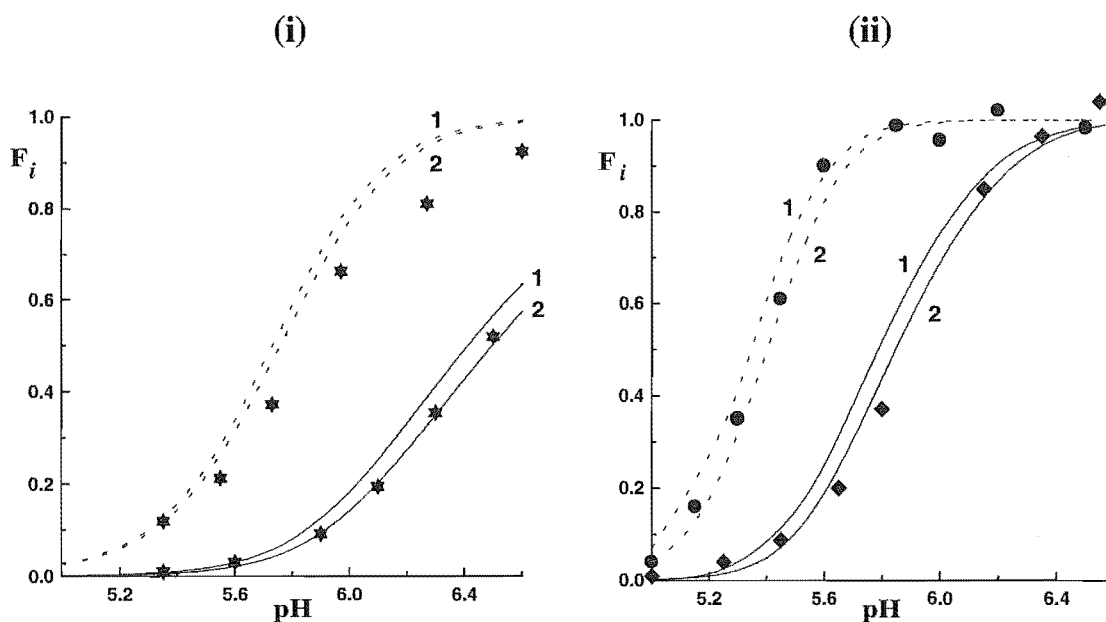


Figure 6.2.5C Sensitivity analysis performed using the current equilibrium model for the systems: (i) H^+ - Al^{3+} -citrate-PCV and (ii) H^+ - Al^{3+} -oxalate-PCV. Refer to Figures 6.2.4B & C for concentrations, equilibrium times and the definition of F_i . Here the calculated curves '1' and '2' refer to the unmodified and modified equilibrium models respectively.

For the H^+ - Al^{3+} -citrate-PCV system the major Al-citrate species forming at both PCV concentrations had the stoichiometry $(-4,1,1)$, *i.e.* $\text{Al}(\text{H}_{-1}\text{Cit})^-$ [Figure 6.2.5A]. The

effect of increasing the $\log \beta_{p,q,r}$ value for this species was investigated. In Figure 6.2.5C(i) curve '2' has been calculated after $\log \beta_{-4,1,1}$ was increased by + 0.2 log units (*i.e.*, from -8.48 to -8.28). These changes result in a near perfect fit for the 20 $\mu\text{mol L}^{-1}$ PCV titration yet have little effect on the 100 $\mu\text{mol L}^{-1}$ PCV titration. In order to obtain a good fit for the 100 $\mu\text{mol L}^{-1}$ PCV titration an increase in this $\log \beta$ of *ca.* + 0.5 would be required; this, however, would result in a very poor fit for the 20 $\mu\text{mol L}^{-1}$ PCV titration. The discrepancies shown here may be due to incomplete equilibration (despite the long equilibration time employed).

In the $\text{H}^+\text{-Al}^{3+}\text{-oxalate-PCV}$ system three major Al-oxalate species form: (-2,1,1), (-4,1,2) and (-6,1,3) [Figure 6.2.5B]. In Figure 6.2.5C(ii) curve '2' has been calculated following increases in $\log \beta_{p,q,r}$ of + 0.1, + 0.2 and + 0.3 for $r = 1$ to 3 respectively, *i.e.* the $\log K$ for the formation of each species (represented here by $\log \beta$) was increased + 0.1 log units. These changes improve the fit between calculated and experimental data in both experiments.

(C) Kinetics of Ligand-Exchange: Enhancements of Rate ? — The experiments in the $\text{H}^+\text{-Al}^{3+}\text{-oxalate-PCV}$ system revealed some interesting results. If a solution containing Al, PCV and oxalic acid equilibrated at pH 5.7 was adjusted (addition of alkali) to pH 5.8-6.6 the absorption spectra changed very quickly and equilibrium appeared (visually) to be reached shortly after. In contrast, for the same experiment in the absence of oxalate equilibrium was not reached for many hours and initially no colour development was observed (no spectral changes) following addition of alkali.

The batch experiments [which compared Al-PCV reaction rates (*i.e.* colour development, pH 6.2) for solutions containing PCV and a second Al-complexing ligand] revealed rates of colour development (upon addition of Al) depended strongly on the 'second ligand'. Rates of colour development were: oxalate $\approx \text{F}^- \approx \text{malonate} > \text{salicylate} \gg \text{no second (competing) ligand} > \text{citrate}$. Following a 24 h equilibration period, PCV displaced Al quantitatively from all of the ligands.

The observations in both of these experiments ($\text{H}^+\text{-Al}^{3+}\text{-oxalate-PCV}$ titration and batch experiments) can be explained in terms of an 'hydrolysis shock'. This occurs when the pH of a solution containing Al is suddenly increased, *i.e.* Al immediately undergoes hydrolysis. In the spectrophotometric titration studies, adjustment of pH (by addition of alkali) results largely in a redistribution of Al between the Al-oxalate equilibria species and partially in hydrolysis of Al before PCV can react. In the absence of oxalate Al hydrolysis is considerably greater which in turn results in longer equilibration times being required for colour development. In the batch experiments the presence of a ligand which reacts quickly with Al counters Al hydrolysis and thus ligand-exchange reactions between PCV and the 'second' ligand can proceed quickly. PCV alone does not react quickly enough with Al to significantly reduce hydrolysis.

The effect of a second ligand is a potential problem in FIA if the sample and PCV are brought together at the analytical pH (a scenario common to many FIA systems for the spectrophotometric detection of metal ions). However, in most FIA methods using PCV for the spectrophotometric determination of Al, the sample (containing Al) is usually merged with acidified (or unbuffered) PCV solution [Røyset, 1986]. In such a solution PCV can complex Al as the 'maltol' complex (see Chapter 4) and upon contact with the buffer (*e.g.* hexamine at pH 6.2) the colour development is quite fast. This would mean that rate enhancing effects are likely to be insignificant.

Although these experiments revealed interesting information relating to reaction kinetics, no further investigations were made. The major interest from this work relates to the possibility of naturally occurring ligands, *e.g.* small organic acids or fluoride, enhancing the rate of reaction in a spectrophotometric analysis. Since analyses are performed under non-equilibrium conditions, the presence of a small amount of F^- , say, might result in rate enhancements relative to Al standards (absence of a 'second-ligand'). For the measurement of total Al or for measurements where changes in solution speciation are not important one could add an 'excess' of a 'catalytic' ligand to ensure consistent product formation, even in the presence of varying amounts of ligands such as F^- , oxalate, malonate *etc.*

CHAPTER 7

A SURVEY OF ELECTROCHEMICAL SENSOR LIGANDS FOR Al^{3+} AND THE DEVELOPMENT OF AN ELECTROCHEMICAL DETECTION SYSTEM FOR Al^{3+}

This chapter describes the evaluation of a series of ligands which exhibit (or could be expected to exhibit) Al-binding and electrochemical properties that may be utilised in the development of an electrochemical method for the determination of Al. It is divided into 2 parts.

SECTION A: A preliminary survey of the electrochemical properties of a series of Al^{3+} -ligand systems using cyclic voltammetry. This was to identify redox-active ligands which may be used as electrochemical probes for Al.

SECTION B: The development of a flow injection analysis (FIA) method for the determination of Al which exploits the indirect electrochemical detection of Al using the ligands pyrocatechol violet (PCV) and rhodizonic acid / tetrahydroxy-1,4-quinone (RHD/THQ).

SECTION A: A SURVEY OF ELECTROCHEMICAL SENSOR LIGANDS FOR Al^{3+}

7.1 INTRODUCTION

The electrode potential at which Al^{3+} is reduced to Al^0 is outside the working range of most electrode materials in aqueous solution. At most electrodes the very negative potentials required for the reduction of Al^{3+} results in the evolution of hydrogen [*i.e.* $\text{H}_2\text{O} + \text{e}^- \rightleftharpoons \text{OH}^- + \frac{1}{2}\text{H}_{2(\text{g})}$]. Furthermore, at reducing potentials, Al has a tendency to form nonconducting oxide or amorphous hydroxide layers. Accurate and reproducible experimental electrode potential data for Al is not abundant.

Possibly the first extensive investigation of the electrode potential of Al was made by Heyrovsky (1920). In these studies hydrogen evolution and oxide formation were minimised by the investigation of dilute Al amalgams in AlCl_3 working solutions. A value of -1.333 V was determined for the formal potential of Al and this potential was attributed to the reaction: $\text{Al}(\text{OH})_3 + 3\text{e}^- = \text{Al}_{(\text{s})} + 3\text{OH}^-$.

A number of studies have now been made of the standard potential of Al [Malachuk, 1976]. The accuracy of these studies is, however, unclear. The accepted value for the standard electrode potential of Al, E° , is -1.66 V:

i.e. $E^\circ [\text{Al}^{3+} + 3\text{e}^- = \text{Al}_{(\text{s})}] = -1.66 \text{ V}$

Direct Determination of Al: The direct determination of Al^{3+} (e.g. with polarographic procedures) is not attractive because of the very negative potential at which it is reduced. However, several early investigations were made of the polarographic behaviour of the Al^{3+} ion. In 0.05 N BaCl_2 solution Prajzler (1931) assigned the Al^{3+} ion to a reduction wave at -1.75 V vs SCE . A method for the determination of Al in magnesium alloys (MgCl_2 , pH 3.2) was developed by Gull (1937) based on this information. Galova and Szmerekova (1973) examined the polarographic behaviour of Al in the presence of several ligands (including fluoride, tartrate and citrate). They observed that as the ratio [complexing anion]/[Al] increased, the $E_{1/2}$ values are shifted to more negative potentials.

Many early voltammetric studies of Al were directed towards elucidating the mechanism for the polarographic reduction of Al^{3+} . Reynolds and Webber (1958) found that the Al^{3+} reduction peak was proportional to Al concentration. It was also observed that peak height was a function of the starting potential and solution composition (salt and buffer concentrations and pH). Kolthoff and Sambucetti (1959) investigated the behaviour of a rotating Al wire electrode in aqueous solutions. The electrode was found to be a function of pOH at pH > 9 in the absence of fluoride. In more acidic solutions and in the presence of fluoride the electrode produced an anodic current at -0.75 V vs SCE which was proportional to the fluoride concentration over the range *ca.* $10\text{--}300 \mu\text{g L}^{-1}$.

Indirect Determination of Al: The direct determination of Al using electrochemical procedures is very difficult. In contrast, the indirect electrochemical determination of Al is a meritorious approach. The first indirect electrochemical method for the determination of Al was a polarographic procedure developed by Willard and Dean (1950). In studies investigating the reduction wave of the 'dye' solochrome violet RS (SVRS) they observed that in the presence of Al the SVRS wave split into two discrete waves. The second wave, attributed to the Al-SVRS complex, was at more negative potentials (*ca.* -0.2 V) than the SVRS wave. The total height of the two waves was equal to that of the SVRS wave alone and the height of the second wave was proportional to the Al concentration.

The method of Willard and Dean was later refined by Florence (1962) and Florence *et al.* (1966). Florence (1962) used the dye superchrome garnet Y (5-sulfo-2',4',2-trihydroxyazobenzene) for the determination of Al in Th compounds using linear-sweep oscillographic polarography. The method had a detection limit (DL) of 1 ppm. In contrast, Florence *et al.* investigated the oxidation of the Al-SVRS complex at a rotating pyrolytic graphite electrode. Well defined oxidation waves for SVRS and the Al-SVRS complex were observed (separated by 0.35 V in acetate buffer). The advantages of this method were that quite simple polarographic equipment could be used to determine Al at 10 ppb concentrations. Furthermore, the deaeration of test solutions was not required and

several metals that interfered in the reduction methods had no effect when oxidation waves were used for measurement.

Hall and Skoumbourdis (1966) investigated the use of an indirect method for Al determination based on an Al-catalysed reduction of the nitrate ion at the dropping mercury electrode. Holleck *et al.* (1969) and Abd El Kader *et al.* (1970) investigated the electrochemistry of Al-dye complexes in methanolic electrolytes. Lendermann *et al.* (1972) used a carbon paste electrode in the oxidative determination of Al via its SVRS complex in 0.2 mol L^{-1} NaOAc electrolyte.

More recently, the technique of adsorptive stripping voltammetry (AdSV, or cathodic stripping voltammetry, CSV) has been investigated for the determination of Al at sub-ppb levels. Wang *et al.* (1985) employed the adsorptive accumulation and oxidation of the Al-SVRS complex at a hanging mercury drop electrode (HMDE). Analysis was carried out over the range 5 to $30 \text{ } \mu\text{g L}^{-1}$ (0.19 - $1.11 \text{ } \mu\text{mol L}^{-1}$) in an acetate electrolyte (pH 4.5) following 60 s adsorption from stirred solution. The estimated DL, based on 10 min adsorption, was $0.15 \text{ } \mu\text{g L}^{-1}$ (5.5 nmol L^{-1}). It was necessary to heat the sample to $90 \text{ }^\circ\text{C}$ (for 10 min) and cool for 15 min to ensure quantitative formation of the Al-SVRS complex. If present in sufficient concentrations, Fe and Cu interfered in the analysis.

In a similar study van den Berg *et al.* (1986) investigated the ligand 1,2-dihydroxyanthraquinone-3-sulfonic acid (DASA) for the determination of Al. The much faster reaction kinetics for this procedure (complex formation at pH 7.1) eliminated the need to heat the sample. Detection was effected by differential pulse CSV and a lower DL of 27 ng L^{-1} (1 nmol L^{-1}) was obtained for 45 s accumulation of $0.1 \text{ } \mu\text{mol L}^{-1}$ DASA. The metal Zn caused significant interference but this could be masked by addition of EDTA. In the analysis of aquatic samples surface active organic species were found to interfere.

Downard *et al.* (1992) modified the method of Wang *et al.* to eliminate the need for the heating (and cooling) steps. This step was replaced with a 10 min degassing of the test solution at pH 8.8 (at room temperature) followed by lowering the pH to 4.6. The DL was 4.5 nmol L^{-1} and the measured reactive fraction of Al was found to approximate total dissolved Al.

An alizarin-modified (1,2-dihydroxyanthraquinone) graphite electrode (CME) was developed by Downard *et al.* (1991) for the voltammetric determination of Al at pH 8.2. An accumulation time of 60 s and differential pulse (DP) measurement of the oxidation peak of the Al-alizarin complex gave a DL of $0.15 \text{ } \mu\text{mol L}^{-1}$ and a linear response up to $10 \text{ } \mu\text{mol L}^{-1}$. Although a significantly higher sensitivity may be obtained using CSV, electrode preparation for the CME method was simpler and more rapid than the CSV method. Interferences were observed for the anions nitrilotriacetic acid (NTA), citrate and PO_4^{3-} and the cations Cu^{2+} , La^{3+} and Fe^{3+} .

An FIA system for the determination of Al utilising the formation of an Al-DASA complex at pH 9.0, followed by amperometric measurement of excess DASA, was developed by Downard *et al.* (1992). Electrode fouling of the gold electrode (used in these studies) was significant but this could be minimised by use of separate detection and cleaning cycles respectively. During the cleaning cycle, cathodic-anodic voltage cycling was used to reactivate the electrode surface. The linear working range (LWR) was dependent on the DASA concentration. For $20 \mu\text{mol L}^{-1}$ DASA the LWR was $0.5\text{--}10 \mu\text{mol L}^{-1}$ and the DL was $0.25 \mu\text{mol L}^{-1}$. Interferences were observed from NTA, tannins and Fe^{3+} .

The voltammetric determination of Al using the adsorptive preconcentration of an Al-PCV complex was investigated by Vukomanovic *et al.* (1991). In a triethanolamine/perchloric acid electrolyte solution the complex was adsorbed onto a mercury drop electrode at -0.5 V (vs SCE). Scanning cathodically gave two well resolved peaks at -0.7 V and -0.9 V for reduction of the adsorbed PCV and Al-PCV complex respectively. For a 60 s adsorption period ($1 \mu\text{mol L}^{-1}$ PCV) a LWR from 1 to $25 \mu\text{g L}^{-1}$ was obtained. The DL was $0.1 \mu\text{g Al L}^{-1}$. Vanadium was found to cause interference in analyses, however this could be overcome by complexation of V with citrate.

Cai and Khoo (1993) utilised 8-hydroxyquinoline (oxine) for the DP AdSV determination of trace amounts of Al. The Al-oxine complex was detected at a glassy carbon (GC) electrode in ammonium acetate buffer (0.024 mol L^{-1} , pH 6.8). The LWR was dependent on the Al concentration and was divided into two segments (ascribed to two processes): (i) oxidative stripping of the adsorbed Al-oxine complex (LWR of $0.04\text{--}5.0 \mu\text{mol L}^{-1}$) and (ii) oxidation of the Al-oxine complex in solution (saturated electrode surface; LWR of $8.0\text{--}40 \mu\text{mol L}^{-1}$). The DL for the method was $0.01 \mu\text{mol L}^{-1}$. A number of potential interferents were tested and procedures for their minimisation suggested.

Recently several AdSV techniques have been applied to the analysis of Al in biological media. Carrera *et al.* (1993) reported the application of a DASA-AdSV technique to the determination of Al in haemodialysis concentrates. Karpiuk *et al.* (1995) utilised a Calmagite-AdSV technique for the determination of Al in human serum-derived products.

7.1.1 SCOPE OF THIS WORK.— The affinity of the Al^{3+} ion for oxygen donor ligands has been well documented [Martell and Smith, 1976-1989; Pearson, 1988; Clevette and Orvig, 1990]. Al also forms strong complexes with a number of hydroxy-arylazo compounds *e.g.* eriochrome black T (EBT), 4-(2-pyridylazo)resorcinol (PAR) [combined nitrogen and oxygen donor molecules].

As discussed above (7.1), the electrochemical analysis of Al generally requires an 'indirect' approach *via* a ligand whose redox chemistry is significantly affected by binding of Al. Many of the dihydroxyaryl, hydroxyquinone and hydroxyarylazobenzene ligands that are known to form stable complexes with Al also exhibit favourable electrochemical responses over the anodic potential range 0 to 1.0 V. Thus such ligands are ideal candidates for investigation with regard to their potential use in developing electrochemical methods for Al determination. The oxidation (anodic) waves of the ligand and metal-ligand complexes are of primary interest because detection systems based on oxidation may be used with flow injection techniques without the requirements of solution deaeration.

A second indirect method for the electrochemical determination of Al may also be considered. This novel procedure could involve probing the electrochemistry of a secondary metal ion bound by a suitable ligand. The ligand's ability to complex Al should be such that, in its presence, the secondary metal ion is displaced quantitatively by Al, thus allowing this metal's electrochemistry to be exploited. The $\text{Cu}^{2+}/\text{Cu}^0$ pair is such a metal ion system. The Cu^{2+} ion can be bound by the same moieties that bind Al and is easily reduced. Ligands such as Tartrazine, which possess functional groups suitable for complexing both Cu and Al, are of possible interest for such work.

In this SECTION a survey of the electrochemical properties of redox active ligands (also known to complex Al) was undertaken. Ligands that may be used for the second indirect procedure described above were also considered. These studies were undertaken using cyclic voltammetry.

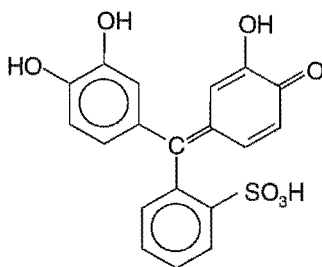
7.1.2 EXPERIMENTAL

(A) Chemicals and Analysis.— All solutions were prepared from Milli-Q water and all working solutions were prepared in $0.10 \text{ mol L}^{-1} \text{ KCl}$ (Merck, *p.a.*), dried at 120°C .

(i) Ligand Solutions: Ligand solutions for electrochemical work were used without further purification (unless otherwise stated) and stored in the dark at 6°C . All ligand stock solutions were prepared by accurately weighing the required amount of dry solid (corrections were made for estimated ligand content). These solutions were *ca.* $5\text{--}10 \text{ mmol L}^{-1}$ ligand and *ca.* $0.01 \text{ mol L}^{-1} \text{ HCl}$ (unless otherwise stated).

Pyrocatechol violet:

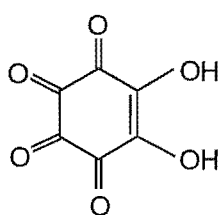
Reagent grade PCV {(i) 2-[(3,4-dihydroxyphenyl)(3-hydroxy-4-oxocyclohexa-2,5-dien-1-ylidene)methyl]benzene sulfonic acid} was obtained from Koch-Light and was used following vacuum drying at 105 °C [as described in Chapter 3 (3.2.6)].



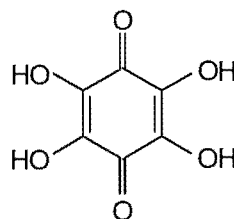
(i)

Rhodizonic acid and tetrahydroxy-1,4-quinone:

Rhodizonic acid [(ii) RHD, 1,2-dihydroxytetraquinone] and tetrahydroxy-1,4-quinone [(iii) THQ] were obtained from Sigma. These solids were used without further purification (RHD solid was stored below 0 °C). RHD solutions were prepared daily under a nitrogen atmosphere to minimise ligand oxidation and decomposition.



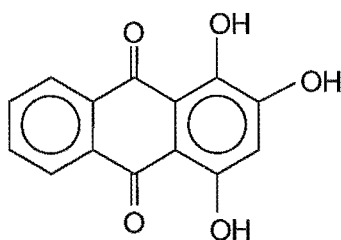
(ii)



(iii)

Purpurin:

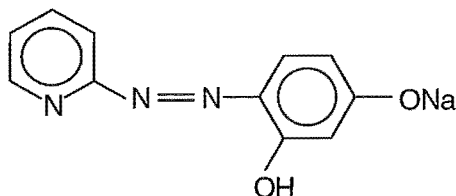
Purpurin [(iv) PPN, 1,2,4-trihydroxyanthraquinone] was obtained from Sigma. The stock solutions were 0.025 μm membrane filtered.



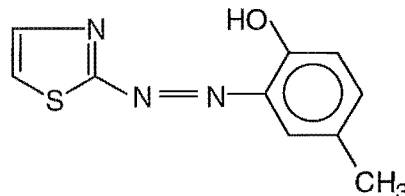
(iv)

4-(2-pyridylazo)resorcinol and 1-(2-thiazolyazo)-2-naphthol:

4-(2-pyridylazo)resorcinol [(v) PAR] and 1-(2-thiazolyazo)-2-naphthol [(vi) TAN] were obtained from Sigma. PAR was quite soluble in H_2O . In contrast, TAN required a drop of KOH (1:1) to provide adequate solubility.



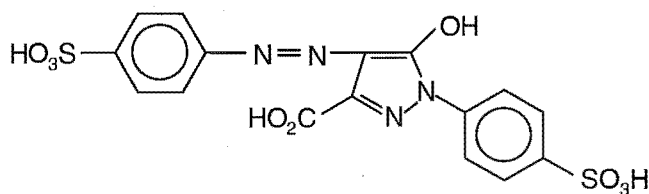
(v)



(vi)

Tartrazine:

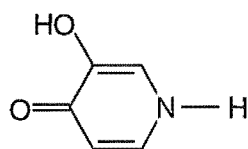
Tartrazine {(vii) TART, 3-carboxy-5-hydroxy-1-*p*-sulphophenyl-4-[(*p*-sulphophenyl)azo]pyrazole} was obtained from BDH as the trisodium salt.



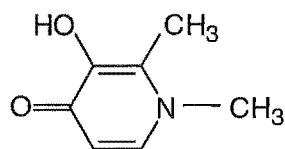
(vii)

Pyridinones Hmpp and Hdpp:

The pyridinones 3-hydroxy-1,2-dimethyl-4-pyridinone [(viii) Hdpp] and 3-hydroxy-2-methyl-4(1H)-pyridinone [(ix) Hmpp] were obtained from Prof. C. Orvig (UBC, Canada) via Prof. S. Sjöberg (Umeå, Sweden).



(viii)



(ix)

(ii) **Metal Ion Solutions:** All metal solutions were prepared by dilution of stock solutions described in Chapter 3 [3.2.5]. These solutions were (i) a 2.0 mmol L^{-1} Al(III) solution, (ii) a 2.0 mmol L^{-1} Fe(III) solution and (iii) a 2.0 mmol L^{-1} Cu(II) solution. All solutions were prepared in 0.02 mol L^{-1} HCl

(iii) **Buffer Solutions:** Three buffer solutions were used throughout these studies: (i) acetate (pH 4.5 - 5.5) [BDH, AnalaR], (ii) ammonium acetate (pH 8.5 - 9.0) [ammonia \ acetic acid; BDH, AnalaR] and MES (pH = 5.9 - 6.2) [Sigma]. All buffer solutions were *ca.* 0.05 mol L^{-1} .

(iv) **Solvents:** The solvent used for dip-coated electrodes was DMF (NN-dimethyl-methanamide) [May and Baker].

(B) Voltammetric Equipment

(i) **Instrumentation:** Cyclic voltammograms (CVs) were obtained using a model 273 A potentiostat (EG & G Princeton Applied Research) with computer recording.

(ii) **Electrodes and Cells:** A three electrode pyrex glass cell was used for all voltammetric studies. It consisted of a glassy carbon (GC) (area = 0.07 cm^2) or graphite (area = 0.28 cm^2) working electrode, a platinum wire counter electrode and a saturated calomel reference electrode (SCE). The laboratory-built cells were 10 mL and 15 mL for the GC and graphite electrodes respectively. The preparation and treatment of the electrodes has been described in Chapter 3 (3.5.2).

(C) **Cyclic Voltammogram Recording Procedures.**— All test solutions were deaerated with oxygen-free nitrogen for 5-10 min before recording voltammograms. Throughout the experiments oxygen-free nitrogen was passed over the top of the test solutions. The concentration of ligand in the test solution was generally $0.3\text{-}1.0 \text{ mmol L}^{-1}$. The addition of the test metal (*e.g.* Al) was made through the 'port' which contained the SCE electrode (following its temporary removal). The GC electrode was not removed during this procedure. A 5 min equilibration period (with deaeration and hence mixing) was effected between each addition to the cell. Care was taken not to create gas bubbles at the surface of the GC electrode. Between repeat 'scans' of a test solution the electrode surface was 'cleaned' by bubbling oxygen-free nitrogen for 2 min through the test solution followed by 30 s with 'no bubbling'. Repeat scans were then effected immediately.

7.1.3 RESULTS.— The electrochemistry of the ligands and their Al (or Cu) complexes were examined using cyclic voltammetry (scan rate = 100 mV s^{-1}) at a GC electrode. For the purposes of these studies, the oxidation waves were of the primary interest. However, in the preliminary studies both oxidation and reduction processes were investigated. The results for ligand and Al-ligand oxidation waves are summarised in Table 7.1.3.

Electrolyte and Buffers: The electrochemical characteristics of the buffer solutions were checked before all ligand and metal-ligand experiments. Cyclic voltammograms of the three buffers used [NaOAc/HOAc (pH 4.5 - 5.5), MES (pH 5.9 - 6.2), NaOAc/ NH_3

(pH 8.5 - 9.0): all $I = 0.10 \text{ mol L}^{-1}$] revealed no electroactive components present. 'Background' signals were negligible over the range $-1.35 \text{ V} \leq E \text{ (vs. SCE)} \leq 1.40 \text{ V}$.

Table 7.1.3 The electrochemistry of the ligands and their Al complexes in aqueous media at a GC electrode.

Ligand concentration	pH	Oxidation waves [E_p^a vs. SCE (V)]	
		ligand	Al-ligand [†]
PCV 0.35 mmol L ⁻¹	6.2	0.35 (0.70) ^b	<i>a</i>
	8.5	0.14	<i>a</i>
RHD 1.0 mmol L ⁻¹	5.0	0.59	1.00
	8.5	0.61	(0.70) 0.95 ^b
THQ 2.5 mmol L ⁻¹	5.0	0.23	<i>a</i>
PPN 1.0 mmol L ⁻¹	5.5	0.55	<i>c</i>
	8.5	0.29	<i>c</i>
PAR 0.5 mmol L ⁻¹	5.5	0.85	<i>a</i>
	8.5	0.75	<i>a</i>
TAN 0.5 mmol L ⁻¹	5.5	0.64	<i>a</i>
	8.5	0.47	<i>a</i>
MPP 1.0 mmol L ⁻¹	5.0	0.90	<i>a</i>
	5.9	0.76	<i>a</i>
	9.0	0.60	<i>a</i>
DPP 1.0 mmol L ⁻¹	5.0	0.83	<i>a</i>
	9.0	0.47	<i>a</i>
TART 0.5 mmol L ⁻¹	5.5	1.02	<i>a</i>
	8.5	0.80	<i>a</i>

[†] The ligand/metal ratio was 3.0 for these E_p^a measurements.

a No shift in potential observed with added Al.

b Two peaks observed (smaller of two bracketed).

c Precipitate observed with added Al.

(A) **Pyrocatechol Violet (PCV).**— Cyclic voltammograms (CVs) were recorded for PCV solutions at pH 6.2 and 8.5. At both of these pHs a linear correlation was observed between the ligand oxidation peak height (i_p^a) and the added Al. PCV is oxidised in air at $\text{pH} > 7$ and the development of an FIA system utilising electrochemical detection with PCV would preferably involve an operating pH of 5.8–6.2. For these reasons pH 6.2 was investigated more thoroughly than pH 8.5 and the CVs recorded for PCV solutions at pH 6.2 are used to illustrate the results. The results for pH 8.5 solutions are shown in the presence of Al [see 'Effect of pH'; Figure 7.1.3B(iii)].

Figure 7.1.3A shows CVs of PCV recorded over the ranges: (i) $-1.0 \text{ V} \leq E \text{ (vs. SCE)} \leq 0.8 \text{ V}$ and (ii) $-0.4 \text{ V} \leq E \text{ (vs. SCE)} \leq 0.5 \text{ V}$. It is apparent from these Figures that electrode fouling is not significant and the peak potentials are stable and reproducible.

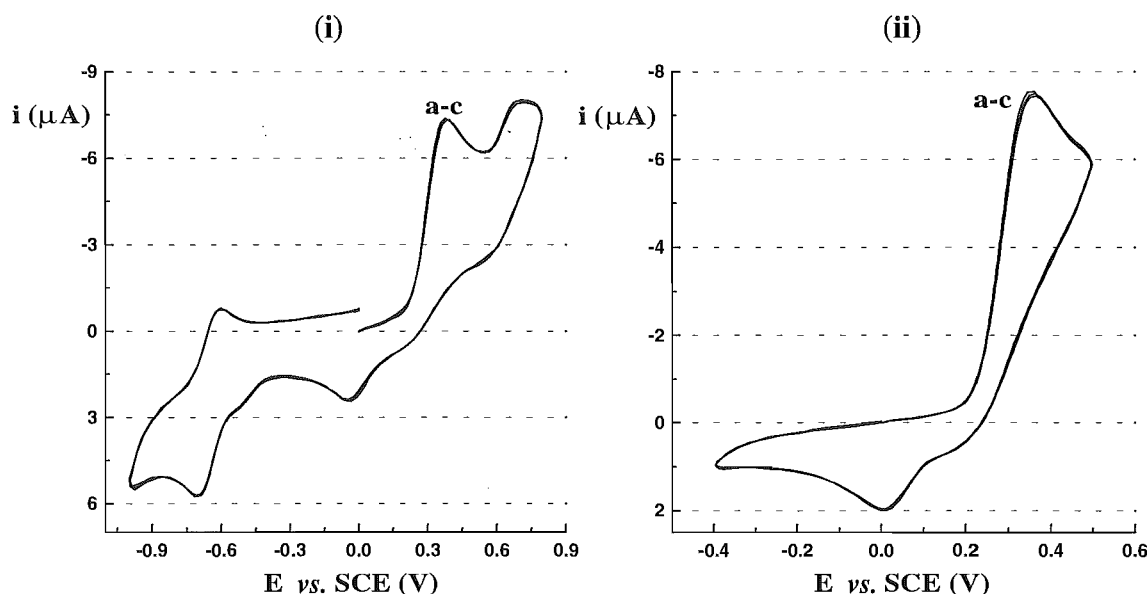
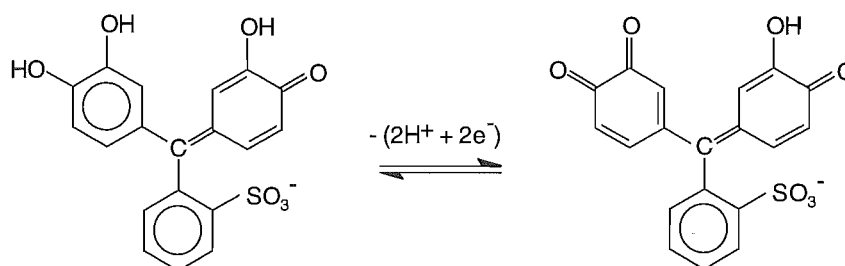


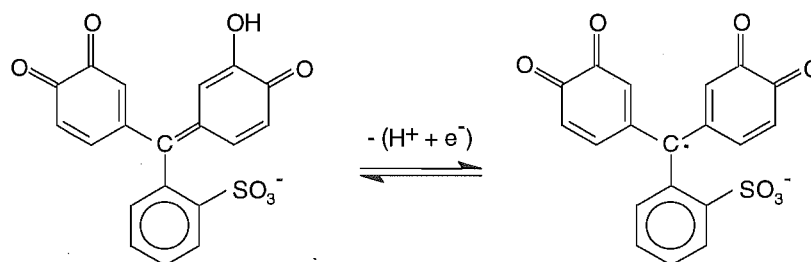
Figure 7.1.3A Cyclic voltammograms of PCV (pH 6.2) recorded over the ranges: (i) $-1.0 \text{ V} \leq E \text{ (vs. SCE)} \leq 0.8 \text{ V}$ and (ii) $-0.4 \text{ V} \leq E \text{ (vs. SCE)} \leq 0.5 \text{ V}$. Both CVs were commenced in the positive direction. The concentration of PCV was 0.35 mmol L^{-1} and three scans are shown for each solution.

The two oxidation waves observed at 0.35 and 0.70 V (vs. SCE) are assigned to the irreversible oxidation of the 1,2-dihydroxyaryl and 2-hydroxy-1-oxocyclo-hexadiene sites respectively. These oxidation processes are depicted below:

(a) Oxidation wave at 0.35 V (vs. SCE): 1,2-dihydroxyaryl site.



(b) Oxidation wave at 0.70 V (vs. SCE): 2-hydroxy-1-oxocyclohexadiene site.



Effect of Al: The effect of Al on the electrochemical response of PCV is shown in Figure 7.1.3B. Also shown in this Figure is a plot of $-i_p^a$ (0.35 V) vs. $[\text{Al}]$.

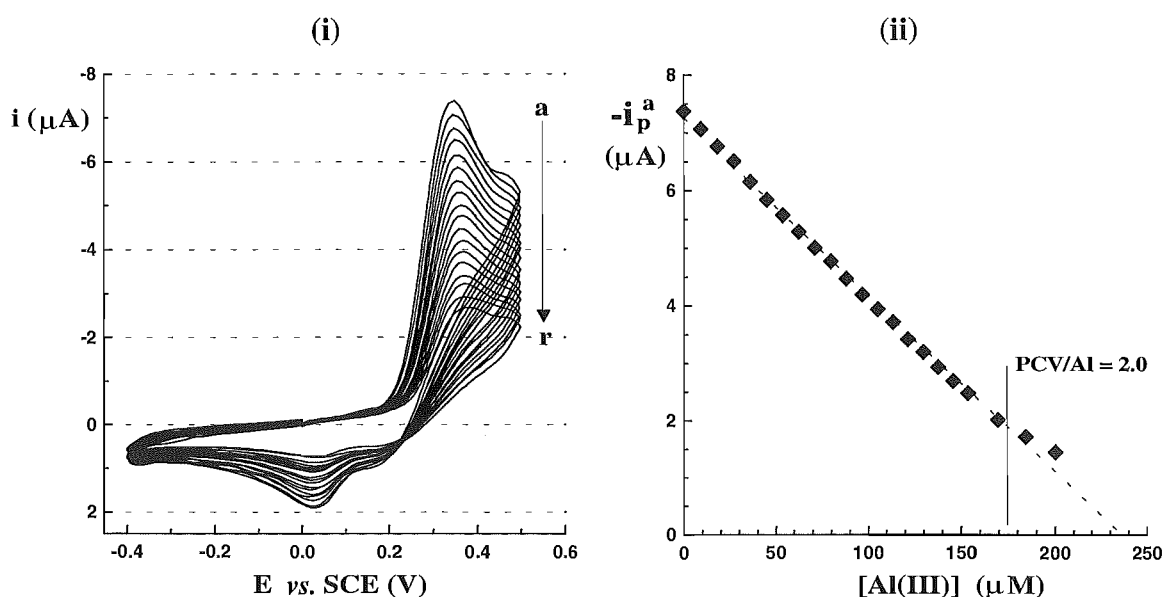


Figure 7.1.3B (i) Cyclic voltammograms recorded over the range $-0.4 \text{ V} \leq E \text{ (vs. SCE)} \leq 0.5 \text{ V}$ [commenced in the positive direction] for solutions containing 0.35 mmol L^{-1} PCV and 'a' 0, 'b' 10, 'c' 20, ... 'r' $200 \text{ } \mu\text{mol L}^{-1}$ Al (pH 6.2). (ii) A plot of i_p^a (0.35 V) vs. $[\text{Al}]$.

It is clear from this Figure that at pH 6.2 PCV complexes Al and that this complex does not exhibit an oxidation signal at the same potential as the uncomplexed PCV. CVs recorded over the range $-1.0 \text{ V} \leq E \text{ (vs. SCE)} \leq 0.8 \text{ V}$ showed no 'second' peak (*i.e.* a peak for the Al-PCV species); such a peak had been observed by Xu [1992] at higher PCV concentrations.

Effect of pH: The effect of Al addition on the voltammetric response of PCV (0.20 mmol L^{-1}) at pH 8.5 is shown in Figure 7.1.3B(iii). This is to be contrasted with Figure 7.1.3B(i).

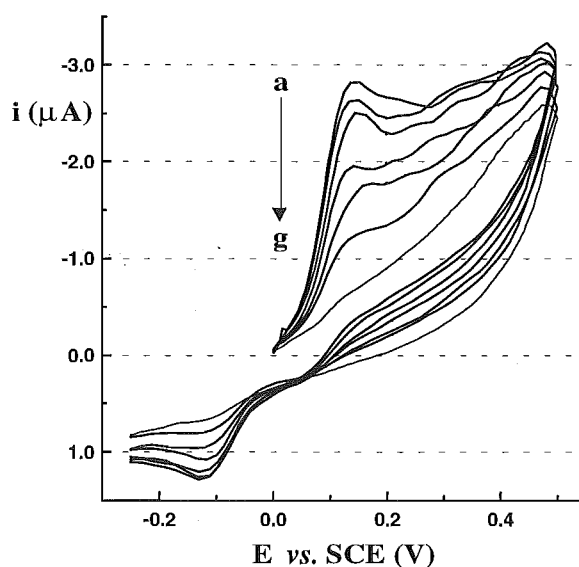


Figure 7.1.3B (iii): Cyclic voltammograms recorded over the range $-0.25 \text{ V} \leq E \text{ (vs. SCE)} \leq 0.5 \text{ V}$ [commenced in the positive direction] for solutions (pH 8.5) containing 0.20 mmol L^{-1} PCV and 'a' 0, 'b' 50, 'c' 100, ... 'g' $300 \mu\text{mol L}^{-1}$ Al.

These results represent a linear decrease in the oxidation peak for PCV, i_p^a , (0.14 V vs. SCE) as a function of Al concentration, *i.e.* as observed in Figure 7.1.3B(ii) (pH 6.2).

Effect of Cu(II): The effect of Cu(II) on the electrochemical response of PCV is shown in Figures 7.1.3C(i)-(ii). In Figure 7.1.3C(i) an increase in the apparent 'PCV' oxidation wave is observed with each consecutive addition of Cu. In (ii) a new oxidation wave is observed at *ca.* -0.05 V ; this wave may be assigned to the Cu(II)/Cu(I) redox couple and indicates the presence of free Cu in the solutions.

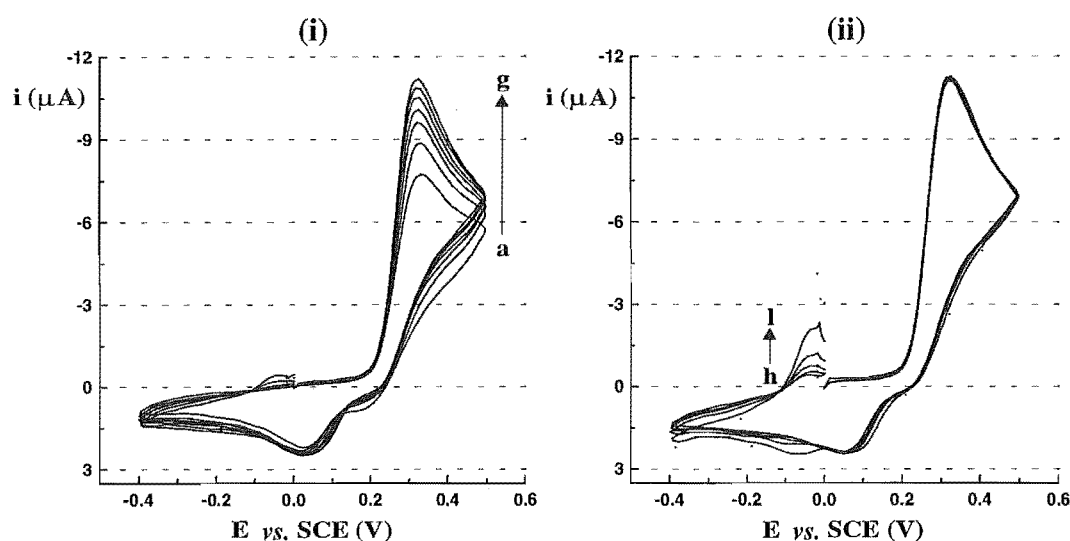


Figure 7.1.3C (i) and (ii): Cyclic voltammograms recorded over the range $-0.4 \text{ V} \leq E$ (vs. SCE) $\leq 0.5 \text{ V}$ [commenced in the positive direction] for solutions (pH 6.2) containing 0.35 mmol L^{-1} PCV and consecutive additions (a \rightarrow l) of Cu(II) (*ca.* 0, 12.5, 25, ... $\mu\text{mol L}^{-1}$ Cu respectively).

It is observed in Figure 7.1.3C that Cu(II) 'enhances' the apparent PCV oxidation peak. Possible explanations to these effects are addressed in the Discussion (7.1.4). Whatever the cause, however, these effects may allow larger detection signals to be obtained in the presence of Al. In Figure 7.1.3C(iii) a plot of $-i_p^a$ (0.35 V and -0.05 V) vs. the PCV/Cu(II) ratio is given. In this Figure the maximum increase in the PCV oxidation peak (0.35 V) is observed at a PCV/Cu ratio *ca.* 0.1. At ratios greater than 0.1 'free' Cu was observed in the solution.

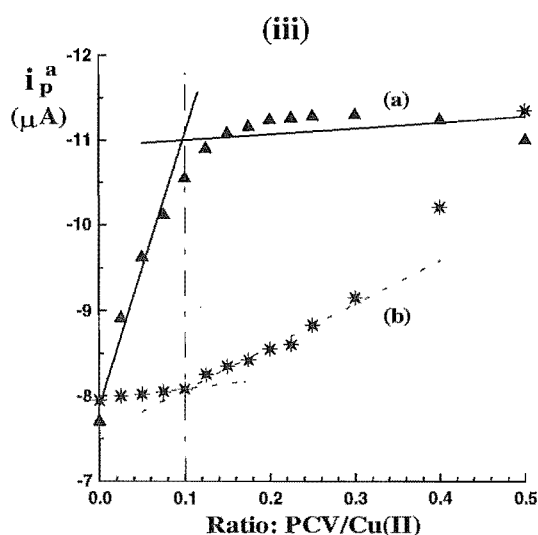


Figure 7.1.3C (iii) A plot of (a) $\{-i_p^a(0.35 \text{ V})\}$ (solid line) and (b) $\{[-i_p^a(-0.05 \text{ V})] - 0.8 \text{ V}\}$ (dashed line) vs. [PCV/Cu(II) ratio] is given.

In a subsequent experiment the effect of Al on a solution containing 0.35 mmol L^{-1} PCV and $0.035 \text{ mmol L}^{-1}$ Cu(II) was studied. The results from these experiments are presented in Figure 7.1.3D.

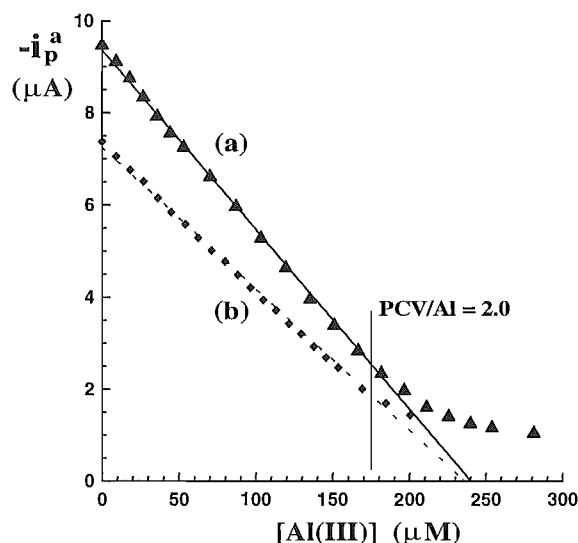


Figure 7.1.3D A plot of $-i_p^a$ (0.35 V) vs. [Al] (a) for cyclic voltammograms recorded over the range $-0.4 \text{ V} \leq E \text{ (vs. SCE)} \leq 0.5 \text{ V}$ [commenced in the positive direction] for solutions containing 0.35 mmol L^{-1} PCV, $0.035 \text{ mmol L}^{-1}$ Cu(II) and 0, 10, 20, ... 200 $\mu\text{mol L}^{-1}$ Al (pH 6.2) and (b) for the results presented in Figure 7.1.3B.

In Figure 7.1.3D the curvature of the plot at ligand/Al ratio of 2.0 indicates that the stoichiometry of the complex forming (pH 6.2) is that predicted from the equilibrium model described in Chapter 4 [*i.e.* $\text{Al}(\text{PCV})_2$].

(B) Rhodizonic Acid (RHD).— CVs were recorded for RHD solutions at pH 5.0 and 8.5. Several features of the chemistry of RHD in aqueous media made the studies of the material difficult. Rhodizonic acid decomposes (*via* oxidation) in the presence of air and for this reason much care was required to exclude oxygen from the cell during all experiments [the decomposition of RHD is addressed in the Discussion (7.1.4)]. The results presented in this Section (pH 5.0) indicate that decomposition of RHD was small. Results in the absence of Al are presented in Figure 7.1.3E.

Figure 7.1.3E shows CVs of RHD recorded over the ranges 'a' $0 \text{ V} \leq E \text{ (vs. SCE)} \leq 0.8 \text{ V}$ and 'b-d' $-0.6 \text{ V} \leq E \text{ (vs. SCE)} \leq 0.3 \text{ V}$. The CV 'a' was not reproducible when using a freshly polished electrode for each scan and further, on repeat scans, both the peak potential (E_p^a) and current (i_p^a) changed significantly. In contrast, CVs 'b-d' were quite

reproducible (as depicted in the Figure by triplicate scans). Electrode fouling was observed not to be significant.

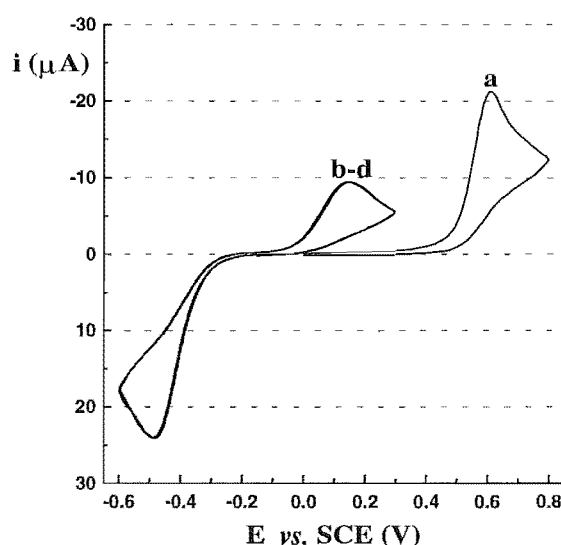
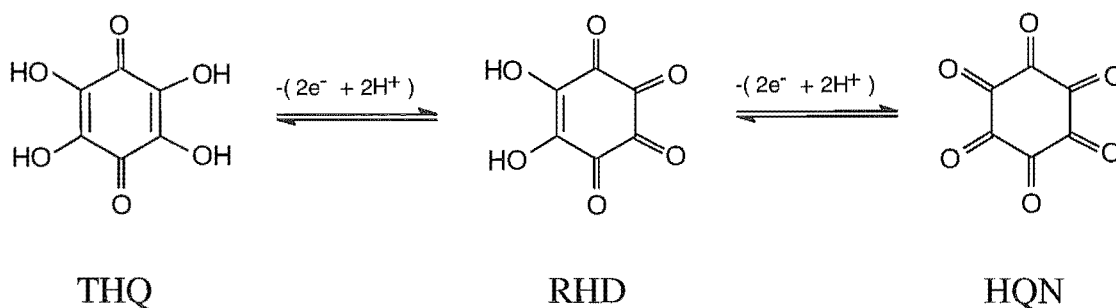


Figure 7.1.3E Cyclic voltammograms of RHD (pH 5.0) recorded over the ranges 'a' $0 \text{ V} \leq E \text{ (vs. SCE)} \leq 0.8 \text{ V}$ [commenced in the positive direction] and 'b'-d' $-0.6 \text{ V} \leq E \text{ (vs. SCE)} \leq 0.3 \text{ V}$ (three repeat scans) [commenced in the negative direction]. The concentration of RHD was 1.0 mmol L^{-1} .

Rhodizonic acid (RHD) may undergo oxidation and reduction; both of these processes are observed in Figure 7.1.3E. The oxidation wave 'a' is consistent with the oxidation of RHD to hexaquinone (HQN). In CVs 'b-d' RHD is reduced to tetrahydroxy-1,4-benzoquinone (THQ), followed by its re-oxidation to RHD. These oxidation and reduction processes are depicted below.



Effect of Al: The effect of Al on the electrochemical response of RHD is shown in Figure 7.1.3F for the reduction process. The oxidation of RHD in the absence of Al was not reproducible. No improvement to the reproducibility (stability of oxidation potential *etc.*)

was observed in the presence of Al. Results for the oxidation of RHD in the presence of Al are not shown.

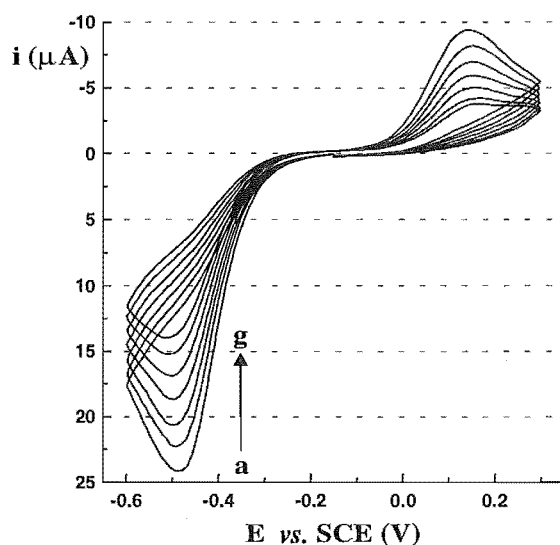


Figure 7.1.3F Cyclic voltammograms recorded over the range $-0.6 \text{ V} \leq E \text{ (vs. SCE)} \leq 0.3 \text{ V}$ [commenced in the negative direction] for solutions containing 0.5 mmol L^{-1} RHD and 'a' 0, 'b' 20, 'c' 40, ... 'g' $120 \text{ } \mu\text{mol L}^{-1}$ Al (pH 5.0).

It is apparent from Figure 7.1.3F that Al complexes RHD and that the Al-RHD complex does not exhibit a reduction signal at the same potential as the uncomplexed RHD. The results were reproducible and a plot of $-i_p^a$ (0.15 V or -0.48 V) vs. [Al] is linear (not shown). Since oxidation processes are preferred over reduction processes for the development of FIA methods (*i.e.* exclusion of oxygen is not required) then oxidation of THQ/Al-THQ (i_p^a at 0.15 V) may be better to investigate than the reduction of RHD/Al-RHD (i_p^c at -0.48 V).

(C) Tetrahydroxy-1,4-quinone (THQ).— CVs were recorded for THQ solutions at pH 5.0. The decomposition of THQ was observed in solutions exposed to the air for prolonged periods of time. The results presented in this Section indicate that decomposition of THQ is likely to be small over the time scale of electrochemical experiments and that THQ should be applicable for FIA use. Results in the absence and presence of Al are shown in Figure 7.1.3G.

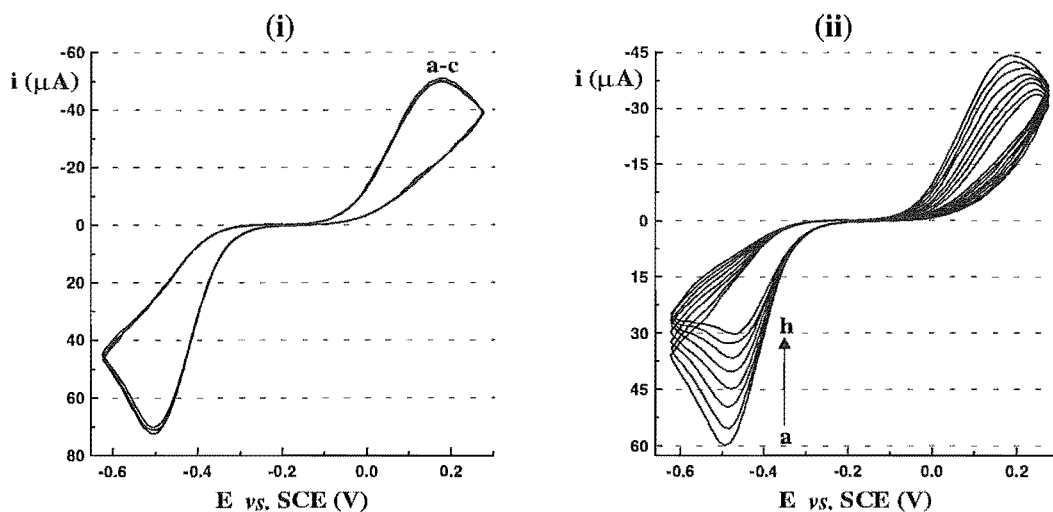


Figure 7.1.3G Cyclic voltammograms recorded over the range $-0.65 \text{ V} \leq E \text{ (vs. SCE)} \leq 0.25 \text{ V}$ [commenced in the positive direction] for solutions containing (i) 3.75 mmol L^{-1} THQ and (ii) 3.75 mmol L^{-1} THQ and 'a' 0.1, 'b' 0.2, 'c' 0.3, ... 'h' 0.8 mmol L^{-1} Al (pH 5.0).

(D) Purpurin (PPN).— Preliminary studies indicated that PPN is sparingly soluble in H_2O . At both pH 5.5 and 8.5 PPN was sufficiently soluble to determine the potential at which the ligand is oxidised (see Table 7.1.3). However the addition of Al resulted in precipitation of the ligand or metal-ligand complex. For these reasons an attempt to investigate the redox chemistry of PPN and the Al-PPN system was made using chemically modified electrodes (CME). This work was performed at pH 8.5. The preparation and characterisation of a 'single-use' PPN-modified graphite electrode (dip coated) is now described.

Preparation of Dip Coated PPN Electrode and Test Solution Analysis: The immobilisation of PPN onto the electrode depends on the electrode material and surface conditions, the solvent and the concentration of PPN in the dip-coating solution. Xu (1992) found that alizarin (1,2-dihydroxyanthraquinone) was most soluble in DMF and dip coating from this medium gave electrodes with the greatest sensitivity (ethanol and acetonitrile were also tested). Because the structures of alizarin and PPN are very similar, DMF was chosen as the solvent for these studies.

Reproducibility depends on electrode surface conditions, therefore surface pretreatment (cleaning and polishing) was most important. This pretreatment of the graphite electrode was described in the Chapter 3 (3.5.2). In these studies the effect of the concentration of PPN (dip concentration) was investigated. PPN concentrations of 20.0, 2.0 and 0.2 mmol L^{-1} (in DMF) were tested. The notation PPN(20 mmol L^{-1}), for example, will be used to describe a CME prepared by dip coating in a DMF solution of 20 mmol L^{-1} PPN.

Test solutions were prepared by addition of an aliquot of Al standard to 5 mL of buffer (NaOAc/NH_3 , pH 8.5) and 5 mL of triply distilled water in the electrochemical cell. The solution was allowed to equilibrate at room temperature for 5 min prior to transferring the CME to the cell. The CME was introduced to the cell and stirring ($\text{N}_2(\text{g})$ bubbling) was initiated for 1 min at open circuit. The CV was then recorded.

Results: CVs were recorded for PPN modified electrodes at pH 5.0 and 8.5. In Figure 7.1.3H(i) the effect of ligand concentration (dip solution) on the voltammetric response of PPN is shown (pH 8.5). Also shown, (ii), is the forward (solid line) and reverse (dashed line) CV for a PPN(20 mmol L^{-1}) CME.

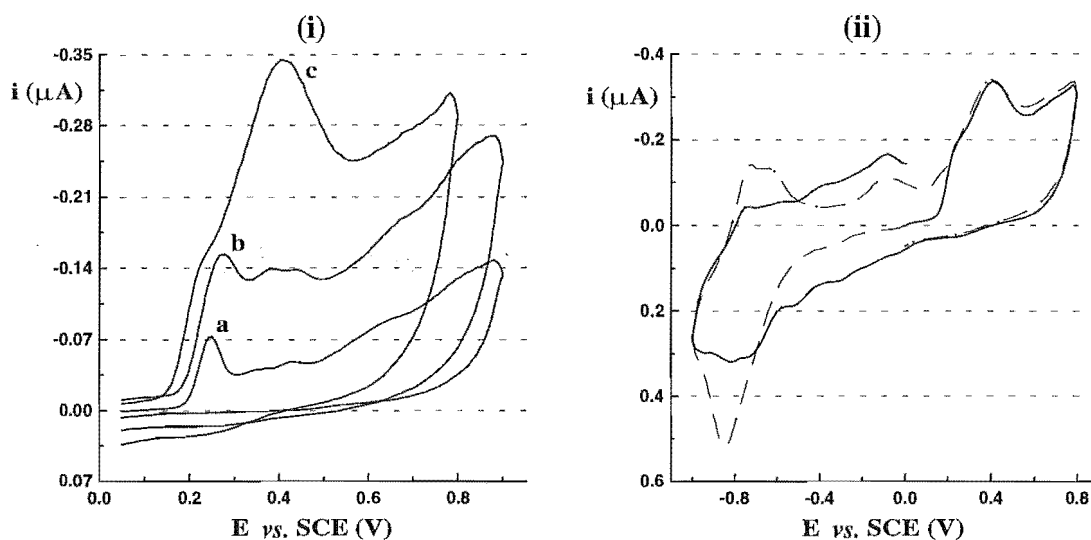
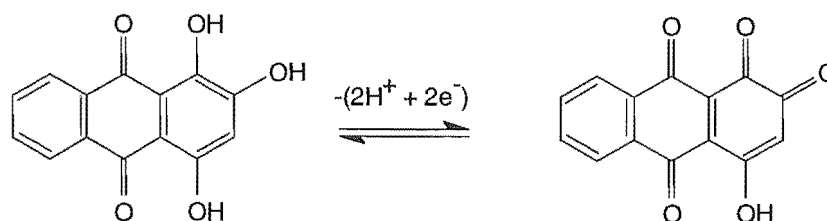


Figure 7.1.3H Cyclic voltammograms of PPN($X \text{ mmol L}^{-1}$) CME's where (i) $X = \text{'a' } 0.2, \text{'b' } 2.0 \text{ and 'c' } 20.0 \text{ mmol L}^{-1}$ [$0.05 \text{ V} \leq E \text{ (vs. SCE)} \leq 0.9 \text{ V}$] and (ii) PPN(20 mmol L^{-1}) CME [$-0.9 \text{ V} \leq E \text{ (vs. SCE)} \leq 0.8 \text{ V}$] (pH 8.5). The voltammograms commenced in the positive direction and negative direction are illustrated by solid lines and dashed lines respectively.

At pH 5.0 the CV for a PPN(20 mmol L^{-1}) CME did not exhibit a sharp and/or well defined peak. In contrast, at pH 5.0, the oxidation peak for a PPN(2 mmol L^{-1}) CME was much sharper and well defined. The oxidation mechanism for the ligand is depicted below:



Effect of Al: Al is expected to bind to the ortho-phenolic oxygens of PPN. After ligand oxidation Al is not expected to remain complexed. The effect of Al on the electrochemical response of PPN is shown in Figures 7.1.3I and 7.1.3J. In Figure 7.1.3J the effect of pH and PPN concentration on the voltammetric response of Al-PPN is also shown.

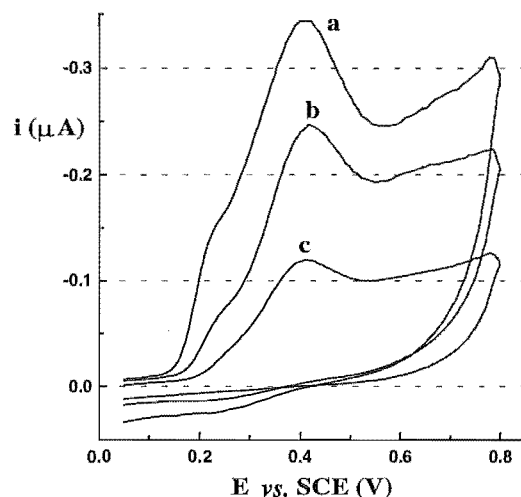


Figure 7.1.3I Cyclic voltammograms recorded over the range $0.05 \text{ V} \leq E \text{ (vs. SCE)} \leq 0.8 \text{ V}$ [commenced in the positive direction] for a PPN(20 mmol L^{-1}) CME and 'a' 0, 'b' 8.0 and 'c' 16 mmol L^{-1} Al (pH 8.5).

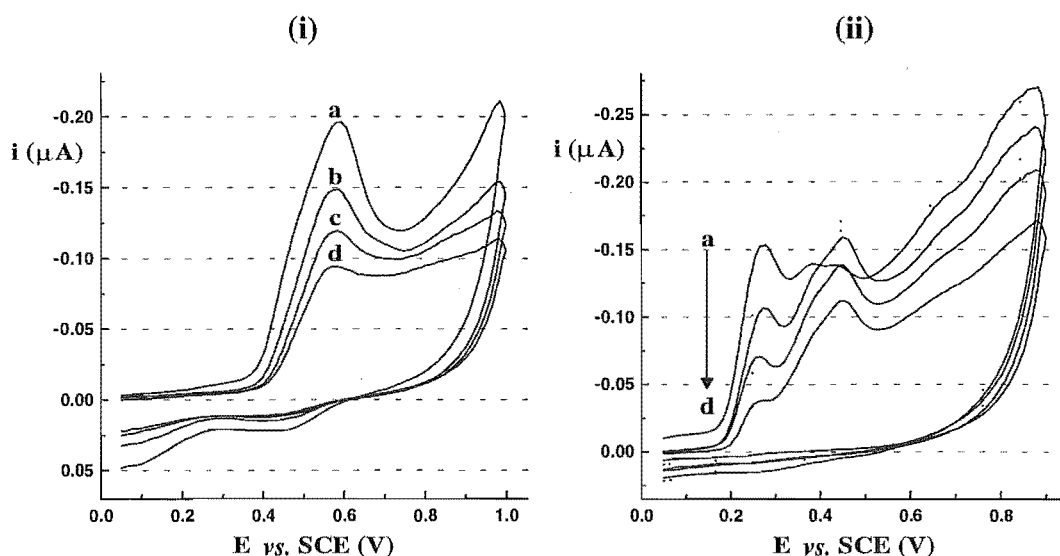


Figure 7.1.3J Cyclic voltammograms recorded over the range $0.05 \text{ V} \leq E \text{ (vs. SCE)} \leq 1.0 \text{ V}$ [commenced in the positive direction] for a PPN(2 mmol L^{-1}) CME at (i) pH 5.0 for and 'a' 0, 'b' 0.9, 'c' 1.8 and 'd' 2.6 mmol L^{-1} Al and (ii) pH 8.5 and 'a' 0, 'b' 1.0, 'c' 2.0 and 'd' 3.0 mmol L^{-1} Al.

(E) Pyridinones: Hmpp and Hdpp.— CVs were recorded for both Hmpp and Hdpp solutions at pH 4.6, 5.0, 5.9, 6.2-6.5 and 9.0. At pH 4.6 and 6.2-6.5 distinct oxidation peaks were not observed for these ligands; the best results are illustrated in Figure 7.1.3K.

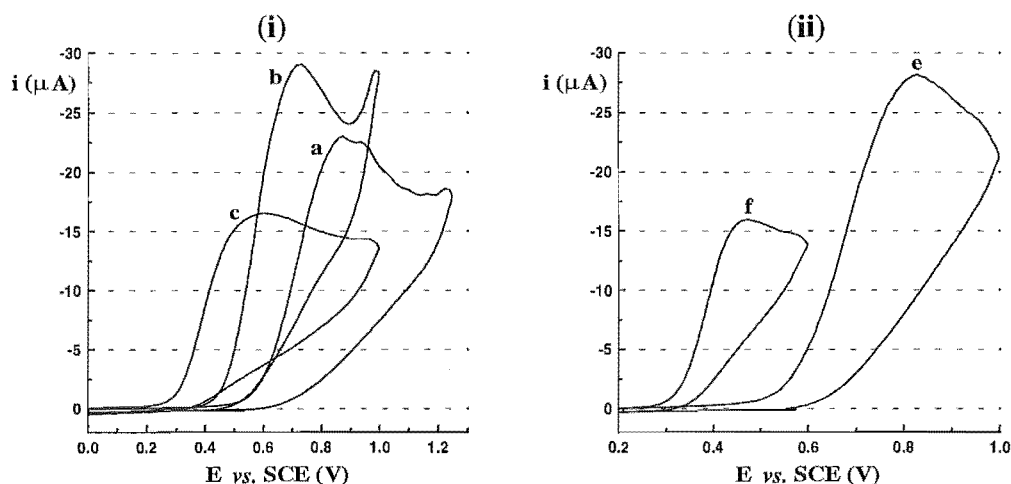


Figure 7.1.3K Cyclic voltammograms recorded for (i) Hmpp at pH 'a' 5.0, 'b' 5.9 and 'c' 9.0 [$0 \text{ V} \leq E$ (vs. SCE) $\leq 1.2 \text{ V}$] and (ii) Hdpp at pH 'e' 5.0 and 'f' 9.0 [$0.2 \text{ V} \leq E$ (vs. SCE) $\leq 1.0 \text{ V}$]. All CVs were commenced in the positive direction. The ligand concentrations were *ca.* 1.0 mmol L^{-1} .

Effect of Cu and Al: The pyridinones were expected to complex both Cu and Al and the effect of each of these metals on the voltammetric response was investigated. In the presence of Cu oxidation waves of both Hmpp and Hdpp were shifted to higher potentials (*ca.* $+0.10$ to 0.15 V). These new peaks were 'sharper' than the ligand only peaks. The effect of added Al on this peak is shown in Figure 7.1.3L for Hmpp.

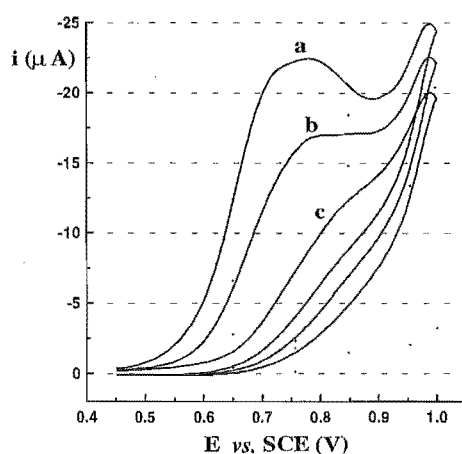


Figure 7.1.3L Cyclic voltammograms recorded over the range $0.45 \text{ V} \leq E$ (vs. SCE) $\leq 1.0 \text{ V}$ [commenced in the positive direction]. All solutions contained 1.0 mmol L^{-1} Hmpp and 0.3 mmol L^{-1} Cu (pH 9.0) and 'a' 0.0, 'b' 0.1 and 'c' 0.2 mmol L^{-1} Al.

(F) Other Ligands.— The results for the ligands 4-(2-pyridylazo)resorcinol (PAR), 1, -(2-thiazolyazo)-2-naphthol (TAN) and Tartrazine (TART) are not shown. The response of these ligands to both Cu and Al was investigated. These results are summarised in Table 7.1.3.

It was intended that these ligands be exploited through the 'second' indirect approach described earlier (7.1.1). For example, TART has an azo group attached to anazole ring which carries a COOH and an OH group in the ortho positions. This type of ligand may be of use in a $\text{Cu}^{2+}/\text{Cu}^0 - \text{Al}^{3+}$ system because the Cu^{2+} is expected to show preference for the azo/COOH binding and the Al^{3+} for azo/OH binding in weakly acidic solution. Similarly PAR and TAN could be expected to complex both Cu and Al.

Unfortunately the electrochemical responses of these ligands were unchanged in the presence of both metals.

7.1.4 DISCUSSION

(A) Pyrocatechol Violet (PCV).— The applicability of PCV for the electrochemical detection of Al at pH 6.2 was clearly demonstrated [7.1.3(A)]. At this pH the Al complexed by PCV would be predominantly the $\text{Al}(\text{PCV})_2$ species [*i.e.* $\text{Al}(\text{HL})_2^{3-}$, *cf.* Figure 4.2.4B (Chapter 4)]. In this species the Al is complexed at the 1,2-dihydroxyaryl sites of both PCV molecules. At pH 8.5 Al was complexed by PCV as one of a possible series of $\text{Al}(\text{PCV})_3$ species [as depicted in Figure 4.2.4B (Chapter 4)].

The results for PCV presented above indicate that the optimum potential for the measurement of Al (at pH 6.2) would be *ca.* 0.35 V *vs.* SCE. At this potential the 1,2-dihydroxyaryl site was oxidised to the corresponding orthoquinone; Al^{3+} was not expected to be complexed by this 'new' site. However, the oxidised PCV may continue to complex Al at the 2-hydroxy-*p*-quinomethide site.

The results for the experiments at pH 6.2 and 8.5 are replotted in Figure 7.1.4A. In this Figure the distribution of the Al-PCV species in solution [calculated (for each CV) from the known solution stoichiometry, the pH and the equilibrium model presented in Chapter 4 for the $\text{H}^+ - \text{Al}^{3+}$ -pyrocatechol violet system] is plotted *vs.* i_p^a for PCV at each pH respectively.

From the earlier calculations it was shown that at both pH 6.2 and 8.5 the oxidation peak, i_p^a , for the oxidation of PCV was a function of the Al concentration. From this Figure it is apparent that the Al-PCV species present in these solutions do not exhibit an electrochemical response at the peak potential of the ligand.

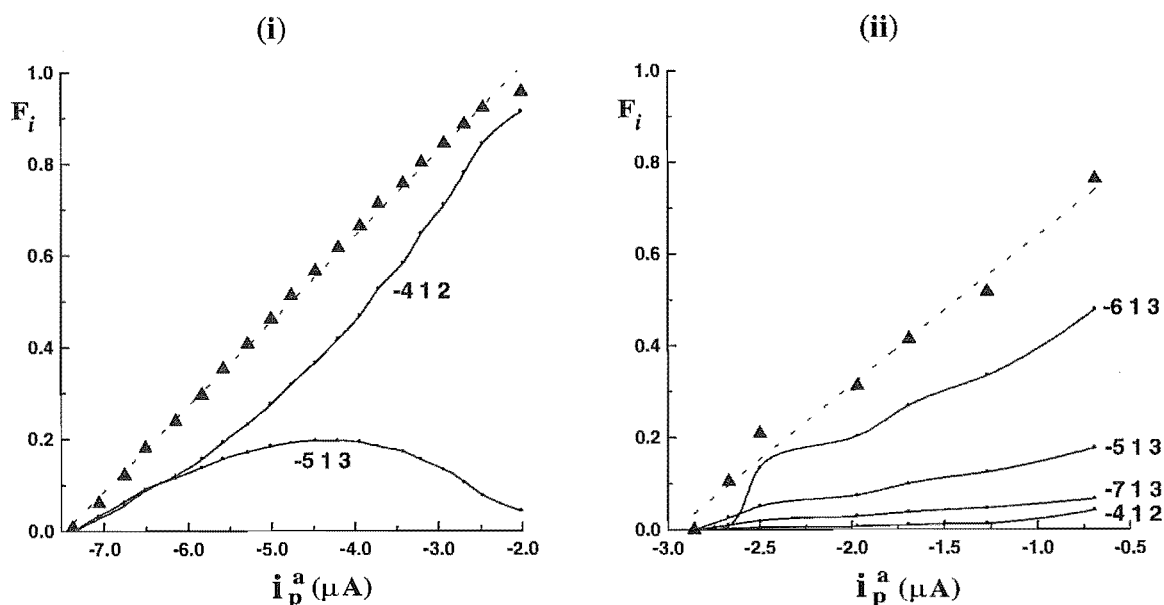


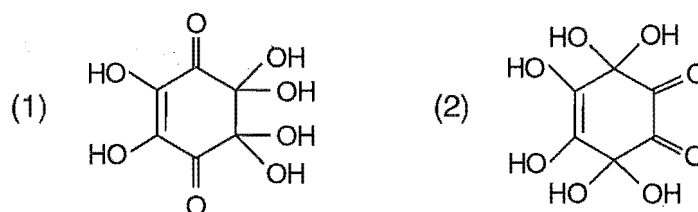
Figure 7.1.4A The distribution of the Al-PCV species present (denoted by p,q,r stoichiometries) in each test solution studied. These distributions are plotted vs. i_p^a (0.35 V and 0.14 V) for PCV at (i) pH 6.2 and (ii) pH 8.5 respectively. The symbols correspond to experimental results plotted vs. the formation sum of all Al-PCV species in solution, *i.e.* $\Sigma(\text{AlPCV})$ (dashed line). Calculations were performed using the computer program SOLGASWATER [Eriksson, 1979] using the equilibrium model presented in Chapter 4 for the H^+ - Al^{3+} -pyrocatechol violet system and the concentrations of PCV and Al and the pH of each solution analysed in this work.

The effect of Cu(II) on the voltammetric response of PCV was surprising. Attempts to further understand this behaviour using adsorptive stripping voltammetric (AdSV) studies of PCV and Al or Cu were not successful. It was not clear whether (i) PCV complexes Cu in solution and the voltammetric response of this species was greater than that of PCV alone or (ii) Cu forms a monolayer [Vassos and Mark, 1967] at the surface of the glassy carbon (GC) electrode and the electrochemical response of PCV at this 'new' surface was significantly greater than that at the clean GC surface. The formation of monolayers at the GC surface using the method of Vassos and Mark was investigated, however no conclusive information was extracted from these studies.

Despite the poor understanding of this behaviour the effect of Cu on the voltammetric response of PCV was significant and may be expected to cause interference in an analysis of Al for solutions which contain significant amounts of Cu.

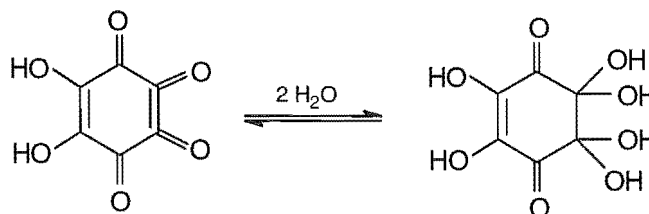
(B) Rhodizonic Acid (RHD) and Tetrahydroxy-1,4-quinone (THQ).— The results presented above indicate that rhodizonic acid (RHD) or tetrahydroxy-1,4-quinone (THQ) may also be appropriate for the development of an electrochemical detection system for Al^{3+} . The biggest drawback in the use of either of these materials was the propensity of these compounds to undergo oxidation upon exposure to air.

Early studies of rhodizonic acid (RHD) indicated the acid was dihydrated in aqueous solutions and at $\text{pH} < 1$ this form dominates. The rhodizonate dianion is unhydrated. The monoanion is an equilibrium mixture of the hydrated and unhydrated forms and RHD exists as the dihydrated structure (1) [Patton and West, 1970]. Slow rates of equilibration of solutions were observed between pH 3 and 6 as a result of these processes. ^{13}C NMR studies have indicated the initially formed ortho-dihydrate structure (1) [Gelb *et al.*, 1978]. Slowly rearranges to the more stable para-dihydrate structure (2) [Gelb *et al.*, 1978]. Studies have shown that the bound water molecules dissociate simultaneously with the second acid dissociation [Gelb *et al.*, 1978].



Rhodizonic acid may decompose in the presence of air by an unknown mechanism [Patton and West, 1970; Alexandersson and Vannerberg, 1972]. Patton and West found that the rhodizonate anion is unstable and decomposes *via* oxidative decarboxylation.

The electrochemistry of the THQ/RHD system is complicated as a result of possible hydration reactions:



The electrochemistry of RHD and THQ has been the subject of several investigations [Kokkinidis *et al.*, 1986; Papadopoulos *et al.*, 1991]. On bare Pt, $\text{RHD} \cdot 2\text{H}_2\text{O}$ was found to undergo irreversible oxidation only; following this the triquinoyl octahydrate was the only product isolated from the electrolysed solution, indicating further hydrolysis [Kokkinidis *et al.*, 1986]. Kokkinidis *et al.* investigated the effect of underpotential deposited layers of Pb, Tl and Bi on Pt electrodes on the voltammetric

response of the RHD/THQ couple at these surfaces. These layers were found to catalyse the oxidation of RHD and THQ and to improve reversibility in the THQ/HHB (hexahydroxybenzene) system.

In the present studies quasi-reversibility was exhibited for the THQ/RHD system at the GC electrode. The complications associated with hydration of RHD and its possible oxidation, even under preventative conditions, may limit the use of this system for the development of an electrochemical system for the determination of Al.

(C) Other Ligands.— Of the other ligands studied, the pyridinones Hmpp and Hdpp showed the greatest prospect for the development of a detection system for Al. Both of these ligands have been shown to form stable complexes with Al [Clevette *et al.*, 1989]. Clevette *et al.* found that the Al-binding efficacy of 3-hydroxy-1-"R"-2-methyl-4-pyridinones was not significantly affected by the N-substituent, "R". In 0.15 mol L^{-1} media the stepwise protonation constants and Al-ligand stability constants determined were $\log K_1 = 9.85$, $\log K_2 = 3.65$ and $\log \beta_1 = 11.8$, $\log \beta_2 = 22.5$, $\log \beta_3 = 32.0$ respectively. A number of studies have investigated the complexation of trivalent metal ions (*e.g.* Fe^{3+} , Ga^{3+} , In^{3+} , Al^{3+}) with different pyridinone ligands [Scarrows *et al.*, 1985; Zhang *et al.*, 1991; Li and Martell, 1993; Kamariotaki *et al.*, 1994; Ma *et al.*, 1994].

Compagnone *et al.* (1992) reported the development of a carbon paste electrode modified with 3-hydroxy-1-methyl-4-pyridinone for the determination of Fe(III). For this electrode, the ligand oxidation peak at 0.335 V (*vs.* SCE) was observed to decrease as a function of Fe concentration. A similar electrode modified with 3-hydroxy-2-methyl-4-pyridinone did not exhibit any electrochemical behaviour in the absence of Fe, however addition of Fe resulted in an oxidation current and a peak at 0.41 V (*vs.* SCE). These results indicate that the position of substituents on the pyridinone ring was likely to influence electrochemical behaviour significantly.

The spectrofluorimetric determination of Al with purpurin (PPN) has been proposed by a number of researchers [Llorente *et al.*, 1989; Maties *et al.*, 1992]. The electrochemical behaviour of anthraquinone derivatives has been investigated [Qureshi *et al.*, 1979], however no studies have been published on the electrochemical behaviour of Al-complexes of these compounds. The electrochemical response of PPN at the GC electrode in aqueous media was not encouraging at either of the pHs studied. The results for PPN at the dip-coated electrode appear promising, however the use of such electrodes in FIA systems would not be very convenient.

The ligands 4-(2-pyridylazo)resorcinol (PAR), 1,6-(2-thiazolyazo)-2-naphthol (TAN) and Tartrazine (TART) did not exhibit useful electrochemical responses in the presence of either Cu(II) or Al(III).



SECTION B: DEVELOPMENT OF AN ELECTROCHEMICAL FLOW INJECTION ANALYSIS METHOD FOR THE DETERMINATION OF Al^{3+}

7.2 INTRODUCTION

Flow injection analysis (FIA) is a micro-technique for solution handling. Based on the concept of controlled dispersion, which allows reproducible development of chemical reactions to occur, it is ideal for combination with many methods of detection. FIA is a technique performed often under non-equilibrium conditions. In FIA a sample plug is injected into a carrier stream where it disperses; on meeting the reagent (present in the carrier or through intersection with another line) dispersion of the reagent occurs into the sample zone. Injection may occur on a time- or volume-based procedure, the latter being the most popular. Injection is usually carried out *via* a multi-port rotary valve.

The technique of FIA originated as a method for rapid sample analysis. However, it is now used routinely for a variety of sample pretreatment procedures including dilution, preconcentration, extraction and dialysis [Ruzicka and Hansen, 1988; Clark *et al.*, 1990]. An example of an FIA manifold and resulting FIA output is shown in Figure 7.2A. The profile developed is unique to the FIA manifold employed and is influenced by a large number of factors (*e.g.* sample size, flow rate, temperature *etc.*). Several good books and reviews have been published on these subjects [Ruzicka and Hansen, 1978; Hansen, 1986; Clark *et al.*, 1990].

In Figure 7.2A(i) a single-line FIA manifold is depicted. In this system a sample (S) is injected into a carrier stream propelled by a pump (P). During the time from sample injection (t_0) to sample detection (t_{det}) the sample passes through a suitable reaction zone (RZ). In this reaction zone the sample undergoes controlled dispersion (characteristic of the manifold) and reacts with reagent (if present) in the carrier stream.

An important feature of FIA is that a sample undergoes dilution and dispersion upon mixing with a carrier stream (and successive reagent lines in multi-line systems). In Figure 7.2(ii) an originally homogeneous sample zone, , of concentration C^0 disperses as it progresses through the reaction zone to the detector. At the detector the dispersed sample plug, , has a maximum concentration C^{max} . The concentration profile of the dispersed sample plug is usually Gaussian in shape [Ruzicka and Hansen, 1988]. The extent of dilution and dispersion is defined according to the dispersion coefficient, D . The (minimum) dispersion coefficient is defined as:

$$D = \frac{C^0}{C^{\text{max}}}$$

where C^0 is the concentration of the injected species prior to dispersion and C^{\max} is the concentration of the species at the time for which D is calculated. C^0 and C^{\max} are depicted in Figure 7.2A(ii).

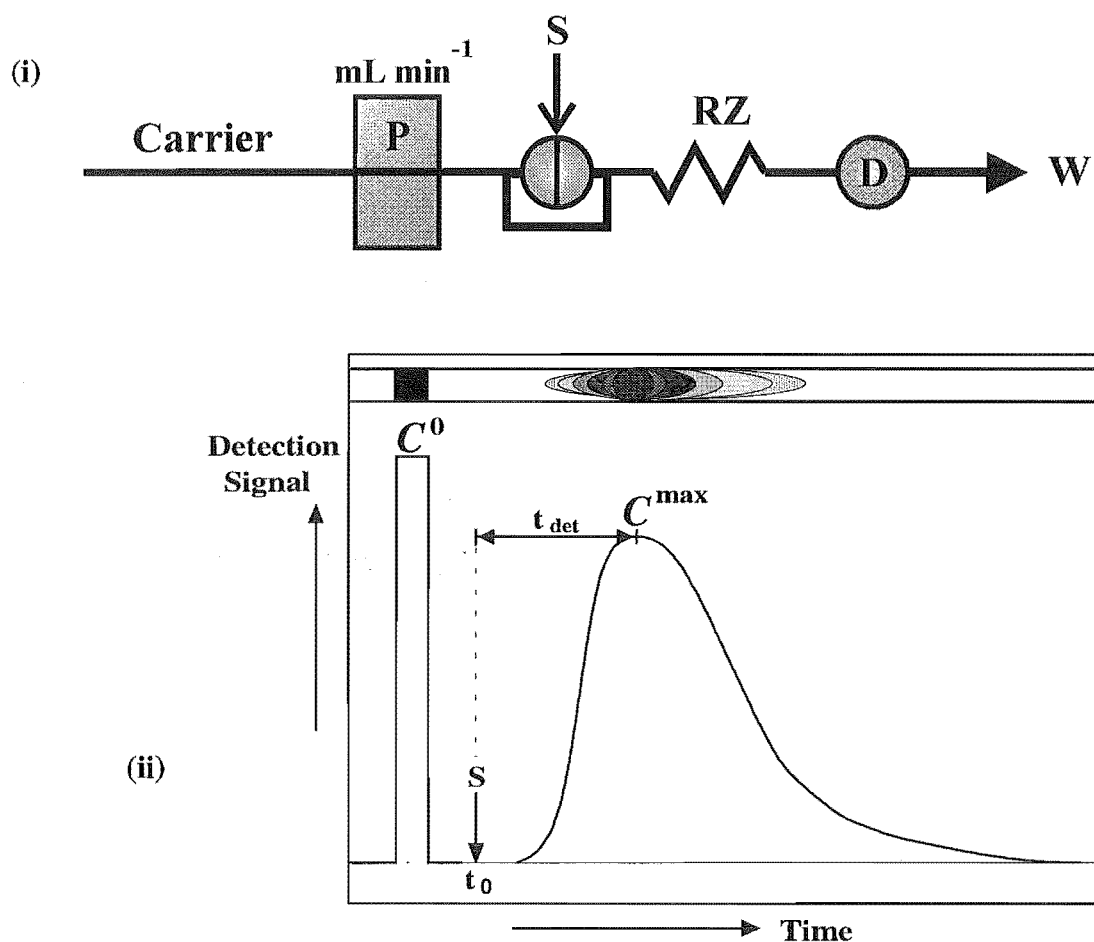


Figure 7.2A (i) A single line FIA manifold where P = pump, S = sample injection point, RZ = reaction zone, D = detector and W = waste. (ii) A typical output from an FIA system where C^0 = initial sample concentration, C^{\max} = maximum sample concentration at detector, S = sample injection, t_0 = time of sample injection and t_{det} = elapsed time to maximum detection signal (C^{\max}).

The design of the FIA manifold influences the dispersion of the sample and hence the sensitivity of the method. Manifolds may be designed with multi-lines to effect the mixing of a number of reagents and sample components. Often these systems require multiple pumps. Several researchers have compared the sensitivity of different manifold configurations [Garn *et al.*, 1988; Chalk and Tyson, 1994].

7.2.1 SCOPE OF THIS WORK.— The direction of this thesis was towards (i) the investigation of processes that influence the determination of Al in environmental samples and (ii) the development of methods for the determination of 'reactive' Al [as described in Chapter 1(1.3)]. Chapters 1-6 were primarily directed towards the first of these objectives. In this Chapter the development of an electrochemical method for the determination of Al was investigated.

In SECTION A of this Chapter the electrochemical properties of a series of ligands (which are known to form stable complexes with Al) were evaluated. Several of these ligands displayed characteristics that may be utilised in the development of an Al detection procedure and incorporated in an FIA technique for the determination of Al. FIA electrochemical detection offers several advantages over other detection procedures (*e.g.* spectrophotometric or fluorimetric detection) in that analyses may be performed rapidly using relatively cheap apparatus.

In the application of amperometric or voltammetric detectors to FIA the interference from oxygen reduction often causes significant problems. In this context, on glassy carbon, in the potential (e.m.f) range 0 to -1.0 V *vs.* SCE, oxygen is reduced to H_2O_2 or water. In the classical procedures of batch voltammetric analysis (*e.g.* ASV, CSV), oxygen is usually removed by bubbling with a suitable gas [*e.g.* $\text{N}_{2(\text{g})}$ or $\text{Ar}_{(\text{g})}$]. These procedures are time consuming and not well suited to FIA. Recently a continuous degassing device designed for FIA applications was presented [Pedrotti *et al.*, 1994], however such a device is likely to be of limited use in the kinetic FIA procedures which are of current preference in Al speciation analyses.

In SECTION A only the oxidation waves of the ligands and Al-ligand complexes were investigated in detail. By utilising a detection procedure based on ligand or Al-ligand oxidation processes the problems associated with dissolved oxygen can be avoided.

In this SECTION the ligands pyrocatechol violet (PCV) and tetrahydroxy-1,4-quinone (THQ) were investigated for the development of electrochemical detection systems applicable to FIA of Al in environmental samples.

(A) Pyrocatechol Violet (PCV).— In Figure 7.2.1A the calculated speciation for the equilibrium between $1 \mu\text{mol L}^{-1}$ Al and $20 \mu\text{mol L}^{-1}$ PCV is given (using the thermodynamic model of the Al-PCV system presented in Chapter 4). The electrochemical analysis of Al is performed under non-equilibrium conditions (*i.e.* FIA conditions). Despite this, equilibrium calculations may be used to estimate the extreme case, *e.g.* the maximum amount of Al that can be complexed and thus measured by PCV. In Figure 7.2.1B the (calculated) effect of pH on the equilibrium determination of Al is shown.

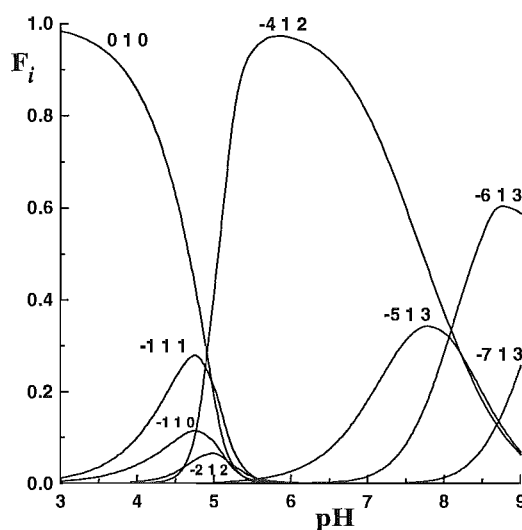


Figure 7.2.1A Distribution diagram for a solution of $20.0 \mu\text{mol L}^{-1}$ PCV and $1.0 \mu\text{mol L}^{-1}$ Al. F_i is defined as the ratio of the Al concentration in an equilibrium species to the total Al concentration. Calculations were performed using the computer program SOLGASWATER [Eriksson, 1979] and the data presented in Table 4.2.3 (Chapter 4).

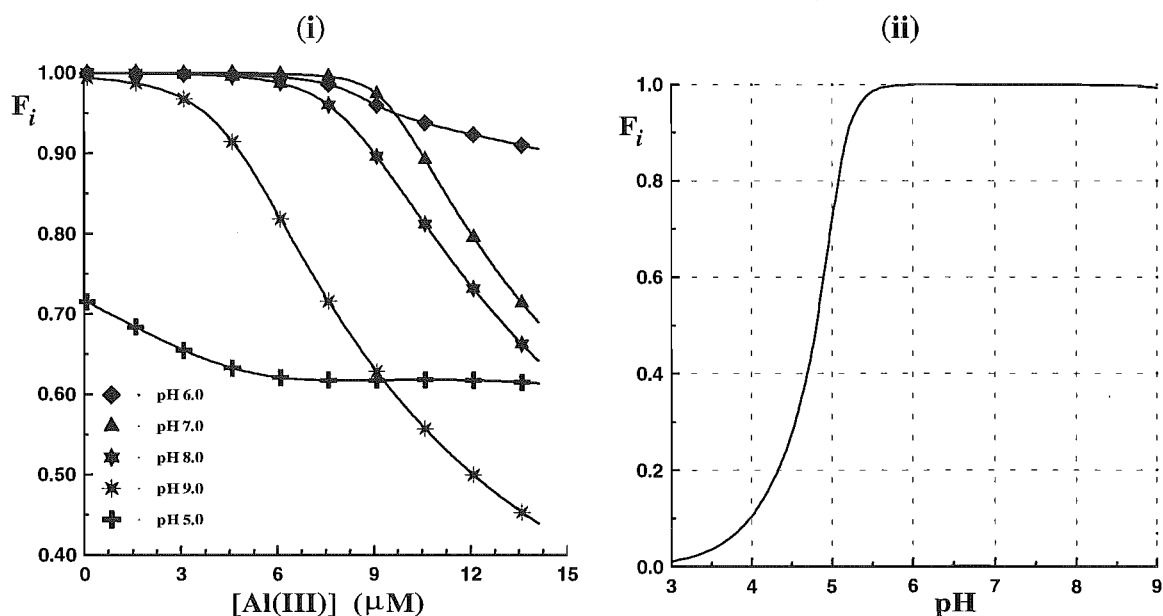


Figure 7.2.1B The total fraction of Al complexed by PCV (*i.e.* the sum of all Al-PCV species) as a function of (i) Al concentration at pH 5.0, 6.0, 7.0, 8.0 and 9.0, and (ii) pH, for a solution of $20.0 \mu\text{mol L}^{-1}$ PCV and $0.1 \mu\text{mol L}^{-1}$ Al. Definitions and method as described in Figure 7.2.1A.

From Figures 7.2.1A and 7.2.1B(i) it is apparent the best determinations of total Al would be made at *ca.* pH 6.0. At pH 6.0 PCV complexes Al strongly and the effects of Al-hydrolysis are not very significant. At higher pH the effect of Al hydrolysis is observed to be more significant, whereas at pH 5.0 Al complexation by PCV is not sufficiently strong. The significance of these results is, however, confused by the kinetics of Al-PCV complex formation and they may be of limited use in estimating effects in the detection method presented here. Figure 7.2.1B(ii) indicates that at higher PCV/Al ratios (200/1) quantitative determinations of Al should be possible over the range $5.75 \leq \text{pH} \leq 8.75$.

(B) Tetrahydroxy-1,4-quinone (THQ).— A significant amount of work has been put into the determination of the protonation constants of rhodizonic acid [Preisler *et al.*, 1947; Patton *et al.*, 1970; Schwartz *et al.*, 1978]. No thermodynamic data have been published on the complexation of Al^{3+} by RHD or THQ, however, some 'unpublished results' for this complexation were obtained from Dr. Tamas Kiss, [Department of Analytical Chemistry, Kossuth Lajos University, Debrecen, Hungary] (personal correspondence). He advised that these "incomplete" results should be regarded as "tentative". These data are given in Table 7.2.1.

Table 7.2.1 Thermodynamic data and equilibrium constants ($\beta_{p,q,r}$) for the system: H^+ - Al^{3+} -rhodizonic acid (L^{2-}) [Unpublished results: *per* Dr. Tamas Kiss, Department of Analytical Chemistry, Kossuth Lajos University, Debrecen, Hungary].

Species	(<i>p,q,r</i>)	$\log \beta_{p,q,r}$
HL^{2-}	(1,0,1)	4.18
H_2L^-	(2,0,1)	8.28
AlHL	(1,1,1)	7.80
AlL	(0,1,1)	5.66
AlLOH	(-1,1,1)	1.02
AlL_2	(0,1,2)	9.78
AlL_2OH	(-1,1,2)	4.20

Despite the potential inaccuracy of these data, they were used to make calculations on the H^+ - Al^{3+} -rhodizonic acid system. The results of these calculations, which were directed towards conditions typical of an FIA analysis system for Al using this ligand (or THQ), are presented in Figures 7.2.1C & D.

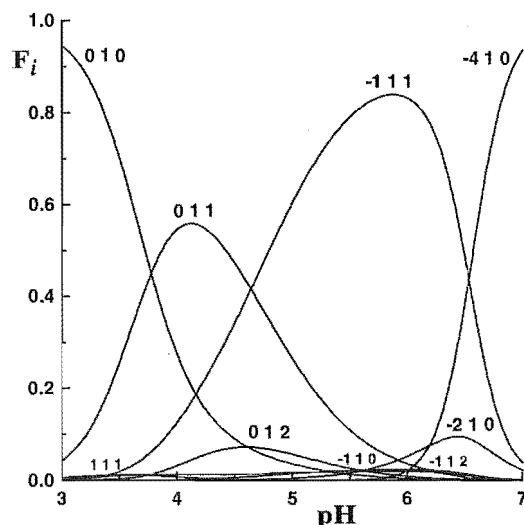


Figure 7.2.1C Distribution diagram for a solution containing $20.0 \mu\text{mol L}^{-1}$ RHD and $1.0 \mu\text{mol L}^{-1}$ Al. Calculations were performed using the computer program SOLGAS-WATER [Eriksson, 1979], the data presented in Table 7.2.1 for the H^+ - Al^{3+} -RHD system and the Al-hydrolysis species presented in Table 6.1.2A (Chapter 6).

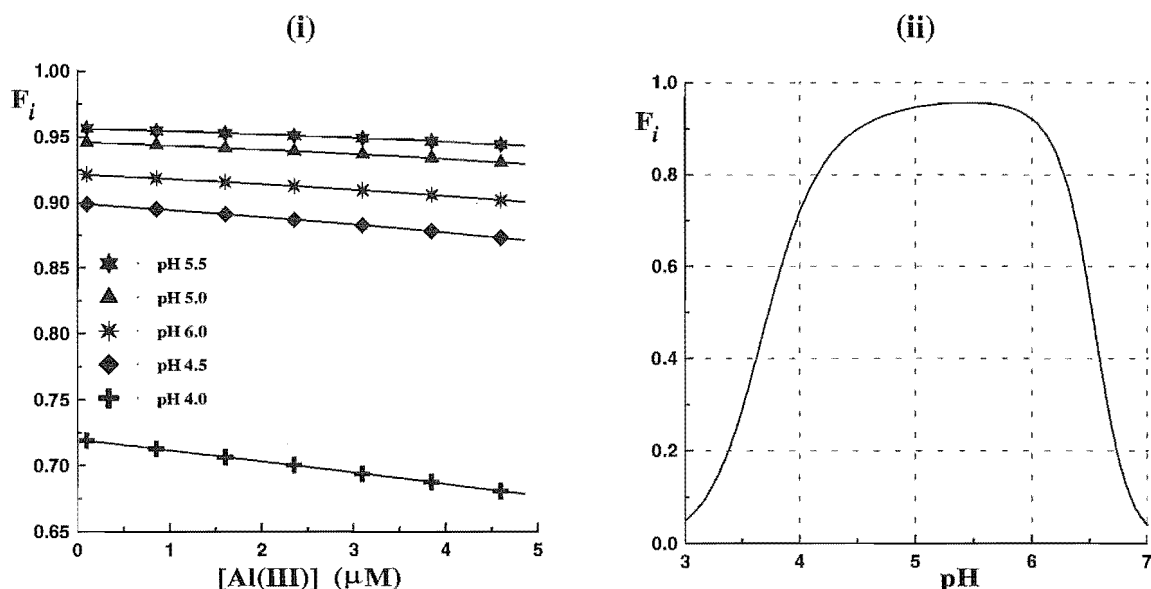


Figure 7.2.1D The total fraction of Al complexed by RHD (calculated) as a function of (i) Al concentration at pH 4.0, 4.5, 5.0, 5.5 and 6.0, and (ii) pH, for a solution of $20.0 \mu\text{mol L}^{-1}$ RHD and $0.1 \mu\text{mol L}^{-1}$ Al. Definitions and method of calculation as described in Figure 7.2.1C.

From these Figures the pH range 5-6 would be predicted as optimum for Al determination, with pH 5.5 being the ideal. The effects of RHD/Al ratio are not expected to affect the result greatly.

7.2.2 EXPERIMENTAL

(A) **Chemicals and Analysis.**— All solutions were prepared from Milli-Q water and all working solutions were prepared in $0.10 \text{ mol L}^{-1} \text{ K}(\text{Cl})$ (Merck, *p.a.*), dried at 120°C .

Reagent and Standard Solutions: Ligand solutions of pyrocatechol violet (PCV) and tetrahydroxy-1,4-quinone (THQ), the metal solutions and buffers were prepared as described in 7.1.2(A).

(B) **FIA Apparatus.**— The materials used for manifold construction, the pump and injection systems have been described in Chapter 3 (3.7). In this Section brief descriptions are given for the manifolds used in the two systems studied. These manifold designs were optimised according to the detection process. Also described is the injection system configuration and the design and fabrication of the wall-jet microflow cell which housed the electrode system.

(i) **Manifold A (PCV System):** In Figure 7.2.2A the FIA manifold used for the PCV studies is depicted.

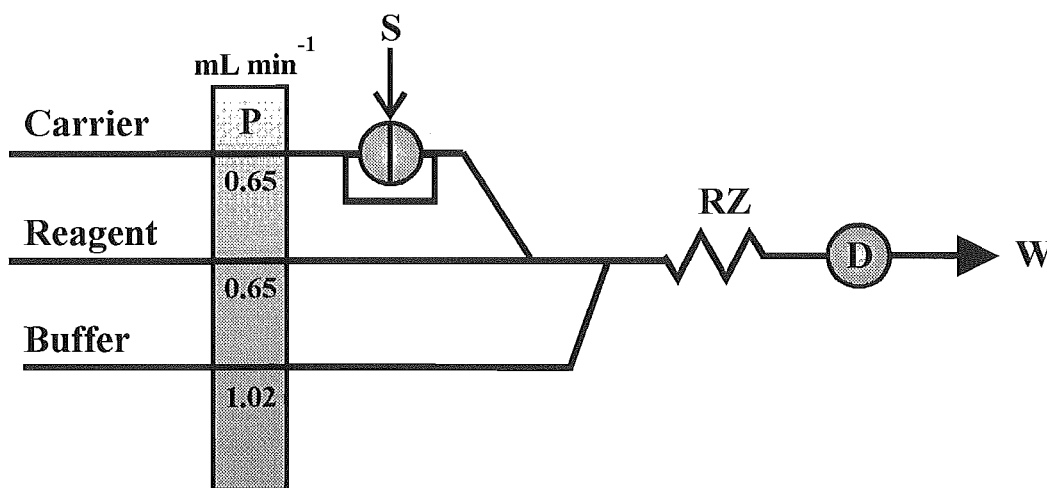


Figure 7.2.2A FIA manifold used for the electrochemical determination of Al with PCV. The chemical components of this system were (i) carrier solution = triple distilled water, (ii) reagent = $20 \mu\text{mol L}^{-1}$ (or $5 \mu\text{mol L}^{-1}$) PCV and (iii) buffer = 0.10 mol L^{-1} MES (pH 6.2; 6.05 - 6.10 at detector). The flow rates of the respective lines are given.

The dispersion coefficient, D [described above (7.2)], was measured for the injected test solution by comparing the peak current for the electroactive ligand when injected (C^{max}) and when pumped through the total manifold (C^0).

(ii) **Manifold B (THQ System):** In Figure 7.2.2B the FIA manifold used for the THQ studies is depicted.

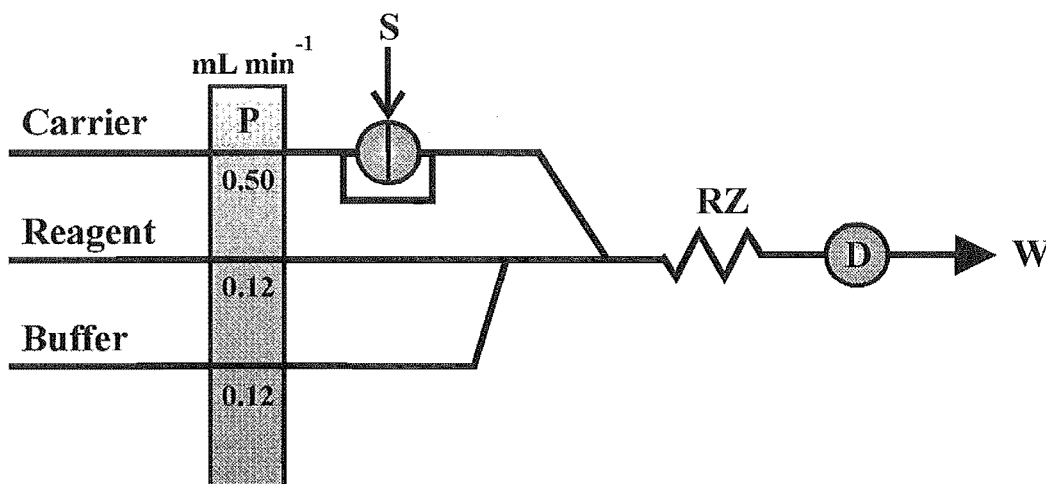


Figure 7.2.2B FIA manifold used for the electrochemical determination of Al with THQ. The chemical components of this system were (i) carrier solution = triple distilled water, (ii) reagent = $200 \mu\text{mol L}^{-1}$ THQ and (iii) buffer = 0.10 mol L^{-1} NaOAc/HOAc buffer (pH 5.10; 5.00 at detector). The flow rates of the respective lines are given.

In each FIA manifold the sample reaction zone was varied by adjusting the size of a reaction coil. Reaction coils consisted of knitted microline tube (0.51 mm i.d.); 25 cm, 50 cm, 100 cm and 200 cm coils were tested. Arrow shaped glass connectors were used at the confluence points of the respective flow lines. These connectors have been reported to achieve high turbulence and maximum dispersion at the confluence point [Karlberg and Pacey, 1989; Chalk and Tyson, 1994].

(iii) **Injection System:** The injection system used in the current studies was a six-port rotary design (Rheodyne). The positions 'LOAD' and 'INJECT' are depicted in Figure 7.2.2C respectively. In the LOAD position, a geometrically defined external volumetric 'sample' loop was filled with the desired test solution. While set in this position the carrier flowed through the valve in a bypass channel. Once the sample loop was filled, the valve position was rapidly turned to the INJECT position. The carrier solution now flowed through the sample loop and the test solution was carried to the detector. In this manner the test solution was 'packaged' between two zones of carrier solution.

During optimisation of the detection procedures, injection loop sizes of 50 μL , 100 μL and 200 μL (microline tubing) were tested.

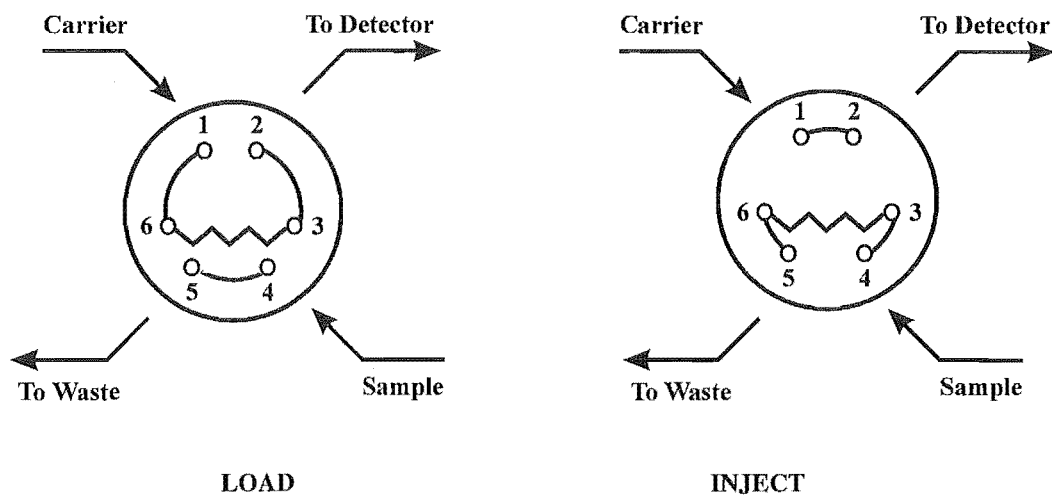
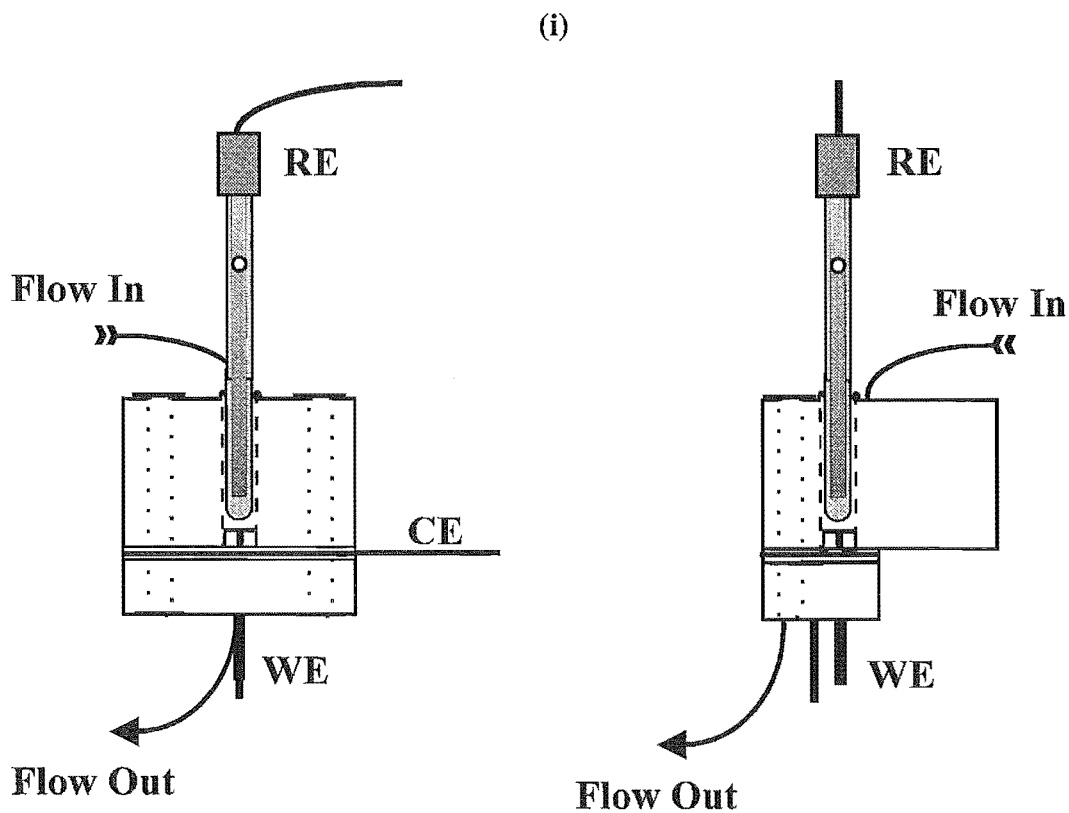


Figure 7.2.2C Six-port injection valve system. Two valve configurations 'LOAD' and 'INJECT' are shown.

(iv) **Wall-jet Microflow Cell:** The design of the wall-jet microflow cell is shown in Figure 7.2.2D. This diagram shows both (i) assembled front and side profiles and (ii) disassembled components.



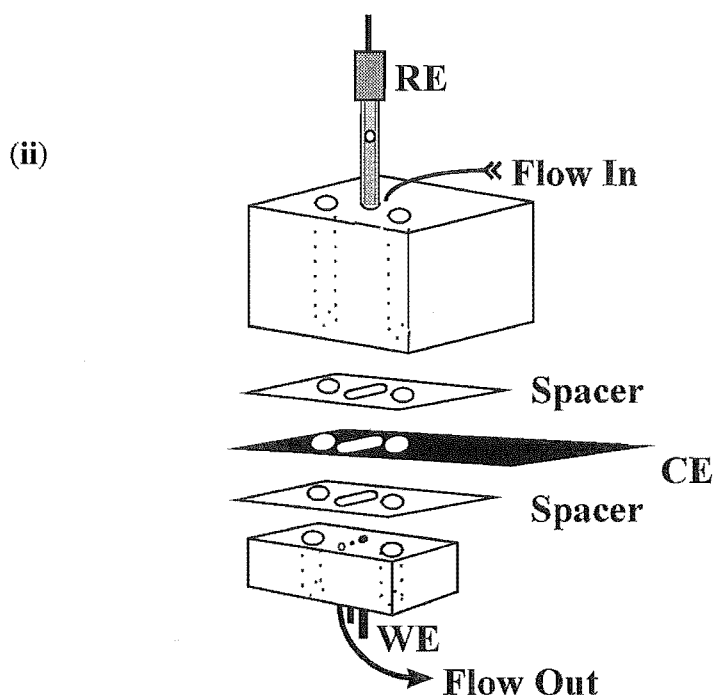


Figure 7.2.2D Diagram of the wall-jet microflow cell. (i) Assembled front and side profiles. (ii) Disassembled components. RE = SCE reference electrode, CE = stainless steel counter electrode, WE = GC working electrode. The blocks (prepared from Dalron) were bolted together *via* the indicated holes (dotted). The spacers were Teflon and the flow 'in' and 'out' tubes were microline. Also shown is a second platinum CE (not used).

The home-made detector was fabricated from two blocks of Dalron (10 x 20 x 32 mm and respectively). Teflon spacers (0.76 mm) were positioned on either side of a stainless steel counter electrode (0.2 mm depth) and the resulting electrochemical cell was *ca.* 50 μL . The three electrodes used were: RE = SCE reference electrode, CE = stainless steel counter electrode and WE = glassy carbon working electrode. The GC working electrode was 0.3 cm diameter and was connected externally *via* a brass rod. The counter electrode was positioned such that it circumferenced the entire cell [A second CE (platinum 0.5 mm diameter) is shown but was not used]. The spacers were Teflon and flow 'in' and 'out' tubes were microline. The entire assembly was interconnected with bolts [via the indicated holes (dotted)].

Prior to use the GC electrode (mounted in the lower block) was hand polished with 1 μm diamond paste. Upon insertion of the SCE care was taken to ensure that the insertion-compartment was completely full of reference electrolyte (excess electrolyte was pushed out through the flow cell). All internal surfaces of the electrode and cell components were washed with acetone (BDH, AnalaR) and dried before assembling. The detection in this system was effected using a laboratory built potentiostat attached to a Graphtec WX 1200 recorder.

7.2.3 RESULTS.

(A) **Pyrocatechol Violet (PCV).**— Before investigating the development of a method for the measurement of Al, the electrochemical response of PCV and the characteristics of the manifold were studied. The dispersion coefficient, D , was measured as 4.0 for the manifold (50 or 100 cm reaction coils). The 'dilution factor' for the system was 2.0 indicating that the real 'dispersion factor' was *ca.* 2.0. Two commercially available PCV materials were tested for purity; Koch-light and Sigma chemicals. Visible absorption spectra (445 nm) of $20 \mu\text{mol L}^{-1}$ PCV solutions (pH 6.2) indicated that the Koch-light material was more pure. Electrochemical comparisons (0.35 V vs. SCE) were made by (i) pumping each PCV solution through and (ii) injecting each PCV solution into the FIA system. These revealed similar results and Koch-light PCV was used for all further experiments.

The preliminary voltammetric studies presented in SECTION A indicated an oxidation peak for PCV at $E_p^a = 0.35 \text{ V}$ (vs. SCE). At this potential it was expected to find a suitable 'voltage window' for the detection of Al (*via* the decrease of the PCV oxidation signal). In the described flow system however, the optimum potential for the measurement of Al (optimum difference in oxidation current in the presence and absence of Al) may be at a slightly different potential, *i.e.* the 'voltage window' will be affected by reaction kinetics and thus manifold design. A hydrodynamic voltammogram (HDV) was measured for a $100 \mu\text{mol L}^{-1}$ PCV solution (Figure 7.2.3A). In this measurement, both the carrier and reagent lines were pumped with carrier solution (triply distilled H_2O); PCV was injected into the system. The buffer line was as shown in Figure 7.2.2A. The HDV for a $20 \mu\text{mol L}^{-1}$ PCV solution is shown in Figure 7.2.3B.

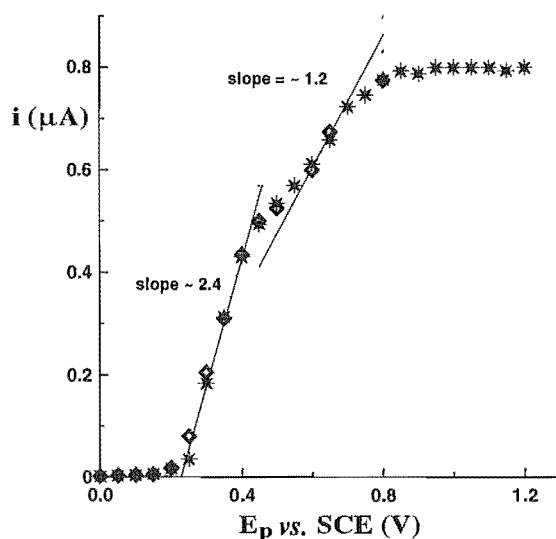


Figure 7.2.3A Hydrodynamic voltammograms for $100 \mu\text{mol L}^{-1}$ PCV solutions. Here ◆ and * denote duplicate experiments (pH 6.2).

From Figure 7.2.3A it was apparent that two oxidation processes occur over the HDV range investigated. These processes may be attributed to the irreversible oxidation of the 1,2-dihydroxyaryl and 2-hydroxy-1-oxocyclohexadiene sites respectively (as described in 7.1.3A).

At $100 \mu\text{mol L}^{-1}$ PCV, fouling of the electrode was apparent, *i.e.* following the recording of the complete HDV, an injection of PCV gave a signal [0.35 V] approximately 85 % of the earlier signal recorded for this potential. For all later experiments $20 \mu\text{mol L}^{-1}$ PCV solutions were used in order to lessen the effects of electrode fouling.

Hydrodynamic Voltammograms of Al-PCV and Fe-PCV Solutions: HDVs were recorded for solutions containing $20 \mu\text{mol L}^{-1}$ PCV and (i) $12 \mu\text{mol L}^{-1}$ Al(III) and (ii) $12 \mu\text{mol L}^{-1}$ Fe(III). These results are presented in Figure 7.2.3B along with the HDV in the absence of the metal ion, (iii). The presence of colloidal matter was observed in Fe-PCV solutions.

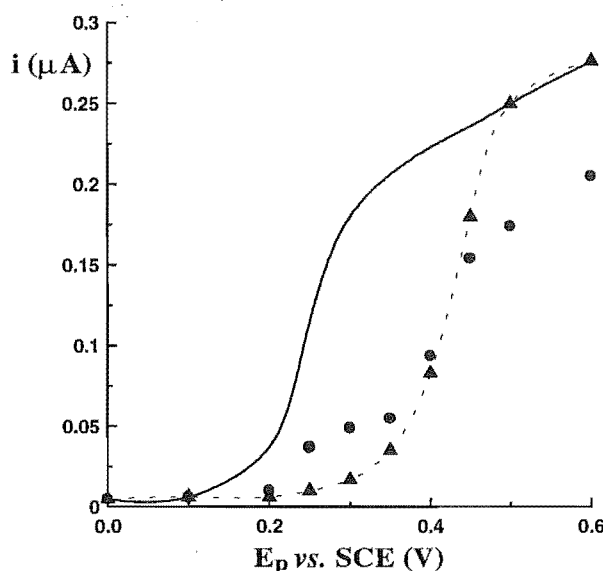


Figure 7.2.3B Hydrodynamic voltammograms for solutions of $20 \mu\text{mol L}^{-1}$ PCV and $12 \mu\text{mol L}^{-1}$ Al(III) [▲], $12 \mu\text{mol L}^{-1}$ Fe(III) [●] and no metals [solid line] (pH 6.2).

The HDV in Figure 7.2.3B indicates that the greatest current change [Δi (μA)] upon addition of Al occurs at 0.325 V (vs. SCE). At potentials greater than 0.5 V the HDV for the Al-PCV solution was very close to the HDV in the absence of Al. The results indicate that Fe(III) may cause significant interference in the use of PCV for the electrochemical analysis of Al.

Linear Working Range and Detection Limit: The linear working range (LWR) and detection limit (DL) for the optimised manifold (Figure 7.1.3A) were determined at 0.325 V by analysis of Al standards over the range 0 - 25 $\mu\text{mol L}^{-1}$ using 5 $\mu\text{mol L}^{-1}$ PCV in the reagent line. The Al standards were prepared in 0.01 $\mu\text{mol L}^{-1}$ HCl.

In the optimised manifold the injection loop was 100 μL and a 100 cm reaction coil was used. For this system a LWR of 0.2 to 10.0 $\mu\text{mol Al L}^{-1}$ was obtained and for 8 successive injections of 1 $\mu\text{mol Al L}^{-1}$ the DL was 0.04 $\mu\text{mol L}^{-1}$ (limit of determination 0.2 $\mu\text{mol L}^{-1}$).

(B) Tetrahydroxy-1,4-quinone (THQ).— THQ solutions were prepared daily from deoxygenated buffer solutions (0.05 M NaOAc/0.05 M NaCl, pH 5.1). Throughout the measurement procedures the THQ reagent solutions were kept continuously under an $\text{N}_2(\text{g})$ atmosphere.

The preliminary voltammetric studies presented in SECTION A indicated an oxidation peak for THQ at *ca.* 0.225 V (vs. SCE). In Figure 7.2.4C HDVs are presented for (i) 50 $\mu\text{mol L}^{-1}$ THQ and (ii) 50 $\mu\text{mol L}^{-1}$ THQ/50 $\mu\text{mol L}^{-1}$ Al solutions.

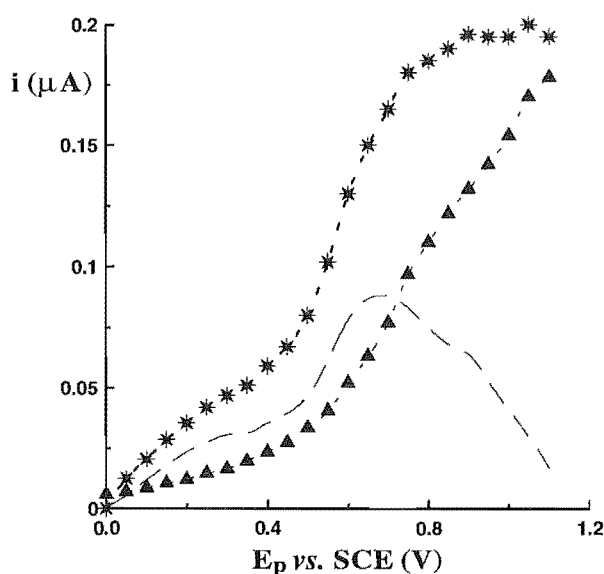


Figure 7.2.3C Hydrodynamic voltammograms for solutions of 50 $\mu\text{mol L}^{-1}$ THQ [*] and 50 $\mu\text{mol L}^{-1}$ THQ/50 $\mu\text{mol L}^{-1}$ Al [▲]. Also shown is a plot of the difference between the two voltammograms, *i.e.* i_p [*(*) - (▲)] (separate dashed line).

From Figure 7.2.3C the greatest current change [Δi (μA)] upon addition of Al occurs at *ca.* 0.7 V (vs. SCE). This potential was quite high and furthermore the slope of

the THQ/Al HDV was 'steep' at this potential. At 0.30 V (vs. SCE) the slope of the two voltammograms was much less and a 'useful' current change (Δi) was observed.

Linear Working Range and Detection Limit: Significant problems were observed for this system in obtaining an acceptable detection signal above that of the background noise. These problems may be, in part, attributed to the quality of the potentiostat. For $200 \mu\text{mol L}^{-1}$ THQ as reagent the LWR for the optimised manifold (Figure 7.1.3B) was determined as 0.5 to $10.0 \mu\text{mol Al L}^{-1}$ (0.30 V). The DL for the optimised manifold was *ca.* $0.5 \mu\text{mol Al L}^{-1}$, however, it was apparent that this may be lowered much further if 'background noise' was reduced.

7.2.4 DISCUSSION.— From Figure 7.2.1A it is clear that PCV complexes Al quantitatively at $\text{pH} > 5.6$. Furthermore it is predicted that the dominant species at $\text{pH} 6.0$ will have the stoichiometry $\text{Al}(\text{PCV})_2$. This second prediction (*i.e.* the stoichiometry) does not, however, match the results observed in the present studies. For $5 \mu\text{mol L}^{-1}$ PCV in the reagent line the LWR extends to $10 \mu\text{mol L}^{-1}$ Al. In this manifold the dispersion coefficient was 4.0, with dilution contributing to half of this value (dilution was the same for both carrier and reagent lines). Thus at the detector the PCV concentration was $2.5 \mu\text{mol L}^{-1}$ and the 'top end' of the LWR corresponded to $2.5 \mu\text{mol L}^{-1}$ Al. This is consistent with the formation of a 1:1 Al-PCV complex. From this it is inferred that the 1:1 complex is formed rapidly, whereas the formation of the 1:2 complex is slow on the FIA timescale. Similar results have been previously observed in investigations of PCV as a spectrophotometric reagent for the kinetic analysis of reactive Al [Hawke and Powell, 1994].

For both the PCV and THQ studies large amounts of background noise were observed at the detector. This noise was particularly troublesome when analyses were made at Al concentrations close to the limit of determination (*i.e.* $\leq 1 \mu\text{mol L}^{-1}$ Al). It may be possible to decrease the DL for these systems by use of better filtering, shielding *etc.*

CHAPTER 8

AN FIA METHOD FOR THE MEASUREMENT OF 'REACTIVE' ALUMINIUM (Al^{3+}) BY 2-s REACTION WITH OXINE-DERIVATISED FRACTOGEL

This Chapter describes the development of an FIA method and speciation protocol for the measurement of reactive aluminium (Al^{3+}) in natural waters and soil solutions. It is divided into 2 parts.

SECTION A: Matrix separation and preconcentration procedures in analytical chemistry are discussed. A review of chelating resins for matrix separation and preconcentration of metals, in particular Fe and Al, is given.

SECTION B: An FIA method for aluminium (Al^{3+}) speciation by 2-s reaction with oxine-derivatised Fractogel is described.

SECTION A: CHELATING RESINS FOR MATRIX SEPARATION AND PRECONCENTRATION OF METALS

8.1 INTRODUCTION

The environmental analysis of trace analytes at the sub-ppm/sub-ppb level is becoming increasingly important. For such analyses, the direct determination of an analyte in the presence of high concentrations of weakly interfering or low concentrations of strongly interfering species is often a significant problem.

Matrix separation and preconcentration techniques may serve to improve many trace analytical procedures. However, in analytical techniques where speciation is important many of the commonly used separation and preconcentration techniques are likely to cause considerable problems. To be applicable to speciation analyses in labile systems, separation procedures should be sufficiently fast so as to prevent significant re-equilibration of analyte species, *i.e.* re-equilibration may result in large changes in the distribution of the analyte. The ideal matrix separation and/or preconcentration procedure for speciation purposes must be one which provides rapid and complete separation of the interfering species immediately before detection of analyte. Flow injection analysis (FIA) is particularly applicable to such procedures.

The most commonly employed techniques for matrix separation and preconcentration of trace metals are solvent extraction, Donnan dialysis, coprecipitation by metal hydroxides, ion-exchange, chelating resins and sorbent extraction onto inorganic

or organic collectors (e.g., SiO₂, activated carbon, C₁₈) [Boniforti *et al.*, 1984; Ruzicka and Arndal, 1989]. The combination of these techniques with FIA has enabled fast and accurate determination of a number of metal ions, which would otherwise only be measurable following long and laborious extraction and preconcentration procedures. The earliest application of on-line flow injection column preconcentration of metal ions was described by Olsen *et al.* (1983) utilising Chelex-100. Since then a large number of FIA matrix separation and/or preconcentration procedures have been developed utilising each of the above techniques [Klinghoffer *et al.*, 1980; Malamas *et al.*, 1984; Sweileh and Cantwell, 1985; Marshall and Mottola, 1985; Cox and McLeod, 1986; Hartenstein *et al.*, 1986; Xie and Christian, 1986]. Procedures have been developed *via* the 'Driscoll's methodology' for fractionation, and thus speciation analysis [as described in Chapter 1 (1.3)], while maintaining all the advantages of a flow system [Canizares *et al.*, 1994].

8.1.1 MATRIX SEPARATION AND PRECONCENTRATION PROCEDURES

Solvent Extraction.— Solvent extraction techniques may be coupled with FIA methods despite the complexity of the separation processes. Much progress has been made in automating liquid-liquid extraction [Backstrom *et al.*, 1986]. However, FIA techniques which utilise solvent extraction often require manifolds with a large array of lines (necessary for segmenting the different solvent zones). Recently FIA solvent extraction has been employed successfully in the determination of 'quick reacting' Al in natural waters [Clarke *et al.*, 1992; Danielsson and Sparén, 1995]. These techniques often utilise organic solvents that are of environmental or toxicological concern.

Ion Exchange Resins.— The use of ion exchange for liquid-solid separations has, for many years, found application in FIA systems. Ion exchange methods are simpler and often less time consuming than solvent extraction procedures. These methods are easily automated and subject to far fewer sources of contamination. Conventional ion exchange resins are formed from cross-linked styrene, divinyl benzene or other functionalised matrices. These materials are widely available and their properties have been well characterised. A drawback of ion exchange resins is that they often exhibit poor selectivity for heavy metals in solutions containing high concentrations of alkali or alkaline earth elements as a result of decreased resin capacity. The high affinity for alkali and alkaline earth elements, may also cause problems during some analysis procedures, *e.g.* matrix problems in AAS. Ion exchange resins commonly require strong mineral acids for adequate elution. Tapparo and Bombi (1990) utilised ion chromatography to preconcentrate Al, followed by post-column spectrophotometric detection using pyrocatechol violet.

Chelating Resins.— These resins offer most of the advantages of ion exchange resins in terms of simplicity and ease of automation of techniques. Chelex-100 resin, containing iminodiacetic acid functional groups, is frequently used in chelating ion-exchange procedures. This material has a lower affinity for alkali or alkaline earth elements than commonly used ion exchange resins. Hyphan cellulose and silica-immobilised 8-hydroxy-quinoline are also frequently used for matrix separation and preconcentration.

Chelating resins which utilise a selective chelating agent covalently bound to a solid support have further advantages over ion exchange resins in that a much higher selectivity for targeted metal ions is possible. However, the limited commercial availability of chelating resins has restricted their use, since preparation in the laboratory is often time consuming and difficult. An interesting feature of these methods is that they exploit the acid-base and metal equilibria properties of the selected ligand (chelating agent) to effect the separation process. The selection of ligand (chelating agent) is therefore of utmost importance if highly selective separation and preconcentration is to be performed. Chelating resins which possess a ligand which forms highly stable complexes with metal ions often require large amounts of acid to elute the metals and even then 100 % elution is sometimes hard to achieve. A disadvantage of chelating resins is that concentrated eluents are often required (e.g. $1-4 \text{ mol L}^{-1} \text{ HCl}$ and/or HNO_3).

Sorbent Extraction.— The technique of sorbent extraction [Ruzicka and Arndal, 1989] combines features of solvent extraction and solid-phase preconcentration. Here, a solid support with hydrophobic functionality is used to preconcentrate a metal complex (e.g. carbamates, 8-quinolates). The robust metal chelates, which are almost indestructible by even strong acids, are readily eluted by a change in solvent polarity. The advantage of this method over the use of chelating resins is that complexes of very high stability may be easily eluted from the column. Elution can often be performed with simple organic solvents like methanol or ethanol. Column packing in FIA techniques has most often utilised silica based C_{18} supports, however several applications have opted for polymeric supports such as Amberlite XAD.

If silica-based solid supports are used in sorbent extraction, then the residual silanol sites on the support provide a second type of site for analytes. These silanol interactions will be disrupted by changes in pH (decreased pH causing release) which is in contrast to C_{18} binding which is disrupted by change in solvent polarity. The silanol groups may retain analyte by complexation, analyte which will not be released in turn by a change in solvent polarity. Typically, metal chelation is performed on-line prior to reaching the solid support at which adsorption occurs (*via* interaction with the hydrophobic C_{18} group). A possible problem with this technique is that because the free chelating agent is likely to be adsorbed with a similar strength to the metal chelate complex, errors will occur once the capacity of the column is reached. Recently,

Lancaster *et al.* (1994) compared sorbent extraction with polymer-based and silica-based C₁₈ supports. The polymer-based support offered significant advantages over the silica-based support (*e.g.* stability to pH, absence of residual silanol groups). The most favourable analyte extraction was accomplished on a polymer-based C₁₈ (hydrophobic) support prepared by pre-adsorption of a suitable chelating agent.

8.1.2 CHELATING RESINS

Metal chelating resins or immobilised chelates (adsorbed or chemically bonded) incorporating ligands with nitrogen, oxygen and sulfur donor atoms on a polymer support have found considerable application in trace metal analysis in recent years. The assortment of ligands that have been immobilised on various substrate backbones is vast. To name a few, this assortment includes alkylamines, diamines and dithiocarbamates [Leyden and Luttrell, 1975; Leyden *et al.*, 1976; Boniforti *et al.*, 1984], hydroxylamines and amides [Vernon and Eccles, 1975; Orf and Fritz, 1978], diaminetetra- and iminodiacetates [Moyers and Fritz, 1977; Pesavento *et al.*, 1993], thioglycolates, dithizone, cysteine [Lorber *et al.*, 1975; Moyers and Fritz, 1976; Elmahadi and Greenway, 1993], amidoxime and dimethylglyoxime [Lee and Halman, 1976; Collela *et al.*, 1980*a,b*], 1,10-phenanthroline, 2,2'-bipyridine and ferrozine [Lungren and Schilt, 1977; King *et al.*, 1991], desferrioxamine and 8-hydroxyquinoline [Jezorek and Freiser, 1979; Marshall and Mottola, 1985; Ljunggren *et al.*, 1992; Resing and Measures, 1994], chelamine and chromotrope [Pesavento *et al.*, 1989; Blain *et al.*, 1993], and the metallochromic dyes pyrocatechol violet and chrome azurol S [Jones and Schwelt, 1989; Quintela, 1993; Hirayama *et al.*, 1994].

These resins are generally of two types: (i) resins utilising a chelating agent that targets a range of metal ions, *e.g.* Hackett and Siggia (1977) introduced a polydithiocarbamate resin (PDTC) which has found widespread application for the determination of over 52 elements [Barnes, 1984], and (ii) chelating resins which incorporate a moiety aimed at targeting just one or a few selected metal ions, *e.g.* 1-nitroso-2-naphthol for uptake of Co(II) and Fe(III) [Gennaro *et al.*, 1986]. Chelating resins that aim to exploit the selective complexing ability of a ligand towards a metal ion usually contain ligands with functional groups having a high affinity for the targeted metal. An ideal ligand for selective preconcentration purposes will have a high capacity for the metal analyte, is unaffected by other analyte constituents (*e.g.* alkali and alkaline earth elements) and does not require strict working conditions (*e.g.* pH control). The use of chelating resins is either by *in situ* modification of a solid support or pre-analysis fabrication of a designer resin. The loading of a chelating reagent onto a support matrix is either by formation of a covalent bond between the reagent and the matrix or by an ion-exchange or π - π interaction.

The resins reviewed in this Section are primarily those dealing with the matrix separation and/or preconcentration of Al and Fe. Particular attention is given to dithiocarbamate and 8-hydroxyquinoline resins. The former of these may be expected to complex Fe but not Al, whereas the latter will complex both Fe and Al strongly. In this section Al and Fe refer to the trivalent ions [Al(III) and Fe(III)] and all other ions are divalent unless otherwise specified [*i.e.* Cu \equiv Cu(II), Zn \equiv Zn(II), ... and Fe(II), Cr(IV), Ag(I), ... are self explicit].

(A) Al Targeting Chelating Resins

(i) **8-hydroxyquinoline Resins:** Landing *et al.* (1986) synthesised an 8-hydroxyquinoline (oxine, 8HQ) resin by immobilisation of oxine on a vinyl polymer. The polymer resin used, Fractogel TSK gel, consisted of intertwined polymer agglomerates exhibiting a hydrophilic character. This polymer gel is highly porous and offers high mechanical and chemical stability. Furthermore, it exhibits no cation exchange capacity and does not adsorb dissolved organic species, *e.g.* humic substances. The ability of the derivatised resin to complex the metals Al, Mn, Fe, Co, Cu, Zn and Cd from organic rich freshwater was demonstrated.

8-hydroxyquinoline immobilised on controlled pore glass (8HQ-CPG) has been used frequently for the preconcentration of metals such as Cd, Co, Cu, Fe, Mn and Ni from natural water and seawater. Mohammad *et al.* (1992) utilised 8HQ-CPG for the on-line column preconcentration of Al from river and sea water (AAS detection). A series of buffers were tested including acetate, malonate, oxalate and citrate; malonate was found to provide the greatest preconcentration efficiency. Collection of Al was effected at pH 10 in a 0.1 mol L⁻¹ malonate buffer and elution was effected using a mixture of 1 mol L⁻¹ HCl/1 mol L⁻¹ HNO₃. The DL was 3 µg Al L⁻¹ and the calibration graph was linear up to 400 µg L⁻¹.

Resing and Measures (1994) utilised the oxine gel developed by Landing *et al.* for the development of an FIA fluorimetric (lumogallion) method for the determination of Al in sea water. This method incorporated an on-line packed oxine-gel column for the preconcentration of Al; the subsequently eluted (0.05 mol L⁻¹ HCl) Al was detected following the formation of the fluorescent lumogallion complex. Maximum uptake of Al by the oxine-gel occurred between pH 5.5 and 5.7. Five interferents, previously reported for lumogallion-Al chemistry, including Cu and Fe were tested. The absence of significant interference from these metals was attributed to their poor retention and/or release (by the resin) achieved through the optimisation of preconcentration conditions. Obata *et al.* (1993) and Measures *et al.* (1995) used this oxine-immobilised TSK-gel for the sorption and subsequent measurement of Fe in seawater. Both methods utilised FIA-type techniques.

Fairman and Sanz-Medel (1993) developed an FIA Al speciation method based on the 'Driscoll protocol' [see Chapter 1 (1.3)] which incorporated a column for the adsorption of 8-hydroxyquinoline-5-sulphonic acid (8-HQS) reactive Al following a short reaction time. In this method an Amberlite IR-120 cation exchange resin was incorporated in the FIA manifold. The *total monomeric* Al was measured by the fluorescent reaction of 8-HQS with Al in a sample that bypassed the column. The *non-labile monomeric* Al was determined as the Al which passed through the column. Hence the *labile monomeric* Al fraction (*i.e.* the oxine-complexed-Al adsorbed by the column) was calculated as the difference between these two fractions. An increased sensitivity was gained by the use of 8-HQS in a micellar media (CTAB). Furthermore, interference from Zn (which had been observed to interfere severely in an earlier fluorimetric method developed using 8-HQS [García Alonso *et al.*, 1989]) was overcome by post-column reaction with 1,10-phenanthroline. The method was compared with the conventional Driscoll batch method [Seip *et al.*, 1984; Sullivan *et al.*, 1986] and was found to be in good agreement.

An FIA method for the measurement of 'fast reactive' Al in natural waters based on the 3 s reaction of Al with oxine (pH 5.0) followed by the sorbent extraction of this complex onto Amberlite XAD-2 mini columns was developed by Fairman *et al.* (1995). The retained Al was eluted with 1.0 mol L^{-1} HCl and subsequently detected with ICP-MS. Applicability of this technique to field use was demonstrated, whereby 'capture' of the fast reactive Al may be performed in the field (thus avoiding sample storage) and subsequent elution and analysis could be undertaken once back in the laboratory.

Recently Yuan and Shuttler (1995) compared (i) oxine immobilised on controlled pore glass (CPG-8HQ) and (ii) adsorption of the Al-8HQ complex on Amberlite XAD-2 resin, for the FIA column preconcentration of Al prior to elution and subsequent detection by ET-AAS. The optimum pH for both systems was found to be 9.3 (at pH > 10 precipitation of Ca and Mg hydroxides occurred in the columns). A change in solvent polarity was used for elution in the XAD-2 system (methanol), whereas for the CPG-8HQ system 10 % (v/v) HNO₃ was used. Both systems were found to exhibit suitable preconcentration. However, the chelating kinetics of CPG-8HQ were not as favourable as the adsorption kinetics of the XAD-2 system. The CPG-8HQ system was also more sensitive to changes in flow-rate. The DL (dependent on preconcentration time) was *ca.* 25 ng L^{-1} .

(ii) **Chromotrope Resins:** Chromotrope-based resins have been used in several investigations for the selective preconcentration of Al from waters and dialysis fluids. Hernández Torres *et al.* (1992) immobilised Chromotrope-2R (disodium salt of 2-phenylazo-1,8-dihydroxynaphthalene-3,6-disulfonic acid, CTR) on Amberlite IRA-400 resin and studied the retention of Al and (a selection of) other metal ions as a function of

pH. Retention under static conditions, *i.e.* batch experiments at pH 4, indicated that Al would be retained by the resin while Fe would not. Their analysis involved an AAS detection system so Fe interference was not problematic.

Pesavento *et al.* (1989) utilised Chromotrope-2B (the acid of Chromotrope-2R) immobilised on an anionic AG1-X8 exchanger. A column preconcentration procedure at pH 6.0 allowed the complete separation of Al from Pb, Zn, Ni, Cd, Ca and Mg. Cu was completely retained whereas Fe was only partially. A similar investigation by Fernández *et al.* (1991) utilised Chromotrope-2B immobilised on the same resin to matrix separate and preconcentrate Al in a chelating microcolumn followed by spectrofluorimetric determination of the complex Al-5,7-dibromo-8-quinolate (extracted into ether). Optimum pH was 5.5 and the elements Cu and Fe were also partially retained by the resin.

(iii) Metallochromic Dyes: In an FIA procedure for speciation of Al in river and tap waters, Quintela (1993) reported the use of pyrocatechol violet (PCV) immobilised on Amberlite IR-120. Fe was found to interfere at the same concentration level as Al. The use of Fe masking agents (*e.g.* 1,10-phenanthroline plus hydroxylammonium chloride) suppressed most interference and a Driscoll-type fractionation procedure was able to be performed. Sarzanini *et al.* (1987) investigated two procedures for uptake of anionic Al-PCV complexes on an anionic exchanger (Bio-Rad AG MP-1 macroporous anion-exchange resin). The first procedure involved pre-formation of Al-PCV complexes followed by pumping through a column containing the exchanger. The second involved loading the resin with PCV and subsequent injection of the sample. The first procedure was deemed to be superior; this may be a result of the slow equilibria between PCV and Al.

Several chromatographic techniques have been developed for speciation of Al in waters [Jones, 1991]. Jones and Schwelt (1989) investigated a number of ion-exchange and chelating exchange coatings for separation of metal ions. Bromophenol blue was found to be the better of the ion-exchangers. The most favourable characteristics were, however, exhibited by chelating exchange materials. The best of these chelators was chrome azurol S (CAS).

Several investigators have studied CAS as a preconcentration agent for Al. Hirayama *et al.* (1994) immobilised CAS on a propylisothiuronium functionalised silica gel (further coated with PTFE resin to obtain greater stability). Al was retained quantitatively above pH 5. Hernández *et al.* (1986) utilised CAS immobilised on a resin for preconcentration of Al from dialysis fluids prior to flame AAS detection. The optimum pH was 8.0 and measurement could be made of Al concentrations lower than $10 \mu\text{g L}^{-1}$.

(iv) Other Resins: Das and Pobi (1991) synthesised a polystyrene-divinylbenzene based resin containing *N*-benzoylphenylhydroxylamine for separation of Be and Al from other

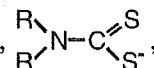
elements. However, Fe binds to this resin at the same pH at which Al complexation occurs, which is likely to cause problems in Al analyses. The target analytes were eluted from the resin using suitable agents (EDTA for Al). To separate eluted Al from Fe a second column was used and at pH 2.5 Fe could be effectively masked with fluoride. The determination of Al in dialysis fluids was investigated by Barnes and Shang-Jing (1983). This procedure involved a pH-dependent uptake of Al on a poly(acrylamidoxime) resin and ICP-AES detection. Both Al and Fe were taken up by the resin; thus it was not ideal for the separate preconcentration of either Fe or Al.

Desferrioxamine was used by Ljunggren *et al.* (1992) for preconcentration of Al *via* immobilisation on a modified porous glass followed by GFAAS detection. Quantitative uptake of Al was restricted to the pH range 5.5 - 6.0. Unfortunately Fe was also complexed strongly, causing interference unless elution conditions were well controlled.

The chelating properties of salicylideneamino-2-thiophenol derivatised glass beads towards Al was investigated by Kobayashi and Miyazaki (1993). A method for FIA column preconcentration of Al at pH 5.5 was developed and interfering ions investigated. Of the ions tested for interference, Fe was the most significant. This problem was overcome by use of the reducing agent hydroxylamine. Vilchez *et al.* (1993) examined the fluorescence of the Al-salicylidene-*o*-aminophenol complex for solid-phase spectrofluorimetric determination of Al in natural waters. The complex was adsorbed on a dextran-type cation-exchange gel (Sephadex CM C-25) and determinations were made by batch procedure (optimum pH was 5.5 - 6). No interference was observed from Fe at a 10,000-fold excess.

Pereiro García *et al.* (1987) investigated the use of a mini-column of Amberlite IRA-400 for the FIA preconcentration of Al in dialysis fluids (AAS and ICP-AES detection). Both the pH and nature of the buffer were found to greatly influence preconcentration efficiency. Maximum retention was obtained at pH 7 for all buffers tested and the greatest retention was observed for the more 'bulky' buffers MES and PIPES. NaOH, HCl and HNO₃ were tested as eluents and 75 µL of 1 mol L⁻¹ NaOH was found to be the most effective. The biologically relevant metals Zn, Cu and Cr(IV) were not observed to interfere in Al determinations. It was verified that Fe was retained by the mini-column but not released by the eluent (1 mol L⁻¹ NaOH); Fe was only eluted with > 2.5 mol L⁻¹ HCl. In a later series of experiments Pereiro García *et al.* (1990) investigated the cation and anion exchangers (Dowex 50W-X2 and Amberlite IRA-400) and chelating resins Chelex 100 and another synthetic version (Kelex 100 adsorbed on Amberlite XAD-7) for this same purpose. Amberlite IRA-400 and Chelex 100 were found to be the most suitable resins, however acetate may interfere in the use of the Amberlite resin. For Chelex 100 a DL of 3 ng Al L⁻¹ and a LWR of 0.015 - 5.0 µg Al L⁻¹ were achievable.

(B) **Dithiocarbamate Resins.**— Early studies by Dingman *et al.* (1974) and further development by Hackett and Siggia (1977) indicated that polydithiocarbamate resins have a strong affinity for a large number of trace metals in natural waters. Dithiocarbamates {*e.g.* diethyl- (DCC), pyrrolidine- (APDC), diethylammonium diethyl- (DDTC), hexamethylene- (HMDC), dibenzyl-dithiocarbamate (DBDC) [Irth *et al.*, 1987; McLeod *et al.*, 1981; Fardy *et al.*, 1984; Smith *et al.*, 1984]} have increasingly been used for matrix separation and preconcentration purposes. The conjugate bases of these acids,



behave as bidentate univalent anionic ligands (complexing *via* the dithiol- moiety) and like most ligands with sulfur and nitrogen donors form metal complexes of low (aqueous) solubility. The order of decreasing DCC complex stabilities is: Hg, Pd, Ag(I), Cu, Tl(III), Ni, Bi(III), Pb, Cd, Tl(I), Zn, In(III), Sb(III), Fe, Te(IV), Mn [Ruzicka and Arndal, 1989].

The resin PDTC synthesised by Hackett and Siggia (1977) has been shown to have no affinity for alkali and alkaline earth elements. This derivatised resin was first prepared by reacting polyethylenimine (molecular weight 1800) with polymethylene-polyphenylene isocyanate to form a cross-linked polyamine-polyurea resin. This polymer has been used to prepare a polydithiocarbamate resin which has been subject of number of investigations. Since then many similarly derivatised resins have been synthesised from different support materials [Barnes and Genna, 1979; Barnes, 1984; Wang and Barnes, 1989; Yebra-Biurrun *et al.*, 1992b]. PDTC resins are non-reversible chelating resins (requiring acid digestion for metal recovery) and are only ideal for analyses in which elution of the targeted metal ion is not a prerequisite. A unique feature of polydithiocarbamate resins is their selective chelating ability for different oxidation states of some metal ions, *e.g.* Fe and Cr [Miyazaki and Barnes, 1981]. Fe(III) and Cr(VI) complex with the resin, whereas Fe(II) and Cr(III) do not.

Burba and Willmer (1987) studied the adsorption of dithiocarbamate-metal complexes on cellulose collectors. At $\text{pH} \leq 4$, the acid concentration only slightly influenced the distribution coefficients (K_d) of the HMDC-metal chelates, whereas K_d values were independent of pH between 5 - 10. Quantitative preconcentration (sorbent extraction) was obtained for reaction times of 15 - 30 min with HMDC. High reproducibility was obtained for all cellulose-HMDC determinations. The system was tested for the determination of trace elements in a high purity Al sample and gave results (after 30 min contact time): 96 % recovery of both Cu and Fe. Barnes *et al.* (1983) used a polydithiocarbamate resin to preconcentrate Fe(II) and Fe(III) from urine at pH 4. Difficulties were found in recovering all Fe(III) from undigested urine.

Amberlite XAD resins exhibit properties of porosity, high surface area, durability and purity. Dithiocarbamates adsorb easily on XAD-4, *e.g.* APDC [Elci *et al.*, 1992]. Yebra-Biurrun *et al.* (1992a,b) synthesised poly(aminophosphonic acid) and poly(dithio-

carbamate) resins from macroreticular Amberlite XAD-4 supports. These resins had considerable advantages over earlier resins because of their larger surface area and resistance to osmotic shock (*e.g.* swelling). A water soluble carbamate, bis(2-hydroxyethyl)dithiocarbamate (NaHEDC), was synthesised by King and Fritz (1985) and used to preconcentrate metals by sorbent extraction with XAD-4. This material formed complexes which were more easily eluted from columns without using large quantities of solvent. The breakthrough capacities for the Cu/HEDC complex on XAD resins, XAD-1, -2, -4, -7 and -8, were investigated. XAD-4 provided the greatest capacity for adsorption and subsequent studies indicated an optimum pH of 6 - 7 for multi-element analysis. 100 % recovery of Fe was obtained for pH 5 - 8.

C₁₈ reverse phase material, a bonded silica with octadecyl functional groups, has been utilised in sorbent extraction techniques with on-line formation of metal dithiocarbamate (NaDDTC) complexes [Sperling *et al.*, 1992]. The method was automated using a 15 μ L conically shaped micro column containing C₁₈ support material; detection limits for Cd, Co, Cu, Pb and Ni were less than 40 ng L⁻¹. Sample loading times of 60 s resulted in a 20-fold preconcentration factor. Lancaster *et al.* (1994) investigated *in situ* modified and pre-analysis adsorption of NaDDC on silica- and polymeric-based C₁₈ supports. The polymeric-based supports were found to offer significant advantages over silica-based supports [see Section (E) 'solid supports'].

Bradford and Bakhtar (1991) used APDC in a chelation-solvent extraction technique for 22 elements including Fe and Cu. The procedure, involving the extraction of APDC metal complexes into chloroform and determination by ICP-OES, provided simple and rapid analyses in the presence of many common alkali and alkaline earth elements. Extraction was effected at pH 5.0 for a total reaction/extraction time of 31 min (25 min reaction with APDC/6 min extraction into chloroform). Recoveries of both Fe and Cu were 100 % (conc. HNO₃). Efficiency of extraction decreased for pH > 6 and pH < 4.

Hsieh and Liu (1993) synthesised several alkylene bisdithiocarbamates which were excellent chelating agents for Fe and Cu. Reaction times of 5 min were required to obtain > 98 % recovery after extraction into IBMK at pH 5.0 - 5.5. A chromatographic method for Fe analysis was developed by Smith and Yankey (1982) utilising diethyldithiocarbamate. A carboxymethylate polyethylenimine polymethylene-polyphenylene isocyanate (CPPI) chelating resin was synthesised by Horváth and Barnes (1986). The resin exhibited retention ability for a large number of metal ions including Al and Fe.

Recently Emteborg *et al.* (1995) developed a solid phase extraction procedure using a dithiocarbamate resin for the determination of Hg species in humic-rich natural waters. The resin was derivatised (using ammonium dithiocarbamate) from a macroporous glycidyl methacrylate material (Spheron E 300).

(C) **8-hydroxyquinoline Chelating Resins.**— The ligand 8-hydroxyquinoline (oxine, 8HQ) has featured in a large number of trace metal matrix separation/preconcentration procedures utilising functionalised resins [Beauchemin and Berman, 1989; Jezorek and Freiser, 1979; Resing and Mottl, 1992; Malamas *et al.*, 1984; Mooney *et al.*, 1987; Porta *et al.*, 1992; Sturgeon *et al.*, 1981; Yuan and Shuttler, 1995]. The chelating properties of oxine and its preference for more highly charged metal ions over alkali and alkaline earth elements are well known. Oxine forms complexes with over 60 metal ions from aqueous solutions with cumulative formation constants (β) ranging from *ca.* 10^4 for Ba to 10^{38} for Fe. Oxine has been immobilised on a variety of different support materials including silica-based and polystyrene-divinylbenzene materials.

Jezorek and Freiser (1979) immobilised oxine on Porasil silica for use in chromatography. Using isocratic and/or continuous gradient elution, the material was found useful for separating the similar metals Co-Ni, Cd-Pd-Zn and La-Gd-Yb at trace levels. Using the same material, Sturgeon *et al.* (1981) investigated the batch preconcentration of trace metals from seawater prior to ET-AAS detection. Large enrichment factors and quantitative recovery were obtained for the elements Cd, Pb, Zn, Cu, Fe, Mn, Ni and Co.

Malamas *et al.* (1984) investigated the use of oxine immobilised on controlled-pore glass (CPG-8HQ) for the FIA on-line enrichment and matrix isolation of trace metals. The porous glass does not swell or shrink upon pH changes and thus offers advantages over other polymer-based ion exchangers. The metals Cu, Co, Cd, Ni, Pb and Zn were recovered quantitatively at pH 6.5 *via* elution with $1 \text{ mol L}^{-1} \text{ HCl}/0.1 \text{ mol L}^{-1} \text{ HNO}_3$. Ca and Mg, even when present in great excess, were not found to interfere. However, Fe and Al bound to the material strongly and may interfere when present in high concentrations if the exchange capacity of the FIA column is not sufficient. Marshall and Mottola (1985) further investigated the performance of silica-immobilised oxine under FIA conditions. The studies, which critically investigated the preconcentration and measurement of Cu, highlighted the promise of this oxine-based material for FIA preconcentration purposes. Nakashima *et al.* (1988) improved the methods of Malamas *et al.* and Marshall and Mottola for the preconcentration of Cd, Pb, Zn, Cu, Fe, Mn, Ni and Co from seawater. The previous methods were unable to achieve adequate detection limits for the determination of these metals in uncontaminated seawater. Elution was effected using much smaller volumes ($< 2 \text{ mL}$) of $2 \text{ mol L}^{-1} \text{ HCl}/0.1 \text{ mol L}^{-1} \text{ HNO}_3$ and allowed detection limits from 0.2 (Co) to 42 (Fe) ng L^{-1} to be reached.

Several investigations have shown CPG-8HQ to be useful for the kinetic measurement of free metal concentrations, M^{n+} , in the presence of kinetically labile complexes [Chow and Cantwell, 1988]. A disadvantage of CPG-8HQ is that it is unstable at high pH and can be prepared with only relatively low metal-complexing capacities. Persaud and Cantwell (1990) investigated the performance of Amberlite XAD-2 as a

polymer substrate for immobilising oxine. In these studies oxine was coupled to the XAD-2 surface *via* a methylene linkage rather than *via* the azo linkage commonly employed [Vernon and Eccles, 1973]. The Mg^{2+} ion was investigated in these studies and the XAD-oxine technique was found to be selective for Mg^{2+} in the presence of hydrophilic complexes but not in the presence of hydrophobic complexes (*e.g.* Mg-picolinate). These studies emphasised that ligands immobilised on hydrophilic substrates (*e.g.* CPG, hydroxyethyl methacrylate) should be more generally useful than those immobilised on hydrophobic substances.

Abollino *et al.* (1990) compared the sorption of 8HQ and 8HQ-5-sulfonic acid (8HQS) on the polymer substrates XAD-2 and Bio-Rad AG MP-1 and their use for uptake and enrichment of trace metal ions. The latter of these substrates coupled with 8-HQS appeared the most promising for metal recovery and enrichment.

As discussed above ['Al targeting chelating resins'] Landing *et al.* (1986) prepared an oxine based resin by immobilisation on an hydrophilic polymer substrate, Fractogel-TSK. The resin was used in the development of a column technique for concentration and, in part, speciation measurements for Al, Mn, Fe, Co, Cu, Zn and Cd in an organic-rich freshwater. This material has been used in a number of subsequent investigations of Al and Fe.

A 'paper chromatography' method for the determination of Fe(II) and Fe(III) ions was developed by Sundd *et al.* (1994) whereby selective separation of the target analyte was performed followed by DP-ASV detection. The ion-exchange approach utilised the chelating agent 7-iodo-8HQS immobilised as counterions on a piperazinium polyelectrolyte matrix. Al was not studied as an interferent since detection was *via* free-metal electrochemistry; Al is not easily oxidised or reduced. However, Al would interact with the paper and possibly cause interference at high concentrations, *i.e.* capacity problems.

(D) Other Chelators and Chelating Resins.— Colella *et al.* (1980a,b) investigated the use of a polyacrylamidoxime chelating resin for the determination of a large range of metal ions. The resin was prepared by reacting divinylbenzene (DVB) cross-linked polyacrylonitrile with hydroxylamine. Initial studies showed Fe was taken up easily at pH 2.5. The resin was applied to the determination of trace metals in natural waters and in particular to the separation and simultaneous concentration of Fe, Cu, Cd, Pb and Zn. A batch technique was used (pH 6.0, 24 h equilibration time); Fe recovery was dependent on concentration, indicating that uptake was not complete.

The chelating resin Chelamine can be easily produced by immobilisation of a pentamine ligand on an organic polymer. Blain *et al.* (1993) used this chelating resin to target transition metals and determine Cu, Mn, Ni, Pb and Zn in natural waters. Groschner and Appriou (1994) further applied this resin to differentiate between neutral

hydrophobic organic-metal complexes, anionic complexes and the 'free ion' concentration of transition metals in natural waters. Their method utilised a three-column procedure with the combination of C₁₈ reverse phase, a Dowex anion-exchange resin and the Chelamine chelating resin. The strong anion-exchange properties of the Dowex 1-X8 resin were shown to be ideal for retention of anionic complexes. However, at high saline concentrations Cl⁻ ions compete with the dissolved anionic complexes.

Singh and Dhingra (1992) investigated the application of two sulfonephthalein dyes bound to Dowex-2 for preconcentration of Cu and Cd. Pyrocatechol violet and xylenol orange were immobilised on the polystyrene-based anion-exchange resin *via* their sulfonate groups and π - π interactions. The adsorption of other competing metal ions was not studied. In previous studies Singh and Rita (1991) had prepared a pyrocatechol violet-loaded resin using Amberlyst A-26 as a support material. A highly stable chelating resin involving alizarin red-S covalently linked with Amberlite XAD-2 was synthesised by Saxena *et al.* (1994). The resin was used to preconcentrate Zn, Cd, Ni and Pb for subsequent AAS determination.

Hase and Yoshimura (1992) investigated the advantages of solid-phase adsorptiometry combined with an FIA system for the determination of trace Fe in highly purified water. The procedure utilised a highly structured FIA system which incorporated purification columns for both reagent and carrier, a preconcentration column and three rotary injection valves for injection of reagent, sample and 'desorbing' solution. The reagent used to complex Fe was 4,7-diphenyl-1,10-phenanthroline disulfonic acid (DPPS) and detection was effected by monitoring this complex adsorbed to the anion exchanger (QAE-Sephadex A-25) at 550 nm.

King *et al.* (1991) investigated the determination of Fe(II) in seawater by complexation with ferrozine adsorbed on a C₁₈ resin. Ferrozine forms a stable coloured complex with Fe(II) but not Fe(III) and the only significantly interfering ion, Cu(I), was removed by complexation with neocuproine.

A thioglycolate modified resin was synthesised by Howard and Danilona-Mirzaians (1989) for the preconcentration of Cd, Zn, Pb and Ni from natural waters. The resin exhibited the strongest affinity for Cd and Pb and these metals could be recovered from seawater.

The ligand 1-nitroso-2-naphthol has been investigated for the retention of a selection of metal ions including Al and Fe. Gennaro *et al.* (1986) found the resin to have a high binding strength for Co, Cu and Hg, however only 5 % of Al was retained under the conditions used. Van den Berg *et al.* (1991) found that sensitive trace analysis of Fe in seawater could be performed following adsorptive deposition of the Fe - 1-nitroso-2-naphthol complex on a mercury drop electrode followed by cathodic stripping voltammetry.

(E) Solid Supports

If chelating resins are to be incorporated in FIA systems it is also important to consider the properties of the solid support on which the chelator is immobilised and parameters relating to the physical separation process itself. The choice of support is often initially made after considering the conditions under which complexation or adsorption occurs. Typically two classes of supports are utilised for the chelation or complexation of analyte (i) supports which respond to changes in solvent polarity and (ii) supports which respond to changes in pH. Many supports respond to both of these processes and selective retention of the chelating agent on the support is achieved by manipulating just one of these properties while the other maintains constant. The more important properties of solid supports include:

- (i) a low degree of swelling and shrinking with change of solvent or pH,
- (ii) high mechanical resistance, *e.g.* unaffected by flow rates,
- (iii) sorbent particles should preferably be of larger size and regular shape,
- (iv) sorbent materials should have favourable kinetic properties regarding the penetration, retention and elution of analyte, and
- (v) sorbent materials should have no affinity for non-targeted free metal ions, *e.g.* alkali or alkaline earth elements.

The polystyrene-divinylbenzene copolymer has been extensively utilised as support for chelating resin polymers. This polymer is readily available and sufficiently durable for many derivatisations. An unfortunate feature of many resins is that their solid support structure undergoes changes, *e.g.* swelling, on contact with different solvent phases or with change in pH. For example, Chelex-100, which has a polystyrene backbone, shrinks as its ionic form and pH change. Any disruption to the resin packing in an FIA column will affect the solution flow rate and the rate of ion-exchange. This is a common feature of most adsorbents synthesised from microreticular resins (styrene-divinylbenzene skeleton).

Yebra-Biurrun *et al.* (1992) reported the synthesis of a selective ion exchange resin with a macroreticular skeleton (Amberlite XAD-4 support) utilising aminophosphonic acid groups for retention and determination of 9 metal ions. These macroreticular support materials exhibit larger inner surface areas and are more resistant to osmotic shock, swelling effects caused by changes in solvent and loss of volume on drying. In addition to these features the resin described above exhibits a low affinity for alkali metals.

Cellulose (short fibre native cellulose weakly cross-linked with formaldehyde) and cellulose derivatised (*e.g.* acetylated cellulose) supports were studied as collectors for

dithiocarbamate metal complexes in sorbent extraction [Burba and Willmer, 1987]. These studies indicated that the K_d values of dithiocarbamates on cellulose sorbents are higher by a factor of 5 to 10 than those on conventional sorbents (*e.g.* C₁₈). Cellulose sorbents appear to be better collectors of hydrophobic organic metal chelates.

The use of C₁₈-based (octadecyl bonded silica gel or polymeric) polymer sorbents is becoming increasingly popular. These materials utilise sorption of metal complexes from aqueous sample streams followed by elution with a suitable solvent, *e.g.* methanol or ethanol. An important feature of all support materials is that they exhibit properties which are particularly selective for the desired chelating agent. Polymeric-based C₁₈ supports have been shown to exhibit greater stability than silica-based C₁₈ supports in solutions of extreme pH values. In addition to this feature, polymeric-based C₁₈ supports lack residual active silanol sites which may adsorb unwanted materials. These polymeric-based C₁₈ supports do not exhibit swelling effects observed with ion exchange supports, chelating resins and silica-based supports.

Inorganic supports with immobilised organic residues behave differently from organic chelating resins or organic supports for adsorbed species. The most commonly employed inorganic support materials are silica gels; these materials can also be functionalised with chelating agents. A substantive review has been written on the use of silica gels (*e.g.* controlled-pore glass and Porasil) and related materials for immobilisation of chelating agents and their application to the adsorption of inorganic species [Biernat *et al.*, 1994].

Solid supports with 'better' properties are continually being developed and many organic- and inorganic-based supports now offer high porosity and high mechanical and chemical stability.

SECTION B: AN FIA METHOD FOR THE MEASUREMENT OF 'REACTIVE' ALUMINIUM (Al^{3+}) BY 2-S REACTION WITH OXINE-DERIVATISED FRACTOGEL

8.2 INTRODUCTION

This SECTION of work addresses the subject of on-line matrix separation and/or preconcentration for flow-through detection systems. The metal ion for analysis is Al and the most important interfering species is Fe. An FIA system incorporating a micro-column packed with a suitable sorbent material is proposed as the best method for this analysis.

In FIA on-line column procedures, when an analyte is introduced to the flow system the operator is interested in (i) the complete (or reproducible) and selective 'capture' of the analyte species with the rejection of the interfering matrix to waste, followed by, the complete release of the analyte species to the detector, or alternatively (ii) the free passage of analyte to the detector and retention of interfering species. In speciation studies the separation and/or capture of the analyte species should occur quickly so as to minimise re-equilibration of the sample. FIA systems utilising a column packed with an analyte- or interferent-specific sorbent material will offer suitable conditions to perform such analyses efficiently.

Manifold And Column Design: The degree of dispersion a volume of analyte undergoes after injection into an FIA manifold and before reaching the detector is an important factor in FIA systems. Parameters affecting dispersion in FIA microcolumns have been described [Ruzicka and Hanson, 1988; Fang, 1991] and include column diameter, column length, column dead volume and sample carrier / eluent flow-rates.

Sample dispersion will occur during both sample sorption and elution from a column. When considering dispersion in columns this should describe both the spatial distribution of the analyte in solution and on the column packing material. The dispersion of analyte during sorption and elution processes may be influenced by:

- (i) the geometric dimensions of the column (*e.g.* length, internal diameter and shape),
- (ii) the properties of the adsorbent material (*e.g.* hydrophilicity/hydrophobicity),
- (iii) the properties of the eluent,
- (iv) the flow rates during analyte adsorption and elution, and
- (v) the manifold design.

The insertion of a column containing an inert packing material usually has little effect on sample dispersion, however, the situation is not so simple when an active sorbing

material is present. In FIA sorption occurs predominantly at the sample injection end of the column, however, the continued application of carrier solution often results in the sorption band being dispersed downstream. Depending on the degree of this dispersion, controlled by the distribution coefficient of the sorbate between the stationary phase and the mobile phase, breakthrough of the sorbate may occur before column saturation has been reached. Provided distribution coefficients are high and the column capacity is not reached, sorption will occur predominantly at the sample injection end of the column. It is therefore often desirable that elution should be performed in the opposite direction to sorption; this will minimise further eluent dispersion. FIA techniques most often analyse eluent peak height and the factors listed above should be optimised to produce sharp elution peaks.

Resin particle size and packing will be of considerable importance in effecting dispersion. Whenever possible manifold designs should be such as to avoid the development of excessive back-pressure due to sorbent packing. Columns have utilised both straight and conical designs. In the latter, the conical shaped column may help minimise dispersion and help to focus the analyte zone as it leaves the column. The studies by Burba and Willmer (1987) on sorbent extraction of HMDC on cellulose collectors indicated that reaction vessels with hydrophobic surfaces (*e.g.*, polytetrafluoroethylene, PTFE) should be avoided in order to minimise loss of HMDC-metal complexes by adsorption.

Column Materials: In SECTION A matrix separation and preconcentration procedures were discussed and particular attention was given to chelation resins or immobilised chelates that may be used for (i) the preconcentration of Al and Fe, and (ii) the preconcentration of Fe (but not Al). 8-hydroxyquinoline (oxine) and dithiocarbamate ligands immobilised on solid supports have been utilised extensively for trace metal matrix separation and preconcentration. These ligands may be useful for achieving the goals '(i)' or '(ii)' above respectively.

Despite dithiocarbamates forming only weak complexes with Fe several studies have highlighted their potential for preconcentration of Fe from waters (see SECTION A). The incorporation of a dithiocarbamate-modified resin into an FIA system would be expected to remove Fe from the carrier stream but not affect the concentrations of Al. In contrast oxine forms very strong complexes with both Al and Fe and the incorporation of a oxine-modified resin into an FIA system would be expected to quantitatively adsorb both of these metals from solution.

Sufficient stability constant data exists for the H^+ - Al^{3+} -oxine and H^+ - Fe^{3+} -oxine systems for modelling calculations to be undertaken to predict the conditions (*i.e.* pH, oxine concentration) that may be useful for the development of an Al speciation system. In Table 8.2 thermodynamic data are given for these systems; the source of these data

follows. Stability constants for the H⁺-Al³⁺-oxine and H⁺-Fe³⁺-oxine systems were obtained from the stability constants database (SC-database) [Pettit and Powell, 1995], Al³⁺ hydrolysis constants were from previous literature sources [see Chapter 6 (6.1.2)] and Fe³⁺ hydrolysis constants were from Baes and Mesmer (1986). The M³⁺ hydrolysis data were for I = 0.1 mol L⁻¹ ionic media (aqueous) whereas the oxine data were for *ca.* 50 % dioxan/H₂O media.

Table 8.2 Thermodynamic data for the systems: H⁺-M³⁺-oxine (where M = Al or Fe) and H⁺-M³⁺ (Al or Fe hydrolysis). The equilibrium constants ($\beta_{p,q,r}$) are given according to the reaction: $p\text{H}^+ + q\text{M}^{3+} + r\text{L}^{2-} \rightleftharpoons \text{H}_p\text{M}_q\text{L}_r^{(p+3q-2r)+}$.

Species	(<i>p,q,r</i>)	log $\beta_{p,q,r}$
Oxine (L²⁻)		
HL ⁻	(1,0,1)	11.12
H ₂ L	(2,0,1)	15.24
AlL ⁺	(0,1,1)	11.17
AlL ₂ ⁻	(0,1,2)	22.59
AlL ₃ ³⁻	(0,1,3)	32.74
FeL ⁺	(0,1,1)	14.01
FeL ₂ ⁻	(0,1,2)	26.77
FeL ₃ ³⁻	(0,1,3)	38.33
Al-hydrolysis (Al³⁺)		
AlOH ²⁺	(-1,1,0)	-5.33
Al(OH) ₂ ⁺	(-2,1,0)	-10.91
Al ₃ (OH) ₄ ⁵⁺	(-4,3,0)	-13.13
Al(OH) ₄ ⁻	(-4,1,0)	-23.30
Al ₁₃ (OH) ₃₂ ⁷⁻	(-32,13,0)	-107.41
Fe-hydrolysis (Fe³⁺)		
FeOH ²⁺	(-1,1,0)	-3.21
Fe(OH) ₂ ⁺	(-2,1,0)	-6.73
Fe ₂ (OH) ₂ ⁴⁺	(-2,2,0)	-4.09
Fe ₃ (OH) ₄ ⁵⁺	(-4,3,0)	-7.58
Fe(OH) ₄ ⁻	(-4,1,0)	-21.60
K _w	(-1,0,0)	-13.78

The computer program SOLGASWATER [Eriksson, 1979] was used to calculate the distribution of species forming in a solution containing $100 \mu\text{mol L}^{-1}$ oxine and $5 \mu\text{mol L}^{-1}$ of each of Al and Fe. Although solution phase oxine will not have the same complexation properties as the oxine-derivatised resin the relative distribution between Al-oxine and Fe-oxine species may be expected to be quite similar [Miyazaki, 1995]. In Figure 8.2 the results from these calculations are presented. The solid lines represent Al species whereas the dashed lines represent Fe species.

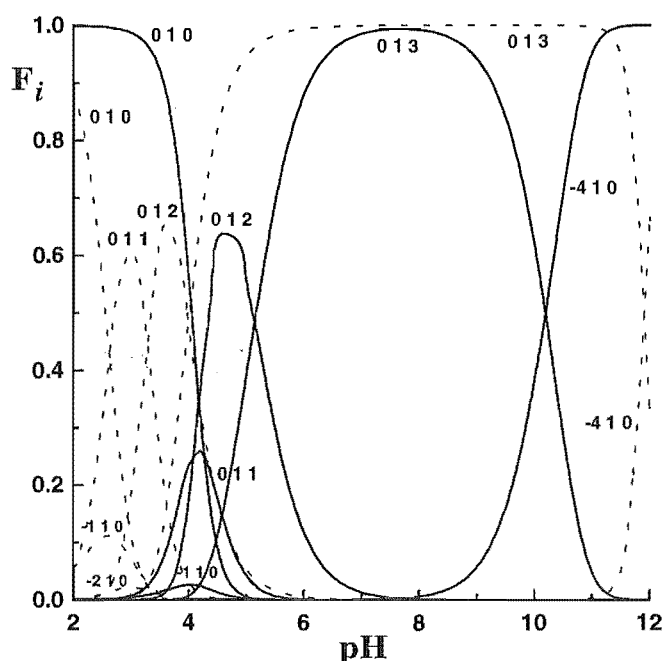


Figure 8.2 Distribution diagram F_i for $100 \mu\text{mol L}^{-1}$ oxine, $5 \mu\text{mol L}^{-1}$ Al and $5 \mu\text{mol L}^{-1}$ Fe. F_i is defined as the ratio of the aluminium concentration in an equilibrium species to the total aluminium concentration. The solid lines represent Al species whereas the dashed lines represent Fe species. The p, q, r stoichiometries are given (where q is Al or Fe respectively).

Figure 8.2 is quite 'busy' at low pH and below pH 6 the species M^{3+} , $\text{M}(\text{OH})_n^{(3-n)+}$ and $\text{M}(\text{Ox})_n^{(3-2n)+}$ (where $\text{M} = \text{Al}$ or Fe and $n = 0 - 2$) are observed to form. Below pH 5.0 there is no region where either (i) oxine complexes 100 % of both Al and Fe, or (ii) oxine complexes 100 % of one of these metals and 0 % of the other. Over the pH range *ca.* 5.0 to 8.0 oxine is observed to complex 100 % of both Al and Fe and at pH *ca.* 11.5 oxine complexes 100 % Fe and 0 % Al. These two 'windows' may be exploited for the development of an Al speciation method in which Fe will not interfere.

8.2.1 SCOPE OF THIS WORK.— Interference from Fe^{3+} in the analysis of Al^{3+} in environmental samples, *e.g.* natural waters and soil solutions, has been a problem faced by research groups for many years. The measurement of Al is most easily performed using an indirect method whereby the response (spectrophotometric, fluorimetric, electrochemical) of a 'probe ligand' which complexes Al can be monitored as a function of Al concentration [as described in Chapter 1 (1.3)]. An unfortunate feature of such analyses is that these methods are prone to interference from other metal ions that interact with the 'probe' ligand. Fe^{3+} binds with the same types of ligands that complex Al^{3+} . In spectrophotometric and fluorimetric procedures interference from Fe^{3+} can often be masked using suitable 'masking agents', *e.g.* bipyridine/ or 1,10-phenanthroline/ascorbic acid. In electrochemical analyses of Al such masking agents are not appropriate because of their inclination to undergo redox reactions. Furthermore, Fe masking agents may also affect Al speciation by disturbing the Fe-NOM equilibria (and hence the Al-NOM equilibria).

This SECTION of work is directed towards the development of an Al speciation technique which may be used without the use of additional masking agents for Fe. This technique will involve the direct measurement of 'reactive' Al through the selective capture of Al on a suitable chelating resin in a microcolumn (incorporated in an FIA system). The factors discussed throughout Chapters 1-7 which affect 'speciation' procedures are considered during the development of this new technique.

The Dithiocarbamate Column: The dithiocarbamate-modified chelating resin was synthesised from the polymer HEMA 100EH (Alltech) following the method described by Emteborg *et al.* (1995). The macroporous hydrophilic HEMA resin was a copolymer of 2-hydroxyethyl methacrylate and ethylene dimethacrylate and had an average particle size of 60 μm . Personal correspondence with Dr. H. Emteborg (Umeå University, Sweden) indicated that this would be a suitable material for this synthesis.

Although previous research had indicated that dithiocarbamate-modified resins were suitable chelating materials for the preconcentration of Fe, preliminary investigations in the present studies indicated that the slow complexation kinetics of this chelating resin with Fe would be not suitable for FIA-based speciation procedures. The immediate promise shown by the oxine-modified chelating resin meant that no further studies were made of the dithiocarbamate chelating resin.

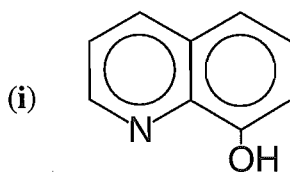
The Oxine Column: In this SECTION an Al^{3+} speciation procedure is described based on a 2 s reaction with oxine-derivatised Fractogel [described by Landing *et al.* (1986)] positioned in a 22 μL column reactor in an FIA manifold. Al^{3+} (pre)concentrated on the column from a 650 μL sample was selectively eluted [*via* the rapid quantitative conversion of resin-bound Al^{3+} to the $\text{Al}(\text{OH})_4^-$ ion] with 150 - 250 μL of 0.02 mol L^{-1} NaOH and detected spectrophotometrically as the Al-CAS (chrome azurol S) complex at pH 5.0.

The resultant FIA method was tested for (i) the extent of separation between reactive Al and Fe, (ii) the sequestering of Al from its citrate, oxalate, malonate and fluoride complexes, and (iii) retention of Al-hydroxy polymers [e.g. $\text{Al}_{13}(\text{OH})_{32}^{7+}$]. The method was applied to humic waters and soil solutions and the results for 'free' Al^{3+} compared with those obtained by the 7-s CAS method. The method's detection limit (DL) and linear working range (LWR) were evaluated.

8.2.2 EXPERIMENTAL

(A) Chemicals and Analysis.— All glass and plasticware was cleaned by soaking in 10 % HNO_3 for 48 h followed by 12 h soaking and repeat rinsing with triply distilled water. All solutions were prepared from Milli-Q water and all working solutions were prepared in 0.10 mol L^{-1} $\text{K}(\text{Cl})$ (Merck, *p.a.*), dried at 120°C . Reagents and model ligand solutions were stored in plastic (polypropylene) bottles. All pH measurements (± 0.03) were performed with a laboratory-built pH meter which was calibrated using standard phthalate (pH 4.01) and phosphate (pH 6.86) buffers.

(i) Oxine Gel: 8-hydroxyquinoline (oxine) [(i), BDH reagent grade] was used for resin preparation. Two gel (vinyl polymer) preparations were made during the course of these studies. The first used the Fractogel material [Supelco, TSK-Gel Toyopearl] HW-65f (30 - 60 μm) while the second used the larger sized material HW-40c (60 - 100 μm). The immobilisation of 8-hydroxyquinoline followed the procedure described by Landing *et al.* (1986). This procedure is described in detail in Chapter 3 (3.2.8). The gel was stored wet in Milli-Q water.



(ii) Chrome Azurol S: CAS (Adrich) was used as supplied. This material had an estimated dye content of 61.5 % by comparison with a double-recrystallised material [Hawke *et al.*, 1995]. CAS solutions *ca.* $1.0 - 3.0 \text{ mmol L}^{-1}$ were prepared as required.

(iii) Bipyridine/Ascorbic Acid Solutions: 2,2'-bipyridine [Baker Analysed Reagent] stock solutions *ca.* 0.5 % were prepared and stored in the dark in plastic bottles. Ascorbic acid [Pharmaceutical Sales & Marketing] was used as supplied. Bipyridine (0.05 %)/ascorbic acid (1 %) solutions were prepared daily in 0.2 mol L^{-1} acetate buffer (pH 4.15).

(iv) **Metal Solutions:** All metal solutions were prepared by dilution of stock solutions described in Chapter 3 [3.2.5]. These solutions were (i) a 2.0 mmol L^{-1} Al(III) solution and (ii) a 2.0 mmol L^{-1} Fe(III) solution. All solutions were prepared in 0.02 mol L^{-1} HCl . Al standard solutions were prepared daily in 0.001 mol L^{-1} $\text{NaOAc}/0.10 \text{ mol L}^{-1}$ NaCl electrolyte with pH 4.5.

(v) **Ligand Solutions:** Citric acid (BDH, AnalaR), oxalic acid (Fisons, AR), malonic acid (Riedel-de Haën, AG) and sodium fluoride (BDH, AnalaR) solids were used after drying (silica gel, 25°C) but without further purification. 5.0 mmol L^{-1} stock solutions were prepared. Fluoride solutions were always stored in plastic bottles.

(vi) **FIA Carrier/Eluent/Buffer Solutions:** Acetate buffer (NaOAc) solutions (pH 4.0 - 5.5) [BDH, AnalaR] were used. The carrier and eluent solutions were the most important regarding purity.

Carrier solution: A 0.05 mol L^{-1} $\text{NaOAc}/0.05 \text{ mol L}^{-1}$ NaCl (pH 5.0) carrier solution was prepared by dissolving NaOAc and NaCl in Milli-Q and pH adjusted with HCl .

Eluent solution: The NaOH eluent (0.02 mol L^{-1} $\text{NaOH}/0.08 \text{ mol L}^{-1}$ NaCl) was prepared with the same ionic strength as the carrier.

Buffer solution: Acetate buffer (2.0 mol L^{-1} , pH 5.3) was prepared in the same manner as the carrier.

(B) FIA System and Protocol.— The material used for manifold preparation, the pump and injection systems have been described in Chapter 3 (3.7). In this Section brief descriptions of the FIA manifold, the oxine micro-column construction and the injection system configuration are given.

(i) **Manifold Design:** The FIA manifold in Figure 8.2.2A was used for all experiments. The manifold system was constructed to minimise dispersion of sample prior to 'Al-capture' and also during sample elution. The distances from injector to column and from column to reaction coil were $< 15 \text{ cm}$. Buffer and chromophore flows were minimised to reduce sample dilution, while maintaining adequate buffer capacity and chromophore concentration ($65 \mu\text{mol L}^{-1}$ at detector). Glass connectors were used at the confluence points of the respective flow lines. These connectors have been reported to achieve high turbulence and maximum dispersion [Karlberg and Pacey, 1989; Chalk and Tyson, 1994].

During optimisation of the manifold, the sample reaction zone was varied by adjusting the size of the reaction coil. Reaction coils consisted of knitted microline tube (0.51 mm i.d.); 50 - 300 cm coils were tested. In the optimised manifold the reaction coil was 300 cm and this provided almost complete colour development for eluted Al.

A GBC model 918 UV-visible spectrophotometer with a 10 mm light path flow cell (3 mm i.d., 70 μL volume) was used as the detector. Absorbance was measured at 545 nm as the FIA peak height using the instrument's computer software. Temperature control, essential for obtaining reproducible standard curves, has been described previously [Hawke and Powell, 1994].

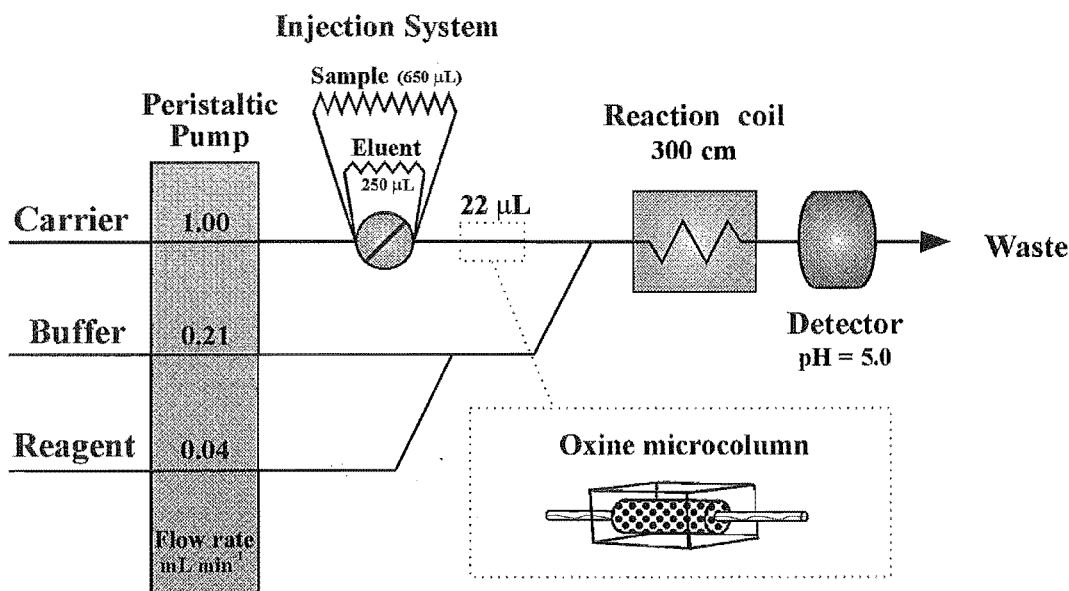


Figure 8.2.2A Schematic diagram for the flow-injection manifold. The chemical components of this system were (i) carrier solution = $0.05 \text{ mol L}^{-1} \text{ NaOAc}/0.05 \text{ mol L}^{-1} \text{ NaCl}$ (pH 5.0), (ii) buffer = 2.0 mol L^{-1} acetate buffer (pH 5.3; 5.00 - 5.05 at detector) and (iii) reagent = 2 mmol L^{-1} CAS. The flow rates of the respective lines are given. Also shown is the sample and eluent injection loop volumes (650 μL and 250 μL respectively). The reaction zone was a 300 cm microline reaction coil.

(ii) Oxine Micro-Column: The microcolumn (incorporating the oxine gel) was prepared from polycarbonate. This material was suitably durable to acid and alkali additions and its transparency allowed any long term degradation of the resin to be observed. No degradation of resin was ever observed, however if the flow direction in the column was not reversed then the resin was observed to compact over long periods of use. The column had a 22 μL volume (7 mm by 2 mm i.d.) and was connected to the FIA system by threaded Teflon-tube end fittings and grippers (Omnifit). At each end of the column (between the oxine gel and the connectors) a small circular disc of fine (nylon) mesh was inserted to secure the resin particles in the column. The gel was packed 'wet' to completely fill the 22 μL volume.

(iii) **Injection System:** The injection system used in these studies was a ten-port VALCO valve with VICI actuator system (rotary design). The system had two injection loops and two positions (i) 'LOAD SAMPLE': load sample and inject eluent, and (ii) 'INJECT SAMPLE': load eluent and inject sample. These positions are depicted in Figure 8.2.2B respectively.

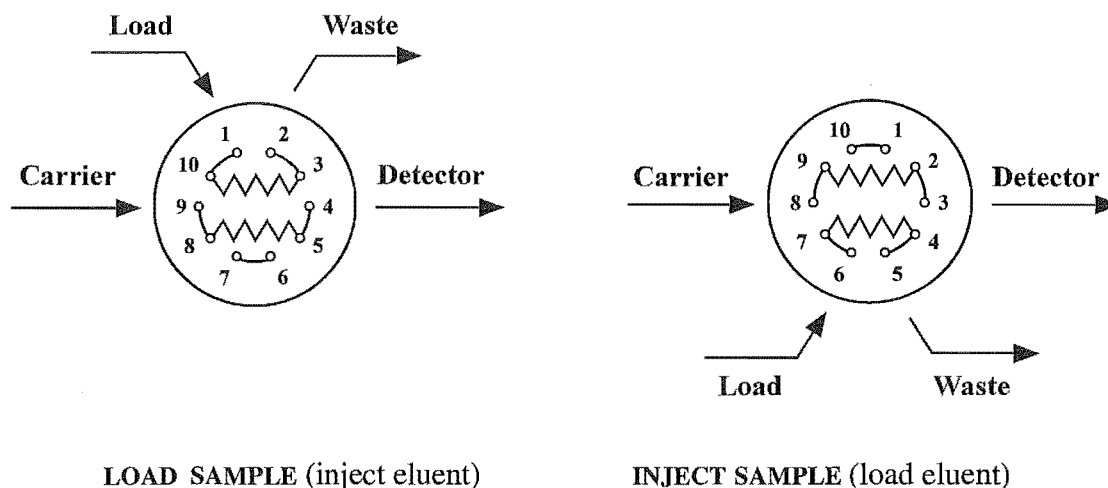


Figure 8.2.2B Two valve configurations of the ten-port injection system.

The use of two injection loops enabled the eluent loop to be filled while the sample was injected. In the LOAD SAMPLE position a geometrically defined external 'sample' loop was filled with the desired test solution. While set in this position the carrier flows through the eluent loop (*i.e.* if present the eluent is injected). Once the sample loop was filled, the valve position was switched (electronic) to the INJECT SAMPLE position. The carrier solution now flows through the sample loop thus injecting the sample into the carrier stream which passes immediately through the oxine microcolumn. If the next step in the procedure was to involve elution of analyte (sorbed sample) from the column the eluent loop was now filled and subsequently injected. Multiple injections of either sample or eluent were made by 'not filling' the opposite loop respectively, but continuing to fill the desired injection loop.

During optimisation of the detection procedures, injection loop sizes (i) sample: 400 - 2000 μL and (ii) eluent: 150 - 400 μL (Teflon) were tested. In the optimised manifold the injection loop sizes were (i) sample: 650 μL and (ii) eluent: 250 μL .

(C) Model Ligand Solutions.— The model ligand solutions were prepared in 0.01 mol L^{-1} NaOAc/0.09 mol L^{-1} NaCl electrolyte (pH 4.5). Stock solutions of the respective ligands were used to spike the electrolyte and Al was added 2 min later. All solutions were allowed to equilibrate for 24 h before analysis.

Modelling calculations were made for solutions of identical composition to those analysed. These calculations were performed using the computer program SOLGAS-WATER [Eriksson, 1979]. The literature sources used for the stability constants for the ligands were: citrate [Öhman, 1988], oxalate [Sjöberg and Öhman, 1985], malonate [Powell and Town, 1993] and fluoride [Nordstrom and May, 1989]. The data for H⁺-Al³⁺-malonate system are given in Table 8.2.2A while data for the other ligands were given in Chapter 6 (Table 6.1.2B). These constants were determined in 0.1 mol L⁻¹ ionic media, however no reliable constants were available for the other Al-L equilibria at this ionic strength. The constants used were for 0.6 mol L⁻¹ media and were considered adequate for the present studies. The data for Al hydrolysis have been described earlier (Table 8.2).

Table 8.2.2A Thermodynamic data for the system: H⁺-Al³⁺-malonate. The equilibrium constants ($\beta_{p,q,r}$) are given according to the reaction: $p\text{H}^+ + q\text{Al}^{3+} + r\text{L}^{2-} \rightleftharpoons \text{H}_p\text{Al}_q\text{L}_r^{(p+3q-2r)+}$.

Malonate (L ²⁻)	(<i>p,q,r</i>)	log $\beta_{p,q,r}$
HL ⁻	(1,0,1)	5.25
H ₂ L	(2,0,1)	7.85
AlL ⁺	(0,1,1)	6.71
AlL ₂ ⁻	(0,1,2)	11.53
AlL ₃ ³⁻	(0,1,3)	14.10
AlL ₂ OH ²⁻	(-1,1,2)	4.85

Acetate forms a weak complex with Al [Marklund *et al.*, 1989]. For Al standards in the presence or absence of acetate buffer, the effects of the acetato complex on the detection signal was found to be insignificant. The acetato complex was not included in model calculations.

(D) Al-Hydrolysis Solutions.— Polymeric Al solutions (100 $\mu\text{mol L}^{-1}$ and 10 $\mu\text{mol L}^{-1}$) were prepared by the partial neutralisation of acidic Al solutions. In each preparation the desired Al was added to 2 L of acidified electrolyte (0.1 mol L⁻¹ NaCl/0.001 mol L⁻¹ HCl). Rapid stirring was effected both magnetically (1x10 cm flea) and mechanically (2x10 cm propeller). The solutions were titrated with 0.005 mol L⁻¹ NaOH to pH 4.0 followed by 0.0002 mol L⁻¹ NaOH to the desired pH.

The titration was automated by use of a computer driven autoburette (Radiometer ABU80) which allowed the slow addition (lowest speed, $0.125 \text{ mL min}^{-1}$) of small volumes of alkali. Two electrode systems were used to monitor pH change (i) a combination pH electrode (Radiometer PHM 64 research pH meter and pHC2005 combination electrode) and (ii) a laboratory pH meter. Both instruments were calibrated using standard buffer solutions [Chapter 3 (3.2.4)] and were observed to function satisfactorily. The former of these electrode systems was interfaced with the computer and monitored pH adjustment to a desired value [pH 'drift conditions' were set as discussed in Chapter 2 (2.3)]. Once satisfactory pH equilibrium was reached a 50 mL sample was removed and stored in the plastic container until analysis (24 h later).

(E) Natural Water and Soil Solutions.— Soil solutions were extracted from *ca.* 100 g soil (roots and stones removed) by centrifugation (20 min at 3000 rpm). Membrane filtration to $-0.025 \mu\text{m}$ was effected immediately. A full description of this extraction protocol is given in Chapter 3 [3.3.2(B)]. Solutions that were not analysed within 4 h were refrigerated until 2 h before analysis. All analyses were performed within 36 h of extraction.

Table 8.2.2A Description of soil sample sites.

Site	Soil type	Parent material	Forest vegetation	Horizon	Depth (cm)
Bealey Spur	typic orthic podzol	greywacke colluvium plus till	silver beech	Oa	0-10
Birchfield	acidic orthic brown soil	greywacke, schist and granite	broadleaf	Oa	0-10
Cave creek & Glentui	-	quartzofeld-spathic	mountain beech	A	0-15
Tekapo	-	glacial moraine	hawkweed, legumes, grasses	A	0-10
Westland Petrel	acidic orthic brown soil	greywacke, schist and granite	broadleaf	A	0-10

8.2.3 RESULTS

(A) **FIA Manifold Optimisation.**— The optimised manifold was shown in Figure 8.2.2A. All sample analyses were performed in triplicate. Prior to sample analysis the absence of 'residual analyte' on the column (*i.e.* sorbed impurities) was checked. This was achieved through multiple injections of eluent ($0.02 \text{ mol L}^{-1} \text{ NaOH}$); the sample loop was only filled (and subsequently injected) if several negative but reproducible elution peaks were obtained. A 'typical signal output' is shown in Figure 8.2.3A.

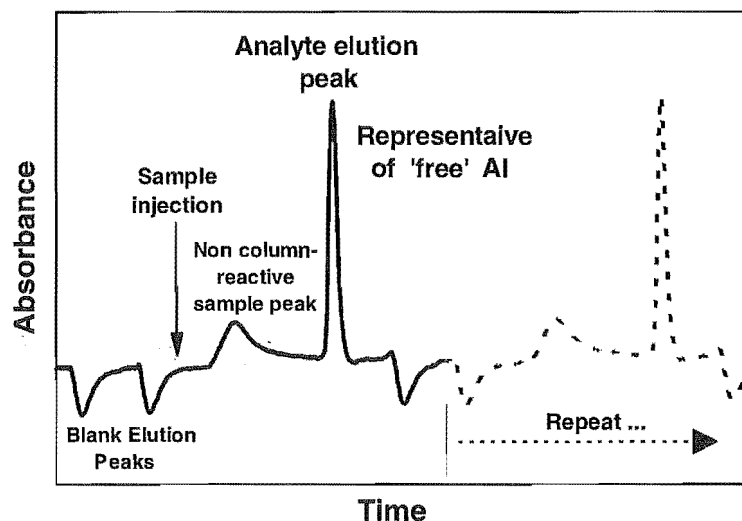


Figure 8.2.3A Typical format of detection signal.

The negative peaks ('blank elution peaks' in Figure 8.2.3A) indicate that buffering of the eluent was not complete and the acid/conjugate base ratio for the CAS reagent has been changed slightly [$\log K_{(\text{HL}+\text{H}=\text{H}_2\text{L})} = 4.64$]. The optimisation of NaOH concentration was focused on the complete elution of Al^{3+} [as the $\text{Al}(\text{OH})_4^-$ ion] from the column without a sufficiently high pH being obtained that would result in the elution of retained Fe^{3+} . In this optimisation the highest signal to noise ratio achievable was obtained by balancing the elution peak height (negative) vs. the concentration of buffer at the detector [higher buffer concentrations reduced the sample elution peak height (detection signal)]. The blank elution peaks (negative) were reproducible. The first blank elution peak following 'analyte elution' always indicated some residual Al (a positive component *before* the negative component); this was attributed to a dead-volume of sample retained in the injection system which was subsequently injected during multiple eluent injections. (Further evidence for this residual Al was its presence even when no column was included in the FIA manifold).

Following the injection of sample ($650 \mu\text{L}$) a peak was observed at the detector. This arose from Al that was not captured by the column but did react with the CAS

reagent. This Al was likely to be 'moderately labile Al' that was not sufficiently labile to be complexed by the oxine column during its short residence time. This peak is discussed further during the Conclusions (8.2.4).

Upon analyte elution a sharp peak was observed at the detector due to eluted Al. This peak was proportional to captured Al^{3+} . The position of this peak relative to the blank elution peak was at the leading edge of the 'elution wave'. To this extent, the uppermost point of the analyte elution peak starts to overlie the 'blank' peak (negative) at *ca.* 25-50 % down the tailing edge of elution wave. At high Al analyte concentrations the 'tail' of the analyte peak extended across the entire blank peak range and no 'dip' was observed. At lower Al concentrations the analyte peak 'dips' as a result of effects from the superimposed negative elution peak. These effects are made clear by comparing peak size *vs.* the 'dip' size (if present) following the sample elution peak for $1\ \mu\text{mol L}^{-1}$, $2\ \mu\text{mol L}^{-1}$ and $16\ \mu\text{mol L}^{-1}$ Al concentrations (Figures 8.2.3B and 8.2.3J respectively). In accord with these observations, the calibration line has a small negative intercept. These effects were important when optimisation of the detection limit was considered. The analyte elution peak was optimised by varying the reagent (CAS) concentration. CAS solutions *ca.* $1.0 - 3.0\ \text{mmol L}^{-1}$ were tested and in the optimised manifold $2.0\ \text{mmol L}^{-1}$ CAS solution was used.

Al Retention and Elution:

Retention of Al^{3+} on the oxine-derivatised Fractogel was quantitative as indicated by zero analyte response at the detector following injection of $650\ \mu\text{L}$ of standard Al^{3+} solution ($0.5 - 16\ \mu\text{mol L}^{-1}$). The capacity of the $22\ \mu\text{L}$ column, measured by saturation with Al^{3+} , then stepwise elution with $0.02\ \text{mol L}^{-1}$ KOH, was $0.113\ \mu\text{mol Al}^{3+}$; this equates to $1.13\ \mu\text{mol Al}^{3+}\ \text{g}^{-1}$ (dry) or $2.34\ \mu\text{mol Al}^{3+}\ \text{g}^{-1}$ (wet). Use of the coarser grade of Fractogel ($50 - 100\ \mu\text{m}$, TSK Toyopearl) was essential to minimise back pressure in the flow system.

The chelating resin was constantly bathed (and conditioned) by carrier solution ($0.05\ \text{mol L}^{-1}$ NaOAc/ $0.05\ \text{mol L}^{-1}$ NaCl, pH 5.0). Therefore purity of this reagent was paramount in order to achieve a low sample blank when the retained Al was eluted with alkali. The buffer was prepared from BDH (AnalaR) NaOAc by addition of BDH (AnalaR) HCl to pH 5.0, and stored in a polypropylene bottle. This reagent had satisfactory purity, but as an added precaution the carrier was passed through an on-line column of Chelex 100 resin in a $2.5 \times 15\ \text{mm}$ column between the peristaltic pump and the injection valve.

Elution of Al^{3+} from the oxine column was effected by $0.02\ \text{mol L}^{-1}$ NaOH/ $0.08\ \text{mol L}^{-1}$ NaCl. This converts Al^{3+} rapidly and quantitatively into the $\text{Al}(\text{OH})_4^-$ ion. The plug of $0.02\ \text{mol L}^{-1}$ NaOH was effectively buffered by the $2\ \text{mol L}^{-1}$ acetate buffer (pH

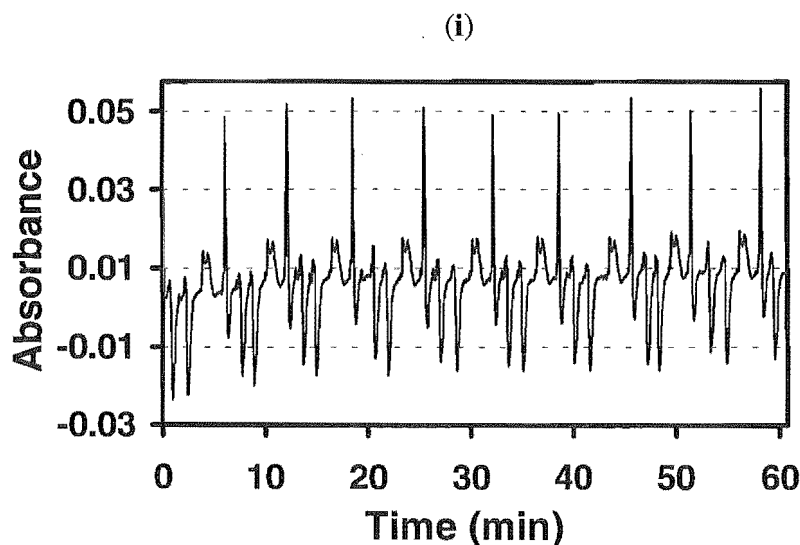
5.3) at the first merging zone to give a final reaction medium of pH 5.0. In contrast, the acid elution of metals from ion exchange or chelating resins requires 1 - 2 mol L⁻¹ acid eluent (HCl or HNO₃) and subsequent buffering of this on-line, if required, is difficult to achieve [Abollino *et al.*, 1990; Blain *et al.*, 1993; Fairman *et al.*, 1995].

FIA Reagents:

The selection of pH 5.0 carrier for the column conditioning and the sample transfer was based on the need to minimise the effect of pH change on speciation of samples likely to be studied for potential Al toxicity (pH 4.5 - 5.4). At pH 5.0, 100 % of both Al^{3+} and Fe^{3+} can be expected to complex with the column. It is believed that buffer retained in the resin pores controls the reaction pH of the oxine-modified resin with Al in the sample. Natural samples are likely to have low buffering capacities and should not influence the pH of the column. Carrier and eluent ionic strengths were 'matched' (0.10 mol L⁻¹) to minimise any ionic strength effects occurring at the detector. The selection of pH 5.0 buffer was based on (i) the optimum pH range for Al-CAS equilibrium spectrophotometric measurements [Hawke and Powell, 1994] and (ii) an adequate pH for Al-CAS kinetics (pH > 5). The reagent CAS provides significantly higher spectrophotometric sensitivity under non-equilibrium conditions than does PCV or ECR.

Analytical Performance:

Figure 8.2.3B indicates the precision achieved from replicate injections of a (i) 1.0 $\mu\text{mol L}^{-1}$ and (ii) 2.0 $\mu\text{mol L}^{-1}$ Al^{3+} standards. The LWR was 0.3 to 16 $\mu\text{mol L}^{-1}$, where the lower limit was five times the DL ($2\sigma = 60 \text{ nmol L}^{-1}$ for a 1.0 $\mu\text{mol L}^{-1}$ standard, $n = 9$). The upper limit was governed by the maximum absorbance that could be accurately measured by the spectrophotometer ($A = 0.8$).



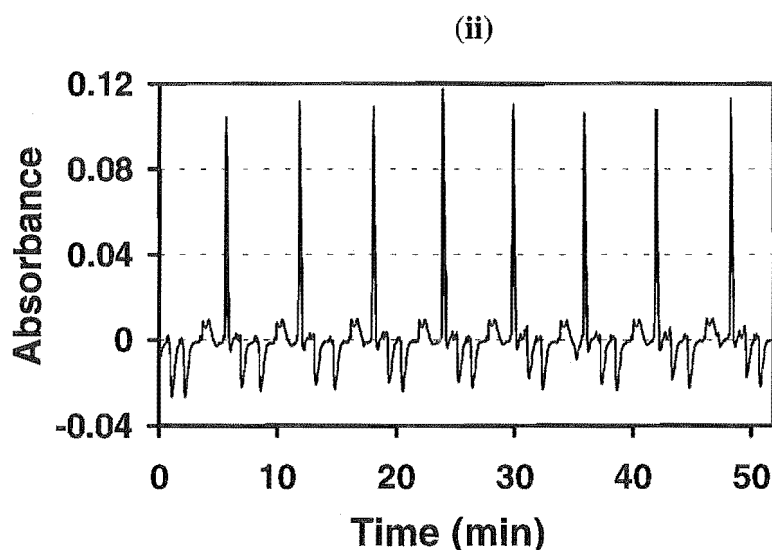


Figure 8.2.3B Precision: replicate injections of a (i) $1.0 \mu\text{mol L}^{-1}$ and (ii) $2.0 \mu\text{mol L}^{-1}$ Al^{3+} standards.

(B) Model Ligand Systems.— To be effective as a method for estimating ‘free’ Al^{3+} it was important that the chelating resin did not sequester significant amounts of Al from simple complexes with organic or inorganic ligands (or from natural organic matter). To establish this property for simple organic and inorganic ligands two experiments were performed; these were as follows. (i) Solutions were prepared at pH 4.5 having $8 \mu\text{mol L}^{-1}$ Al^{3+} with the ligands citrate, oxalate, malonate and fluoride at concentrations such that less than 1 % of the Al present was uncomplexed (predicted from thermodynamic calculations). These ligand concentrations were $15 \mu\text{mol L}^{-1}$, $50 \mu\text{mol L}^{-1}$, $100 \mu\text{mol L}^{-1}$ and $40 \mu\text{mol L}^{-1}$ respectively. (ii) For each of the ligands fluoride, oxalate and malonate *ca.* 10 solutions were prepared at pH 4.5 having $15 \mu\text{mol L}^{-1}$ Al^{3+} and ligands concentrations in the range 0 – $100 \mu\text{mol L}^{-1}$. Results were compared with those for Al standard solutions and with the calculated solution speciation.

For the former of these experiments (pump speed = 20 rpm) the Al signal observed (in each case) was less than 5 % of the signal from an $8 \mu\text{mol L}^{-1}$ Al standard solution. For citrate virtually no Al signal was observed, indicating that Al was not sequestered from the Al-citrate complex by the oxine resin. The results from the second series of experiments are presented in the following Figures (8.2.3C-E).

In these Figures the measured response for each solution relative to the response for a $15 \mu\text{mol L}^{-1}$ Al standard, F_i , is plotted (datum points) as a function of ligand concentration. Also drawn is a curve for $\Sigma \{[\text{Al}^{3+}] + [\text{Al}(\text{OH})^{2+}] + [\text{Al}(\text{OH})_2^{+}]\}$ calculated from the thermodynamic models using SOLGASWATER. For each ligand the response is shown for a range of pump speeds, 10 - 80 rpm, corresponding to carrier flow rates 0.5 - 2.0 mL min^{-1} and sample-resin contact times of 2.8 - 0.7 s respectively.

Fluoride: For fluoride, Figure 8.2.3C, the calculated curves were for the sum of (i) Al^{3+} and monomeric Al-OH species (solid line), (ii) AlF^{2+} , Al^{3+} and monomeric Al-OH species (dashed line) and (iii) all monomeric cationic species (dotted line). The comparison between experimental and calculated values indicated that the dominant fluoride complex, AlF^{2+} , and possibly the complex AlF_2^+ , contributes to the Al retained by the resin.

There are disparate values for the Al-F stability constants in the literature. In Figure 8.2.3C(ii) curves are shown calculated using Al-F stability constants obtained from a variety of literature sources [Driscoll, 1984; Hodges, 1987; LaZerte, 1984; Martin, 1988; Noble *et al.*, 1988].

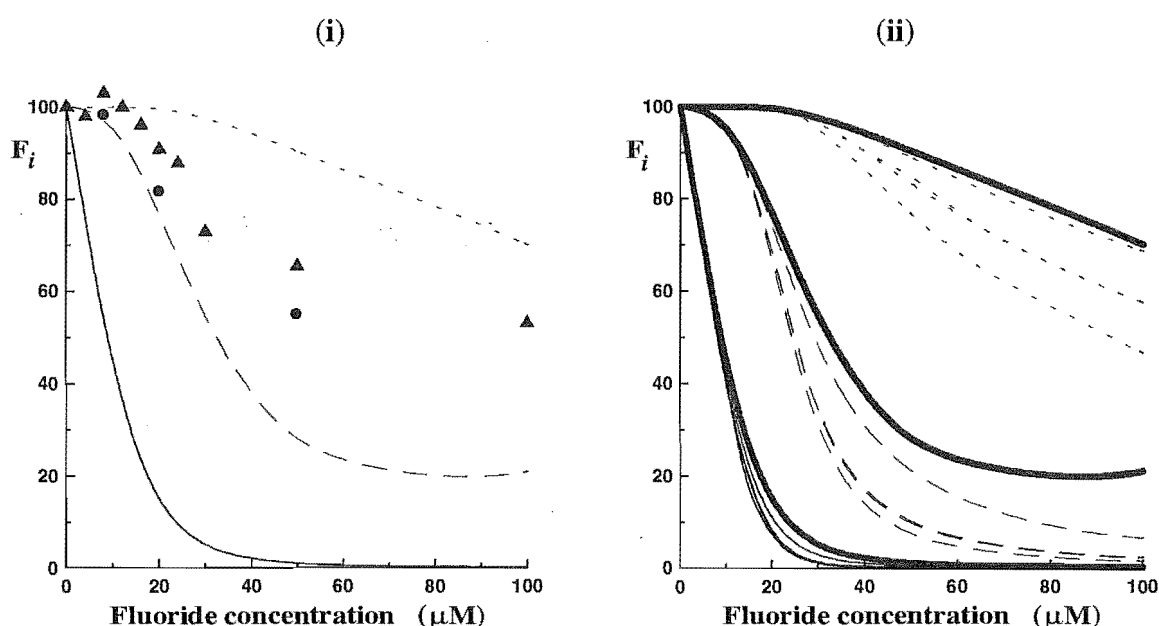


Figure 8.2.3C (i) The fraction of Al measured in solutions containing $15 \mu\text{mol L}^{-1}$ Al and $0 - 100 \mu\text{mol L}^{-1}$ fluoride is plotted as a function of fluoride concentration. This 'fraction', F_i , was calculated as the measured response for each solution relative to the response for a $15 \mu\text{mol L}^{-1}$ Al standard. Data are presented for experiments at pump speeds; 40 rpm (\blacktriangle) and 80 rpm (\bullet). The three calculated curves were for the sums (a) solid line: $\Sigma \{[\text{Al}^{3+}] + [\text{Al}(\text{OH})^{2+}] + [\text{Al}(\text{OH})_2^+]\}$, (b) dashed line: $\Sigma \{[\text{Al}^{3+}] + [\text{Al}(\text{OH})^{2+}] + [\text{Al}(\text{OH})_2^+] + [\text{AlF}^{2+}]\}$ and (c) dotted line: $\Sigma \{[\text{Al}^{3+}] + [\text{Al}(\text{OH})^{2+}] + [\text{Al}(\text{OH})_2^+] + [\text{AlF}^{2+}] + [\text{AlF}_2^+]\}$. These curves were calculated from the thermodynamic model for this H^+ - Al^{3+} -ligand system using the computer program SOLGASWATER. (ii) Curves are shown calculated using Al-F stability constants obtained from a variety of literature sources [Driscoll, 1984; Hodges, 1987; LaZerte, 1984; Martin, 1988; Noble *et al.*, 1988]; the thicker lines represent the model line shown in Figure 8.2.3C (i).

Oxalate: For oxalate the agreement between the experimental data and calculated curve obtained for the faster pump speed (sample-resin contact time of 1.4 s) shown in Figure 8.2.3D was very good. It was apparent that at slower pump speeds Al was sequestered from the Al-oxalate complexes and an overestimation of free Al, $\Sigma \{[\text{Al}^{3+}] + [\text{Al}(\text{OH})^{2+}] + [\text{Al}(\text{OH})_2^+]\}$, was obtained. Further increases to higher pump speeds (80 rpm, not shown) did not result in a significant change relative to the results for 40 rpm.

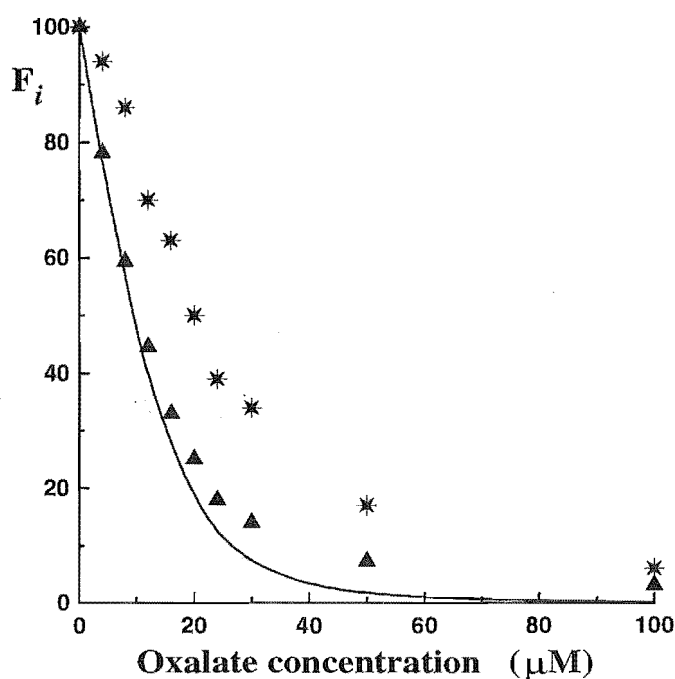


Figure 8.2.3D The fraction of Al measured in solutions containing $15 \mu\text{mol L}^{-1}$ Al and $0 - 100 \mu\text{mol L}^{-1}$ oxalate plotted as a function of oxalate concentration. Data are presented for experiments at pump speeds 20 rpm (*) and 40 rpm (▲). The definition of F_i and the method by which the curve, $\Sigma \{[\text{Al}^{3+}] + [\text{Al}(\text{OH})^{2+}] + [\text{Al}(\text{OH})_2^+]\}$, was calculated were given in Figure 8.2.3C.

Malonate: Results from the experiment for malonate are shown in Figure 8.2.3E. For the weaker malonate complexes measurable (10 - 20%) sequestering of complexed Al by the resin occurred for 1.4 s contact time (40 rpm). At higher flow rates sequestering was lowered but not eliminated.

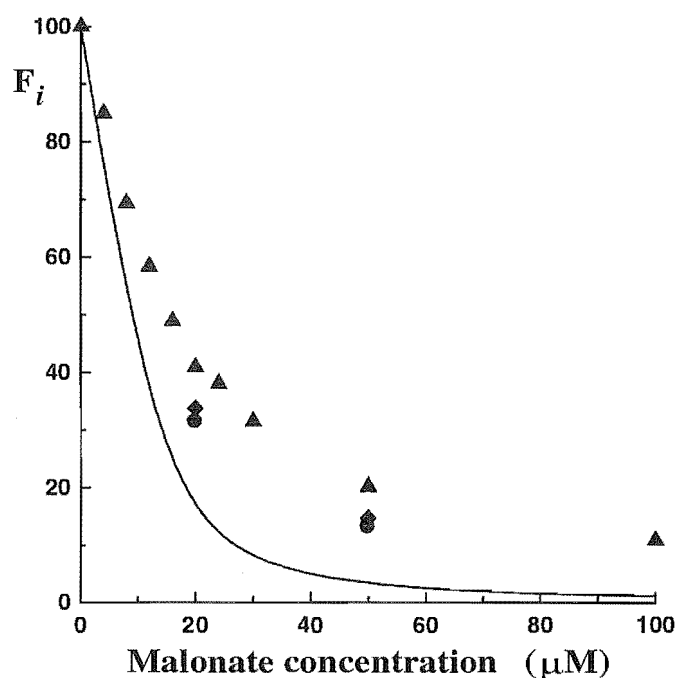


Figure 8.2.3E The fraction of Al measured in solutions containing $15 \mu\text{mol L}^{-1}$ Al and 0 - $100 \mu\text{mol L}^{-1}$ malonate is plotted as a function of malonate concentration. Data are presented for experiments at pump speeds 40 rpm (▲), 60 rpm (◆) and 80 rpm (●). Definitions and methods were given in Figure 8.2.3D.

(C) **Fe(III) Interferences.**— The principal interferent for analysis of Al^{3+} in environmental samples is Fe^{3+} . In spectrophotometric analyses this can be masked by reduction to Fe^{2+} (*e.g.* with ascorbic acid) and complexation with bipyridine or 1,10-phenanthroline. This route is not applicable to determining Al by amperometric or voltammetric measurements. In the present work three issues were addressed: (i) does the elution protocol achieve an analytically useful separation of Al and Fe, (ii) does the resin sequester Fe from its complexes in natural waters, and (iii) can Fe^{3+} , if complexed by the resin, be subsequently eluted for determination of $[\text{Fe}^{3+}]$ in the sample?

Two experiments were performed to elucidate the extent to which Fe^{3+} may interfere in analyses of natural water or soil solution samples. The first experiments were performed in a similar manner to the 'model ligand' experiments described above. Here solutions were prepared at pH 4.5 having $8 \mu\text{mol L}^{-1}$ Fe^{3+} with the ligand citrate at a concentration such that (i) less than 1 % or (ii) 20 % of the Fe present was uncomplexed (predicted from thermodynamic calculations - data not shown). These solutions showed negligible detection signals upon sample elution (CAS detection system).

In a second series of experiments, FIA measurements for Fe used 0.05 mol L^{-1} NaOAc (pH 5.0) as carrier and 0.05 % bipyridine/1 % ascorbic acid/ 0.05 mol L^{-1} acetate buffer (pH 4.15) in the reagent line. The product $\text{Fe}(\text{bpy})_3^{2+}$ was monitored at 515 nm.

Elution of Fe by NaOH and by bipyridine/ascorbic acid was studied for natural water solutions containing moderate to high NOM levels (Fe spiked and unspiked). NaOH elution profiles indicated that Fe^{3+} retained by the resin was not eluted with 0.02 mol L^{-1} NaOH and was thus removed as an interferent in down-line Al chemistry. This result was consistent with the much lower stability of the ferrate complex $[\text{Fe}(\text{OH})_4^-]$ in comparison with aluminate $[\text{Al}(\text{OH})_4^-]$. Using bipyridine/ascorbic acid eluent it was possible to elute oxine-bound Fe from the column. No attempt was made to quantify the eluted Fe.

(D) Polymeric Hydroxy-Aluminium Species.— Hydrolysed Al solutions were prepared by the slow incremental addition of NaOH (0.005 or $0.0005 \text{ mol L}^{-1}$) to a solution of 10 or $100 \mu\text{mol L}^{-1}$ Al in 0.10 mol L^{-1} NaCl to achieve solution pH values in the range 4.4 to 6.0 . The slow addition of alkali from an autotitrator was under computer control. In the analysis of the $100 \mu\text{mol L}^{-1}$ Al solutions the test sample was diluted 10-fold (and shaken) immediately prior to injection. Turbidity (light-dispersion) measurements of test solutions found negligible turbidity thus indicating the absence of solid phase Al-hydroxy species. The results are presented in Figure 8.2.3F.

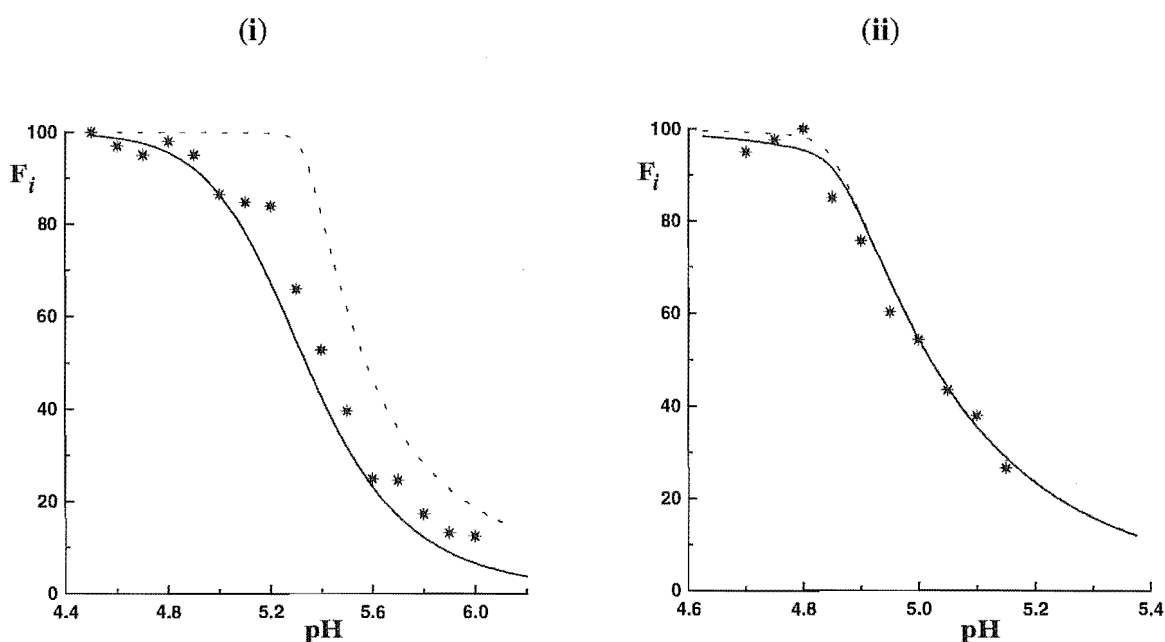
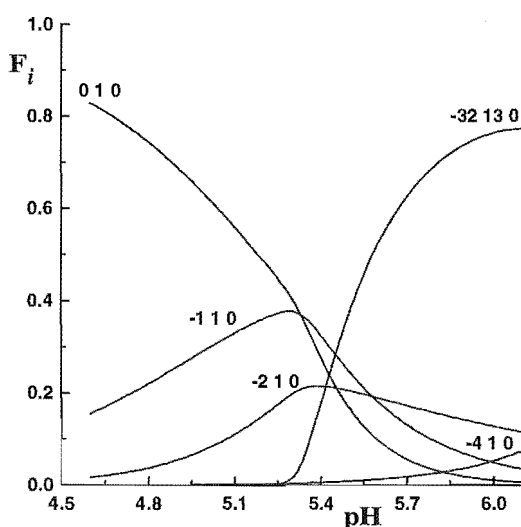


Figure 8.2.3F The fraction of Al measured in solutions containing (i) $10 \mu\text{mol L}^{-1}$ and (ii) $100 \mu\text{mol L}^{-1}$ Al. This fraction, F_i , (plotted as a function of pH) was defined in Figure 8.2.3C. Two curves are shown for the different Al-hydrolysis models 'A' and 'B' respectively (described below).

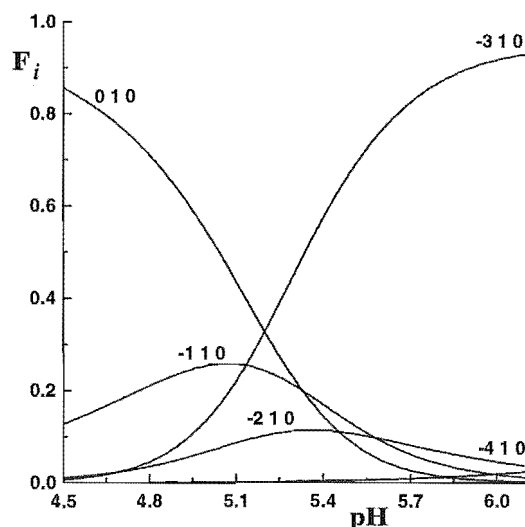
In Figure 8.2.3F the agreement between the measured response and the calculated sum of $[\text{Al}^{3+}] + [\text{Al}(\text{OH})^{2+}] + [\text{Al}(\text{OH})_2^+]$ for (i) $10 \mu\text{mol L}^{-1}$ and (ii) $100 \mu\text{mol L}^{-1}$ Al solutions is shown. The two curves shown in this Figure were for two Al-hydrolysis models respectively. The first model (A: dashed line) included the Al hydrolysis species presented in Table 8.2 earlier, *i.e.* AlOH^{2+} , $\text{Al}(\text{OH})_2^+$, $\text{Al}_3(\text{OH})_4^{5+}$, $\text{Al}(\text{OH})_4^-$ and $\text{Al}_{13}(\text{OH})_{32}^{7-}$. The second model (B: solid line) included all the Al hydrolysis species of the first model plus the species $\text{Al}(\text{OH})_3^0$ [$\log \beta_{-3,1,0} = -15.60$; Baes and Mesmer (1986)]. In the presence of complexing ligands this additional Al-hydrolysis species does not form due to its relatively low thermodynamic stability (hence it was not included in earlier models). However, in the absence of complexing ligands and at low Al concentrations this species may form.

In Figure 8.2.3G the distribution of Al species for each of these experiments is shown. Al-hydrolysis models 'A' and 'B' respectively (described above) for experiments at (i) $10 \mu\text{mol L}^{-1}$ (pH 4.5 - 6.1) and (ii) $100 \mu\text{mol L}^{-1}$ (pH 4.6 - 5.2) Al are shown. Also given are the p, q, r stoichiometries.

(i) $10 \mu\text{mol L}^{-1}$ Al: 'Model A'



'Model B'



(ii) $100 \mu\text{mol L}^{-1}$ Al : 'Model A'

'Model B'

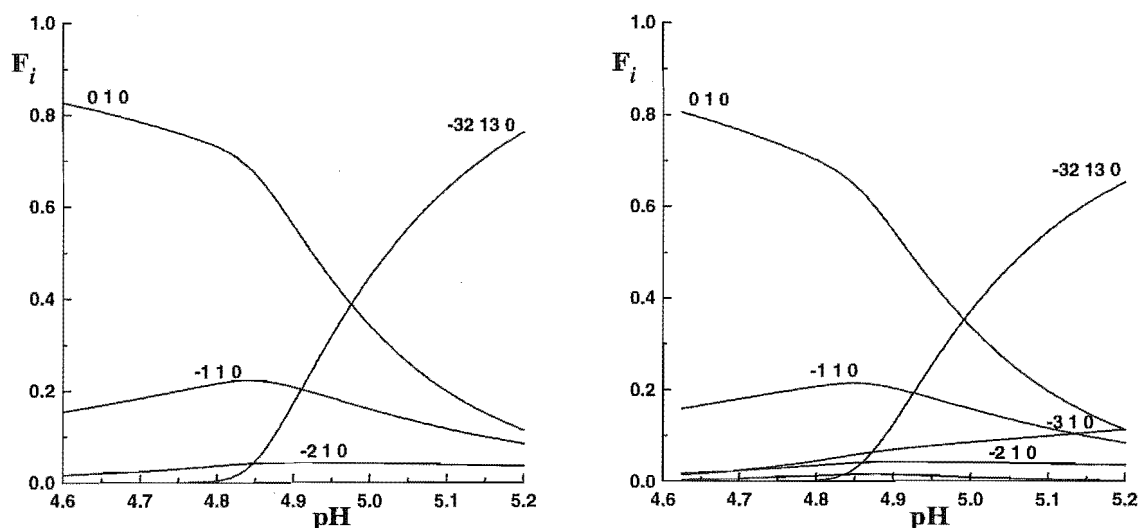


Figure 8.2.3G Distribution diagrams for Al-hydrolysis models 'A' and 'B' respectively (described above) for (i) $10 \mu\text{mol L}^{-1}$ and (ii) $100 \mu\text{mol L}^{-1}$ Al solutions. F_i is defined as the ratio of the aluminium concentration in an equilibrium species to the total aluminium concentration. The p,q,r stoichiometries are given.

The $\text{Al}_{13}(\text{OH})_{32}^{7+}$ species does not react measurably with CAS at pH 5 on the FIA timescale. Thus, if it was not retained by the chelating resin it would not produce a pre-elution signal at the detector, as demonstrated in Figure 8.2.3F. Further, if eluted from the resin without conversion to monomers, it would not provide an elution signal. At low Al concentrations the formation of $\text{Al}(\text{OH})_3$ is thermodynamically favoured over $\text{Al}_{13}(\text{OH})_{32}^{7+}$ [as indicated in Figure 8.2.3G(i)B]. This species is non-charged and it is possible that it may precipitate in the oxine column rather than be complexed. The results in Figure 8.2.3F established that if $\text{Al}_{13}(\text{OH})_{32}^{7+}$ and/or $\text{Al}(\text{OH})_3$ were retained by the resin they were not eluted significantly by each injection of 0.02 mol L^{-1} NaOH. That is to say, they do not appear to contribute to the first analyte elution peak. Anomalies apparent from these studies are described in the following Section (8.2.3E).

(E) Column Fouling \ Stop-Flow Cleaning.— Experiments established that the $\text{Al}_{13}(\text{OH})_{32}^{7+}$ and/or $\text{Al}(\text{OH})_3$ were retained quantitatively by the resin and only a minor fraction was eluted by each injection of 0.02 mol L^{-1} NaOH. The output signals for multiple elution from the most highly polymerised (high pH) $100 \mu\text{mol L}^{-1}$ (1/10 diluted as described) are shown in Figure 8.2.3H.

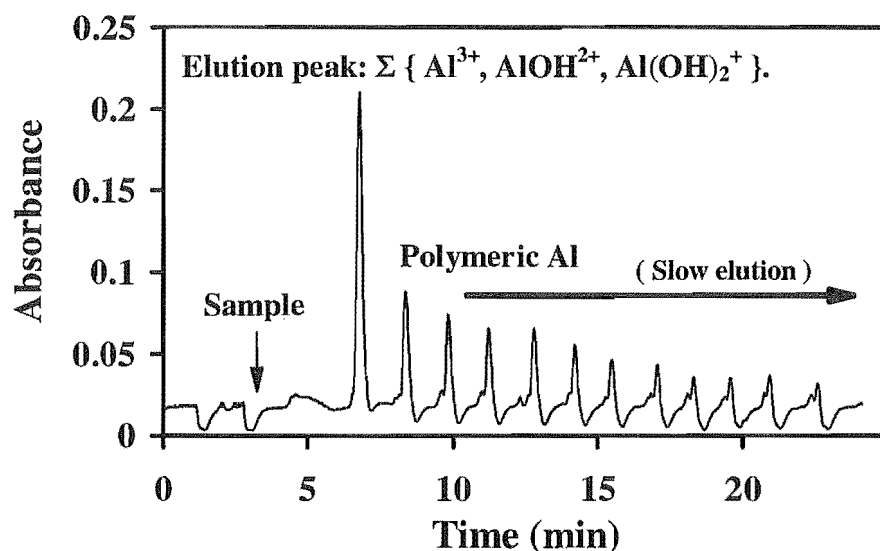


Figure 8.2.3H Output signals for $100 \mu\text{mol L}^{-1}$ Al sample at *ca.* pH 5.15 (most highly polymerised sample).

It is apparent from this Figure that an undefined Al species is eluted from the column after the first sample elution. The subsequent signals observed upon multiple elution steps (0.02 mol L^{-1} NaOH) were observed to slowly decrease. These elution peaks have been attributed to ' Al_{13} ' complexed by, or $\text{Al}(\text{OH})_3$ complexed and/or precipitated in, the column. Much time was spent 'cleaning' the column in this manner. To quantitatively remove the polymer from the resin it was necessary to use 0.2 mol L^{-1} NaOH eluent coupled with a 2 min stop-flow protocol. By this method a single aliquot of eluent removed all polymer from the resin. This may be a basis for its quantitative determination by down-line reaction with CAS. The output for the same solution analysed in Figure 8.2.3H but using this stop-flow cleaning protocol is shown in Figure 8.2.3I. It is clear that one cleaning step was effective in removing polymeric species from the column.

This stop-flow cleaning protocol reduced 'carry-over effects' for the analysis of Al solutions of high concentration ($> 15 \mu\text{mol L}^{-1}$) and increased the reproducibility for analysis of these samples. The reproducibility of the stop-flow procedure is shown in Figure 8.2.3J for a $16 \mu\text{mol L}^{-1}$ Al standard solution. The relative standard deviation (RSD) for the seven sample injections was $< 1 \%$. In this Figure, two 'large' peaks are observed. The first of these peaks is the 'analyte' elution peak, while the latter peak ('off-scale') is the 'stop-flow' cleaning peak. This latter peak has a very large absorbance (545 nm) because the reagent CAS, upon mixing with the stop-flow eluent (0.2 mol L^{-1} NaOH), is converted to the deprotonated form (which absorbs strongly at 545 nm).

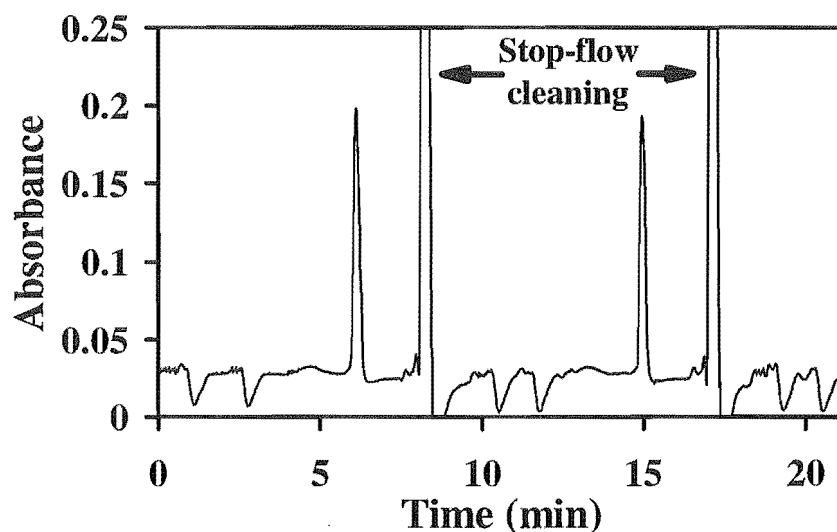


Figure 8.2.3I Typical output signal for 'stop-flow cleaning': same solution analysed as in Figure 8.2.3H.

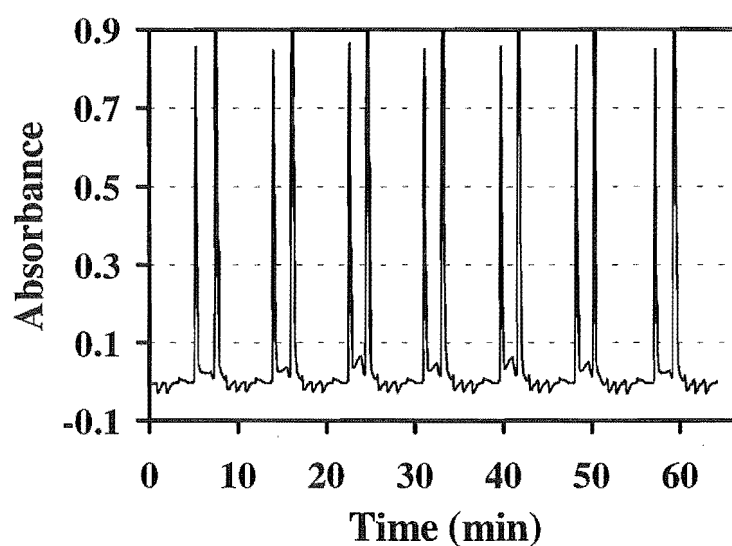


Figure 8.2.3J 'Stop-flow cleaning': reproducibility for a $16 \mu\text{mol L}^{-1}$ Al standard solution.

(F) Application to Humic Waters and Soil Solutions.— The determination of 'free' Al, $\{[\text{Al}^{3+}] + [\text{Al}(\text{OH})^{2+}] + [\text{Al}(\text{OH})_2^{+}]\}$, in humic waters and soil solutions involved a comparison between the 2 s oxine-derivatised Fractogel method and the 7 s CAS method of Hawke and Powell (1994). The results are shown in Figure 8.2.3K.

This Figure indicates that on average the 2 s oxine method determines some 20 % less Al than does the 7 s CAS method. This is consistent with experiments with model ligand systems which established that the method with the shorter analyte-reagent contact time is less aggressive in sequestering Al from its complexes.

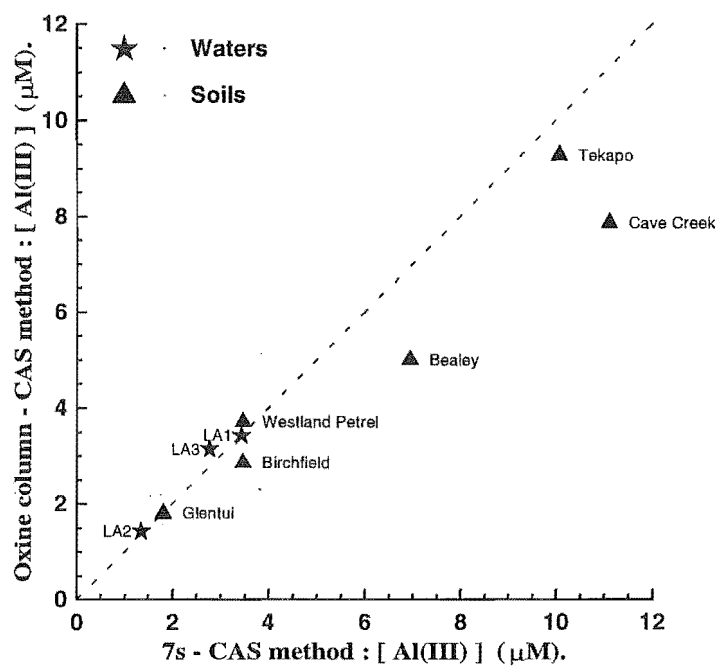


Figure 8.2.3K A comparison between the 2 s oxine-derivatised Fractogel method and the 7 s CAS method of Hawke and Powell (1994) for the determination of 'reactive' Al in natural waters and soil solutions.

8.2.4 CONCLUSIONS

Speciation of Al^{3+} is effected by 2 s reaction with oxine-derivatised Fractogel in a 22 μL column reactor in an FIA manifold. Al^{3+} (pre)concentrated on the column from a 650 μL sample is selectively eluted with 150-250 μL 0.02 mol L^{-1} NaOH and detected spectrophotometrically as the Al-CAS (chrome azurol S) complex at pH 5.0. Tests with synthetic solutions established that Al is not significantly sequestered from the citrate, oxalate and malonate complexes. Al-hydroxy polymers [$\text{Al}_{13}(\text{OH})_{32}^{7+}$] are quantitatively retained by the column but are not desorbed by 0.02 mol L^{-1} NaOH in the time frame of the FIA method; therefore they do not contribute to the analytical signal. The AlF^{2+} and AlF_2^+ complexes are retained quantitatively and therefore contribute to the measurement of reactive Al. The method has been applied to humic waters and soil solutions and the results for 'free' Al^{3+} compared with those obtained by the 7 s CAS method. The method

has a DL of $60 \text{ nmol Al L}^{-1}$, a linear working range of $0.3\text{--}16 \text{ }\mu\text{mol Al L}^{-1}$ and RSD of 3 % and 1 % at 1.0 and $16 \text{ }\mu\text{mol Al L}^{-1}$ respectively.

Several channels exist for the further of development this Al speciation method. Following the injection of sample a peak is observed at the detector due to Al that was not captured by the column but 'does' react with the CAS reagent. This Al is likely to be 'moderately labile Al' which was not sufficiently labile to be complexed by the oxine column during its short residence time. It may be possible to quantify this peak and relate it to *moderately labile Al*. The investigation of polymeric Al (*e.g.* Al_{13}) revealed that Al-polymers may be complexed by the oxine column but not eluted upon the 'first' elution step. Subsequent work by several colleagues has indicated that it may be possible to obtain a 'useful' elution signal from the adsorbed polymeric Al (using a different volume of 'stop-flow' eluent) and quantify this fraction of Al in samples immediately following the determination of 'reactive Al'. If a total of three fractions of Al can be estimated from a single sample injection, *i.e.* those of (i) *fast reactive Al*, (ii) *moderately reactive Al* and (iii) *polymeric Al*, then this method may offer a novel opportunity to analysts probing the speciation of Al in natural waters and soil solutions.

Furthermore, potential exists for the use of micro-columns of oxine in field studies whereby sample collection is made in the field by injection of a sample through a suitable column and analysis is made at a later time back in the laboratory. Such procedures may offer advantages regarding sample collection and storage prior to analysis.

CHAPTER 9

CONCLUSIONS

The primary objective of this thesis was to develop a speciation protocol for Al in natural waters and soil solution. A significant component of this work involved the investigation of factors that might influence the accuracy of the speciation results. To this extent, it was of primary importance that any speciation protocol developed should be thoroughly tested. This was to ensure that the detection signal was a result of the 'targeted Al-species' and not from known interferents or 'unspecified' Al species. It was desired that the approach taken in method development work should be based on a sound knowledge of the equilibrium reactions between the reagent and Al.

9.1 INTERACTIONS OF PCV WITH Al^{3+} AND THE Al-OXIDE HYDROXIDE BOEHMITE

Pyrocatechol violet (PCV) is a metallochromic ligand that has been used extensively as a reagent for the determination of Al. An integral part of this thesis was a detailed investigation the equilibria in the H^+ - Al^{3+} -PCV system by potentiometry (and spectrophotometry). These studies allowed the development of a complete thermodynamic model describing these equilibria. The results indicate a complex, yet logical, speciation of this system over the pH range 2.0 - 10.0. PCV was found to complex Al strongly over this entire pH range; complexation was predominantly *via* the 2-hydroxy-*p*-quinomethide moiety at $\text{pH} < 4.5$, whereas at $\text{pH} > 6.0$ complexation occurs *via* the 1,2-dihydroxyaryl moiety. At low PCV/Al molar ratios polynuclear mixed hydroxo species were required in the model to adequately explain the data. Spectrophotometric studies showed that the model, determined for millimolar solutions, was also valid for micromolar concentrations. The dominant species, forming to greater than 95 %, from $5.7 \leq \text{pH} \leq 6.3$ was $\text{Al}(\text{HL})_2^{3-}$; consistent with spectrophotometric molar ratio plots.

Colloids in natural waters, sediments and soil solution represent large surface areas on which adsorption (of anions or cations) or complexation (of organic or inorganic anions) may occur. These surfaces carry a significant proportion of the humic substances 'dissolved' in natural waters and so could control the availability of ligands that mask Al toxicity. Such surfaces have the potential to interfere in the use of metallochromic or redox active ligands for the speciation of Al^{3+} . The adsorption behaviour of PCV on the surface of the aluminium-oxide hydroxide boehmite [α - $\text{AlO}(\text{OH})$] was investigated.

In these studies surface complexation of PCV at the boehmite-water interface was evaluated on the basis of the electrostatic constant capacitance model. This model allowed thermodynamic equilibria to be evaluated in the same manner as solution equilibria. As a prerequisite to studying the ligand adsorption behaviour the acid/base

properties of the surface hydroxy groups at the boehmite-solution interface were investigated. The results from these preliminary studies were in excellent agreement with those obtained previously. In the studies of the 3-component system, H^+ -{boehmite}-PCV, binuclear complexes were observed to form, *i.e.* the PCV molecule bridged two metal centres. The treatment of these species required the re-formulation of the mass balance equations to describe a binuclear binding site at the boehmite surface where adjacent hydroxy groups were identical and dependent. Surface complexation of PCV was observed to be weak and surface saturation could not be reached. Adsorption behaviour was described by the formation of two species.

A calculation, using the developed model, indicated that in the presence of excess PCV, 1 mg L^{-1} ($\mu\text{g L}^{-1}$) of boehmite will remove approximately 0.1 mmol (μmol) PCV from solution. Typical natural water concentrations of Fe and Al oxide materials are *ca.* 10 mg L^{-1} . Studies of the adsorption of PCV at micromolar concentrations on boehmite (at concentrations typical of a natural water) revealed that PCV was adsorbed at only *ca.* 60 % of that predicted by the model. The significant discrepancy between the model predictions and the experimental results was related to the use of a buffer (MES) in the latter experiments. It is likely that the buffer (at millimolar concentrations) is electrostatically attracted to the boehmite surface and blocks sufficient surface sites to affect the adsorption of PCV. The results from these studies indicated that reagents like PCV could be expected to be adsorbed by naturally occurring Fe and Al oxide surfaces. However, it was also observed that buffer present in reagent solutions may block much of this adsorption behaviour. Since test solutions are usually filtered prior to storage or immediately before analysis then the effects of reagent-adsorbing materials on the analysis results are likely to be negligible. The effect of PCV on the dissolution of boehmite was observed to be negligible over the pH range 5.0 - 8.0 and, as a result, errors due to oxide particle dissolution would be expected to be negligible on the time scale used in Al analysis techniques.

9.2 EVALUATION OF INTERFERENCES BY COMPUTER MODELLING AND EFFECTS OF COMPLEXATION KINETICS ON THE DETERMINATION OF 'LABILE' Al

The evaluation of interferences and the optimisation of analysis conditions for analytical methods is usually carried out *via* a trial-and-error approach whereby the parameters such as pH and reagent concentration are manipulated to achieve minimal effect from interferents and the greatest detection signal. In speciation analyses, this optimisation procedure is further complicated by the need to target a single analyte species.

An alternative to the trial-and-error approach is to use equilibrium constants to model the effects of interferents. Thermodynamic speciation calculations allow an analyst

to predict the behaviour of metal ions in complex multi-ligand environments. In these calculations, thermodynamic data (usually determined in non-competitive, H^+-M^{n+} -ligand, systems) are used together with total and/or free concentrations of reacting components in order to calculate the equilibrium concentrations of individual species. In this work the data determined for the H^+-Al^{3+} -PCV system, appropriate data for the H^+-Al^{3+} -chrome azurol S (CAS) and H^+-Al^{3+} -eriochrome cyanine R (ECR) systems respectively, and equilibrium data for H^+-Al^{3+} -ligand systems were used to calculate results for the competitive equilibria system: H^+-Al^{3+} -reagent-ligand. The ligands (potential interferents) used were citrate, oxalate, salicylate and fluoride (representing ligands with Al-complexing properties 'typical' of soils and natural waters) and calculations were performed over the pH range 4.5 - 6.5.

The equilibrium calculations showed that PCV is the chromophore that could be used most effectively for the determination of total Al (least susceptible to interference from Al-binding ligands). The results of the equilibrium interference calculations showed that PCV's susceptibility to interference decreased with increasing pH, regardless of the competing ligand. In contrast, CAS and ECR reflected the pH dependence of Al complexing by the interferent ligand. Organic matter from soils and natural waters contains both salicylate and carboxylate functional groups. Therefore, manipulating pH to minimise interference when using CAS or ECR is a futile exercise in soil and water analysis.

The focus of this thesis is aimed at measuring the 'labile' and hence toxic fraction of Al in environmental samples. However, since these analyses usually utilise 'kinetic' methodologies to distinguish between species of differing reactivity then thermodynamic calculations provide significantly less information on the potential of a ligand for this purpose. In natural water and soil environments, Al exists in competitive equilibria with a large number of naturally occurring ligands. Natural systems are quite 'dynamic' and the kinetics of chemical processes may be particularly important in controlling speciation at any instant. For speciation measurements it is desirable that the reagent should only interact with free Al, *i.e.* Al^{3+} , $Al(OH)^{2+}$, $Al(OH)_2^+$. Unfortunately, most reagents used for the determination of Al (which react rapidly and form strong complexes with Al) are likely to sequester significant amounts of Al from both weak and moderate strength Al complexes.

The kinetics of complexation and dissociation processes affect the results obtained during the analysis of 'labile Al' and these effects may be different for different sample compositions. The time scales for the establishment of equilibrium in competitive H^+-Al^{3+} -ligand(L)-PCV systems were investigated. The ligands citrate and oxalate were investigated in detail whereas a series of other ligands were investigated through simple batch experiments. The former of these experiments further validated the Al-PCV thermodynamic model for spectrophotometric conditions. The establishment of

equilibrium in the $H^+ - Al^{3+} - L - PCV$ systems required greater than 300 min (180 min) for $L =$ citrate (oxalate). These results indicate that thermodynamic approximations of speciation in analyses utilising kinetic (non-equilibrium) methods are not expected to be very useful.

In a series of batch experiments the effect of the mixing-order for the sample (in the presence or absence of a 'second' Al-complexing ligand), reagent and buffer on speciation results was investigated. These experiments revealed that rates of colour development (upon addition of Al) depended strongly on the 'second ligand'. Rates of colour development were: oxalate $\approx F^- \approx$ malonate $>$ salicylate \gg no second (competing) ligand $>$ citrate. Following a 24 h equilibration period, PCV displaced Al quantitatively from all of the ligands. The observations in these experiments can be explained in terms of an 'hydrolysis shock'. This occurs when the pH of a solution containing Al is suddenly increased, *i.e.* Al immediately undergoes hydrolysis. In the presence of a ligand which reacts quickly with Al, Al-hydrolysis is countered and then ligand-exchange reactions between PCV and the 'second' ligand can proceed quickly. PCV alone does not react quickly enough with Al to significantly reduce hydrolysis.

The effect of a second ligand is a potential problem in FIA if the sample and PCV are brought together at the analytical pH (a scenario common to many FIA systems for the spectrophotometric detection of metal ions). Since analyses are performed under non-equilibrium conditions, the presence of a small amount of F^- , say, might result in rate enhancements relative to Al standards (absence of a 'second-ligand').

9.3 DEVELOPMENT OF CHEMICAL AND/OR ELECTROCHEMICAL PROBES FOR THE AQUEOUS Al^{3+} ION (Al^{3+})

Flow injection techniques utilising electrochemical detection may offer several advantages over other detection procedures (*e.g.* spectrophotometric or fluorimetric detection) in that analyses may be performed rapidly using relatively cheap apparatus. The initial focus of this thesis was towards the development of an electrochemical method (amperometric or voltammetric) for the determination of Al in environmental samples. Electrochemical analysis of Al generally requires an 'indirect' approach *via* a ligand whose redox chemistry is significantly affected by binding of Al.

The Al-binding and electrochemical properties of a series of ligands were evaluated with the intention that suitable ligands could be utilised in the development of an electrochemical method for the determination of Al. Of the ligands examined, PCV and tetrahydroxy-1,4-quinone (THQ) showed a linear decrease in the oxidation peak i_p^a (*vs.* SCE) as a function of Al concentration. These results indicated that all Al-PCV species present in solution at pH 6.2 and 8.5 are not electroactive. These ligands were investigated for the development of electrochemical detection systems applicable to FIA of

Al in environmental samples. It was apparent that PCV has the greater potential for this application. The detection limit (DL) was $0.04 \mu\text{mol Al L}^{-1}$ and a linear working range (LWR) was observed from 0.2 to $10.0 \mu\text{mol Al L}^{-1}$. Results for THQ were not as promising. However, provided care was taken to thoroughly exclude oxygen from the reagent solution, a DL of $0.5 \mu\text{mol Al L}^{-1}$ and a LWR of 0.5 to $10.0 \mu\text{mol Al L}^{-1}$ was obtainable.

An unfortunate feature of indirect methods of analysis (whereby the response of a 'probe ligand' which complexes Al is monitored as a function of Al concentration) is that these methods are prone to interference from other metal ions that interact with the 'probe' ligand. Fe^{3+} binds with the same types of ligands that complex Al^{3+} . In spectrophotometric and fluorimetric procedures interference from Fe^{3+} can often be masked using suitable 'masking agents', *e.g.* bipyridine/ or 1,10-phenanthroline/ascorbic acid. However, in electrochemical analyses of Al such masking agents are not appropriate because of their inclination to undergo redox reactions. Furthermore, Fe masking agents are less appropriate to speciation analyses because disruptions caused to Fe-NOM equilibria will also affect Al-NOM equilibria (NOM = natural organic matter).

The final section of work in this thesis addressed the subject of on-line matrix separation and/or analyte preconcentration for the flow-through speciation of Al in natural waters and soil solutions. In this work, the development of an Al speciation technique which may be used without the use of additional masking agents for Fe was investigated. An FIA system incorporating a micro-column packed with a suitable sorbent material was proposed as the best method for this analysis. This technique involved the direct measurement of 'reactive' Al through the selective capture of Al on an oxine-derivatised gel in a microcolumn (incorporated in an FIA system).

In this method the speciation of Al^{3+} was effected by 2 s reaction with oxine-derivatised Fractogel in a $22 \mu\text{L}$ column reactor in an FIA manifold. Al^{3+} (pre)concentrated on the column from a $650 \mu\text{L}$ sample was selectively eluted with $150\text{--}250 \mu\text{L}$ 0.02 mol L^{-1} NaOH and detected spectrophotometrically as the Al-CAS (chrome azurol S) complex at pH 5.0. Consequently, both Al and Fe were selectively retained by the chelating resin, however only the 'captured' Al was eluted and subsequently detected.

Tests with synthetic solutions established that Al was not significantly sequestered from the citrate, oxalate and malonate complexes. Al-hydroxy polymers $[\text{Al}_{13}(\text{OH})_{32}^{7+}]$ were quantitatively retained by the column but were not desorbed by 0.02 mol L^{-1} NaOH in the time frame of the FIA method; therefore they do not contribute to the analytical signal. The AlF^{2+} and AlF_2^+ complexes were retained quantitatively and therefore contribute to the measurement of reactive Al. The method was applied to humic waters and soil solutions and the results for 'free' Al^{3+} were compared with those

obtained by the 7 s CAS method. The method had a DL of 60 nmol L^{-1} , a LWR of 0.3 to $16 \text{ } \mu\text{mol L}^{-1}$ and RSD of 3 % and 1 % at 1.0 and $16 \text{ } \mu\text{mol L}^{-1}$ respectively.

In regard to the speciation of Al in natural waters (*i.e.* the measurement of 'reactive Al') this method is possibly the most effective currently available. The limitations of many of the earlier methods [Driscoll, 1984; Clarke *et al.*, 1992; Hawke and Powell, 1994; Clarke and Danielsson, 1995] are discussed in Chapter 1 (1.3). In the currently described method, analysis is rapid in comparison to Driscoll's method and free Al is measured directly (not as the difference between two other fractions). The methods by Clarke *et al.* and Hawke and Powell measure similar fractions to this method. However, Clarke *et al.* use reagent concentrations which may promote sequestering of Al from organic complexes. Furthermore, the buffer contained significant concentrations of Fe^{3+} masking agents. This can result in ligands that were initially complexing Fe^{3+} becoming free and immediately capturing free Al and resulting in further disturbances to the samples' natural equilibria. The method of Hawke and Powell has insufficient on-line buffering for the analysis of moderately acidic or alkaline samples.

Several channels exist for the further development of the currently described Al speciation method. Following the injection of sample a peak is observed at the detector due to Al that was not captured by the column but 'does' react with the CAS reagent. This Al is likely to be 'moderately labile Al' which was not sufficiently labile to be complexed by the oxine column during its short residence time. It may be possible to quantify this peak and relate it to *moderately labile Al*. The investigation of polymeric Al (*e.g.* Al_{13}) revealed that Al-polymers may be complexed by the oxine column but not eluted upon the 'first' elution step. If a total of three fractions of Al can be estimated from a single sample injection, *i.e.* those of (i) *fast reactive Al*, (ii) *moderately reactive Al* and (iii) *polymeric Al*, then this method may offer a novel opportunity to analysts probing the speciation of Al in natural waters and soil solutions.

Furthermore, potential exists for the use of micro-columns of oxine-derivatised gel in field studies whereby sample collection is made in the field by injection of a sample through a suitable column and analysis is made at a later time back in the laboratory. Such procedures may offer advantages for sample collection and storage prior to analysis.

REFERENCES

- Abd El Kader, J. M., Shams El Din, A. M., Kastening, B. and Holleck, L. (1970) Polarographic behaviour of alizarin and alizarin S and formation of aluminium complexes in methanolic solution. *J. Electroanal. Chem. Interfacial Electrochem.*, **26**, 41-51.
- Abollino, O., Mentasti, E., Porta, V. and Sarzanini, C. (1990) Immobilised 8-oxine units on different solid sorbents for the uptake of metal traces. *Anal. Chem.*, **62**, 21-26.
- Abreo, K. and Glass, J. (1993) Cellular, biochemical and molecular mechanisms of aluminium toxicity. *Nephrol. Dial. Transplant*, **8**, 5-11.
- Ågren, A. (1955) The complex formation between Iron(III) ion and some phenols, IV. The acidity constant of the phenolic group. *Acta Chem. Scand.*, **9**, 49-56.
- Alexandersson, D. and Vannerberg, N.-G. (1972) The stability constants of squaric acid and rhodizonic acid. *Acta. Chem. Scand.*, **26**, 1909-1920.
- Alfrey, A. C., Mishell, J. M., Burks, J., et al. (1972) Syndrome of dyspraxia and multifocal seizures associated with chronic haemodialysis. *Trans. Amer. Soc. Artif. Int. Organs*, **18**, 257-261.
- Alva, A. K., Blamey, F. P. C., Edwards, D. G. and Asher, C. J. (1986a) An evaluation of aluminium indices to predict aluminium toxicity to plants grown in nutrient solutions. *Commun. Soil Sci. Plant Anal.*, **17**, 1271-1280.
- Alva, A. K., Edwards, D. G., Asher, C. J. and Blamey, F. P. C. (1986b) Effects of phosphorous/aluminium molar ratio and calcium concentration on plant response to aluminium toxicity. *Soil Sci. Soc. Am. J.*, **50**, 133-137.
- Alva, A. K., Edwards, D. G., Asher, C. J. and Blamey, F. P. C. (1986c) Relationships between root length of soybean and calculated activities of aluminium monomers in solution. *Soil Sci. Soc. Am. J.*, **50**, 959-962.
- Alva, A. K., Summer, M. E., Li, Y. C. and Miller, W. P. (1989) Evaluation of three aluminium assay techniques for excluding aluminium complexed with fluoride or sulfate. *Soil Sci. Soc. Am. J.*, **53**, 38-44.
- Alveteg, M., Sverdrup, H. and Warfvinge, P. (1995) Developing a kinetic alternative in modelling soil aluminium. *Water Air Soil Pollut.*, **79**, 377-389.
- Anderson, M. A. and Malotky, D. T. (1979) The adsorption of protolysable anions on hydrous oxides at the isoelectric pH. *J. Colloid Interface Sci.*, **72**, 413-427.
- Anderson, H. A., Berrow, M. L., Farmer, V. C., et al. (1982) A re-assessment of the podzol formation process. *J. Soil Sci.*, **33**, 125-136.

- Anderson, M. A. and Bertsch, P. M.** (1988) Dynamics of aluminium complexation in multiple ligand systems. *Soil Sci. Soc. Am. J.*, **52**, 1597-1602.
- Andersson, M.** (1988) Toxicity and tolerance of aluminium in vascular plants. *Water Soil Air Pollut.*, **39**, 439-462.
- Ares, J.** (1986) Identification of aluminium species in acid forest soil solution on the basis of Al:F reaction kinetics: 2. An example at the Solling area. *Soil Sci.*, **142**, 13-19.
- Ares, J.** (1990) Fluoride-aluminium water chemistry in forest ecosystems of Central Europe. *Chemosphere*, **21**, 597-612.
- Arp, P. A. and Strucel, I.** (1989) Water uptake by black spruce seedlings from rooting media (solution, sand, peat) treated with inorganic and oxalated aluminium. *Water Air Soil Pollut.*, **44**, 57-70.
- Arrigan, D. W. M., Deasy, B., Glennon, J. D., Johnston, B. and Svehla, G.** (1993) Incorporation of hydroxamic acid ligands into nafion film electrodes. *Analyst*, **118**, 355-359.
- Bache, B. W. and Sharp, G. S.** (1976) Soluble polymeric hydroxy-aluminium ions in acid soils. *J. Soil. Sci.*, **27**, 167-174.
- Bache, B. W.** (1986) Aluminium mobilisation in soils and waters. *J. Geological Soc. (London)*, **143**, 699-706.
- Backes, C. A. and Tipping, E.** (1987) An evaluation of the use of cation-exchange resin for determination of organically-complexed Al in natural acid waters. *Int. J. Environ. Anal. Chem.*, **30**, 135-143.
- Backstrom, K., Danielsson, L. and Nord, L.** (1986) Design and evaluation of a new phase separator for liquid-liquid extraction in flow systems. *Anal. Chim. Acta*, **169**, 43-49.
- Backstrom, K., Danielsson, L. and Nord, L.** (1986) Dispersion in phase separators for flow injection systems. *Anal. Chim. Acta*, **187**, 255-269.
- Baes, C. F. and Mesmer, R. E.** (1986) *The hydrolysis of cations*. Wiley, New York.
- Bailey, S. W., Driscoll, C. T. and Hornbeck, J. W.** (1995) Acid-base chemistry and aluminium transport in an acidic watershed and pond in New Hampshire. *Biogeochem.*, **28**, 69-91.
- Baker, J. P. and Schofield, C. L.** (1982) Al toxicity to fish in acidic waters. *Water Air Soil Pollut.*, **18**, 289-309.
- Baksi, K. and Pal, B. K.** (1994) Non-extractive spectrophotometric determination of aluminium in real, environmental and biological samples using chromotropic acid. *Talanta*, **41**, 81-87.

- Baligar, V. C., Wright, R. C., Kinraide, T. B., Foy, C. D. and Elgin, J. H. (1987) Aluminium effects on growth, mineral uptake and efficiency ratios in red clover cultivars. *Agron. J.*, **79**, 1038-1044.
- Baligar, V. C., Campbell, T. A. and Wright, R. J. (1993a) Differential responses of alfalfa clones to aluminium-toxic acid soil. *J. Plant Nutrition*, **16**, 219-233.
- Baligar, V. C., Schaffert, R. E., Dos Santos, H. L., Pitta, G. V. E. and Bahia Filho, A. F. (1993b) Soil aluminium effects on uptake, influx and transport of nutrients in sorghum genotypes. *Plant Soil*, **150**, 271-277.
- Barcelo, J., Guevara, P. and Poschenrieder, C. (1993) Silicon amelioration of aluminium toxicity in teosinte (*Zea mays* L. sp. *mexicana*). *Plant Soil*, **154**, 249-255.
- Barnes, R. B. (1975) The determination of specific forms of aluminium in natural water. *Chem. Geol.*, **15**, 177-191.
- Barnes, R. M. and Genna, J. S. (1979) Concentration and spectrochemical determination of trace metals in urine with a poly(dithiocarbamate) resin and inductively coupled plasma-atomic emission spectrometry. *Anal. Chem.*, **51**, 1065-1070.
- Barnes, R. M., Fodor, P., Inagaki, K. and Fodor, M. (1983) Determination of trace elements in urine using inductively coupled plasma spectroscopy with a poly(dithiocarbamate) chelating resin. *Spectrochim. Acta*, **38B**, 245-257.
- Barnes, R. M. and Shang-Jing, L. (1983) Application of a poly(acrylamidoxime) resin for concentration and inductively coupled plasma spectroscopy for determination of trace elements in reagent-grade chemicals and dialysis solution. *Can. J. Spectrosc.*, **28**, 139-145.
- Barnes, R. M. (1984) Determination of trace elements in biological materials by inductively coupled plasma spectroscopy with novel chelating resins. *Bio. Trace Element Res.*, **6**, 93-103.
- Barrero, J. M., Moreno-Bondi, M. C., Pérez-Conde, M. C. and Cámara, C. (1993) A biosensor for ferric ion. *Talanta*, **40**, 1619-1623.
- Barrero, J. M., Cámara, C., Pérez-Conde, M. C., San José, C. and Fernández, L. (1995) Pyoverdine-doped Sol-Gel glass for the spectrofluorimetric determination of iron(III). *Analyst*, **120**, 341-435.
- Bartlett, R. J., Ross, D. S. and Magdoff, F. R. (1987) Simple kinetic fractionation of reactive aluminium in soil "solutions". *Soil Sci. Soc. Am. J.*, **51**, 1479-1482.
- Bassett, J., Denney, R. C., Jeffery, G. H. and Mendham, J. (1978) *Vogel's textbook of quantitative inorganic analysis, including elementary instrumental analysis (4th edition)*. Longman, New York.

- Bates, R. G.** (1973) *Determination of pH, theory and practice (2nd edition)*. John Wiley & Sons, New York.
- Baylis, A. D., Gragopoulou, C., Davidson, K. J. and Birchall, J. D.** (1994) Effect of silicon on the toxicity of aluminium to soybean. *Commun. Soil Sci. Plant Anal.*, **25**, 537-546.
- Beauchemin, D. and Berman, S. S.** (1989) Determination of trace metals in reference water standards by inductively coupled plasma mass spectrometry with on-line preconcentration. *Anal. Chem.*, **61**, 1857-1862.
- Berggren, D. and Fiskesjö, G.** (1987) Aluminium toxicity and speciation in soil liquids - experiments with *allium cepa* L. *Environ. Toxicol. Chem.*, **6**, 771-779.
- Berggren, D.** (1989) Speciation of aluminium, cadmium, copper, and lead in humic soil solutions - a comparison of the ion exchange column procedure and equilibrium dialysis. *Int. J. Environ. Anal. Chem.*, **35**, 1-15.
- Berry, D. F., Zelazny, L. W. and Walker, H. L.** (1990) Aluminium and organic matter mobilisation from forest soil infiltrated with acidified calcium sulfate solutions. *Soil Sci. Soc. Am. J.*, **54**, 1757-1762.
- Bertsch, P. M.** (1987) Conditions for Al_{13} polymer formation in partially neutralised aluminium solutions. *Soil Sci. Soc. Am. J.*, **51**, 825-829.
- Bertsch, P. M.** (1989) Aqueous polynuclear aluminium species. **In:** *The environmental chemistry of aluminium*. (Ed: G. Sposito) CRC Press, Boca Raton, Florida.
- Bertsch, P. M.** (1990) The hydrolytic products of aluminium and their biological significance. *Environ. Geochem. Health*, **12**, 7-14.
- Bi, S.** (1995) Investigation of the factors influencing aluminium speciation in natural water equilibria with the mineral phase gibbsite. *Analyst*, **120**, 2033-2039.
- Biedermann, G. and Sillén, L. G.** (1952) Studies on the hydrolysis of metal ions. IV. Liquid junction potentials and constancy of activity factors in $NaClO_4$ - $HClO_4$ ionic medium. *Ark. Kemi.*, **5**, 425-440.
- Biedermann, G.** (1975) The nature of seawater. **In:** *The nature of seawater*. (Ed: E. D. Goldberg) Dahlem Konferenzen, Berlin.
- Biernat, J. F., Konieczka, P., Tarbet, B. J., Bradshaw, J. S. and Izatt, R. M.** (1994) Complexing and chelating agents immobilised on silica gel and related materials and their application for sorption of inorganic species. *Separation Purification Methods*, **23**, 77-348.
- Birchall, J. D., Exley, C., Chappell, J. S. and Phillips, M. J.** (1989) Acute toxicity of aluminium to fish eliminated in silicon-rich acid waters. *Nature*, **338**, 146-148.

- Birchall, J. D. and Chappell, J. S.** (1989) Aluminium, water chemistry, and Alzheimer's disease. *Lancet*, **1**, 953.
- Birchall, J. D.** (1990) The role of silicon in biology. *Chem. Brit.*, 141-144.
- Biryuk, E. A. and Ravitskaya, R. V.** (1970) Ionisation constants of pyrocatechol violet in solutions with ionic strengths ranging from 0 to 1. *Zh. Anal. Khim.*, **25**, 576-578.
- Bjerrum, N.** (1915) *Kgl. Danske Videnskab. Selskabs Skrifter.*, **12**, 4.
- Blain, S., Appriou, P. and Handel, H.** (1993) Preconcentration of trace metals from sea water with the chelating resin chelamine. *Anal. Chim. Acta*, **272**, 91-97.
- Blamey, F. P. C., Edwards, D. G. and Asher, C. J.** (1983) Effects of aluminium, OH:Al and P:Al molar ratios, and ionic strength on soybean root elongation in solution culture. *Soil Sci.*, **136**, 197-207.
- Blamey, P. and Asher, C.** (1993) Aluminium toxicity - a treat to food production. *Search*, **24**, 296-298.
- Blamey, F. P. C., Asher, C. J., Edwards, D. G. and Kerven, G. L.** (1993a) Factors affecting aluminium sorption by calcium pectate. *Plant Soil*, **149**, 87-94.
- Blamey, F. P. C., Asher, C. J., Edwards, D. G. and Kerven, G. L.** (1993b) *In vitro* evidence of aluminium effects on solution movement through root cell walls. *J. Plant Nutr.*, **16**, 555-562.
- Bloom, P. R., McBride, M. B. and Weaver, R. M.** (1979) Aluminium organic matter in acid soils: buffering and solution aluminium activity. *Soil Sci. Soc. Am. J.*, **43**, 488-493.
- Bloom, P. R.** (1981) Metal-organic matter interactions in soil. **In:** *Chemistry in the environment*. (Ed: Am. Soc. Agronomy, Soil Sci. Soc. Am., Madison, WI).
- Bloom, P. R.** (1983) The kinetics of gibbsite dissolution in nitric acid. *Soil Sci. Soc. Am. J.*, **47**, 164-168.
- Bond, A. M. and Wallace, G. G.** (1984) Liquid chromatography with electrochemical and/or spectrophotometric detection for automated determination of lead, cadmium, mercury, cobalt, nickel, and copper. *Anal. Chem.*, **56**, 2085-2090.
- Boniforti, R., Ferraroli, R., Frigieri, P., Heltai, D. and Queirazza, G.** (1984) Intercomparison of five methods for the determination of trace metals in seawater. *Anal. Chim. Acta*, **162**, 33-46.
- Booth, C. E., McDonald, D. G., Simons, B. P. and Wood, C. M.** (1988) Blood gases, acid-base status, ions and haematology in adult brook trout (*Salvelinus fontinalis*) under acid/aluminium exposure. *Can. J. Fish. Aquat. Sci.*, **45**, 1563-1574.

- Boutot, J.-P., Merlet, D., Rouiller, J. and Maitat, O.** (1994) Validation of an operational procedure for aluminium speciation in soil solution and surface waters. *Sci. Tot. Environ.*, **158**, 237-252.
- Bowen, H. J. M.** (1966) *Trace elements in biochemistry*. Academic Press, New York.,
- Bowers, A. R. and Huang, C. P.** (1985) Adsorption characteristics of polyacetic amino acids onto hydrous γ -Al₂O₃. *J. Colloid Interface Sci.*, **105**, 197-215.
- Bradford, G. R. and Bakhtar, D.** (1991) Determination of trace metals in saline irrigation drainage waters with inductively coupled plasma optical emission spectrometry after preconcentration by chelation-solvent extraction. *Environ. Sci. Technol.*, **25**, 1704-1708.
- Brown, A. S.** (1934) A type of silver chloride electrode suitable for use in dilute solutions. *J. Am. Chem. Soc.*, **56**, 646-647.
- Brown, P. L., Sylva, R. N., Batley, G. E. and Ellis, J.** (1985) The hydrolysis of metal ions. Part 8. Aluminium(III). *J. Chem. Soc. Dalton Trans.*, 1967-1970.
- Brown, J. A. and Whitehead, C.** (1995) Catecholamine release and interrenal response of brown trout, *Salmo-trutta*, exposed to aluminium in acidic water. *J. Fish Biol.*, **46**, 524-535.
- Browne, B. A., McColl, J. G. and Driscoll, C. T.** (1990a) Aluminium speciation using morin: I. Morin and its complexes with aluminium. *J. Environ. Qual.*, **19**, 65-72.
- Browne, B. A., Driscoll, C. T. and McColl, J. G.** (1990b) Aluminium speciation using morin: II. Principles and procedures. *J. Environ. Qual.*, **19**, 73-82.
- Browne, B. A. and Driscoll, C. T.** (1992) Soluble aluminium silicates: stoichiometry, stability, and implications for environmental geochemistry. *Science*, **256**, 1667-1670.
- Buckler, D. R., Cleveland, L., Little, E. E. and Brumbaugh, W.** (1995) Survival, sublethal responses, and tissue residues of Atlantic salmon exposed to acidic pH and aluminium. *Aquat. Toxicol.*, **31**, 203-216.
- Burba, P. and Willmer, P. G.** (1987) Multielement preconcentration for atomic spectroscopy by sorption of dithiocarbamate-metal complexes (e.g., HMDC) on cellulose collectors. *Fresenius' J. Anal. Chem.*, **329**, 539-545.
- Burrows, W. D.** (1977) Aquatic aluminium: chemistry, toxicity, and environmental prevalence. *CRC Crit. Rev. Environ. Control*, **7**, 167-216.
- Cai, Q. and Khoo, S. B.** (1993) Determination of trace aluminium by differential pulse adsorptive stripping voltammetry of aluminium(III)-8-hydroxyquinoline complex. *Anal. Chim. Acta*, **276**, 99-108.

- Cameron, R. S., Ritchie, G. S. P. and Robson, A. D.** (1986) Relative toxicities of inorganic aluminium complexes to barley. *Soil Sci. Soc. Am. J.*, **50**, 1231-1236.
- Campbell, P. G. C., Bisson, M., Bougie, R., Tessier, A. and Villeneuve, J.-P.** (1983) Speciation of aluminium in acidic freshwaters. *Anal. Chem.*, **55**, 2246-2252.
- Candy, J. M., Klinowski, J., Perry, R. H., et al.** (1986) Aluminosilicates and senile plaque formation in Alzheimer's disease. *Lancet*, **1**, 354-357.
- Cañizares, P. and Luque de Castro, M. D.** (1994) Fluorometric flow-through sensor for aluminium speciation. *Anal. Chim. Acta*, **295**, 59-65.
- Carr, S. J., Ritchie, G. S. P. and Porter, W. M.** (1991) A soil test for aluminium toxicity in acidic subsoils of yellow earths in Western Australia. *Aust. J. Agric. Res.*, **42**, 875-892.
- Carr, S. J. and Ritchie, G. S. P.** (1993) Al toxicity of wheat grown in acidic subsoils in relation to soil solution properties and exchangeable cations. *Aust. J. Soil Res.*, **31**, 583-596.
- Carrera, M. E., Rodríguez, V., Toral, M. I. and Richter, P.** (1993) Voltametric determination of aluminium in haemodialysis concentrates using the adsorption of the Al(III)-1,2-dihydroxyanthraquinone-3-sulphonic acid complex in presence of calcium. *Anal. Lett.*, **26**, 2575-2585.
- Chalk, S. J. and Tyson, J. F.** (1994) Comparison of the maximum sensitivity of different flow injection manifold configurations: alternating variable search optimisation of the iron(II)/1,10-phenanthroline system. *Anal. Chem.*, **66**, 660-666.
- Chappell, J. S. and Birchall, J. D.** (1988) Aspects of the interaction of silicic acid with aluminium in dilute solution and its biological significance. *Inorg. Chim. Acta*, **153**, 1-4.
- Chazan, J. A., Lew, N. L. and Lowrie, E. G.** (1991) Increased serum aluminium. An independent risk factor for mortality in patients undergoing long-term haemodialysis. *Arch. Intern. Med.*, **151**, 319-322.
- Chiacchierini, E., Marini, D. and Gagli, A.** (1974) The reaction of pyrocatechol violet with iron(III) and aluminium(III) in aqueous medium. *Gazz. Chim. Ital.*, **104**, 1257-1267.
- Childs, C. W., Parfitt, R. L. and Lee, R.** (1983) Movements of aluminium as an inorganic complex in some podsolised soils. *Geoderma*, **29**, 139-155.
- Chow, P. Y. T. and Cantwell, F. F.** (1988) Calcium sorption by immobilised oxine and its use in determining free calcium ion concentration in aqueous solution. *Anal. Chem.*, **60**, 1569-1573.

- Clark, G. D., Whitman, D. A., Christian, G. D. and Ruzicka, J. (1990) Sample handling and pretreatment using flow injection analysis. *Crit. Rev. Anal. Chem.*, **21**, 357-375.
- Clarke, N., Danielsson, L.-G. and Sparén, A. (1992) The determination of quickly reacting aluminium in natural waters by kinetic discrimination in a flow system. *Intern. J. Environ. Anal. Chem.*, **48**, 77-100.
- Clarke, N. (1994) *Speciation of aluminium and iron in natural fresh waters*. Ph.D. Thesis, The Royal Institute of Technology (KTH), Sweden.
- Clarke, N. and Danielsson, L.-G. (1995) The simultaneous speciation of aluminium and iron in a flow-injection system. *Anal. Chim. Acta*, **306**, 5-20.
- Clarke, N., Danielsson, L.-G. and Sparén, A. (unpub.) Analytical methodology for the determination of aluminium species in natural fresh waters. *Pure Appl. Chem.* (submitted).
- Cleveland, L., Little, E. E., Hamilton, S. J., Buckler, D. R. and Hunn, J. B. (1986) Interactive toxicity of aluminium and acidity to early life stages of brook trout. *Trans. Am. Fish. Soc.*, **115**, 610-620.
- Clevette, D. J., Nelson, W. O., Nordin, A., Orvig, C. and Sjöberg, S. (1989) Complexation of aluminium with N-substituted 3-hydroxy-4-pyridinones. *Inorg. Chem.*, **28**, 2079-2081.
- Clevette, D. J. and Orvig, C. (1990) Comparison of ligands of differing denticity and basicity for the *in vivo* chelation of aluminium and gallium. *Polyhedron*, **9**, 151-161.
- Cline, G. R. and Senwo, Z. N. (1994) Tolerance of lespedeza *bradyrhizobium* to acidity, aluminium and manganese in culture media containing glutamate or ammonium. *Soil Biol. Biochem.*, **26**, 1067-1072.
- Colella, M. B., Siggia, S. and Barnes, R. M. (1980a) Poly(acrylamidoxime) resin for determination of trace metals in natural waters. *Anal. Chem.*, **52**, 2347-2350.
- Colella, M. B., Siggia, S. and Barnes, R. M. (1980b) Synthesis and characterisation of a poly(acrylamidoxime) metal chelating resin. *Anal. Chem.*, **52**, 967-972.
- Conyers, M. (1990) The control of aluminium solubility in some acidic Australian soils. *J. Soil Sci.*, **41**, 147-156.
- Cotton, F. A. and Wilkinson, G. (1988) *Advanced inorganic chemistry (Fifth Edition)*. John Wiley & Sons, New York.
- Covington, A. K. and Prue, J. E. (1955) Precise measurement with the glass electrode. I. The cell: glass electrode|HCl|AgCl|Ag. *J. Chem. Soc.*, 3696-3700.

- Covington, A. K., Dobson, J. V. and Wynne-Jones, L. (1967) The calomel electrode-II. Further studies at 25 °C and measurements at other temperatures. *Electrochim. Acta*, **12**, 525-534.
- Covington, A. K. (1969) *Reference electrodes*. Nat. Bur. Stand., Washington, D.C.
- Covington, A. K., Bates, R. G. and Durst, R. A. (1983) Definition of pH scales, standard reference values, measurement of pH and related terminology. *Pure Appl. Chem.*, **55**, 1467-1476.
- Cox, A. G. and McLeod, C. W. (1986) Preconcentration and determination of trace Cr(III) by flow injection/inductively-coupled plasma emission spectrometry. *Anal. Chim. Acta*, **179**, 487-490.
- Cronan, C. S. and Schofield, C. L. (1979) Aluminium leaching response to acid precipitation: effects on high-elevation watersheds in the Northeast. *Science*, **204**, 304-306.
- Cronan, C. S., Walker, W. J. and Bloom, P. R. (1986) Predicting aqueous aluminium concentrations in natural waters. *Nature*, **324**, 140-143.
- Cronan, C. S., April, R., Bartlett, R. J., et al. (1989) Aluminium toxicity in forests exposed to acidic deposition: the ALBIOS results. *Water Air Soil Pollut.*, **48**, 181-192.
- Crosby, S. A., Butler, E. I., Turner, D. R., et al. (1981) Phosphate adsorption onto iron oxyhydroxides at natural concentrations. *Environ. Technol. Lett.*, **2**, 371-378.
- Crush, J. R. and Caradus, J. R. (1992) Response to soil aluminium of two white clover (*trifolium-repens* L) genotypes. *Plant Soil*, **146**, 39-43.
- Dahlgren, R. A. and Ugolini, F. C. (1989) Aluminium fractionation of soil solutions from unperturbed and Tephra-treated spodosols, Cascade Range, Washington, U.S.A. *Soil Sci. Soc. Am. J.*, **53**, 559-566.
- Dahlgren, R. A. and Walker, W. J. (1993) Aluminium release rates from selected Spodosol Bs horizons: effect of pH and solid-phase aluminium pools. *Geochim. Cosmochim. Acta*, **57**, 57-66.
- Dalziel, T. R. K., Morris, R. and Brown, D. J. A. (1986) The effects of low pH, calcium concentrations and elevated aluminium concentrations on sodium fluxes in brown trout, *Salmo trutta* L. *Water Air Soil Pollut.*, **30**, 569-577.
- Danielsson, L.-G. and Sparén, A. (1995) A mechanised system for the determination of low levels of quickly reacting aluminium in natural waters. *Anal. Chim. Acta*, **306**, 173-181.
- Das, A. K. (1989) Studies on mixed ligand complexes of cobalt(II), nickel(II), copper(II) and zinc(II) involving 8-hydroxyquinoline-5-sulphonic acid as a primary ligand and substituted catechols as secondary ligands. *Transition Met. Chem.*, **14**, 200-202.

- Das, J. and Pobi, M.** (1991) Separation of beryllium and aluminium from other elements using an ion-exchange resin with N-benzolphenylhydroxylamine as a functional group. *Anal. Chim. Acta*, **242**, 107-111.
- David, M. B. and Driscoll, C. T.** (1984) Aluminium speciation and equilibria in soil solutions of a haplorthod in the Adirondack mountains (New York, U.S.A.). *Geoderma*, **33**, 297-318.
- Davis, J. A., James, R. O. and Leckie, J. O.** (1978) Surface ionisation and complexation at the oxide/water interface 1. Computation of electric double layer properties in simple electrolytes. *J. Colloid Interface Sci.*, **63**, 480-499.
- Davis, J. A. and Leckie, J. O.** (1978) Effect of adsorbed complexing ligands on trace metal uptake by hydrous oxides. *Environ. Sci. Technol.*, **12**, 1309-1315.
- Davis, J. A. and Leckie, J. O.** (1980) Surface ionisation and complexation at the oxide/water interface 3. Adsorption of anions. *J. Colloid Interface Sci.*, **74**, 32-43.
- Davis, J. A. and Gloor, R.** (1981) Adsorption of dissolved organics in lake water aluminium oxide. Effect of molecular weight. *Environ. Sci. Technol.*, **15**, 1223-1229.
- Davis, J. A.** (1982) Adsorption of natural dissolved organic matter at the oxide/water interface. *Geochim. Cosmochim. Acta*, **46**, 2381-2393.
- Davis, J. A.** (1984) Complexation of trace metals by adsorbed natural organic matter. *Geochim. Cosmochim. Acta*, **48**, 679-691.
- Davis, J. A. and Kent, D. B.** (1990) Surface complexation modelling in aqueous geochemistry. In: *Mineral-Water Interface Geochemistry* (Ed: M. F. Hochella and White, A. F.) Reviews in mineralogy Mineralogical Society of America, Washington, DC.
- Deevey, E. S.** (1970) Mineral cycles. *Scientific American*, **223**, 148-158.
- Delhaize, E., Craig, S., Beaton, C. D., et al.** (1993a) Aluminium tolerance in wheat (*Triticum aestivum* L.) I. Uptake and distribution of aluminium in root apices. *Plant Physiol.*, **103**, 685-693.
- Delhaize, E., Ryan, P. R. and Randall, P. J.** (1993b) Aluminium tolerance in wheat (*Triticum aestivum* L.) II. Aluminium-stimulated excretion of malic acid from root apices. *Plant Physiol.*, **103**, 695-702.
- Delhaize, E. and Ryan, P. R.** (1995) Aluminium toxicity and tolerance in plants. *Plant Physiol.*, **107**, 315-321.
- Dietrich, D. and Schlatter, C.** (1989) Aluminium toxicity to rainbow trout at low pH. *Aquatic Toxicol.*, **15**, 197-242.

- Dingman, J., Gloss, K. M., Milano, E. A. and Siggia, S. (1974) Concentration of heavy metals by complexation on dithiocarbamate resins. *Anal. Chem.*, **46**, 774-779.
- Djane, N.-K., Malcus, F., Martins, E., Sawula, G. and Johnansson, G. (1995) Hollow fiber cartridges for removal of particulate matter from natural waters prior to matrix isolation and trace metal enrichment using an 8-quinolinol chelating ion exchanger in a flow system. *Anal. Chim. Acta*, **316**, 305-311.
- Doll, R. (1993) Review: Alzheimer's disease and environmental aluminium. *Age Ageing*, **22**, 138-153.
- Domingo, J. L., Gomez, M., Llobet, J. M. and Corbella, J. (1991) Influence of some dietary constituents on aluminium absorption and retention in rats. *Kidney Int.*, **39**, 598-601.
- Dougan, W. K. and Wilson, A. L. (1974) The absorptiometric determination of aluminium in water. A comparison of some chromogenic reagents and the development of an improved method. *Analyst*, **99**, 413-430.
- Downard, A. J., Powell, H. K. J. and Xu, S. (1991) Voltammetric determination of aluminium(III) using a chemically modified electrode. *Anal. Chim. Acta*, **251**, 157-163.
- Downard, A. J., Powell, H. K. J. and Xu, S. (1992) Flow injection analysis for aluminium with indirect amperometric detection. *Anal. Chim. Acta*, **256**, 117-123.
- Downard, A. J., Powell, H. K. J. and Xu, S. (1992) Modification of the solochrome violet RS method for the cathodic stripping voltammetric determination of aluminium. *Anal. Chim. Acta*, **262**, 339-343.
- Driscoll, C. T., Baker, J. P., Bisogni, J. J. and Schofield, C. L. (1980) Effect of aluminium speciation on fish in dilute acidified waters. *Nature*, **284**, 161-164.
- Driscoll, C. T. (1984) A procedure for the fractionation of aqueous aluminium in dilute acidic waters. *Intern. J. Environ. Anal. Chem.*, **16**, 267-283.
- Driscoll, C. T. (1985) Aluminium in acidic surface waters: chemistry, transport, and effects. *Soil Sci. Soc. Am. J.*, **49**, 437-444.
- Driscoll, C. T., van Breemen, N. and Mulder, J. (1985) Aluminium chemistry in a forested spodosol. *Soil Sci. Soc. Am. J.*, **49**, 437-444.
- Driscoll, C. T. (1989) The chemistry of aluminium in surface waters. In: *The environmental chemistry of aluminium*. (Ed: G. Sposito) CRC Press, Boca Raton, Florida.
- Driscoll, C. T. and Schecher, W. D. (1990) The chemistry of aluminium in the environment. *Environ. Geochem. Health*, **12**, 28-49.

- Durst, R. A., Koch, W. F. and Wu, Y. C. (1987) pH theory and measurement. *Ion-Selective Electrode Rev.*, **9**, 173-196.
- Eastwood, J. B., Levin, G. E., Pazianas, M., et al. (1990) Aluminium deposition in bone after contamination of drinking water supply. *Lancet*, **336**, 462-464.
- Ehrlich, H. A. (1990) *Geomicrobiology, 2nd Ed. revised and expanded*. Marcel Dekker Inc., New York.
- Elci, L., Soylak, M. and Dogan, M. (1992) Preconcentration of trace metals in river waters by the application of chelate adsorption on Amberlite XAD-4. *Fresenius' J. Anal. Chem.*, **342**, 175-178.
- Elliott, H. A. and Huang, C. P. (1979) The adsorption characteristics of Cu(II) in the presence of chelating agents. *J. Colloid Interface Sci.*, **70**, 29-45.
- Elmahadi, H. A. M. and Greenway, G. M. (1993) Immobilised cysteine as a reagent for preconcentration of trace metals prior to determination by atomic absorption spectrophotometry. *J. Anal. At. Spectrom.*, **8**, 1011-1014.
- Emteborg, H., Baxter, D. C., Sharp, M. and Frech, W. (1995) Evaluation, mechanism and application of solid-phase extraction using a dithiocarbamate resin for the sampling and determination of mercury species in humic-rich natural waters. *Analyst*, **120**, 69-77.
- Epstein, S. G. (1990) Human exposure to aluminium. *Environ. Geochem. Health*, **12**, 65-70.
- Eriksson, G. (1979) An algorithm for the computation of aqueous multicomponent, multiphase equilibria. *Anal. Chim. Acta*, **112**, 375-383.
- Eriksson, E. (1981) Aluminium in groundwater. Possible solution equilibria. *Nordic Hydrol.*, **12**, 43-50.
- Evans, L. J. (1989) Chemistry of metal retention by soils. *Environ. Sci. Technol.*, **23**, 1046-1056.
- Exley, C., Chappell, J. S. and Birchall, J. D. (1991) A mechanism for acute aluminium toxicity in fish. *J. theor. Biol.*, **151**, 417-428.
- Exley, C. and Birchall, J. D. (1992) Hydroxyaluminosilicate formation in solutions of low total aluminium concentration. *Polyhedron*, **11**, 1901-1907.
- Exley, C. and Birchall, J. D. (1992) The cellular toxicity of aluminium. *J. theor. Biol.*, **159**, 83-98.
- Exley, C., Wicks, A. J., Hubert, R. B. and Birchall, J. D. (1994) Polynuclear aluminium and acute aluminium toxicity in the fish. *J. theor. Biol.*, **167**, 415-416.

- Fahal, I. H., Yaqoob, M., Williams, P. S., et al.** (1994) Does silicon protect against aluminium toxicity in dialysis patients ? *Lancet*, **343**, 122-123.
- Fairman, B. and Sanz-Medel, A.** (1993) Improved determination of aluminium species in waters using FIA separation/fluorometric detection techniques. *Intern. J. Environ. Anal. Chem.*, **50**, 161-171.
- Fairman, B., Sanz-Medel, A., Gallego, M., et al.** (1994) Method comparison for the determination of labile aluminium species in natural waters. *Anal. Chim. Acta*, **286**, 401-409.
- Fairman, B., Sanz-Medel, A. and Jones, P.** (1995) Field sampling technique for 'fast reactive' aluminium fraction in waters using a flow injection mini-column system with inductively coupled plasma atomic emission spectrometric and inductively coupled plasma mass spectrometric detection. *J. Anal. At. Spectrom.*, **10**, 161-171.
- Fang, Z.** (1991) Flow-injection on-line column preconcentration in atomic spectrometry. *Spectrochim. Acta Rev.*, **14**, 235-259.
- Fardy, J. J., McOrist, G. D. and Florence, T. M.** (1984) Rapid radiochemical separation in neutron activation analysis. Part 1. The use of C₁₈-bonded silica gel and selective complexation for determinations of manganese, copper and zinc in biological materials. *Anal. Chim. Acta*, **159**, 199-209.
- Farmer, V. C.** (1982) Significance of the presence of allophane and imogolite in podzol Bs-horizons for podzolisation mechanisms: a review. *Soil Sci. Plant Nutrit.*, **28**, 571-578.
- Farmer, V. C., Adams, M. J., Fraser, A. R. and Palmieri, F.** (1983) Synthetic imogolite: properties, synthesis and possible applications. *Clay Minerals*, **18**, 459-472.
- Faust, B. C., Labiosa, W. L., Dai, K. H., et al.** (1995) Speciation of aqueous mononuclear Al(III)-hydroxo and other Al(III) complexes at concentrations of geochemical relevance by aluminium-27 nuclear magnetic resonance spectroscopy. *Geochim. Cosmochim. Acta*, **59**, 2651-2661.
- Fernández, P., Pérez-Conde, C., Gutiérrez, A. and Cámara, C.** (1991) On-line aluminium preconcentration on chelating resin and its FIA-spectrofluorometric determination in foods and dialysis concentrates. *Talanta*, **38**, 1387-1392.
- Fischer, R. B. and Peters, D. G.** (1970) *Chemical equilibria*. W.B. Saunders Company, Philadelphia.
- Flaten, T. P.** (1990) Geographical associations between aluminium in drinking water and death rates with dementia (including Alzheimer's disease), Parkinson's disease and amyotrophic lateral sclerosis in Norway. *Environ. Geochem. Health*, **12**, 152-167.
- Flaten, T. P. and Garruto, R. M.** (1992) Polynuclear ions in aluminium toxicity. *J. theor. Biol.*, **156**, 129-132.

- Florence, T. M.** (1962) Determination of aluminium in thorium compounds by linear-sweep oscillographic polarography. *Anal. Chem.*, **34**, 496-499.
- Florence, T. M., Miller, F. J. and Zittel, H. E.** (1966) Voltammetric determination of aluminium by oxidation of its solochrome violet RS complex at the rotated pyrolytic graphite electrode. *Anal. Chem.*, **38**, 1065-1067.
- Forbes, W. F., Hayward, L. M. and Agwani, N.** (1991) Dementia, aluminium, and fluoride. *Lancet*, **338**, 1592-1593.
- Forsling, W., Hietanen, S. and Sillen, L. G.** (1952) Studies on the hydrolysis of metal ions. III. The hydrolysis of mercury(I) ion, Hg_2^{2+} . *Acta Chem. Scand.*, **6**, 901-999.
- Foy, C. D.** (1983) The physiology of plant adaptation to mineral stress. *Iowa State J. Res.*, **57**, 355-392.
- Fredriksson, E.** (1993) *CVD of Titanium oxides and Aluminium Oxides*. Ph.D. Thesis, Uppsala University, Sweden.
- Frick, K. G. and Herrmann, J.** (1990) Aluminium accumulation in a lotic mayfly at low pH - a laboratory study. *Ecotoxicol. Environ. Safety*, **19**, 81-88.
- Froment, D. H., Molitoris, B. A., Buddington, B., Miller, N. and Alfrey, A. C.** (1989) Site and mechanism of enhanced gastrointestinal absorption of aluminium by citrate. *Kidney Int.*, **36**, 978-984.
- Furrer, G. and Stumm, W.** (1983) The role of surface coordination in the dissolution of $\delta\text{-Al}_2\text{O}_3$ in dilute acids. *Chimia*, **37**, 338-341.
- Furrer, G. and Stumm, W.** (1986) The coordination chemistry of weathering: I. Dissolution kinetics of $\delta\text{-Al}_2\text{O}_3$ and BeO. *Geochim. Cosmochim. Acta*, **50**, 1847-1860.
- Furrer, G., Trusch, B. and Müller, C.** (1992) The formation of polynuclear Al^{13} under simulated natural conditions. *Geochim. Cosmochim. Acta*, **56**, 3831-3838.
- Gahoonia, T. S.** (1993) Influence of root-induced pH on the solubility of soil aluminium in the rhizosphere. *Plant Soil*, **149**, 289-291.
- Galova, M. and Szmerekova, V.** (1973) Polarography of aluminium(III) in the presence of complexing agents. *Chem. Zvesti*, **27**, 437-445.
- Gamble, D. S., Schnitzer, M., Kerndorff, H. and Langford, C. H.** (1983) Multiple metal ion exchange equilibria with humic acid. *Geochim. Cosmochim. Acta*, **47**, 1311-1323.
- Gans, P., Sabatini, A. and Vacca, A.** (1985) SUPERQUAD: An improved general program for computation of formation constants from potentiometric data. *J. Chem. Soc. Dalton Trans.*, **6**, 1195-1200.

- García Alonso, J. I., López García, A., Sanz-Medel, A., Ebdon, L. and Jones, P.** (1989) Flow-injection and liquid chromatographic determination of aluminium based on its fluorimetric reaction with 8-hydroxyquinoline-5-sulphonic acid in a micellar medium. *Anal. Chim. Acta*, **225**, 339-350.
- García Alonson, J. I., García, A. L., Sanz-Medel, A. and Gonzalez, E. B.** (1989) Flow-injection and liquid chromatographic determination of aluminium based on its fluorimetric reaction with 8-hydroxyquinoline-5-sulfonic acid in a micellar medium. *Anal. Chim. Acta*, **225**, 339-350.
- Garn, M. B., Gisin, M., Gross, P., Schmidt, W. and Thommen, C.** (1988) Extensive flow-injection dilution for in-line sample pretreatment. Comparison between single-stage and dual-stage modules. *Anal. Chim. Acta*, **207**, 225-230.
- Garruto, R. M.** (1991) Pacific paradigms of environmentally-induced neurological disorders: clinical, epidemiological and molecular perspectives. *Neurotoxicology*, **12**, 347-378.
- Gee, A. S. and Stoner, J. H.** (1989) A review of the causes and effects of acidification of surface waters in Wales and potential mitigation techniques. *Arch. Environ. Contam. Toxicol.*, **18**, 121-130.
- Gelb, R. I., Schwartz, L. M. and Laufer, D. A.** (1978) The structure of aqueous rhodizonic acid. *J. Phys. Chem.*, **82**, 1985-1988.
- Gennaro, M. C., Mentasti, E. and Sarzanini, C.** (1986) Immobilised ligands on silica: uptake of cobalt and other metals by 1-nitroso-2-naphthol. *Polyhedron*, **5**, 1013-1015.
- Gherini, S. A., Mok, L., Hudson, R. J. M., et al.** (1985) The ILWAS model: formulation and application. *Water Air Soil Pollut.*, **26**, 425-459.
- Giltelman, H. J.** (1989) *Aluminium and Health. A critical review*. Marcel Dekker, Inc, New York.
- Goina, T., Olariu, M. and Bocaniciu, L.** (1970) Stability constants of metal-ion complexes. In: *Part B. Organic Ligands*. (Ed: IUPAC) Pergamon, Oxford.
- Good, P. F., Perl, D. P., Bierer, L. M. and Schmeidler, J.** (1992) Selective accumulation of aluminium and iron in the neurofibrillary tangles of Alzheimer's disease: a laser microprobe (LAMMA) study. *Ann. Neurol.*, **31**, 286-292.
- Gran, G.** (1952) Determination of the equivalence point in potentiometric titrations. *Analyst*, **77**, 661-671.
- Greenland, D. J.** (1971) Interactions between humic and fulvic acids and clays. *Soil Sci.*, **111**, 34-41.
- Greenwood, N. N. and Earnshaw, A.** (1984) *Chemistry of the elements*. Pergamon Press, Oxford.

- Gregor, J. E. and Powell, H. K. J. (1988) Protonation reactions of fulvic acids. *Soil Sci.*, **39**, 243-252.
- Groschner, M. and Appriou, P. (1994) Three-column system for preconcentration and speciation determination of trace metals in natural waters. *Anal. Chim. Acta*, **297**, 369-376.
- Grzyb, K. R. (1995) NOAEM (natural organic anion equilibrium model): A data analysis algorithm for estimating functional properties of dissolved organic matter in aqueous environments: Part I. Ionic component speciation and metal association. *Org. Geochem.*, **23**, 379-390.
- Gull, H. C. (1937) Polarographic analysis of magnesium alloys. *J. Soc. Chem. Ind.*, **56**, 177-190.
- Gundersen, D. T., Bustaman, S., Seim, W. K. and Curtis, L. R. (1994) pH, hardness and humic acid influence aluminium toxicity of rainbow trout (*Oncorhynchus mykiss*) in weakly alkaline waters. *Can. J. Fish. Aquat. Sci.*, **51**, 1345-1355.
- Gunneriusson, L. (1993) *Aqueous speciation and surface complexation to goethite (α -FeOOH) of divalent mercury, lead and cadmium*. Ph.D. Thesis, Umeå University, Sweden.
- Gutzman, D. W. and Langford, C. H. (1993) Kinetic study of the speciation of copper(II) bound to a hydrous ferric oxide. *Environ. Sci. Technol.*, **27**, 1388-1393.
- Hackett, D. S. and Siggia, S. (1977) *Selective concentration and determination of trace metals using poly(dithiocarbamate) chelating ion-exchange resins*. Academic Press, London.
- Häkkinen, P. (1984a) Formation of copper(II) and zinc(II) complexes of 1,2-dihydroxy-4-nitrobenzene in aqueous solution. *Finn. Chem. Lett.*, 9-12.
- Häkkinen, P. (1984b) Studies on the formation of manganese(II), iron(III), cobalt(II) and nickel(II) complexes of 1,2-dihydroxy-4-nitrobenzene in aqueous solution. *Finn. Chem. Lett.*, 59-62.
- Häkkinen, P. (1984c) Studies on the formation of Al(III), Cd(II) and Be(II) complexes of 1,2-dihydroxy-4-nitrobenzene in aqueous solution. *Finn. Chem. Lett.*, 151-154.
- Häkkinen, P. (1985) Formation of magnesium(II), calcium(II), strontium(II) and barium(II) complexes of 1,2-dihydroxy-4-nitrobenzene in aqueous solution. *Finn. Chem. Lett.*, 17-20.
- Hakoila, E. J., Kankare, J. J. and Sharp, T. (1972) Chelation of boric acid with nitropyrocatechols and the photometric determination of boric acid. *Anal. Chem.*, **44**, 1857-1860.
- Hall, M. E. and Skoumbourdis, C. T. (1966) Indirect polarographic determination of aluminium. *Anal. Chem.*, **38**, 64-66.

- Hall, R. J., Driscoll, C. T., Likens, G. E. and Pratt, J. M. (1985) Physical, chemical and biological consequences of episodic aluminium additions to a stream. *Limnol. Oceanogr.*, **30**, 212-220.
- Hall, R. J., Driscoll, C. T. and Likens, G. E. (1987) Importance of hydrogen ions and aluminium in regulating the structure and function of stream ecosystems: an experimental test. *Freshwater Biol.*, **18**, 17-43.
- Hall, R. J., Bailey, R. C. and Findeis, J. (1988) Factors affecting survival and cation concentration in the blackflies *Prosimulium fuscum/mixtum* and the mayfly *Leptophlebia cupida* during spring snowmelt. *Can. J. Fish Aquat. Sci.*, **45**, 2123-2131.
- Hansen, E. H. (1986) *Flow injection analysis*. Technical University of Denmark, Copenhagen.
- Hartel, P. G., Whelan, A. M. and Alexander, M. (1983) Nodulation of cowpeas and survival of cowpeas rhizobia in acid, aluminium-rich soils. *Soil Sci. Soc. Am. J.*, **47**, 514-517.
- Hartenstein, S. D., Christian, G. D. and Ruzicka, J. (1986) Applications of an on-line preconcentrating flow injection analysis system for inductively coupled plasma atomic emission spectrometry. *Can. J. Spectrosc.*, **30**, 144-148.
- Hase, A., Kawabata, T. and Terada, K. (1990) Preconcentration of trace metals with dithiocarbamate-chitin. *Anal. Sci.*, **6**, 747-751.
- Hase, U. and Yoshimura, K. (1992) Determination of trace amounts of iron in highly purified water by ion-exchanger phase absorptiometry combined with flow analysis. *Analyst*, **117**, 1501-1506.
- Haug, A. (1984) Molecular aspects of aluminium toxicity. *Crit. Rev. Plant Sci.*, **1**, 345-373.
- Havas, M. (1985) Aluminium bioaccumulation and toxicity to *Daphnia magna* in soft water at low pH. *Can. J. Fish Aquat. Sci.*, **42**, 1741-1748.
- Havas, M. and Likens, G. E. (1985) Toxicity of aluminium and hydrogen ions to *Daphnia catawba*, *Holopedium gibberum*, *Chaoborus punctipennis* and *Chironomus anthrocinus* from Mirror lake, New Hampshire. *Can. J. Zool.*, **63**, 1114-1118.
- Hawke, D. J. and Powell, H. K. J. (1994) Flow injection analysis applied to the kinetic determination of reactive (toxic) aluminium: comparison of chromophores. *Anal. Chim. Acta*, **299**, 257-268.
- Hawke, D. J., Powell, K. J. and Sjöberg, S. (1995) A potentiometric and spectrophotometric study of the system H^+-Al^{3+} -Chrome Azurol S. *Polyhedron*, **14**, 377-385.

- Hawke, D. J., Powell, H. K. J. and Gregor, J. E. (1996) Determination of aluminium complexing capacity of fulvic acids and natural waters, with examples from five New Zealand rivers. *Mar. Freshwater*, **47**, (in press).
- Hawke, D. J., Powell, H. K. J. and Simpson, S.L. (1996) Equilibrium modelling of interferences in the visible spectrophotometric determination of aluminium(III) : comparison of the chromophores chrome azurol S, eriochrome cyanine R and pyrocatechol violet, and stability constants for eriochrome cyanine R - aluminium complexes. *Anal. Chim. Acta*, **319**, 305-314.
- Hedlund, T. and Öhman, L.-O. (1988) Equilibrium and structural studies of silicon(IV) and aluminium(III) in aqueous solution 19. Composition and stability of aluminium complexes with kojic acid and maltol. *Acta Chem. Scand.*, **42A**, 702-709.
- Hefter, G. T. (1982) calculation of liquid junction potentials for equilibrium studies. *Anal. Chem.*, **54**, 2528-2524.
- Helliwell, S., Batley, G. E., Florence, T. M. and Lumsden, B. G. (1983) Speciation and toxicity of aluminium in a model fresh water. *Environ. Technol. Lett.*, **4**, 141-144.
- Henry, R. P., Prue, J. E., Rossotti, F. J. C. and Whewell, R. J. (1971) Precise potentiometric titrations using glass electrodes. *Chem. Commun.*, 868-869.
- Hering, J. G. and Morel, F. M. M. (1990) Kinetics of trace metal complexation: ligand-exchange reactions. *Environ. Sci. Technol.*, **24**, 242-252.
- Hering, J. G. and Stumm, W. (1991) Fluorescence spectroscopic evidence for surface complex formation at the mineral-water interface: Elucidation of the mechanism of ligand-promoted dissolution. *Langmuir*, **7**, 1567-1570.
- Hernandéz, P., Hernández, L. and Losada, J. (1986) Determination of aluminium in haemodialysis fluids by a flow injection system with preconcentration on a synthetic chelate-forming resin and flame atomic absorption spectrophotometry. *Fresenius' Z. Anal. Chem.*, **325**, 300-203.
- Hernandéz Torres, O., Jiménez Moreno, F., Jiménez Abizanda, A. and Arias Leon, J. J. (1992) Use of an azo derivative immobilised on an anionic resin for the determination of aluminium in water and dialysis fluids. *Clin. Chim. Acta*, **209**, 35-46.
- Herrmann, J., Degerman, E., Gerhardt, A., et al. (1993) Acid-stress effects on stream biology. *Ambio*, **22**, 298-307.
- Heyrovsky, J. (1920) The electroaffinity of aluminium. I. The ionisation and hydrolysis of aluminium chloride. *J. Chem. Soc.*, **117**, 11-26.
- Hill, U. T. (1966) New direct spectrophotometric determination of aluminium in steel, spelter and iron ores. *Anal. Chem.*, **38**, 654-656.

- Hirayama, K., Sekine, T. and Unohara, N. (1994) Determination of trace aluminium in natural waters by ICP-AES after separation and preconcentration using chrome azurol S immobilised silica gel. *Bunseki Kagaku*, **43**, 1065-1070.
- Hodges, S. C. (1987) Aluminium speciation: A comparison of five methods *Soil Sci. Soc. Am. J.*, **51**, 57-64.
- Hohl, H. and Stumm, W. (1976) Interaction of Pb^{2+} with hydrous $\gamma-Al_2O_3$. *J. Colloid Interface Sci.*, **55**, 281-288.
- Holleck, L., Abd El Kader, J. M. and Shams El Din, A. M. (1969) Polarographic reduction of solochrome violet RS and the complex forming mechanism with aluminium in methanolic solution. *J. Electroanal. Chem. Interfacial Electrochem.*, **20**, 287-296.
- Horváth, Z. and Barnes, R. M. (1986) Carboxymethylated polyethylenimine-polymethylenepolyphenylene isocyanate chelating ion exchange resin preconcentration for inductively coupled plasma spectrometry. *Anal. Chem.*, **58**, 1352-1355.
- Howard, A. G. and Danilona-Mirzaïans, R. (1989) Trace metal preconcentration using thioglycolate chelating resin. *Anal. Lett.*, **22**, 257-267.
- Hsieh, T.-S. and Liu, J. K. (1993) Alkylene bisdithiocarbamates as complexing agents for the preconcentration of trace metals in aquatic samples. *Anal. Chim. Acta*, **282**, 221-225.
- Huang, P. and Stumm, W. (1972) The specific surface area of $\gamma-Al_2O_3$. *Surface Sci.*, **32**, 287-296.
- Huang, P. and Stumm, W. (1973) Specific adsorption of cations on hydrous $\gamma-Al_2O_3$. *J. Colloid Interface Sci.*, **43**, 409-420.
- Huang, J. W., Grunes, D. L. and Kochian, L. V. (1992) Aluminium effects on the kinetics of calcium uptake into cells of the wheat root apex. *Planta*, **188**, 414-421.
- Hue, N. V., Craddock, G. R. and Adams, F. (1986) Effect of organic acids on aluminium toxicity in subsoils. *Soil Sci. Soc. Am. J.*, **50**, 28-34.
- Hughes, S., Norris, D. A., Stevens, P. A., et al. (1994) Effects of forest age on surface drainage water and soil solution aluminium chemistry in stagnopodzols in Wales. *Water Air Soil Pollut.*, **77**, 115-139.
- Hunter, D. and Ross, D. S. (1991) Evidence for a phytotoxic hydroxy-aluminium polymer in organic soil horizons. *Science*, **251**, 1056-1058.
- Ingri, N., Andersson, I., Pettersson, L., et al. (1996) LAKE - A program system for the equilibrium analytical treatment of multimethod data, especially combined potentiometric and NMR data. *Acta Chem. Scand.*, (Accepted).

- Irth, H., de Jong, G. J., Brinkman, U. A. T. and Frei, R. W.** (1987) Trace enrichment and separation of metal ions as dithiocarbamate complexes by liquid chromatography. *Anal. Chem.*, **59**, 98-101.
- James, B. R., Clark, C. J. and Riha, S. J.** (1983) An 8-hydroxyquinoline method for labile and total aluminium in soil extracts. *Soil Sci. Soc. Am. J.*, **47**, 893-897.
- Jameson, R. F. and Wilson, M. F.** (1972) Thermodynamics of catechol with transition metals. Part III. The effect of 4-chloro- and 4-nitro-substitution on proton and metal catechol complex formation. *J. Chem. Soc. Dalton.*, 2617-2621.
- Jeffries, D. S. and Hendershot, W. H.** (1989) Aluminium geochemistry at the catchment scale in watersheds influenced by acidic precipitation. In: *The environmental chemistry of aluminium*. (Ed: G. Sposito) CRC Press, Boca Raton, Florida.
- Jezorek, J. R. and Freiser, H.** (1979) Metal-ion chelation chromatography on silica-immobilised 8-hydroxyquinoline. *Anal. Chem.*, **51**, 366-373.
- Johnson, N. M.** (1979) Acid rain: neutralisation within the Hubbard Brook ecosystem and regional implications. *Science*, **204**, 497-499.
- Johnson, N. M., Driscoll, C. T., Eaton, J. S., Likens, G. E. and McDowell, W. H.** (1981) 'Acid rain', dissolved aluminium and chemical weathering at the Hubbard Brook experiment forest, New Hampshire. *Geochim. Cosmochim. Acta*, **45**, 1421-1437.
- Johnson, N. M., Likens, G. E., Feller, M. C. and Driscoll, C. T.** (1984) Acid rain and soil chemistry. *Science*, **225**, 1424-1425.
- Jones, P., Ebdon, L. and Williams, T.** (1988) Determination of trace amounts of aluminium by ion chromatography with fluorescence detection. *Analyst*, **113**, 641-644.
- Jones, P. and Schwedt, G.** (1989) Dyestuff-coated high-performance liquid chromatographic resins for the ion-exchange and chelating-exchange separation of metal ions. *J. Chromatogr.*, **482**, 325-334.
- Jones, P.** (1991) The investigation of aluminium speciation in natural and potable waters using short-column ion chromatography. *Intern. J. Environ. Anal. Chem.*, **44**, 1-10.
- Kamariotaki, M., Karaliota, A., Stabaki, D., et al.** (1994) Coordination complexes of iron(III) with 3-hydroxy-2(1H)-pyridinone, 2,3-dihydroxybenzoic acid and 3,4-dihydroxybenzoic acid: preparation and characterisation in the solid state. *Trans. Metal Chem.*, **19**, 241-247.
- Karlberg, B. and Pacey, G. E.** (1989) *Flow injection analysis: a practical guide*. Elsevier, Amsterdam.

- Karpiuk, M., Politowicz, M., Stryjewska, E. and Rubel, S. (1995) Adsorptive voltammetry for the determination of trace amounts of aluminium in blood serum derived products. *Fresenius' J. Anal. Chem.*, **351**, 693-695.
- Kennedy, J. A., Munro, M. H. G., Powell, H. K. J., Porter, L. J. and Yeap Foo, L. (1984) The potentiometric reactions of catechin, epicatechin and related compounds. *Aust. J. Chem.*, **37**, 885-92.
- Kennedy, J. A. and Powell, H. K. J. (1985) Aluminium(III) and iron(III) 1,2-diphenolato complexes: a potentiometric study. *Aust. J. Chem.*, **38**, 659-67.
- Kerven, G. L., Edwards, D. G., Asher, C. J., Hallman, P. S. and Kokot, S. (1989) Aluminium determination in soil solution. II. Short-term colorimetric procedures for the measurement of inorganic monomeric aluminium in the presence of organic acid ligands. *Aust. J. Soil. Res.*, **27**, 91-102.
- King, E. J. (1965) Acid-base equilibria. In: *The international encyclopedia of physical chemistry and chemical physics. Topic 15. Equilibrium properties of electrolyte solutions.* (Ed: R. A. Robinson) Pergamon Press, London.
- King, J. N. and Fritz, J. S. (1985) Concentration of metal ions by complexation with sodium bis(2-hydroxyethyl)dithiocarbamate and sorption on XAD-4 resin. *Anal. Chem.*, **57**, 1016-1020.
- King, D. W., Lin, J. and Kester, D. R. (1991) Spectrophotometric determination of iron(II) in sea water at nanomolar concentrations. *Anal. Chim. Acta*, **247**, 125-132.
- Kinraide, T. B. and Parker, D. R. (1987) Cation amelioration of aluminium toxicity in wheat. *Plant Physiol.*, **83**, 546-551.
- Kinraide, T. B. and Parker, D. R. (1989) Assessing the phytotoxicity of mononuclear hydroxy-aluminium. *Plant Cell Environ.*, **12**, 479-487.
- Kinraide, T. B. and Parker, D. R. (1990) Apparent phytotoxicity of mononuclear hydroxy-aluminium to four dicotyledonous species. *Physiol. Plant.*, **79**, 283-288.
- Kinraide, T. B. (1991) Identity of the rhizotoxic aluminium species. *Plant Soil*, **134**, 167-178.
- Kinraide, T. B., Ryan, P. R. and Kochian, L. V. (1992) Interactive effects of Al^{3+} , H^{+} and other cations on root elongation considered in terms of cell-surface electrical potential. *Plant Physiol.*, **99**, 1461-1468.
- Kinraide, T. B., Ryan, P. R. and Kochian, L. V. (1994) Al^{3+} - Ca^{2+} interactions in aluminium rhizotoxicity. II. Evaluating the Ca^{2+} -displacement hypothesis. *Planta*, **192**, 104-109.
- Klatzo, I., Wisniewski, H. and Stretcher, E. (1965) Experimental production of neurofibrillary degeneration. *J. Neuropathol. Exp. Neurol.*, **24**, 187-199.

- Klinghoffer, O., Ruzicka, J. and Hansen, E. H. (1980) Flow injection analysis of traces of lead and cadmium by solvent extraction with dithizone. *Talanta*, **27**, 169-175.
- Kobayashi, J. and Miyazaki, M. (1993) Synthesis of salicylideneamino-2-thiophenol immobilised glass beads and their application to a preconcentration of trace aluminium. *Chem. Pharm. Bull.*, **41**, 919-922.
- Kokkinidis, G., Sazou, D. and Moutzizis, I. (1986) Electrocatalytic influence of underpotential Tl, Pb and Bi monolayers on the electrochemical behaviour of rhodizonic acid and tetrahydroxy-1,4-benzoquinone on Pt in acid solutions. *J. Electroanal. Chem.*, **213**, 135-147.
- Kolthoff, I. M. and Sambucetti, C. J. (1959) Amperometric determination of fluoride at a rotated aluminium electrode. *J. Am. Chem. Soc.*, **81**, 1516-1517.
- Kolthoff, I. M. and Sambucetti, C. J. (1959) Voltammetric, potentiometric and amperometric studies with a rotated aluminium wire electrode (R.AIE). I. Voltammetric behaviour of R.AIE. *Anal. Chim. Acta*, **21**, 17-24.
- Kotowski, M., Pawlowski, L., Seip, H. M. and Vogt, R. D. (1994) Mobilisation of aluminium in soil columns exposed to acids or salt-solutions. *Ecological engineering*, **3**, 279-290.
- Kramer, J. R., Hummel, J. and Gleed, J. (1986) Speciation of aluminium and its toxicity to fish. In: *Proceedings of the international conference on chemicals in the environment*. (Ed: J. N. Lester, Perry, R. and Sterritt, R. M.) Selper Ltd, London.
- Krishnan, S. S., McLachlan, D. R., Krishnan, B., Fenton, S. S. A. and Harrison, J. E. (1988) Aluminium toxicity to the brain. *Sci. Tot. Environ.*, **71**, 59-64.
- Kummert, R. and Stumm, W. (1980) The surface complexation of organic acids on hydrous γ - Al_2O_3 . *J. Colloid Interface Sci.*, **75**, 373-385.
- Laiti, E. and Öhman, L.-O. (unpub.) Acid/base properties and phenylphosphonic acid complexation at the boehmite/water interface. *J. Colloid Interface Sci.*, (submitted).
- Laitinen, M. and Valtonen, T. (1995) Cardiovascular, ventilatory and haematological responses of brown trout (*Salmo trutta* L.) to the combined effects of acidity and aluminium in humic water at winter temperatures. *Aquat. Toxicol.*, **31**, 99-112.
- Lancaster, H. L., Marshall, G. D., Gonzalo, E. R., Ruzicka, J. and Christian, G. D. (1994) Trace metal atomic adsorption spectrometric analysis utilising sorbent extraction on polymeric-based supports and renewable reagents. *Analyst*, **119**, 1459-1465.
- Landing, W. M., Haraldsson, C. and Paxeus, N. (1986) Vinyl polymer agglomerate based transition metal cation chelating ion-exchange resin containing the 8-hydroxyquinoline functional group. *Anal. Chem.*, **58**, 3031-3035.

- Landsberg, J. P., McDonald, B. and Watt, F.** (1992) Absence of aluminium in neuritic plaque cores in Alzheimer's disease. *Nature*, **360**, 65-68.
- Langford, C. H. and Cook, R. L.** (1995) Kinetic *versus* equilibrium studies for the speciation of metal complexes with ligands from soil and water. *Analyst*, **120**, 591-596.
- Laxen, D. P. H.** (1985) Trace metal adsorption/coprecipitation on hydrous ferric oxide under realistic conditions. *Water Res.*, **19**, 1229-1236.
- LaZerte, B. D.** (1984) Forms of aqueous aluminium in acidified catchments of Central Ontario: A methodological analysis. *Can. J. Fish. Aquat. Sci.*, **41**, 766-776.
- LaZerte, B. D., Chun, C. and Evans, D.** (1988) Measurement of aqueous aluminium species: Comparison of dialysis and ion-exchange techniques. *Environ. Sci. Technol.*, **22**, 1106-1108.
- Lee, D. W. and Halman, M.** (1976) Selective separation of nickel(II) by dimethylglyoxime-treated polyurethane foam. *Anal. Chem.*, **48**, 2214-2218.
- Lee, J. and Pritchard, M. W.** (1984) Aluminium toxicity expression on nutrient uptake, growth and root morphology of *Trifolium repens* L. cv. 'Grasslands Huia'. *Plant Soil*, **82**, 101-116.
- Lendermann, B., Monien, H. and Specker, H.** (1972) Inverse voltammetric determination of traces of aluminium and beryllium. *Anal. Lett.*, **5**, 837-842.
- Lenihan, R. J.** (1994) *Indirect electrochemical determination of aluminium(III) using 4-nitrocatechol*. Masters Thesis, University of Canterbury, New Zealand.
- Lewis, T. E., Dobb, D. E., Henshaw, J. M., Simon, S. J. and Heitmar, E. M.** (1988) Apparent monomeric aluminium concentrations in the presence of humic and fulvic acid and other ligands: an intermethod comparison study. *Int. J. Environ. Anal. Chem.*, **34**, 69-87.
- Leyden, D. E. and Luttrell, G. H.** (1975) Preconcentration of trace metals using chelating groups immobilised *via* silylation. *Anal. Chem.*, **87**, 1612-1617.
- Leyden, D. E., Luttrell, G. H., Sloan, A. E. and DeAngelis, N. J.** (1976) Characterisation and application of silylated substrates for the preconcentration of cations. *Anal. Chim. Acta*, **84**, 97-108.
- Li, Y. J. and Martell, A. E.** (1993) Potentiometric and spectrophotometric determination of stabilities of the 1-hydroxy-2-pyridinone complexes of trivalent and divalent metal ions. *Inorg. Chim. Acta*, **214**, 103-111.
- Lindsay, W. L.** (1979) *Chemical equilibria in soils. V. Aluminosilicate minerals*. Wiley-Interscience, New York.

- Ljunggren, L., Alttrell, I., Risinger, L. and Johansson, G.** (1992) Trace enrichment of aluminium ions on immobilised desferrioxamine. *Anal. Chim. Acta*, **256**, 75-80.
- Llorente, A. R., Castillo, P. D. and Stockert, J. C.** (1989) Aluminium binding to chromatin DNA as revealed by formation of fluorescent complexes with 8-hydroxyquinoline and other ligands. *J. Microsc.*, **1552**, 277-230.
- López-Quintela, A. M., Knoche, W. and Veith, J.** (1984) Kinetics and thermodynamics of complex formation between aluminium(III) and citric acid in aqueous solution. *J. Chem. Soc. Faraday Trans. I*, **80**, 2313-2321.
- Lorber, K., Müller, K. and Spitz, H.** (1975) Column extraction chromatography with dithizone in *o*-dichlorobenzene. Possibilities for separating metal traces in the nanogram region. *Microchim. Acta*, **2**, 603-615.
- Lövgren, L., Hedlund, T., Öhman, L.-O. and Sjöberg, S.** (1987) Equilibrium approaches to natural systems 6. Acid-base properties of a concentrated bog-water and its complexation reactions with aluminium(III). *Water Res.*, **21**, 1401-1407.
- Lövgren, L., Sjöberg, S. and Schindler, P. W.** (1990) Acid/base reactions and Al(III) complexation at the surface of goethite. *Geochim. Cosmochim. Acta*, **54**, 1301-1306.
- Lövgren, L.** (1991) Complexation reactions of phthalic acid and aluminium(III) with the surface of goethite. *Geochim. Cosmochim. Acta*, **55**, 3639-3645.
- Lu, Y., Chakrabarti, C. L., Back, M. H., Grégoire, D. C. and Schroeder, W. H.** (1994) Kinetic studies on aluminium and zinc speciation in river water and snow. *Anal. Chim. Acta.*, **293**, 95-108.
- Lundbäck, H. and Olsson, B.** (1985) Amperometric determination of galactose, lactose and dihydroxyacetone using galactose oxidase in a flow system with immobilised reactors and on-line dialysis. *Anal. Lett.*, **18**, 871-889.
- Lundgren, J. L. and Schilt, A. A.** (1977) Analytical studies and applications of ferrion type chromogens immobilised by adsorption on a styrene-divinylbenzene copolymer. *Anal. Chem.*, **49**, 974-980.
- Lundström, U. S.** (1993) The role of organic acids in the soil solution chemistry of a podsolised soil. *J. Soil Sci.*, **44**, 121-133.
- Lydersen, E., Salbu, B. and Polò, A. B. S.** (1992) Size and Charge Fractionation of Aqueous Aluminium in Dilute Acidic Waters: Effects of Changes in pH and Temperature. *Analyst*, **117**, 613-617.
- Lydersen, E., Polò, A. B. S., Oughton, D. H. and Salbu, B.** (1993) Addition of sulfuric-acid to high organic-carbon lake water - effects on macro-chemistry, aluminium, and iron. *Water Air Soil Pollut.*, **66**, 349-363.

- Ma, R., Reibenspies, J. J. and Martell, A. E. (1994) Stabilities of 1,2-diethyl-3-hydroxy-4-pyridinone chelates of divalent and trivalent metal ions. *Inorg. Chim. Acta*, **223**, 21-29.
- Macdonald, T. L. and Martin, R. B. (1988) Aluminium ion in biological systems. *Trends Biochem. Sci.*, **13**, 15-19.
- MacFall, J. S., Ribeiro, A. A., Cofer, G. P., et al. (1995) Design and use of background-reduced ^{27}Al NMR probes for the study of dilute samples from the environment. *Appl. Spectrosc.*, **49**, 156-162.
- Mackie, G. L. (1989) Tolerances of five benthic invertebrates to hydrogen ions and metals (Cd, Pb, Al). *Arch. Environ. Contam. Toxicol.*, **18**, 215-233.
- MacLean, D. C., Hansen, K. S. and Schneider, R. E. (1992) Amelioration of aluminium toxicity in wheat by fluoride. *New Phytol.*, **121**, 81-88.
- Madsen, L. and Blokhus, A. M. (1994) Adsorption of benzoic acid on α -alumina and γ -boehmite. *J. Colloid Interface Sci.*, **166**, 259-262.
- Mak, M. K. S. and Langford, C. H. (1983) Kinetic analysis applied to aluminium citrate complexing. *Inorg. Chim. Acta*, **70**, 237-246.
- Malachuk, P. A. (1976) *Aluminium (Chapter 6)*. Marcel Dekker, New York.
- Malamas, F., Bengtsson, M. and Johansson, G. (1984) On-line trace enrichment and matrix isolation in atomic absorption spectrometry by a column containing immobilised 8-quinolinol in a flow injection system. *Anal. Chim. Acta.*, **160**, 1-10.
- Marjerrum, D. W., Cayley, G. R., Weatherburn, D. C. and Pagenkopf, G. K. (1978) *Kinetics of and mechanisms of complex formation and ligand exchange*. ACS, Washington, DC.
- Marklund, E., Sjöberg, S. and Öhman, L.-O. (1986) Equilibrium and structural studies of silicon(IV) and aluminium(III) in aqueous solution. 14. Speciation and equilibria in the aluminium(III)-lactic acid- OH^- system. *Acta Chem. Scand.*, **40A**, 367-373.
- Marklund, E., Öhman, L.-O. and Sjöberg, S. (1989) Equilibrium and structural studies of silicon(IV) and aluminium(III) in aqueous solution. 20. Composition and stability of aluminium complexes with propionic and acetic acid. *Acta Chem. Scand.*, **43**, 641-646.
- Marklund, E. and Öhman, L.-O. (1990) Equilibrium and structural studies of silicon(IV) and aluminium(III) in aqueous solution 24. A potentiometric and ^{27}Al NMR study of polynuclear aluminium(III) hydroxo complexes with lactic acid. *Acta Chem. Scand.*, **44**, 228-234.
- Marklund, E. (1990) *Equilibrium studies of aqueous aluminium(III) complexes with "alfa"-substituted low molecular weight carboxylic acids*. Ph.D. Thesis, Umeå University, Sweden.

- Marshall, M. A. and Mottola, H. A.** (1985) Performance studies under flow conditions of silica-immobilised 8-quinolinol and its application as a preconcentration tool in flow injection/atomic absorption determinations. *Anal. Chem.*, **57**, 729-733.
- Martell, A. E. and Smith, R. M.** (1974-1989) *Critical stability constants*. Plenum Press, New York.
- Martin, R. B.** (1986) The chemistry of aluminium as related to biology and medicine. *Clin. Chem.*, **32**, 1797-1806.
- Martin, R. B.** (1988) Ternary hydroxide complexes in neutral solutions of Al^{3+} and F^- . *Biochem. Biophys. Res. Commun.*, **155**, 1194-1200.
- Martin, R. B.** (1990) Aluminosilicate stabilities under blood plasma conditions. *Polyhedron*, **9**, 193-197.
- Martin, R. B.** (1991) Fe^{3+} and Al^{3+} hydrolysis equilibria. Cooperatively in Al^{3+} hydrolysis reactions. *J. Inorg. Biochem.*, **44**, 141-147.
- Martin, R. B.** (1994) Aluminium: a neurotoxic product of acid rain. *Acc. Chem. Res.*, **27**, 204-210.
- Martín-Esteban, A., Fernández, P., Pérez-Conde, C., Gutiérrez, A. and Cámara, C.** (1995) On-line preconcentration of aluminium with immobilised chromotrope 2B for the determination by flame atomic absorption spectrometry and inductively coupled plasma mass spectrometry. *Anal. Chim. Acta*, **304**, 121-126.
- Martyn, C. N., Barker, D. J. P., Osmond, C., et al.** (1989) Geographical relation between Alzheimer's disease and aluminium in drinking water. *Lancet*, **1**, 59-62.
- Masion, A., Thomas, F., Tchoubar, J. Y., Bottero, F. and Tekeley, P.** (1994) Chemistry and structure of $\text{Al}(\text{OH})_3$ /organic precipitates. A small angle X-ray scattering study. 3. Depolymerisation of the Al_{13} polycation by organic ligands. *Langmuir*, **10**, 4353-4356.
- Mason, J. and Seip, H. M.** (1985) The current state of knowledge on acidification of surface waters and guidelines for further research. *Ambio*, **14**, 45-51.
- Maties, R., Arias, J. J., Jiménez, F. and Román, M.** (1992) Spectrofluorometric determination of aluminium in blood serum using 1,2,4-trihydroxyanthraquinone. *Anal. Lett.*, **25**, 851-864.
- May, H. M., Helmke, P. A. and Jackson, M. L.** (1979) Gibbsite solubility and thermodynamic properties of hydroxy-aluminium ions in aqueous solution at 25 °C. *Geochim. Cosmochim. Acta*, **43**, 861-868.
- McAvoy, D. C., Santore, R. C., Shosa, J. D. and Driscoll, C. T.** (1992) Comparison between pyrocatechol violet and 8-hydroxyquinoline procedures for the determining aluminium fractions. *Soil Sci. Soc. Am. J.*, **56**, 449-455.

- McBride, M. B.** (1982) Cu^{2+} -adsorption characteristics of aluminium hydroxide and oxyhydroxides. *Clays Clay Miner.*, **30**, 21-28.
- McBride, M. B. and Wessellink, L. G.** (1988) Chemisorption of catechol on gibbsite, boehmite, and noncrystalline alumina surfaces. *Environ. Sci. Technol.*, **22**, 703-708.
- McCahon, C. P., Brown, A. F., Poulton, M. J. and Pascoe, D.** (1989) Effects of acid, aluminium and lime additions on fish and invertebrates in a chronically acidic Welsh stream. *Water Soil Air Pollut.*, **45**, 345-359.
- McCahon, C. P. and Pascoe, D.** (1989) Short-term experimental acidification of a Welsh stream: toxicity of different forms of aluminium at low pH to fish and invertebrates. *Arch. Environ. Contam. Toxicol.*, **18**, 233-242.
- McLaughlin, A. I. G., Kazantzis, G., King, E., et al.** (1962) Pulmonary fibrosis and encephalopathy associated with the inhalation of aluminium dust. *Brit. J. Industr. Med.*, **19**, 253-263.
- McLeod, C. W., Otsuki, A., Okamoto, K., Haraguchi, H. and Fuwa, K.** (1981) Simultaneous determination of trace metals in sea water using dithiocarbamate preconcentration and inductively coupled plasma emission spectrometry. *Analyst*, **106**, 419-428.
- Measures, C. I., Yuan, J. and Resing, J. A.** (1995) Determination of iron in seawater by flow injection analysis using in-line preconcentration and spectrophotometric detection. *Mar. Chem.*, **50**, 3-12.
- Meyer, J. M. and Abdallah, M. A.** (1978) The fluorescent pigment of *Pseudomonas fluorescens*: Biosynthesis, purification and physicochemical properties. *J. Gen. Microbio.*, **107**, 319-328.
- Miller, J. R. and Andelman, J. B.** (1987) Speciation of aluminium in an acidic mountain stream. *Water Res.*, **21**, 999-1005.
- Millero, F. J. and Schreiber, D. R.** (1982) Use of the ion pairing model to estimate activity coefficients of the ionic components of natural waters. *Am. J. Sci.*, **282**, 1508-1540.
- Millero, F. J., Yao, W. and Aicher, J.** (1995) The speciation of Fe(II) and Fe(III) in natural waters. *Marine Chem.*, **50**, 21-39.
- Miyasaka, S. C., Buta, J. G., Howell, R. K. and Foy, C. D.** (1991) Mechanism of aluminium tolerance in snapbeans. Root exudation of citric acid. *Plant Physiol.*, **96**, 737-743.
- Miyazaki, A. and Barnes, R. M.** (1981) Complexation of some transition metals, rare earth elements, and thorium with a poly(dithiocarbamate) chelating resin. *Anal. Chem.*, **53**, 299-304.

- Miyazaki, Y.** (1995) NMR studies on the complexation of aluminium ion with inorganic ligands in crosslinked polysaccharide gel. *Polyhedron*, **14**, 1961-1964.
- Mohammad, B., Ure, A. M. and Littlejohn, D.** (1992) On-line preconcentration of aluminium with immobilised 8-hydroxyquinoline for determination by atomic absorption spectrometry. *J. Anal. At. Spectrom.*, **7**, 695-699.
- Molitoris, B. A., Froment, D. H., MacKenzie, T. A., Huffer, W. H. and Alfrey, A. C.** (1989) Citrate: A major factor in the toxicity of orally administered aluminium compounds. *Kidney Int.*, **36**, 949-953.
- Mookherji, S. and Floyd, M.** (1991) The effect of aluminium on growth of and nitrogen fixation in vegetable soybean germplasm. *Plant Soil*, **136**, 25-29.
- Mooney, J. P., Meaney, M., Smyth, M. R., Leonard, G. L. and Wallace, G. G.** (1987) Determination of copper(II) and iron(III) in some anaerobic adhesive formulations using high-performance liquid chromatography. *Analyst*, **112**, 1555-1558.
- Moyers, E. H. and Fritz, J. S.** (1976) Separation of metal ions using a hexylthioglycolate resin. *Anal. Chem.*, **48**, 1117-1120.
- Moyers, E. H. and Fritz, J. S.** (1977) Preparation and analytical applications of a propylenediaminetetraacetic acid resin. *Anal. Chem.*, **49**, 418-423.
- Munns, D. N., Helyar, K. R. and Conyers, M.** (1992) Determination of aluminium activity from measurements of fluoride in acid soil solutions. *J. Soil Sci.*, **43**, 441-446.
- Mustafin, I. S., Molot, L. A. and Arkhangelskaya, A. S.** (1967) Polyhydroxytriphenylmethane dyes as reagents for aluminium, Communication 1. Pyrocatechol violet and its aluminium complex. *Zh. Anal. Khim.*, **22**, 1808-1811.
- Nakashima, S., Sturgeon, R. E., Willie, S. N. and Berman, S. S.** (1992) Determination of trace metals in seawater by graphite furnace atomic absorption spectrometry with preconcentration on silica-immobilised 8-hydroxyquinoline in a flow system. *Fresenius' Z. Anal. Chem.*, **330**, 592-595.
- Neal, C., Reynolds, B., Stevens, P. and Hornung, M.** (1989) Hydrogeochemical controls for inorganic aluminium in acidic stream and soil waters at two upland catchments in wales. *J. Hydrol.*, **106**, 155-175.
- Netter, P., Steinmetz, J., Gillet, P., et al.** (1991) Amorphous aluminosilicates in synovial fluid in dialysis-associated arthropathy. *Lancet*, **337**, 545-555.
- Ngila, J. C., Alexander, P. W. and Hibbert, D. B.** (1994) Determination of aluminium ions by indirect potentiometry in a flow system. *Electroanalysis*, **6**, 990-995.
- Nilsson, S. I. and Bergkvist, B.** (1983) Aluminium chemistry and acidification processes in a shallow podsol on the Swedish Westcoast. *Water Air Soil Pollut.*, **20**, 311-329.

- Nilsson, N., Lövgren, L. and Sjöberg, S. (1992) Phosphate complexation at the surface of goethite. *Chemical Speciation Bioavail.*, **4**, 121-130.
- Nilsson, N. (1995) *Inner/outer sphere complexation of phosphate and organic ligands at the goethite-water interface*. Ph.D. Thesis, Umeå University, Sweden.
- Noble, A. D., Sumner, M. E. and Alva, A. K. (1988) Comparison of aluminium and 8-hydroxyquinoline methods in the presence of fluoride for assaying phytotoxic aluminium. *Soil Sci. Soc. Am. J.*, **52**, 1059-1063.
- Nordin, J., Persson, P., Laiti, E. and Sjöberg, S. (unpub.) Outer sphere complexation of *o*-phthalate at the boehmite-water interface.
- Nordstrom, D. K. (1982) The effect of sulfate on aluminium concentrations in natural waters: some stability relations in the system $\text{Al}_2\text{O}_3\text{-SO}_3\text{-H}_2\text{O}$ at 298 K. *Geochem. Cosmochim. Acta*, **46**, 681-692.
- Nordstrom, D. K. and May, H. M. (1989) Aqueous equilibrium data for mononuclear aluminium species. In: *The environmental chemistry of aluminium*. (Ed: G. Sposito) CRC Press, Boca Raton, Florida.
- Nyholm, N. E. I. (1981) Evidence of involvement of aluminium in causation of defective formation of eggshells and of impaired breeding in wild Passerine birds. *Environ. Res.*, **26**, 363-371.
- Obata, H., Karatani, H. and Nakayama, E. (1993) Automated determination of iron in seawater by chelating resin concentration and chemiluminescence detection. *Anal. Chem.*, **65**, 1524-1528.
- Oden, W. I., Amy, G. L. and Conklin, M. (1993) Subsurface interactions of humic substances with Cu(II) in saturated media. *Environ. Sci. Technol.*, **27**, 1045-1051.
- Ogawa, H. (1991) Orientation of benzoic acid and terephthalic acid on an alumina surface and their reactivities observed by infrared spectroscopy. *J. Phys. Org. Chem.*, **4**, 346-352.
- Öhman, L.-O. and Forsling, W. (1981) Equilibrium and structural studies of silicon(IV) and aluminium(III) in aqueous solution 3. A potentiometric study of aluminium(III) hydrolysis and aluminium(III) hydroxo carbonates in 0.6 M NaCl. *Acta Chem. Scand.*, **A35**, 795-802.
- Öhman, L.-O., Sjöberg, S. and Ingri, N. (1983) Equilibrium and structural studies of silicon(IV) and aluminium(III) in aqueous solution. 7. Redox, hydrolysis and complexation equilibria in the system Al^{3+} -1,2-naphthoquinone-4-sulfonate/1,2-dihydroxy-naphthalene-4-sulfonate- OH^- . A potentiometric study in 0.6 M NaCl. *Acta Chem. Scand.*, **37A**, 561-568.
- Öhman, L.-O. and Sjöberg, S. (1983) Equilibrium and structural studies of silicon(IV) and aluminium(III) in aqueous solution. 8. A potentiometric study of aluminium(III)

- salicylates and aluminium(III) hydroxo salicylates in 0.6 M NaCl). *Acta Chem. Scand.*, **37A**, 875-880.
- Öhman, L.-O. and Sjöberg, S.** (1983) Equilibrium and structural studies of silicon(IV) and aluminium(III) in aqueous solution 10. A potentiometric study of aluminium(III) pyrocatecholates and aluminium(III) hydroxo pyrocatecholates in 0.6 M NaCl). *Polyhedron*, **2**, 1329-1335.
- Öhman, L.-O. and Sjöberg, S.** (1988) Thermodynamic calculations with special reference to the aqueous aluminium system. **In:** *Metal speciation: theory, analysis and application*. (Ed: J. R. Kramer and Allen, H. E.) Lewis Publishers, Chelsea.
- Öhman, L.-O.** (1988) Equilibrium and structural studies of silicon(IV) and aluminium(III) in aqueous solution. 17. Stable and metastable complexes in the system $H^+ - Al^{3+}$ -citric acid. *Acta Chem. Scand.*, **37A**, 875-880.
- Olsen, S., Pessenda, L. C., Ruzicka, J. and Hansen, E. H.** (1983) Combination of flow injection analysis with flame atomic-adsorption spectrophotometry: determination of trace amounts of heavy metals in polluted seawater. *Analyst*, **108**, 905-917.
- Orf, G. M. and Fritz, J. S.** (1978) Preparation and chromatographic applications of an amide resin. *Anal. Chem.*, **50**, 1328-1330.
- Pakalns, P.** (1965) Spectrophotometric determination of aluminium with chrome azurol S. *Anal. Chim. Acta*, **32**, 57-63.
- Palmer, D. A. and Wesolowski, D. J.** (1992) Aluminium speciation and equilibria in aqueous solutions: II. The solubility of gibbsite in acidic sodium chloride solutions from 30 to 70 °C. *Geochim. Cosmochim. Acta*, **56**, 1093-1111.
- Pankow, J. F. and Morgan, J. J.** (1981) Kinetics for the aquatic environment. *Environ. Sci. Technol.*, **15**, 1155-1164.
- Papadopoulos, N., Hasiotis, C., Kokkinidis, G. and Papanastasiou, G.** (1991) Three-dimensional electrochemistry. Utilisation of i-E-t curves for elucidation of electrochemical reactions. *J. Electroanal. Chem.*, **308**, 83-96.
- Parker, D. R., Kinraide, T. B. and Zelazny, L. W.** (1988) Aluminium speciation and phytotoxicity in dilute hydroxy-aluminium solutions. *Soil Sci. Soc. Am. J.*, **52**, 438-444.
- Parker, D. R., Zelazny, L. W. and Kinraide, T. B.** (1988) Comparison of three spectrophotometric methods for differentiating mono- and polynuclear hydroxy-aluminium complexes. *Soil Sci. Soc. Am. J.*, **52**, 67-75.
- Parker, D. R., Kinraide, T. B. and Zelazny, L. W.** (1989) On the phytotoxicity of polynuclear hydroxy-aluminium complexes. *Soil Sci. Soc. Am. J.*, **53**, 789-796.

- Parkinson, I. S., Ward, M. K., Feest, T. G., Fewcett, R. W. P. and Kerr, D. N. S. (1979) Fracturing dialysis osteodystrophy and dialysis encephalopathy: an epidemiological survey. *Lancet*, **1**, 406-409.
- Parkinson, I. S., Ward, M. K. and Kerr, D. N. S. (1981) Dialysis encephalopathy, bone disease and anaemia: the aluminium intoxication syndrome during regular haemodialysis. *J. Clin. Pathol.*, **34**, 1285-1294.
- Patton, E. and West, R. (1970) New aromatic anions. VIII. Acidity constants of rhodizonic acid. *J. Phys. Chem.*, **74**, 2512-2518.
- Pavan, M. A., Bingham, F. T. and Pratt, P. F. (1982) Toxicity of aluminium to coffee in ultisols and oxisols amended with CaCO_3 , MgCO_3 and $\text{CaSO}_4 \cdot 2\text{H}_2\text{O}$. *Soil Sci. Soc. Am. J.*, **46**, 1201-1207.
- Pearson, R. G. (1988) Absolute electronegativity and hardness: application to inorganic chemistry. *Inorg. Chem.*, **27**, 734-740.
- Pedrotti, J. J., Angnes, L. and Gutz, I. G. R. (1994) A fast, highly efficient, continuous degassing device and its application to oxygen removal in flow-injection analysis with amperometric detection. *Anal. Chim. Acta*, **298**, 393-399.
- Pereiro García, M. R., Diaz García, M. E. and Sanz-Medel, A. (1987) Flow injection ion-exchange pre-concentration for the determination of aluminium by atomic absorption spectrometry and inductively coupled plasma atomic emission spectrometry. *J. Anal. At. Spectrom.*, **2**, 699-703.
- Pereiro García, M. R., López García, A., Diaz García, M. E. and Sanz-Medel, A. (1990) On-line aluminium pre-concentration and its application to the determination of the metal in dialysis concentrates by atomic absorption spectrometric methods. *J. Anal. At. Spectrom.*, **5**, 15-19.
- Perl, D. P., Gajdusek, D. C., Garruto, R. M., Yanagihara, R. T. and Gibbs, C. J. (1982) Intraneuronal aluminium accumulation in Amyotrophic Lateral Sclerosis and Parkinsonism-Dementia of Guam. *Science*, **217**, 1053-1055.
- Perrin, D. D., Dempsey, B. and Serjeant, E. P. (1981) *pK_a prediction for organic acids and bases*. Chapman and Hall, New York.
- Persaud, G. and Cantwell, F. F. (1992) Determination of free magnesium ion concentration in aqueous solution using 8-hydroxyquinoline immobilised on a nonpolar adsorbent. *Anal. Chem.*, **64**, 89-94.
- Pesavento, M., Profumo, A., Riolo, C. and Soldi, T. (1989) Separation of trace amounts of aluminium on a strong anion-exchange resin loaded with a sulphonated azo dye. *Analyst*, **114**, 623-626.
- Pesavento, M., Biesuz, R., Gallorinin, M. and Profumo, A. (1993) Sorption mechanism of trace amounts of divalent metal ions on a chelating resin containing iminodiacetate groups. *Anal. Chem.*, **65**, 2522-2527.

- Pesavento, M. and Biesuz, R. (1995) Simultaneous determination of total and free metal ion concentration in solution by sorption on iminodiacetate resin. *Anal. Chem.*, **67**, 3558-3563.
- Pettit, L. D. and Powell, H. K. J. (1995) *SC-database, stability constant database*. IUPAC; Academic Software, Oxford.
- Pichet, P. and Benoit, R. L. (1967) Complexes of germanium(IV) with anions of *o*-diphenols and their stability constants. *Inorg. Chem.*, **6**, 1505-1509.
- Plankey, B. J., Patterson, H. H. and Cronan, C. S. (1986) Kinetics of aluminium fluoride complexation in acidic waters. *Environ. Sci. Technol.*, **20**, 160-165.
- Plankey, B. J. and Patterson, H. H. (1987) Kinetics of aluminium fulvic acid complexation in acid waters. *Environ. Sci. Technol.*, **21**, 595-601.
- Plankey, B. J., Patterson, H. H. and Cronan, C. S. (1995) Kinetic analysis of aluminium complex formation with different soil fulvic acids. *Anal. Chim. Acta*, **300**, 227-236.
- Playle, R. C. and Wood, C. M. (1989) Water pH and aluminium chemistry in the gill micro-environment of rainbow trout during acid and aluminium exposures. *J. Comp. Physiol. B*, **159**, 539-550.
- Playle, R. C., Goss, G. G. and Wood, C. M. (1989) Physiological disturbances in rainbow trout (*Salmo gairdneri*) during acid and aluminium exposures in soft water of two calcium concentrations. *Can. J. Zool.*, **67**, 314-324.
- Playle, R. C. and Wood, C. M. (1990) Is precipitation of aluminium fast enough to explain aluminium deposition on fish gills? *Can. J. Fish. Aquat. Sci.*, **47**, 1558-1561.
- Pol  , A. B. S. (1995) Aluminium polymerisation - a mechanism of acute toxicity of aqueous aluminium to fish. *Aquat. Toxicol.*, **31**, 347-356.
- Porta, V., Sarzanini, C., Mentasti, E. and Abollino, O. (1992) On-line preconcentration system for inductively coupled plasma atomic emission spectrometry with quinolin-8-ol and Amberlite XAD-8 resin. *Anal. Chim. Acta*, **258**, 237-244.
- Powell, H. K. J. and Town, R. M. (1993) Aluminium(III)-malonate equilibria - a potentiometric study. *Aust. J. Chem.*, **46**, 721-726.
- Powell, H. K. J. and Hawke, D. J. (1995) Free aluminium and aluminium complexing capacity of natural organic matter in acidic forest soil solutions from Canterbury, New Zealand. *Aust. J. Soil Res.*, **33**, 611-620.
- Prajzler, J. (1931) Simultaneous estimation in the groups iron, chromium, aluminium, nickel, cobalt, zinc and manganese. *Collect. Czech. Chem. Commun.*, **3**, 406-417.

- Preisler, P. W., Berger, L. and Hill, E. S.** (1947) Oxidation-reduction potentials and ionisation constants of the reversible series: Hexahydroxybenzene-tetrahydroxyquinone-rhodizonic acid. *J. Am. Chem. Soc.*, **69**, 326-329.
- Prosser, I. P., Hailes, K. M., Melville, M. D., Avery, R. P. and Slade, C. J.** (1993) A comparison of soil acidification and aluminium under *Eucalyptus* Forest and unimproved pasture. *Aust. J. Soil Sci.*, **31**, 245-254.
- Quintela, M. J., Gallego, M. and Valcarcel, M.** (1993) Flow injection spectrophotometric method for the speciation of aluminium in river and tap waters. *Analyst*, **118**, 1199-1203.
- Qureshi, G. A., Svehla, G. and Leonard, M. A.** (1979) Electrochemical studies of strongly chelating anthraquinone derivatives. *Analyst*, **104**, 705-722.
- Reiber, S., Kukull, W. and Standish-Lee, P.** (1995) Drinking water aluminium and bioavailability. *J. AWWA*, **87**, 86-100.
- Rengel, Z. and Robinson, D. L.** (1989) Aluminium effects on growth and macronutrient uptake by annual ryegrass. *Agron. J.*, **81**, 208-215.
- Rengel, Z.** (1992) Role of calcium in aluminium toxicity. *New Phytol.*, **121**, 499-513.
- Resing, J. A. and Mottl, M. J.** (1992) Determination of manganese in seawater using flow injection analysis with on-line preconcentration and spectrophotometric detection. *Anal. Chem.*, **64**, 2682-2687.
- Resing, J. A. and Measures, C. I.** (1994) Fluorometric determination of Al in seawater by flow injection analysis with on-line preconcentration. *Anal. Chem.*, **66**, 4105-4111.
- Reuss, J. O. and Johnson, D. W.** (1985) Effect of soil processes on the acidification of water by acid deposition. *J. Environ. Qual.*, **14**, 26-31.
- Reuss, J. O., Walthall, P. M., Roswall, E. C. and Hopper, R. W. E.** (1990) Aluminium solubility, calcium-aluminium exchange, and pH in acid forest soils. *Soil Sci. Soc. Am. J.*, **54**, 374-380.
- Reynolds, G. F. and Webber, T. J.** (1958) Oscillographic polarography of aluminium in calcium chloride solution. *Anal. Chim. Acta*, **18**, 293-298.
- Ritchey, K. D., Baligar, V. C. and Wright, R. J.** (1988) Wheat seedling responses to soil acidity and implications for subsoil rooting. *Commun. Soil Sci. Plant Anal.*, **19**, 1285-1293.
- Ritchie, G. S. P.** (1994) Role of dissolution and precipitation of minerals in controlling soluble aluminium in acidic soils. *Water Air Soil Pollut.*, **53**, 47-83.
- Ritchie, G. S. P.** (1995) Soluble aluminium in acidic soils: principles and practicalities. *Plant Soil*, **171**, 17-27.

- Robards, K., Starr, P. and Patsalides, E. (1991) Metal determination and metal speciation by liquid chromatography. *Analyst*, **116**, 1247-1273.
- Robarge, W. P. and Corey, R. B. (1979) Adsorption of phosphate by hydroxy-aluminium species on a cation exchange resin. *Soil Sci. Soc. Am. J.*, **43**, 481-487.
- Rönngren, L., Sjöberg, S., Sun, Z. X., Forsling, W. and Schindler, P. W. (1991) Surface reactions in aqueous metal sulfide systems. 2. Ion exchange and acid/base reactions at the ZnS/H₂O interface. *J. Colloid Interface Sci.*, **145**, 396-404.
- Rönngren, L. (1992) *Acid/base and complexation properties of hydrous zinc- and lead sulfide surfaces*. Ph.D. Thesis, Umeå University, Sweden.
- Rosemond, A. D., Reice, S. R., Elwood, J. W. and Mulholland, P. J. (1992) The effects of stream acidity on benthic invertebrate communities in the south-eastern United States. *Freshwater Biol.*, **27**, 193-209.
- Rosseland, B. O., Eldhuset, T. D. and Staurnes, M. (1990) Environmental effects of aluminium. *Environ. Geochem. Health*, **1/212**, 17-27.
- Rosseland, B. O., Blakar, I. A., Bulger, A., et al. (1992) The mixing zone between limed and acidic river waters: complex aluminium chemistry and extreme toxicity for salmonids. *Environ. Pollut.*, **78**, 3-8.
- Rossotti, F. J. C. and Rossotti, H. (1961) *The determination of stability constants: and other equilibrium constants in solution*. McGraw-Hill, New York.
- Roy, A. K., Sharma, A. and Talukder, G. (1988) Some aspects of aluminium toxicity in plants. *Bot. Rev.*, **54**, 145-178.
- Røyset, O. (1985) Comparison of four chromogenic reagents for the flow-injection determination of aluminium in water. *Anal. Chim. Acta*, **178**, 223-230.
- Røyset, O. and Sullivan, T. J. (1986) Effect of dissolved humic compounds on the determination of aqueous aluminium by three spectrophotometric methods. *Intern. J. Environ. Anal. Chem.*, **27**, 305-314.
- Ruzicka, J. and Hansen, E. H. (1978) Flow injection analysis. X. Theory, techniques and trends. *Anal. Chim. Acta*, **99**, 37-76.
- Ruzicka, J. and Hansen, E. H. (1988) *Flow injection analysis, 2nd Edition*. John Wiley & Sons, New York.
- Ruzicka, J. and Arndal, A. (1989) Sorbent extraction in flow injection analysis and its application to enhancement of atomic spectrometry. *Anal. Chim. Acta*, **216**, 243-255.
- Ryan, P. R., Kinraide, T. B. and Kochian, L. V. (1994) Al³⁺-Ca²⁺ interactions in aluminium rhizotoxicity. I. Inhibition of root growth is not caused by reduction of calcium uptake. *Planta*, **192**, 98-103.

- Sadler, K. and Turnpenny, A. W. H.** (1986) Field and laboratory studies of exposures of brown trout to acid waters. *Water Air Soil Pollut.*, **39**, 593-599.
- Salbu, B., Bjornstad, H. E., Lindstrom, N. S., et al.** (1985) Size fractionation techniques in the determination of elements associated with particulate or colloidal material in natural fresh waters. *Talanta*, **32**, 907-913.
- Saraswat, I. P., Sharma, C. L. and Sharma, A.** (1979) Thermodynamical functions of pyrocatechol violet complexes with bivalent transition metal ions. *J. Indian Chem. Soc.*, **56**, 928-929.
- Sarzanini, C., Mentasti, E., Porta, V. and Gennaro, M. C.** (1987) Comparison of anion-exchange methods for preconcentration of trace aluminium. *Anal. Chem.*, **59**, 484-486.
- Saxena, R., Singh, A. K. and Sambi, S. S.** (1994) Synthesis of a chelating polymer matrix by immobilising alizarin red-S on Amberlite XAD-2 and its application to the preconcentration of lead(II), cadmium(II), zinc(II) and nickel(II). *Anal. Chim. Acta*, **295**, 199-204.
- Scarrow, R. C., Riley, P. E., Abu-Dari, P., White, D. L. and Raymond, K. N.** (1985) Ferric ion sequestering agents. 13. Synthesis, structures, and thermodynamics of complexation of cobalt(III) and Iron(III) tris complexes of several chelating hydroxypyridinones. *Inorg. Chem.*, **24**, 954-967.
- Schartz, L. M. and Gelb, R. I.** (1978) Statistical analysis of titration data. *Anal. Chem.*, **50**, 1571-1576.
- Schautman, M. A. and Morgan, J. J.** (1994) Adsorption of aquatic humic substances on colloidal-size aluminium oxide particles: influence of solution chemistry. *Geochim. Cosmochim. Acta*, **58**, 4293-4303.
- Schecher, W. D. and Driscoll, C. T.** (1987) An evaluation of uncertainty associated with aluminium equilibrium calculations. *Water Resour. Res.*, **23**, 525-534.
- Schecher, W. D. and Driscoll, C. T.** (1988) An evaluation of the equilibrium calculations within acidification models: the effect of uncertainty in measured chemical components. *Water Resour. Res.*, **24**, 533-540.
- Schindler, P. W. and Gamsjäger, H.** (1972) Acid-base reactions of TiO_2 (Anatase) - water interface and the point of zero charge of TiO_2 suspensions. *Kolloid-Z. u. Z. Polymere*, **250**, 759-765.
- Schindler, P. W.** (1981) Adsorption of inorganics at solid-liquid interfaces. (Ed: M. A. Anderson and Rubin, A. J.) Ann Arbor Science, Ann Arbor, MI.
- Schindler, P. W. and Stumm, W.** (1987) The surface chemistry of oxides, hydroxides, and oxide minerals. In: *Aquatic Surface Chemistry*. (Ed: W. Stumm) John Wiley and Sons, New York.

- Schindler, P. W.** (1990) Co-adsorption of metal ions and organic ligands: formation of ternary surface complexes. **In:** *Mineral-Water Interface Geochemistry* (Ed: M. F. Hochella and White, A. F.) Mineralogical Society of America, Washington, DC.
- Schindler, P. W. and Sposito, G.** (1991) Surface complexation at (hydr)oxide surfaces. **In:** *Interactions at the soil colloid - soil solution interface*. (Ed: G. H. Bolt et al) NATO ASI Series; Series E, Applied Sciences, Kluwer Academic Publishers, Netherlands.
- Schnitzer, M., Ripmeester, J. A. and Kodama, H.** (1988) Characterisation of the organic matter associated with a soil clay. *Soil Sci.*, **145**, 448-454.
- Schofield, C. L. and Trojnar, J. R.** (1980) Aluminium toxicity to brook trout (*Salvelinus fontinalis*) in acidified waters. *Environ. Sci. Res.*, **17**, 341-366.
- Schulten, H.-R.** (1995) The three-dimensional structure of humic substances and soil organic matter studied by computational analytical chemistry. *Fresenius' J. Anal. Chem.*, **35**, 62-73.
- Schulthess, C. P. and Sparks, D. L.** (1987) Two-site model for aluminium oxide with mass balanced competitive pH + salt/salt dependent reactions. *Soil Sci. Soc. Am. J.*, **51**, 1136-1144.
- Schulthess, C. P. and McCarthy, J. F.** (1990) Competitive adsorption of aqueous carbonic and acetic acids by an aluminium oxide. *Soil Sci. Soc. Am. J.*, **54**, 688-694.
- Schulthess, C. P. and Huang, C. P.** (1991) Humic and fulvic acid adsorption by silicon and aluminium oxide surfaces on clay minerals. *Soil Sci. Soc. Am. J.*, **55**, 34-42.
- Seip, H. M.** (1980) Acidification of freshwaters: sources and mechanisms. **In:** *Ecological impact of acid precipitation*. (Ed: D. Drablos and Trollan, A.) Johs. Grefslie Trykkeri A/S, Mysen.
- Seip, H. M., Müller, L. and Naas, A.** (1984) Aluminium speciation: comparison of two spectrophotometric analytical methods and observed concentrations in some acidic aquatic systems in Southern Norway. *Water Air Soil Pollut.*, **23**, 81-95.
- Shann, J. R. and Bertsch, P. M.** (1993) Differential cultivar response to polynuclear hydroxo-aluminium complexes. *Soil Sci. Soc. Am. J.*, **57**, 116-120.
- Sigg, L. and Stumm, W.** (1981) The interactions of anions and weak acids with the hydrous goethite (α -FeOOH) surface. *Colloids Surf.*, **2**, 101-117.
- Simon, L., Kieger, M., Jones, J. B. and Lasseigne, F. T.** (1994a) Aluminium toxicity in tomato. Part 1. Growth and mineral nutrition. *J. Plant Nutr.*, **17**, 293-306.
- Simon, L., Kieger, M., Sung, S. S. and Smalley, T. J.** (1994b) Aluminium toxicity in tomato. Part 2. Leaf gas exchange, chlorophyll content, and invertase activity. *J. Plant Nutr.*, **17**, 307-317.

- Singh, A. K. and Rita, P.** (1991) Amberlyst A-26 resin loaded with pyrocatechol violet-preparation and applications as a preconcentrator in the atomic adsorption spectrophotometric determination of lead and cadmium. *Microchem. J.*, **43**, 112-115.
- Singh, A. K. and Dhingra, S. K.** (1992) Application of Dowex-2 loaded with sulfonephthalein dyes to the preconcentration of Cu(II) and Cd(II). *Analyst*, **117**, 889-891.
- Sjöberg, S., Hägglund, Y., Nordin, A. and Ingri, N.** (1983) Equilibrium and structural studies of silicon(IV) and aluminium(III) in aqueous solution - V. Acidity constants of silicic acid and the ionic product of water in the medium range 0.05-2.0 M NaCl at 25 °C. *Mar. Chem.*, **13**, 35-44.
- Sjöberg, S. and Öhman, L.-O.** (1985) Equilibrium and structural studies of silicon(IV) and aluminium(III) in aqueous solution. 13. A potentiometric and ²⁷Al nuclear magnetic resonance study of speciation and equilibria in the aluminium(III)-oxalic acid-hydroxide system. *J. Chem. Soc. Dalton Trans.*, 2665-2669.
- Sjöberg, S. and Lövgren, L.** (1993) The application of potentiometric techniques to study complexation reactions at the mineral/water interface. *Aquatic Sci.*, **55**, 324-335.
- Slanina, P., Frech, W., Ekström, L. G., et al.** (1986) Dietary citric acid enhances absorption of aluminium in antacids. *Clin. Chem.*, **32**, 539-541.
- Smith, R. M. and Yankey, L. W.** (1982) Determination of metal ions by liquid chromatography incorporating dithiocarbamates in the eluent. *Analyst*, **107**, 744-748.
- Smith, C. L., Motooka, J. M. and Wilson, W. R.** (1984) Analysis of trace metals in water by inductively coupled plasma emission spectrometry using sodium dibenzyldithiocarbamate for preconcentration. *Anal. Lett.*, **17**, 1715-1730.
- Sparén, A.** (1994) *Analytical methodology for aluminium fractionation in aqueous media*. Ph.D. Thesis, The Royal Institute of Technology (KTH), Sweden.
- Sperling, M., Yin, X. and Welz, B.** (1992) Determination of ultra-trace concentrations of elements by means of on-line solid sorbent extraction graphite furnace atomic adsorption spectrometry. *Fresenius' J. Anal. Chem.*, **343**, 754-755.
- Sposito, G.** (1983) On the surface complexation model of the oxide-aqueous solution interface. *J. Colloid Interface Sci.*, **91**, 329-340.
- Sposito, G.** (1989) *The environmental chemistry of aluminium*. CRC Press, Boca Raton, Florida.
- Stern, O.** (1924) The theory of the electric double layer. *Z. Elektrochem.*, **30**, 508-516.

- Stevenson, F. J. and Vance, G. F.** (1989) Naturally occurring aluminium-organic complexes. *In: The environmental chemistry of aluminium.* (Ed: G. Sposito) CRC Press, Boca Raton, Florida.
- Stone, A. T.** (1991) Oxidation and hydrolysis of ionisable organic pollutants at hydrous metal oxide surfaces. *In: Rates of Soil Chemical Processes.* (Ed: SSSA Spec. Publ., Madison, WI.
- Stone, A. T., Torrents, A., Smolen, J., Vasudevan, D. and Hadley, J.** (1993) Adsorption of organic compounds possessing ligand donor groups at the oxide/water interface. *Environ. Sci. Technol.*, **27**, 895-909.
- Stumm, W., Huang, C. P. and Jenkins, S. R.** (1970) Specific chemical interactions affecting the stability of dispersed systems. *Croat. Chem. Acta*, **48**, 491-504.
- Stumm, W. and Morgan, J. J.** (1981) *Aquatic Chemistry.* Wiley-Interscience, New York, N.Y.
- Stumm, W.** (1986) Coordinative interactions between soil solids and water - An aquatic chemist's point of view. *Geoderma*, **38**, 19-30.
- Sturgeon, R. E., Berman, S. S., Willie, S. N. and Desaulniers, J. A. H.** (1981) Preconcentration of trace elements from seawater with silica-immobilised 8-hydroxyquinoline. *Anal. Chem.*, **53**, 2337-2340.
- Sullivan, T. J., Seip, H. M. and Muniz, I. P.** (1986) A comparison of frequently used methods for the determination of aqueous aluminium. *Intern. J. Environ. Anal. Chem.*, **26**, 61-75.
- Sun, Z. X., Forsling, W., Rönngren, L., Sjöberg, S. and Schindler, P. W.** (1991) Surface reactions in aqueous metal sulfide systems. 3. Ion exchange and acid/base properties of hydrous lead sulfide. *Colloid Surfaces*, **59**, 243-254.
- Sundd, S., Prasad, S. K., Kumar, A. and Prasad, B. B.** (1994) Chelating resin-impregnated paper chromatography, applications to trace element collection of ferrous and ferric ions, and determination by differential pulse anodic stripping voltammetry. *Talanta*, **41**, 1943-1949.
- Sutheimer, S. H. and Cabaniss, S. E.** (1995a) Aqueous Al(III) speciation by high-performance cation exchange chromatography with fluorescence detection of the aluminium-lumogallion complex. *Anal. Chem.*, **67**, 2342-2349.
- Sutheimer, S. H. and Cabaniss, S. E.** (1995b) Determination of trace aluminium in natural waters by flow-injection analysis with fluorescent detection of the lumogallion complex. *Anal. Chim. Acta*, **303**, 211-221.
- Sweileh, J. A. and Cantwell, F. F.** (1985) Sample introduction by solvent extraction/flow injection to eliminate interferences in atomic adsorption spectroscopy. *Anal. Chem.*, **57**, 420-424.

- Sweileh, J. A., Lucyk, D., Kratochvil, B. and Cantwell, F. F. (1987) Specificity of the ion exchange/atomic absorption method for free copper(II) species determination in natural waters. *Anal. Chem.*, **59**, 586-592.
- Takahashi, T., Fukupka, T. and Dahlgren, R. A. (1995) Aluminium solubility and release rates from soil horizons dominated by aluminium-humus complexes. *Soil Sci. Plant Nutr.*, **41**, 119-131.
- Tan, K. H. and Binger, A. (1986) Effect of humic acid on aluminium toxicity in corn plants. *Soil Sci.*, **141**, 20-25.
- Tanaka, A., Tadano, T., Yamamoto, K. and Kanamura, N. (1987) Comparison of toxicity to plants among Al^{3+} , AlSO_4^+ , and Al-F complex ions. *Soil Sci. Plant Nutr.*, **33**, 43-55.
- Tapparo, A. and Bombi, G. G. (1990) Ion chromatographic determination of trace amounts of aluminium with on-line preconcentration and spectrophotometric detection. *Anal. Chim. Acta*, **238**, 279-284.
- Tapparo, A., Solda, L., Bombi, G. G., et al. (1995) Analytical validation of a general protocol for the preparation of dose-controlled solutions in aluminium toxicology. *Analyst*, **120**, 2425-2429.
- Taugbøl, G., Seip, H. M., Bishop, K. and Grip, H. (1994) Hydrochemical modelling of a stream dominated by organic-acids and organically bound aluminium. *Water Air Soil Pollut.*, **78**, 103-139.
- Thomas, F., Bottero, J. Y. and Cases, J. M. (1989a) An experimental study of the adsorption mechanisms of aqueous organic acids on porous aluminas. 1. The porosity of the adsorbent: A determining factor for the adsorption mechanisms. *Colloids Surf.*, **37**, 269-280.
- Thomas, F., Bottero, J. Y. and Cases, J. M. (1989b) An experimental study of the adsorption mechanisms of aqueous organic acids on porous aluminas. 2. Electrochemical modelling of salicylate adsorption. *Colloids Surf.*, **37**, 281-294.
- Tikhonov, V. N. and Bakhtina, V. V. (1984) Complexation of aluminium, gallium and indium with pyrocatechol violet. *Zh. Anal. Khim.*, **39**, 2126-2132.
- Tipping, E., Ohnstad, M. and Woof, C. (1989) Adsorption of aluminium by stream particles. *Environ. Pollut.*, **57**, 85-96.
- Tipping, E., Berggren, D., Mulder, J. and Woof, C. (1995) Modelling the solid-solution distributions of protons, aluminium, base cations and humic substances in acid soils. *Eur. J. Soil Sci.*, **46**, 77-94.
- Torres, H. O., Moreno, J. F., Abizanda, J. A. and Leon, A. J. J. (1992) Use of an azo derivative immobilised on an anionic resin for the determination of aluminium in water and dialysis fluids. *Clin. Chim. Acta*, **209**, 35-46.

- Town, R. M.** (1991) *Studies on the hydrophobic and hydrophilic properties of humic substances*. Ph.D. Thesis, University of Canterbury, New Zealand.
- Town, R. M. and Powell, H. K. J.** (1993) Ion-selective electrode potentiometric studies on the complexation of copper(II) by soil-derived humic and fulvic acids. *Anal. Chim. Acta*, **279**, 221-233.
- van den Berg, C. M. G., Murphy, K. and Riley, J. P.** (1986) The determination of aluminium in seawater and freshwater by cathodic stripping voltammetry. *Anal. Chim. Acta*, **188**, 177-185.
- van der Berg, C. M. G., Nimmo, M., Abollino, O. and Mentasti, E.** (1991) The determination of trace levels of iron in seawater using adsorptive cathodic stripping voltammetry. *Electroanalysis*, **3**, 477-484.
- Vassos, B. H. and Mark, H. B.** (1967) The anodic dissolution of thin films of copper metal from pyrolytic graphite. A study of the dissolution current peaks. *Electroanal. Chem. Interfacial Electrochem.*, **13**, 1-9.
- Vernon, F. and Eccles, H.** (1975) Chelating ion exchangers containing N-substituted hydroxylamine functional groups. I. N-arylphenylhydroxylamines. *Anal. Chim. Acta*, **77**, 145-152.
- Vilchez, J. L., Navalon, A., Avidad, R., García-López, T. and Capitán-Vallvey, L. F.** (1993) Determination of trace amounts of aluminium in natural waters by solid-phase spectrofluorimetry. *Analyst*, **118**, 303-307.
- Violante, A., Colombo, C. and Buondonno, A.** (1991) Competitive adsorption of phosphate and oxalate by aluminium oxides. *Soil Sci. Soc. Am. J.*, **55**, 65-70.
- Vukomanovic, D. V., Page, J. A. and Vanloon, G. W.** (1991) Voltammetric determination of Al(III) with adsorptive preconcentration of the pyrocatechol violet complex. *Can. J. Chem.*, **69**, 1418-1426.
- Wagatsuma, T., Kaneko, M. and Hayasaka, Y.** (1987) Destruction process of plant root cells by aluminium. *Soil Sci. Plant Nutr.*, **33**, 161-175.
- Wakley, W. D. and Varga, L. P.** (1972) Stability constants of tin pyrocatechol violet complexes from computer analysis of absorption spectra. *Anal. Chem.*, **44**, 169-178.
- Walker, W. J., Cronan, C. S. and Bloom, P. R.** (1990) Aluminium solubility in organic soil horizons from northern and southern forested watersheds. *Soil Sci. Soc. Am. J.*, **54**, 369-374.
- Wang, J., Farias, P. A. M. and Mahmoud, J. S.** (1985) Stripping voltammetry of aluminium based on adsorptive accumulation of its solochrome violet RS complex at the static mercury drop electrode. *Anal. Chim. Acta*, **172**, 57-64.

- Wang, X. and Barnes, R. M. (1989) Chelating resins for on-line flow injection pre-concentration with inductively coupled plasma atomic emission spectrometry. *J. Anal. At. Spectrom.*, **4**, 509-517.
- Waring, C. P. and Brown, J. A. (1995) Ionoregulatory and respiratory responses of brown trout, *Salmo-trutta*, exposed to lethal and sublethal aluminium in acidic soft waters. *Fish. Physiol. Biochem.*, **14**, 81-91.
- Weatherly, N. S., Rogers, A. P., Goenaga, X. and Ormerod, S. J. (1990) The survival of early life stages of brown trout (*Salmo trutta* L.) in relation to aluminium speciation in upland Welsh streams. *Aquat. Toxicol.*, **17**, 213-230.
- Welz, B., Yin, X. and Sperling, M. (1992) Time-based and volume based sampling for flow-injection on-line sorbent extraction graphite furnace atomic adsorption spectrometry. *Anal. Chim. Acta*, **261**, 477-487.
- Westall, J. C. and Hohl, H. (1980) A comparison of electrostatic models for the oxide/solution interface. *Adv. Colloid Interface Sci.*, **12**, 265-294.
- Westall, J. C. (1986) Reactions at the oxide-solution interface: chemical and electrostatic models. In: *Geochemical processes at mineral surfaces*. (Ed: J. A. Davis and Hayes, K. F.) ACS symposium series American Chemical Society, Washington.
- Westall, J. C. (1987) Adsorption mechanisms in aquatic surface chemistry. In: *Aquatic Surface Chemistry*. (Ed: W. Stumm) John Wiley and Sons, New York.
- Wheller, D. M. (1994) Effects of growth period, plant age and changes in solution aluminium concentrations on aluminium toxicity in wheat. *Plant Soil*, **166**, 21-30.
- Whitten, M. G. and Ritchie, G. S. P. (1991a) A comparison of soil tests to predict the growth and nodulation of subterranean clover in aluminium-toxic topsoils. *Plant Soil*, **136**, 11-24.
- Whitten, M. G. and Ritchie, G. S. P. (1991b) Soil tests for aluminium toxicity in the presence of organic matter: laboratory development and assessment. *Commun. In Soil Sci. Plant Anal.*, **22**, 343-368.
- Wilkinson, K. J., Bertsch, P. M., Jagoe, C. H. and Campbell, P. G. C. (1993) Surface complexation of aluminium on isolated fish gill cells. *Environ. Sci. Technol.*, **27**, 1132-1138.
- Willard, H. H. and Dean, J. A. (1950) Polarographic determination of aluminium. *Anal. Chem.*, **22**, 1264-1267.
- Wills, M. R. and Savory, J. (1983) Aluminium poisoning: dialysis encephalopathy, osteomalacia, and anaemia. *Lancet*, **2**, 29-34.
- Wilson, M. J. (1986) Mineral weathering processes in podsollic soils on granitic materials and their implications for surface water acidification. *J. Geological Soc.*, **143**, 691-697.

- Winship, K. A. (1993) Toxicity of aluminium: a historical review. Part 2. *Adverse Drug React. Toxicol.*, **12**, 177-211.
- Witters, H. E. (1986) Acute acid exposure of rainbow trout, *Salmo Gairdneri* Richardson: effects of aluminium and calcium on ion balance and haematology. *Aquat. Toxicol.*, **8**, 197-210.
- Wood, C. M., Playle, R. C., Simons, B. P., Goss, G. G. and McDonald, D. G. (1988) Blood gases, acid-base status, ions and haematology in adult brook trout (*Salvelinus fontinalis*) under acid/aluminium exposure. *Can. J. Fish. Aquat. Sci.*, **45**, 1575-1586.
- Wren, C. D. and Stephenson, G. L. (1991) The effect of acidification on the accumulation and toxicity of metals to freshwater invertebrates. *Environ. Pollut.*, **71**, 205-241.
- Wright, R. J., Baligar, V. C. and Wright, S. F. (1987) Estimation of phytotoxic aluminium in soil solution using three spectrophotometric methods. *Soil Sci.*, **144**, 224-232.
- Xie, R. Y. and Christian, G. D. (1986) Serum lithium analysis by coated wire lithium ion selective electrodes in a flow injection analysis dialysis system. *Anal. Chem.*, **58**, 1806-1810.
- Xu, S. (1992) *Development and application of chemically modified electrodes for analysis*. Ph.D. Thesis, University of Canterbury, New Zealand.
- Yates, D. E., Levine, S. and Healy, T. W. (1974) Site-binding model of the electrical double layer at the oxide/water interface. *J. Chem. Soc. Faraday Trans.*, **70**, 1807-1818.
- Yebra-Biurrun, M. C., Bermejo-Barrera, A. and Bermejo-Barrera, P. (1992a) Synthesis and characterisation of a poly(aminophosphonic acid) chelating resin. *Anal. Chim. Acta*, **264**, 53-58.
- Yebra-Biurrun, M. C., Bermejo-Barrera, A. and Bermejo-Barrera, P. (1992b) Application of a poly(dithiocarbamate) resin to the determination of trace copper, iron and zinc in natural waters. *Mikrochim. Acta*, **109**, 243-251.
- Yuan, D. and Shuttler, I. L. (1995) Flow-injection column preconcentration directly coupled with electrothermal atomisation atomic absorption spectrometry for the determination of aluminium. Comparison of column packing materials. *Anal. Chim. Acta*, **316**, 313-322.
- Zelazny, L. W. and Jardine, P. M. (1989) Surface reactions of aqueous aluminium. In: *The environmental chemistry of aluminium*. (Ed: G. Sposito) CRC Press, Boca Raton, Florida.
- Zernichow, L. and Lund, W. (1995) Size exclusion chromatography of aluminium species in natural waters. *Anal. Chim. Acta*, **300**, 167-171.

-
- Zhang, Z., Rettig, S. J. and Orvig, C.** (1991) Lipophilic coordination compounds: Aluminium, gallium, and indium complexes of 1-aryl-3-hydroxy-2-methyl-4-pyridinones. *Inorg. Chem.*, **30**, 509-515.
- Zusman, R., Rottman, C., Ottolenghi, M. and Avnir, D.** (1990) Doped sol-gel glasses as chemical sensors. *J. Non-cryst. Solids*, **122**, 107-109.
-